Research Highlights 1997-2010

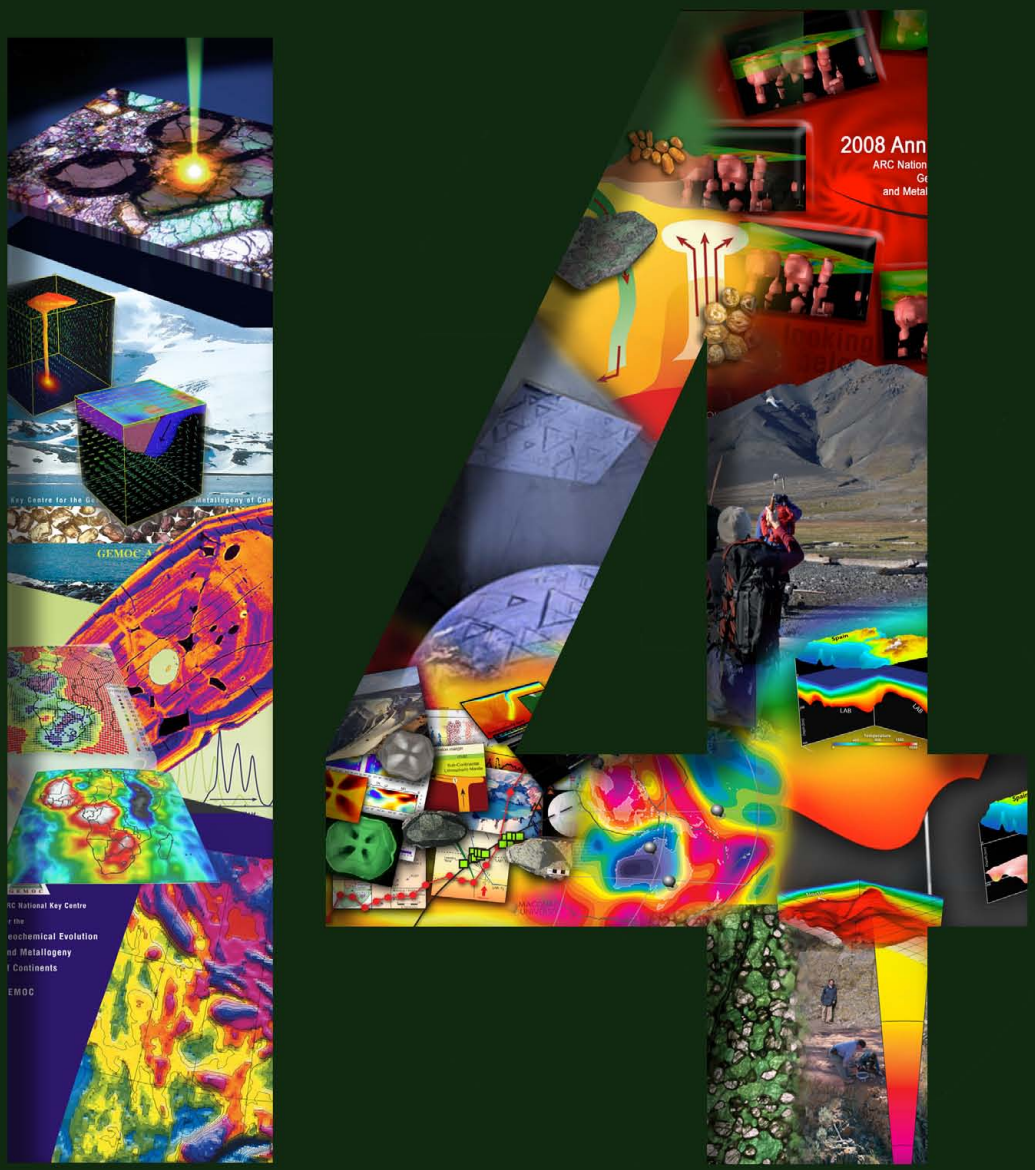

ARC National Key Centre for the Geochemical Evolution and Metallogeny of Continents

MACQUARIE UNIVERSITY

GEMOC

- **GEMOC information is accessible on WWW at: http://www.gemoc.mq.edu.au/**
- **Contact GEMOC via email at: gemoc@mq.edu.au**

Contact details

http://www.gemoc.mq.edu.au/
gemoc@mq.edu.au

GEMOC
Department of Earth and Planetary Sciences
Macquarie University NSW 2109
AUSTRALIA

Carol McMahon
Administrator
Phone: 61 2 9850 8953
Fax: 61 2 9850 8943 or 6904
Email: carol.mcmahon@mq.edu.au

Professor Suzanne Y. O'Reilly
Director
Phone: 61 2 9850 8362
Fax: 61 2 9850 8943
Email: sue.oreilly@mq.edu.au

Professor W.L. Griffin
Program Leader
Phone: 61 2 9850 8954
Fax: 61 2 9850 8943
Email: bill.griffin@mq.edu.au

Dr Norman Pearson
Manager, Geochemical Analysis Unit
Phone: 61 2 9850 8361
Fax: 61 2 9850 8943 or 6904
Email: norman.pearson@mq.edu.au

Contents

1997 Research Highlights	1
1998 Research Highlights	11
1999 Research Highlights	23
2000 Research Highlights	39
2001 Research Highlights	59
2002 Research Highlights	84
2003 Research Highlights	110
2004 Research Highlights	136
2005 Research Highlights	161
2006 Research Highlights	186
2007 Research Highlights	211
2008 Research Highlights	237
2009 Research Highlights	273
2010 Research Highlights	303

The complete GEMOC Annual Reports can be viewed in html at: http://www.gemoc.mq.edu.au/

Established and supported under the Australian Research Council's Research Centres Program

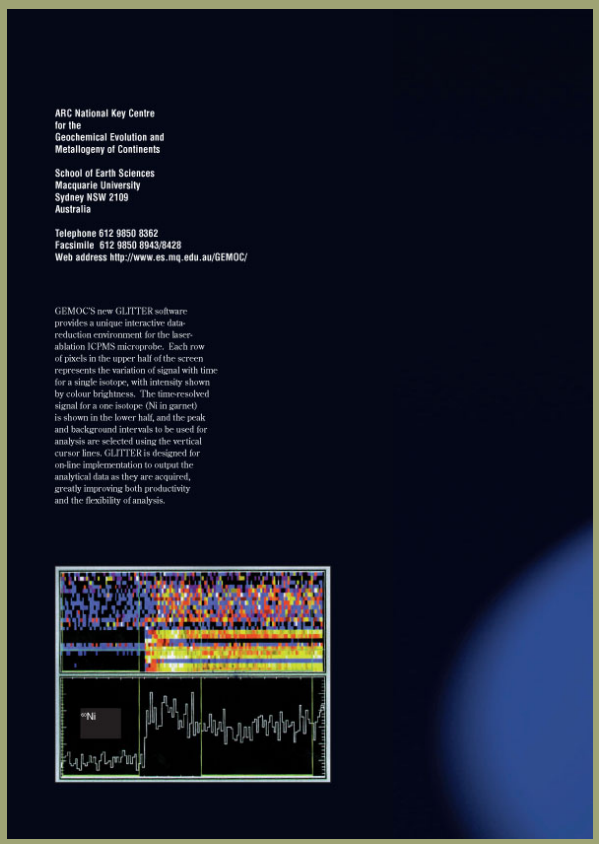

1997 Contents

Chromites from ultramafic rocks: guides to nickel, diamonds and the lithosphere	2
Unique mantle history of eastern Australian diamonds: products of stress in a slab?	3
Are lithospheres forever?	4
Chemical tomography of the northern Siberian Platform: imaging the lithosphere	6
All cratons are not created equal: Lithosphere Structure and Mantle Terranes, Slave Craton, Canada	8
Zircon — a brilliant petrological recorder	9
Island Arc-Oceanic Plateau Collision;Santa Isabel, Solomon Islands	10
The petrology and mineralisation of the plutonic roots of an island arc magmatic system - the Greenhills Complex, New Zealand	10

Cover: A thin section of garnet lherzolite, the most common rock type in Earth's upper mantle, is being ablated by a focussed laser beam for in situ trace element microanalysis. In 1997 GEMOC's laser-ablation ICPMS microprobe analysed more than 8000 mineral grains for academic and industrial research.

Chromites from ultramafic rocks: guides to nickel, diamonds and the lithosphere

CHROMITE [(Mg,Fe)(Al,Cr,Fe)2O4] is a ubiquitous and important accessory mineral in mantle-derived ultramafic magmatic and metamorphic rocks, which are potential source rocks of diamond and other commodities such as Ni. Chromite has long been used as an indicator mineral in diamond exploration because it is very resistant to weathering and remains in the regolith after other indicators such as garnet are destroyed. However, other ultramafic rocks such as komatiites, which may host Ni deposits, also contain abundant chromite, which is similar in major-element composition to those from diamondiferous rocks. The GEMOC laser-ablation ICPMS microprobe (LAM-ICPMS) is being used to develop trace-element discriminants to improve the use of chromites in exploration for diamonds and komatiite-hosted Ni deposits. Detailed studies over the last two years have shown that the abundances of several trace elements, such as Co, Zn and Mn are closely related in mantle-derived chromites of all ages and tectonic setting, reflecting temperature-dependent partitioning between chromite and olivine. This Mantle Array we have defined for chromites has become a basic tool for distinguishing between mantle-derived xenocrysts and the chromites of ultramafic magmas such as komatiites. On a more detailed level, trace element analyses show marked differences in the chromites of Ni-bearing and barren komatiites, which appear to reflect the contamination of the Ni-bearing magmas with crustal material.

"The GEMOC laser-ablation ICPMS microprobe (LAM-ICPMS) is being used to develop trace-element discriminants to improve the use of chromites in exploration"

These "fingerprints" can be used to recognise potentially mineralised flow units, before the ore has been found.

Kimberlites and other volcanic rocks generated near the lithosphere-asthenosphere boundary penetrate the whole lithosphere stratigraphy as they ascend to the surface, and carry up mantle xenocrysts, including chromite. If the chemistry of the chromite xenocrysts can be interpreted, they become tracers of mantle composition. The elements in the Mantle Array record temperature differences, and allow the original depth of each grain to be estimated. Our other studies show that the composition of lithospheric mantle has changed through time, and these differences also are showing up in the chromites. For example, chromites from Phanerozoic lithosphere generally are higher in Al and Ga than those from older lithosphere, reflecting lower degrees of depletion in basaltic components, while chromites from Archean lithosphere are significantly richer in V and Nb than those from younger mantle. Chromites will become progressively more important to our Lithosphere Mapping work as these studies proceed.

"trace element analyses show marked differences in the chromites of Ni-bearing and barren komatiites"

Contact: Bill Griffin and Shixin Yao; funded by Rio Tinto, Macquarie University, Industry consulting
Part of GEMOC's Lithosphere Mapping and Metallogenesis strands

Unique mantle history of eastern Australian diamonds: products of stress in a slab?

OVER 1000 ALLUVIAL DIAMONDS from several localities in eastern Australia have revealed that while all diamonds have similar surface textures that indicate transport to the surface in a magma, there are two distinctive groups (*Publication 89*). Group A (for Airly Mtn) is similar to diamonds from conventional kimberlitic occurrences in cratons in their inclusions, carbon isotopic compositions, internal morphology and old formation ages (from Re/Os compositions of sulphide inclusions).

However, Group B (for Bingara) is unique: forms are irregular and show strong deformation; their mineral inclusions reflect a Ca-rich eclogitic environment; and their carbon is isotopically heavy. Furthermore internal growth structures revealed in cathodoluminescence (CL) images (*Figures 1, 2*) show evidence of unstable and dynamic growth histories during which deformation has occurred simultaneously with diamond growth (*Publication 110 Appendix 2*). This ubiquitous deformation in Group B diamonds is evident not as the fine cross-hatched linear features typical of plastic deformation in diamond, but as brittle displacements of layers, commonly with cataclastic disruption of layers and brecciation of internal structures (*Figure 2*).

"Cathodoluminescence images show evidence of unstable and dynamic growth histories during which deformation has occurred simultaneously with diamond growth"

Internal structures typical of the Group B diamonds include non-planar growth facets (*Figure 1*), resorption and disrupted central structures that have annealed and show subsequent overgrowths. Many diamonds show N-rich rounded cores (light CL) overgrown by N-poor (dark CL) diamond that may be overgrown, in turn, by an oscillating sequence of N-bearing and N-free layers with sharp contacts, suggesting growth under rapidly changing conditions. These structures are consistent with episodic growth and fluctuating fluid compositions and physical conditions (eg temperature and oxygen fugacity); a high strain field is necessary to explain the deformation features and is consistent with growth in an active subduction environment.

Contact: Rondi Davies; funded by Rio Tinto. Part of GEMOC's Lithosphere Mapping and Metallogenesis strands:

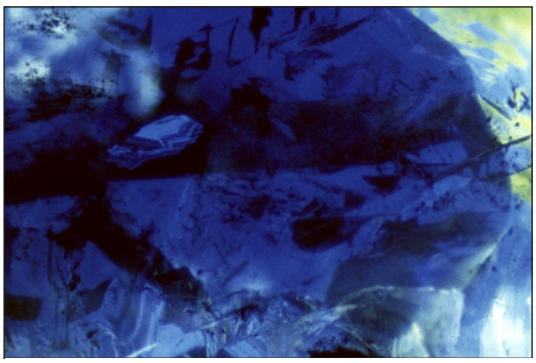

Figure 1.

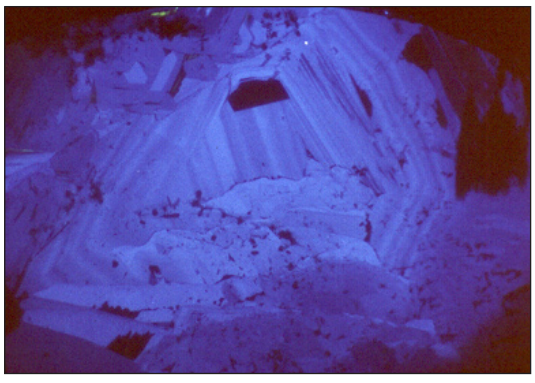

Figure 2.
Cataclastic deformation structures.

Eastern Australian diamonds

Are lithospheres forever?

THE SUBCONTINENTAL LITHOSPHERIC mantle (SCLM) carries a geochemical, thermal and chronological record of large-scale tectonic events that have shaped the Earth's crustal geological terrains. The SCLM is part of the continental plate, and moves with the plates over the less rigid asthenosphere. Development of the 4-D Lithosphere Mapping methodology (*Publication 1, Appendix 2*) has provided tools for constructing realistic geological sections of the SCLM and for following the evolution of the lithosphere through time. Xenoliths and garnet and chromite xenocrysts from mantle-derived volcanics (eg basalts, lamproites, kimberlites) provide samples of the lithospheric mantle at the time of eruption. Where sufficient xenoliths and/or xenocrysts of appropriate composition are available, we can determine the paleogeotherm, the depth to the crust-mantle boundary, the detailed distribution of rock types with depth, the spatial distribution of fluid-related (metasomatic and anatectic) processes and the depth to the lithosphere-asthenosphere boundary within the tectosphere. Volcanic episodes of different ages in one region provide this information for different time-slices corresponding to ages of the volcanism, while geophysical data (seismic, gravity, magnetic, thermal) can be used to extend the geologically-derived profiles laterally or to interpret lithospheric domains with geophysical signatures that can be matched with geologically mapped sections.

Applications of 4-D lithosphere mapping have resulted in several new fundamental conclusions about lithosphere processes through time. *Secular variation* in lithosphere composition is revealed from the geochemical fingerprints of mantle xenoliths and disaggregated garnets. These data show that there have been episodic and irreversible changes in the composition of the SCLM from the Archean to the Phanerozoic and that the Archean/Proterozoic boundary represents a major change in the nature of lithosphere-forming processes *(Publication 109, Appendix 2)*. *Lithosphere evolution and destruction* mechanisms have been defined in some regions and appear to be characterised by lithosphere thinning and geochemical and thermal erosion.

"there have been episodic and irreversible changes in the composition of the SCLM from the Archean to the Phanerozoic"

The Sino-Korean craton provides an excellent example: Ordovician kimberlites have sampled deep (200 km), cool, depleted (buoyant) Archean type mantle lithosphere while younger basaltic and kimberlitic volcanics contain mantle samples characterising thin (80 km), hot, fertile mantle with relatively low Vp of about 7.7 km/sec. A tomographic model of this region by Yuan (1996) is shown in figure 1, suggesting thinning and disruption of old mantle with high seismic velocity and replacement by new fertile, asthenospheric mantle. The new mantle corresponds to the fertile Phanerozoic type and would metasomatise and mix into the older disrupted SCLM. This disruption and dispersal of a 200 km thick Archean root was accompanied by uplift, basin formation and widespread magmatism.

Figure 1

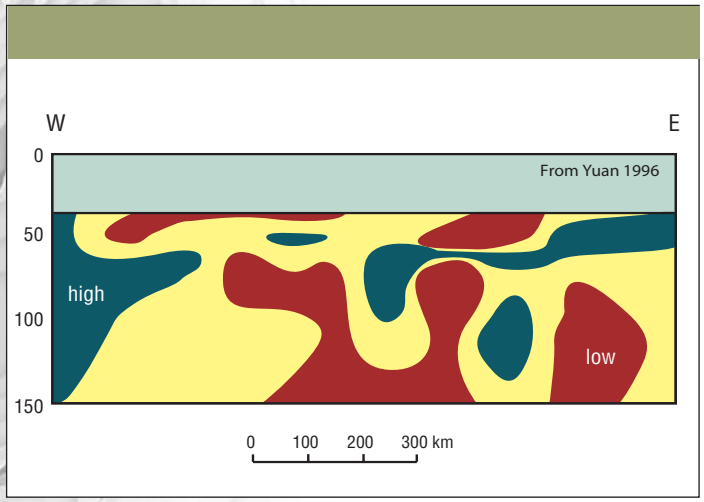

“events that lead to the replacement of old SCLM by such younger material cause changes in the density and geotherm of the lithospheric column, with major effects at the surface”

Tectonic or magmatic events that lead to the replacement of old SCLM by such younger material cause changes in the density and geotherm of the lithospheric column, with major effects at the surface. In the Kaapvaal Craton (Figure 2, with icons showing fields for diamond and graphite) thermal and chemical erosion produced in a thinner, hotter and chemically recharged (metasomatised) lithosphere at about 90 million years, and led to significant uplift of the craton *(Brown et al., 7IKC Abstract, 1998, Appendix 4)*.

In summary, correlations between mantle type and crustal age indicate that continental crust and its underlying SCLM were formed together and remain coupled for geologically long times. Destruction of Archean SCLM is difficult, but where it occurs, by thermal and chemical erosion and/or rifting, thinning and displacement, it has major thermal and tectonic consequences and affects geophysical properties (*Publications 90, 109 Appendix 2*).

“Destruction of Archean SCLM has major thermal and tectonic consequences and affects geophysical properties”

Contact: S.Y. O’Reilly and W. L. Griffin and the Lithosphere Modelling Group: funded by ARC, Macquarie University, Collaborative research with industry, ACILP, DEETYA TIL Part of GEMOC’s Lithosphere Mapping strand

Figure 2

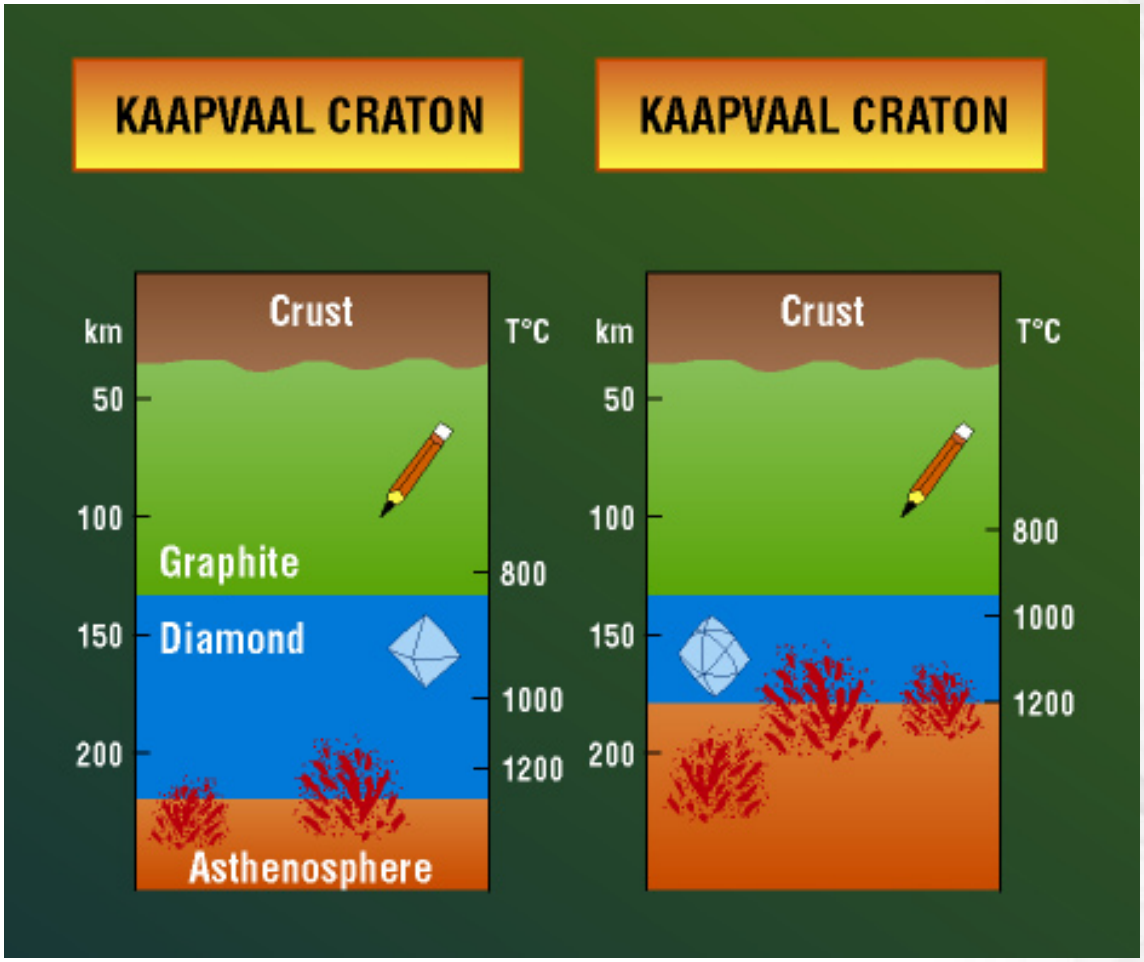

Chemical tomography of the northern Siberian Platform: imaging the lithosphere

THE KIMBERLITE FIELDS of the northern Siberian Platform sample the mantle to depths of about 200 km along a 1000 km traverse stretching from the Malo-Botuobiya field in the SW to the Kuoika field in the NE. This traverse crosses several major terrane boundaries mapped using surface geology and geophysics, including a major discontinuity between the Archean part of the craton in the south and the Proterozoic part in the north. Over 6,000 garnet and chromite xenocrysts from 14 of these fields have been used to map the distribution of mantle rock types along this traverse. Nickel and Zinc Thermometry have been used to derive the paleogeotherm at each point *(Publication 92, Appendix 2)* and a depth of derivation for each xenocryst. The garnets have been assigned to one of 5 rock types, using their Ca and Cr contents. The figure (next page) shows the vertical and lateral distribution of these rock types along the traverse, and outlines several important geological features. Harzburgitic rocks are restricted to the southern portions of the craton which have Archean crust; the Archean-Proterozoic boundary is clearly visible in the central portion of the figure. Under the Archean part of the traverse, the lithosphere-asthenosphere boundary is delineated by the Ca-harzburgites, and shows significant topography.

"Large vertical offsets in mantle stratigraphy within the Archean part of the craton reflect mapped surface terrane boundaries"

The low-Cr rocks are fertile lherzolites, and appear especially in the right centre, where the traverse crosses an Upper Precambrian rift zone. The low-Cr rocks at depths >150 km probably represent magmatic intrusion into the lower lithosphere, and show the rise in the lithosphere-asthenosphere boundary beneath the rift. Large vertical offsets in mantle stratigraphy within the Archean part of the craton reflect mapped surface terrane boundaries, which appear to be translithospheric sutures.

Images like this let us map major lithospheric structures, their boundaries (likely to be the sites of world-class ore deposits of such commodities as nickel) and provide new data about how continents form. The next stage of this work will use regional geophysics to map these structures laterally into areas where kimberlites are not available.

"Images like this let us map major lithospheric structures, their boundaries and provide new data about how continents form"

Contact: W.L. Griffin, S. Y. O'Reilly, C. Ryan: original project funded by ARC and RTZ Exploration; next stage funded by Western Mining Corp. and Macquarie University.
Part of GEMOC's Lithosphere Mapping and Geotectonics strands.

Window to the lithosphere
The Mir diamond mine has yielded some of the mantle xenoliths, mineral concentrates and diamonds that have been some of the tools for constructing the chemical tomography section across northern Siberia.

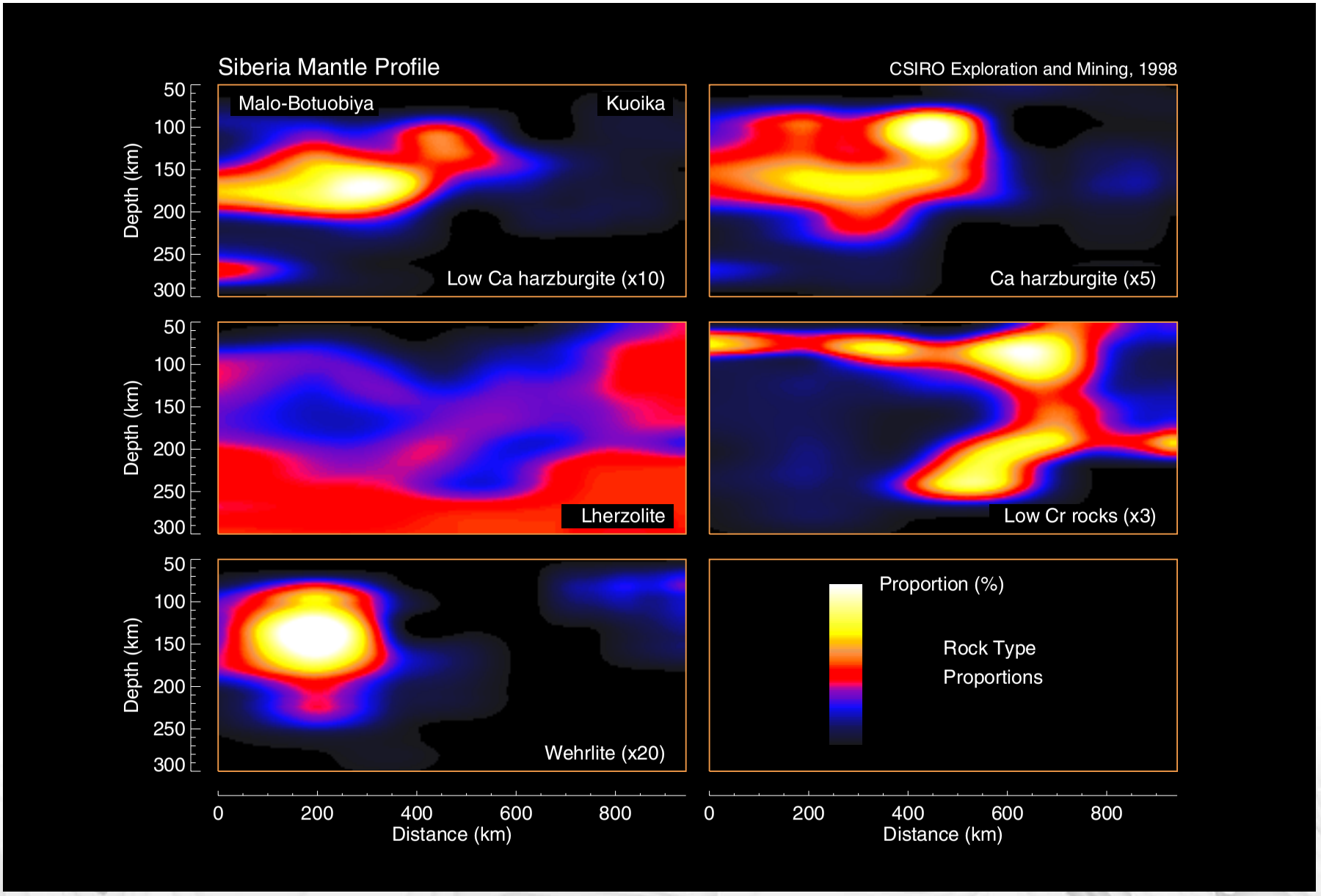

See text on facing page for explanation

All cratons are not created equal: Lithosphere Structure and Mantle Terranes, Slave Craton, Canada

XENOLITHS AND HEAVY MINERAL concentrates have been used to map the composition, structure and thermal state of the lithospheric mantle beneath the Slave craton in northwestern Canada. Beneath the Lac de Gras area in the centre of the craton, the lithosphere is 200-220 km thick, and a sharp boundary between two layers of the lithospheric mantle is defined by plots of trace- and major-element data vs Nickel Temperature (T_{Ni}) for concentrate garnets. Projection of the temperature of this boundary (~900 °C) to the geotherm derived from xenoliths and concentrates places it at a depth of 150±10 km. Above this boundary, the mantle consists of ultradepleted rocks dominated by harzburgites, while from 150 km to the lithosphere-asthenosphere boundary (LAB) the major rock type is a moderately depleted lherzolite. Testimates on eclogite xenoliths show that they are concentrated in the deeper layer, and especially near the LAB. Our studies of the diamonds from this area show that a large proportion contain a "superdeep" inclusion suite, with minerals that have formed at depths >650 km (Davies et al., 1998). This suggests that the deeper layer of the lithosphere rose as a diapir from near the core-mantle boundary, and spread out below a thinner pre-existing lithosphere that may have been formed during craton assembly (>2.6 Ga).

"diamonds from this area show that a large proportion contain a "superdeep" inclusion suite"

"the deeper layer of the lithosphere rose as a diapir from near the core-mantle boundary"

The heat supplied by the lithospheric underplating may have helped generate the extensive 2.6 Ga granite suite of the Slave Craton. The two-layered lithosphere has been traced over an area of ca 1800 km^2 around Lac de Gras; at greater distances the shallow ultradepleted layer appears to thin, and the deeper layer and the LAB rise to shallower depths.

This integrated study of diamonds (and their inclusions), xenoliths and concentrate minerals has shown that the Slave craton has a unique lithosphere structure, and gives us clues to the interpretation of other cratons worldwide.

"the Slave craton has a unique lithosphere structure, and gives us clues to the interpretation of other cratons worldwide"

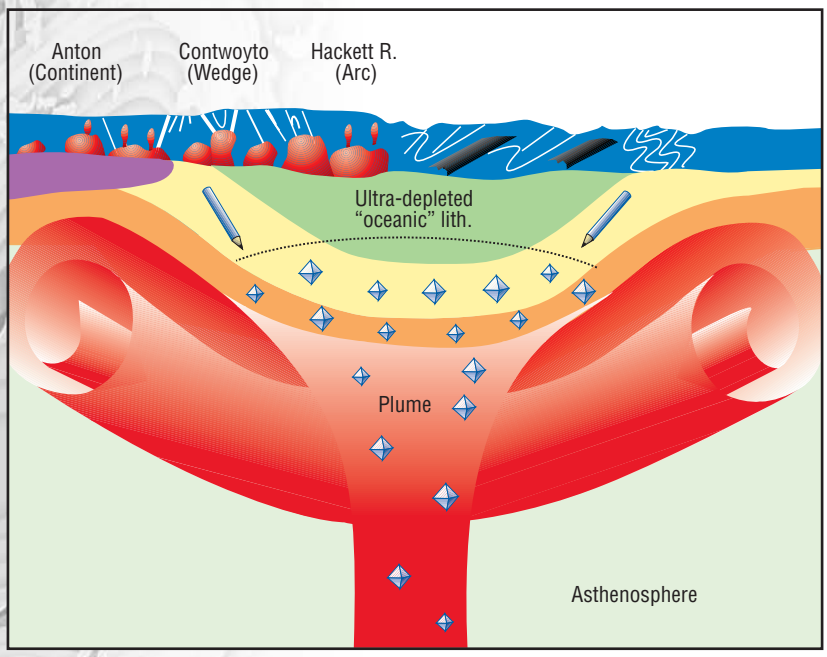

Contact: W.L. Griffin, S. Y. O'Reilly, N.J. Pearson; project funded by Kennecott Canada Inc. and Macquarie University. Part of GEMOC's Lithosphere Mapping, Metallogenesis and Geotectonics strands

Zircon — a brilliant petrological recorder

Zircon ($ZrSiO_4$) is a common accessory in a wide range of igneous rocks ranging from basic to felsic in composition. It is highly stable and resistant, so that it can survive partial melting processes and hydrothermal activity as well as weathering and transport. Magmatic zircon typically shows pronounced internal zoning, which can be observed in polished sections using a combination of high-resolution backscattered-electron (BSE) and cathodoluminescence (CL) imaging. (See zircon image in the *Technology Development* section).

This zoning, which reflects minor compositional variations, records changes in the external morphology of the crystals during their growth in the magma. The morphology of zircon is complex, with the development of different crystal forms related to both temperature and magma composition, and the internal zoning thus provides a qualitative tape recorder of changes in these parameters. The GEMOC laser-ablation ICPMS microprobe (LAM ICPMS) allows us to analyse up to 30 elements in zircon at low ppb detection limits, with a spatial resolution of 30-40 microns. With these data, we can correlate changes in internal morphology with changes in trace element chemistry, and the composition of the magma at each stage of crystallisation then can be calculated by using experimentally-derived and empirical distribution coefficients. In several Australian examples, this approach has provided clear evidence of complex magmatic histories, with linked changes in temperature and magma composition.

The technique now will be used, together with analysis of Hf and Pb isotopes by the new multi-collector ICPMS laser-ablation microprobe, to study the evolution of granites in eastern China, as part of a study of crust-mantle interactions.

Most crustal zircons show yellow excitation colours under the cathodoluminescence microscope, while most mantle-derived zircons (from kimberlites) show blue-violet colours. These differences appear to be related to trace-element contents. LAM-ICPMS data show that kimberlite zircons have distinctive trace element patterns, with well defined ranges for REE, Y, U, Th and P as well as chondrite-normalised REE patterns with low and flat HREE. Rare yellow-luminescing zones in kimberlitic zircons have higher U, Th, Y, and REE than those with blue-violet CL. This suggests that variations in luminescence colours reflect an interplay between elements such as the REE, which give blue colours, and lattice defects, which give yellow colours.

"This study is providing base-line data using our new technology to provide a framework for mineral exploration"

This study is providing base-line data using our new technology to provide a framework for mineral exploration.

Contact: Bill Griffin, Elena Belousova; funded by Rio Tinto, BHP, Macquarie University
Part of GEMOC's Crustal Generation and Metallogenesis strands

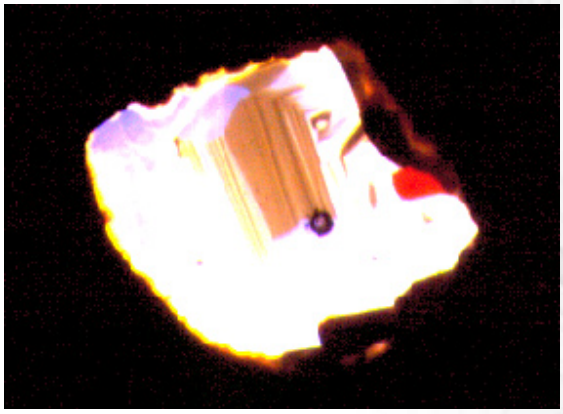

Cathodoluminescence image of zircon from Yakutian kimberlite (Russia) shows inherited core with thin oscillatory zoning overgrown by a homogeneous rim.

Island Arc-Oceanic Plateau Collision; Santa Isabel, Solomon Islands

ON SANTA ISABEL in the northeastern Solomon Islands arc, exposed rock units include: pillow basalts of the world's largest known "flood basalt" province, the Ontong Java Plateau (OJP); gabbros and refractory peridotites (representing the upper mantle residues from melting during formation of the pillow basalts); fault-slices and serpentinite diapirs of supra-subduction zone mantle. These rock sequences comprise the essential components of an ophiolite, except that sheeted dykes are not present, and represent the first reported occurrence of deep portions of the OJP. A 2 km stratigraphic lava sequence yields strictly bi-modal 40Ar/39Ar ages of 122±1 and 90±1 Ma, the same as basalts recovered by Ocean Drilling Program Leg 130 ~ 2000 km away on the OJP. Four chemically-distinctive basalt groups occur on Santa Isabel, three of which are similar to ODP Leg 130 basalts. Lavas erupted at 122 and 90 Ma are modelled as high degree melts of peridotite, most likely within a mantle plume head which impacted beneath thin oceanic lithosphere. The peridotites have origins ranging from harzburgite residues from a supra-subduction zone setting to lherzolite residues of melting processes which generated the OJP. Of particular interest is the nature of the spinel phases included within the various peridotite types - these vary in composition from abyssal-peridotite-like through highly refractory Cr-rich to highly oxidised (Fe3+-rich). Juxtaposition of peridotites with contrasting melting histories may be diagnostic of oceanic plateau collision at a convergent margin. The exposed OJP shows limited signs of being subducted, and may form a thick lithospheric cap under which subduction zone melts will be generated. Modification of the OJP by these melts and eventual collision with a continent will complete a sequence of continental crustal growth formed both by mantle plume and supra-subduction zone processes.

"The exposed OJP shows limited signs of being subducted, and may form a thick lithospheric cap under which subduction zone melts will be generated"

Contact: R. J. Arculus; project funded by ARC Part of GEMOC's Crustal Generation strand

The petrology and mineralisation of the plutonic roots of an island arc magmatic system - the Greenhills Complex, New Zealand

THE GREENHILLS COMPLEX is an Early Permian, ultramafic-mafic layered igneous intrusion comprising thick sequences of dunite, olivine clinopyroxenite, olivine gabbro and hornblende gabbro-norite, enclosed by a ring dyke and cut by numerous other doleritic dykes. The complex is part of the Brook Street Terrane, probably originally formed in an intra-oceanic arc setting, correlative with the Gympie Province of northeastern Australia, and accreted to the eastern margin of Gondwana. The bulk of the complex was formed by fractional crystallisation of mafic magma. On the basis of the crystallisation sequence, mineral compositions, calculated oxygen fugacities, and trace element compositions of (re-heated, homogenised) former melt inclusions in chromite, we infer that the parental melts of the Greenhills rocks were primitive, low-K island arc tholeiites. Both primary and secondary platinum group element (PGE) minerals are preserved in chrome spinel-rich pods in dunite, and are likely the source of alluvial platinum minerals distributed along the coast to the east of the complex.

"primary and secondary platinum group element (PGE) minerals are preserved in chrome spinel-rich pods in dunite"

Contact: C. Spandler, R. J. Arculus, S.M. Eggins & J. Mavrogenes; project funded by ARC in collaboration with R.C. Price (University of Waikato) and A. Reay (University of Otago) Part of GEMOC's Crustal Generation and Metallogenesis strands

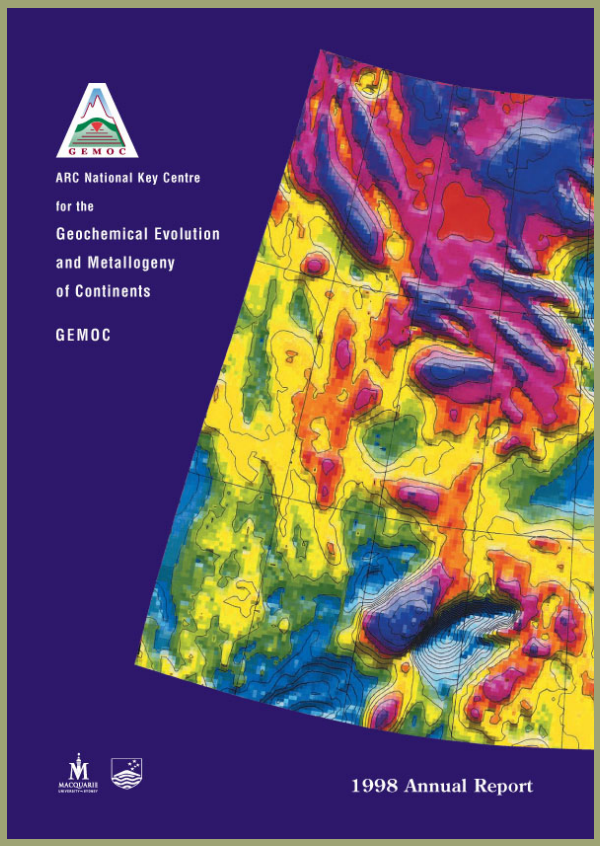

ARC National Key Centre
for the
Geochemical Evolution and
Metallogeny of Continents

Department of Earth and Planetary Sciences
Macquarie University
Sydney NSW 2109
Australia

Telephone 612 9850 8362
Facsimile 612 9850 8943/6904
Web address http://www.es.mq.edu.au/GEMOC/
Email address gemoc@mq.edu.au

GEMOC'S new Nu Plasma multi-collector magnetic sector ICPMS is manufactured by Nu Instruments Ltd and the GEMOC instrument is the first of its kind in the southern hemisphere. It combines an argon-plasma ionisation source with a multicollector magnetic sector mass spectrometer to make an instrument specifically designed for high-precision analysis of isotope ratios. The instrument features a revolutionary design with an electrostatic "zoom lens" that allows it to analyse most of the elements in the periodic table with a series of fixed detectors.

1998 Contents

Where has the mantle under Australia been? 12

Diamonds from the Deep and Shallow 13

Apatite: a sensitive indicator of crystallisation environment 14

Other Worlds: Deep Space 2 15

Detecting lithosphere-scale structures: Siberian Platform 16

From the micro to the macro or: has the Earth changed? 18

Continental fragments within an oceanic plateau? The Agulhas Plateau, SW Indian Ocean 20

Where has Australia been? 21

Trace elements in the carbon of your choice by LAM-ICP-MS 22

Granites hot and cold 22

Established and supported under the Australian Research Council's Research Centres Program

Research highlights 1998

Where has the mantle under Australia been?

THE GLOBAL-SCALE MANTLE CONVECTION CELLS in the asthenosphere are not geochemically homogeneous. The heterogeneity is most prominently reflected in the isotopic compositions (Pb-Sr-Nd) of the mid-ocean ridge basalts (MORB) that are direct partial melts from the underlying asthenosphere. Of particular relevance to Australia's geodynamic evolution from about 100 million years, is the distinctive geochemical signatures of the asthenosphere beneath the Pacific Ocean (Pacific MORB) and Indian Ocean (Indian MORB). Therefore, delineation of the boundary between the two distinct mantle reservoirs and any change in that boundary with time provides information about the patterns of global-scale asthenospheric mantle convection from the base of the lithosphere to the core-mantle boundary. This information also allows us to track global-scale mantle chemical reservoirs such as the distinctive Gondwana lithospheric mantle and hence better understand the geodynamic evolution of the Australian continent from the time of Gondwana dispersal.

Pb-Sr-Nd isotope data for Cenozoic basalts in eastern Australia indicate that Pacific-MORB type mantle isotopic signatures characterise the lava-field basalts (55-14 Ma) in southeastern Australia, whereas Indian-MORB type mantle isotopic signatures characterise younger basalts (6-0 Ma) from northeastern Australia. This discovery helps to constrain the changing locus of major asthenospheric mantle convection cells represented by the Pacific and Indian MORB sources during and following the breakup of the eastern part of Gondwana, and locates, for the first time, the locus of the boundary of these convection cells beneath the Australian continent. These new data also indicate that the Indian-MORB source is a long-term asthenospheric reservoir beneath most of the Gondwana lithosphere and that the westward migration of the Pacific MORB source may have been associated with the Tasman Sea opening (ca 85-60 Ma) along a broad front southeast of the Australian continent.

Publication: 133

Contact: Ming Zhang and Sue O'Reilly
Funded by: ARC, Macquarie University, ACILP
Part of GEMOC's Lithosphere Mapping and Geotectonics strands.

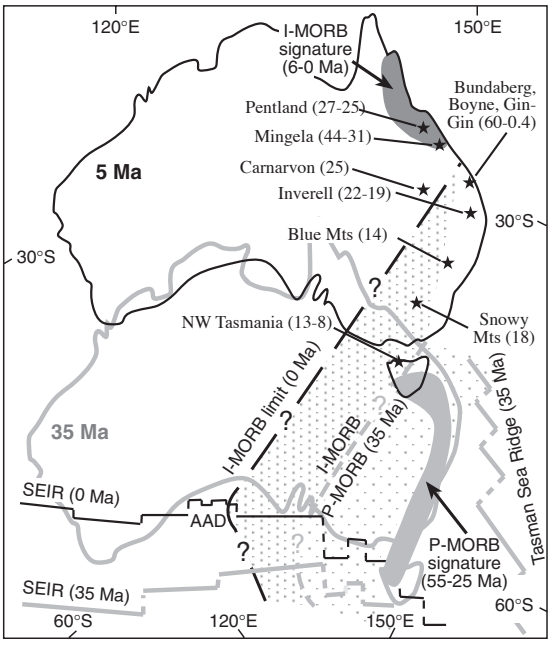

Shaded fields show distribution of the Australian basalts with Pacific-MORB and Indian-MORB geochemical signatures at 35 Ma and 5 Ma. Solid stars represent present-day locations of basalts. Numbers in brackets are ages of the basalts in Ma.

Diamonds from the Deep and Shallow

DIAMONDS from kimberlites recently discovered in the Slave Craton (Canada) were compared with alluvial diamonds from eastern Australia using mineral inclusions, morphological characteristics, carbon isotopes, nitrogen contents and nitrogen aggregation states of the diamonds. Diamonds from the DO-27 kimberlite pipe (Canada), largely contrast with the characteristics of those from eastern Australia, and have provided new information about the mantle from the Lac de Gras region in the central Slave Craton.

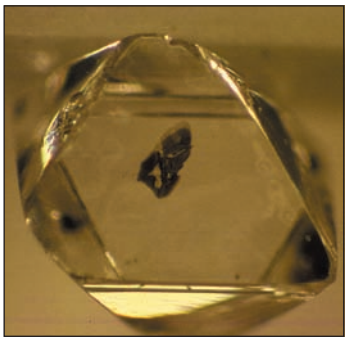

Figure 1. Octahedral diamond with peridotitic inclusion, Slave Craton, Canada

The syngenetic mineral inclusions encased in diamond preserve pristine samples of the ancient cratonic mantle from the time of diamond crystallisation. The combined inclusion and diamond studies show that about half of the diamonds from the DO-27 kimberlite formed in an eclogitic environment, 35% in peridotite environments and the remaining 15% are from the "super-deep" paragenesis, recognised from only eleven diamond localities worldwide.

Super-deep minerals include ferropericlase ((Mg, Fe)O) and Mg, Fe-perovskite ((Mg, Fe)SiO_3) with inferred formation conditions in excess of 1000˚C and 200 kbars, equivalent to lower mantle depths of more than 650 km. The super-deep diamonds may be evidence for the activity of ancient deep plumes in the construction of the Slave Craton. A parallel GEMOC study of xenoliths and heavy mineral concentrates from kimberlites across the central region of the Slave Craton found that the mantle lithosphere has a two-layered structure. The lower layer, (about 150 to 220 km), may host the super-deep and eclogitic assemblages, while the peridotitic diamonds may derive from the higher levels with more depleted and older mantle.

The diamonds from the Slave Craton contrast in morphology with those from eastern Australia (see the octahedral diamond from the Slave Craton and the dodecahedral diamond with resorbed and glossy surfaces. Their low nitrogen contents do not allow cathodoluminescece imaging as do the eastern Australian diamonds (Fig. 3). The fundamental differences between the diamonds of these two occurrences have led to our conclusions that some of the Canadian diamonds originated in the lower mantle, while some eastern Australian ones formed at shallow levels, probably in a subduction environment.

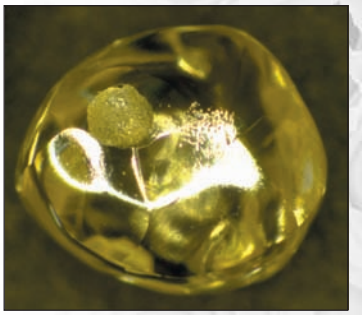

Figure 2. Dodecahedral diamond with resorbed, glossy surfaces, Bingara, eastern Australia.

Publications: 89, 110, 123, 124, 137

Contact: Rondi Davies, Bill Griffin, Sue O'Reilly
Partly funded by Rio Tinto.
Part of GEMOC's Lithosphere Mapping and Metallogenesis strands.

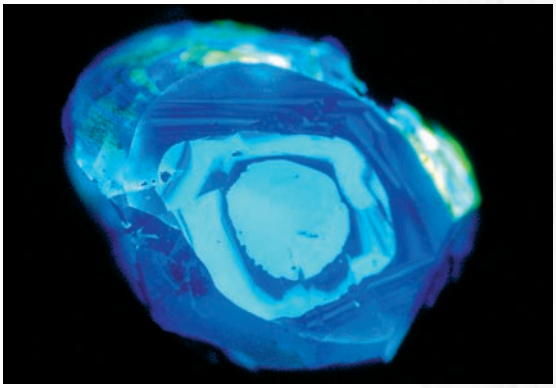

Figure 3. A cathodoluminescence image of a diamond from Bingara, eastern Australia, with high nitrogen content.

Apatite: a sensitive indicator of crystallisation environment

APATITE is a ubiquitous accessory mineral in magmatic, metamorphic and sedimentary rocks.

It is found in mafic to felsic rocks, in carbonatites and in many mineralised environments including magmatic iron-ore deposits. Apatite may concentrate a high proportion of the whole-rock REE, Y, Sr, U, Th and thus, apatite is a sensitive recorder of the trace element chemistry of the rock at the time of its crystallisation. Where crystallisation has taken place over an extended time, differences between generations of apatite and/or compositional zoning within individual grains, record the evolution of the chemical environment.

The GEMOC laser-ablation ICPMS microprobe has allowed analysis of about 30 trace elements (including REE, Y, Sr, U, Th, Pb, Fe, Mn) from 30-50 µm spots on a single apatite crystal. In a broad survey of apatite variability, representative samples have been analysed from granites (from Australia and Norway), larvikites and pegmatites (Norway), dolerites (Ukraine), as well as from less common rock types such as carbonatites (Fen, Norway; Palabora, S. Africa; Kovdor, Russia; Mud Tank, Australia), jacupirangite (Kodal, Norway), and iron ore deposits (Kiruna, Sweden and Durango, Mexico).

"The trace element patterns of apatite in the highly fractionated and highly oxidised granitoids related to Cu-Au mineralisation were found to be distinct"

Trace-element signatures specific for apatite of different origins have been defined, and show that the distribution of trace elements, especially REE, Y, Mn and Th in apatite depends not only on the mineral structure, but on the abundance of these trace elements and the chemical characteristics of the melt or fluid from which the apatite crystallised.

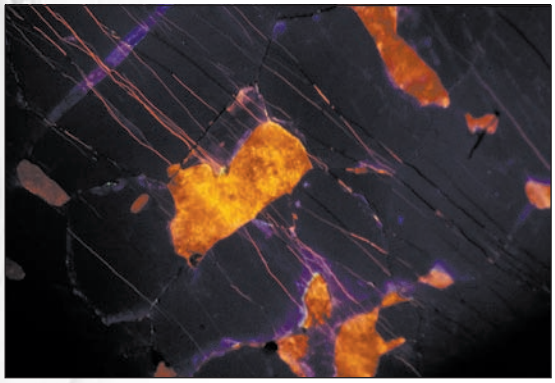

Figure 1. Cathodoluminesence image of an apatite with veinlets of calcite from Palabora carbonatite complex, South Africa.

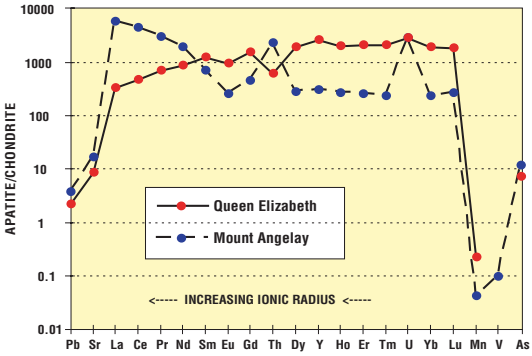

Figure 2. Apatite trace element patterns from Mount Isa granitoids.

Particular attention has been paid to the study of primary magmatic apatites from granitoid rocks, to determine how the chemistry of this mineral reflects granite fractionation and composition, and to test whether apatite composition can be used to characterise granite suites related to Cu-Au mineralisation. This study focused on the Proterozoic granite suites of the Mount Isa Inlier, using the extensive AGSO granite collection. Preliminary results suggest that the variation in trace element concentrations within apatites is directly correlated with whole rock parameters such as the SiO_2 and alkali contents and the aluminium saturation index, as well as fO_2 and the presence of other accessory phases. The trace element patterns of apatite in the highly fractionated and highly oxidised granitoids related to Cu-Au mineralisation were found to be distinct from those of apatites in the less fractionated, less oxidised barren granites (Figure 2). Apatite turns out to be a highly sensitive indicator of the mineralisation potential of a granite body or suite, and is a potentially useful exploration tool.

Publications: Belousova et. al.

Contact: E. Belousova, W. L. Griffin, S. Y. O'Reilly.
Funded by: APA, BHP, Macquarie University
Part of GEMOC's Metallogenesis and Crustal Generation strands.

Other Worlds: Deep Space 2

WITH AN ON TIME LAUNCH on the 3rd of January, 1999, GEMOC started its first excursion to another planet, Mars. Mars is near the end of its lithospheric evolution and represents an end-member in lithospheric studies. It is also an extreme remote environment, and technology developed for remote studies on Mars may find application in exploration in remote areas of Earth's continents. Deep Space 2, or DS-2, is the second in a series of missions jointly conceived by NASA and the Jet Propulsion Laboratory under the umbrella of the New Millennium Program with the program motto, "Faster, Cheaper, Better." This concept is something for which many organisations are striving as we enter the third millennium: Faster – less time between conception and implementation; Cheaper – use existing resources and knowledge wherever possible; Better – focus on achieving the goal not the process. DS-2 admirably meets these criteria.

Paul Morgan is one of nine scientists to lead the science data acquisition for DS-2, the first NASA mission to penetrate the surface of another planet.

The DS-2 mission is two microprobes that are flying piggyback on another spacecraft, the Mars Polar Lander. The microprobes are small enough (basketball-size) and light enough (about 2 kg each) to use payload and space that would have been otherwise wasted on the Delta II launch vehicle (the ultimate cheap launch - a free ride). They will be released just prior to the insertion of the parent vehicle into Mars orbit and will free fall to the surface. The microprobes are enclosed in thin ceramic aeroshells that protect the probes from heat generated during entry through the atmosphere and orient the probes to impact the surface nose first. On impact the aeroshells will shatter, and the probes will penetrate the Mars surface.

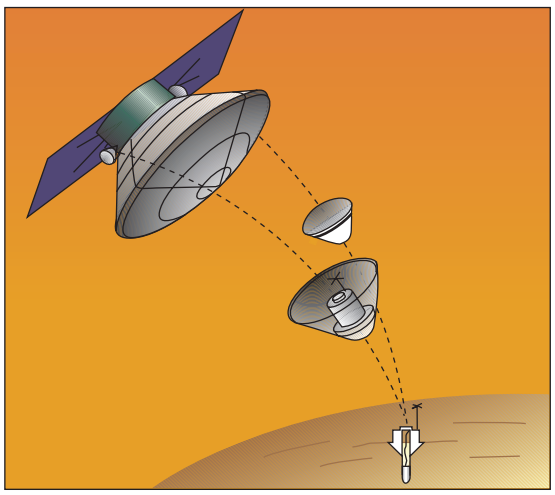

Figure 1. Separation of DS-2 aeroshells from the Mars Polar Lander spacecraft.

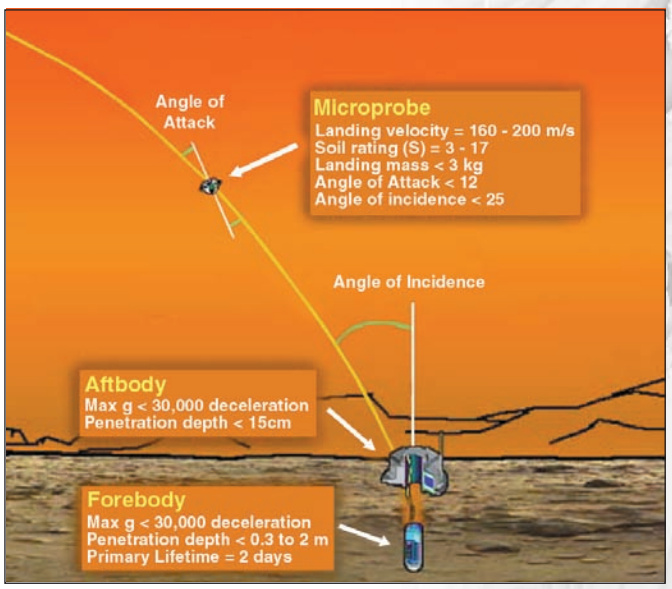

Figure 2. DS-2 microprobe parameters.

The principle scientific goal of the probes is to detect volatile compounds in the Mars soil. Cooling from the heat of entry and penetration of the probes will be used to determine the thermal properties of the Mars soil, a parameter that is sensitive to the presence of any ice or water. In addition, a small drill in the probe will collect a small sample of the soil, heat it, and pass any evolved gas in front of a laser to detect water or carbon dioxide.

"The principle scientific goal of the probes is to detect volatile compounds in the Mars soil."

Surface morphology indicates that Mars had abundant surface water at some time in the past, but its current atmosphere is so thin and so cold that modern surface water cannot exist for more than a short time. DS-2 will be the first exploration into the subsurface for the missing water on Mars.

Contact: Paul Morgan Funded by: NASA

Detecting lithosphere-scale structures: Siberian Platform

THE SIBERIAN PLATFORM is one of GEMOC's key natural laboratories – a place where mantle petrology, geophysics and crustal terranes can be integrated to study the relationships between crustal and mantle processes, and the geophysical signatures of both. A formal collaboration with VSEGEI (St. Petersburg) brought Dr Yuriy Erincheck to Sydney to work with GEMOC Postdoctoral Fellow Yvette Poudjom Djomani and GEMOC Associate Lev Natapov on the analysis of geophysical data from an area of 1.4 million km^2 in the NE part of the platform (Fig. 1, and front cover).

Basement exposures in the Anabar Shield, and regional aeromagnetic data, have previously been used to map a series of Archean and Proterozoic basement terranes across the study area. We have analysed garnet concentrates and xenoliths from the chain of Paleozoic to Mesozoic kimberlites that crosses the region, to look at the thickness, composition and thermal state of the mantle lithosphere beneath these terranes. These studies showed that the Archean terranes are underlain by typical depleted Archean lithosphere up to 220 km thick, while the Proterozoic terranes to the north are underlain by thinner and less depleted lithosphere. Large differences in mantle "stratigraphy" between closely-spaced kimberlite fields suggest that the crustal terrane boundaries are near-vertical and cut through the whole lithosphere.

"The Bouguer pattern ....reflects the greater thickness of less dense Archean lithospheric mantle beneath the Archean terranes, and the thinner, denser Proterozoic mantle beneath the northern end of the traverse."

The gravity data were upward-continued to 16 km to examine large-scale structure in a traverse along the main chain of kimberlites (Fig. 2). The Archean terranes are characterised by negative Bouguer anomalies, and the Proterozoic terranes by positive anomalies. The boundary between the two is well-marked. The Bouguer pattern is expected from the mantle-petrology data; it reflects the greater thickness of less dense Archean lithospheric mantle beneath the Archean terranes, and the thinner, denser Proterozoic mantle beneath the northern end of the traverse. The results show that the Bouguer anomaly signature of these two mantle types can be used to map their distribution well away from the "drill holes" provided by the kimberlites.

An analysis of the flexural strength (Effective Elastic Thickness, or Te) was done, using gridded gravity and topography data. The most striking observation is that most of the study area, though geologically a stable Precambrian craton, has low Te values (<30 km), indicating a weak lithosphere like that of geologically much younger and more active zones. Paradoxically, the highest values of Te (30-40 km) are found over the Vilyui Aulacogen, a major Devonian rift zone in the SE quadrant of the study area where the lowest values would have been expected. The reasons for the low Te values

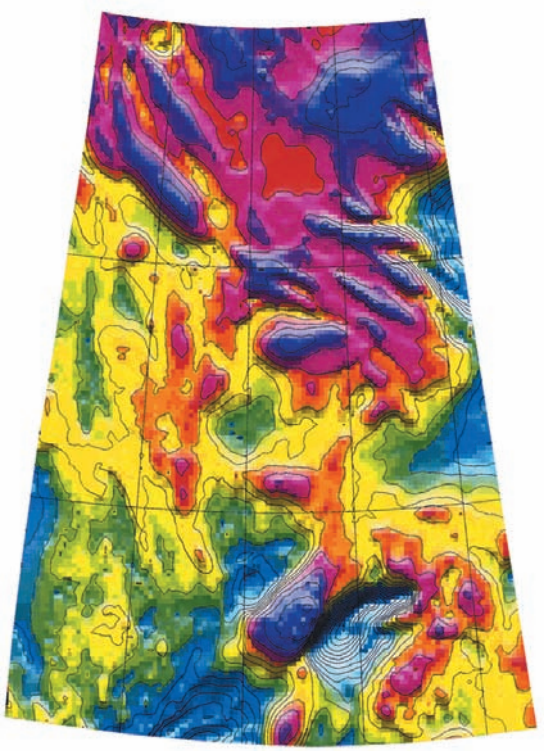

Figure 1. Map of the vertical gradient of the Bouguer gravity data over the northeastern part of the Siberian Craton.

are not clear, but a tectonic analysis suggests that they may be related to lithosphere deformation during accretion of the craton, or to the effects of several later episodes of crustal extension in the area.

The extension of this study to the west, planned for 1999, will examine the signature of the deep structure(s) (lithospheric) that have controlled the emplacement of the world-class Nor'ilsk nickel deposit.

Publications: 139, 154

Contact: W.L. Griffin, Y. Poudjom Djomani, L. Natapov, S. Y. O'Reilly
Funded by: Western Mining and Macquarie University
Part of GEMOC's Lithosphere Mapping, Metallogenesis and Geotectonics strands.

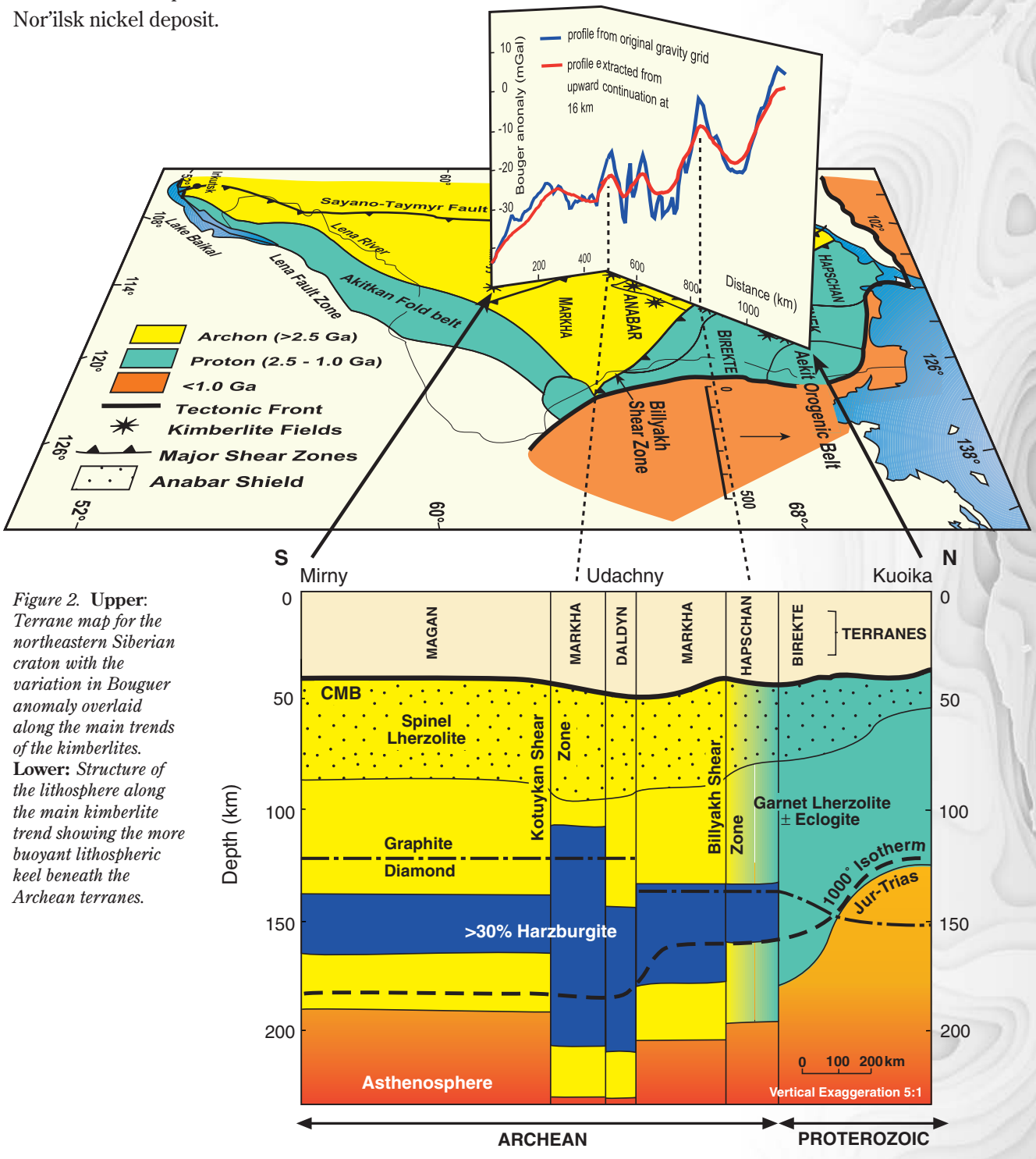

Figure 2. **Upper**: *Terrane map for the northeastern Siberian craton with the variation in Bouguer anomaly overlaid along the main trends of the kimberlites.* **Lower:** *Structure of the lithosphere along the main kimberlite trend showing the more buoyant lithospheric keel beneath the Archean terranes.*

From the micro to the macro or: has the Earth changed?

ONE OF GEMOC'S RESEARCH TOOLS is a very large database of major- and trace-element analyses of garnet xenocrysts from volcanic rocks, built up through research related to diamond exploration. Statistical analysis of this database (with GEMOC Associate Nick Fisher of CSIRO Mathematics and Information Technology and Jerry Friedman of Stanford University) documented large differences in the types and composition of garnets derived from beneath various regions, and correlated these differences with the age of the last major thermal event in the crust. When statistically defined garnet populations were correlated with garnet compositions in real rocks (mantle-derived peridotite xenoliths) it became obvious that these small grains were carrying a very large-scale story about the way the Earth works.

In lithospheric mantle made after ca 2.5 Ga (billion years) ago, some kinds of rocks, especially strongly depleted harzburgites and lherzolites, simply do not occur, and the garnets of the main rock type in the younger mantle, the common lherzolites, become progressively less depleted in "incompatible" trace elements such as Y, Ti and Ga over the time span from 2.5 Ga to the present.

In the next step of this research, a correlation between the compositions of garnets and their host xenoliths showed that the composition of a lithospheric mantle section can be reliably calculated from the mean composition of its garnets. These calculations confirmed major changes in the composition of lithospheric mantle beneath terranes with Archean, Proterozoic and Phanerozoic crustal ages; younger lithospheric mantle is progressively less depleted in "basaltic" components. Using average mineral compositions measured in xenoliths, these compositions have been recast into mineral assemblages (modes), and used to derive the mean density and seismic velocities for mantle lithosphere of different ages. Archean

"[There are] major changes in the composition of lithospheric mantle between terranes with Archean, Proterozoic and Phanerozoic crustal ages"

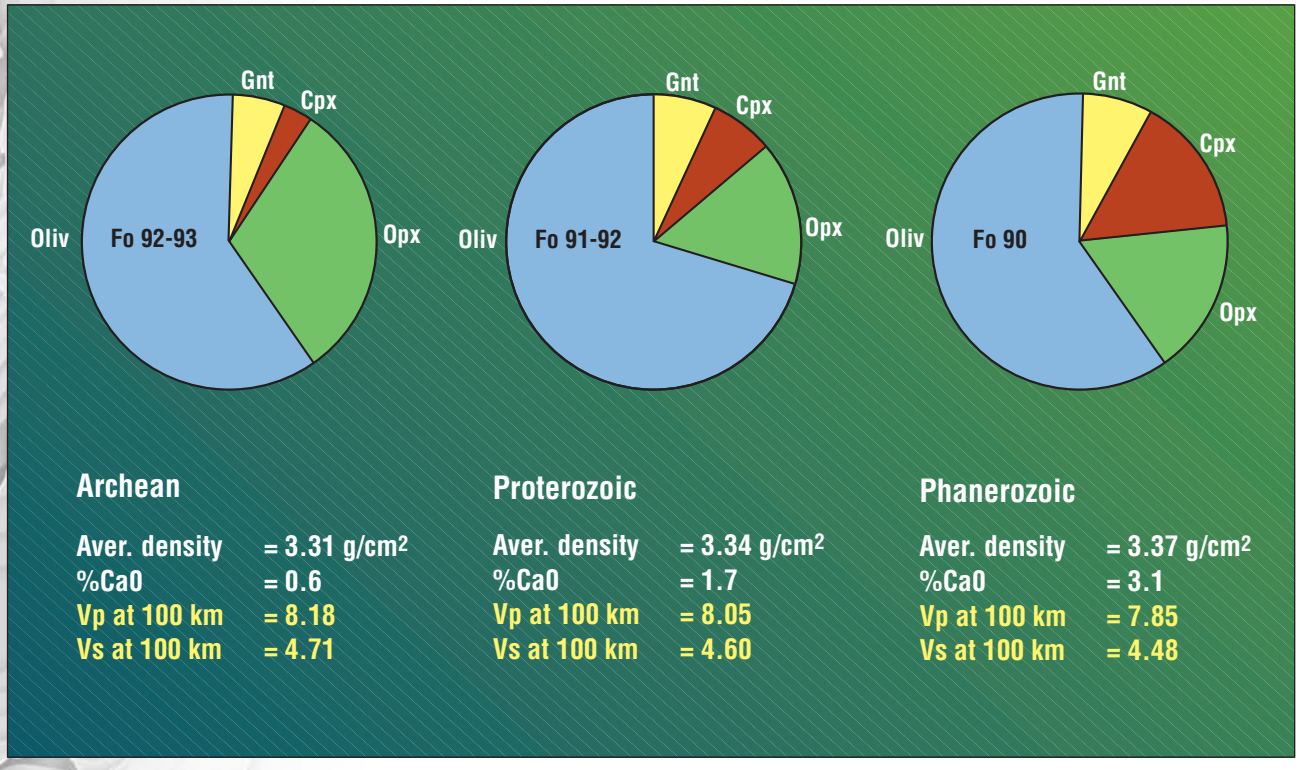

Differences in Archean, Proterozoic and Phanerozoic mantle composition and physical properties

lithospheric mantle is much less dense than Phanerozoic mantle, but has higher seismic velocities at any temperature; Proterozoic mantle lies between these two end-members.

The correlation of mantle composition with crustal age has important implications:

- the crust and the underlying lithospheric mantle must have formed quasi-simultaneously, and they typically have stayed coupled for periods of aeons
- there must have been major changes in Earth's geodynamics about 2.5 Ga ago, which changed the way continents and their roots are formed
- since 2.5 Ga, the continent-forming processes have evolved toward lower degrees of partial melting; this suggests a link to the secular cooling of Earth
- regional variations in gravity and seismic velocity (as shown in seismic tomography) must reflect compositional as well as thermal variations
- Archean and Proterozoic lithospheric mantle are too buoyant to "delaminate" and sink into the deeper mantle, as suggested in many tectonic models
- processes such as thermal erosion that can replace old lithosphere with younger and hotter, but denser lithosphere will have major effects on regional tectonics

Lithosphere replacement events may be important in producing fluids and structures controlling crustal economic concentrations.

Publications: 90, 132, 139, 154

Contact: W. L. Griffin and S.Y. O'Reilly
Funded by: ARC, Macquarie University, collaborative research with industry, ACILP, DIST
Part of GEMOC's Lithosphere Mapping strand.

Mantle-derived garnet concentrate

Continental fragments within an oceanic plateau? The Agulhas Plateau, SW Indian Ocean

OCEANIC PLATEAUX play a significant role in the growth of continents through the process of accretion. The Agulhas Plateau is one of the key structures within the reconstructions of the break-up of Gondwana with its crustal structure and palaeo-position still under debate. A new set of seismic reflection and deep crustal refraction lines has been interpreted to shed more light on the Late Cretaceous development of the plateau. Based on the ocean-bottom seismograph recordings, a deep crustal/upper mantle velocity-depth model has been produced which yields relatively high P-wave velocities of 7 km/s beginning at crustal depths of only 6-7 km. Observations of large-amplitude, high-velocity phases from shallow levels are consistent throughout the records from the central plateau. Prominent lower-crustal wide-angle reflections and refracted phases with apparent velocities of more than 8 km/s constrain the crust-mantle boundary (Moho) to a maximum depth of 24-25 km below sea-floor. An important result is the distribution of velocities between 7.0 and 7.6 km/s for the mid- to lower crust. As velocities of over 7 km/s represent mostly rock material of predominantly mafic and ultramafic composition, we interpret the Agulhas Plateau as of oceanic origin. Although a continental affinity was implied in earlier studies, based on the quartzo-feldspathic composition, high metamorphic grades and Cambrian and Proterozoic ages of some dredge samples, we do not see evidence for such materials in the seismic data. However, continental micro-fragments might be part of the western plateau which started to move from its attachment to the Falkland Plateau toward its present position at about 108-105 Ma. A large number of extrusive centres formed on the southern Agulhas Plateau, documenting the overprinting of the already overthickened oceanic crust. The high seismic velocities in the middle and lower crust and the evidence for major extrusive centres across the plateau are indicative of voluminous emplacement of predominantly mafic extrusive and intrusive rocks, the defining characteristics of Large Igneous Provinces.

Contact: Karsten Gohl
Funded by: MURG in collaboration with the Alfred Wagner Institute
Part of GEMOC's Lithosphere Mapping, Crustal Generation and Geotectonics strands.

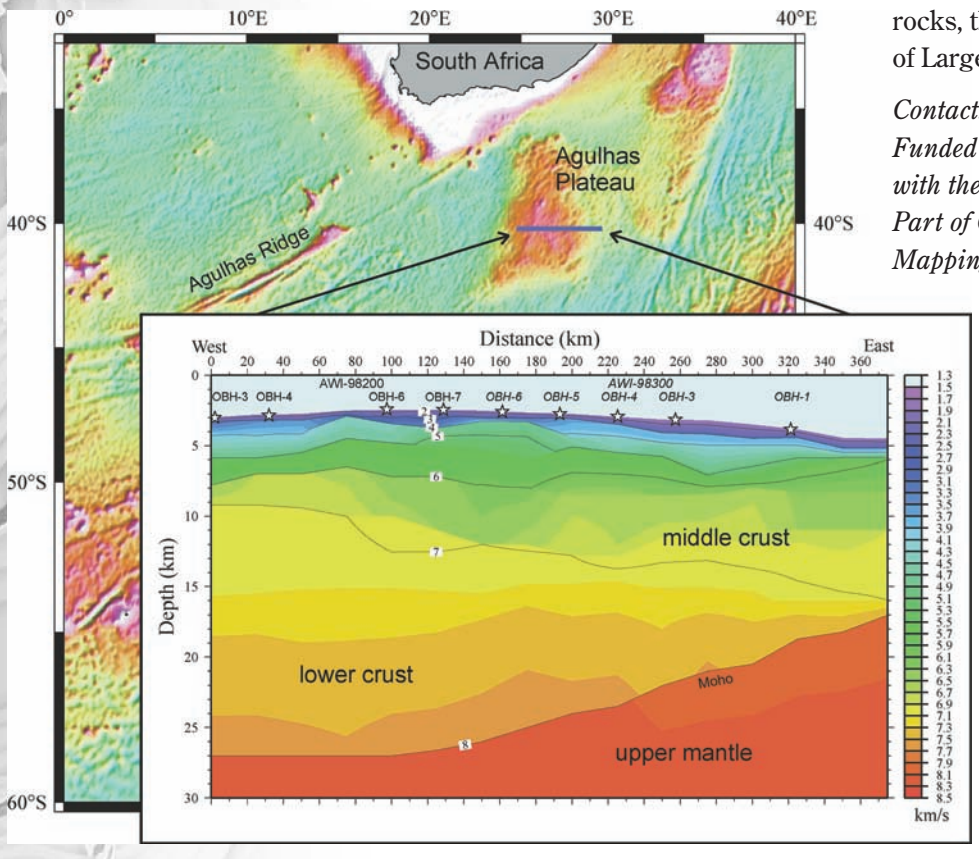

A recently-modelled velocity-depth distribution across the central Agulhas Plateau shows high P-wave velocities of above 7 km/s for up to 70% of its crustal thickness. The map represents a model of the sea-floor topography of the SE Atlantic and SW Indian Ocean region derived from satellite gravity.

Where has Australia been?

DURING THE CARBONIFEROUS TO PERMIAN, Australia moved from low to high latitudes. The apparent polar wander path (APWP) for Australia for this period is not well defined so a palaeomagnetic study of volcanic units from the southern part of the Connors-Camboon Province, of the Late Palaeozoic Northern New England Orogen in Queensland was carried out. The age range of the Province is 320 - 280 Ma, and this study concentrated on the Late Carboniferous Torsdale Volcanics and the Early Permian Camboon Volcanics from the Cracow area. The Camboon Volcanics sampled were generally andesitic ignimbrites and lavas yielding a primary direction in both magnetite and haematite carriers. All directions were reversed and initial analysis of the data shows a southerly steep down direction of Dec = 171.7°, Inc = 76.6° (α_{95} = 6.1°, k = 52, N=12) which results in a palaeomagnetic south pole of 50.4°S, 155.9°E (dp = 10.5, dm = 11.3; 11 in figure). This is consistent with other Australian Early Permian data such as the Mount Leyshon Complex and the Tuckers Igneous Complex. The Torsdale Volcanics sampled were generally silicic ignimbrites that yielded a primary direction in both magnetite and haematite carriers. Initial analysis shows that the directions are generally reversed, although some normal polarities are observed. The directions are not as steep as those observed for the Camboon Volcanics and show a more westerly character, with a mean direction of Dec = 217.8°, Inc=68.8° (α_{95} = 7.9°, k = 59, N=7) which results in a south pole of 50.9°S, 113.8°E (dp = 11.4, dm = 13.4; 10 in figure). The pole is consistent with the Late Carboniferous age of the unit.

Contact: Mark Lackie
Funded by: ARC, Macquarie University
Part of GEMOC's Lithosphere Mapping, and Geotectonics strands.

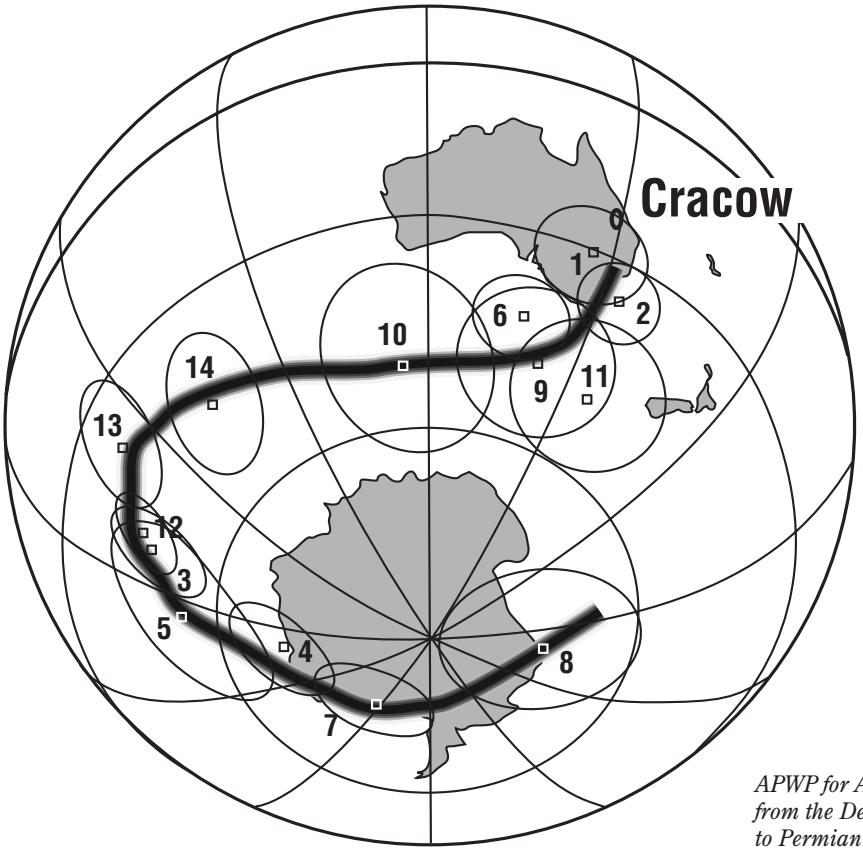

APWP for Australia from the Devonian (8) to Permian (1).

Trace elements in the carbon of your choice by LAM-ICP-MS

CARBONACEOUS SUBSTANCES are commonly associated with economically important mineral resources - from inclusions of trapped liquid hydrocarbons to bituminous materials associated with major metalliferous deposits to diamonds.

The historical lack of trace element information on carbonaceous materials has been due to the lack of a reliable technique for in situ determination of low level trace elements in small volumes of these materials. We have recently developed a technique for analysis of both liquid and solid carbon-bearing substances using the GEMOC LAM-ICP-MS and have applied it to analysis of bituminous materials associated with the Oklo uranium deposits in Gabon and diamonds from several localities.

"Calibration of the analyses is achieved by direct ablation of a synthetic oil standard encapsulated in a capillary tube"

Calibration of the analyses is achieved by direct ablation of a synthetic oil standard encapsulated in a capillary tube; correction for ablation yield differences between calibration oil and sample is performed using carbon as an internal standard.

Our chemical analysis of trace elements in the bitumens at Okla has allowed identification of six different types, providing a major contribution to the understanding of the Oklo deposit.

The ability to rapidly and accurately determine a wide suite of trace elements in diamonds with high spatial resolution now offers the possibility of better understanding the genesis of diamonds and addressing such questions as:

- the nature of source regions and fluids, and the ultimate source of the carbon.
- are micro- and macro-diamonds generated by similar or different processes?
- are all diamond-forming processes similar, or are they dependent on mantle age, composition and environment?

Contact: Simon Jackson and Rondi Davies
Part of GEMOC's Lithosphere Mapping, Metallogenesis, and Technology and Development strands.

Granites hot and cold

I-TYPE GRANITES of the Paleozoic fold belts of Eastern Australia were recognised to form two groups formed at high and low magmatic temperatures. The distinction is made on the absence or presence, respectively, of zircon with inherited ages in the more mafic rocks, and related differences in Zr variation patterns with SiO_2. The high-temperature I-type granites, which include close analogues of Cordilleran tonalites, formed from a magma that was completely or largely molten, and in which crystals of zircon were not initially present because the melt was undersaturated in zircon. In contrast with the low-temperature I-type granites, the compositions extend to lower SiO_2 contents and the abundances of Ba, Zr and the rare earth elements initially increase with increasing SiO_2 in the more mafic rocks. While the high-temperature granite magmas were produced by the partial melting of mafic source rocks and represent a comparatively primitive addition to the upper crust, the low-temperature I-type granites resulted from the partial melting of quartzofeldspathic rocks such as older tonalites. In that second case the melt produced was felsic and the more mafic low-temperature granites have that character because of the presence of entrained and magmatically equilibrated restite which includes older zircon crystals. These low-temperature granites are effectively what Pitcher called Caledonian I-types. They may occur in close association with S-type granites since both are products of the magmatic recycling of older crust. There are also broad differences in composition between the I-type groups, with the Caledonian granites being more typically granodiorites and monzogranites. In contrast, tonalites and low-K granodiorites characterise the high-temperature Cordilleran granites, which have inherited that and associated features from their less evolved source materials.

Publication: 141

Contact: Bruce Chappell
Part of GEMOC's Crustal Generation strand.

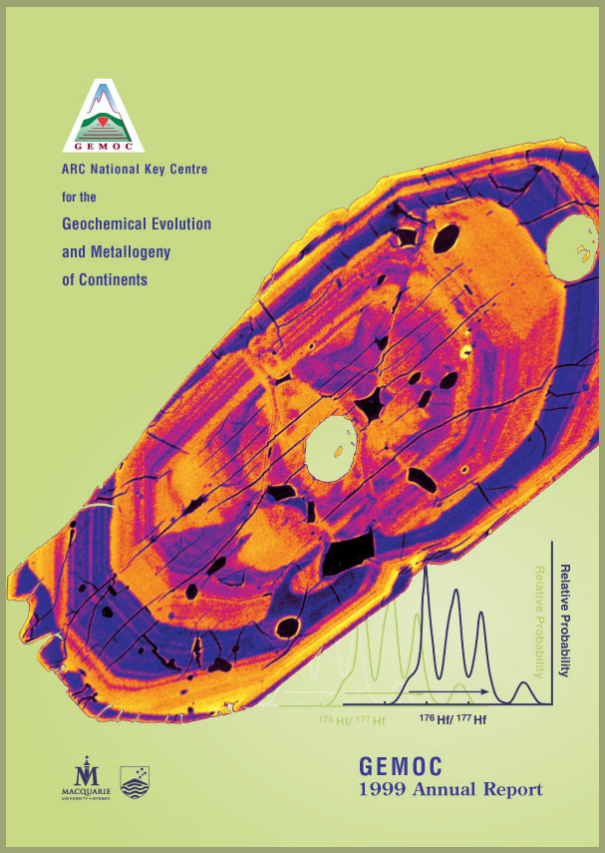

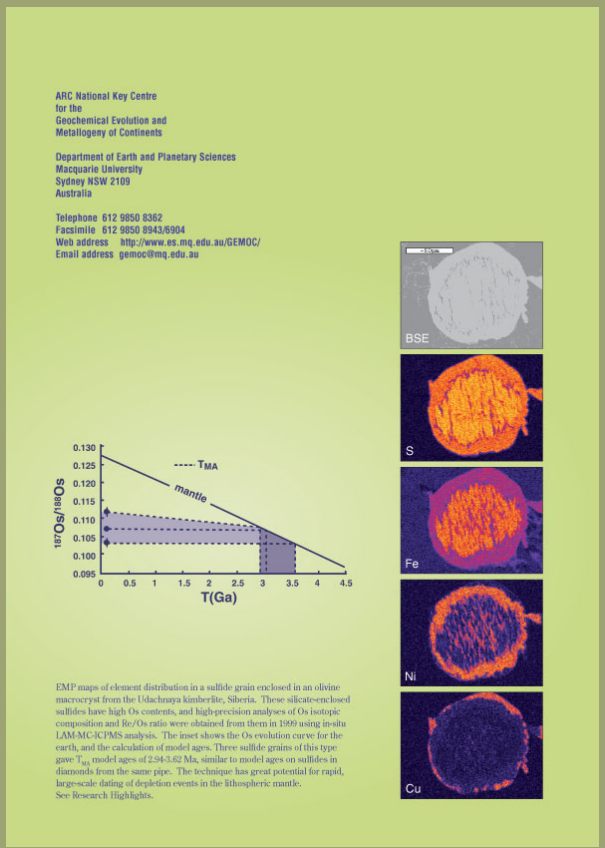

1999 Contents

Carbonatites and kimberlites ? melt inclusions from the deep lithosphere	24
Sulfides - a shining tracer of lithosphere evolution	26
News Flash: in situ dating of mantle events	27
Composition of groundwaters: geochemical fingerprints of aquifer lithology	28
Copper isotope geochemistry - new tools for exploration and research	29
What is the origin of the diamonds from eastern Australia?	30
Event signatures - tracing crustal growth with detrital zircons	32
What role did oceanic plateaux play in the Gondwana break-up?	33
Xenoliths from the Kerguelen islands: mantle metasomatism and continent formation	34
News Flash: Isochrons in minuits: SM-ND in titanite	35
Shell Games: Sr isotopes and Permian Terranes in New Zealand	36
Defining the APWP for Paleozoic eastern Gondwana paleopoles from the Northern TASMAN orogen, Queensland	37
Reading Granite Recipes from Zircon Tapes	38

Front cover:
Zircon was a major focus of research at GEMOC in 1999; the trace element and isotopic zoning of this resistant mineral record its magmatic and metamorphic history. The holes in the zircon are ablation pits from LAM-ICPMS analyses, which yielded U-Pb ages and the trace element compositions of different zones. LAM-MC-ICPMS analyses gave high-precision spot analyses of Hafnium isotope composition (inset), which showed that many granitoid rocks retain isotopic evidence of mixing between several components. The arrow shows the direction of isotopic zoning recorded in core-to-rim analyses of individual zircon grains in a quartz diorite from the Pingtandao complex, SE China. The technique is now being applied to zircon populations from sediments, for analysis of crustal genesis over large continental areas. See Research Highlights

Research highlights 1999

Carbonatites and kimberlites – melt inclusions from the deep lithosphere

GEMOC'S ONGOING COLLABORATION with Kennecott Canada Inc. has shown that the lithosphere beneath the Lac de Gras area of the Slave Craton (northern Canada) consists of two distinct layers (figure 1, Publication 137). Among the xenoliths brought up by the kimberlites in this area there are many cm- to dm-sized megacrysts of chrome-diopside pyroxene (figure 2).

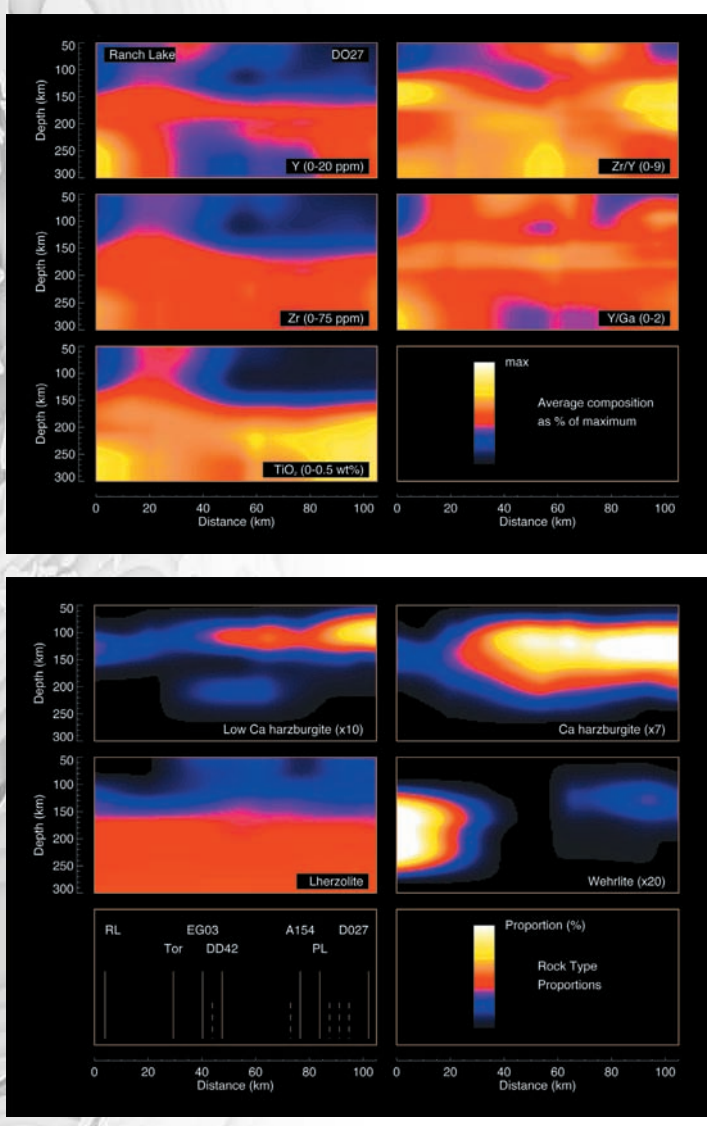

Mineral inclusions in the pyroxenes show that they are fragments of very coarse-grained garnet peridotites derived from the base of the lithosphere (180-200 km depth). Many of these contain abundant inclusions of quenched carbonatite melts, as well as inclusions of ultramafic silicate melts and Fe-Ni sulfide melts. These melts were trapped as fluid inclusions in the clinopyroxene, which shielded them from interaction with kimberlite and mantle and crustal wall-rocks during ascent. The microstructures of the carbonatites, in particular, show that they were quenched in near-surface conditions. The relationships between the carbonatitic, ultramafic silicate and sulfide melts are complex, with all three types occurring along apparent single inclusion trails through the pyroxenes. At present, the data suggest that all of the inclusions were derived from a carbonated ultramafic parent melt by progressive degrees of liquid immiscibility, while cooling through a small temperature range near 1250 °C.

GEMOC's work on these unique samples has integrated data from several components of the Facility for Integrated Microanalysis (see *Technology Development*). The electron microprobe and the scanning nuclear microprobe have been used to image the structure and the distribution of major and trace elements, and the LAM-ICPMS has been used for detailed trace-element analysis at low levels. Sr isotope ratios will be measured using

Figure 1. Chemical tomography images of the lithospheric mantle beneath the Lac de Gras area of the Slave Craton. Top: Zr, Y and Ti contents of garnets show the boundary between the ultradepleted upper layer of the lithosphere and the less depleted deeper layer. Bottom: Rock types deduced from garnet chemistry show that depeted harzburgites are restricted mostly to the shallow layer, while lherzolites dominate the lower layer.

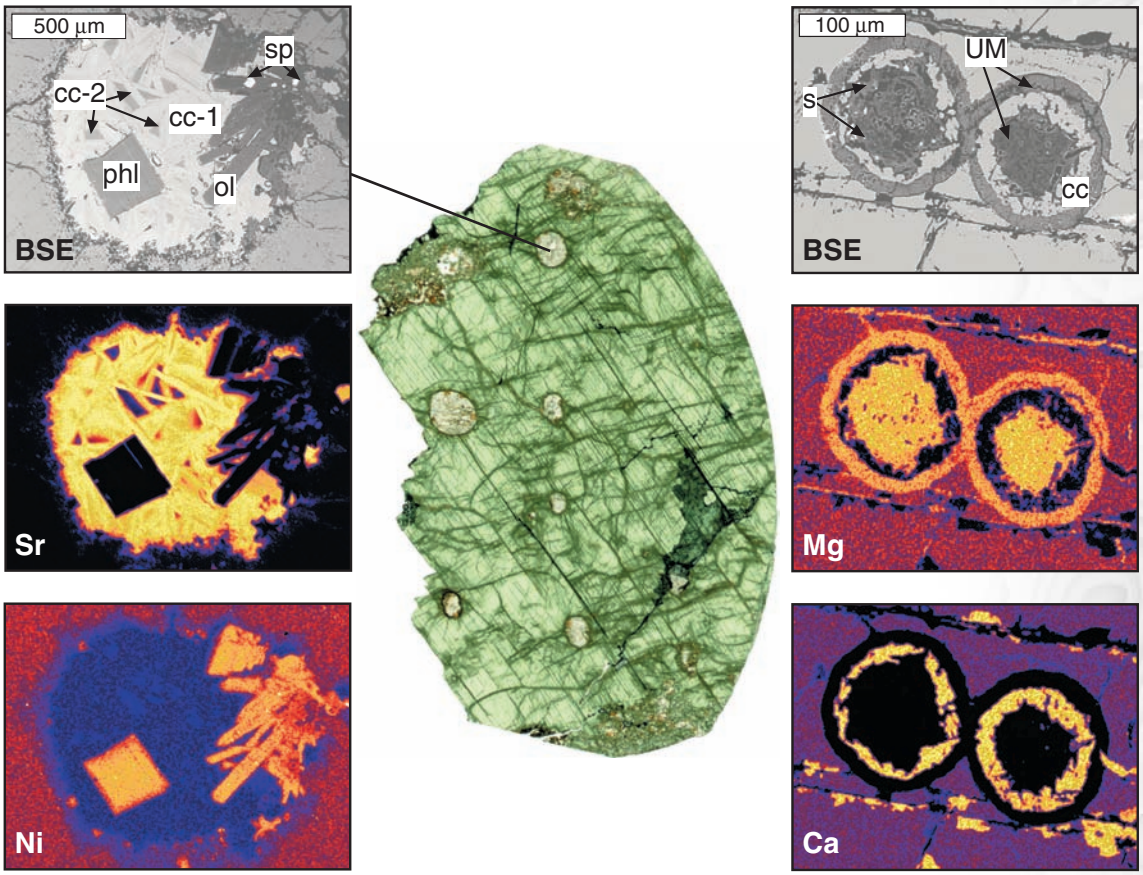

Figure 2. Centre: Carbonatite inclusions in a chrome-diopside megacryst (1.5 x actual size). Left: Backscattered electron (BSE) image and maps of Sr and Ni distribution in a carbonatite bleb, produced with the CSIRO-GEMOC Scanning Nuclear Microprobe. Right: BSE image of composite carbonatite-kimberlite blebs, and maps of Mg and Ca distribution produced by energy-dispersive electron microprobe analysis.

the LAM-MC-ICPMS.

The carbonatite inclusions show radiating "spinifex" olivine and blocky phlogopite crystals, set in a matrix of calcite; two generations of calcite with different Sr and Ba contents are present, reflecting the concentration of these elements in the first carbonate to crystallise. Detailed image analysis of modal compositions, combined with analysis of the individual phases, shows the bulk composition of the melts to be a magnesian silico-carbonatite.

In some ultramafic inclusions, the silicate and carbonate components have unmixed into concentric rings in a single globule (figure 2), where the carbonatite separates an outer ring of ultramafic melt (UM) from a more magnesian silicate melt in the core. Many of these inclusions contain abundant dispersed Fe-Ni sulfide. The scanning nuclear microprobe images show the partitioning of different elements among these components. The calculated bulk compositions of these inclusions closely resembles that of many kimberlites. The study of these unusual samples is providing new insights into the processes that produce both kimberlites and carbonatites, and on their metasomatic effects in the mantle.

Contact: Esmé van Achterbergh, Bill Griffin, Sue O'Reilly, Norm Pearson
Funded by: ARC, Kennecott Canada Inc. and Macquarie University.
Part of GEMOC's Lithosphere Mapping, Geotectonics and Metallogenesis strands.

Sulfides — a shining tracer of lithosphere evolution.

THE PLATINUM GROUP ELEMENTS (Os, Ir, Ru, Rh, Pt, Pd), together with Au and Re, comprise the Highly Siderophile Elements (HSE). The relative abundances of these elements are important for models of the formation and evolution of the Earth. Because of their siderophile and variably chalcophile nature they also provide, along with the Re-Os isotopic system, a different perspective on the formation and evolution of the different parts of the Earth (Core, Mantle and Crust).

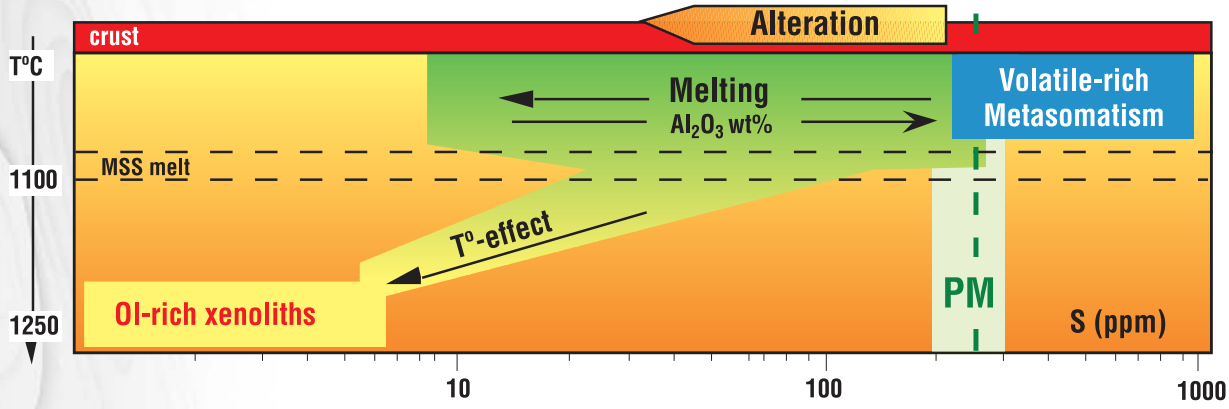

Figure 1. Effects of different processes on mantle sulfides

Sulfide minerals are ubiquitous in the mantle and, despite their very low modal abundance (<0.1%), have been inferred to be the main host phases for the HSE. However, the behaviour and trace element contents of these sulfides is very poorly known.

A detailed study of several mantle xenolith suites world wide (in collaboration with Dr. J.P. Lorand, Muséum National d'Histoire Naturelle de Paris), has shown that sulfides are sensitive to many processes, including melt removal and metasomatism (figure 1). Heating events and extensive melt/rock reaction trigger sulfur loss because of the low melting temperature of sulfide, while volatile-rich metasomatism may add significant amounts of sulfide. All these features suggest that the HSEs, hosted in sulfides, can be significantly mobile in the mantle.

The *in situ* analytical capabilities of the GEMOC Facility for Integrated Microanalysis (Laser ablation microprobe (LAM) –ICPMS, LAM-MC-ICPMS and Scanning Nuclear Microprobe) have allowed us to make a breakthrough in the understanding of the behaviour of the HSEs. *In situ* analyses of enclosed and interstitial sulfides yield contrasting HSE patterns. Silicate-enclosed sulfides, shielded from fluid percolation processes, have mono-sulfide solid solution compositions, high HSE abundances and Pd/Ir ratio less than chondrites (figure 2). In contrast, interstitial sulfides have a Cu-rich pentlandite composition, lower HSE contents and high Pd/Ir ratios (figure 2). Both sulfides often occur in the same sample. Our data indicate that silicate-enclosed sulfides are the residua of melting process(es), while interstitial sulfides are the result of crystallisation of sulfide-bearing fluids. Hence, we suggest that non-chondritic HSE patterns are due to process(es) occurring in the upper mantle (i.e. melting and sulfide addition via metasomatism), and are not evidence of core material addition or 'exotic' meteoric bombardments as has been recently proposed.

The results are also significant for the interpretation of Re-Os depletion ages on mantle xenoliths, because the mobility of sulfide implies the mobility of Os, and the mixing of material from different sources will produce ambiguous age data. Preliminary *in situ* Re-Os dating of mantle sulfides (see *News_Flash*, page 27) shows that enclosed and interstitial sulfides may have widely different Os isotope compositions, and that whole rock $^{187}Os/^{188}Os$ may reflect mixing between several sulfide populations rather than "young" melt

depletion ages. A detailed knowledge of the petrography and chemistry of the sulfide component of the rock has become essential to understanding and interpreting Re-Os data.

Contact: Olivier Alard, Simon Jackson, Bill Griffin, Sue O'Reilly.
Funded by: ARC and Macquarie University
Part of GEMOC's Lithosphere Mapping and Metallogenesis strands.

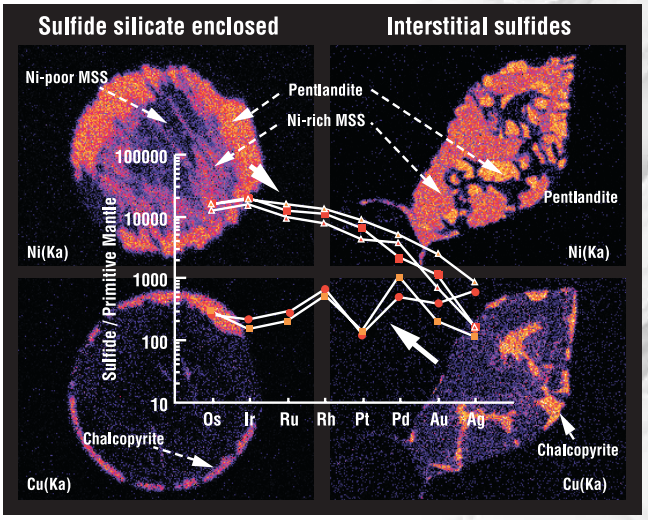

Figure 2. Sulfide inclusions in mantle silicate have PGE patterns showing Os enrichment and may date mantle depletion events. Interstitial sulfides in mantle rocks show PGE patterns that are flat to Pd-enriched and track metasomatic effects.

NEWS FLASH

IN SITU DATING OF MANTLE EVENTS:

The Re-Os isotopic system has rapidly become an important tool for dating the timing of melt-extraction events in the upper mantle. The recognition and definition of two types of Platinum Group Element (PGE) patterns in mantle sulfides (see elsewhere in *Research Highlights*) has important implications for the interpretation of Re-Os ages on mantle-derived xenoliths. That work also has shown that many grains of Fe-Ni sulfides enclosed in the primary minerals of mantle xenoliths have very high Os contents.

Late in 1999, we demonstrated that these grains could be dated by *in situ* laser-ablation analysis on the GEMOC MC-ICPMS. A series of test analyses on a synthetic Fe-Ni sulfide standard spiked with PGEs and with Os of known isotopic composition showed that these analyses could be done in a few minutes, with precision and accuracy comparable to standard TIMS analyses. The technique was then applied to large (200 micron) sulfide grains included in olivine xenocrysts from the Udachnaya kimberlite, Siberia (via Prof. Y. Barashkov) and the A481 kimberlite, Slave Province (via Jennifer Burgess of Diavik Diamond Mines). These gave similar model ages (T_{MA}) for melt removal: 3.07±0.05 Ga (2sd) for Udachnaya and 3.01±0.07 Ga for A481. Both are equivalent to the oldest ages reported for xenoliths from these areas by conventional TIMS Re-Os analysis. Preliminary analyses of interstitial sulfides in several types of mantle xenoliths show that these have much more radiogenic Os than the enclosed sulfides. Conventional whole-rock analyses will represent mixtures of these types, with ambiguous ages.

The LAM-MC-ICPMS technique is very rapid and inexpensive, compared to conventional TIMS analysis, so that dating of mantle sections can be done on a statistical basis. Even more important, the spatial resolution of the *in situ* technique means that the data can be interpreted with less ambiguity, since a single generation of sulfide is being analysed with each shot. The new technique also will make dating of single diamonds a relatively simple matter – and sulfides are the most common inclusion in diamonds!

Contact: Bill Griffin, Norm Pearson, Olivier Alard, Sue O'Reilly
Funded by: ARC
Part of GEMOC's Lithosphere Mapping and Metallogenesis strands.

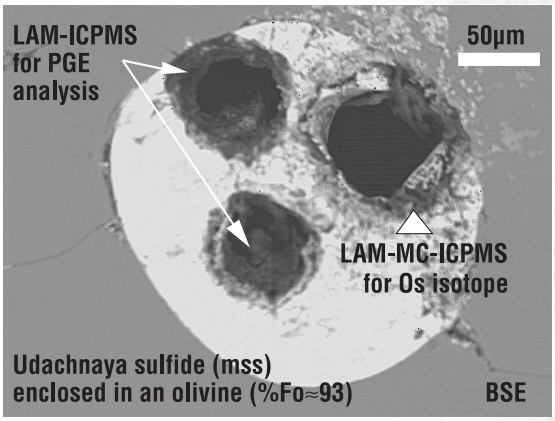

Composition of groundwaters: geochemical fingerprints of aquifer lithology

TRANSPORTED SOIL presents an exploration problem in many parts of Australia, hiding geological outcrop and obscuring the geochemical signatures of ore deposits. Groundwaters offer a unique opportunity to see beneath cover and interpret basement geology. Groundwaters are active exploration media in that they can move vertically and laterally, sampling large volumes of rock by dissolving major and trace elements in amounts depending on the local geological and geothermal environment. Until recently there has been a problem in relating aquifer rock type with groundwater major element chemistry in a simple way that is amenable to exploration. A GIS approach with large groundwater geochemical databases is addressing this problem.

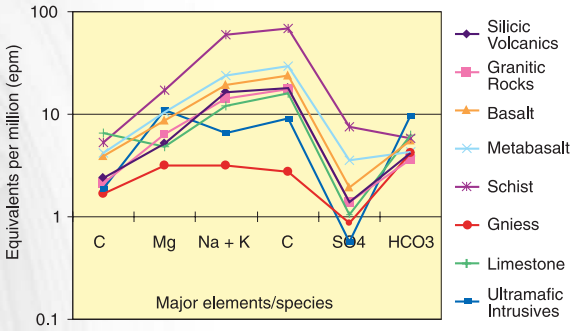

Figure 1. Schoeller plot of groundwater geochemistry with respect to aquifer lithology.

By considering approximately 37,000 groundwaters and linking their locations with known surface geology, a series of major element concentration plots (Schoeller plots) have been made (figure 1). Each Schoeller plot gives a distinct groundwater signature of the rock type with which it is assumed to be associated. Both the position and shape of the line traces can be used to distinguish between signatures. Schist, gneiss, limestone and ultramafic aquifers result in unique patterns. The relative ratios of consecutive ions (e.g. SO_4^{2-} and HCO_3^-) are particularly important when establishing differences between basalts and metabasalts. No differences were expected (or found) between granitic and silicic volcanic aquifers.

Schoeller plots provide a simple, effective way of distinguishing groundwaters from different sources. This can have exploration applications and has been demonstrated for paleochannel uranium deposits. Schoeller plots from mineralised paleochannels are significantly different from those from the surrounding area, even when close to uranium mineralisation of a different style.

Aquifer lithology dictates the most appropriate geothermometer to apply in a particular environment. Current research is using groundwater geochemistry to suggest aquifer lithology in parts of the Great Artesian Basin (figure 2). This information will be used to select the most appropriate geothermometer prior to making an estimation of subsurface temperature. This, combined with bore depths and thermal conductivity measurements, will allow heat flow to be estimated across the basin. New field data, combined with data from state government databases in NSW, Qld and SA are being used to achieve this.

Contact: Mark C Pirlo, Sue O'Reilly
Project funded and supported by: Queen's Trust for Young Australians Achievement Award, GEMOC National Key Centre, APA award, MUPR Grant Part of GEMOC's Lithosphere Mapping and Metallogenesis strands.

Figure 2. Blanche Cup (foreground) and Hamilton Hill (background): natural discharge points of the Great Artesian Basin, South Australia.

Copper isotope geochemistry - new tools for exploration and research

STABLE ISOTOPES have long been used to study the sources of O, C and S in mineralising systems. The isotopes of the commodity elements have been ignored because of the analytical limitations of conventional mass spectrometry. However, the extremely high ionising efficiency of the ICP ion source of the MC-ICPMS now makes precise determination of the isotope ratios of these elements relatively straightforward.

We have recently developed procedures for *in situ* determination of copper isotope ratios in chalcopyrite using the new GEMOC LAM-MC-ICPMS system. An important new finding was that laser ablation/transport processes can cause very significant isotopic fractionation. This required development of operating conditions that minimise such fractionation and of a chalcopyrite standard to calibrate the analyses. The technique has been applied to a study of copper-bearing ores from a wide range of depositional settings, to establish the range of copper isotope fractionation in ore forming processes. A preliminary study on the Cadia porphyry copper-gold deposit examined how

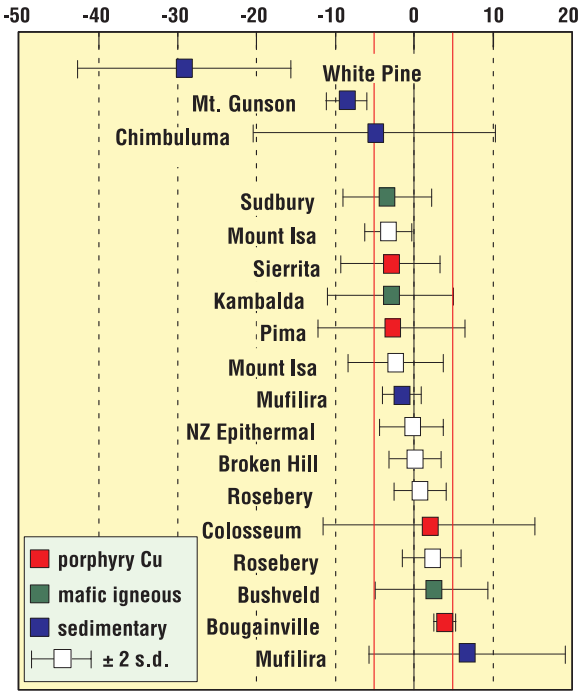

Figure 1. Epsilon ^{65}Cu for chalcopyrite

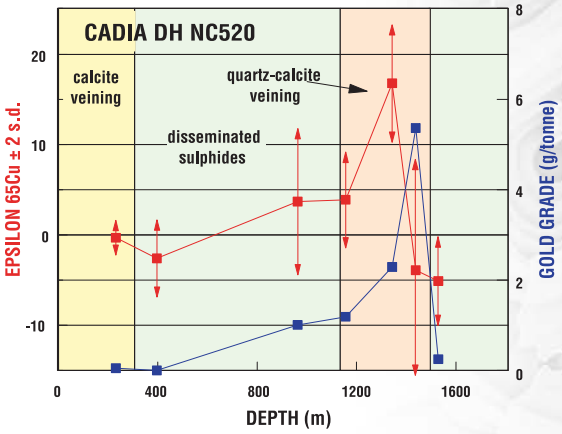

Figure 2. Variation of Cu isotope composition and gold grade with depth, Cadia deposit.

Cu isotope compositions vary on the scale of one ore system (figure 2).

This preliminary study has resulted in two major findings:

- copper derived from igneous sources has a relatively limited spread of copper isotopic compositions (figure 1). However, notable ^{65}Cu depletion occurs in low-temperature sedimentary deposits, suggesting that biogenic fractionation of copper may be an important process.
- significant variations in copper isotopic compositions occur within the Cadia porphyry Cu-Au deposit (figure 2). Significantly, copper isotope variation correlates with alteration style and gold grade.

We are now applying similar techniques to other isotopic systems (e.g., Sb, Ag) and an application has been submitted to AMIRA for funding to study the isotopic systematics of copper and other important commodity metals (e.g., Fe, Zn, Ni, Mo). This work is expected to yield information that can be used as a tool to:

- constrain the type of deposit that has contributed to a surface exploration anomaly
- alert explorationists to the presence of different domains within a buried ore body
- allow metals source(s) and fluid pathways in ore systems to be traced, thereby furthering our understanding of ore genesis.

Contact: Simon Jackson, Bill Griffin, Norm Pearson
Part of the Metallogenesis and & Technology Development programs. Based on the Honours Thesis study carried out by Andrew Botfield (1999).

What is the origin of the diamonds from eastern Australia?

ECONOMIC CONCENTRATIONS of diamonds, both *in situ* and as alluvial deposits, are mainly associated with kimberlitic and lamproitic intrusions in Archean and Proterozoic continental crust worldwide. The kimberlites and lamproites have transported xenoliths and xenocrysts from the cool cratonic roots (>150 km depth) of the upper mantle to the upper crust so rapidly that the metamorphic minerals, including diamonds, do not have an opportunity to re-equilibrate to crustal temperatures and pressures.

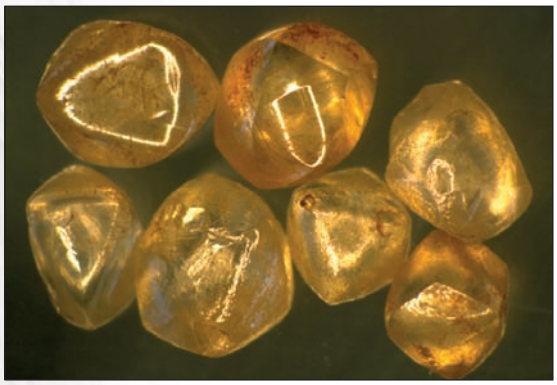

Resorbed dodecahedral diamonds from Wellington, NSW.

Occurrences of diamond in metamorphic and ophiolitic rocks are of less commercial significance, but are important in understanding lithosphere processes. They provide evidence that rocks once at great depth have been tectonically transported to the Earth's surface. All of the tectonically emplaced metamorphic diamond deposits are younger than Proterozoic, and are characterised by micro-diamonds (< 1mm), or graphitised relics of larger diamonds. None contains unaltered macrodiamond.

In eastern Australia, diamonds occur in Cenozoic alluvium overlying Paleozoic and Mesozoic crust. Similar deposits are known from Burma, Thailand, Kalimantan, the Ural Mountains and California, but the origin of such diamond deposits is not well established. There is no trace of a primary source, nor are they associated with the usual diamond indicator minerals.

A wide variety of imaging and analytical techniques was used to characterise diamonds from a number of localities in New South Wales and has distinguished two Groups (A and B) with distinctive characteristics and origins (Publication numbers 89, 110, 124). Group A diamonds are Precambrian (but represent two different episodes based on Re/Os age determinations (2.1Ma and 3.4 Ga, Pearson et al, 1998). Group A diamonds are similar to those from kimberlites and lamproites from cratonic regions worldwide. Group B diamonds have physical and chemical characteristics that are unique among diamonds worldwide and are inferred to have formed in a Paleozoic subduction slab. However, all diamonds show evidence of emplacement at the surface by igneous, rather than tectonic processes despite their inferred different origins of formation.

Group A diamonds are similar in their primary crystal forms, internal growth structures, mineral inclusion compositions and carbon isotope ratios to diamonds found in kimberlitic/lamproitic hosts in Archean and Proterozoic cratons worldwide. Mineral inclusions are dominantly peridotitic and carbon isotope ratios have a typical mantle range and distribution.

Furthermore, the Re–Os ages constrain the origin of these diamonds to formation in ancient mantle sources. This, along with the nature of the surface abrasion structures and radiation damage, suggests that the Group A diamonds may represent an older group of diamonds that have been in secondary collectors for a significant time. If this is so,

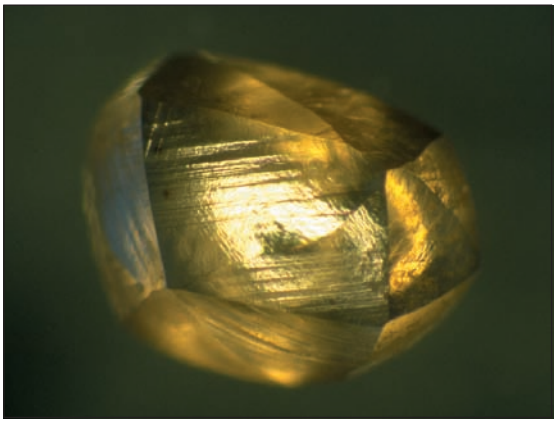

A Group A diamond with strong plastic deformation

it is feasible that the Group A diamonds may be derived from a number of primary sources (both in terms of the mantle and magmatic hosts).

The age and location of the primary host rocks of the Group A diamonds has not been identified. There is evidence for possible Proterozoic lithospheric components in eastern Australia but none for Archean components. At this stage it is not possible to identify a source region or a time of transportation to the surface for the Group A diamonds. However, Veevers (1994) has traced Lower Permian fluvio-glacial drainage patterns from east Antarctica to southeastern Australia prior to the breakup of Gondwanaland, and has shown that the distribution of ca. 600 Ma zircons in the Lachlan Fold Belt sediments is consistent with their derivation from Antarctica. Therefore Precambrian Antarctic terrains are a possible location for diamond-bearing kimberlites or lamproites that could be the primary sources for the Group A diamonds.

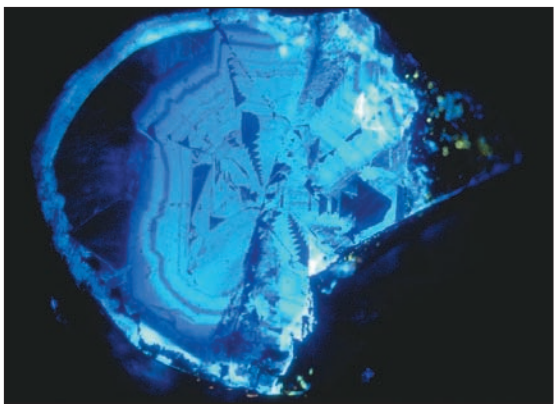

A cathodoluminescence image of the internal structure of a Group B diamond showing concentric growth zoning, sector structures and strong deformation

Group B diamonds are unique among documented diamond suites worldwide in their combination of surface features, strained and irregular internal structures, enriched carbon and nitrogen isotopic signatures, and the eclogite/calc-silicate suite of mineral inclusions. These features are consistent with their formation in a subducting slab (Publications 89, 110, 124 and unpub. PhD Thesis by R. Davies). A provenance for the Group B

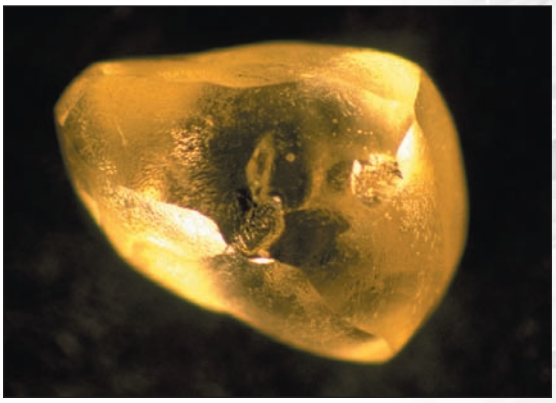

A typical Group B diamond with an irregular resorbed form, corroded surfaces and a frosted pit.

diamonds could be linked to subduction and subsequent magmatic emplacement within eastern Australia related to Carboniferous to early Permian subduction and arc accretion in the New England Fold Belt. This is consistent with diamond emplacement ages obtained from mineral inclusions, which constrain transport of the diamonds to the Earth's surface between ~300 Ma and ~220 Ma. Provided that the diamonds have a subduction origin, formation ages would be similar to emplacement ages because the stability of diamond in a subducting slab is transient, with only a small window in which they could survive. The majority of Group B diamonds occurring on basement terrains of the New England Fold Belt (at Copeton and Bingara) and Group B diamonds at Wellington (on basement of the Lachlan Fold Belt) are less abundant and show stronger evidence of surface abrasion, possibly corresponding to more alluvial reworking. However, all Group B diamonds clearly have been transported. They show abrasion, are well sorted and occur in mature alluvium preserved by Cenozoic basalts.

"diamond emplacement ages....from mineral inclusions ....constrain transport of the diamonds to the earth's surface between ≈300 Ma and ≈220 Ma."

Contact: Rondi Davies, Sue O'Reilly, Bill Griffin
Funded by: CRA (now Rio Tinto), GEMOC, ARC, Kennecott Canada
Part of GEMOC's Lithosphere Mapping and Metallogenesis strands.

Event signatures - tracing crustal growth with detrital zircons

1999 MARKED SOME BIG STEPS toward GEMOC's goal of understanding the links between mantle processes and crustal generation. One was the development of a new approach to the analysis of crustal formation processes, using zircon from sediments.

Understanding the genesis of a block of crust means answering three big questions:

- *When* was material added to the crust?
- *How* did it get there – juvenile addition from the mantle, or reworking of old crust?
- *What* sort of material was added?

This knowledge traditionally requires a long and expensive effort - field mapping, petrography, geochemistry and isotopic dating. In recent years, one shortcut has been to use ion-probe dating of zircon grains in sediments derived from the block of crust being studied. The age spectra that come from this kind of study can answer the *when?* but not the *how?* or the *what?*

GEMOC has developed a more integrated approach, based on the *in situ* analytical capabilities of the Geochemical Analysis Unit (see section on Technology Development). Zircons are concentrated from a sediment sample, mounted and polished for several stages of analysis.

(1) GEMOC's Electron Microprobe is used to collect backscattered electron/ cathodoluminescence images of the internal structure of each grain (see cover), to recognise different growth zones. At the same time, each grain is analysed for a series of trace elements (Hf, Y, U, Th). With these elements, each grain can be assigned to a restricted range of rock types, using a series of discriminant plots (figure 1).

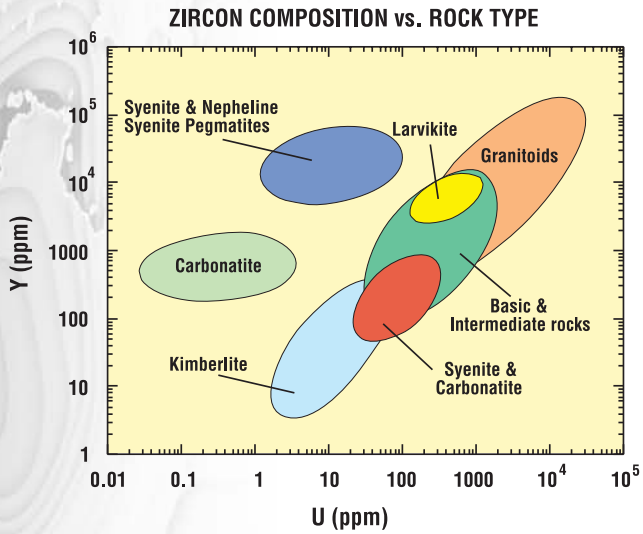

Figure 1. Relation of trace element composition of zircon to host-rock chemistry

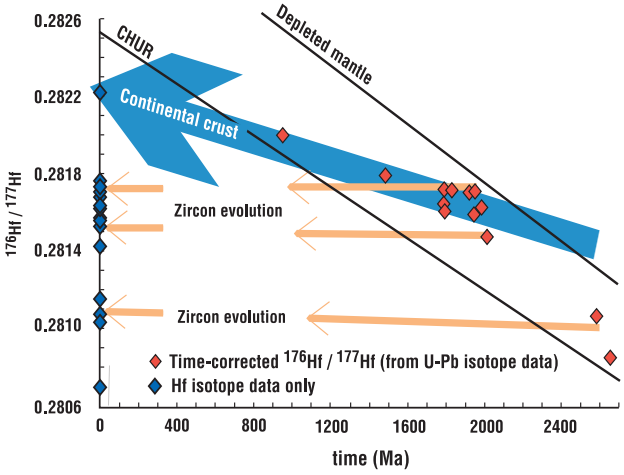

Figure 2. U-Pb age vs Hf isotope composition in zircons from East Greenland sandstones.

(2) U-Pb ages for each grain (or zone) are measured using GEMOC's quadrupole ICPMS-laser ablation microprobe, to produce an age spectrum. A rigorous analytical protocol provides U-Pb ages with precision and accuracy equivalent to ion-probe analysis, but at significantly lower cost and reduced analysis time.

(3) The Hf isotope composition of each grain is measured using GEMOC's new multi-collector ICPMS with laser-ablation microprobe (LAM-MC-ICPMS). The Hf-isotope data have precision and accuracy comparable to that obtained using standard TIMS analysis on zircon concentrates. These data, combined with the U-Pb ages, are used to identify the relative proportions of juvenile (mantle-derived) material and recycled older crust, and to place a minimum age on the recycled component. As a by-product, the analysis gives concentrations of Yb and Lu, which help to identify the parent rock type for each grain.

The integration of these different types of data gives Event Signatures — detailed pictures of crustal formation events, including their age, the degree of crust-mantle interaction

and crustal reworking, and the range of rock types generated at each stage. For example, data from Devonian sediments on E. Greenland (figure 2) , from a collaboration with Dr. T.-L. Knudsen, University of Oslo, show a major addition to the crust around 1900 Ma. Other significant igneous events occurred around 1000 Ma and 500 Ma, but the Hf-isotope data indicate that these mainly involved reworking of the 1900 Ma crust.

In addition to large-scale crustal-generation studies, applications include correlation between different terranes for mineral exploration and tectonic analysis, and mapping the provenance of basin sediments. Studies of crustal genesis in the Yilgarn Craton and the Mt. Isa Province are planned for 2000, with support from industry.

Contact: Bill Griffin, Simon Jackson, Sue O'Reilly, Elena Belousova
Funded by: ARC, BHP Exploration
Part of GEMOC's Crustal Generation, Metallogenesis and Geotectonics strands.

What role did oceanic plateaux play in the Gondwana break-up?

A NUMBER OF OCEANIC PLATEAUX cover the southern Atlantic and southwest Indian Ocean region. Their geographical positions can be reconstructed close to the zone of the Gondwana break-up between Antarctica, South America and Africa. Were these plateaux parts of the pre-break-up continent or did they evolve within the newly formed oceanic crust? As part of a collaborative project, we conducted an extensive seismic survey over one of the larger plateaux, the Agulhas Plateau south of South Africa, with the aim to help solve the questions about its crustal structure, origin, and role in a plate tectonic reconstruction context. Seismic reflection data show clear indications of numerous volcanic extrusion centres with random distribution. We are able to date this phase of voluminous volcanism to Late Cretaceous time, a period when numerous other Large Igneous Provinces (LIP) formed. Travel time inversion of ocean-bottom seismograph records reveals a crust up to 25 km thick with velocities between 7.0 and 7.6 km/s for the lower 50-70% of its crustal column. We do not find indications for continental affinity, as suggested in previous studies, but rather a predominantly oceanic origin of the Agulhas Plateau, similar to that inferred for the Northern Kerguelen and the Ontong-Java Plateaux. In Late Cretaceous time, its main crustal growth was controlled by the proximity of the spreading centres and by the passage over the Bouvet hot spot at 80-100 m.y. A new reconstruction of the southern Atlantic and southwest Indian Ocean region also demonstrates that neither the Agulhas Plateau nor the Maud Rise could have existed before the break-up. Future work will include geophysical investigations of the Maud Rise, the Mozambique Plateau and the Crozet Plateau.

Contact: Karsten Gohl
Funded by: MURG in collaboration with the Alfred Wegener Institute, Germany.
Part of GEMOC's Lithosphere Mapping, Crustal Generation and Geotectonics strands.

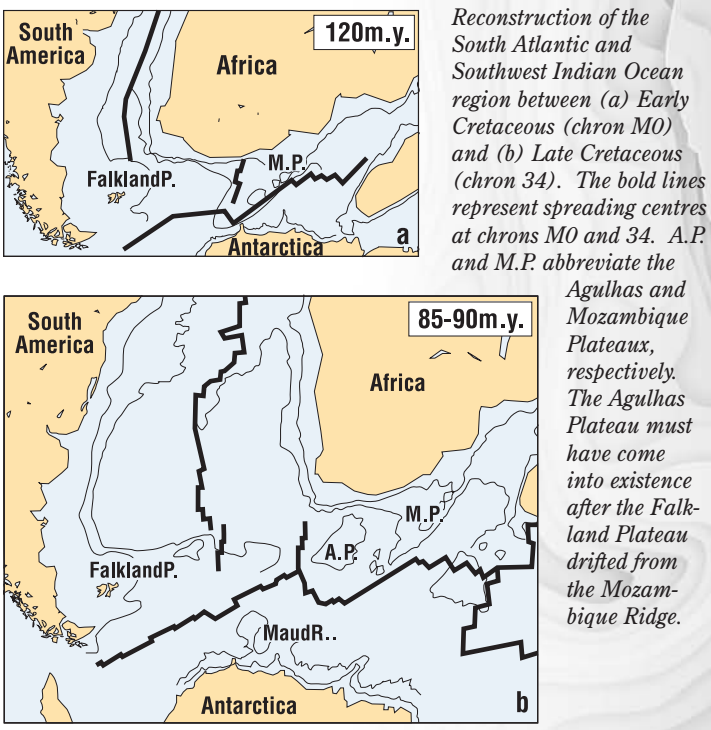

Reconstruction of the South Atlantic and Southwest Indian Ocean region between (a) Early Cretaceous (chron M0) and (b) Late Cretaceous (chron 34). The bold lines represent spreading centres at chrons M0 and 34. A.P. and M.P. abbreviate the Agulhas and Mozambique Plateaux, respectively. The Agulhas Plateau must have come into existence after the Falkland Plateau drifted from the Mozambique Ridge.

Xenoliths from the Kerguelen islands: mantle metasomatism and continent formation

THE KERGUELEN ARCHIPELAGO in the southern Indian Ocean sits atop a very large oceanic volcanic plateau, and the extensive basalts are intruded by granitic and syenitic rocks. Is this a model for the initiation of continent formation? An ongoing cooperation between GEMOC and the University of St. Etienne has concentrated on the study of xenoliths in the basaltic rocks, to map the structure and composition of the lithosphere beneath the plateau.

The ultramafic and mafic xenoliths occur in the youngest and more alkaline lavas, and include many of the types of ultramafic and mafic xenoliths entrained by within-plate basalts in continental and oceanic settings. Type I spinel-bearing harzburgites and dunites are samples of the lithospheric mantle equilibrated in the spinel peridotite stability field beneath the thick oceanic crust (14-20 km). Three groups of ultramafic to mafic xenoliths are interpreted as deep crustal and upper mantle segregates from the basaltic magmas of the archipelago. A clinopyroxene + orthopyroxene + spinel series varies from clinopyroxene-rich lherzolites, through pyroxenites to metagabbros ± garnet ± sapphirine. A second clinopyroxene + ilmenite + spinel series is represented by clinopyroxenites ± garnet and by garnet + spinel + ilmenite metagabbros. A third clinopyroxene + ilmenite series is represented by garnet-bearing metagabbros.

The Type I harzburgites can be divided into two distinct types: Cr-diopside-bearing protogranular harzburgites and Mg-augite-bearing poikilitic harzburgites. Both carry evidence for several mantle metasomatic events. The first produced LREE-enrichment in both types of harzburgite and Cr-Na-rich Mg-augite ± phlogopite in the poikilitic ones, and is ascribed to metasomatic reactions between previously depleted harzburgites and highly alkaline magmas. The second type of metasomatism results in formation of alkali-rich (K_2O: 1-10 wt%) feldspar + olivine (2) + Ti-chromite + Nb-rutile + ilmenite + Cr-armalcolite + Cr-Ca-armalcolite, in reaction zones close to opx and spinel or in thin veins cross-cutting the olivines. The formation of this exotic mineral assemblage is probably related to percolation of TiO_2-rich, H_2O-poor alkaline silicate melts into harzburgites. The dunites show similar mg# and REE patterns to the poikilitic harzburgites. Dunites in some composite xenoliths are wall rocks to magmatic dykes of tholeiitic or alkaline affinity. The dunites appear to have formed by interaction between depleted harzburgites and basaltic melts, producing metasomatic reactions such as: (1) opx + liquid 1 —> ol + liquid 2 and (2) opx + liquid 1 –> cpx + liquid 2.

All the plagioclase-bearing xenoliths have reequilibrated under granulite facies conditions, in the Kerguelen oceanic lower crust and upper mantle. These mafic granulites are the first examples reported from an oceanic environment. The existence of oceanic granulites beneath the Kerguelen islands is consistent with the presence of a thickened crust detected by seismic studies, and the calculated and measured Vp values (collaboration with I. Jackson, RSES, ANU)

Model for the evolution of the Kerguelen lithosphere

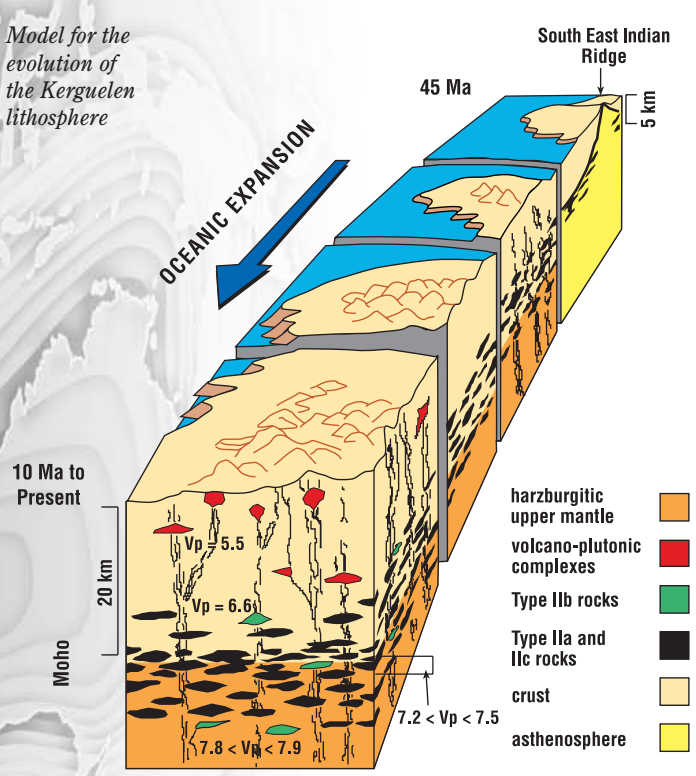

for the basic granulites are similar to those observed in the low-velocity region beneath the oceanic crust (Vp = 7.2-7.5 k/s). Thus, this first study of the Kerguelen ultramafic and mafic xenoliths indicates that crustal thickening developed as basalts intruded at different levels of the lithosphere. The synergy between the young East-Indian Ridge and the Kerguelen hot spot (≈ 45 Ma ago) produced voluminous tholeiitic-transitional magmas with resultant intrusion and formation of associated cumulates in the vicinity of the Moho. This process of crustal thickening by deep intrusion (underplating) was later amplified by the extrusive volcanic sequences related to the longevity of the hot spot activity (≈ 45 Ma), leading to granulite-facies metamorphism of the lower crust.

Publications: 117, 175 and 176
Contact: Sue O'Reilly, Michel Grégoire
Funded by: ARC, Macquarie University
Part of GEMOC's Crustal Generation and Lithosphere Mapping strands.

NEWS FLASH

ISOCHRONS IN MINUTES: SM-ND IN TITANITE:

A demonstration of the power of the new laser ablation MC-ICPMS technology emerged late in 1999, as an unexpected by-product of a study of Sm-Nd and Rb-Sr systems in apatite and titanite (sphene) from granitoid rocks in the Mt Isa inlier, done in collaboration with Dr. Geordie Mark of James Cook University. The project is using trace element chemistry (by LAM-ICPMS) of apatite to link crystallisation and mineralisation processes in granitoids and associated hydrothermal systems. The same samples were then analysed for Sr and Nd isotopes using the LAM-MC-ICPMS. To obtain the initial Nd isotope composition of the granitoids, we analysed separated grains of titanite; the analysis gives both the Sm-Nd ratio and the isotopic composition of the Nd. At the levels of Nd in these grains (2000-5000 ppm) the *in situ* analysis of single points typically produces data with precision and accuracy equivalent to conventional TIMS analysis of bulk samples ($^{143}Nd/^{144}Nd \pm 0.00003$ (2sd)). In the titanite concentrate from the Mt. Angelay quartz monzonite, we found an unexpectedly large degree of heterogeneity in both Sm/Nd and Nd isotopic composition. The data define an excellent isochron (MSWD = 1.7) with an age of 1533 ±70 (2sd), identical to a SHRIMP zircon U-Pb age on the quartz monzonite of 1525 Ma. The initial $^{143}Nd/^{144}Nd$ of 0. 51030±6 is similar to the value determined by whole-rock analysis of samples from the same intrusion. The T_{DM} model age of ca 2500 Ma indicates a late Archean age for the source of the granitoid. The precision of the isochron age and the initial ratio, despite the relatively small spread in Sm/Nd, attests to the accuracy of the individual analyses.

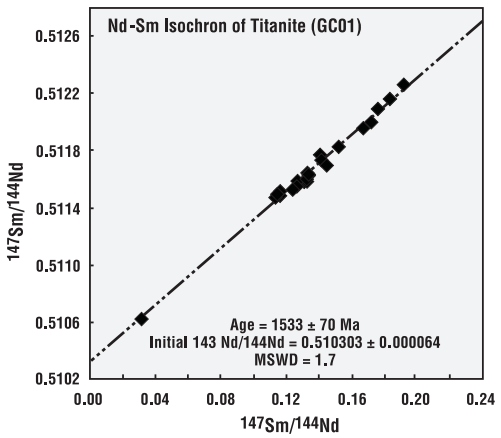

The total analysis time used for this work was two hours. The technique may be applicable to a wider range of samples, and could offer a rapid and cost-effective tool for reconnaissance geochronological studies, and for determining the age and provenance of detrital titanites in sediments.

Contact: Bill Griffin, Geordie Mark (JCU)
Funded by: ARC and AMIRA
Part of GEMOC's Crustal Generation strand.

Shell Games: Sr isotopes and Permian Terranes in New Zealand

THE ISOTOPIC COMPOSITION of Sr in marine fossils reflects that of the sea water in which they grew, and the large variations in the $^{87}Sr/^{86}Sr$ of sea water throughout the Phanerozoic offer an indirect method of dating calcareous sediments. Previously, this approach has wrestled with problems of identifying pristine carbonate material. The analysis of the Sr also commonly required laborious and time-consuming microdrilling of individual fossil fragments, followed by chemical separation of Sr and analysis by conventional mass-spectrometry. The new LAM-MC-ICPMS technique overcomes many of these problems, by providing rapid high-precision *in situ* Sr isotope analyses on a 200-micron scale, so that isotopic variations within single fossil fragments, and differences or similarities between fossils and matrix, can be used to recognise fossils whose isotopic composition has been modified by diagenesis.

Provenance studies of the Permian-Jurassic volcanic arc terranes of New Zealand require dating of the extensive volcaniclastic sediments, many of which contain few fossils. However, the distinctive prismatic calcite shell debris of the bivalve Atomodesma is widespread from Early-Late Permian, and over this period the $^{87}Sr/^{86}Sr$ of sea water fell from 0.7081 (275 Ma) to 0.7068 (265 Ma), then rose to ca 0.7071 (251 Ma). LAM-MC-ICPMS analyses of Sr isotopes were done on Atomodesma debris from several known sections, and a variety of matrix types, to test the methods and the stratigraphic usefulness of the data.

> "The new LAM-MC-ICPMS technique [provides] .... high-precision Sr isotope analyses on a 200-micron scale [which]...can be used for detailed stratigraphic correlation"

Atomodesma fragments contained 300-1200 ppm Sr. A laser beam of 200-400 microns in diameter, rastered over a 1-5 mm length, gave signals high enough to provide $^{87}Sr/^{86}Sr$ data with an external precision better than ±0.00004 (2sd). This is equivalent to a stratigraphic precision of ca ±300,000 years, which is very useful. At a given stratigraphic time horizon, we found consistent $^{87}Sr/^{86}Sr$ ratios for Atomodesma fragments, irrespective of their matrices; in one case concordant results were found for coexisting echinoid debris. Large differences were found between the fossils and their clastic matrices. The data obtained so far are consistent with the accepted sea-water curve for the Permian, and show that Atomodesma, while not a very good marker fossil in itself, can be used for detailed stratigraphic correlation by analysis of its $^{87}Sr/^{86}Sr$.

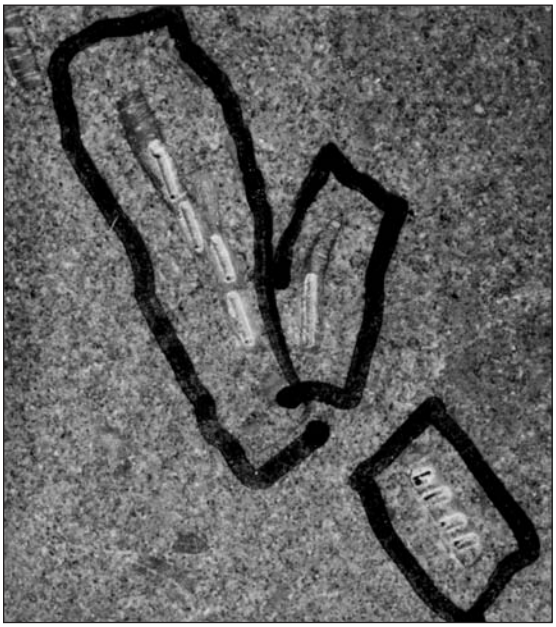

Section of Tramway Sandstone containing marine fossils (the bivalve Atomodesma, marked in black). The whitish grooves within the fossils are laser ablation tracks produced during Sr isotope analysis using GEMOC's LAM-MC-ICPMS. Width of photo = 1.5 cm

Contact: *Bill Griffin, Dr. C.J. Adams (Inst. Geological & Nuclear Sciences, Lower Hutt, NZ (argon@gns.cri.nz), Norm Pearson*
Funded by: GEMOC and the Institute of Geological and Nuclear Sciences
Part of GEMOC's Crustal Genesis strand.

Defining the APWP for Paleozoic eastern Gondwana: paleopoles from the Northen TASMAN orogen, Queensland

THE MID-CARBONIFEROUS segment of Gondwana's Apparent Polar Wander Curve (APWP) is still poorly defined and it is suggested that resolution of the preliminary data presented herein could provide a key pole in the definition of this part of the path. Ignimbritic sequences from the Permo-Carboniferous Newcastle Range (NRV), central Queensland (18.3 S, 143.7 E), were sampled for paleomagnetic investigation. Mid-Carboniferous volcanics display a characteristic magnetisation direction for the majority of sites: D_C=202.7, I_C=62.6, with an antipodal direction of D_C=8.7, I_C=-57.5. These directions indicate a mid-Carboniferous paleomagnetic pole of Plat=-58.6, Plong=115.8. This well-defined pole is supported by results from Africa and South America as reported in the Global Paleomagnetic Database. (See figure)

Sediments from a site in the Devonian Gilberton Formation (DGF) exhibited two magnetic components, one which is described as the mid-Carboniferous overprint (D_C=191.1, I_C=55.7) and the second, a hematite (high-temperature) component, has a direction of D_D=355.9, I_D=-10. This high-temperature component gave a VGP of Plat=-76.1, Plong=306.5, a pole that is, seemingly, in concordance with that of the Late Devonian Comerong Volcanics (CV), Plat=-76.9, Plong=330.7.

The coupling of paleomagnetic analysis with detailed rock magnetic tests is an integral part of the geophysics research conducted at Macquarie. An enhanced understanding of paleogeodynamics is the aim of this program for which the collaboration between GEMOC and CSIRO is vital. Mid-2000 will see an additional field excursion to northern Queensland, followed by one to the Georgina Basin of far western Queensland. It is this second trip that will best exemplify the collaborative effort that is necessary in paleogeodynamics as reinvestigation of the Cambrian/Ordovician Black Mountain carbonates, key units in the recently proposed IITPW event, will depend heavily upon chemical analyses for correlation of paleomagnetisations with earlier studies.

Contact: Kari Anderson
Mark Lackie
Funded by: Macquarie University, Small ARC
Part of GEMOC's Geotectonics strand.

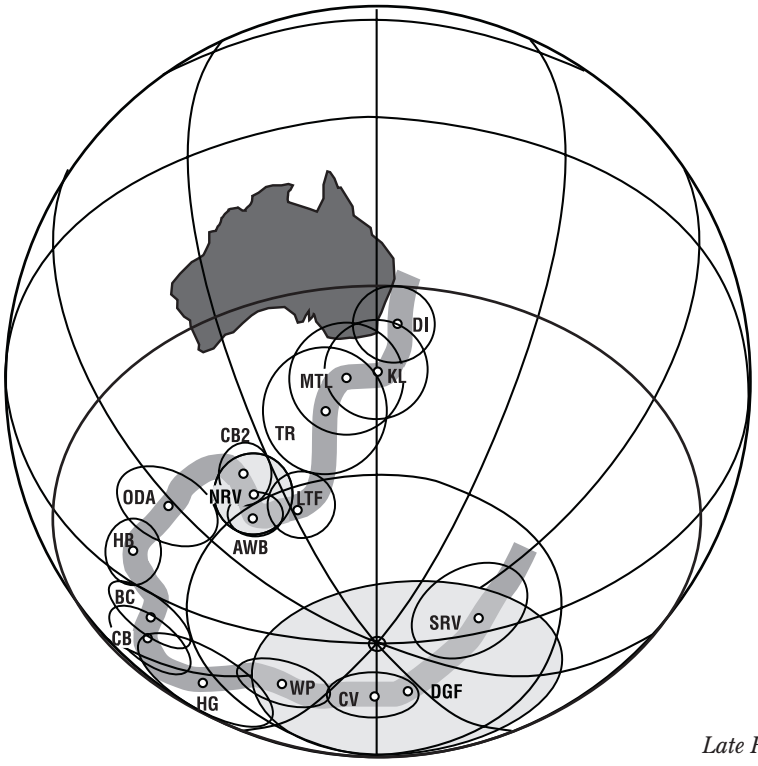

Late Paleozoic APWP for Australia

Reading Granite Recipes from Zircon Tapes

ISOTOPIC ANALYSIS of elements such as Sr, Nd and Hf is widely used to evaluate the sources of igneous rocks. Many granites have isotopic compositions that imply they are made up of material from two or more sources, such as remelted older rocks and juvenile mantle material (see Event Signatures). Unfortunately, these analyses only tell us the final state, and leave us in the dark about when and how these different components got together to make up the magma that crystallised into the sample.

But many of these rocks contain grains of zircon, and the zoning in single zircon crystals acts like a tape recorder, preserving a record of changes in magma composition and physical conditions such as temperature. The challenge has been to read this information at a useful scale.

Backscattered electron/cathodoluminescence images (figure 1) of sectioned zircon grains show changes in zircon growth forms that reflect changes in the crystallisation environment, and detailed work by GEMOC, using electron microprobe and LAM-ICPMS techniques, has documented large changes in trace-element patterns from zone to zone. These changes appear to reflect major shifts in magma composition, which can be related to mixing of different magmas, or to changes in fractional crystallisation patterns.

GEMOC's new multi-collector ICPMS, with its attached laser microprobe, lets us test whether magma mixing was being recorded in such zircons. Crystallisation of a single magma can produce changes in magma composition,

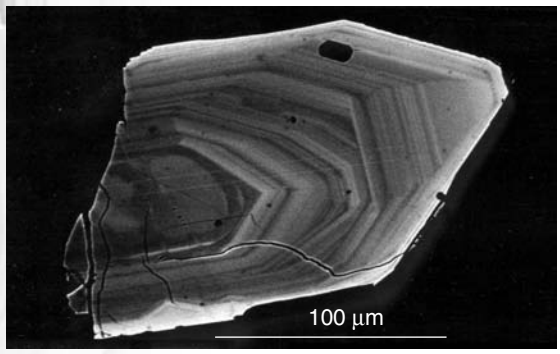

Figure 1. BSE/CL image of a zircon, showing changes of crystal morphology during growth

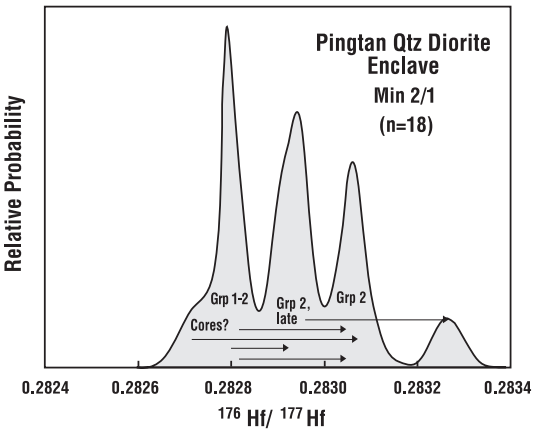

Figure 2. Cumulative probability curve of Hf isotope compositions in zircons from a Pingtan quartz diorite. Arrows show zoning within single grains.

but will not affect the isotopic composition of a single element such as Hf, which is abundant in zircon. However, mixing of two magmas with different sources could produce a change in the isotopic composition of Hf. Isotopic heterogeneity in the Hf of the zircons from one rock would be good evidence of magma mixing.

As part of GEMOC's China collaboration program, we have carried out a detailed morphological and geochemical study of zircons from a series of rocks from the Jurassic Pingtan igneous complex in Fujian, China, where field relations indicate the mingling of mafic and felsic magmas. When the LAM-MC-ICPMS was used to analyse Hf isotopes in these zircons, we found significant heterogeneity from grain to grain, and from zone to zone within single grains (figure 2). The data show that relatively felsic magmas, derived from remelting of crustal rocks 600-800 Ma older, were mixed with more juvenile magmas derived from the depleted mantle, during their crystallisation. Such mixing may have occurred several times.

These are the first studies of this kind. This new type of data provides a new dimension to studies of magma genesis and mechanisms of crust-mantle interaction, and illustrates how the new LAM-MC-ICPMS technology is going to revolutionise many areas of petrology and geochemistry in the next few years.

Contact: Bill Griffin, Simon Jackson, Wang Xiang and Sue O'Reilly. Part of GEMOC's Crustal Generation strands. Funded by ARC and AusAID.

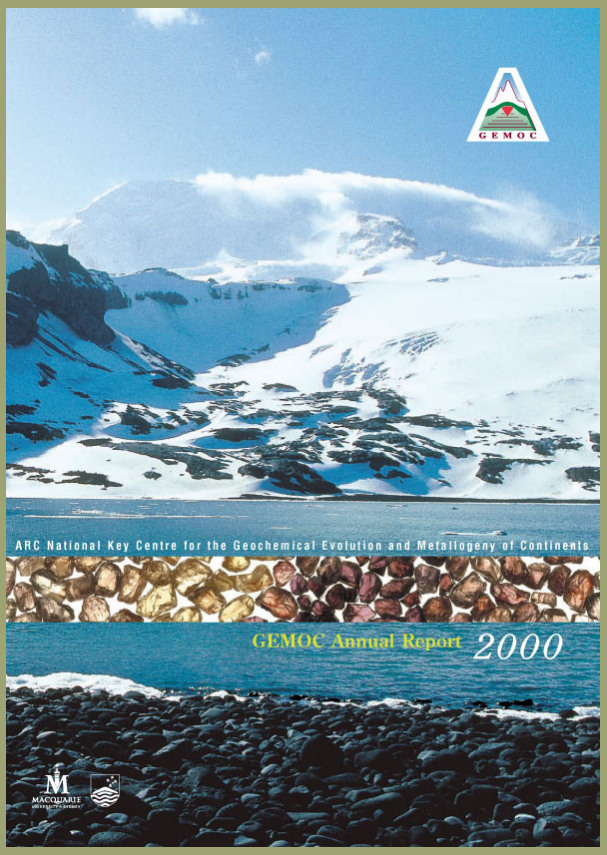

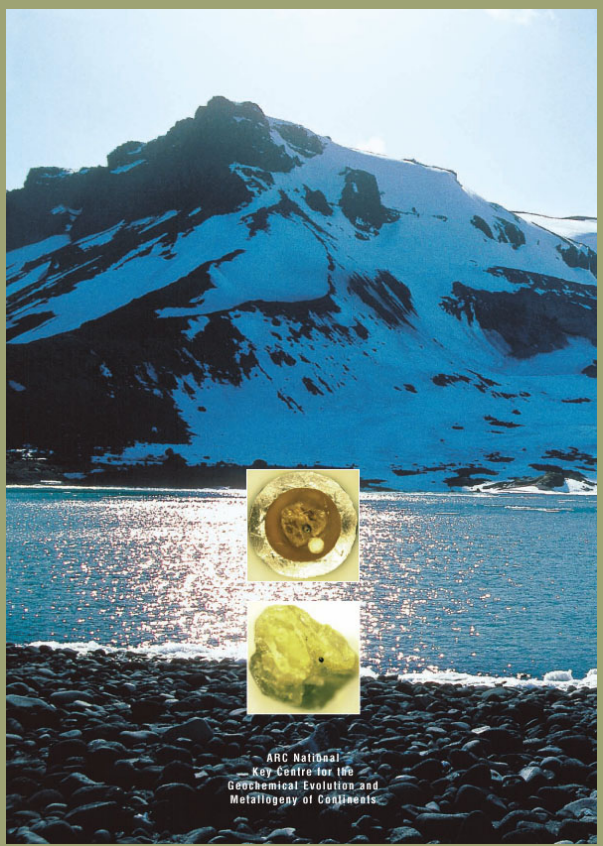

2000 Contents

TerraneChron™ reveals the development of the Mt Isa Eastern Succession	40
How to make a Craton: TerraneChron™ in the Yilgarn	42
Zircons reveal magma source rocks for the New England Batholith granites	43
How old is the Slave Craton mantle?	44
Diamond fingerprints - for science and peace	45
Heard Island: piecing together the evolution of the Kerguelen-Heard plateau	46
Composition of groundwaters: an insight into sub-surface temperatures	47
Barcoding the mantle: basalts as probes to Earth's geodynamics	48
The Slave Craton (Canada) in deep analysis	50
The new GEM in GEMOC - the GJ-1 zircon standard	51
Superdeep diamonds	52
A key palaeomagnetic pole for the Early Permian for Australia and Gondwana	53
Sorting out the mantle: In situ measurement of Re-Os isotopes in mantle sulfides by LAM-MC-ICPMS	54
Partition coefficients-essential ingredients for modelling the geochemical evolution of the crust-mantle system.	56

Front and Back Cover: Big Ben on Heard Island. Will Powell joined an Australian National Antarctic Research expedition to Heard Island in 2000, to collect mantle xenoliths from the basalts. The analysis of these xenoliths will be linked with ongoing studies of similar material from Kerguelen Island to trace the evolution of the mantle lithosphere beneath this major oceanic plateau, and provide analogies to the early development of continents (see Research Highlights)

Front cover frieze: Grains (average size 1 cm) of the GEMOC GJ-1 zircon standard for U-Pb dating, donated by Jerry Yakoumelos of G & J Gems Pty Ltd, Sydney (see Research Highlights).

Back cover inset: A sulfide inclusion in mantle-derived olivine from the Slave Province kimberlites, for in-situ analysis of Re and Os isotopes by LAM-MC-ICPMS. Bottom, the raw material; top, mounted and polished, ready for analysis (see Research Highlights).

Research highlights 2000

TerraneChron reveals the development of the Mt Isa Eastern Succession

ESTABLISHING A GEOCHRONOLOGICAL FRAMEWORK is an important component in characterising terrane evolution and correlating events. This can include time slices associated with known metallogenic endowment or recognition of 'fertile' crustal histories of direct interest for terrane assessment in regional mineral exploration. Recent advances in laser ablation microprobe ICPMS (LAM-ICPMS) make it possible to obtain *in situ* U-Pb age data comparable in quality with ion microprobe analyses, but more quickly and at lower unit cost, making it feasible to analyse large grain populations. The TerraneChron concept developed by GEMOC and Advantage Geochemical Solutions (AGS) (and described in a separate feature article in the *Research Highlights*) has been used to define a detailed Event Signature for the Soldiers Cap 'Terrane' in the Mount Isa Eastern Succession based on detrital heavy mineral sampling.

The area was selected due to its obvious economic interest as host to the world-class Cannington Ag-Pg-Zn deposit and several Iron Oxide Cu-Au deposits. The region has been the focus of intensive research including SHRIMP U-Pb dating that has defined a broad chronostratigraphic framework. Ten heavy mineral samples (ca 500 zircons) were collected to cover the main outcrop extent of the mapped Soldiers Cap Group and adjacent units.

The TerraneChron U-Pb results show good agreement with the age spectra predicted from correlations of SHRIMP data with the mapped geology of

TerraneChron – zircons barcode the crust for correlation and exploration

Modern field geology, based on an understanding of plate tectonics, has shown that most of our continents are made up of fragments (terranes), assembled at different times, then broken up, moved and re-assembled. The ambiguity of many plate reconstructions, particularly back beyond Phanerozoic time, can be constrained if we have a way of recognising blocks of crust with equivalent genetic histories. This has practical consequences as well – if we want to find the next Broken Hill or Mt. Isa, we need to look for blocks of crust with similar histories of crustal development. In effect, we need be able to match up geological "barcodes" of individual terranes. Field geology, even assisted by geochronology, can only go part of the way – commonly there are too few bars in the code to provide unambiguous matches.

GEMOC, working together with Dr Steve Walters of Advantage Geochemical Solutions (AGS) has applied its in situ analytical capabilities to develop a better barcoding method, applicable at scales from individual drainages to large continental areas. The technique uses suites of detrital zircons from modern drainages. Each zircon is precisely dated using GEMOC's LAM-ICPMS techniques; this tells When material was added to the crust. Then in situ analysis of Hf isotopes in each grain by LAM-MC-ICPMS tells How the material got there – juvenile addition from the mantle, or reworking of old crust. A suite of trace elements (Hf, Y, Th, U, Lu, Yb) collected during the other analyses identifies the original host rock of each zircon, telling What sort of material was added. The resulting Event Signature (see Mt Isa and Yilgarn Research Highlights) gives a detailed picture of the formation of the block of crust, which can be compared with similar data from other blocks. Beyond the direct correlation applications, there lies the possibility of predictive mineral exploration, based on the recognition of the Event Signatures of "fertile" and "barren" metallogenic provinces globally. GEMOC is in discussion with the mineral industry and other end-users to raise support for a program of comparative analysis of such provinces.

sample drainages. Individual lithostratigraphic units can be recognised not only by their age spectra, but also in several cases by distinctive zircon chemistry (trace elements, Hf-isotope signature). Metasediments in the Soldiers Cap-Fullarton River Groups commonly show multiple populations that reflect provenance. The presence of abundant inherited zircons allows reconstruction of a crustal evolution history extending back to Late Archean time, despite the fact that the host units do not substantially outcrop in the sampled areas. Modelling of composite age spectra allows definition of eight major Proterozoic geochronological events in the Eastern Succession, spanning the period 1400-1950 Ma, and these correspond broadly to events recognisable in the existing SHRIMP database. A more sophisticated Event Signature has been defined by integration of the Hf-isotope and trace element data (Fig. 1). This suggests four major stages of crustal evolution – 2550-2330 Ma, 1950-1825 Ma, 1800-1600 Ma and 1590-1420 Ma. Each stage has a distinct pattern of crustal generation: the relative importance of juvenile mantle input relative to reworking of older crust increases with time, as does the degree of mixing between older crust and juvenile material, and the first three cycles each ends with a period of crustal homogenisation. This history of cyclic rifting with juvenile additions followed by homogenisation is a distinctive pattern of crustal evolution; in the case of the Mount Isa Inlier it is linked to world-class metal endowment involving a range of metallogenic styles. The challenge for the future is to develop a 'library' of comparative Event Signatures for known endowed versus barren terranes within these time slices to determine the predictive economic significance of this pattern.

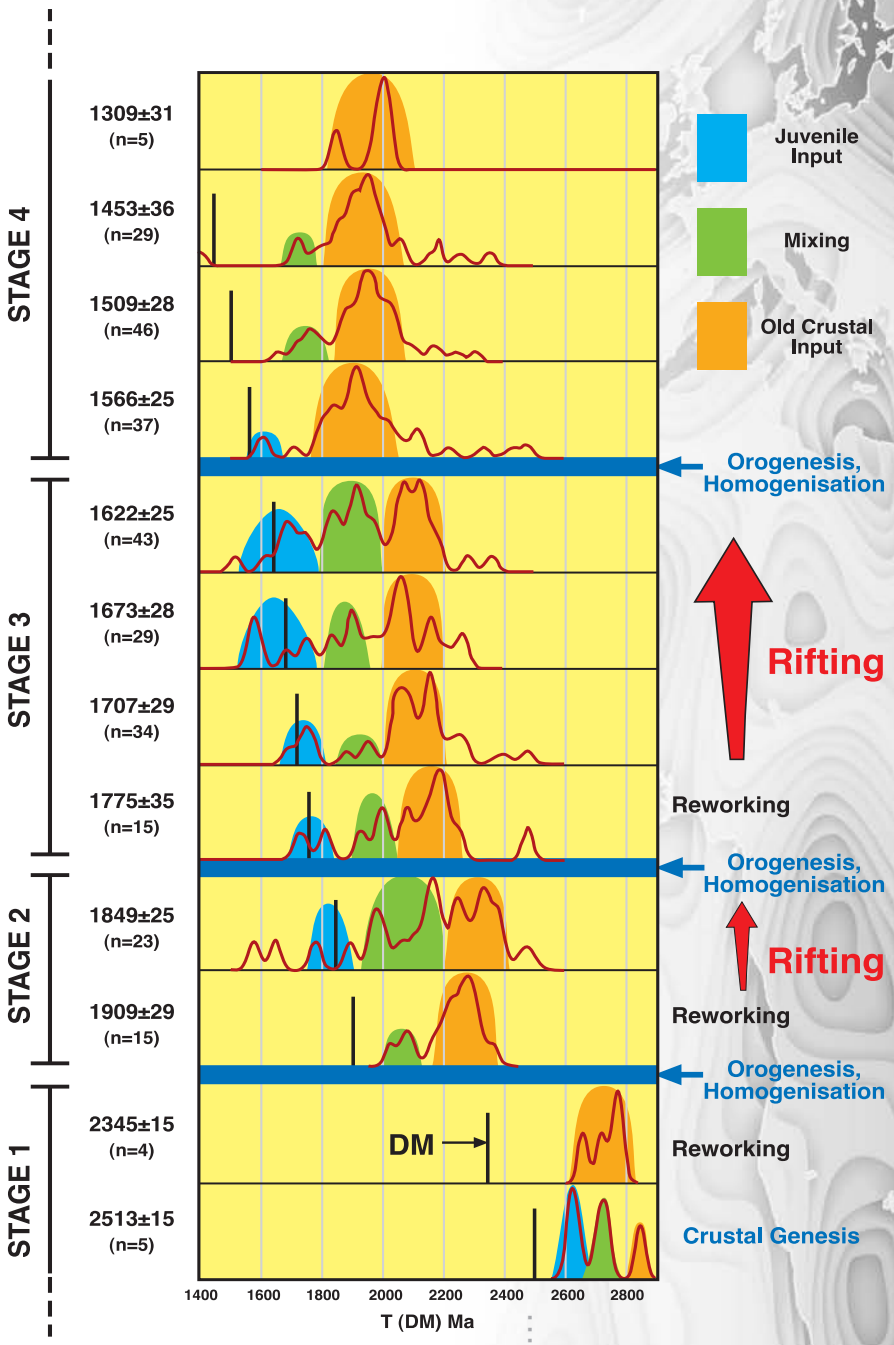

'Event Signatures' at the Mount Isa Eastern Succession. Time slices determined by zircon U-Pb dating are plotted against $T_{(DM)}$ model ages, where DM represents the depleted mantle line. Age peaks are grouped into material derived from juvenile (depleted mantle) sources, reworked old crust and mixtures of both, for each period.

Contact: Bill Griffin, Elena Belousova, Simon Jackson, Sue O'Reilly, Steve Walters
Funded by: Industry Collaborative projects (BHP, Anglo, WMC), Macquarie University

How to make a Craton: TerraneChron in the Yilgarn

THE TERRANECHRON APPROACH (integrated U-Pb dating, Hf-isotope analysis and trace-element spectra on suites of detrital zircons – see TerraneChron Feature Article) offers a new way to look at the development of Precambrian cratons. In a reconnaissance study, GEMOC has analysed over 600 zircons from modern drainages along a traverse across the northern end of the Yilgarn Craton; the zircon separates were prepared from diamond exploration samples by DeBeers Australia Exploration Pty Ltd. The samples cover the NW Gneiss Terrane, the Murchison Province, the Southern Cross Province and the Eastern Goldfields Province. The results show major differences in crustal evolution and the history of crust-mantle interaction among the different provinces.

In the Eastern Goldfields Province continental crust probably did not exist before 2.9 Ga ago, and most of the magmatic rocks produced at 2.6-2.8 Ga were derived from a Depleted Mantle source. In the Southern Cross Province (Barlee Terrane), juvenile crust formed at 3.6-3.7 Ga and again at 3.3-3.4 Ga, and this older crust was reworked to produce granitoid magmas at 2.5-2.7 Ga. In contrast to the adjacent Eastern Goldfields Province, there is no evidence of a juvenile (mantle) contribution to the crust during the major 2.5-2.7 Ga magmatism. In the Murchison Province, juvenile crust formed at least by 3.3-3.5 Ga; this older crust was reworked at 2.6-2.8 Ga, but significant juvenile crust was also added during this time. In the NW Gneiss Province, juvenile crust probably formed by 3.5 Ga, and again between 2.8-3.0 Ga, but younger granitoids (2.4-2.8 Ga) were derived mainly by crustal reworking. These different crustal evolution histories suggest that the NW Gneiss Province, Murchison Province and Southern Cross Province represent separate micro-continental fragments with very different geological histories. These older fragments were swept together to form the nucleus of the Yilgarn continent, and the Eastern Goldfields Province was accreted (as a series of arcs?) to the continental margin between 2.8-2.9 Ga.

The data also contribute to a picture of the development of the early Earth. The oldest rocks in the Murchison and Southern Cross provinces were derived from a chondrite-like mantle source, suggesting that little continental crust had been extracted before 3.5 Ga. A Depleted Mantle source had developed beneath the Southern Cross Province ca 3.3 Ga ago, but may not have appeared under the NW Gneiss Terrane and the Murchison Province until ca 3.1 Ga ago.

The data on the zircons from the 2.5-2.7 Ga granitoids suggest that the presence of older crust strongly influenced the nature of crust-mantle interaction during the assembly of the craton and the accompanying major magmatism. These differences in the style of crust-mantle interaction also correlate strongly with known mineral potential: more mantle input, more mineralisation.

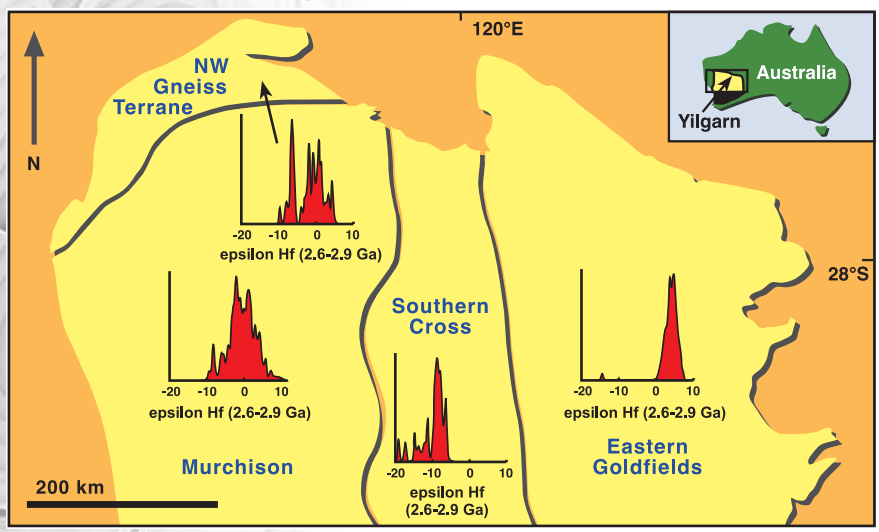

Distribution of ε_{Hf} in detrital zircons with U-Pb ages of 2.6-2.8 Ga, from different terranes of the northern Yilgarn Craton. High values of ε_{Hf} show that little ancient crust was involved in the generation of 2.6-2.8 Ga granites in the Eastern Goldfields, while low values show that the granites in the Southern Cross terrane were melted from crust formed at ca 3.6-3.8 Ga.

Contact: Bill Griffin, Elena Belousova, Sue O'Reilly
Funded by: ARC, Stockdale Prospecting

Zircons reveal magma source rocks for the New England Batholith granites

GRANITES MAY CRYSTALLISE from a single magma or from several magmas that mix. The relative importance of magma(s) sourced from either the crust or mantle is a major debate with important implications for the mechanism of continental growth. New micro-analysis techniques for hafnium isotopes in zircons from granite allow the recognition of those zircons that have crustal signatures and those that have mantle signatures. In addition, the TerraneChron technique developed recently in GEMOC (see item in *Research Highlights*) can provide rapid *in situ* zircon U/Pb age determination as well as the Hf^{176}/Hf^{177} ratios. The granites of the New England Batholith have few zircons that are inherited from older rocks and therefore the $^{176}Hf/^{177}Hf$ zircon data provide a measure of the time since the source rock was generated from the mantle.

Bald Rock: a huge outcrop of the Stanthorpe Granite close to the N.S.W. - Queensland border (also pictured below).

Preliminary data for one I-type granite have resolved a major controversy by confirming that it is formed mainly from a melt with a distinctively crustal Hf isotopic signature. However, a second group of zircons from the more felsic part of the granite was found to have Hf isotopic ratios indicating involvement of a magma derived either from the mantle or a very young crustal source (eg young mantle-derived mafic intrusions into the lower crust). The surprise was not that at least two magma types are involved but rather that the magma derived from the mantle (or very young crust) is felsic and not mafic. Thus the zircon evidence suggests the mixing of two felsic magmas without a mafic melt component. This observation has potentially significant implications for the origin of most granites and the type of melts involved in mixing processes. New data are expected to resolve unambiguously whether granites that form so much of the upper crust in eastern Australia are (a) formed by recycling older crustal materials or (b) are significantly new material added from the mantle below.

We will now examine the other five supersuites (groups) of New England Batholith granites to determine if this source rock diversity is general. Our aim is to find whether a mix of magma types is common in other granite types of the New England Batholith and especially whether a mantle-derived felsic magma may be a significant component of S-type granites, thus explaining chemical differences between S-type granites and the regional metasediments. The extent to which the Hf isotopic data differ in the six different granite groups is important and we would predict from the available other isotopic data that the age of the crustal source rocks and/or the relative importance of the mantle component will vary.

If mixing of felsic magmas (one reworked crustal and one "juvenile") is common to many or all of these granites it will result in a major change to the way the geochemical variation in granites is interpreted. In particular this may explain why most granites that have a dominantly metasedimentary source rock region do not have the composition expected if the regional sedimentary rocks are perceived to be the source.

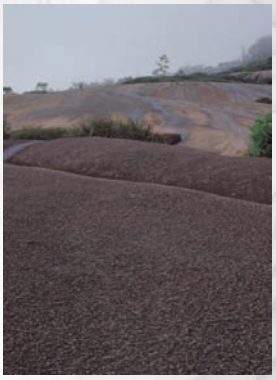

Contact: Dick Flood, Stirling Shaw; Funded by: MURG

How old is the Slave Craton mantle?

MACROCRYSTS OF OLIVINE in kimberlites are commonly interpreted as fragments of the rocks that make up the lithospheric mantle. One in several hundred of these olivine grains contains inclusions of sulfide minerals that are residues from the melting events that differentiated primitive mantle into crust and depleted lithospheric mantle. Because they are mostly shielded from post-melting processes by their hosts, these sulfides may carry information about these initial melting events – especially their age. Sulfides have high concentrations of highly siderophile elements, among them Re and Os, a radioactive parent-radiogenic daughter pair useful in dating and geochemical tracing.

The recent development of high-precision *in situ* laser-ablation techniques (see *Research Highlights 1999*) enables us to rapidly obtain Re and Os isotopic ratios in single sulfide grains. We have combined this innovation with a new approach to retrieving and preparing statistically meaningful numbers of sulfide inclusions. Olivine grains with sulfide inclusions are hand-picked from heavy-mineral concentrate under the binocular microscope and mounted in aluminium sleeves filled with resin which is then hardened at about 150° C. The sleeves are then polished to expose the the sulfide, which is characterised by electron microprobe analysis and X-ray imaging. The Re and Os isotopic ratios are collected by laser ablation multicollector inductively coupled mass spectrometry (LAM-ICPMS) using GEMOC's Nu Plasma instrument. Repolishing of the samples after laser ablation reveals that for about 75% of the samples, enough material is left for the determination of platinum group elements by quadrupole LAM-ICPMS. This added geochemical information allows us to assess whether the sulfides are of primary or metasomatic origin and puts the isotopic data in a more specific context.

Preliminary results reveal that the lithosphere beneath the Lac de Gras area, Slave craton, Canada, contains at least two distinct sulfide assemblages, one with Ni-Fe mono-sulfide solid solution (mss) ± pentlandite (pn) ± chalcopyrite (cp), the other with Co-rich (up to 17.5 wt%) phases ± mss ± pn ± cp. The Re-Os systematics of about 20 mss-dominated inclusions have been analysed. One population gives plausible model ages (T_{CHUR}), ($0 < T_{CHUR} < 4.5$ Ga) testifying to undisturbed Re-Os isotope systematics. These sulfides may have formed during several melting episodes. The Re-Os model age spectrum shows two main peaks at 2.8 Ga and 3.3 Ga, ages that can be correlated with tectonothermal events in the area. Alternatively, the strong positive correlation shown by some of these inclusions can be interpreted as an isochron, yielding an age of 3.45 ± 0.25 Ga and an enriched initial $^{187}Os/^{188}Os$ of 0.1072 ± 0.0016. Recent Re addition is shown in some grains with low Os isotopic compositions combined with elevated Re/Os. This group may still yield meaningful Re-depletion ages

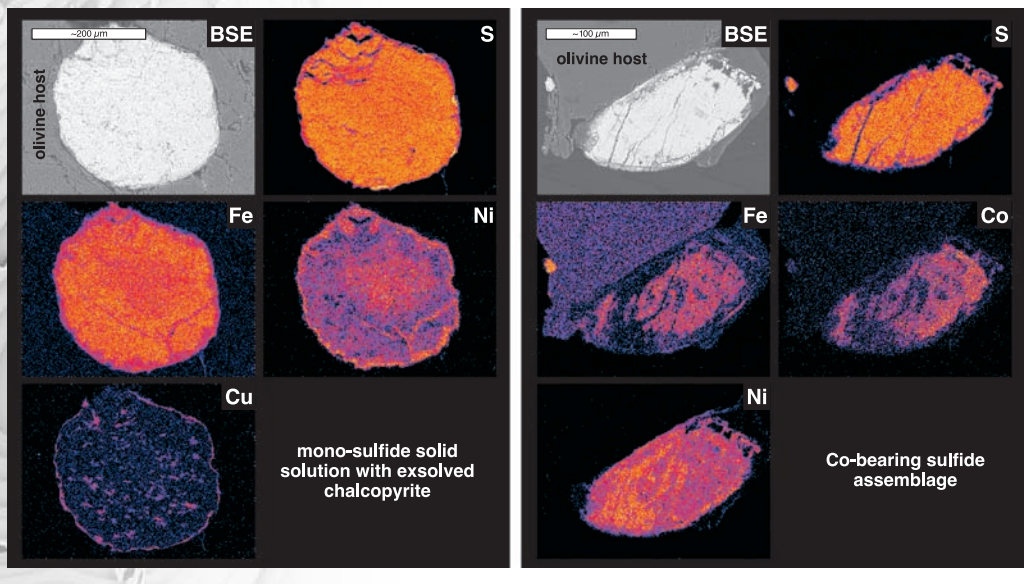

X-ray images showing the relative abundance of major elements in an Fe-rich (a) and a Co-Ni-rich assemblage (b)

(assumption: all Re has been lost during partial melting and any Re present is secondary), all of which are older than 3 Ga. The results suggest that the lithospheric mantle beneath the central part of the Slave Craton formed in a small time interval around 3-3.5 Ga ago.

Contact: Sonja Aulbach, Bill Griffin, Sue O'Reilly, Norm Pearson
Funded by: ARC SPIRT, Kennecott Canada, GEMOC, MUPRF, IPRS, MUIPRA

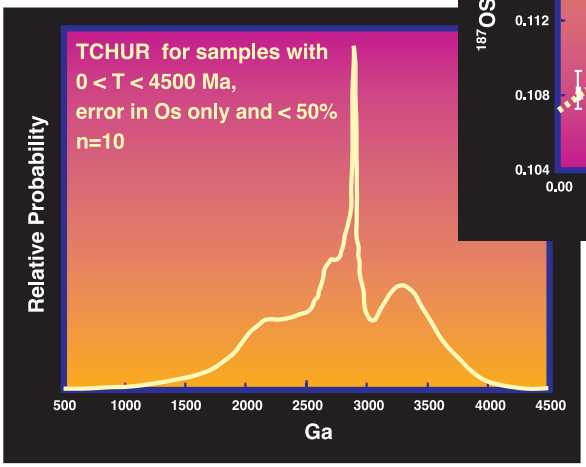

(a) Plot of relative probability of T_{CHUR} model ages showing two distinct modes, at ~2.8 and 3.3 Ga.

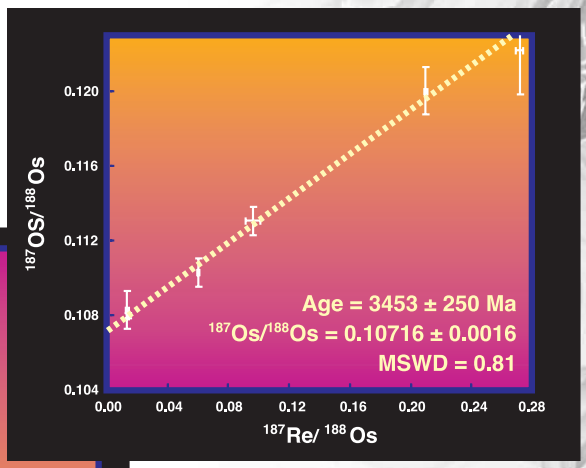

(b) The Re-Os isotope data for a subset of sulfide inclusions lies on an isochron yielding a Meso-Archean age and an enriched initial Os isotopic composition.

Diamond fingerprints – for science and peace

Diamonds are the mantle's time capsules – they are strong and chemically inert (until exposed to oxygen and high temperature), and their mineral inclusions yield unique information on the composition and history of the mantle where and when the diamonds formed. But the nature of the medium from which the diamonds themselves crystallised remains poorly understood. However, even gem-quality diamonds contain minute quantities of trace elements, and crystal-chemical considerations suggest that most of these must be in submicroscopic inclusions, which might represent the diamond growth medium.

In the current chaotic situation in parts of Africa, control of diamond deposits has become a potent factor in financing civil wars; "conflict diamonds" from war-torn areas are smuggled into countries with legimitate production, and laundered through various channels until they appear in the open market. World-wide efforts by DeBeers and other legitimate producers to assure that they are not contributing to this situation demand a means of identifying the source of individual stones. The trace-element patterns of diamonds have been suggested as a possible means of fingerprinting stones from different sources, and identifying "conflict diamonds".

GEMOC's highly sensitive Agilent 7500 ICPMS, and New Wave Research laser-ablation microprobes, allow the determination of many elements down to parts per trillion. Quantitative calibration uses a synthetic oil as a primary standard and a synthetic glass as a secondary standard to extend the range of calibrated elements to more than sixty. Important trace elements, such as the rare earths, have now been measured in diamonds with sufficient precision to provide complete and smooth trace-element patterns. A comprehensive program of analysis is underway, designed both to evaluate the potential of "diamond fingerprinting" for forensic purposes, and to learn more about the origin of diamond. We have established a baseline for comparisons, by analysing "fibrous" or "coated" diamonds (several provided by Dr Oded Navon of the Hebrew University). Unlike most diamonds, these unusual stones have grown very rapidly in the kimberlite magma itself, during its ascent to the surface, and their fibrous structure has trapped samples of the growth medium. Stones from several localities show very similar trace-element patterns, and the average pattern is strikingly close to that of an average kimberlite magma (Fig. 1). The data confirm that these stones have included the kimberlite melt, and this pattern will serve as a template for the interpretation of data from other, more typical diamonds. Contact: Simon Jackson, Rondi Davies, Bill Griffin; Funded by: ARC SPIRT, Kennecott Canada

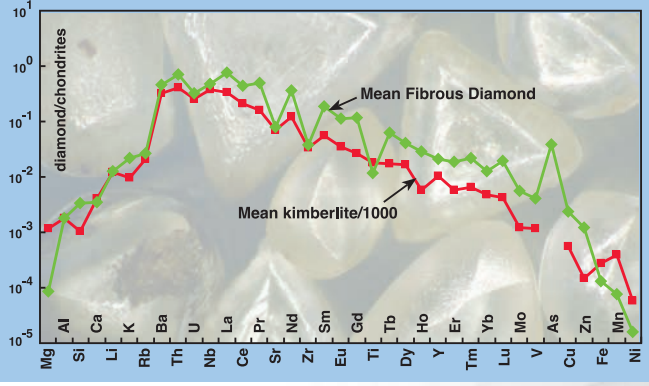

Heard Island: piecing together the evolution of the Kerguelen-Heard plateau

THE AUSTRALIAN TERRITORY of Heard and McDonald Islands lies in the windswept Southern Ocean, at 53 degrees south, 4500 km southwest of Perth. It is one of the few places where the enormous Kerguelen-Heard plateau breaks the water's surface (see front cover), the other being the Kerguelen Archipelago, 460 km to the north. Heard is dominated by the volcanic cone of Big Ben, rising from sea level to over 2700 m in less than 10 km. Big Ben and McDonald Island are Australia's only two active volcanoes – the last major eruption of Big Ben took place in 1992, producing a flow on the SW slopes around 4.5 km long.

The Kerguelen-Heard Plateau began to form around 110 Ma ago over the southeast Indian ridge, with volcanism from the ridge and the Kerguelen Plume combining to produce the enormous volume of material that makes up the plateau. The plateau was split apart 43 Ma ago to form the submarine Broken Ridge plateau to the north, and the Kerguelen-Heard plateau, which remained over the hotspot on the Antarctic plate. Kerguelen has a large part of its volcanic history exposed at the surface – the oldest lavas are around 40 million years old, and the most recent eruptions have taken place in the last 20 thousand years, at Mt Ross. Kerguelen is an unusual oceanic island in that granitic rocks are exposed at the surface – rocks normally associated with continental settings. This has led workers to believe that the Kerguelen-Heard plateau may be neo-continental – representing a transitional stage between oceanic and continental crust. An alternative view is that the plateau represents a small fragment of the Gondwana supercontinent, left isolated as Africa, India, Australia and Antarctica began to break apart around 130 million years ago.

Round Hill, on Heard Island's north coast, one of the xenolith localities with the red tent of the field camp visible at the lagoon edge.

Olivine-rich xenoliths in basalt from Round Hill.

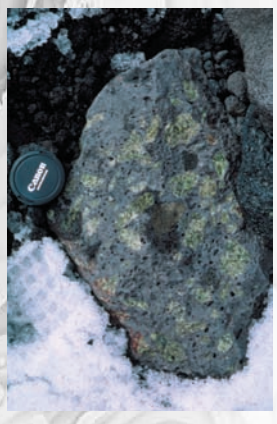

Near-vertical basaltic dyke on the south coast of the Laurens Peninsula

The volcanic sequence exposed on Heard Island is considerably younger than that on Kerguelen; the main volcanic landforms of the island – Big Ben and the Laurens Peninsula – are thought to be less than 1 million years old.

In the summer of 2000/2001 William Powell participated in the ANARE expedition to Heard Island, with the aim of collecting mantle-derived xenoliths to complement an ongoing GEMOC project in collaboration with the Université Jean Monnet, which already has provided insights into the lithospheric composition and structure of the northern part of the Kergeulen-Heard plateau (Publications 175, 184).

The fieldwork was very succesful and many xenoliths were collected from new localities: they were found in volcanic flows, and in basaltic boulders in moraine and sedimentary deposits. Xenolith types range from olivine-rich, coarse grained types to finer-grained xenoliths with relatively iron-rich olivines, and rare composite xenoliths of lherzolite with pyroxenite. Electron microprobe analysis of the constituent minerals will be used be used for thermometry, to infer the depth from which the xenoliths originated, and give an idea of the thickness of the crust beneath Heard Island. Trace element analyses using *in situ* laser ablation ICPMS will provide information on the melting and fluid-interaction history of the lower crust and upper mantle beneath the island, and Re-Os dating of sulphides *in situ* will be used to estimate the age of the underlying mantle, and help constrain the evolution of the Kerguelen-Heard plateau.

Contacts: Sue O'Reilly, Will Powell; Funded by: ASAC (AAD), MURG

Composition of groundwaters: an insight into sub-surface temperatures

HEAT FLOW is the driving force behind plate tectonics and it is ultimately responsible for much of the geology observed on the surface of the earth. Unfortunately, heat flow is relatively poorly determined across Australia, particularly when compared to North America and Europe. Heat flow is expressed as a function of geothermal gradient and thermal conductivity. Determining geothermal gradients requires a measurement or estimation of sub-surface temperature. Chemical geothermometers applied to groundwaters can give an insight into sub-surface temperatures. These are believed to be as accurate as temperatures obtained from conventional measurements in sedimentary basins.

Although it covers approximately 20% of Australia, there are very few heat flow measurements in the Great Artesian Basin (GAB). A transect has been evaluated from Birdsville in Queensland, near the deepest part of the GAB, to Marree in South Australia, near the shallowest part of the basin (Fig. 1). Various silica and cation geothermometers have been applied to groundwater analyses obtained from samples that were collected from flowing artesian bores (Fig. 2) during fieldwork, and from government sources. Geotemperatures returned by the respective geothermometers have been compared and evaluated. The correlation with measured (emergence) temperature at the surface for many of the geothermometers suggests that water-rock equilibrium in the reservoir has been attained.

Figure 1. Variation in total dissolved major elements, wellhead temperature and geotemperature with depth for a series of bores along the Birdsville Track

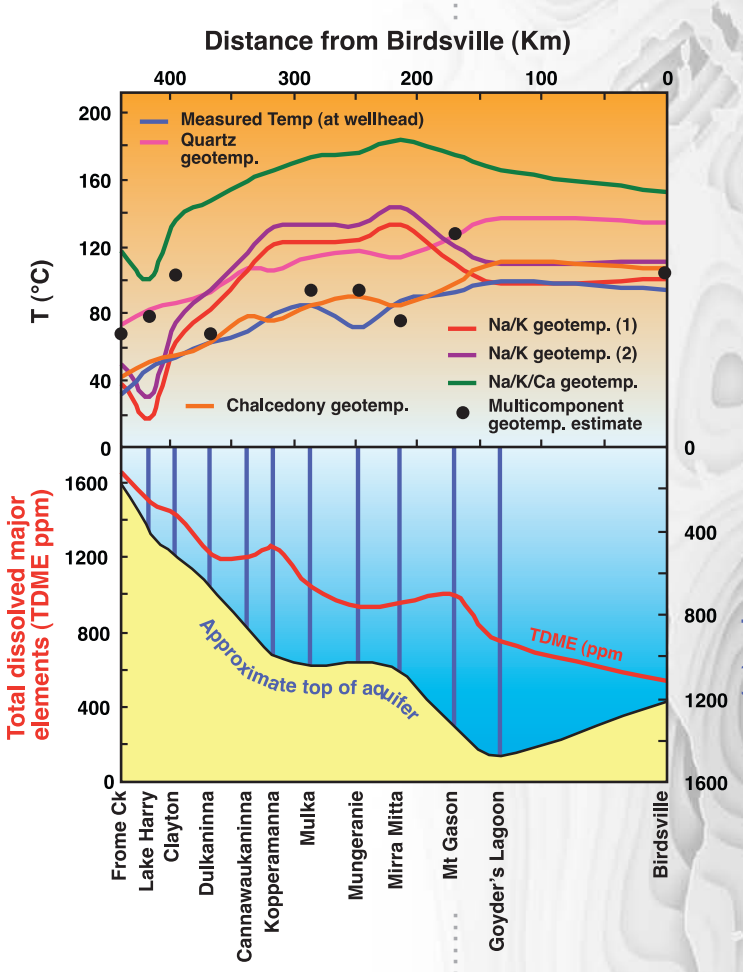

Current research is evaluating the applicability of multicomponent geotemperature estimates obtained through computer modeling of the groundwater. This type of geotemperature can be difficult to interpret, but it can offer useful information concerning the evolution of groundwaters in sedimentary basins.

Figure 2. Clayton bore - a flowing artesian bore on the Birdsville Track

Contact: Mark C. Pirlo, Sue O'Reilly
Project funded and supported by: Queen's Trust for Young Australians Achievement Award, GEMOC National Key Centre, APA award, MUPR Grant

Barcoding the mantle: basalts as probes to Earth's geodynamics

PRIMITIVE BASALTS are our best geochemical probes (so far) of the Earth's mantle below the lithosphere. The asthenosphere redistributes heat by convection cells and plumes that change in intensity in space and time. Basalts sample these reservoirs at the time and place of melting.

At the simplest level, there are three main geochemical reservoirs (Fig. 1): the convecting mantle or *asthenosphere*, commonly considered to be the mantle source that yields the mid-ocean ridge basalts and which may have its own heterogeneous domains; *plumes*, which may have different geochemical signatures depending on their ultimate origins; and the *lithosphere* which is non-convecting and does not homogenise easily, and thus carries a geochemical, thermal and chronological record of large-scale tectonic events.

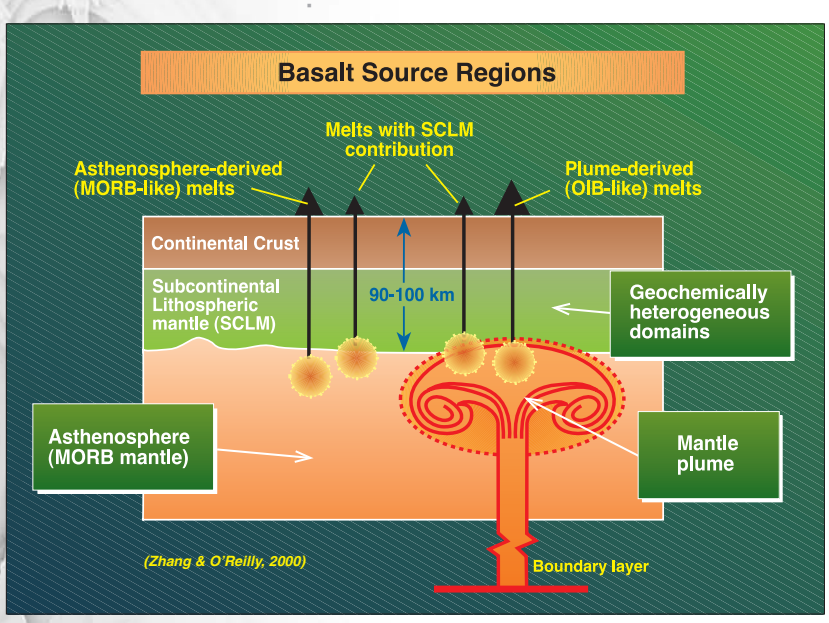

Figure 1: Source regions for primitive basalts

Eastern Australia is an ideal natural laboratory to assess the geochemical signatures of different types of basalt sources, their locations and the role of lithospheric mantle in modifying basalt composition. Primitive basalts extend for over 4,000 km along the east coast and across fundamentally different tectonic domains. They have erupted over a timespan from about 100 Ma to the present day and commonly contain mantle xenoliths that are direct samples of the rock types in the lithospheric mantle. Therefore integrated studies of basalts and xenoliths from the same locality can be used to unravel the contribution of the lithosphere to basalt compositions. Identifying specific types of lithosphere geochemical signatures in this way helps to recognise lithospheric contributions to basalts that lack xenoliths.

We have identified three major source regions contributing to the eastern Australian basalts (Publications # 133 and 219). *Firstly,* there are the distinctive geochemical signatures of the Pacific Ocean and Indian Ocean asthenospheric cells. The boundary between the "westerly" Indian and more "easterly" Pacific cells has moved eastward across the Australian continent over about the last 50 Ma so that young basalts in Queensland have an Indian cell signature. *Secondly*, there is the distinctive Australian plume (that has tracked southwards from central Queensland to the southern ocean over the last 45 Ma) and *thirdly,* there is the lithospheric component.

The different Australian basalt provinces also show different regional geochemical fingerprints that mirror the regional variations in composition that we see in xenoliths from lithospheric mantle. These lithospheric fingerprints are superimposed on the main geochemical signatures, which reflect the relative contribution from the asthenosphere and the Australian plume as the Australian plate has moved northwards. The geochemical characteristics of each lithospheric domain are in turn the combined imprint of different episodes of anatexis and fluid fluxes (metasomatism) of different origins (including primitive mantle fluids and

subduction-derived fluids), related to different tectonic events through time. Each major episode appears to have resulted in distinctive geochemical signatures and a given lithospheric domain may record multiple events.

Geochemical fields for Nd-Sr and Pb systems are shown (Fig. 2) for basalts from different provinces. These contrasts in Sr-Nd-Pb isotopic trends reflect not only the influence of the Pacific- and Indian-asthenospheric mantle convection cells, but also the principal regional geochemical heterogeneity of the lithospheric mantle domains (EM1 for New South Wales and EM2 for North Queensland). This heterogeneity appears to be fractal and detailed work on basalts within the North Queensland Province has identified different source contributions for younger and older basalts. The older ones (44-25 Ma) have isotopic signatures requiring contributions from the Australian plume and an EM2-type lithospheric mantle while the Sr-Nd-Pb isotopic trends for younger North Queensland basalts can be explained by mixing of Indian asthenosphere and EM2-type lithospheric mantle sources derived from late Paleozoic regional orogenesis (Publication #219). At a more detailed level, the high U/Pb ratios (negatively correlated with Pb isotopic ratio) shown by some highly undersaturated North Queensland basalts may have been generated from amphibole- and apatite-bearing lithospheric mantle affected by young (≤ 40 Ma) metasomatism caused by the early Tertiary subduction of the Phoenix-Pacific plate under that region.

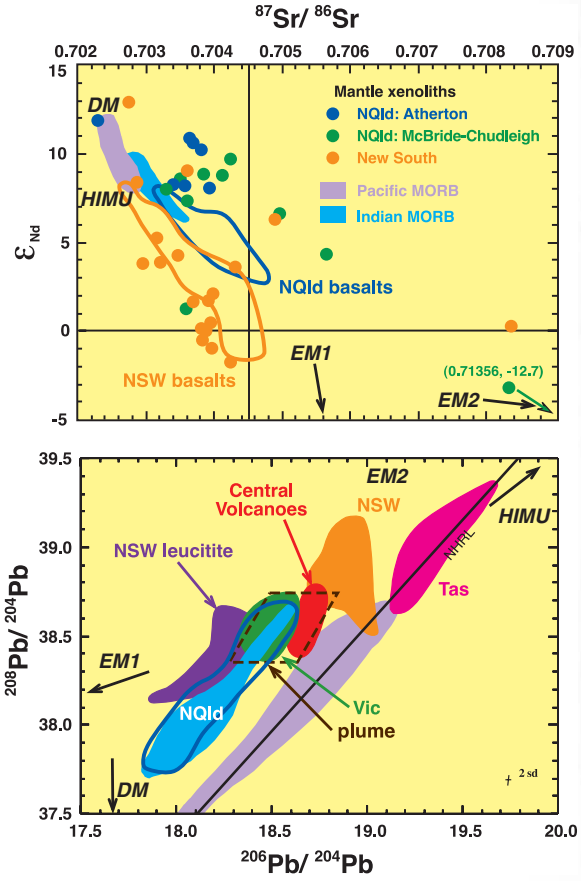

Figure 2: Nd-Sr-Pb isotopic fields for eastern Australian basalts and Nd-Sr data for mantle xenoliths. Geochemical abbreviations are explained in Publication # 219.

Figure 3: Barcoding of the eastern Australian mantle domains. SCLM = subcontinental lithospheric mantle; geochemical abbreviations are explained in Publication # 219.

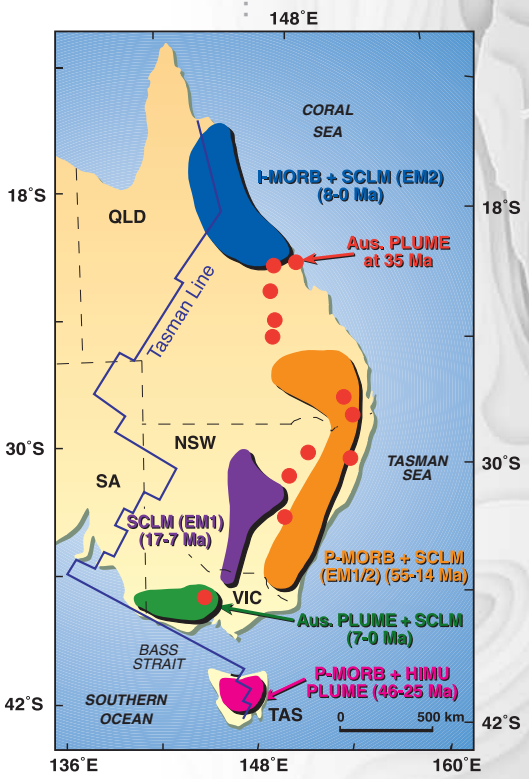

Figure 3 gives a summary of this work in progress and emphasises that primitive continental basalt compositions may reflect both mantle composition at the source of melting and additions from the lithospheric mantle. Components such as EM1, EM2, HIMU may reside in the continental lithospheric mantle and reflect metasomatism due to specific tectonic events. Mapping mantle geochemical reservoirs *in timeslices* can provide constraints for the geodynamic evolution of continental regions.

Contact: Sue O'Reilly, Ming Zhang
Funded by: ARC, Macquarie University, ACILP (AusAID)

The Slave Craton (Canada) in deep analysis

THE SLAVE PROVINCE in Canada is one of GEMOC's natural laboratories, where we can integrate geochemical, tectonic and geophysical data to map major lithospheric domains. This project is part of a SPIRT grant with Kennecott Canada. The Slave craton is a small Archean nucleus within the larger North American craton. Xenoliths and heavy mineral concentrates have been used to map the composition, structure and thermal state of the lithospheric mantle beneath the Lac de Gras area on the craton. This analysis revealed a distinct two-layered lithosphere beneath the Slave craton: a shallow ultradepleted layer and a deeper less depleted layer. The two layers are separated by a sharp boundary at 140-150 km depth (Fig 1). Griffin et al. (1999) interpreted the lower layer as plume material accreted from the lower mantle. This interpretation is consistent with the presence of abundant lower-mantle inclusions in diamonds from the region (Davies et al., 1999).

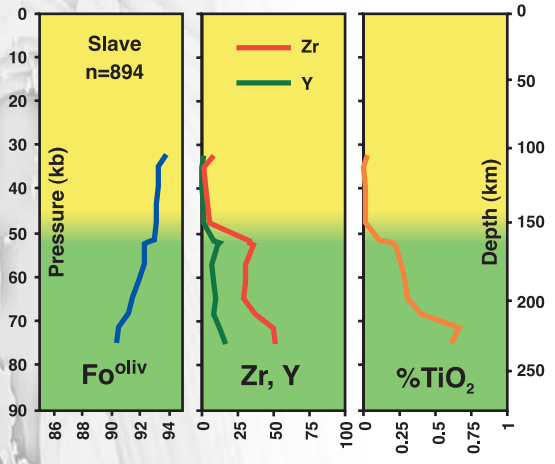

Figure 1: The layered structure of the Slave lithospheric mantle shown by key geochemical indicators. Note the ultra-depleted composition of the upper layer down to about 150 km.

Gravity data have been enhanced to map large-scale structures on the Slave craton. A map of the gravity data upward continued to 100 km (Fig. 2) shows long wavelength negative Bouguer anomalies on the central part of the craton, correlating with the major kimberlite fields. The northern part of the craton is characterised by relative positive anomalies, which probably reflect the head of the MacKenzie plume that produced major dyke swarms across the craton. Maps of vertical and horizontal derivatives of the Bouguer anomalies highlight NS-oriented structures (eg the eastern and western margins of the craton), as well as near EW-oriented structures (eg Great Slave Shear Zone).

Gravity and topographic data have been inverted to estimate the flexural strength or effective elastic thickness (*Te*) of the lithosphere of the Slave craton. The regional *Te* map shows variations from 14 km to 66 km (Fig. 3). The northern part of the craton is characterised by a relatively weak lithosphere (*Te* < 25 km) surrounded by stronger lithosphere, the strongest being in the eastern part of the craton (*Te* > 56 km). A zone of low *Te* (oriented N-S) defines the western edge of the strong lithosphere to the east of the craton. This feature may map the deep extension of the suture between the ancient continental block (up to 4 Ga old) making up the western part of the craton, and the younger (2.7-2.9 Ga) accreted terranes that make up

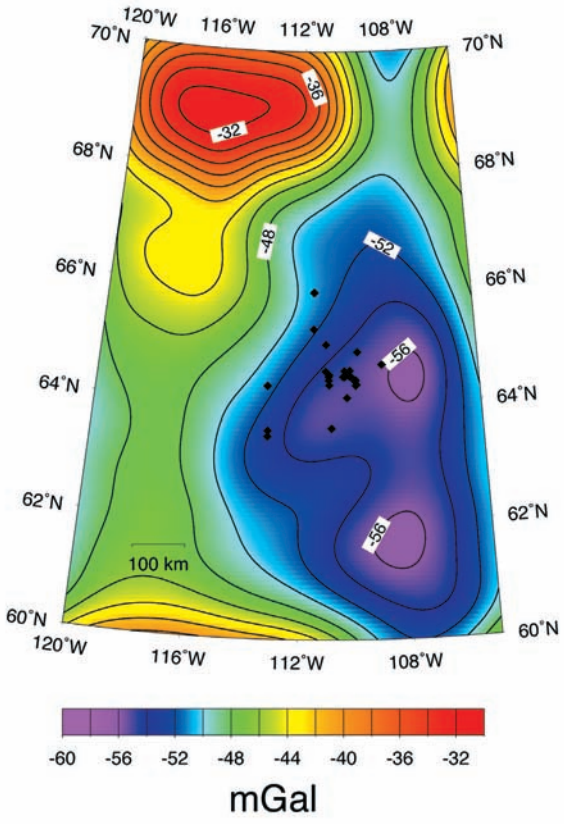

Figure 2: Colour contour map of the Bouguer gravity anomalies on the Slave craton, upward continued at 100 km. The filter applied to the gravity data in this case attenuates shallow features and enhances long wavelength or regional features > 100 km. Note that most of the diamond-bearing kimberlites (black diamonds) coincide with located an area of large negative Bouguer anomalies (less dense lithosphere).

the eastern part. The zone of low *Te* gradient corresponds to the area where long-period magnetotelluric studies have defined a strongly conductive upper mantle (Jones et al., Geology, 2001). At this stage of the work, the reasons for the correlation between *Te* and the conductive upper mantle are not obvious. The diamond fields on this part of the Slave Province are concentrated within the zone of low *Te* and anomalous mantle conductivity. This zone appears to be geochemically and geophysically anomalous and to represent a major lithospheric discontinuity on the Slave craton.

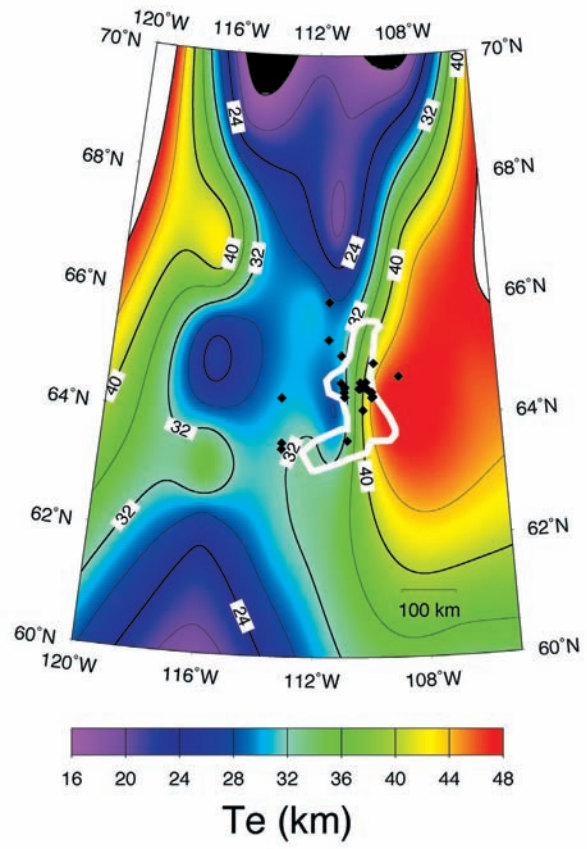

Figure 3: Color contour map of the Effective Elastic Thickness (Te) of the lithosphere on the Slave craton showing a zone of low Te gradient (oriented N-S), defining the western edge of the strong lithosphere (Te > 56 km) to the east of the craton. The white polygon outlines the area where magnetotelluric studies have defined a strongly conductive upper mantle.

Contact: Yvette Poudjom Djomani, Bill Griffin, Sue O'Reilly, Norm Pearson; Funded by: ARC SPIRT, Kennecott Canada Inc. and Macquarie University

The new GEM in GEMOC – the GJ-1 zircon standard

The large volume of laser-ablation ICPMS (LAM-ICPMS) U-Pb dating of zircons carried out at GEMOC during 2000 emphasized the need for a reliable "standard" zircon. The dating method depends on the regular analysis of a zircon with known lead-isotope composition and U/Pb ratio, to correct for elemental fractionation in the laser and mass bias in the ICPMS. Since each analysis uses up a small volume of zircon, a standard tends to disappear with time. A standard needs to be very homogeneous in isotopic composition, and to contain enough U and Pb that good counting statistics can be attained during analysis. Much of the dating done in the world today, either by ion microprobe or LAM-ICPMS, relies on a small number of standards, all of them in very short supply. In 2000 GEMOC approached Jerry Yakoumelos of G & J – The Gem Merchants, of Sydney. The firm had earlier helped Jingfeng Guo with sapphire material for his PhD thesis work at Macquarie, and Jerry responded to our plea for a "big, old, homogeneous, high-uranium zircon" by producing a large bag of gem-quality rough zircons 1-2 cm across, colored from pale yellow through red to chocolate brown. Their exact locality is lost in the mists, but they probably are derived from granulite-facies pegmatites in E. Africa. Testing so far indicates that they are very homogeneous isotopically, range from 100-250 ppm U, and have excellent laser-ablation characteristics. Several grains have been dated using conventional high-precision mass spectrometric techniques by Dr F. Corfu at the University of Oslo; they showed little variation and gave an age of 608.5 Ma. All indications are that the "GJ-1" zircon will be a very useful standard. If further tests confirm this, GEMOC will distribute the standard to other laboratories.

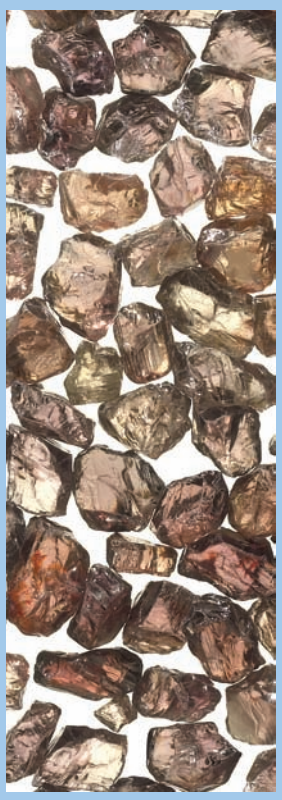

Superdeep diamonds

TO CHARACTERISE the deep Earth's physical properties and composition we rely on seismologists and experimental petrologists to provide theoretical models and data from experiments. Direct sampling of material from more than 400 kilometres below the earth's surface to test and build on such models has not been feasible.

That is, until recent years – when it was found that rare diamonds contain assemblages of mineral inclusions that require pressures and temperatures corresponding to at least 670 km below the Earth's surface.

As diamonds grow, they trap minerals from the surrounding rocks. Provided that no cracks form in the diamonds later, these minerals remain inert to later processes that may modify the mantle. Diamond inclusions thus allow us to study the composition of ancient mantle environments, including the age of entrapment, and to speculate on processes in oldest parts of the Earth. In addition, diamond inclusion data can be directly used as a tool in diamond exploration.

Octahedral diamond from the Slave Craton

Most diamonds have formed at depths of 150-200 km in ancient thickened continental roots. Diamonds with deep mantle mineral inclusions have been recognised from only about eleven localities worldwide. At GEMOC we have had the opportunity to study diamonds and their inclusions from two of these regions, the Juina alluvial deposit in Mato Grosso, Brazil and kimberlites at Lac de Gras in the Northwest Territories, Canada.

Mineral assemblages in these superdeep diamonds correspond to formation depths of the seismically defined transition zone between about 400 and 670 km, the base of which defines the Upper–Lower mantle boundary. The transition zone marks the transformation of upper mantle silicate phases with orthorhombic structures, to denser spinel and perovskite structured phases. Seismic models suggest that the mantle is dominantly peridotitic in composition, and that these structural transformations in olivine define global seismic discontinuities at 410 and 670 km.

Inclusions in diamonds from Juina, Brazil are essentially all from the lower mantle (ca 670 km) and have compositions consistent with peridotitic host rocks. In addition to the known superdeep inclusion types, we found some new phases including Ti-Fe rich chrome-spinel and Mn-ilmenite.

Resorbed dodecahedron with deformation. Superdeep diamond from the Slave Craton.

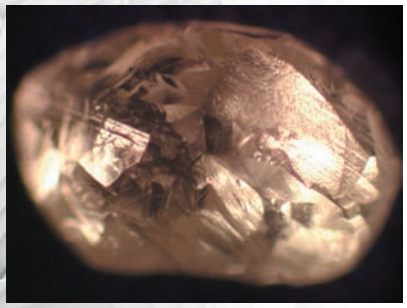

About 10% of diamonds from Lac de Gras contain superdeep phases, and these also have peridotitic compositions. Interestingly, most of the lithospheric diamonds from the same deposits are from the eclogitic paragenesis. However, there are also a few eclogitic diamonds that contain majoritic garnets, suggesting that some formed below the cratonic roots, in the upper transition zone. It appears that eclogitic diamonds also are common at other superdeep diamond localities around the world, although in general eclogitic diamonds only comprise a small fraction of most deposits.

The link between eclogitic diamonds sourced from the upper mantle through the transition zone, and superdeep diamonds with peridotitic compositions from below the Upper –Lower mantle boundary, provides new insights into the composition and structure of the mantle and the formation of diamond, with many parallels to the megalith model of Ringwood (1991).

Contact: Rondi Davies, Bill Griffin
Funded by: GEMOC

A key palaeomagnetic pole for the Early Permian for Australia and Gondwana

PALAEOGEOGRAPHIC RECONSTRUCTIONS for pre-Mesozoic times rely heavily on well-defined apparent polar wander paths from each of the continental blocks involved in the reconstructions. The tightness of the fit of the southern continents into the supercontinent of Gondwana during the Palaeozoic, and the degree of subsequent intraplate deformation in Africa, can only be tested with precise, well-dated, essentially coeval, palaeomagnetic poles from its constituent continents. Similarly, differing hypotheses regarding the relative configuration of Gondwana and Laurasia within Pangaea in the Late Palaeozoic require comparison of well-defined coeval poles from the two constituent supercontinents. Unfortunately, high quality palaeomagnetic data for the Late Palaeozoic have been scarce for the Gondwanan continents. Over the last decade, a few relatively high quality palaeomagnetic poles for Permian rocks of Africa have been reported, with no similar quality poles from other Gondwana components. Recent work at GEMOC has provided reliable, precisely defined and well-dated Early Permian (286 ± 5 Ma) palaeomagnetic poles for Australia from the Mount Leyshon Igneous Complex (MLIC) and the Tuckers Igneous Complex (TIC) that will enable such comparisons to be made.

The characteristic remanence carried by the intrusive phases and by locally remagnetised contact metamorphosed host rocks has ubiquitous reversed polarity, consistent with acquisition during the Permo-Carboniferous (Kiaman) Reverse Superchron. The corresponding palaeopoles confirm that Australia occupied high latitudes in the Early Permian. The pole positions are: MLIC: Lat = 43°S, Long = 137°E (dp = 6.0°, dm = 6.4°; Q = 6); TIC: Lat = 49°S, Long = 142°E (dp = 10.3°, dm = 11.4°; Q = 6). The primary nature of the Early Permian palaeomagnetic signature is established by full-baked contact aureole tests at both localities.

The new poles are more consistent with Pangaea B type reconstructions of Gondwana and Laurasia than with the Pangaea A2 configuration. Systematic differences between approximately coeval poles from Africa, South America and Australia, require a tighter fit than is found in standard Gondwana reconstructions. This suggests that some attenuation of continental margins, not accounted for in the reconstructions, has taken place during the breakup of Gondwana. If stretching of continental margins during breakup of supercontinents is a general phenomenon, it may help to resolve the longstanding controversy regarding Pangaea reconstructions.

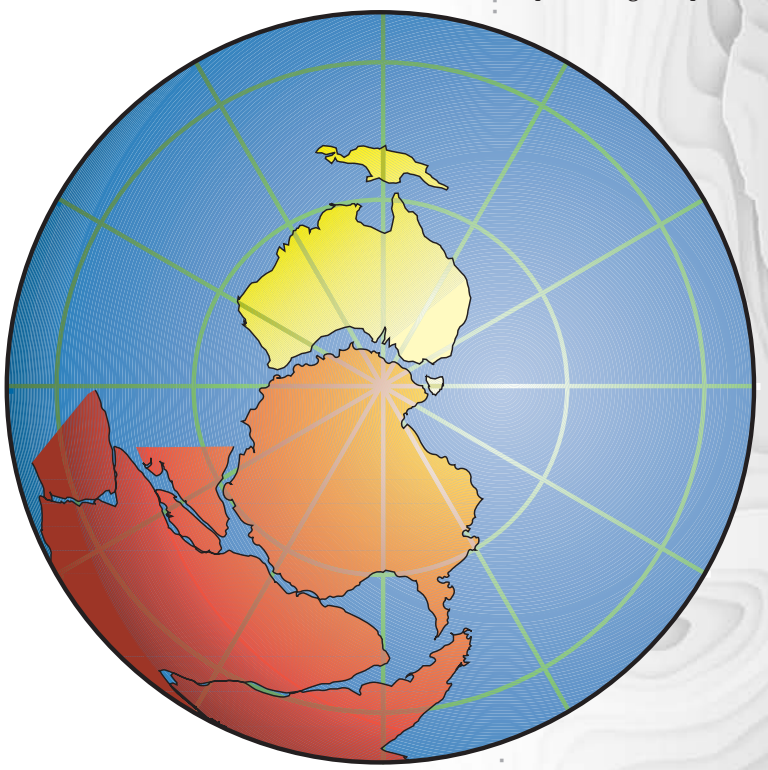

The position of Gondwana in the Permian (~285 Ma), based on the MLIC palaeomagnetic pole.

Contact: Mark Lackie, Dave Clark
Funded by: Macquarie University, AMIRA

Sorting out the mantle: In situ measurement of Re-Os isotopes in mantle sulfides by LAM-MC-ICPMS

THE *IN SITU* RE-OS ISOTOPE analysis of mantle sulfides was developed at GEMOC during 1999-2000, and has rapidly become the most powerful method available for dating mantle events – the time framework essential to 4-D lithosphere mapping. The method, which uses GEMOC's multi-collector ICPMS laser microprobe (LAM-MC-ICPMS) has a great advantage over conventional Re-Os analysis because it analyses single sulfide grains, and preserves the microstructural context necessary for interpretation of the analytical data. Another advantage is that each analysis takes a few minutes, without the need for the difficult and time-consuming separation of the sulfides and micro-chemical extraction of Os.

Using LAM-ICPMS analyses of sulfides in mantle-derived peridotites, Alard et al. (2000; see 1999 *Research Highlights*) showed that sulfides enclosed in primary silicate minerals typically have high Os and Ir contents (≥ 100,000 x PM) and low Pd/Ir ratios (Pd/Ir < 0.5), whereas interstitial sulfides have low Os and Ir contents and high Pd/Ir ratios (up to 1000). Both types of sulfide commonly occur in the same sample. The silicate-enclosed sulfides are thought to represent the residues of partial melting, and the intersitial sulfides the crystallisation products of sulfide-bearing metasomatic fluids. During 2000, the analysis of Os isotopes in these two sorts of sulfides in xenoliths from ancient and young lithospheric mantle has shown its usefulness in understanding the complexity of mantle rocks.

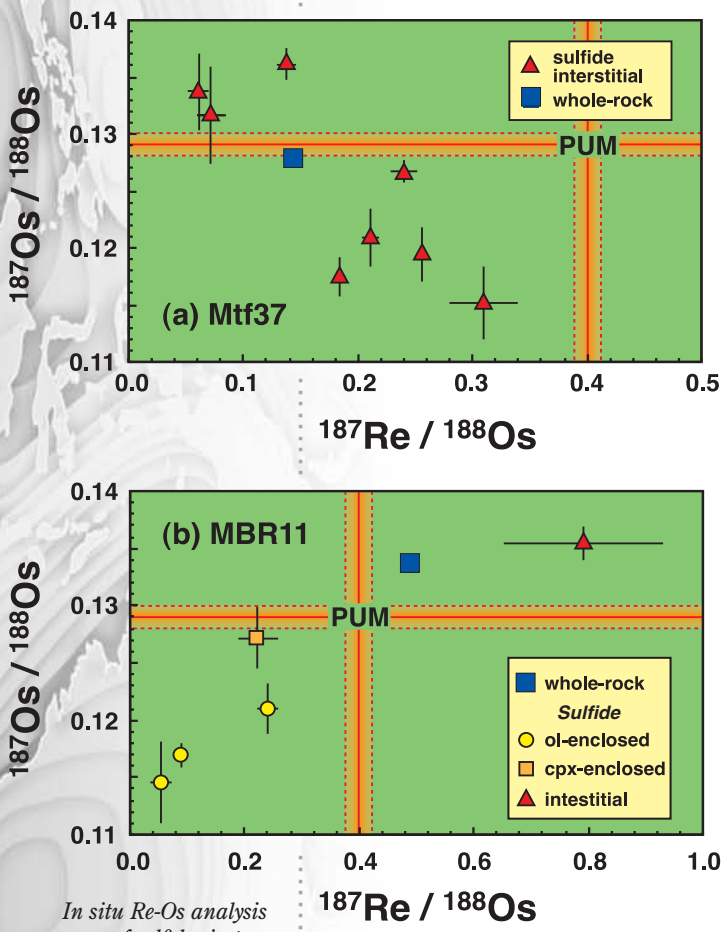

In situ Re-Os analysis of sulfides in two Massif Central peridotite xenoliths

The best precision for the *in situ* Os isotope technique is obtained from sulfides with > 40 ppm Os and > 100 µm in size. Such sulfides are common as inclusions in macrocrystic olivine in kimberlites (e.g. Udachnaya pipe, Siberian craton, Russia; Lac de Gras, Slave craton, Canada; see *Research Highlight*). *In situ* LAM-ICPMS showed that the sulfides from Udachnaya can have very high PGE contents (up to ≈ 900 ppm) and very low Pd/Ir (0.0002-0.0093). $^{187}Os/^{188}Os$ ratios of these sulfides range between 0.1033 ± 0.0002 and 0.1118 ± 0.0013, while the low $^{187}Re/^{188}Os$ ratios (0.006 to 0.081) are consistent with their low Pd/Ir. The unradiogenic Os isotopic ratios require that these sulfides have evolved in a low Re/Os environment since roughly 3 Ga ago. The *in situ* results are in good agreement with data for diamond-enclosed sulfides from the same pipe (Pearson et al., 1999) and have demonstrated the reliability of the *in situ* method relative to the already established micro-chemistry method.

The results from two spinel lherzolites from the Massif Central, France highlight the power of the *in situ* technique in understanding processes within the mantle. A low-temperature spinel lherzolite from the Montferrier alkali basalt (Sample Mtf37; Languedoc, southern France) contains interstitial sulfides that produce an inverse correlation between $^{187}Os/^{188}Os$ and Re/Os ratio (Fig. 1a).

The low $^{187}Os/^{188}Os$ of some of these sulfides yields T_{RD} ages down to ≈ 1.8 Ga. The relationship between sulfide and whole-rock data indicates that the whole-rock Os isotopic composition represents the mixing of Proterozoic components and younger radiogenic Os. The negative $^{187}Os/^{188}Os$ – Re/Os correlation suggests that the radiogenic Os, but not Re, has been transported from a high Re/Os reservoir via a metasomatic fluid. A coarse, granular spinel-lherzolite (MBR11) from Mont Briancon, Massif Central, France has a whole-rock Os isotopic composition and $^{187}Re/^{188}Os$ ratio more radiogenic than the primitive mantle; the usual interpretation would call upon host lava contamination. However, *in situ* Os-isotope data show that silicate-enclosed sulfides have a wide range of $^{187}Os/^{188}Os$, correlated with $^{187}Re/^{188}Os$. The analysed interstitial sulfide shows an even more radiogenic Os signature and higher Re/Os ratio (Fig. 1b). In both of these samples it is clear that the whole-rock Re-Os signature reflects a mixing of several sulfide populations, and that Os is mobile within the lithosphere, contrary to general belief.

Olivier Alard brandishes his icon - a sulfide grain from the Udachnaya kimberlite, analysed twice for trace elements and once for Re-Os, by LAM-ICPMS. Olivier Alard was part of the GEMOC team that developed this methodology during his PhD project.

The work carried out so far shows that the LAM-MC-ICPMS technique can provide Os-isotope analyses of individual sulfide grains with precision and accuracy comparable to whole-rock analyses using Carius tube digestion and N-TIMS analysis, provided the grains contain ≥ 40 ppm Os. Grains with lower Os contents yield data with lower precision, but the analyses of Massif Central peridotites demonstrate that these data still provide valuable information on the movement of Os within the lithosphere. Our analyses of sulfides in peridotite xenoliths confirm that sulfides enclosed in silicates preserve significantly less radiogenic Os isotopic compositions than interstitial sulfides. Whole-rock Os-isotope compositions will generally reflect the proportions of these different types of sulfides, and this casts doubt on the significance of many published "depletion ages". However, analysis of sulfides enclosed in primary silicates can produce more realistic estimates of depletion ages in the lithospheric mantle. These data will allow more detailed correlation between events in the mantle and the overlying crust, and a better understanding of Earth's dynamics.

"The work carried out so far shows that the LAM-MC-ICPMS technique can provide Os-isotope analyses of individual sulfide grains with precision and accuracy comparable to whole-rock analyses..."

Contact: Bill Griffin, Norm Pearson, Sue O'Reilly
Funded by: ARC, GEMOC, IPRS, MUIPRA, MUPRF, MURG

Partition coefficients—essential ingredients for modelling the geochemical evolution of the crust-mantle system.

TRACE ELEMENT PARTITION COEFFICIENTS (D) for up to 13 REE, Nb, Ta, Zr, Hf, Sr and Y have been determined by SIMS analysis of 7 garnets, 4 clinopyroxenes, 1 orthopyroxene and 1 phlogopite crystallized from an undoped basanite and a lightly doped (200 ppm Nb, Ta and Hf) quartz tholeiite. Experiments were conducted at 2-7.5 GPa, achieving near-liquidus crystallization at relatively low temperatures of 1080-1200 °C under strongly hydrous conditions (5-27% wt. added water). Garnet and pyroxene D_{REE} show a parabolic pattern when plotted against ionic radius, and conform closely to the lattice strain model of Blundy and Wood. Comparison, at constant pressure, between hydrous and anhydrous values of the strain-free partition coefficient (D_0) for the large cation sites of garnet and clinopyroxene reveals the relative importance of temperature and melt water content on partitioning. In the case of garnet the effect of lower temperature, which serves to increase D_0, and higher water content, which serves to decrease D_0, counteract each other to the extent that water has little effect on garnet-melt D_0 values. In contrast, the effect of water on clinopyroxene-melt D_0 overwhelms the effect of temperature, so that D_0 is significantly lower under hydrous conditions. For both minerals, however, the lower temperature of the hydrous experiments tends to tighten the partitioning parabolas, increasing fractionation of light from heavy REE compared to anhydrous experiments.

Three sets of near-liquidus clinopyroxene-garnet two-mineral D values increase the range of published experimental determinations, but show significant differences from natural two-mineral Ds determined for subsolidus mineral pairs. Similar behaviour is observed for the first experimental data for orthopyroxene-clinopyroxene two-mineral Ds when compared with natural data. These differences are in large part a consequence of the subsolidus equilibration temperatures and compositions of natural mineral pairs. Great care should therefore be taken when using natural mineral-mineral partition coefficients to interpret magmatic processes.

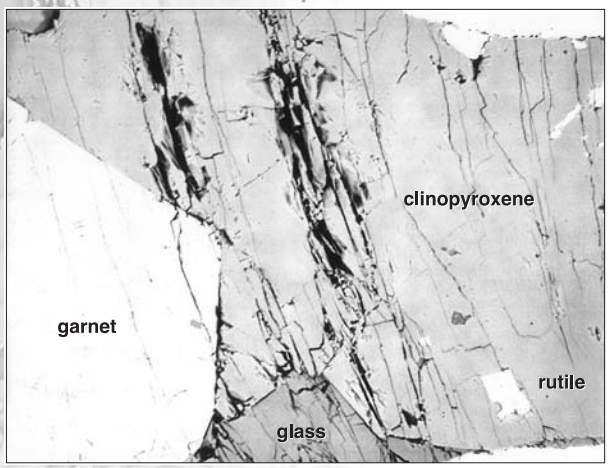

Basalt at 4.0 Gpa, 1100 °C with 15% added water.

The new data for strongly hydrous compositions suggest that fractionation of Zr-Hf-Sm by garnet decreases with increasing depth. Thus melts leaving a garnet-dominated residuum at depths of about 200 km or greater may preserve source Zr/Hf and Hf/Sm. This contrasts with melting at shallower depths where both garnet and clinopyroxene will cause Zr-Hf-Sm fractionation. Also, at shallower depths clinopyroxene-dominated fractionation may produce a positive Sr spike in melts from spinel lherzolite, but for garnet lherzolite melting no Sr spike will result. Conversely, clinopyroxene megacrysts with negative Sr spikes may crystallize from magmas without anomalous Sr contents when plotted on mantle compatibility diagrams. Because the characteristics of strongly hydrous silicate melt and solute-rich aqueous fluid converge at high pressure, the hydrous data presented here are particularly pertinent to modelling processes in subduction zones, where aqueous fluids may have an important metasomatic role.

Rutile—a minor mineral with a big geochemical punch

Mass balance calculations involving the Earth's crust and estimated compositions for the primitive (Chondritic) and depleted mantle produce several conundrums; one is that there appears to be less Nb and Ta in the continental crust than is required, and that the continental crust has a significantly lower Nb/Ta ratio than the mantle. Rutile has been proposed as a key to explaining the "missing" Nb and Ta in the crust, by sequestering these elements in the subducted oceanic crust as this transforms to rutile-bearing eclogite, loses a melt or fluid component and travels into the lower mantle. A detailed study of the partitioning of Nb, Ta, Zr and Hf between rutile and a range of melts (basalt through to rhyolite and carbonatite) and aqueous fluid at high pressure and temperature (1.5-3.5 Gpa and 900-1050 °C) has revealed that rutile consistently favours Ta over Nb relative to melt or fluid. Thus these results limit the role proposed for rutile to equilibration with a highly silicic melt at lower temperature (800 °C), where other researchers have shown that rutile has a higher Nb/Ta than the coexisting melt.

"these results limit the role proposed for rutile"

Carbonatite—a popular mantle metasomatic agent

Trace element-rich carbonatite generated in the mantle has often been called upon as a metasomatic agent, modifying the trace element composition of affected mantle domains. However although it has been demonstrated that mantle derivation of carbonatites is possible, it has not been shown that such melts will have the appropriate trace element composition. Such testing requires knowledge of partition coefficients between relevant silicate minerals and carbonatitic melts.

The GEMOC laser-ablation ICPMS microprobe was used to analyse concentrations of K, Rb, Cs, Sr, Ba, Ti, Zr, Hf, Nb, La, Ce, Sm, Ho, Yb and Lu in experimentally produced garnet, clinopyroxene, amphibole and magnesiocarbonatitic melt. The experiment was conducted at 1050 °C and 2.5 GPa on a synthetic composition designed to simulate natural peridotite melting. Crystal/melt partition coefficients determined from the experiment were used to calculate minor and trace element concentrations in a hypothetical carbonatitic melt equilibrated with a garnet-bearing amphibole lherzolite of primitive mantle composition. The resulting melt is strongly enriched in alkaline earths and rare earths relative to high field strength elements and alkalis, and plots within the compositional range of natural carbonatites. However, the fractionation of alkaline earths and REE from alkalis and HFSE is usually larger in natural carbonatites than in the calculated composition. The absolute concentrations of many incompatible elements are also much larger in some natural carbonatites. Because of these features, processes in addition to peridotite melting (such as crystal fractionation, wall rock reactions, and variations in source chemistry) are needed to fully account for the minor and trace element characteristics of carbonatites.

Contact: T. Green, J. Adam
Funded by: MURG and ARC

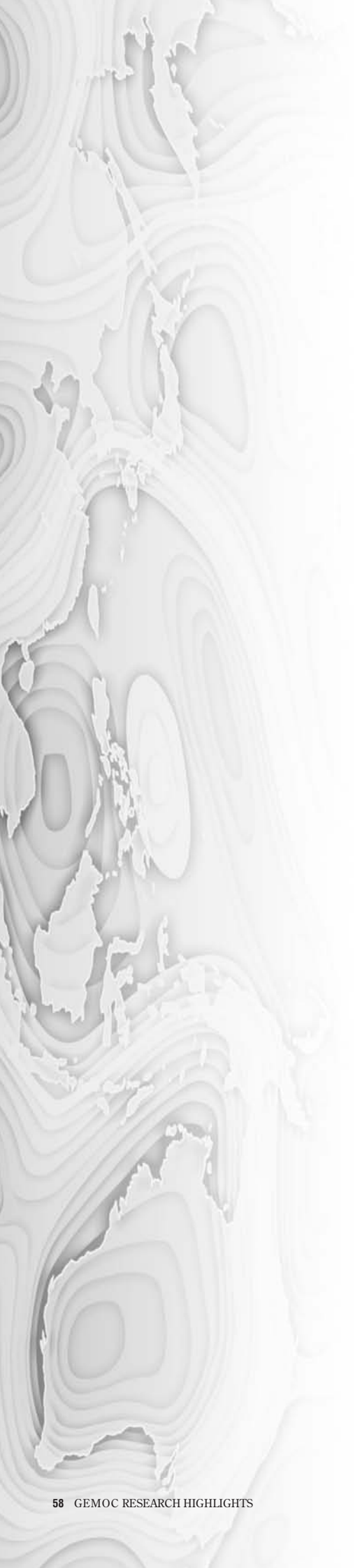

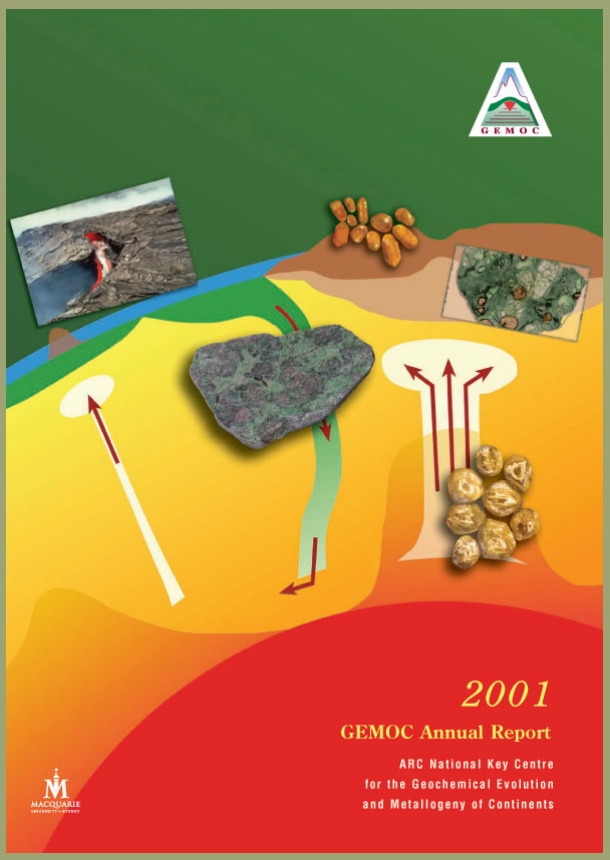

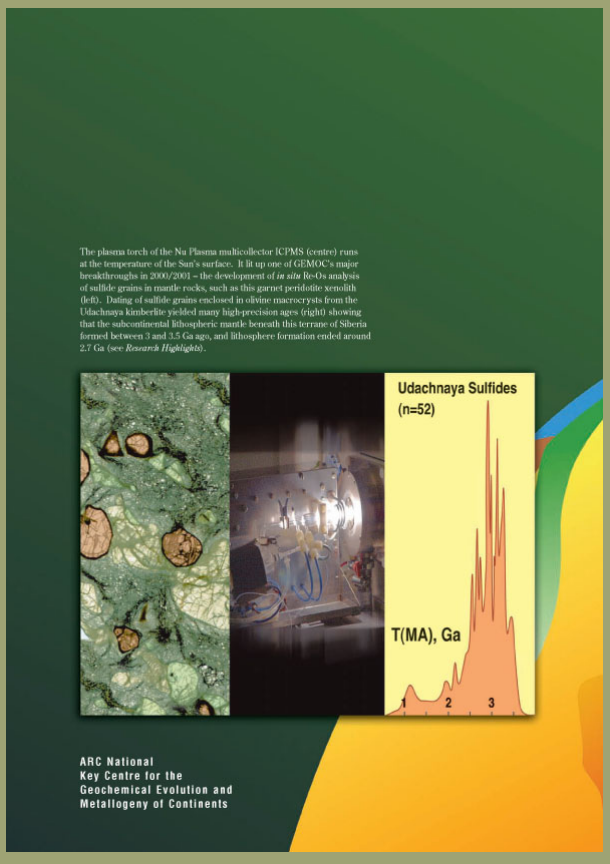

2001 Contents

Geochemical remote sensing of the deep Earth - 4D lithospheric mapping 2001	60
Mapping the Mantle with garnet variables - order from complexity	62
Chemical tomography beneath the Kalahari Craton	64
Sulfides - more evidence for plumes from the lower mantle?	66
Metal isotopes lead the way to riches	68
How old are diamonds?	70
Microdiamonds and microminerals - Slave Craton, Canada	71
Green and gold: sulfides in olivine date the Siberian lithosphere	72
Archean mantle hiding under Proterozoic crust in western Norway	73
Ancient mantle beneath New England	74
Wandering poles in the Late Cambrian	76
Structure and chemistry of the Australian lithosphere	77
Hafnium isotopes and the Baltic Margin jigsaw puzzle	78
TerraneChron™ takes off	79
Mantle mixup beneath Tasmania	80
Plateaus, plumes and fluids in Kerguelen xenoliths	81
Cooking mantle fluids - trace element mobility during subduction	82

Front Cover: GEMOC studies Earth materials down to the micron scale, to answer global-scale questions about the Earth's dynamics and evolution. From lower right: rising plumes bring up diamonds from the lower mantle, and contribute to the formation of subcontinental lithosphere (garnet peridotite; see back cover); U-Pb and Hf-isotope analyses of zircon fingerprint the evolution of crustal rocks on a terrane scale (TerraneChron™; see Research Highlights); subduction turns basalts into beautiful eclogites; oceanic hotspot volcanism (Hawaii) and oceanic plateaus like Kerguelen (see Research Highlights) give insights into the origin of continents.

Research highlights 2001

Geochemical remote sensing of the deep Earth - 4D lithospheric mapping 2001

GEOPHYSICAL DATASETS record the physical properties of Earth's interior at the present day. Translating this information into actualistic Earth models requires petrological and geochemical data on real samples of deep-earth materials. GEMOC has developed a range of tools, collectively termed 4-D Lithosphere Mapping (eg Publications 1, 234), to study the lithospheric mantle and its evolution, by defining its composition, architecture and the location of its important discontinuities (eg crust-mantle and lithosphere-asthenosphere boundaries). This methodology is based on the integration of geochemical and petrophysical analyses of mantle-derived materials with tectonic syntheses and geophysical datasets. It has provided some important constraints on fundamental questions such as the compositional evolution of sub-continental lithospheric mantle (SCLM; see Fig. 1, p.62), the lateral variability of SCLM composition and its effects on tectonics, and the extent to which lithospheric mantle can be recycled into the convecting mantle, or is irreversibly differentiated from it. One of the most important results has been the demonstration that the composition of the SCLM varies in a systematic way that correlates with the age of the last major tectonothermal event in the overlying crust (Publications 90, 132, 234; Fig, 1).

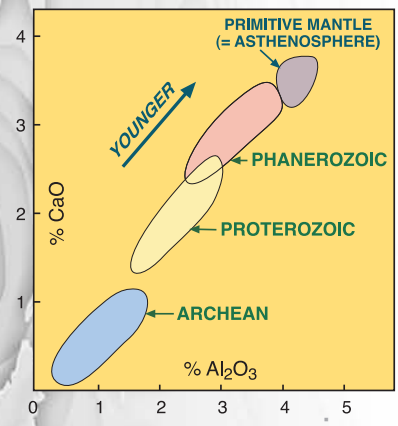

Figure 1. Secular evolution in SCLM composition.

The compositional variations within the SCLM result in differences in the density and elastic properties of lithospheric mantle of different age (Publication 228, Fig. 2). *Archean and Proterozoic* mantle roots are highly buoyant; they cannot be "delaminated" and recycled. This buoyancy, combined with the refractory nature and low heat production of Archean SCLM, may explain the thickness and longevity of Archean lithospheric keels. However, 4-D Lithosphere Mapping (using mantle fragments sampled by magmas of different ages in regions such as eastern China) documents the dispersion of old, buoyant SCLM and the upwelling of fertile asthenospheric mantle, consistent with detailed tomographic imaging (Publications 64, 234; Fig. 3). Modelling of regional lithospheric strength (elastic thickness) in the eastern Siberian craton has shown a N-S lithosphere-scale weak zone within the lithospheric mantle that suggests lithosphere modification related to deformation (Publication 250; Fig. 4).

Typical *Phanerozoic SCLM sections* (about 100 km thick) are buoyant under conditions of high geothermal gradient (eg during their formation). However, they are at best neutrally buoyant after cooling to typical stable conductive geotherms; they become vulnerable to Rayleigh-Taylor instability and will tend to delaminate. Asthenospheric material welling up into the resulting "space" will cool to form a new, little-depleted SCLM; this will raise geotherms and may cause crustal melting. As this new SCLM cools, it in turn will become unstable, and start the cycle again. This cyclic delamination may explain the ubiquitous presence of fertile xenolith suites in young basalts erupted through Paleozoic-Mesozoic orogenic belts.

Figure 2. Density of SCLM sections as a function of thickness and geotherm, compared to the density of the asthenosphere. Stars show typical SCLM thicknesses.

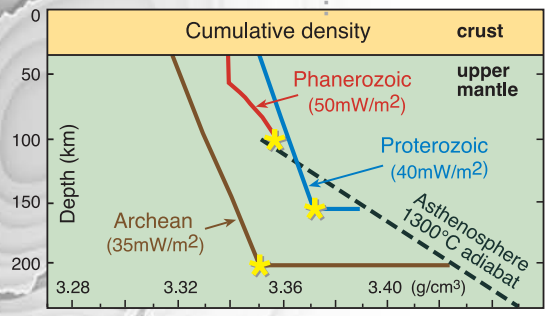

Olivine is the most abundant mineral in all SCLM sections, and the Fe/Mg ratio of olivine is important in controlling the

physical properties of the lithosphere (density, Vp, Vs). Decreasing Fe/Mg results in lower density but *higher* seismic velocity. Because olivine is rarely preserved (and contains little P or T information), we have inverted a garnet-olivine Fe-Mg exchange geothermometer to calculate the Fe/Mg of olivine coexisting with each xenocrystic garnet grain (Publication 222). This inversion has been used to track the compositional variation of olivine through well-characterised SCLM regions. It provides an independant confirmation that Archean SCLM is characterised by much more Mg-rich olivine than Phanerozoic SCLM. In many SCLM sections worldwide the Fe/Mg of olivine increases with depth (Fig. 5), paralleling an increase in Zr and Ti of garnet with depth. This pattern probably reflects the transformation (refertilisation) of SCLM over time by addition of asthenosphere-derived material.

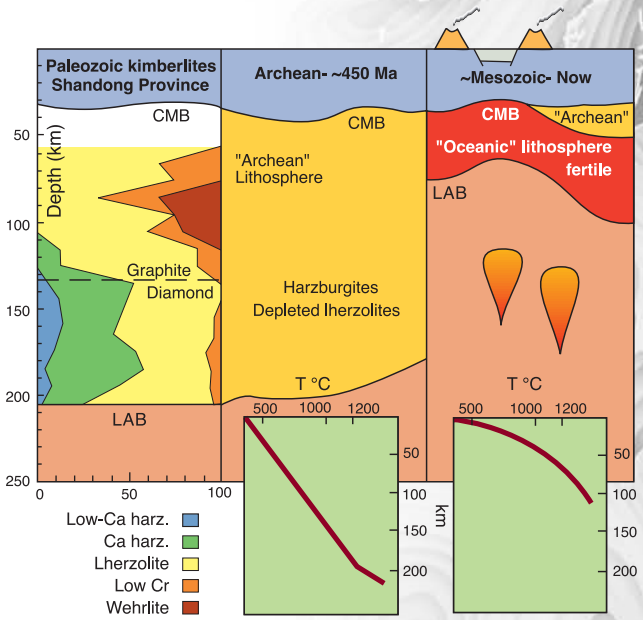

Figure 3. Evolution of SCLM under the eastern Sino-Korean Craton, from thick, depleted Archean SCLM in Ordovician time to thin, hot and fertile SCLM now.

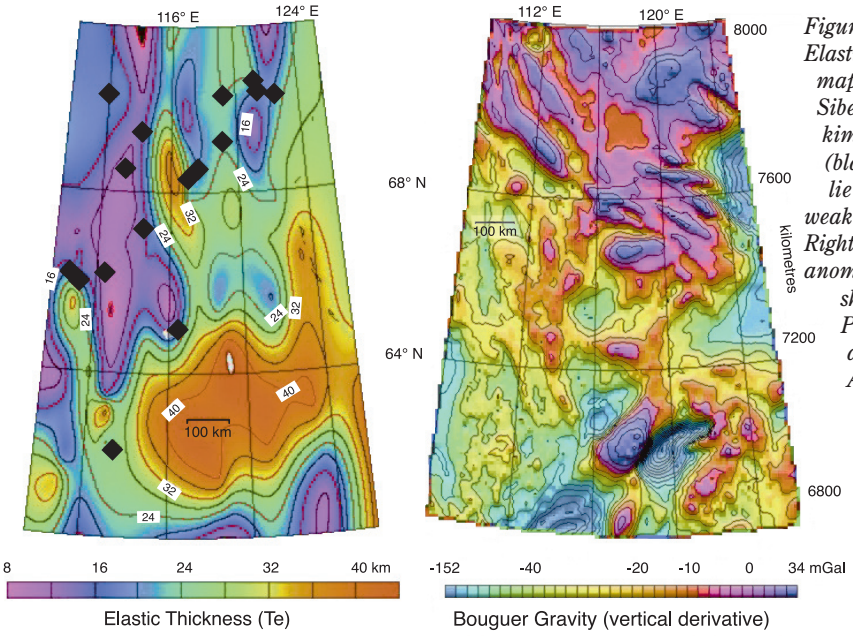

Figure 4. Left: Elastic thickness map of the eastern Siberian Craton; kimberlite fields (black diamonds) lie on flanks of weak zones. Right: Bouguer anomaly map shows highs over Proterozoic areas, lows over Archean areas.

The contrasting properties of different mantle domains require lateral contrasts in composition, density, thickness and seismic response in the present-day SCLM. They also suggest a secular evolution in Earth's geodynamics from Archean to Proterozoic time, and an increased importance for lithosphere-delamination processes in Phanerozoic orogens. The intrinsic buoyancy of Archean SCLM places major constraints on the tectonic behaviour of old continents; some dynamic models indicate that without this buoyancy in their cratonic cores, continents would not have survived on the convecting Earth.

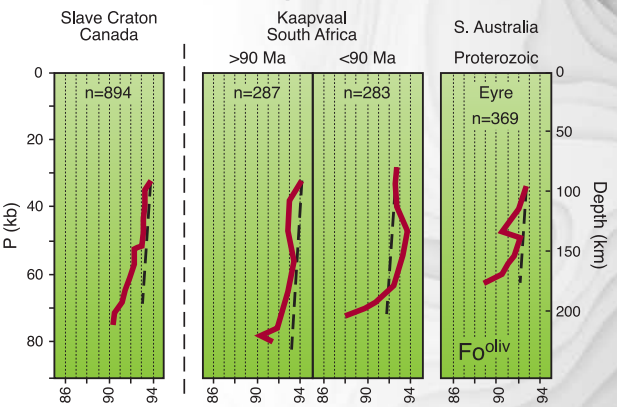

Figure 5. Variation of olivine composition with depth in SCLM sections, as mapped from garnet data.

Contacts: Sue O'Reilly, Bill Griffin
Funded by: GEMOC, ARC, Industry, Macquarie University

Mapping the Mantle with garnet variables – order from complexity

GEMOC'S DATABASE on mantle-derived garnets, built up during 15 years of work with the diamond exploration industry, long since grew to over 30,000 analyses. Up to 1995, trace-element data were acquired with the CSIRO proton microprobe, in collaboration with Dr. Chris Ryan. Since 1995, we have exploited the greater sensitivity of GEMOC's laser-ablation ICPMS microprobes to gather data on a wider range of trace elements. This database has provided fertile ground for collaborating with statisticians Nick Fisher (formerly CSIRO) and Jerry Friedman (Stanford University). They have used the large array of variables in the dataset to develop new ways to recognise populations and anomalies within large data sets, with an emphasis on techniques that give simple and easily interpreted rules. The distribution of these populations can then be combined with temperature (depth) estimates for each grain to map spatial occurrence and thus to analyse mantle structure.

Three of these novel statistical approaches (CARP, PRIM and ModeMap) were used to define compositional populations within a database (n >13,000) of Cr-pyrope garnets from the subcontinental lithospheric mantle (SCLM). The variables used are the major oxides, and proton-probe data for Zn, Ga, Sr, Y and Zr. Because the rules defining these populations (classes) are expressed in simple compositional variables, they are easily applied to new samples and other databases. The classes defined by the three methods show strong similarities and cross-correlations, suggesting that they are statistically meaningful.

The geological significance of the classes has been tested by classifying the garnets from 184 mantle-derived peridotite xenoliths, and from a smaller database (n >5000) of garnets analysed by LAM-ICPMS. Several classes reflect different degrees of depletion (melt extraction) of mantle peridotites, others reflect different styles of metasomatism, and several show the metasomatic

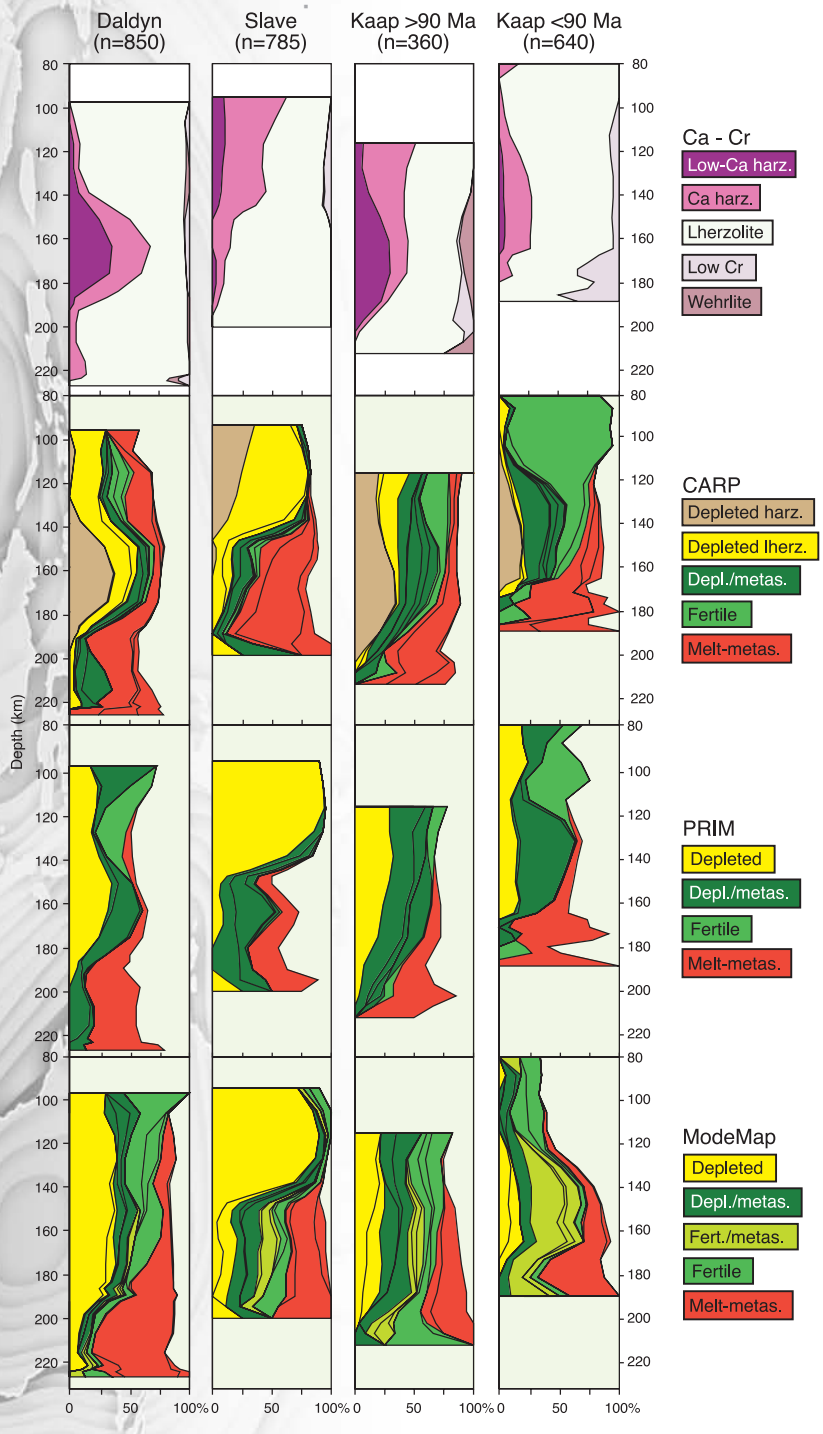

Figure 1. Chemical tomography sections for the lithosphere beneath the Siberian craton (Daldyn kimberlite field), Slave Craton and Kaapvaal Craton (in two time slices), showing the distribution with depth of garnet classes defined by classical Ca-Cr relationships (top) and three statistical tools described here, grouped according to their geological interpretation. "metas." = metasomatised.

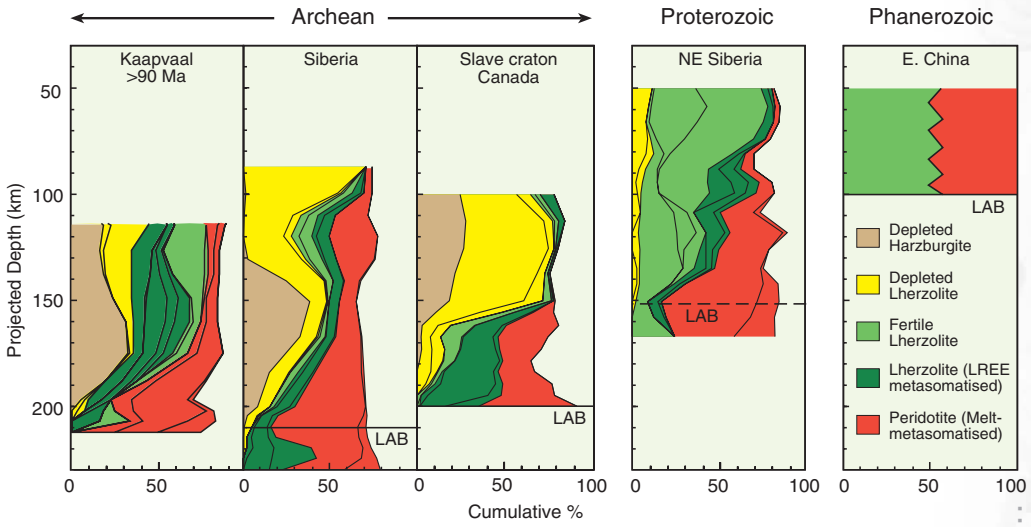

Figure 2. Distribution of CARP groups (see Fig. 1) in "typical" Archean, Proterozoic and Phanerozoic SCLM sections.

re-enrichment of formerly depleted rocks. The distribution of these classes with depth has been mapped by measuring the temperature of each grain (from its nickel content) and deriving a depth by reference of the temperature to the local paleogeotherm (Fig. 1).

The relative abundances of these classes in the SCLM vary widely across different tectonic settings and define intrinsically distinct compositional mantle domains: some classes are completely absent in either Archean or Phanerozoic SCLM (Fig. 2). The distribution of classes can vary widely with depth within individual lithospheric sections. For instance, the SCLM section for the Daldyn kimberlite field in Siberia (Fig. 1) shows a thick layer of strongly depleted harzburgites and lherzolites, overlain by more fertile lherzolites, and the base of the section has been metasomatised by asthenosphere-derived silicate melts.

Phanerozoic garnet peridotites are uniformly fertile (Fig. 2). Archean SCLM sections generally show high degrees of depletion and varying degrees of metasomatism, and commonly are strongly layered. Proterozoic SCLM sections appear quite different (Fig. 2). Many show a concentration of more depleted material near their base, grading upward into more fertile lherzolites. The distribution of garnet classes reflecting low-T phlogopite-related metasomatism and high-T melt-related metasomatism suggests that some of these Proterozoic SCLM sections actually consist of strongly metasomatised Archean SCLM. If this proves to be true, at least part of the observed secular evolution of SCLM composition (Fig. 1, p.18) probably reflects reworking and refertilisation of SCLM that formed in Archean time, and has survived due to its buoyant and refractory nature.

Contacts: Bill Griffin, Sue O'Reilly
Funded by: DIST, Macquarie University Visiting Fellowship, numerous industry collaborations and ARC sources

Chemical tomography beneath the Kalahari Craton

CHROME-PYROPE GARNETS brought up from the mantle by kimberlites and basalts carry large amounts of information on the subcontinental lithospheric mantle (SCLM). The garnet-classification schemes developed by GEMOC (see *"Mapping the Mantle", p.62*) now give us a powerful new tool for mapping the compositional structure of the SCLM, anywhere that enough volcanic rocks have sampled it.

In 2001, GEMOC mapped the SCLM in space and time, beneath the Kalahari Craton of southern Africa and its surrounding mobile belts (Fig. 1). The project used >3500 garnet xenocrysts from >60 kimberlites intruded over the period 520-80 Ma. Figure 2 shows the distribution of classes defined by the new classification scheme, CARP (developed by Nick Fisher and Jerry Friedman using the large garnet dataset and described on p.62-63), along a NE-SW traverse from the Limpopo Belt through the Kimberley area in the SW, and into the Proterozoic Namaqua-Natal Fold Belt. In order to image mantle composition laterally and vertically, we mapped the distribution of different classes at 150 km depth, along with the mean olivine composition, calculated from the garnet compositions and temperatures (Fig. 3).

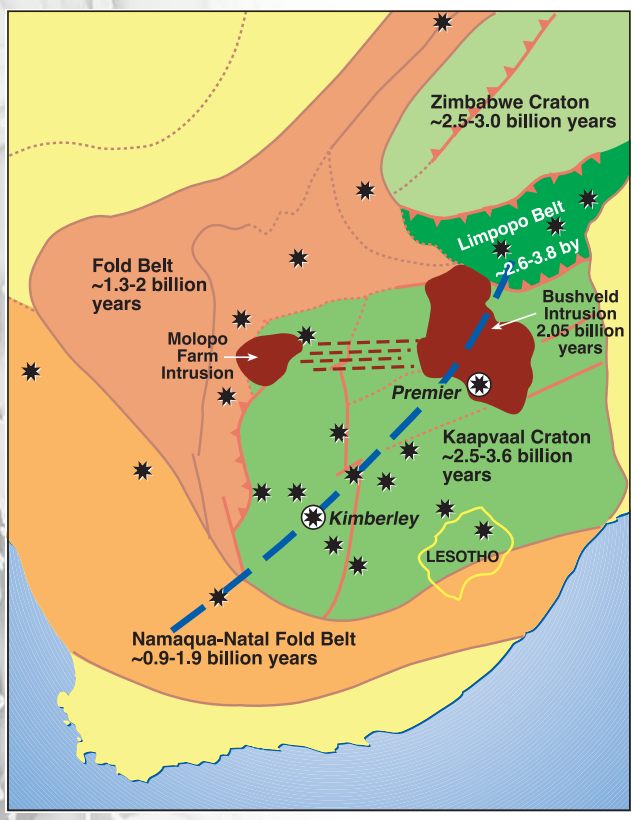

Figure 1. Tectonic map of southern Africa (by Lev Natapov) showing locations of sampled kimberlites (stars) and the traverse shown in Fig. 2 (dashed line).

The trace-element patterns of many garnets reflect the metasomatic refertilisation of originally highly depleted harzburgites and lherzolites, and much of the lateral and vertical heterogeneity in the SCLM observed within the craton is the product of this metasomatism. The SCLM beneath the Limpopo Belt is the most depleted section yet studied. It was sampled by early Paleozoic kimberlites, and the SCLM beneath other parts of the craton may represent similar material modified by metasomatism during Phanerozoic time.

The 1200 Ma Premier kimberlite intruded through the massive 2050 Ma

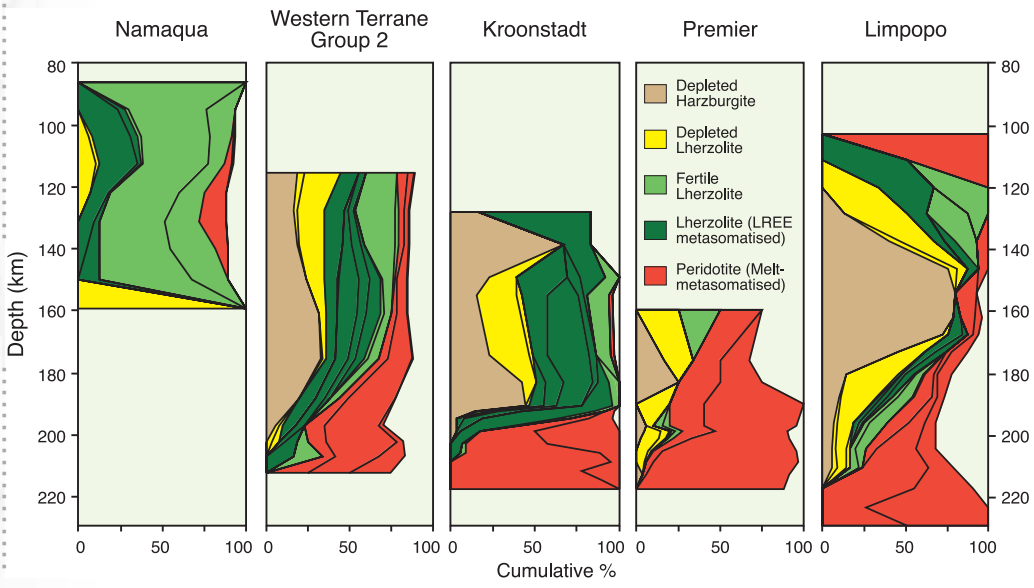

Figure 2. Chemical tomography sections for areas along the traverse shown in Fig. 1, showing the distribution with depth of garnet groups defined by CARP.

Bushveld complex (Fig. 1). The SCLM under Premier was strongly metasomatised and refertilised by the Bushveld event, to produce a much more iron-rich mantle than in the other sections. In the SW part of the craton, the SCLM sampled by "Group 2" kimberlites (>110 Ma) is thicker, cooler and less metasomatised than that sampled by "Group 1" kimberlites (mostly ≤95 Ma) in the same area (Fig. 1, p.62). That result affects our use of xenolith data in a wider perspective - it implies that the extensively studied xenolith suites from the "Group 1" kimberlites probably are not representative of primary Archean SCLM compositions.

The relatively fertile SCLM beneath the mobile belts surrounding the craton is interpreted as largely Archean SCLM, metasomatised and mixed with younger material during Proterozoic rifting and compression. There are strong correlations between mantle composition and the lateral variations in seismic velocity (Vp) shown by detailed tomographic studies (James et al., 2001, G.R.L. 28). Our study showed very small lateral temperature differences within the craton, so the seismic data can be used to map the lateral extent of different types of SCLM. Areas of relatively low Vp within the craton largely reflect the progressive refertilisation (resulting in Fe-enrichment) of the Archean root during episodes of intraplate magmatism, including the Bushveld (2 Ga) and Karroo (ca 180 Ma) events; areas of high Vp map out the distribution of less metasomatised Archean SCLM. The relatively low Vp of the SCLM beneath the mobile belts is consistent with its fertile composition.

Contacts: Bill Griffin, Sue O'Reilly
Funded by: ARC large grant, Macquarie University and Industry

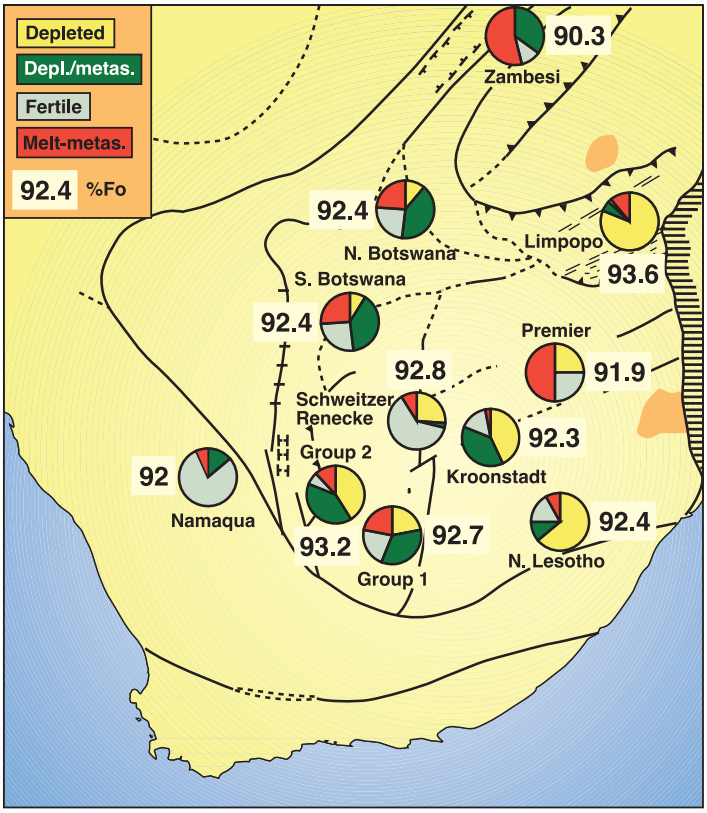

Figure 3. Chemical tomography map showing relative abundances of CARP groups in the 140-160 km depth slice, and the mean Fo content of olivine, calculated from the garnet data by the method of Gaul et al. (2000; Publication No. 222).

Sulfides – More Evidence For Plumes From The Lower mantle?

"The distinct ultra-high pressure signature of sulfides included in concentrate minerals represents a new tool to recognise sublithospheric influences... "

Re-Os DATING of sulfide inclusions in mantle minerals opens new perspectives on the origin of the mantle (see *Research Highlight "Green and gold - sulfides in olivine date the Siberian lithosphere", p.72)*. As part of this new research direction, we have recovered a suite of sulfide inclusions in concentrate minerals (mostly olivine) from the Lac de Gras kimberlites in the Slave craton, Canada (see *Research Highlights 2000 at www.es.mq.edu.au/GEMOC/*). A distinct population of these sulfides, with a non-stoichiometric structural formula of $[(Ni,Co,Fe)_{3-x}S_2]$ has a high metal/sulfur ratio [(Fe+Co+Ni)/S], unusually high Ni/Fe and Co, and low Ni/Co relative to the common monosulfide solid solution (mss) that is more typical of mantle peridotites (Fig. 1). These Ni-Co sulfides also contain up to several percent of tungsten; this is unusual because W is not generally compatible in mantle minerals under common (lithospheric) conditions. These major and trace element systematics imply an unusual origin for the sulfides from Lac de Gras.

One inclusion of Fe metal also has been recovered. This has negative Co- and Ni-anomalies relative to elements of similar siderophile (metal-seeking) character (Fig. 2) and is more enriched in W than the sulfides, suggesting a related and complementary origin for the Fe metal and the Ni-Co sulfides.

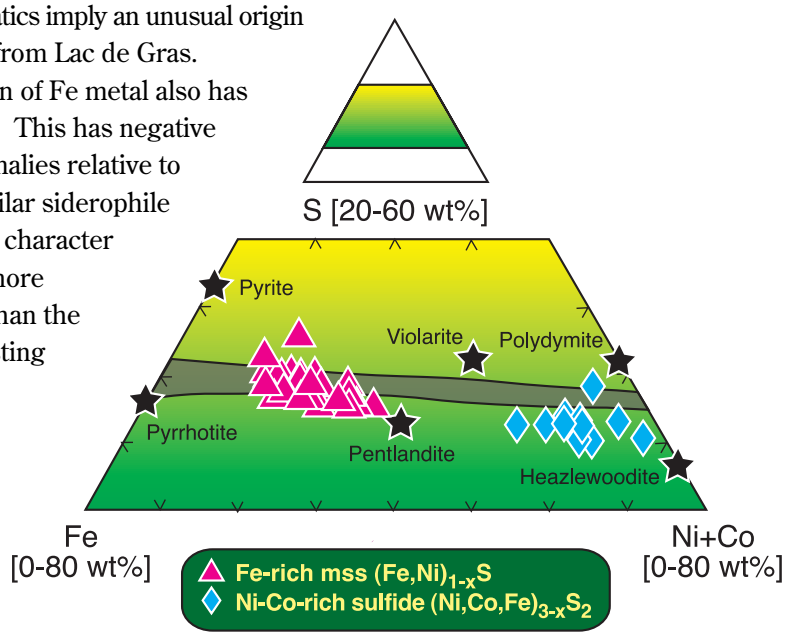

Figure 1. Reconstructed compositions of Fe rich and Ni-Co rich sulfides from Lac de Gras concentrate in the Fe-S-(Ni+Co) quadrilateral. Shaded field delimits mss compositions at 300° C. Highlighted area in small triangle indicates position of the quadrilateral in the ternary diagram. Stars show stoichiometric (with exception of pentlandite which has variable Ni/Fe) sulfide phases.

Both phases may have formed under reducing conditions (corresponding to high metal/sulfur) where metal melts and sulfide melts are immiscible. After unmixing, Ni and Co will be concentrated in the sulfide melt, consistent with their chalcophile (sulfur-seeking) nature, whereas the chalcophobic (sulfur-avoiding) W partitions into the S-poor metal. The presence of Fe metal and the W-enrichment in Ni-Co sulfides indicate very reducing conditions, at or below the iron-wüstite oxygen buffer, and suggests sources deeper than the subcontinental lithospheric mantle, such as the transition zone or lower mantle where metal saturation is thought to be reached.

However, reducing conditions alone are not sufficient to explain the major and trace element systematics of the Ni-Co sulfides. In particular the enrichment in Co and the resulting low Ni/Co (~8.5) of the Ni-Co sulfides relative to the primitive mantle (18.7; McDonough and Sun, 1995, Chem. Geol.) require conditions where more Co than Ni partitions into the sulfide. This is not the case for the simple

unmixing scenario described above, but may occur in equilibrium with a silicate melt at pressures corresponding to the lower mantle. The strong W-enrichment in the sulfides cannot be attained by simple equilibrium processes, such as partitioning between sulfide melt and silicate liquid, but may require an open system process, where W is continuously scavenged from surrounding silicates during percolation of a mobile sulfide melt. This enrichment mechanism would be far more effective at lower mantle depths because sulfide equilibrating with lower mantle phases can take up more W than sulfide equilibrating with silicate melt. Hence, both low Ni/Co and high W concentrations are consistent with formation of the sulfides at ultra-high pressures.

The Ni-Co sulfides and Fe metal may have been emplaced in the upper mantle during upwelling of a plume originating at the core-mantle boundary. A lower mantle component has previously been suggested for the Lac de Gras lithosphere based on the occurrence of lower mantle inclusions in diamond (Davies et al., see *Research Highlights 1998, 2000*). The distinct ultra-high pressure signature of sulfides included in concentrate minerals represents a new tool to recognise sublithospheric influences where diamonds and their inclusions are not (yet) available. Deep-seated mantle plumes may entrain diamond as they rise through the convecting mantle, including the transition zone. Thus, in 'cool' cratonic regions, which have low geotherms favourable to the preservation of diamonds, ultra-high pressure sulfides recovered from kimberlite concentrate may also be an indicator for the presence of abundant diamond in the mantle root.

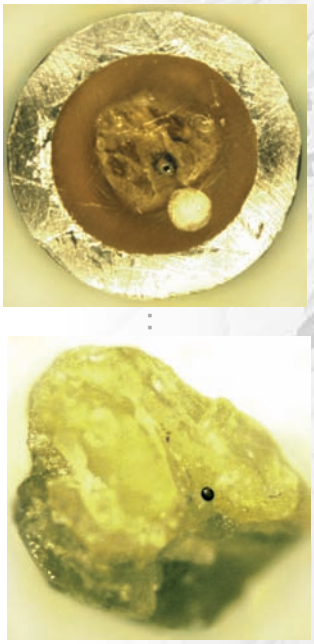

Sulfide inclusion in olivine grain (bottom) and after mounting and polishing in an aluminium tube (top)

Contacts: Sonja Aulbach, Norm Pearson, Bill Griffin
Funded by: ARC SPIRT (with Kennecott Canada), Macquarie University and GEMOC

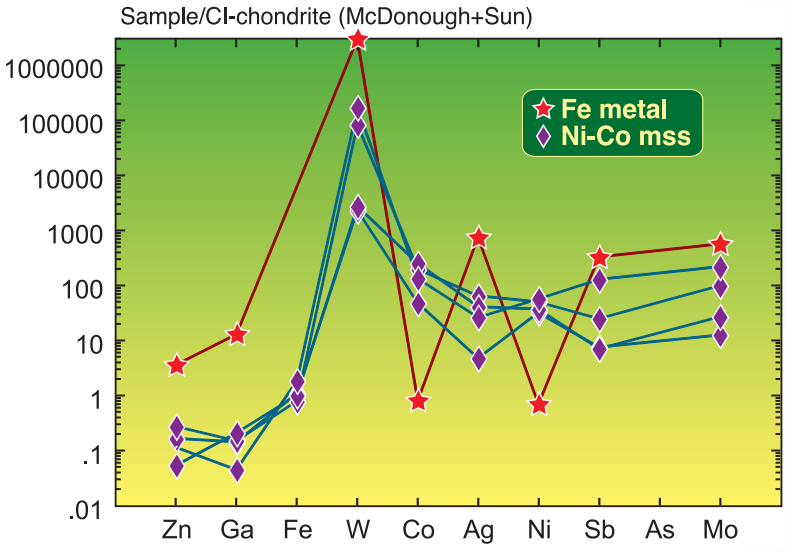

Figure 2. Chondrite-normalised trace element abundances of Fe metal and Ni-Co sulfides. Element order corresponds to increasing siderophile character.

Metal isotopes lead the way to riches

ISOTOPE GEOCHEMISTRY is a basic tool for understanding ore-forming processes. Data on variations in the stable isotopes of carbon, oxygen, sulfur and hydrogen have been used to identify the sources of hydrothermal fluids and to model the mechanisms that drive hydrothermal circulation systems. But not all fluids carry metals, and the sources of the fluids and the ore metals could be quite different. Many of the important commodity metals (Cu, Zn, Fe, etc.) have two or more stable isotopes, whose fractionation could carry more direct information on the sources, movements and precipitation of these elements.

Until recently, there have been few reliable data on the isotopic composition of these metals, because their high ionisation potentials made them very difficult to measure by conventional thermal ionisation mass spectrometry. Now the multi-collector ICPMS makes it possible to do high-precision analyses of the isotopic ratios of Cu, Fe and many other metals. With the addition of a laser-ablation microprobe, these analyses can be done *in situ*, adding information on the spatial context of isotopic variations.

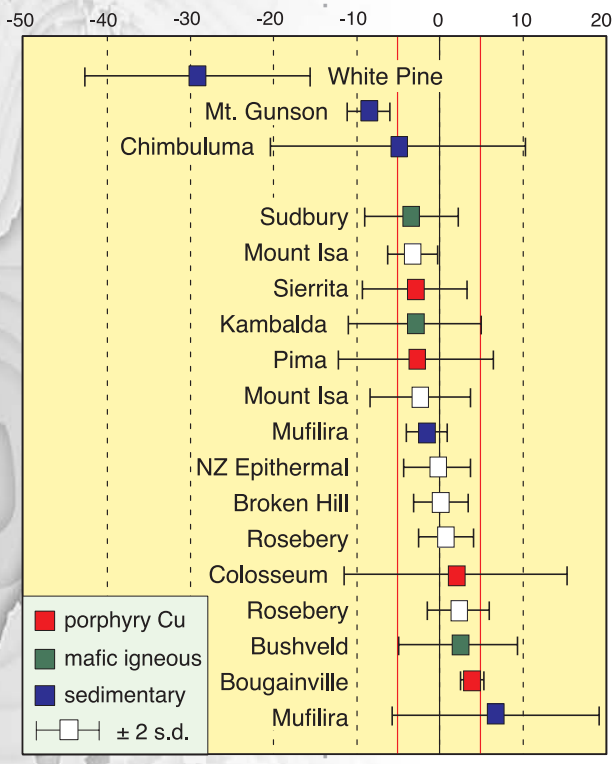

Figure 1. Distribution of copper-isotope ratios, expressed as $\varepsilon^{65}Cu$, in chalcopyrite from worldwide sources. After Botfield (1999; Honours Thesis, Macquarie Univ.)

In 1999, Andrew Botfield completed an Honours thesis on Cu isotopes in chalcopyrite from a wide variety of ore samples, that increased the world-wide database by a factor of five and showed that there were large and significant variations in Cu-isotope ratios within and between deposits (Fig. 1).

In 2001 GEMOC, supported by a consortium of five mineral exploration companies, has carried out a study of Cu and Fe isotopes in chalcopyrite, and Fe isotopes in pyrite, from several types of ore deposit. The results show large variations that can be correlated with parameters such as ore grade, temperature, and spatial position within the ore bodies.

The 1640 Ma McArthur River (also known as HYC) deposit is an unmetamorphosed stratiform Pb-Zn-Ag deposit in northern Australia (Fig. 2). The geological preservation and size of this deposit make it an ideal location to study the primary geological characteristics of a Proterozoic sedimentary-hosted Pb-Zn-Ag deposit. Sediment deposition and mineralisation occurred in a quiet marine environment below the wave base, as ore-bearing fluids percolated through the basin. Earlier studies of metal zoning, sulfur isotopes and organic chemistry have defined a temperature gradient, and suggest that bacterial reduction of sulfate was an important process in the cooler parts of the ore body, away from a main vent where the metal-bearing fluids entered the basin.

Chalcopyrite Cu-isotopes (115 analyses) and pyrite Fe-isotopes (140 analyses) were measured over a horizontal distance of approximately 1200 metres through the ore body and reflect changes in the chemistry of the brine as it passed through the basin. Chalcopyrite and pyrite in the hot Cu-rich section of the ore body have isotopically light Cu and Fe. As the brine moved and cooled, it became enriched in the heavy Cu and Fe isotopes (^{65}Cu and ^{57}Fe) as the light isotopes (^{63}Cu and ^{54}Fe) were preferentially removed from the solution by thermochemical sulfate reduction (TSR; Fig. 3). Beyond about 800 metres from the vent, a much greater range in

both $^{65}Cu/^{63}Cu$ and $^{57}Fe/^{54}Fe$ is observed, and this spread may indicate the beginning of bacterial sulfate reduction. Iron- and copper-reducing bacteria are expected to preferentially remove the light isotopes from solution, with the result that the solution becomes isotopically heavy. The similar proportions of isotopically heavy and light pyrites and chalcopyrites above and below the TSR trend in Figure 3 suggest that up to 50% of the sulfides in this part of the deposit were formed as a direct result of bacterial reduction. This conclusion is supported by palaeontological evidence in this region of the deposit.

The use of metal isotopes in ore-genesis studies is in its infancy, but it shows great promise. In deposits like HYC, the isotopic data also can be important in mineral exploration – they point toward the source regions of the ore metals.

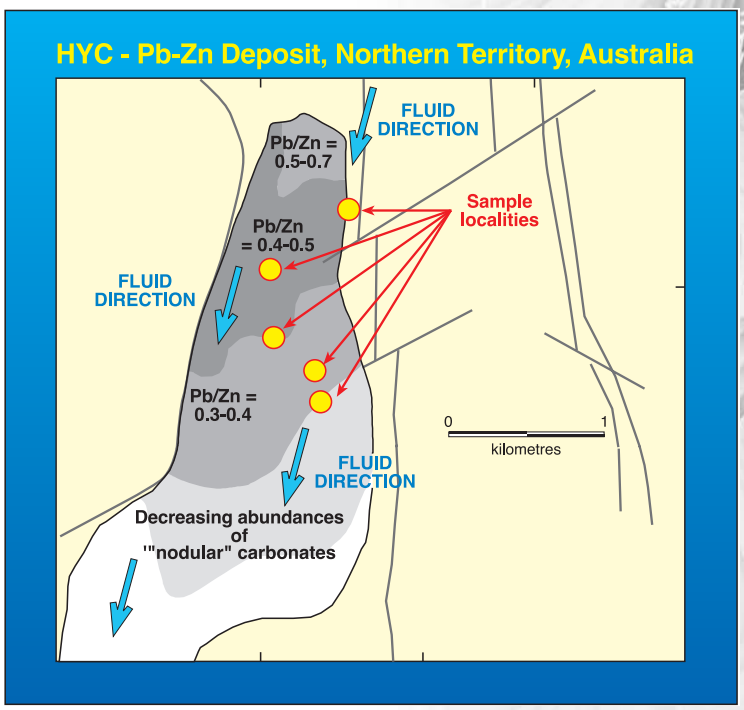

Figure 2. Map of the HYC Pb-Zn deposit, showing inferred flow direction of metal-bearing basinal brines, Pb/Zn zoning pattern and the location of samples analysed for Cu and Fe isotopes.

Contacts: Bill Griffin, Simon Jackson, Stuart Graham, Norm Pearson
Funded by: Industry partners, Macquarie University, GEMOC

Figure 3. Variation in $\varepsilon^{65}Cu$ and $\varepsilon^{57}Fe$ in pyrite and chalcopyrite along the HYC ore deposit, showing trends possibly related to temperature (TSR) and scatter that may reflect bacterial sulfate reduction (BSR) in the cooler brines.

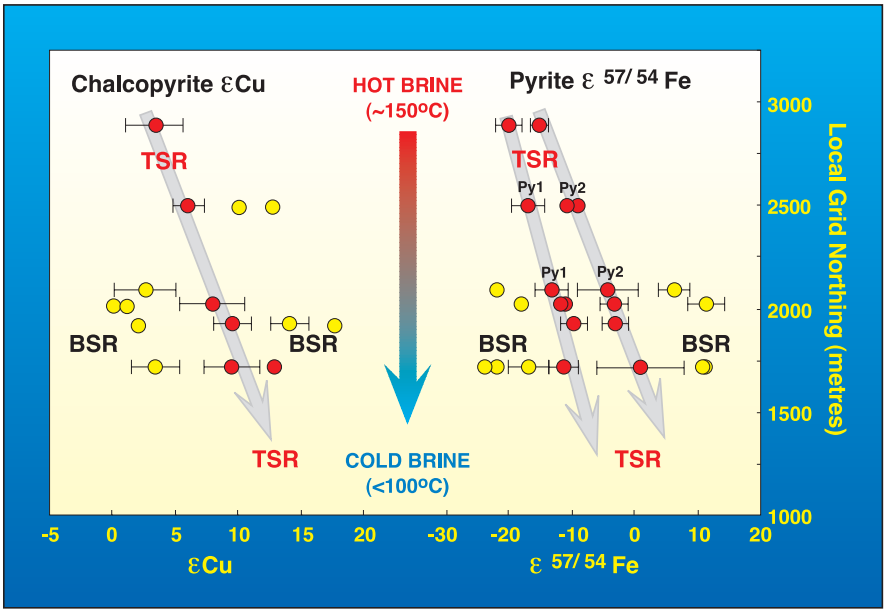

How old are diamonds?

DIAMONDS often are described as mantle time capsules - mineral inclusions, once trapped inside a diamond, are protected from the environment, and give us one of our best windows into mantle conditions. But which conditions? When did the diamonds actually crystallise? The most direct way of finding out might be to date the inclusions, assuming that the diamond crystallisation process reset the isotopic clocks in the minerals that became included in the diamond. In the last few years,

Figure 1. Aerial view of the Mir diamond mine in Siberia. High-rise apartment buildings near rim of pit give scale.

a lot of time and technology has been spent on determining the Re-Os model ages of sulfide inclusions in diamonds. The results have been used to argue that most diamonds crystallised in Archean time.

This approach required rethinking after Slava Spetsius arrived at GEMOC during 2001 with a collection of large zircon crystals from the Mir kimberlite in Siberia. These zircons contain inclusions of peridotitic minerals —chromite, olivine, chrome-diopside, phlogopite — that tell us the zircons grew in the mantle wall-rocks, as part of a metasomatic process. Some of these zircons also contain inclusions of typical peridotitic sulfides, with negative-crystal forms (Fig. 2) showing that they underwent grain boundary adjustment during formation of the surrounding zircon. *In situ* LAM-ICPMS U-Pb dating and Hf-isotope analysis showed that the zircons probably crystallised 355 Ma ago, and in any case cannot be older than 600 Ma. But *in situ* Re-Os dating of three sulfide inclusions gave mean depletion ages of more than 3000 Ma! It appears that the growth of the zircon did *not* reset the Os isotope compositions of the sulfides; the metasomatic fluids probably carried little Os, while the sulfides contain 50-250 ppm Os.

This result implies that the ages of analogous sulfides in diamonds date the formation of the wall-rock in which the diamond crystallised, but would only date the formation of the diamond if the sulfide inclusion and diamond coincidentally formed at the same time. With our current knowledge and methodologies we cannot unequivocally know when a diamond itself actually crystallised, and can only know that it is younger than its sulfide inclusions.

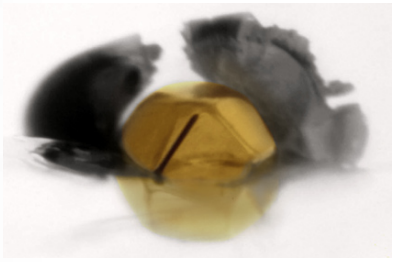

Figure 2. 100µm sulfide inclusion in a zircon megacryst from Mir, showing negative-crystal form; the "wings" are expansion cracks lined with sulfide and formed during decompression. The sulfide gives a Re-Os age of 3 Ga.

Contacts: Bill Griffin, Elena Belousova, Sue O'Reilly
Funded by: Macquarie University visiting Fellow Research Grant, de Beers Australia, GEMOC

Microdiamonds and microminerals - Slave Craton, Canada

MINERAL INCLUSIONS within diamonds represent pristine mantle material trapped at the time of diamond growth –they have been protected from the processes that modify the mantle during its tectonic history. Mineral inclusions in microdiamonds from kimberlites at Lac de Gras in the Slave Craton, Canada have been studied to investigate unmodified compositions of the diamond bearing mantle, constrain the proportions of diamond bearing rock types and provide key information that brings us closer to understanding the evolution of the Slave Craton in this region.

Microdiamonds, defined as less than 1 mm in cross section, were selected because they are more abundant and less valuable than macrodiamonds, and are used as indicators to evaluate the prospectivity of a kimberlite body in diamond exploration. Macrodiamonds from one pipe have been studied previously, and we wanted to find out if the two diamond types at Lac de Gras differed. Over two hundred mineral inclusions were extracted from 500 microdiamonds, representing eight kimberlite localities in the central Slave craton, and analysed for major and minor elements.

We found that although some diamond characteristics differ between macro- and microdiamond groups, inclusion compositions and the relative abundances of different paragenetic types of inclusions do not. Microdiamonds from Lac de Gras typically have low nitrogen aggregation states, suggesting that they formed at a late stage in the history of the mantle, possibly just prior to kimberlite emplacement. In contrast, the nitrogen contents and carbon-isotope compositions of micro- and macrodiamonds are similar.

At Lac de Gras a large proportion of microdiamonds contain inclusions from the eclogitic paragenesis (70%), followed by the peridotitic paragenesis (16%); diamonds containing unusual phases derived from the transition zone and lower mantle make up 14% of the microdiamond population. Inclusions in diamonds of lower mantle origin are the oxide ferropericlase, $MgSiO_3$ and $CaSiO_3$- perovskite, SiO_2 and Mg_2SiO_4; the last is likely to have formed as a spinel-structured polymorph of olivine. The lower mantle phases, which occur in combination with one another in single diamonds, suggest a deep origin for these diamonds (~670 km). A small number of diamonds of both eclogitic and peridotitic paragenesis were identified as having possible transition zone origins.

The inclusion data suggest that mantle plumes transported diamonds from the transition zone and lower mantle to the base of the Slave Craton at Lac de Gras. Although lower mantle diamond inclusions typically reflect peridotitic bulk compositions, the abundance of eclogitic diamonds at Lac de Gras, also noted at other localities where transition zone/lower mantle diamonds occur, suggests the presence of eclogites is significant to the processes of mantle formation and dynamics in regions where deep mantle material has been transported to the Earth's surface.

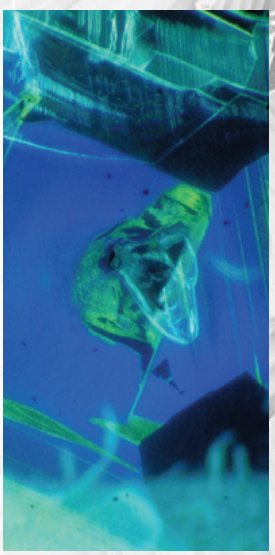

Figure 1. Cathodoluminescence image of a diamond, showing internal structure around a mineral inclusion

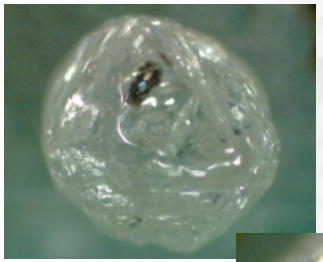

Figure 2. Ferropericlase inclusion in a microdiamond from Lac de Gras

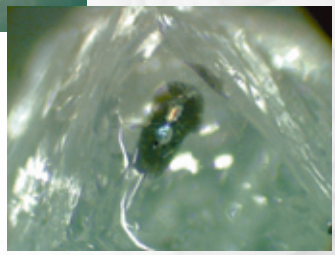

Contacts: Rondi Davies (now at the American Museum of Natural History, New York), Bill Griffin, Sue O'Reilly
Funded by: ARC SPIRT with Industry Partner Kennecott Canada

Green and gold: sulfides in olivine date the Siberian lithosphere

GEMOC'S DEVELOPMENT of *in situ* Re-Os analysis of sulfide grains (using the LAM-MC-ICPMS) has provided new insights into the timing of stabilisation and modification of continental roots. As we analyse sulfide populations in more mantle xenoliths, it becomes obvious that most of these rocks have complex histories, with many generations of sulfides and mixtures of Re-Os components, that make whole-rock ages difficult to interpret. The *in situ* analysis of sulfides in single rocks can sort out this confusion, but it requires painstaking serial sectioning to locate and analyse the small and widely scattered individual sulfide grains.

In 2001, we took a new approach to surveying the age spectrum of a lithospheric section, by picking sulfide-bearing olivine grains (perhaps 1 in 10,000) out of concentrates prepared from kimberlites. Dr. Zdislav Spetsius, mineralogist/petrologist with the Siberian diamond miner Alrosa (Mirny), scanned many litres of coarse olivine concentrate from the Udachnaya kimberlite. He arrived at GEMOC with over 100 grains, some containing up to 6 sulfide inclusions. Over 90 of these inclusions were successfully analysed for Re-Os and 26 could also be analysed (by LAM-ICPMS) for their contents of Platinum Group Elements and other trace elements.

The sulfides are mixtures of Ni-rich and Fe-rich monosulfide solid solutions (MSS), pentlandite and chalcopyrite, exsolved from MSS bulk compositions (Fig. 1). They can be divided into 5 populations (1, 2, 3A-3C) on the basis of Os content, Os/Pt and Re/Os. By comparison with published experimental data, Group 1 sulfides can be identified as MSS residual after low degrees of melting of a primitive mantle source, under sulfur-saturated conditions. Group 2 sulfides are best modelled as mixtures of MSS and alloy phases, formed under sulfur-undersaturated conditions. The other groups can be modelled as sulfide liquids, or as the products of reaction between these liquids and the MSS of Groups 1 and 2. Inclusions of different groups may occur within single olivine grains, suggesting repeated introduction of sulfide melts, followed by annealing and grain growth.

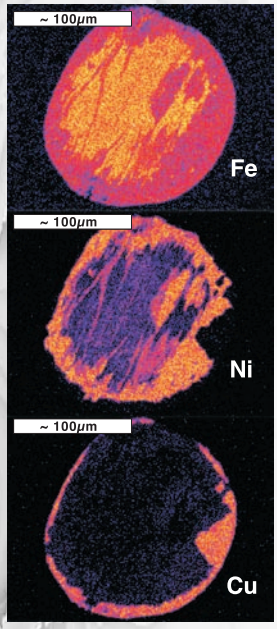

Figure 1. Element distribution maps showing exsolution textures in a typical "enclosed" sulfide from Udachnaya.

Sulfides of Groups 1 and 2 give geologically reasonable (0-4 Ga) Os model ages (T_{MA}). Most Group 3 sulfides contain unsupported ^{187}Os, implying a two-stage history. Our modelling shows that sulfides with $^{187}Re/^{188}Os$ <0.07 are unlikely to have been disturbed. 52 grains satisy this criterion; 45 of these give T_{MA} ages between 2.5 and 3.6 Ga (Fig. 2). These data suggest that most of the lithospheric mantle beneath the Daldyn kimberlite field formed during the period 3 - 3.5 Ga, and that lithosphere formation culminated in a major event at ca 2.9 Ga. There is little evidence in the Re-Os data for significant further additions to the lithosphere after this time.

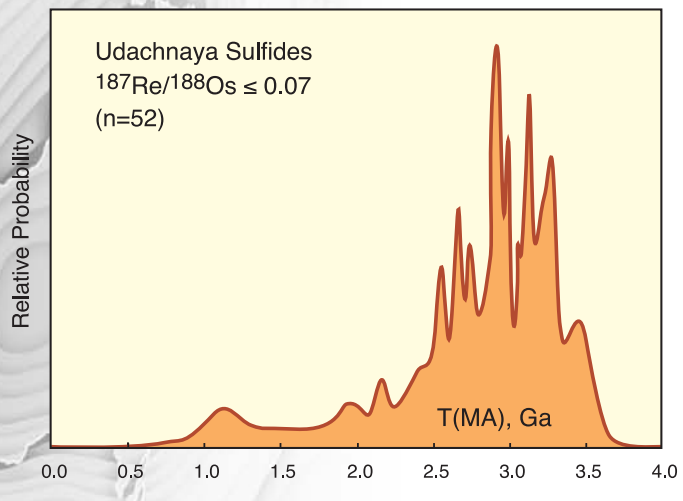

Figure 2. Re-Os model ages of "undisturbed" sulfides from Udachnaya.

This analysis of sulfides from olivine concentrates gives us a (relatively) rapid way to assess the spectrum of depletion ages in a lithosphere section, and that will be a very valuable guide to interpretation of more detailed work on individual xenoliths. GEMOC has started a program of sampling worldwide, with the help of friends from the diamond exploration industry.

Contacts: Bill Griffin, Norm Pearson, Sue O'Reilly
Funded by: Macquarie University, GEMOC, Industry

Archean mantle hiding under Proterozoic crust in western Norway

OROGENIC PERIDOTITE MASSIFS occur in many mountain systems. Most are spinel-bearing peridotites, or their retrograded, hydrated equivalents (chlorite peridotites or serpentinites). Garnet-bearing peridotites are much less common, but many of these rocks bear a remarkable resemblance to some kimberlite-borne mantle xenoliths and they appear to represent slices of lithospheric mantle tectonically emplaced into continental crust during subduction.

Coarse-grained garnet-bearing peridotites have been documented at several localities in the Western Gneiss Region (WGR) of southwest Norway (Fig. 1). Mantle sequences from the WGR mainly comprise minor garnet-bearing peridotites (including lherzolites, wehrlites and cpx-free harzburgites) and dominant, very depleted garnet-free dunites.

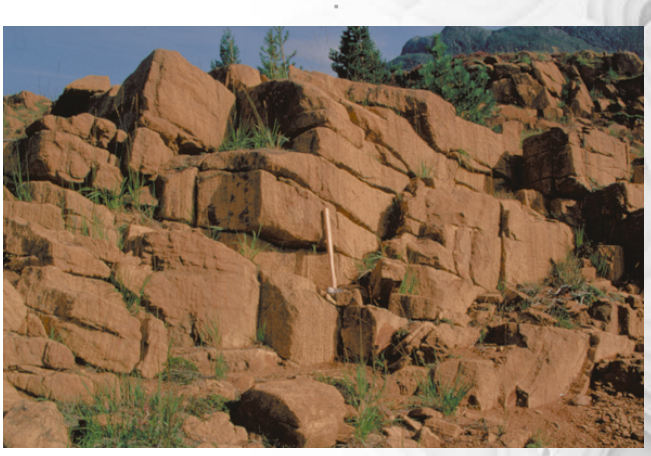

Figure 1. Garnet peridotite outcrop at Helgehornsvatn

The recent development of high-precision *in situ* laser-ablation techniques enables us to rapidly obtain Re-Os isotopic ages from single sulfide grains in such peridotites. Where the sulfides contain significant amounts of Re, the calculation of Re-Os model ages ("Re-depletion ages" or T_{RD}) requires back-calculation to the likely time of Re addition, to correct for any in-growth of ^{187}Os. In xenoliths, this generally is taken as the time of eruption. In massif peridotites, the correction is less straightforward, and must be based on the age of major magmatic or tectonic events that affected the peridotites.

Two main events may have affected the WGR peridotites. The first is the Gothian orogeny between 1600-1750 Ma, which saw widespread magmatic activity and crust-building in Norway. The second is the Caledonian ultra-high pressure metamorphic event at about 410 Ma, which marks continental subduction and probably the emplacement of the peridotites into the crust. The Sveconorwegian (Grenvillian) orogeny at ca 1000 Ma had a limited effect on the WGR.

Sulfides in the WGR garnet peridotites are predominantly pentlandite ± heazelwoodite and occur both interstitially and as inclusions in silicate phases. Re-Os model ages were measured for twenty-three sulfides from peridotites at Almklovdalen in the southern WGR. On a cumulative probability diagram the TRD ages (calculated at 400 Ma) define several peaks, some of which can be matched to major crust-building events in Norway. There are no obvious Caledonian sulfide ages. Sveconorwegian ages also are poorly represented in the sulfide population, which suggests that this crustal event was not very effective in resetting the ages in the sulfides. Ages greater than 1000 Ma are clearly resolved into distinct Proterozoic and Archean peaks with little overlap. The Proterozoic peak has a maximum at ~1700 Ma which falls within the age range for the Gothian orogeny

Figure 2. Relative-probability plot of T_{RD} model ages calculated assuming Re addition at 1600 Ma.

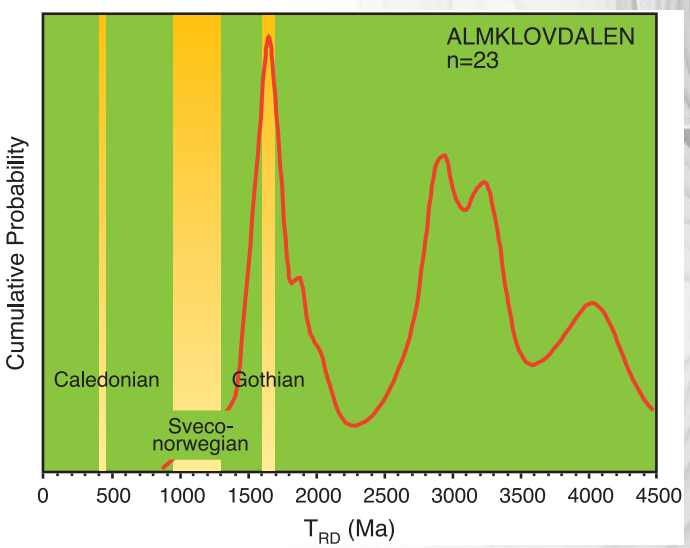

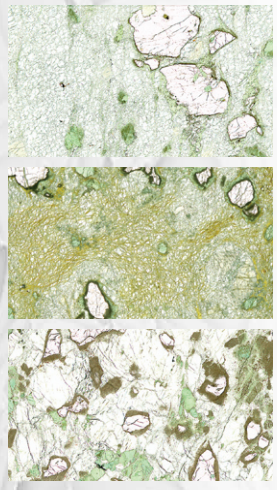

Garnet peridotites from the Western Gneiss region, SW Norway.

(1600-1750 Ma) and is close to the calculated Sm-Nd mineral age of 1703 ± 29 Ma for garnet peridotites from the Raudkleivane locality in Almklovdalen.

The greatest surprise, and perhaps the most exciting result of this study, is the significant number of Archean ages (peaks at 2900 - 3200 Ma). These ages are greater than known crustal ages in the region, and may suggest that the peridotites reflect a mantle depletion event that was not associated with crustal growth in this part of the Baltic Shield. Alternatively, the Archean crust corresponding to this mantle depletion event may have been reworked in Proterozoic time, to the point of being unrecognisable. In either case, it appears that mantle material that underwent depletion (melt extraction) in Archean time has survived in relatively shallow parts of the lithospheric mantle through a major episode of crustal generation in Proterozoic time. Its survival is almost certainly linked to the buoyancy of these highly depleted peridotites, relative to the underlying asthenosphere. This conclusion has major implications for our understanding of mantle evolution, and the linkages between crustal and mantle tectonics.

Contacts: Eloise Beyer, Sue O'Reilly, Bill Griffin
Funded by: ARC, Macquarie University Postgradutae Grant, GEMOC

Ancient mantle beneath New England

THE NEW ENGLAND OROGEN, northern NSW (Fig. 1) was assembled during a convergent tectonic regime, active along the eastern margin of the Australian continent in Paleozoic time. It can be divided into two regions: the Tamworth Belt represents the sediments deposited at the continental margin inboard of the subduction zone, and the Tablelands Complex represents a collage of terranes accreted to and dispersed along the convergent margin. The two regions are separated by the Peel Fault and the Great Serpentinite Belt, which appear to be relics of the suture along which oceanic crust was subducted.

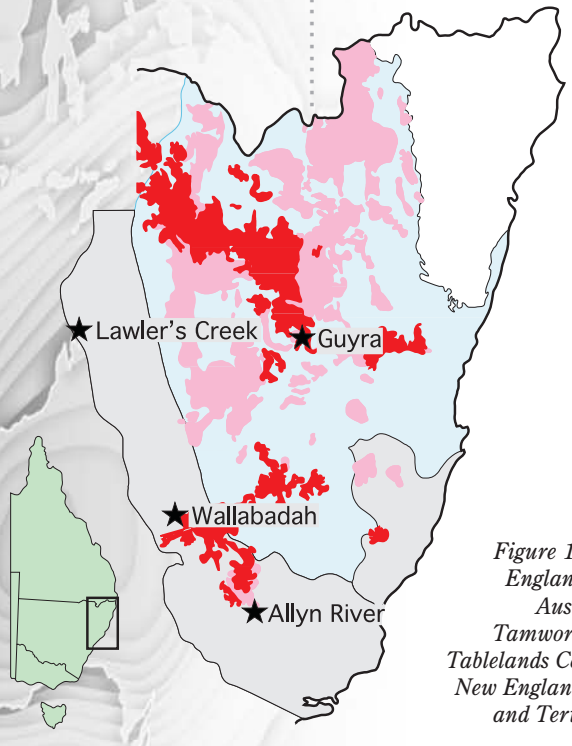

Figure 1. Map of the New England Orogen, eastern Australia showing the Tamworth Belt (grey), the Tablelands Complex (blue), the New England batholith (pink) and Tertiary basalts (red)

Traditional methods of dating surface geology show that tectonic activity in the orogen ceased with the emplacement of the New England Batholith in Carboniferous and Permian time; in the Cretaceous the Tasman Sea was opened, and during Tertiary time abundant basaltic lavas were erupted. The oldest materials recognised thus far are 'exotic' blocks tectonically emplaced close to the Peel Fault. U-Pb dating (plagiogranites and eclogites) and fossils (limestones) give dates that stretch back as far as the Early Cambrian and late Neoproterozoic, but little is known about their affinities or position on the margin of eastern Gondwana.

Mantle xenoliths brought to the surface by erupting basalts represent samples of the upper mantle and lower crust. Xenoliths from several locations in the New Engand Orogen

have been characterised as part of this study, and *in situ* Re-Os dating of sulfide grains found in the peridotites has been carried out using the GEMOC multi-collector ICPMS laser microprobe. The Re-Os data can be used to calculate model ages that correspond to periods of melt extraction from the peridotitic mantle.

Re-Os ages for the xenoliths in this study far exceed the ages determined for the surface rocks (Fig. 2). Xenoliths from Allyn River and Wallabadah Rocks, in the southern end of the Tamworth Belt, give ages in the range 0.8 to 1.8 Ga, and samples from Guyra, in the central part of the Tablelands Complex give ages in the range 0.6 to 1.8 Ga. Model ages for samples from Lawler's Creek, at the north western margin of the Tamworth Belt are significantly older, in the range 1.4 to 3.4 Ga.

These new data show that old mantle can persist beneath younger terrains, probably because of the inherent buoyancy of depleted peridotites (see *Research Highlight p.60*). The ages also raise questions about the early history of Eastern Australia, prior to the breakup of Gondwana. Why is the mantle beneath the orogen so much older than the rocks at the surface? Is it inherited from a precursor terrane that was broken up and dispersed prior to the onset of subduction along the eastern Gondwana margin? What is the association with other Proterozoic-age blocks now located in Antarctica and elsewhere?

Research is continuing on the subject ….

Contacts: Will Powell, Sue O'Reilly
Funded by: Macquarie University postgraduate grant, GEMOC

Mt Kaputar, in the northwest of the New England Orogen. Numerous spectacular trachyte plugs remain as evidence of the volcanism here, which took place around 17-20 million years ago, bringing xenoliths to the surface at the nearby Lawler's Creek locality.

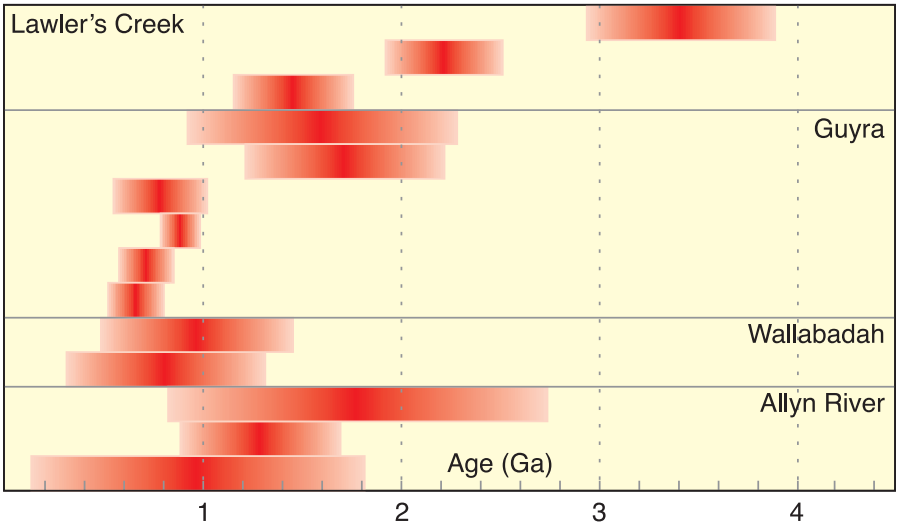

Figure 2. Re-Os model ages for sulfides from the New England xenolith localities. Coloured bars are centred on the calculated age, with the length covering the 2-sigma uncertainty.

Wandering poles in the Late Cambrian

PALAEOMAGNETIC STUDIES of rocks measure the direction of the magnetic pole at the time a rock crystallised or was deposited. The apparent movement of the magnetic pole between different time periods usually is interpreted in terms of the continental plates moving relative to the pole – but what if the pole itself, and not just the plates, really was wandering?

A palaeomagnetic investigation of Cambro-Ordovician limestones from Black Mountain in western Queensland is being carried out to assess the possibility of a large-scale true polar wander event during the Late Cambrian. Inertial Interchange True Polar Wander (IITWP) is a special case of true polar wander; it describes the rapid rotation of the solid lithosphere of up to 90° by the physical crossing, or interchange, of the earth's intermediate and maximum moments of inertia.

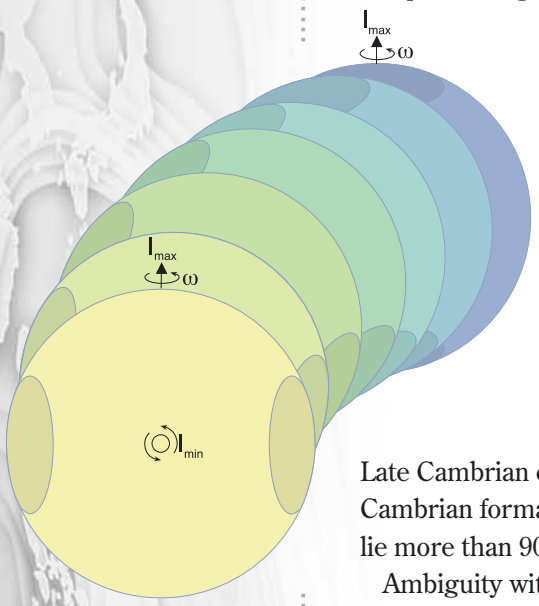

Figure 1. Visual representation of IITPW.

For such a large-scale shift the earth must be modelled as a quasi-rigid spinning spheroid in which a concentration of mass at the poles would produce an inherent instability, leading to the realignment of mass towards the equator (Fig. 1). Palaeomagnetic evidence to support an IITPW event in the Late Cambrian comes from selected groups of palaeopoles from Vendian to earliest Cambrian formations in Laurentia, Baltica, Siberia and Australia. These palaeopoles lie more than 90° away from similarly derived Late Cambrian-Early Ordovician poles.

Ambiguity with respect to the polarity of Early Palaeozoic and older palaeopoles presents a large degree of uncertainty when we attempt to define the directions of ancient apparent polar wander paths (APWPs). For the pole path presented in Figure 2, polarities of the ancient palaeopoles (>400 Ma) were invoked to minimise the length of the generated polepath, and IITPW is not supported.

However, a shorter path is not necessarily a better path. Before a more detailed APWP can be presented as a part of this study, identification of the age of magnetisations carried by limestones at and around Black Mountain will need to be ascertained. For example, GB1 in Figure 2 is the characteristic palaeomagnetic direction obtained from specimens at Black Mountain. Petrophysical tests will aid in the distinction between an authigenic magnetite, supporting the Silurian remagnetisation age suggested by the presented APWP, and primary remanence, which will support IITPW. If the IITPW hypothesis is sustained by this investigation, it will require a radical restructuring of palaeogeodynamics and the Earth system as we know it.

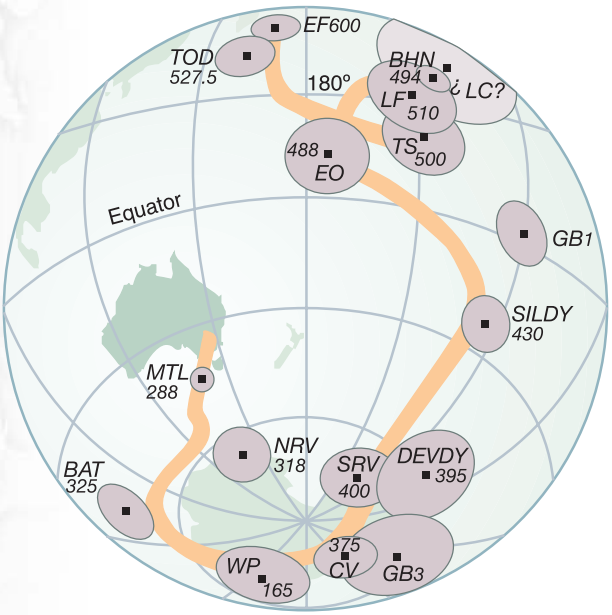

Figure 2. Latest Proterozoic-Earliest Palaeozoic APWP for Australia. Selected Australian palaeopoles taken from the palaeomagnetic database maintained by M.R. McElhinny & J. Lock on-line at "http://dragon.ngu.no/Palmag/paleomag.htm"

Contacts: Kari Anderson, Mark Lackie

Funded by: Macquarie University postgraduate grant, GEMOC

Structure and chemistry of the Australian lithosphere

GARNET XENOCRYSTS from a series of localities in southern Australia have been used to construct a lithospheric transect across one of the major tectonic boundaries of the Australian continent, the Tasman Line. The localities, from Jugiong in central NSW to the Eyre Peninsula in South Australia, cover a range of tectonic environments, from Phanerozoic fold belt to Proterozoic craton.

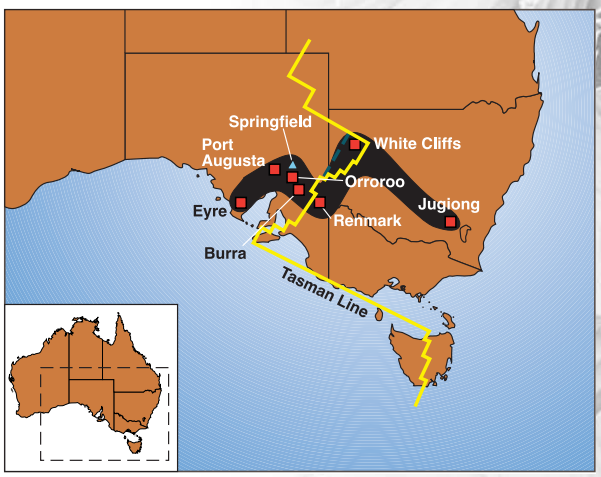

Figure 1. Map of southern Australia showing sample localities relative to the Tasman line.

At each of these localities garnet data have been used to estimate the pressure-temperature regime within the lithosphere and the depth to the lithosphere/asthenosphere boundary (LAB).

These sections reveal thicker lithosphere and lower geothermal gradients with increasing tectonothermal age of the lithosphere domains. The paleogeotherm decreases from greater than 50 mW/m^2 at Jugiong to around 40 mW/m^2 in South Australia and the depth to the LAB changes from ca 100 km to 180 km. These physical changes are paralleled by higher MgO and lower CaO and Al_2O_3 contents in progressively older lithospheric mantle, consistent with the global secular variation in mantle composition (Publications 132, 234).

Comparison of the adjacent Springfield (Permian) and Orroroo (Jurassic) sections indicates lithosphere thinning by about 10-15 km over this time period, attributed to the effect of Pangean rifting.

A method of estimating olivine Mg content from garnet composition via an inversion of O'Neill and Wood's (1979) geothermometer has been developed (Publication 222). This method reproduces xenolith olivine compositions in the mantle to within ± 0.5 mol%.

Application of this inversion to the southern Australian transect shows high XMg_{ol} (Mg/(Mg+Fe)) in the shallow parts of the Proterozoic westerly sections and lower XMg_{ol} in the Phanerozoic eastern sections, reflecting greater degrees of melt extraction during formation of older lithosphere. There also is an overall trend to lower Mg# with increasing depth in each section, which may reflect infiltration by asthenospheric melts near the LAB. Olivine density varies inversely with Mg#, and the Proterozoic lithosphere in this traverse therefore is more buoyant relative to the asthenosphere than the Phanerozoic sections, despite the lower geotherm beneath the craton. As Vp and Vs also vary with Mg# (the higher the Mg#, the higher the Vp and Vs) these compositional differences are important in the interpretation of seismic tomography.

Figure 2. Contour plots of XMg_{ol} against depth for sections on the southern Australian transect.

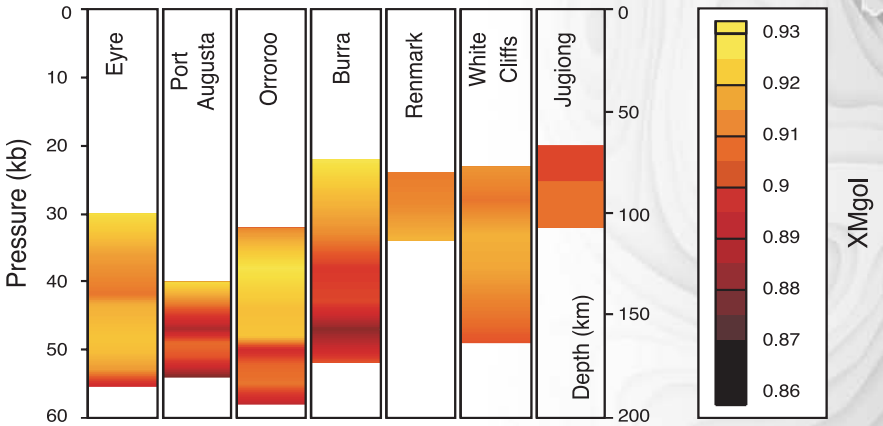

Contacts: Oliver Gaul, Sue O'Reilly, Bill Griffin
Funded by: GEMOC, ARC APA(I), Industry partners

Hafnium isotopes and the Baltic Margin jigsaw puzzle

THE INTEGRATED ANALYSIS of U-Pb ages and Hf-isotope composition in zircon is proving to be a valuable tool in sorting out tectonic relationships in complex terrains. A collaborative project between GEMOC and the Precambrian Geochemistry research group at the University of Oslo, Norway has used this approach to analyse the relationships between the different crustal blocks that now make up the Southwest Scandinavian Domain of the Baltic Shield.

Two contrasting tectonic models have dominated the recent debate about this region. In one, the part of south Norway west of the Oslo Rift was an exotic microcontinent, accreted onto the Baltic Shield between 1.58 and 1.50 Ga along a suture, now conveniently masked by the Paleozoic rocks of the Oslo Rift. In the competing model, South Norway has been part of the Baltic Shield since the early Proterozoic, but the crustal terranes building up the area have been displaced southwards along the margin of the Baltic Shield during the Sveconorwegian (i.e. Grenvillian, ca 1000 Ma) orogeny.

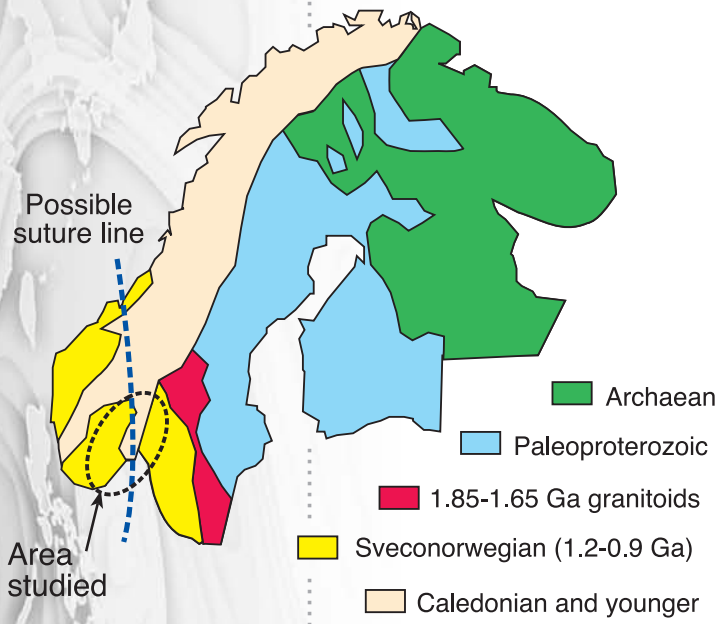

Figure 1. Tectonic map of the Baltic Shield and adjacent parts of the Caledonides, showing the hypothetical suture line through the Permian Oslo Rift in the study area

LAM-ICPMS U-Pb dating of Mesoproterozoic intrusions from South Norway in the GEMOC laboratories showed that extensive calcalkaline magmatism occurred in the period *1500 -1600 Ma*, and this magmatism can be traced on both sides of the Oslo Rift (Fig. 1). The major and trace element characteristics of the 1500-1600 Ma intrusive rocks indicate that they formed in a moderately evolved continental margin volcanic arc setting.

Zircons from these intrusions show a range of initial Hf isotopic compositions (Fig. 2). In the western part of the area, furthest from the Mesoproterozoic continent, the $^{176}Hf/^{177}Hf$ values are close to the depleted mantle at the time of intrusion. In the east, significantly lower values indicate that rising batches of magma may have interacted directly with Paleoproterozoic continental rocks. The

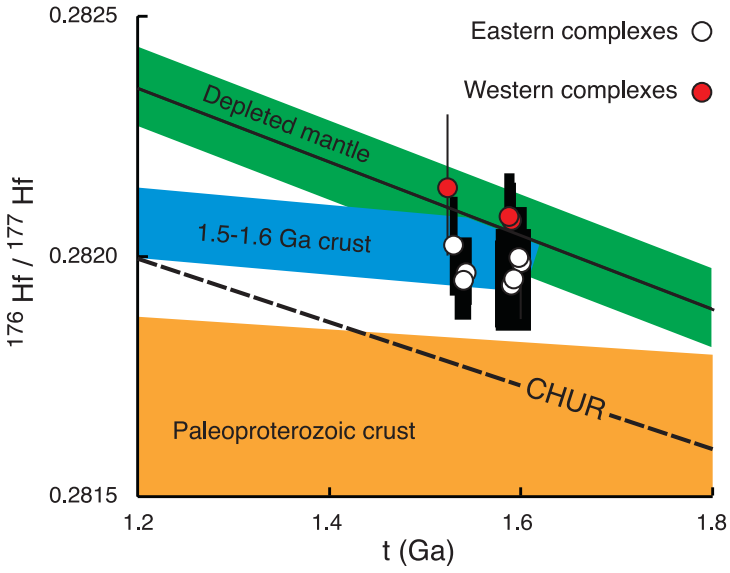

Figure 2. U-Pb ages vs Hf isotope composition for S. Norwegian igneous complexes. Calcalkaline rocks of 1500-1600 Ma age occur both east and west of the Oslo rift. The lower $^{176}Hf/^{177}Hf$ of the eastern complexes indicates a greater contribution of old crustal material during magma generation.

distribution of Hf-isotope values is consistent with a Cordillieran-type model for the mid-Proterozoic evolution of the margin of the Baltic Shield.

Hf isotope data on other intrusions across southern Norway show that today, rocks with a crustal history extending back to early Proterozoic time and carrying a continental geochemical signature are present at depth west of the areas dominated by the Mesoproterozoic calkalkaline rocks. This supports suggestions that these western terranes originally lay farther north along the ancient Baltic continental margin, and were displaced southward along that margin during the Sveconorwegian orogeny (Fig. 3).

Contacts: Tom Andersen (Univ. of Oslo), Bill Griffin
Funded by: GEMOC, Norwegian Research Council

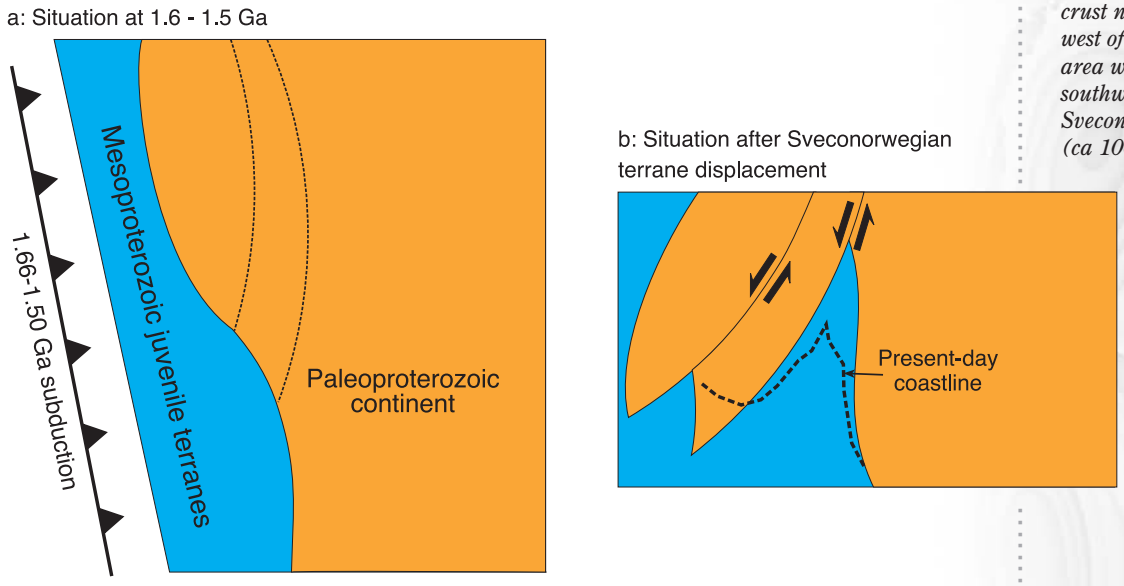

Figure 3. Cartoon showing tectonic model implied by the U-Pb and Hf-isotope data. (a) The study area (in blue) was generated at a continental margin, with subduction offshore. (b) Older crust now occurring west of the study area was displaced southward during Sveconorwegian time (ca 1000 Ma).

TerraneChron™ takes off

***TerraneChron*™ is GEMOC's unique approach to terrane evaluation and the study of crustal evolution, based on the integrated *in situ* analysis of U-Pb age, Hf-isotope composition and trace-element patterns in single zircon grains. The zircons can come from modern drainages sampling a terrane of interest, from ancient sedimentary rocks, or from individual igneous rocks. Using GEMOC's EMP, LAM-ICPMS and LAM-MC-ICPMS facilities (see *Technology Development*), this methodology gives the age, the host magma type, and the source of the magma (crustal or mantle), for each zircon grain analysed. Applied to zircon suites from ancient or modern sediments, it generates an 'event signature' that defines the evolution of the area in terms of the timing and nature of the magmatic events that have formed its crust (Publications 215, 251, 262).**

In 2001, the interest in *TerraneChron*™ as a tool in mineral exploration, basin analysis and crustal evolution studies took off to an exhilarating extent, with funded projects in Scandinavia, India, South America and Australia. More discussions about collaborative projects are in progress with exploration companies, and state and national geological surveys in Australia and overseas. The advocacy of Dr. Steve Walters from Advantage Geochemical Solutions has been a significant factor in generating this interest. The Geochemical Analysis Unit now reserves one of its laser-probe ICPMS instruments for the U-Pb work, and Ayesha Sayeed recently joined Elena Belousova to add increased capacity for the *TerraneChron*™ work. The "brand name" is now going through the copyright process, and a series of papers on the results of projects will begin to appear in 2002.

Contact: Bill Griffin, Elena Belousova, Sue O'Reilly

Mantle mixup beneath Tasmania

MANTLE XENOLITHS provide a basic but very powerful tool for investigating the nature of the lithosphere in space and time. A study of spinel peridotite xenoliths in Tasmanian basalts has revealed marked heterogeneity in the lithospheric mantle beneath the northern part of the island. Tasmania can be broadly divided into two terrains: a Proterozoic terrain in the west, and a Phanerozoic terrain in the east (Fig. 1). The Proterozoic terrain can be further divided into six regions or "Crustal Elements" based on geological and geophysical mapping (GSA Abstracts, 49, 1998). The Phanerozoic terrain is defined as the Northeast Element. Each of the Elements has a distinct geological history and internal structure. An east-west traverse across northern Tasmania sampled xenoliths from the Rocky Cape (RC), Sheffield (SH) and Northeast (NE) Elements.

Figure 1. "Crustal Elements" of Tasmania (after GSA Abstracts, 49, 1998).

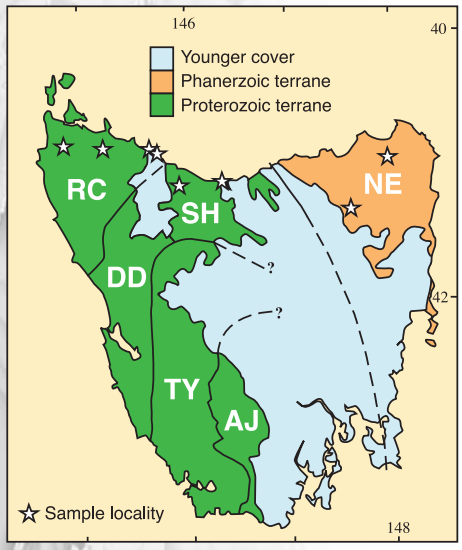

A correlation between mantle composition and the age of the overlying crust has been observed in numerous terrains around the world and has been interpreted as evidence that crustal volumes and their underlying lithospheric mantle formed at least quasi-contemporaneously, and can remain coupled for periods of eons. In Tasmania it was expected that the mantle xenoliths sampled in the Proterozoic Elements would resemble depleted Proterozoic lithosphere elsewhere in the world, while those erupted through Phanerozoic crust would be more fertile and representative of typical Phanerozoic lithosphere.

However, in Tasmania the majority of mantle peridotites are fertile, even in regions where they have been erupted through Proterozoic crust. In fact, the xenoliths with the most fertile compositions are found in the Rocky Cape Element, which has yielded some of the oldest crustal ages in Tasmania. This suggests that the Proterozoic depleted lithosphere has been either removed and replaced by younger, chemically fertile lithosphere, or refertilised by the infiltration of asthenospheric melts. Rare depleted xenoliths found at some localities may represent remnant Proterozoic lithospheric mantle that has persisted at least to the Tertiary, the time of xenolith entrainment. The seismic velocity of peridotite increases with its degree of depletion (see *Research Highlight p.60)*, and the overall fertile nature of the mantle beneath northern Tasmania is consistent with the relatively low mantle velocities recorded by recent Geoscience Australia seismic surveys.

Figure 2. Xenolith localities in Tasmania

The presence of unexpectedly fertile lithosphere in northern Tasmania may be related to rifting between Australia and Antarctica during Jurassic time. Crustal extension would thin and disrupt the old depleted lithosphere, providing space for upwelling asthenospheric material that would later cool to form new, little-depleted lithospheric mantle. In this regard, northern Tasmania may be a good model for the generation of young lithospheric mantle beneath many terrains affected by Phanerozoic extensional tectonics.

Contacts: Eloise Beyer, Sue O'Reilly, Ming Zhang
Funded by: ARC, Macquarie University Postgraduate Grant, GEMOC

Plateaus, plumes and fluids in Kerguelen xenoliths

OCEANIC PLATEAUS are vast outpourings of lava on the ocean floor, and may be good analogues for the development of continents on the early Earth. The Kerguelen Archipelago (South Indian Ocean) lies on Earth's second largest oceanic plateau, and is being studied at GEMOC in a joint research program with an international consortium, headed by the Université Jean Monnet (St. Etienne). The formation of the plateau is related to interaction between the South East Indian Ridge (SEIR) and the long-lived Kerguelen plume, and makes Kerguelen a unique laboratory for studying the generation of thickened lithospheric mantle in an oceanic setting.

Figure 1. Lac Michèle, on the Loranchet Peninsula (NW Kerguelen).

Mantle xenoliths provide key information on the geochemistry of the mantle, that can be used to understand the dynamics, physical properties and evolution through time of the lithosphere. On the Kerguelen Islands, mantle xenoliths usually are found in dikes or pipes of young alkaline basalts. However, harzburgite xenoliths recently were found in tholeiitic-transitional basalt dykes at Lac Michèle, on the Loranchet Peninsula (NW Kerguelen, Fig. 1). Their bulk-rock and mineral compositions (e.g $Mg\#_{Ol} = 90.7\text{-}92.2$, $CaO_{WR} < 1$wt %) indicate that these harzburgites are residues from an extensive partial melting event, possibly related to the early formation of the Kerguelen Islands when the plume hit the SEIR 40 Ma ago.

Secondary metasomatic processes that modify the original composition of the xenoliths are well documented in Kerguelen xenoliths and reflect metasomatism by alkaline melts and carbonated fluids. Some of the very depleted harzburgites contain an unusual metasomatic assemblage, composed of sodium-rich feldspar ($Ab_{78\text{-}83}An_{14\text{-}19}Or_{2\text{-}4}$), low Ca-spongy clinopyroxenes, olivine and apatite, that forms reaction rims on Cr-spinel grains (Fig. 2). To our knowledge, this is the first description of such Na-rich feldspars in mantle xenoliths. LAM-ICPMS analyses show that the clinopyroxene is extremely enriched in the light Rare Earth Elements, Sr ± Th ± U, and depleted in High Field Strength Elements (Nb, Ta, Zr, Hf, Ti). This geochemical signature strongly suggests that the metasomatic agent was a carbonated fluid. The crystallization of this unusual assemblage probably reflects the percolation of small volumes of volatile and Na-CO_2-rich fluids through the peridotitic matrix, reacting with the peridotite to crystallise the metasomatic assemblage.

Figure 2. Element distribution maps of a metasomatic "pocket" with Na-feldspar (Fs), clinopyroxene (Cpx), apatite (Ap) and olivine (OlII) in spinel (Sp).

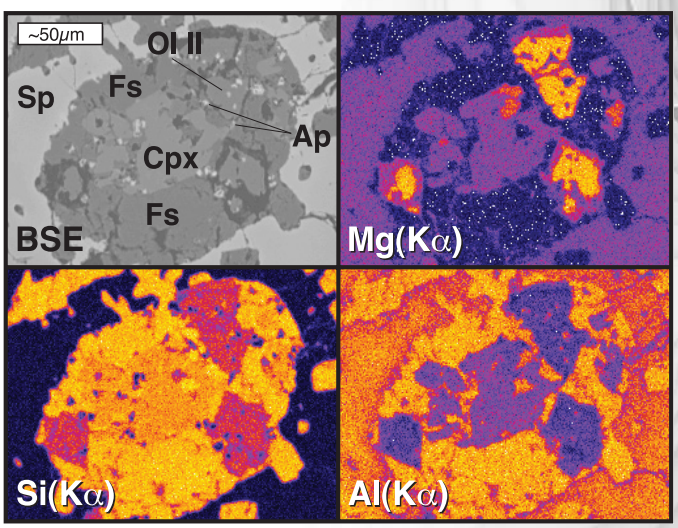

These observations have important implications for the diversity of geochemical signatures that can be generated in the oceanic mantle above a mantle plume. They show that the percolation of small volumes of fluids can lead to extreme trace element enrichment of previously very depleted oceanic mantle on a very small scale (i.e < mm scale). Further understanding of the processes will require evaluation of the petrogenesis of carbonatitic magmas in an Albite-Calcite ($NaAlSi_3O_8$-$CaCO_3$) system.

Contacts: Guillaume Delpech, Sue O'Reilly
Funded by: ARC, Macquarie University, GEMOC

Cooking mantle fluids - trace element mobility during subduction

SUBDUCTION of oceanic crust is a crucial step in the generation of new continental crust, because it promotes magmatic processes in the mantle wedge above the subduction zone. The generation of these magmas is linked to water derived from dehydration and/or melting reactions in the subducted slab. This water is thought to enrich the magma source region with large ion lithophile elements (LILE), but not

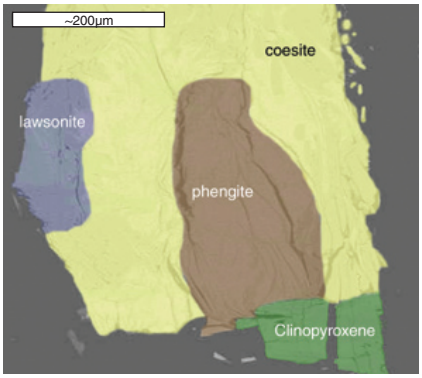

Figure 1. Crystal aggregate grown in fluid in outer capsule, 650 °C. The outer capsule contained 500 ppm Ni and 200 ppm Zn as impurities and these were very selectively taken up by silicate minerals grown in this capsule (eg pyroxene contains 0.6-1.7%, chloritoid 5-6%, phengite 3-4% NiO). No Ni and Zn were evident in the inner capsule, nor in minerals there.

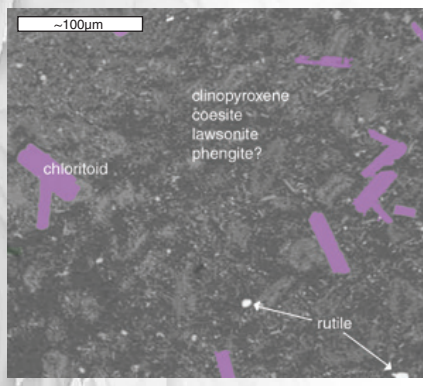

Figure 2. Large chloritoid (with <0.1% ZnO) in fine grained matrix, inner capsule, 650 °C.

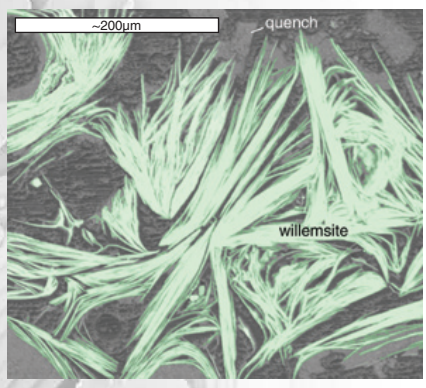

Figure 5. Talc aggregate and quench solute from fluid in outer capsule, 650 °C. N.B. This is actually Ni-talc (willemsite) with Ni coming from the outer capsule (see Fig. 1).

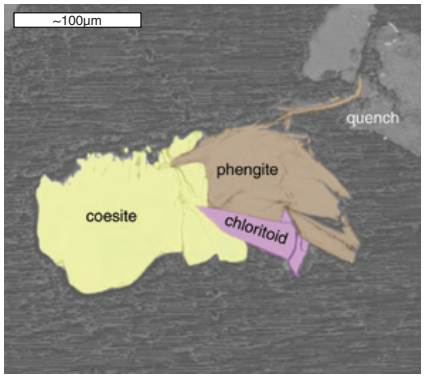

Figure 3. Crystal aggregate grown in fluid and quenched solute from fluid in outer capsule, 650 °C. Chloritoid contains 4% ZnO.

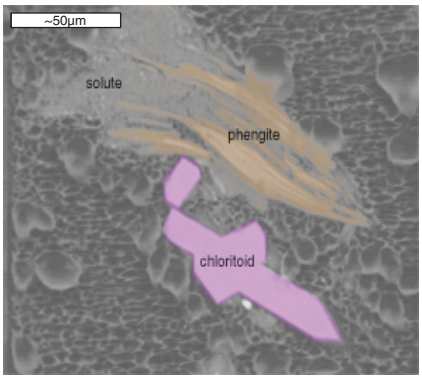

Figure 4. As for Fig.3. Chloritoid contains 9-11% ZnO.

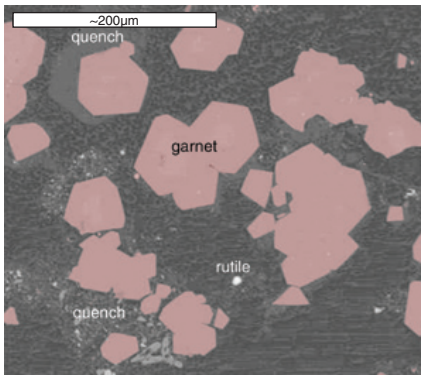

Figure 6. Upper zone of sample in inner capsule, 700 °C.

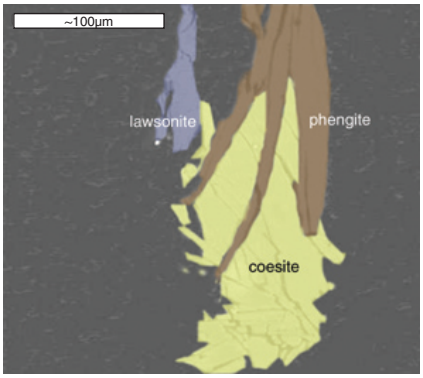

Figure 7. Crystal aggregate grown in fluid in outer capsule, 700 °C. Phengite contains 3% NiO.

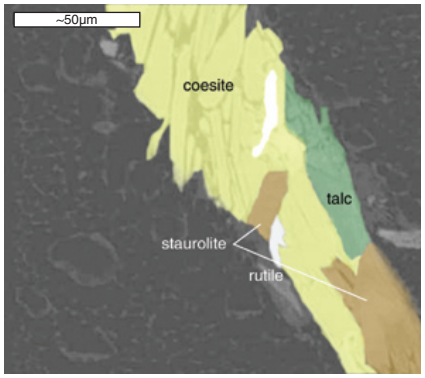

Figure 8. Crystal aggregate grown in fluid in outer capsule, 700 °C. Talc contains 13% NiO, staurolite contains 3-5% ZnO, 3-4% NiO.

with high field strength (HFSE) or rare earth elements (REE). Early experiments have confirmed this model on a bulk rock scale for a few trace elements, but did not discriminate the effects of different mineralogies.

We carried out new experiments on an oceanic tholeiite (MORB) enriched (10-100 ppm) in 25 trace elements; it was crystallized at 3.0 GPa, 650 and 700 °C for 2 weeks, with 30-50 wt.% added water. One set of experiments used a double capsule configuration, with fluid in the outer sealed Ag-Pd capsule and powdered MORB glass in the unsealed inner Ag-Pd capsule. These produced a clearcut separation of solid and fluid, with growth of some large crystals in the fluid, and the solute could be quenched for study. Experiments in a single sealed Ag-Pd capsule produced a remarkable separation of fluid and solid. The solid component in both capsule configurations showed a distinct mineralogical zoning. At 650 °C the fluid coexists with omphacite (Figs. 1, 2), lawsonite (Figs. 1, 2), chloritoid (Figs. 2-4), coesite (Figs. 1-3) and accessory phengite (Figs. 1-4), rutile (Fig. 2), Ti-magnetite and talc (Fig. 5). At 700 °C garnet is conspicuous as a coarse layer at the top (Fig. 6), below which omphacite, coesite, phengite (Fig. 7), minor staurolite (Fig. 8), and rare lawsonite (Fig. 7), rutile (Fig. 8) and talc (Fig. 8) occur; chloritoid is absent.

The LAM-ICPMS microprobe lets us examine the trace element contents of individual minerals coexisting with fluid in these experimental charges, and the changes in trace element ratios for the fluid as the coexisting mineralogy changes. LAM-ICPMS spectra also indicate the presence of minute crystals of zircon and allanite, the latter commonly included in garnet or chloritoid crystals. Most importantly the LAM-ICPMS analyses establish *patterns* of trace element partitioning between minerals (data for omphacite, lawsonite, phengite, chloritoid and garnet) and fluid, if not absolute values.

The fluid shows strong enrichment of LILE relative to HFSE and REE. Rb/Sr, Cs/Sr and Ba/Sr decrease from 650 to 700 °C, apparently controlled by residual lawsonite; an increase in La/Lu is clearly controlled by garnet. Omphacite fractionates both Zr/Nb and La/Lu, so that Zr/Nb decreases and La/Lu increases in the fluid. Rutile strongly takes up Nb and Ta, but cannot explain an almost 4-fold increase in Nb/Ta observed in the fluid relative to the bulk sample.

These results indicate that the movement of a fluid derived by dehydration processes may increase LILE/HFSE, LILE/REE and decrease Zr/Nb in the mantle wedge, and thus in magmas derived from the wedge. The fluid may impart different Rb/Sr, Cs/Sr and Ba/Sr to the magmas, depending on the temperature at which dehydration took place. Residual rutile may explain Nb and Ta depletion without significantly affecting Nb/Ta ratios. The observed lack of fractionation in La/Lu restricts the role of garnet in the melting. Thus close examination of key trace element ratios in subduction zone magmas may point to a broad pressure/temperature gradient in the dehydrating slab, giving rise to the fluids that ultimately drove the magma generation.

"....close examination of key trace element ratios in subduction zone magmas may point to a broad pressure/temperature gradient in the dehydrating slab, giving rise to the fluids that ultimately drove the magma generation."

Contacts: Trevor Green, John Adam
Funded by: Macquarie University Grants

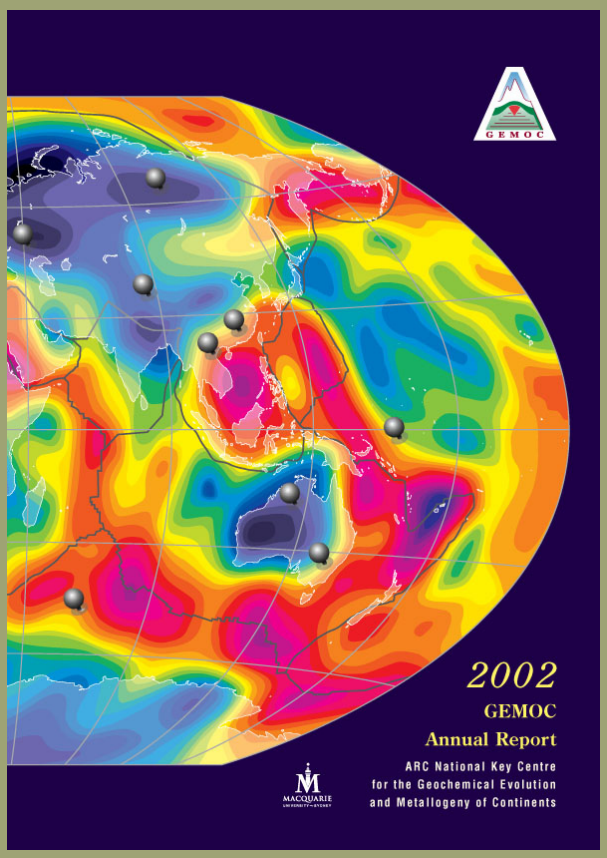

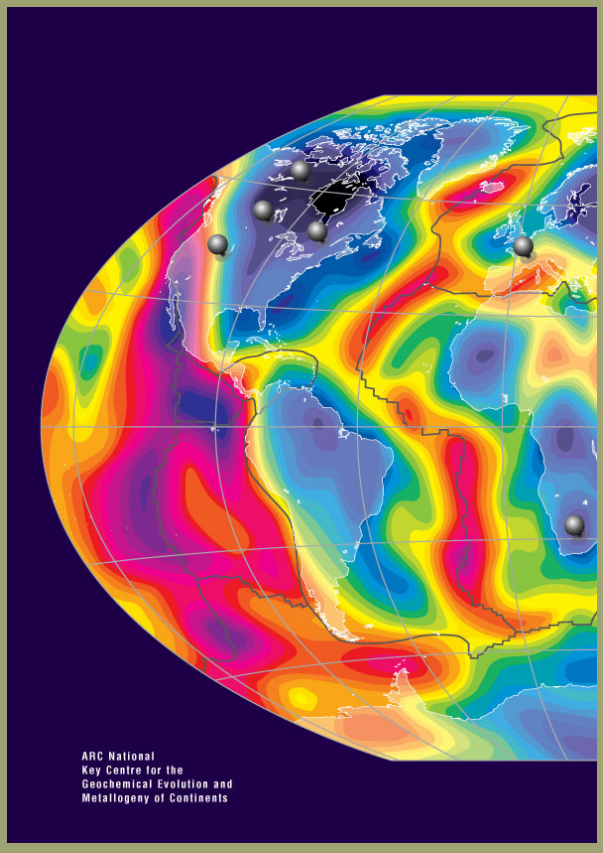

2002 Contents

Journey to the centre of the Earth	85
Lithosphere mapping beneath the North American Plat	86
Taking the pulse of the Earth: Lithosphere events tracked by *in situ* geochronology	88
Not so stable after all? High-temperature deformation induces resetting in zircon	90
From dunite to lherzolite: tracking refertilisation of Archean peridotite in Norway	92
Fingerprinting diamonds	94
TerraneChronTM success keeps soaring	95
Lower crustal terranes in the North China Craton - new surprises from xenoliths	96
La plume de mon Massif ?	98
Hafnium in rutile frees Slave secrets	99
Mantle composition and processes beneath the Taiwan Strait, SE Asi	101
Waves of fluid invade the mantle beneath western Victoria	102
Ore grades correlate with Cu and Fe isotopic data	104
Mg isotopes in olivine track fluid flow in the mantle	106
Trace elements in mantle rocks revisited - a warning to modellers	108
Trace element partitioning - time for the detail	109

Front Cover: Global tomography image at 150 km based on dataset of Ritsema (Ritsema et al., 2000. Sci. Prog, 83, 243-259). Highlighted points identify some regions where GEMOC has detailed petrologic and geochemical controls on the composition and architecture of the lithospheric mantle that can provide anchor points to groundtruth tomographic models.

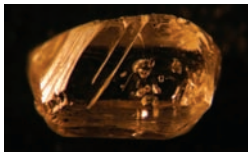

Research highlights 2002

Journey to the centre of the Earth

GEMOC'S FIRST SIX YEARS concentrated heavily on mapping the composition and architecture of the lithosphere in 4 dimensions, using mantle-derived rock samples and mineral debris brought to the surface in host magmas. Time provides the 4th dimension and is measured by the age of the host magmas. We have mapped the crust-mantle boundary and the lithosphere-asthenosphere boundary in different lithospheric sections in space and time, and have the most detailed information for the points shown.

This work has made some significant conceptual discoveries (eg Publication #234) including:

- Lithospheric mantle composition and thermal structure have changed with time (apparently episodically) and three major mantle types can now be recognised, reflecting major episodes of formation. Progressive reworking of early lithosphere provides a continual geochemical evolution trend towards the present.
- Archean and Proterozoic mantle roots are highly buoyant; they cannot be delaminated but require mechanical disaggregation (lithospheric thinning and/or rifting) and infiltration of upwelling fertile material to be destroyed or transformed.
- Phanerozoic SCLM is denser than the asthenosphere for observed thicknesses (~100 km) and can "delaminate" under stress.

The availability of refined seismic tomography datasets allows us to move on to the next phase of lithosphere mapping and to investigate large-scale problems such as:

- the implications of lateral variability between physical properties due to the compositional difference in lithospheric mantle domains
- the nature of domain boundaries identifiable in the lithospheric mantle; these may be important pathways for mantle fluids and relevant to metallogenesis
- the density variability of global lithospheric domains vertically and laterally
- the tectonic histories of coupled crust and mantle lithosphere terranes, assisted by input from *TerraneChron*™ studies (see *Research Highlights*)

Our aim is the compilation of a global map of Earth's lithosphere

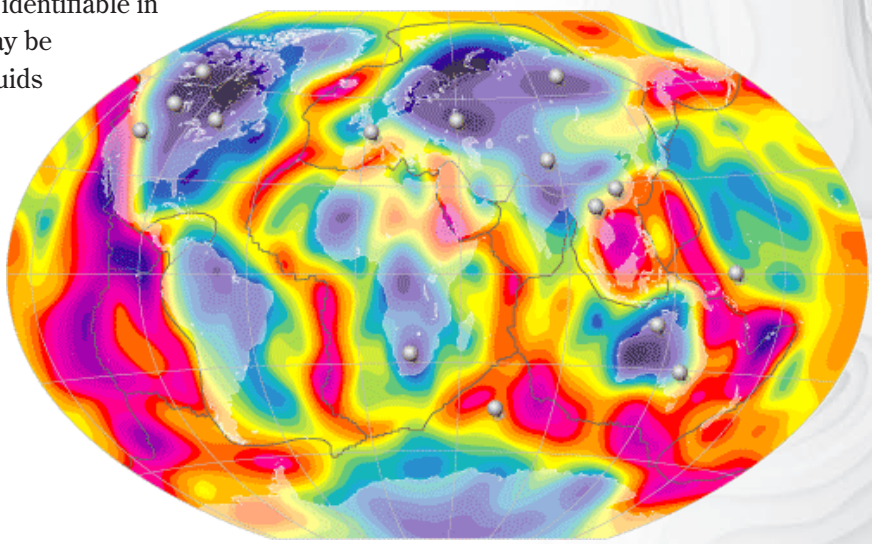

Global tomography image at 150 km based on dataset of Ritsema (Ritsema et al., 2000. Sci. Prog, 83, 243-259). Highlighted points identify some regions where GEMOC has most detailed petrologic and geochemical controls on the composition and architecture of the lithospheric mantle.

Lithosphere mapping beneath the North American Plate

THE COMPOSITIONAL STRUCTURE of the subcontinental lithospheric mantle (SCLM) beneath the North American Plate (USA, Canada, W. Greenland) has been mapped in 3D using major- and trace-element data on Cr-pyrope garnets from ca 100 kimberlites, lamproites and lamprophyres in 26 areas (Fig. 1). A statistical classification scheme (Publication #299) allows mapping of garnet compositional populations with depth to produce SCLM sections, which show the distribution of rock types and metasomatic processes. Inversion of a garnet-olivine thermometer (Publication #222) has been used to map the variation in mean $X_{Mg}^{olivine}$ with depth.

Analysis of seismic tomography (Fig. 1) shows that known kimberlites do not sample the thickest and most depleted part of the North American SCLM; on a continental scale, as well as the regional scale, kimberlites and related rocks tend to be concentrated near major changes in lithospheric thickness. Available SCLM samples therefore represent the thinner and modified outer parts of the continental root.

SCLM composition shows broad correlations with the tectonothermal age of the crust at each locality, and strong correlations with seismic velocity at 100-175 km depths. The thickness of the depleted SCLM varies from >200 km (Paleozoic in State Line District, Mesozoic in Saskatchewan), to 120-130 km in strongly modified younger areas (Colorado Plateau, N. Montana), and to ca 60 km beneath young orogens (Appalachians). The SCLM thickness is closely related to the geotherm, as reflected in the temperature at 150 km depth (Fig. 1).

Mean $X_{Mg}^{olivine}$ is typically 92.6-93.2 in the upper parts of the SCLM beneath Archons, and beneath Protons with significant Archean prehistory (Figs. 1, 2); many Proton SCLM sections probably represent metasomatically modified Archean SCLM. Tectons and possible "juvenile" Protons have less magnesian SCLM even at shallow depths (eg Colorado Plateau, 91.3; Kansas, 91.2; Virginia, 90.2). The highest mean $X_{Mg}^{olivine}$ is found in localities (Michigan, Hudson Bay) on the edge of the highest-velocity part of the root, where magnesian compositions also extend to greatest depth (Fig. 2); this suggests that the central cratonic "root" represents the extension of this highly depleted material to depths >175 km.

Many SCLM sections are relatively homogeneous in terms of rock type distribution and $X_{Mg}^{olivine}$, except for a rise in fertility and a drop in $X_{Mg}^{olivine}$ to asthenospheric values (≤90.5) over distances of 10-50 km toward the lithosphere-asthenosphere boundary. The transition from depleted lithosphere to asthenosphere is relatively sharp under the eastern part of the craton, and broader beneath Protons (Fig. 2); this may reflect more extensive metasomatism beneath the Protons.

Several sections show marked stratification, typically with the upper layer being more depleted, and one or more sharply defined discontinuities at 120-160 km depth. In terms

Figure 1. Map of N. America with contour outlines of the high-velocity lithospheric root at 100-175 km (red) and 175-250 km (green) after dataset of S. Grand. Symbols indicate temperature at 150 km (as derived from geotherms). The traverse line referred to in the text is also shown.

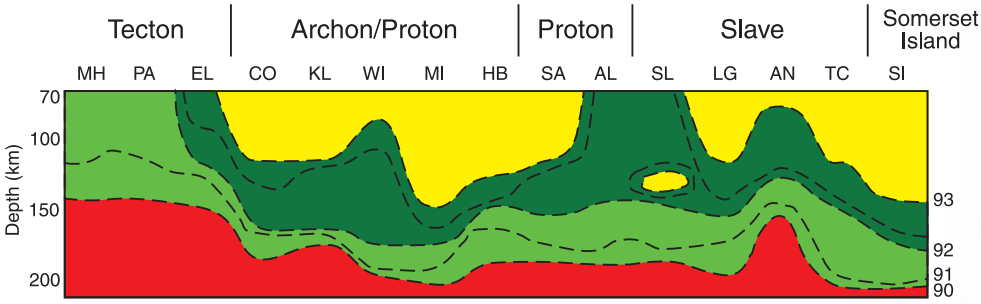

Figure 2. Distribution of X_{mg} of olivine with depth along the traverse shown in Figure 1.

of trace-element depletion, the upper part of the central Slave Craton stands out dramatically from other parts of the craton (Fig. 3); this appears to reflect greater degrees of later metasomatic re-enrichment outside the Slave Province. In West Greenland, interleaving of depleted and fertile SCLM may reflect tectonic stacking, related to the development of the nearby major Proterozoic suture zone. Other cases (Lac de Gras, N. Michigan, Saskatchewan; Fig. 3) are interpreted as the result of plume subcretion beneath a depleted SCLM of moderate thickness. Synchroneity between kimberlite intrusion and basin subsidence in the latter two cases is consistent with suggestions (Kaminski and Jaupart, 2000. EPSL, 178, p.139) that plume modification of the SCLM caused the development of these major intracratonic basins.

This analysis reveals strong correlations between the degree of depletion ($X_{Mg}^{olivine}$), the geotherm and tectonothermal age. Depletion and lithospheric temperature are negatively correlated, and thus have mutually reinforcing effects on seismic velocity. These correlations simplify the interpretation of seismic tomography in terms of lithosphere composition and history. The central core of the North American continent has an extensive, highly depleted root that extends well below 175 km, but is poorly sampled by known kimberlites. This root is essentially continuous beneath the Early-Mid Proterozoic mobile belts of the Canadian Shield. The outer parts of the root have been modified by introduction of material from the asthenosphere in both Archean and later time, producing a belt of varying thickness in which the SCLM has a less magnesian mean composition, and tends to be thinner. The intermediate seismic velocity of Tecton areas such as the Appalachians reflects both the fertile nature of the SCLM, and moderately elevated geotherms. Areas such as the Colorado Plateau, which has a moderately fertile mantle and is currently experiencing thermally driven uplift, show anomalously low seismic velocity in the 100-175 km depth range.

The present lithospheric architecture reflects an interplay between the buoyancy of Archean SCLM, its modification along rifts and mobile belts, the generation of juvenile Proterozoic and Phanerozoic SCLM, and the subcretion of plume head material. Lithospheric mapping, combined with interpretation of seismic tomography, indicates that relict Archean SCLM probably is present, at least at shallow levels, beneath much of the Proterozoic part of the N. American plate. This conclusion has important tectonic implications and is being tested by *in situ* Re-Os analysis of sulfides in mantle-derived xenoliths.

Contacts: Bill Griffin, Sue O'Reilly, Norman Pearson
Funded by: ARC, Industry, Macquarie University

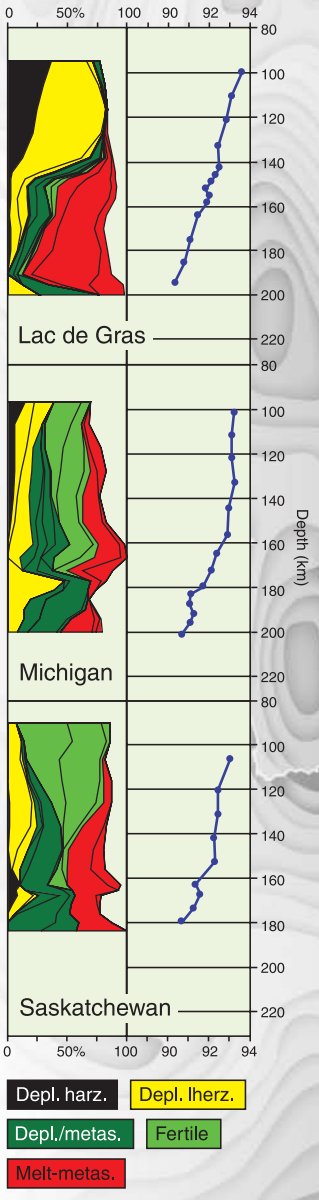

Figure 3. Rock-type sections for the Slave (Lac de Gras), Michigan and Saskatchewan regions.

Taking the pulse of the Earth: Lithosphere events tracked by *in situ* geochronology

THE DELIVERY of mantle fragments to the surface by kimberlitic and other deep-seated volcanics has allowed the mapping of compositional domains and architecture of the lithospheric mantle and lower crustal regions, as well as ground-truthing of geophysical datasets and modelling. New techniques for *in situ* dating of mantle wall-rocks using the Re-Os isotopic system (Publication #267) are revealing that these peridotites contain sulfides that record many events in the lithosphere. These range from the original depletion event(s) that formed the lithospheric domain to subsequent episodes of fluid addition that accompanied large-scale metasomatic transport, lithosphere reworking and/or younger lithospheric additions. The timing pattern of such events can also be used to test if different cratonic lithosphere domains had common evolution histories or if they docked or separated discretely.

Sulfides with high Os contents but low $^{187}Os/^{188}Os$ (γOs <1) and low Re/Os and Pt/Os ratios commonly are enclosed in primary silicates. If they have $^{187}Re/^{188}Os$ <0.08 and Pt/Os <0.5 they are inferred to represent monosulfide solid solution phases that are residual from partial melting or have crystallised from sulfide melts (ie primary; Publication #218 and Publication #292). It is these sulfides that potentially provide information on the timing of lithosphere stabilisation episodes, ie when domains of uppermost mantle were isolated from the convecting mantle by mechanisms such as:

- the partial melting residue from primordial mantle
- cooling of upwelling asthenosphere
- plume accretion to existing lithosphere
- crystallisation from a magma ocean

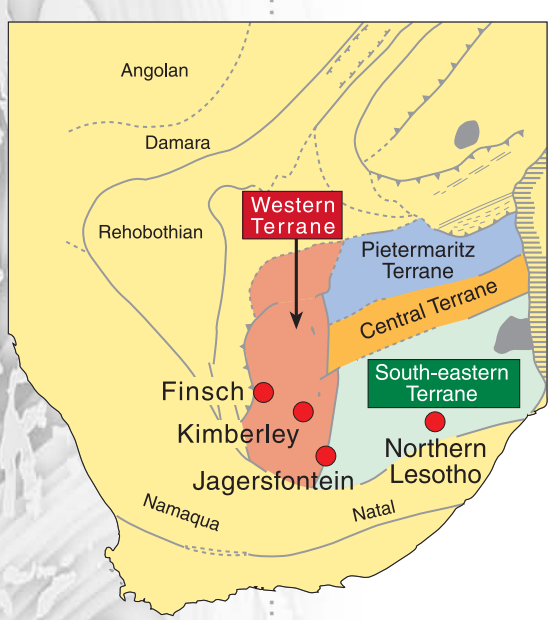

Figure 1. Terrane structure of the Kaapvaal Craton, showing localities sampled in this study; (after Publication #303).

Sulfides with low Os contents but highly radiogenic Os isotopic values and high Pt/Os ratios are inferred to represent trapped sulfide melts (Publication #292) that have scavenged radiogenic Os from older lithosphere (Publication #218 and Publication #290). They probably were originally interstitial to mantle silicate phases but recrystallisation of mantle peridotites may lead to their subsequent inclusion in the silicates. They record post-stabilisation lithospheric events.

The Kaapvaal craton can be divided into terranes based on crustal geological and geophysical data (Fig. 1) and provides a good natural laboratory for the application of this technique. Primary sulfides in mantle peridotites from N. Lesotho (*the SE Terrane*) show a major peak of *in situ* Re-Os ages from 3.0 to 3.6 Ga corresponding with crustal formation ages in the overlying crust (Fig. 2). There are also broad peaks around 2.2 and 1 Ga and a distinct spike at 2.65-2.75 Ga. Those from the Finsch and Kimberley kimberlites (*Western Terrane)* show a distinctive age profile with a pronounced peak at 2.8-3.1 Ga (Fig. 2), again coinciding with the oldest ages in the overlying crust, and other clear peaks at 2.5-2.6 Ga and 1.8-2.0 Ga.

Whole-rock Re-Os analyses of our samples give ages lying within the spread of those obtained by *in situ* analysis, reflecting the presence in the bulk sample of multiple generations of sulfides. The *in situ* data push back the earliest age of SCLM stabilisation, and indicate the potential for dating individual episodes of SCLM modification on a terrane scale and for identifying mantle terranes with

different histories.

Data obtained so far on mantle rocks from other old terranes (eg Siberia, Slave Craton and exposed sequences in Norway) indicate that significant volumes of lithosphere in cratonic regions were formed by 3 Ga. However, it has been demonstrated that very large volumes of juvenile crust were formed at ca 2.7 Ga. So far, the *in situ* Re-Os data do not suggest that there was a major episode of lithospheric mantle stabilisation directly corresponding to this dominant crustal event. This may be explained by the apparent distribution of kimberlites around the margins of coherent mantle domains identified by geophysical modelling, and overlain by 2.7 Ga crust, resulting in a biased xenolith sampling.

Detailed elastic thickness modelling (using gravity and topographic datasets) in the Slave Craton, Canada (8IKC abstract, Poudjom Djomani et al., 2003) and in N. Siberia (Publication #250) have shown that kimberlites occur at features identified as gradients in lithosphere strength and tend to outline coherent mantle structures (Fig. 3). This marginal distribution biases the sampling of mantle domains and it may be that the lithospheric mantle beneath the 2.7 b.y. juvenile crustal terranes is rarely penetrated by kimberlites and thus is poorly sampled.

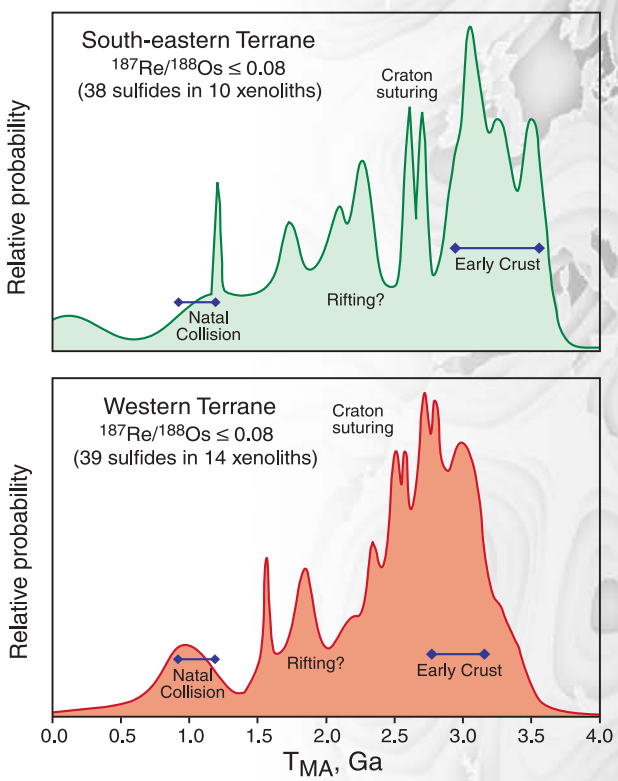

Figure 2. Cumulative-probability plots of the T_{MA} model ages of low-Re/Os sulfides from the SE Terrane (N. Lesotho) and the Western Terrane.

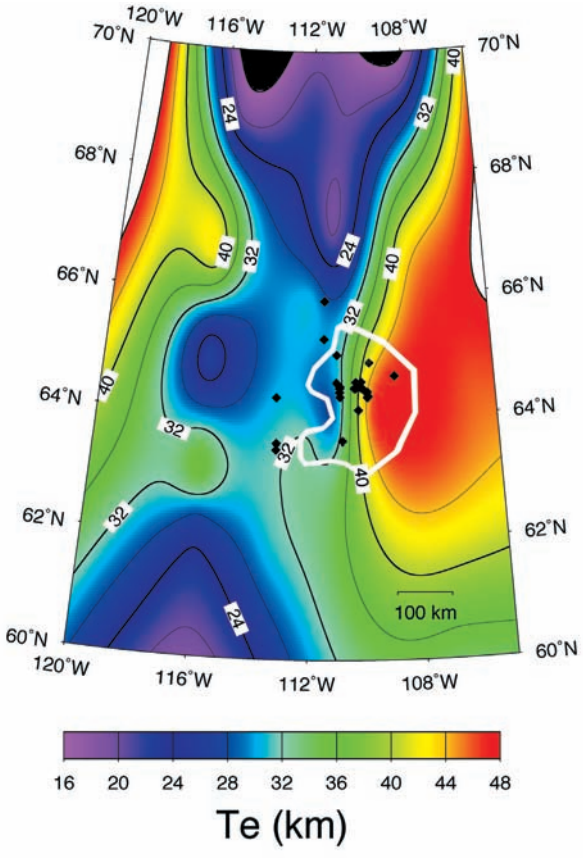

Figure 3. Elastic thickness (Te) contours for the Slave Craton. Kimberlite fields (black diamonds) lie on the flanks of weak zones (see Research Higlights, 2000).

Contacts: Sue O'Reilly, Bill Griffin, Norman Pearson
Funded by: ARC, Industry, Macquarie University

Not so stable after all? High-temperature deformation induces resetting in zircon

BECAUSE OF ITS chemical and physical resistance under most geological conditions, zircon has become one of the most important tools used by geochemists and geochronologists to determine the age, origin and thermal history of crustal igneous and metamorphic rocks. However, as studies of zircon systematics multiply, it has become evident that many zircons in metamorphic and igneous rocks show complex internal structures and disturbed U-Pb ages, making interpretation of the radiometric data ambiguous. Igneous and metamorphic overgrowths, inheritance, annealing of radiation damage, hydrothermal alteration, precipitation and dissolution, are all processes that can severely affect the isotopic system, leading to mixtures of age components within single grains.

Aerial view of the Howard Peaks Intrusion.

The application of high-precision *in situ* laser ablation techniques to obtain trace-element, U-Pb and Lu-Hf compositions in the same zircon grains, combined with a detailed study of the zircon's internal structures, has proved indispensable in discriminating between different types of zircon growth and alteration mechanisms. This approach has been applied to zircons extracted from metaluminous, calc-alkaline monzogranites, granodiorites and tonalites, affected by pervasive high-temperature solid-state ductile deformation, in the Howard Peaks Intrusive Complex in the Deep Freeze Range, Antarctica (Fig. 1). The aim of the project is to reconstruct the processes that affected the crust of this sector of Antarctica during the Late Cambrian – Early Ordovician Ross Orogenesis and to constrain the source regions of the granite magmas. This project is based on a collaboration between GEMOC and Università degli Studi di Siena, Italy.

The analyzed zircons show complex internal stuctures with inherited components, euhedral concentric zonation, convoluted zones and patches of unzoned zircons sometimes retaining ghost zones (Fig. 2). Ignoring the inherited components, a wide scatter in concordant and discordant ages between 518 and 440 Ma is observed, and two or three main age populations are found in all the analyzed samples (Fig. 3). Discordant ages are often exhibited by strongly zoned domains characterized by adjacent zones with high contrast in brightness, while grains with complex zoning, weak zoning or no zoning at all may show

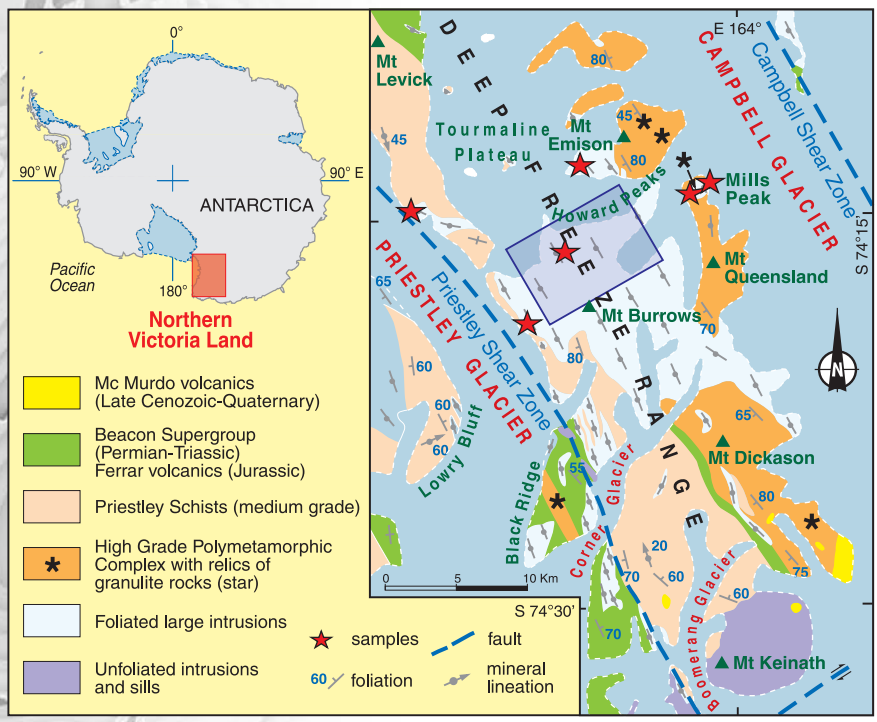

Figure 1. Geological map of the Deep Freeze Range, Northern Victoria Land – Antarctica, showing sample localities.

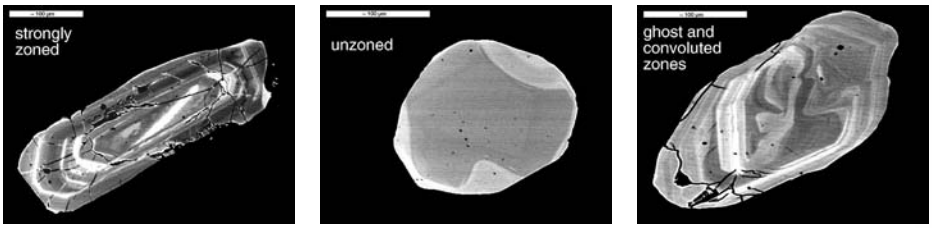

Figure 2. Back-scattered electron/ cathodoluminescence images showing secondary structures in the studied zircons.

a wide range of concordant ages.

Another striking feature of these zircons is the wide range of trace-element compositions with large variations in U, Th, Y and LREE contents, and limited variability in HREE (Fig. 4). Light REE enrichment is often related to the occurrence of bright domains in BSE images and/or relatively younger ages in zircon. The lack of a positive correlation between Yb and Th/U indicates that the trace-element variations are not related to fractional crystallisation processes. A simple volume diffusion cannot, on the other hand, be responsible for the observed variations in trivalent and tetravalent cations, as it should produce larger variations in HREE relative to LREE, and a higher mobility of Hf than of U and Th, which is not observed.

In contrast, a relatively narrow range of initial $^{176}Hf/^{177}Hf$ ratios has been obtained in distinct zircon populations within each sample. The lack of correlation between Hf ratios and zircon age populations suggests that the Lu-Hf system was left relatively undisturbed, while other elements including U, Th and Pb migrated within the grains. The similar low $^{176}Hf/^{177}Hf$ ratios in all the samples suggest a common parental derivation from old recycled crust for the different selected intrusives.

Figure 3. Plot of relative probability of concordant ages.

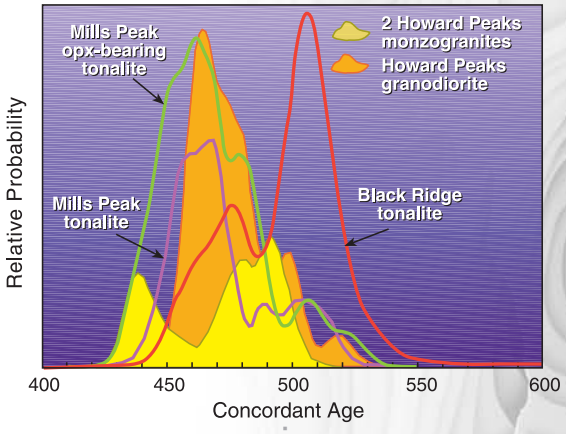

Our preferred explanation of the textural and compositional features of the studied zircons is that isotopic and elemental resetting occurred in the analyzed grains, and was related to sub-solidus recrystallisation, producing a strong modification of the trace-element distributions and the U-Pb system. The wide range of trace-element compositions is not always related to different age or structural domains; eg similar Th/U ratios are found in different types of growth or age domains in zircons. This suggests that the mobility of elements during the secondary processes causing resetting was variable and probably related to the degree of fluid access, aided by the occurrence of numerous fractures in the studied grains.

There appear to be two main processes responsible for the great variety in zircon age signatures, the modification of zircon zonation and trace-element redistribution:

1) pervasive deformation and sub-solidus recrystallisation related to the occurrence of a dextral strike-slip shear zone in this area
2) slow cooling of the pluton, probably associated with new mafic magmatic pulses

Figure 4. Chondrite-normalised trace-element abundances of zircons. The dark field contains the unreset compositions.

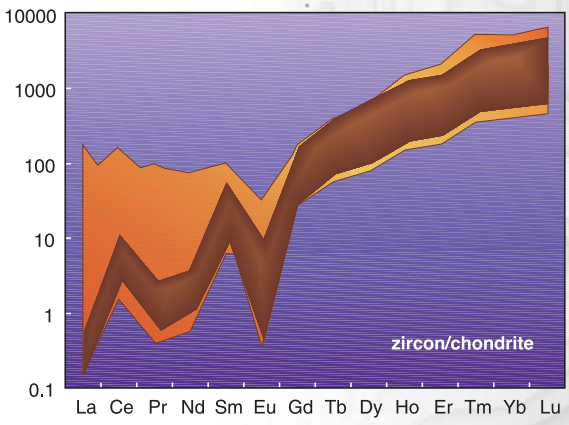

Contacts: Rosa Maria Bomparola, Bill Griffin, Sue O'Reilly
Funded by: Università degli Studi di Siena, Italy

From dunite to lherzolite: tracking refertilisation of Archean peridotite in Norway

GARNET PERIDOTITES are widely distributed across the Proterozoic Western Gneiss Region (WGR) of western Norway and typically occur as discrete zones within larger masses of dunite. Previous work on the WGR peridotites has tended to focus on the garnet peridotites as the most interesting rock type, but this disregards the volumetrically most significant part of the peridotite bodies. The dunites have long been interpreted as retrograded garnet peridotites, based on the close spatial relationship between the two rock types and evidence for retrogression of garnet and clinopyroxene to chlorite and amphibole (also minor phases in some dunites) along the margins of the garnet peridotite bodies. However, analyses carried out at GEMOC, at the Technical University of Trondheim and by A/S Olivin (the company that mines the dunite for refractory material) show that this interpretation is very unlikely. In fact, the bulk of the dunites at the major Almklovdalen locality in the southern WGR are highly refractory and cannot represent retrograded garnet peridotite.

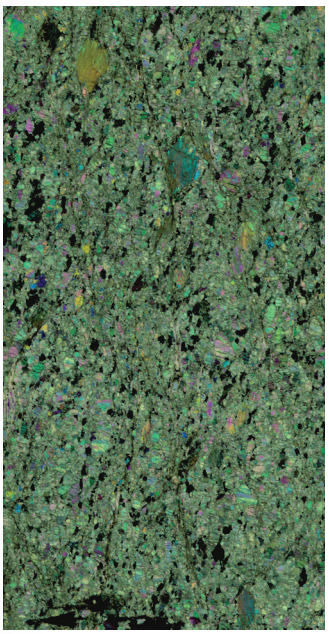

FROM DUNITE.....

Dunite quarry at Ekremseter, Western Gneiss Region, Norway, and thin section image of a garnet-free dunite.

This poses the problem of how to explain the presence of small volumes of relatively fertile material (the garnet peridotites) within large bodies of extremely depleted dunite. Melt modelling suggests that the Almklovdalen dunites formed at significantly higher pressures (5-7 GPa) than the garnet lherzolites at the same locality (2 GPa) which rules out a simple melt-depletion relationship. Another possibility is that the garnet peridotite bodies represent zones of melt percolation and subsequent refertilisation of the dunite. This is supported by the common association of the garnet peridotites with bands of eclogite and garnet pyroxenite, which might represent the crystallisation of percolating mafic melts. Another line of evidence is the compositional

resemblance between the Almklovdalen garnet peridotites and the high-T sheared garnet peridotite xenoliths found in many kimberlites; the latter are widely regarded as representing refertilisation of ancient depleted cratonic lithosphere.

Whole-rock compositions for the garnet peridotites show that they are moderately depleted in most basaltic components but show an overall enrichment in Fe relative to the low-T peridotites typical of cold, melt-depleted lithospheric mantle. This pattern is characteristic of high-T sheared xenoliths and suggests re-enrichment of a depleted precursor. Furthermore, rare earth element patterns for the Almklovdalen garnets are enriched in heavy rare earth elements (REE) but depleted in light REE, similar to garnets from high-T sheared peridotite xenoliths.

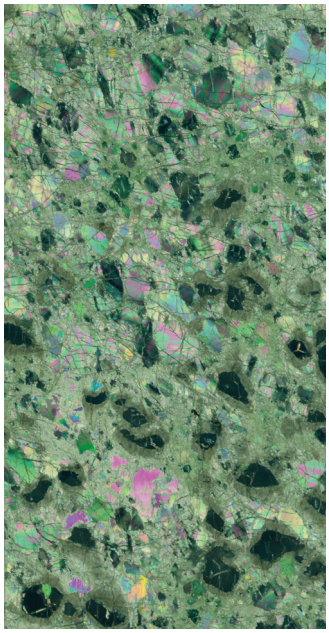

.....TO LHERZOLITE

Garnet peridotite block from a quarry in Gusdal, Western Gneiss Region, Norway. The thin section image is a garnet-rich lherzolite.

Similar garnets are abundant in shallow layers of many Archean and Proterozoic mantle sections investigated by GEMOC, and are interpreted as evidence for the progressive refertilisation of depleted harzburgites to yield more fertile lherzolites. Recognition of this process has led to speculation that at least some Proterozoic lithosphere may represent strongly reworked Archean lithospheric mantle. The WGR peridotite bodies are widely considered to be contemporaneous in age with their Proterozoic host rocks. However, a mixture of both Archean and Proterozoic Re-Os model ages determined for the Almklovdalen garnet peridotites (see *Research Highlights 2001*) suggests that these bodies may in fact represent Archean lithospheric mantle reworked during the Proterozoic. During 2002, whole-rock Re-Os dating of several very depleted WGR dunites has yielded Archean model ages, adding further weight to the sulfide data. The presence of Archean mantle fragments in the Proterozoic crust of the WGR has major implications for the evolution of the western part of the Baltic Shield and may require a reassessment of crustal growth history in this region.

Contacts: Eloise Beyer, Sue O'Reilly, Bill Griffin
Funded by: ARC, Macquarie University Postgraduate Research Grant, GEMOC

Fingerprinting diamonds

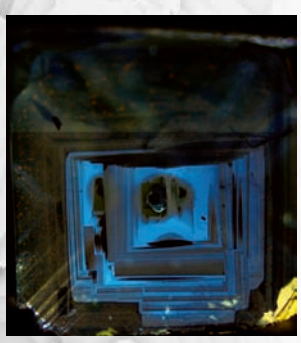

Figure 1. A cathodoluminescence image of the internal structure of a diamond from Koffiefontein, South Africa, showing growth zoning. Trace-element variations can be correlated with zonal patterns imaged by CL.

THE CHEMICAL COMPOSITION of diamond can be expressed very simply as almost 100% carbon. But is there anything that makes each diamond unique? Can we distinguish between diamonds formed from different sources in different parts of the world? Even within a single locality, the diamonds may differ from each other because of variations in the mantle host rock compositions, depth of formation, and conditions of growth. Studying the trace elements in diamonds may provide an answer.

Most diamonds, during crystallisation, incorporate minute amounts of trace elements, either in their crystal lattice or as submicroscopic inclusions, and may represent the medium/fluid from which the diamonds grew. Once they are trapped inside the diamond, the inclusions do not react with the environment unless exposed to oxygen and/or high temperatures. Characterisation of the trace-element (especially rare earth element) patterns of diamond has been suggested as a possible means of "fingerprinting" stones from different sources. The question is more than scientifically interesting - it has geopolitical implications. "Conflict diamonds", mined illegally in war zones, are used to launder illicit funds and to finance wars, and represent a major headache for the legitimate diamond industry. The ability to identify the sources of diamonds on the market could help to limit this trade.

To test these ideas and to find out more about how diamonds form, the trace-element compositions of diamonds are being determined by laser ablation ICPMS (LAM ICPMS), using a two stage analytical technique developed at GEMOC by Simon Jackson. Both gem-quality and industrial-quality stones are being studied; the latter have higher trace element contents. Many of the diamonds are prepared as polished plates, where trace-element variations can be studied in a spatial context and correlated with zoning patterns imaged by cathodoluminescence (CL; Fig. 1).

The diamonds come from a range of localities including Siberia, Eastern Australia (Wellington and Bingara), Brazil (Juina), Canada (Slave Province), Thailand, and South Africa (Koffiefontein, Finsch, and Premier mines). Fibrous diamonds from Jwaneng and Central Africa are also being studied. Mineral inclusions are used to classify the diamonds into eclogitic, peridotitic and superdeep parageneses, and diamonds of different paragenesis from the same locality are being studied.

Preliminary results indicate broad similarities in trace-element patterns (but differences in abundances) of the samples analysed. The patterns of many diamonds, and especially those of fibrous diamonds, strongly resemble those of average carbonatite and average kimberlite (Fig. 2), but the strong negative anomalies for elements such as Zr, Ti and Nb in these patterns are more similar to the carbonatite pattern. This exciting result suggests a genetic link between these mantle melts and diamond genesis. Despite the broad similarities, there appear to be some consistent differences

TerraneChron™ success keeps soaring

GEMOC's TerraneChron™ is delivering a valuable new tool to the exploration industry. Integrated with our methodology for dating mantle sulfides in situ, it is also providing an additional novel solution to tracking the timing of formation of crust and mantle components in the same lithospheric column.

Industry tool ***TerraneChron*™ has been shown to be able to map the tectonic history of complex regions with "uncanny accuracy" according to one of our Industry partners exploring an extensive, difficult and largely unmapped terrain. *TerraneChron*™ analyses zircon concentrates from defined drainages using three instrumental *in situ* techniques to provide the zircon ages (U-Pb method), their host rock type (from our trace-element database) and the type of tectonic event that produced the host rock (the Hf isotopic composition defines whether crust recycling and/or mantle input was important). This information yields a synthesis of the tectonic history represented in the drainage area (Publications #251, 261, 288, 289, 291, 300).**

Unravelling crust-mantle connections **Understanding the complexity of continental assembly, breakup and rearrangement requires tracking the timing of events that have affected the crust and mantle components. Important questions include:**

- **Was formation of the crust and the underlying lithospheric mantle contemporaneous?**
- **How long have crust-mantle sections been coupled?**

GEMOC has also developed a method for measuring Re-Os *in situ* in mantle sulfides (see *Technology Development*), thus determining the model ages recorded by each sulfide with an identified petrological spatial relationship. This is a breakthrough in unravelling the timing of significant mantle events that precipitated new sulfides, or interacted with existing ones. Thus *TerraneChron*™ provides timing and tectonic style information for crustal terranes and the sulfide Re-Os *in situ* method yields timing and context information for multiple mantle events recorded in single rock types (Publications #267, 268, 290, 292).

THE COMBINATION OF THESE TWO NOVEL METHODOLOGIES CAN NOW BE APPLIED TO UNDERSTANDING CRUST-MANTLE RELATIONSHIPS DURING LITHOSPHERE FORMATION AND THROUGH SUBSEQUENT LITHOSPHERE EVOLUTION EVENTS.

between diamonds of different parageneses, and between diamonds of similar paragenesis from different localities. If these variations prove to be statistically significant, they may offer a possibility of fingerprinting diamonds from different sources, and of unravelling the mechanisms of diamond formation.

Contacts: Sonal Rege, Bill Griffin, Sue O'Reilly
Funded by: GEMOC, Macquarie University

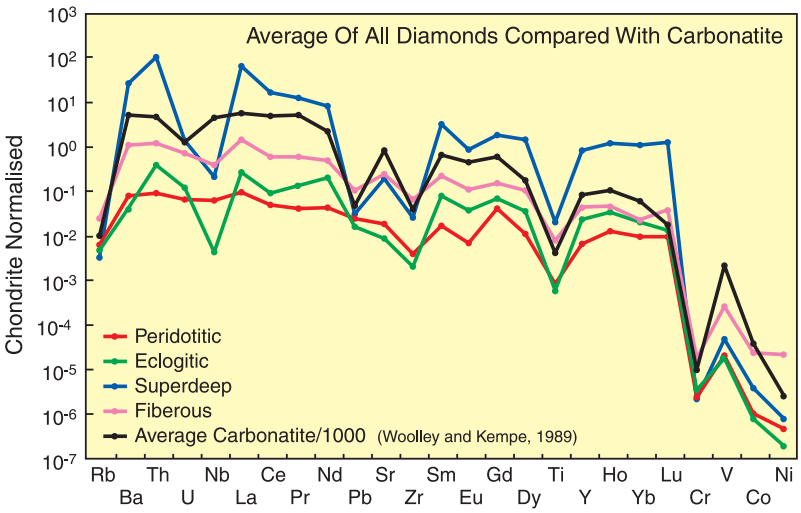

Figure 2. Trace-element compositions of diamonds from different parageneses analysed by LAM-ICPMS.

Inclusions in a diamond from Finsch, South Africa.

Lower crustal terranes in the North China Craton – new surprises from xenoliths

THE LOWER CRUST is an important lithospheric layer, that may integrate the history of crust-mantle interaction through time. Some of the best direct evidence about this history comes from the examination of lower-crustal xenoliths, usually granulites, brought up in volcanic eruptions. In 2002 GEMOC and the China University of Geosciences (Wuhan) collaborated on integrated U-Pb and Hf-isotope studies of zircons in such xenoliths from two widely spaced localities in the North China Craton (Fig. 1): Fuxian in the northeast, and Henan along the southern margin. The craton consists of several nuclei; ancient rocks (>3.5 Ga) are known in the northeastern part, whereas the oldest rocks in the Henan region are ca 2.8 Ga.

Figure 1.

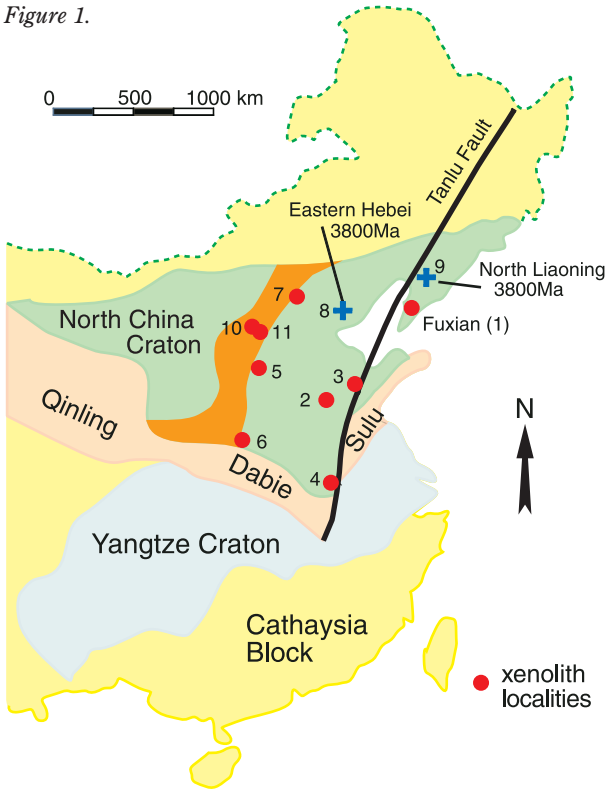

Mafic granulite, amphibolite and garnet-metagabbro xenoliths in the Paleozoic Fuxian kimberlites (locality 1) contain zircons with an obvious multistage history, which is strikingly revealed in their BSE/CL images (Fig. 2) – older strongly zoned cores are overgrown by wide structureless rims. U-Pb dating using LAM-ICPMS yielded concordant ages ranging from 2620-2430 Ma for the strongly zoned portions, and near-concordant ages of 1927-1852 Ma for rims and structureless grains. One granulite contained two populations of structureless grains, dated at 1927 ± 55 Ma and 600-700 Ma.

The interpretation of the U-Pb ages was enhanced by measuring the Hf-isotope ratios of the same grains, using GEMOC's LAM-MC-ICPMS facility. In each sample zircons with 2620-2430 Ma ages showed no variation in their $^{176}Hf/^{177}Hf$ ratios (ie their ε_{Hf} lie on the evolution curves in Fig. 3). This suggests that the spread in ages reflects semicontinuous loss of radiogenic Pb (but no exchange of Hf with the surroundings) during slow cooling of the mafic magmas in the lower crust. In this case the oldest ages are closest to the magmatic intrusion age. In some granulites, the younger zircons have much higher $^{176}Hf/^{177}Hf$ than the older ones (ie their ε_{Hf} lie above the evolution curves in Fig. 3). This pattern strongly suggests that they grew from Zr and Hf liberated by breakdown of the older silicate minerals, in which radiogenic ^{176}Hf had grown from ^{176}Lu over the intervening time. In other samples, the younger and older zircons have similar $^{176}Hf/^{177}Hf$, and the younger ages thus appear to represent recrystallisation of the older zircons, rather than growth of new zircon.

The 2.6 Ga ages in the Fuxian xenoliths are similar to many ages from upper-crustal rocks in the area, and represent a major period of crustal growth in the

Figure 2.

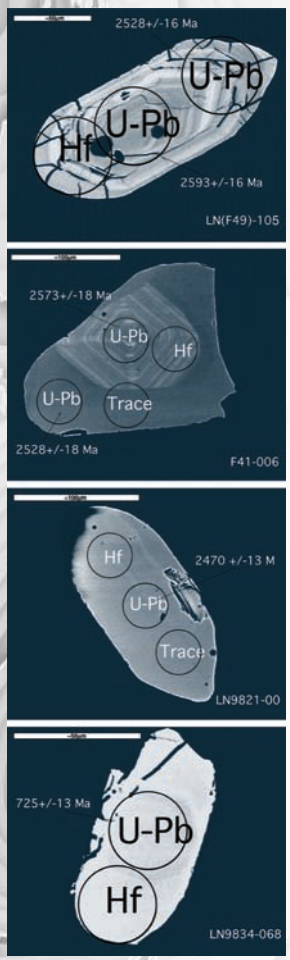

craton; it appears that mafic magmas were being added to the lower crust during this episode. The 1.8-1.9 Ga ages correspond to the collision between the Eastern and Western Blocks that led to the final assembly of the North China Craton. The growth of metamorphic zircon at ≈600 Ma may be related to an asthenospheric upwelling and crustal heating in Neoproterozoic time, which produced a regional disconformity across the North China Craton.

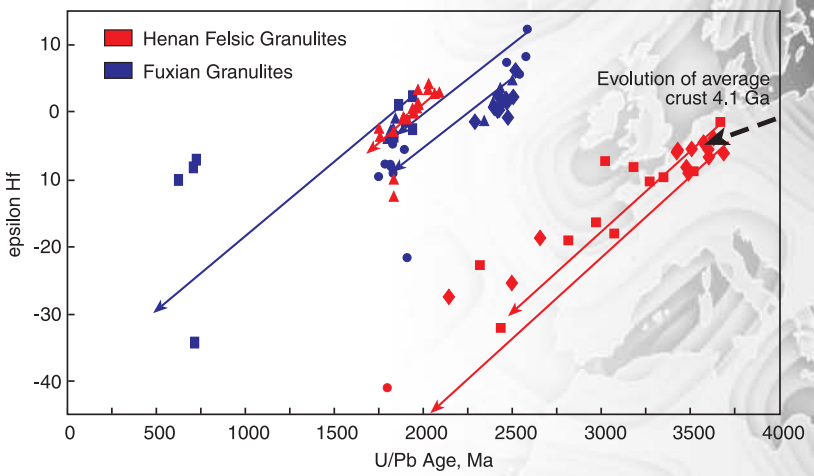

Figure 3. Hf-isotope evolution lines (reflecting simple Pb loss) and data points for zircons from N. China granulite xenoliths.

While the Fuxian granulites recorded the expected major crustal events in the NE part of the craton, a greater surprise awaited us in the felsic granulite xenoliths from Mesozoic lamprophyres in Henan (locality 6). LAM-ICPMS dating at GEMOC, and single-grain U-Pb dating in China, combined with Hf-isotope analysis, showed that two granulites crystallised at ca 3.6 Ga (near-concordant upper intercept dates), and grew new, concordant metamorphic zircon at several stages between 2.8 and 1.7 Ga (Fig. 3). A third granulite contained only metamorphic zircons, with an upper-intercept age of 1991 ± 50 Ma and a poorly defined lower intercept age of 830 ± 290 Ma; all lie on the evolution line predicted for simple Pb loss. However, this sample contains two zircons with lower ε_{Hf}, suggesting an older component.

The older group of zircons has $^{176}Hf/^{177}Hf$ below the mantle evolution line (Fig. 2; $\varepsilon_{Hf} \approx -5$), which indicates derivation by remelting of an older source rock. Whether this source was felsic or mafic, its age must be more than 3.9 Ga, and almost certainly more than 4.1 Ga, similar to the oldest crustal ages known on Earth. What makes this finding extraordinary is that the oldest rocks now exposed in the upper crust of the Henan part of the North China Craton are only ca 2.6 Ga old, and the nearest exposed 3.5 Ga rocks are found over 1000 km to the NE (Fig. 1).

The Henan xenolith data show that parts of the lower crust may be not only more felsic than expected from similar data worldwide, but also much older than the overlying upper crust. It this finding is repeated in many other places, it will affect our ideas on the composition of the crust, and especially on the rates of crustal generation through time.

Dr Ming Zhang at a spectacular outcrop of granulite and peridotite xenoliths, Hannuoba, North China Craton.

Contacts: Bill Griffin, Sue O'Reilly, Jianping Zheng and Ming Zhang
Funded by: ARC, GEMOC, AusAID ACICP, Macquarie University

La plume de mon Massif ?

THE FRENCH MASSIF CENTRAL region (Fig. 1) is an uplifted area of Hercynian (400-250 Ma) metamorphic and granite rocks, originally part of a convergent mountain belt. Alkaline volcanism occurred from the late Tertiary into Quaternary time, bringing abundant mantle and crustal xenoliths to the surface. The uplift, volcanism and high regional heat flow have been attributed to a mantle plume beneath the recently active volcanic areas such as Cantal, Velay and Devès. The plume has been imaged by seismic tomography (Fig. 2), but its existence is still controversial and other suggestions are that the mantle upwelling could be the result of the Alpine orogeny. The penetration of the Alpine root could imply asthenospheric flow and thermal-mechanical erosion of the lithosphere which could be responsible for extension and subsequent Tertiary-Quaternary volcanism. Recent geophysical studies by French geophysicists have shown that the Massif Central is made of two different lithospheric domains separated by a lithospheric fault (Sillon Houiller; Fig. 1).

Figure 1. Simplified geological map of the French Massif Central.

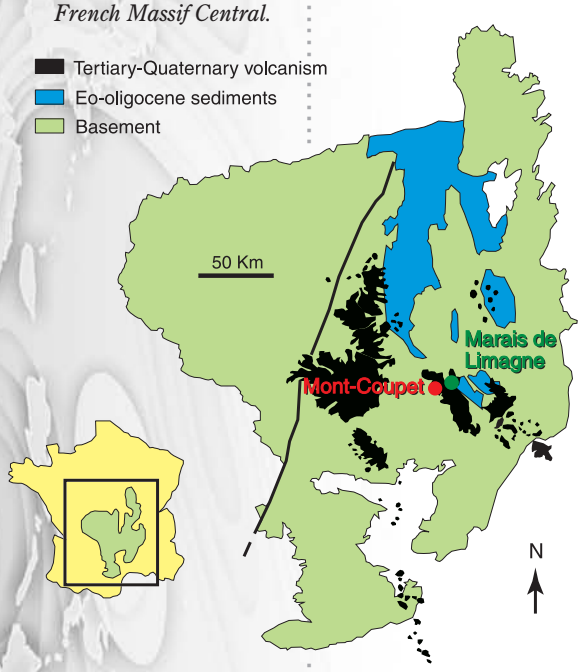

The petrographic and geochemical analysis of the mantle and crustal xenoliths in the basalts provides a unique opportunity to understand the nature of the mantle diapir associated with lithospheric thinning, lithospheric mantle heterogeneity and metasomatic processes beneath the French Massif Central. A research program, part of the international collaboration between GEMOC and Jean Monnet University, Saint-Etienne (France) and the University of Clermont-Ferrand, is investigating the regional heterogeneity in the mantle of the Massif Central.

The primary aims of the project are to relate geochemical data for the French peridotites to the available geophysical data in order to answer questions such as: What are the metasomatic agents percolating through the mantle? What is the contribution of the lithospheric mantle to the Tertiary and Quaternary alkaline volcanism? The work so far has focused on spinel-bearing peridotites from two localities, Marais de Limagne (Fig. 3) and Mont-Coupet (Fig. 4), located in Devès volcanic district; both are dated as erupting at 1.9 Ma.

Figure 2. Tomographic image beneath Cantal and Velay volcanic districts, after Granet et al., Bull. Soc. Geol. France, 2000, 171, 149-167: SH = Sillon Houiller.

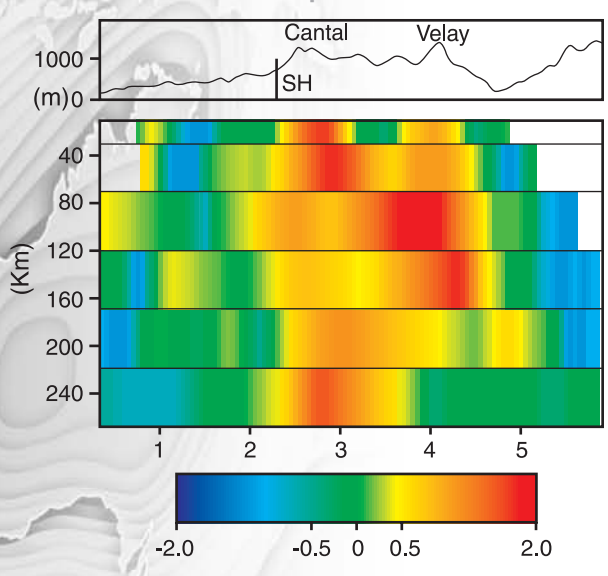

Petrographic studies show that peridotites from Marais de Limagne contain more volatile-bearing phases (such as amphibole and phlogopite) and cover a larger range of microstructures than those from Mont-Coupet. The major element compositions in the mineral phases (Mg# vs Al_2O_3, SiO_2, CaO) do not show systematic trends in samples from Marais de Limagne, whereas those from Mont-Coupet show a trend that is compatible with partial melting. The calculated equilibrium temperatures are higher in samples from Marais de Limagne than from Mont-Coupet. Trace-element compositions in both clinopyroxene and amphibole phases show variability at both outcrop scale and sample scale.

The lherzolites from Marais de Limagne are inferred to come from deeper levels (higher temperatures) and they are more affected by complex metasomatism than the ones

from Mont-Coupet. The mantle beneath Devès volcanic district therefore shows significant heterogeneity between two closely-spaced localities of similar age.

Stable isotope analyses (Jean Monnet University) and radiogenic isotope analyses (GEMOC) are starting to provide more information about the metasomatic agent.

Contacts: Stephanie Touron, Sue O'Reilly, Jean-Yves Cottin, Gilles Chazot
Funded by: ARC Discovery and IREX, Macquarie University, Eurodoc and the French Government Co-tutelle program

Figure 4. Mont-Coupet Locality

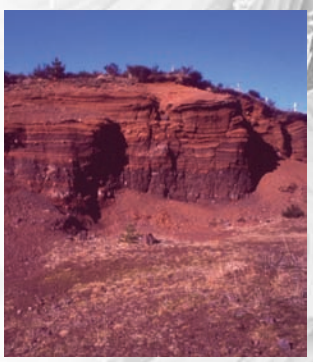

Figure 3. Marais de Limagne Locality.

Hafnium in rutile frees Slave secrets

THE KIMBERLITES of the Slave province in northern Canada contain abundant, but small (1-3 cm) xenoliths of eclogites, many of which contain diamonds. As part of a collaborative project with Kennecott Canada, GEMOC is carrying out a detailed investigation of eclogite xenoliths from the Lac de Gras kimberlites. We hope to find out when and where they formed, and their spatial relationship to other lithologies in the lithospheric mantle. Many of these samples, including the rutile-bearing varieties, have major and trace-element signatures, eg positive Eu and Sr anomalies, suggesting that an origin as subducted oceanic crust should be considered.

Because the samples are so small, and commonly altered, it is difficult to date the eclogites by conventional means. Eclogitic rutile is a major carrier of Hf, and its Hf isotopic composition can be measured *in situ*, for age determinations and to constrain the nature of the eclogite source. We have used a New Wave/Merchantek LUV266 laser microprobe attached to GEMOC's Nu Plasma multicollector ICP-MS to measure the Hf-isotope composition of individual rutile grains in polished sections. We also have measured the abundances of Lu and Hf, as well as other trace elements, in the rutile (Fig. 1) and the major minerals (garnet and clinopyroxene) of the eclogites, using a laser microprobe attached to an Agilent

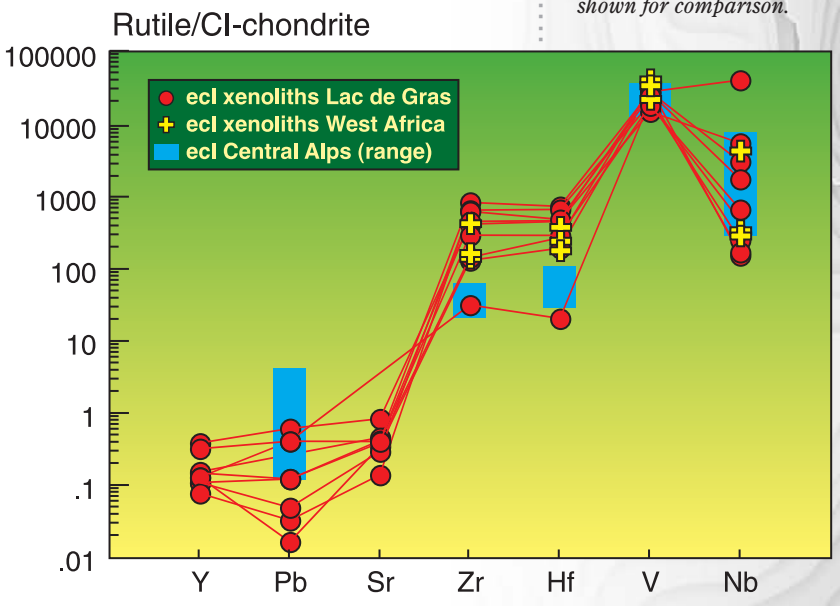

Figure 1. Chondrite-normalised trace-element patterns of rutile in eclogites and pyroxenites. Element order corresponds to increasing compatibility of the elements in the rutile. Trace-element patterns of eclogitic rutile from the literature are shown for comparison.

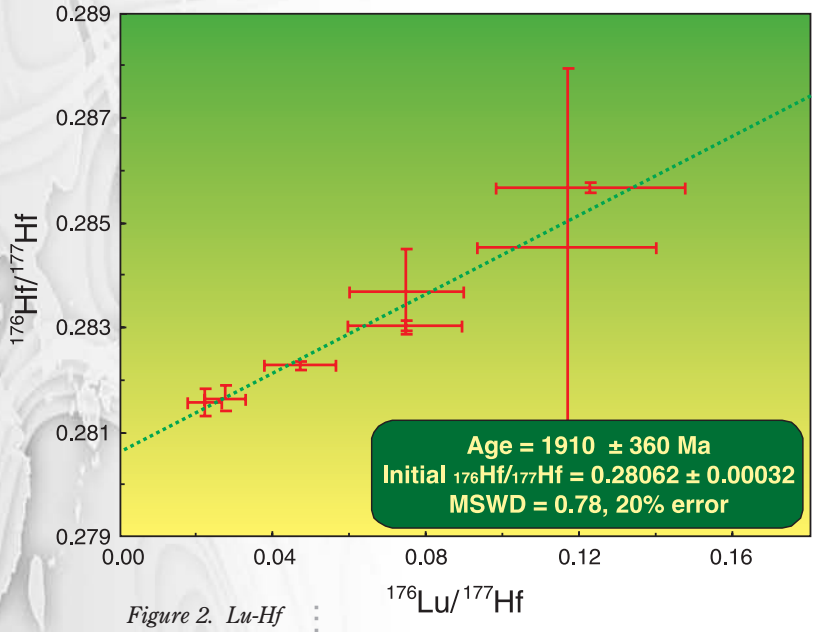

Figure 2. Lu-Hf isochron diagram.

7500 ICPMS (see *Technology Development section*). These analyses, and the modal abundances of the minerals, have been used to reconstruct the bulk Lu/Hf ratios of the whole rocks. The values we determined are comparable to those obtained in other studies, supporting the validity of our analytical method.

$^{176}Hf/^{177}Hf$ in the rutiles ranges from 0.28156 ± 0.00026 to 0.28567 ± 0.00010. Rutile contains very little Lu, and the variability in Hf isotopic composition is most easily explained by isotopic equilibration with coexisting high-Lu/Hf phases such as garnet. If the eclogites resided in the lithospheric mantle above the closure temperature, the Hf isotopic composition of rutile should reflect that of the eclogite at the time of entrainment in the kimberlite. Using the Lu/Hf of the reconstructed whole rocks and $^{176}Hf/^{177}Hf$ of rutile, seven of eight samples define an isochron (Fig. 2). The excluded sample, in contrast to the others, has trace-element abundances consistent with the loss of partial melt.

The isochron gives an age of 1.91 ± 0.36 Ga, with an initial Hf isotopic composition of 0.28062 ± 0.00032 (MSWD = 0.78, assuming 20% uncertainties on the reconstructed whole-rock $^{176}Lu/^{177}Hf$). What does the age record? One interpretation is that the eclogites represent subducted oceanic crust of Proterozoic age. After its amalgamation at ~2.7 Ga, the Slave Craton was involved in several collisions along its western and eastern margin (Fig. 3). The isochron age is very close to the age of eastward oriented subduction that produced the Great Bear magmatic arc at 1.875 to 1.840 Ga west of the Slave craton, following collision with the Hottah arc. However, the initial $^{176}Hf/^{177}Hf$ is very depleted, and corresponds to the ratio expected in the upper mantle at ca 3.2 Ga – similar to the age recorded by the Re-Os systematics of sulfide inclusions in the Slave peridotites (*see Research Highlights 2001*). This could suggest isotopic equilibration between the eclogites and the peridotites, which would make the meaning of the isochron age questionable. Several other interpretations remain open, and are being tested by Re-Os analysis of the eclogites.

Figure 3. Structural provinces of northwestern Canada. Star denotes sample locality.

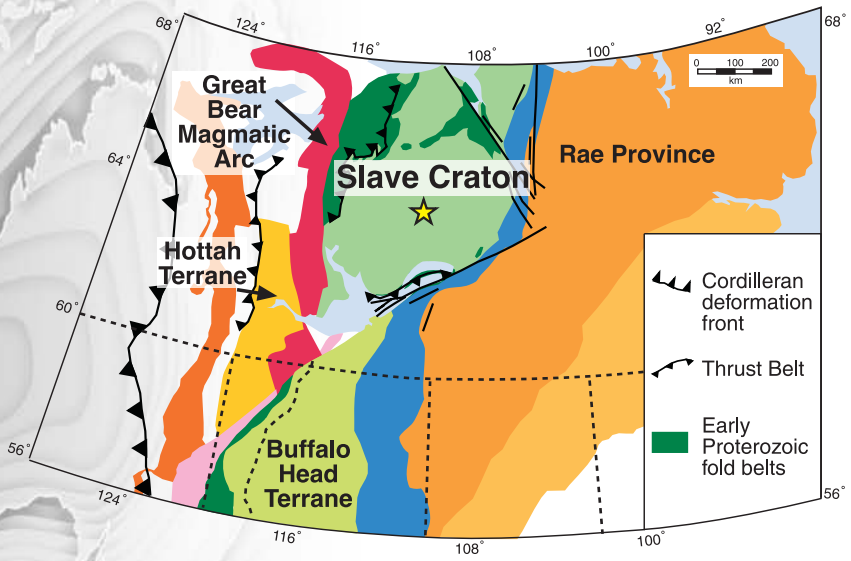

Contacts: Sonja Aulbach, Bill Griffin, Sue O'Reilly
Funded by: ARC SPIRT, ARC Discovery, Macquarie University

Mantle composition and processes beneath the Taiwan Strait, SE Asia

THE EVOLUTION of the subcontinental lithospheric mantle (SCLM) is of fundamental importance to understanding the growth and stability of continents and long-term mantle evolution. Studies of mantle xenoliths from continental areas have shown that the SCLM has a complex history of depletion and enrichment, related to multiple episodes of partial melting and metasomatism. Extensive and widespread Cenozoic basaltic volcanism in Eastern China captured abundant mantle xenoliths, which make it possible to evaluate the compositional heterogeneity of the SCLM beneath the region, and the processes that produced it.

The region underwent major lithospheric thinning and extension in Miocene time, leading to submergence of the crust. Mantle xenoliths occur in Miocene (~16-8 Ma) intraplate basalts from Taiwan and Penghu Islands, SE China (Fig. 1). The generation of the basalts is generally attributed to Cenozoic lithospheric extension which could have resulted in thermo-mechanical erosion of the basal SCLM by convective upwelling of the asthenosphere. Consequently, during ascent, the extension-induced basalts that are derived mainly from the asthenosphere may tap the SCLM beneath this region.

The xenoliths are dominantly spinel peridotites with rare spinel and spinel-garnet pyroxenites and one reported garnet peridotite. The equilibration temperatures of spinel peridotites range from 879°C to 1250°C. Most peridotites have fine to coarse-grained porphyroclastic or equigranular microstructures, and some are foliated. They commonly show textural disequilibrium with clinopyroxene exsolution lamellae in orthopyroxenes, spinel exsolution in clinopyroxenes, and strained clinopyroxene grains coexisting with strain-free clinopyroxene neoblasts. Some orthopyroxenes have cores with high Ca contents, indicating partial equilibration of the rims to lower temperatures. These observations suggest that the peridotites have originated from upwelling of deeper mantle materials.

The peridotites show a large range in modal clinopyroxene contents; some have more clinopyroxene (>20%) than most estimated primitive mantle compositions. Rare depleted peridotites contain amphibole and/or apatite. However, the major-element data suggest that some of the lithospheric mantle beneath this region is quite refractory. The Fo contents of olivine in spinel peridotites range from 86.0 to 91.6, but most fall between 90.0 and 91.0; mg# of olivine is correlated with cr# (0.11~0.55) in spinel.

Trace-element patterns of clinopyroxene in these peridotites can be divided into three types: depleted, enriched and intermediate. The depleted patterns ($(La/Yb)_N \approx 0.1\sim0.3$; $(La)_N \approx 0.2\sim0.7$) are typical of unmetasomatised, refractory, lithospheric mantle. The enriched and intermediate ones provide fingerprints of different metasomatic episodes. At least two episodes of metasomatism can be recognized. High La/Yb and low Ti/Eu ratios in clinopyroxenes

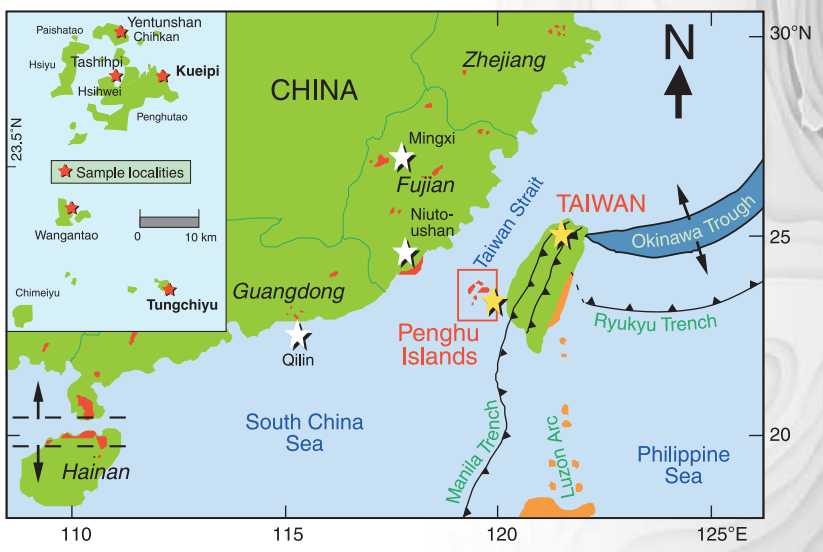

Figure 1. Simple tectonomagmatic map of South China and adjacent regions. Red areas mark outcrops of late Cenozoic intraplate basalts. Stars mark localities of mantle xenoliths: yellow, samples studied here; white, samples from other GEMOC projects. Inset: sample localities.

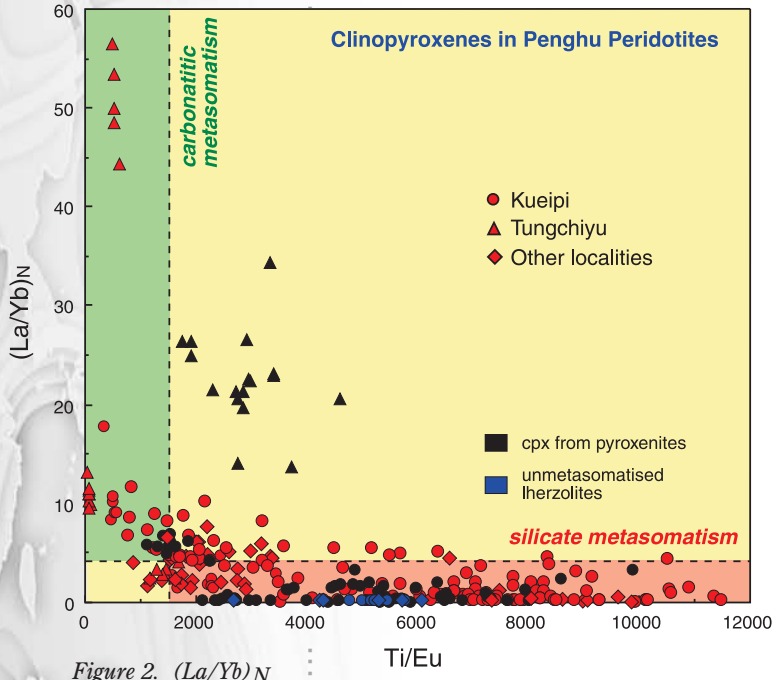

Figure 2. $(La/Yb)_N$ vs Ti/Eu ratios of clinopyroxenes from Penghu Islands peridotites and pyroxenites.

indicate carbonatitic metasomatism, which the GEMOC database shows to be typical for extensional settings worldwide (Fig. 2). The other metasomatic signature is geochemically characteristic of silicate melt interaction.

Further work will map the distribution of these two processes with depth. Preliminary *in situ* Re-Os analysis of sulfides in the mantle peridotites reveals old ages for the original lithospheric mantle formation and suggests that some Proterozoic mantle domains have survived, but may have been subjected to metasomatic re-enrichment during the Miocene extension and thinning in this region.

Contacts: Kuo Lung Wang, Sue O'Reilly
Funded by: ARC, Macquarie University, National Taiwan University

Waves of fluid invade the mantle beneath western Victoria

METASOMATIC EFFECTS have been widely recognised and described in mantle samples delivered to the Earth's surface as xenoliths in deeply-derived magmas. The thin and shallow lithospheric mantle beneath western Victoria, sampled by basaltic volcanics, records multiple and varied episodes of fluid percolation. Modal metasomatism by the fluids deposited different generations of metasomatic minerals including amphibole, phlogopite, clinopyroxene and apatite. Cryptic metasomatism altered the trace-element abundances of phases already present in the mantle wall-rock by partitioning of elements between the minerals and the metasomatising fluid, imparting a 'signature' characteristic of the fluid type.

Foliated amphibole-bearing xenolith from Bullenmerri, western Victoria.

Clinopyroxene is the main host phase for trace elements in the (common) mantle assemblage olivine + orthopyroxene + clinopyroxene + spinel, which makes it most important for identifying trace-element signatures of cryptic metasomatic agents. However in modally-metasomatised lithospheric mantle, phases such as amphibole, phlogopite or apatite contain significant parts of the whole-rock trace-element budget, and must be included in attempts to characterise metasomatic agents.

Samples from Bullenmerri and Gnotuk, Western Victoria provide a unique opportunity to study the effects of multiple episodes of modal metasomatism on a lithospheric volume. The xenolith suite at these localities contains a diverse range of rock types and assemblages from the garnet- and spinel stability fields, including peridotites, pyroxenites and granulites, some of which contain amphibole ± phlogopite ± apatite. Previous studies of xenoliths from western Victoria have ascribed their features

to several metasomatic agents, including silicic- and carbonate-rich types. A selection of amphibole (± apatite) bearing xenoliths was chosen for this study, to further characterise the metasomatic episodes undergone by the lithospheric mantle in western Victoria.

The xenoliths in this study can be divided into groups that show differences in geochemical, isotopic, modal, and petrographic features, inferred to reflect differences in metasomatic agent(s). Samples in *Group A* have features consistent with silicate metasomatism, *Group B* has features consistent with metasomatism by a carbonate-rich fluid (such as a carbonatite), and *Group C* samples have features overlapping those of groups A and B, although metasomatism by a silicic metasomatising agent with a hydrous component appears likely.

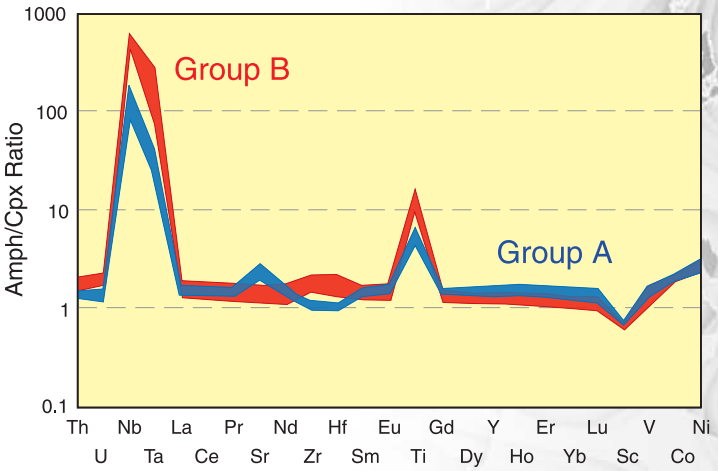

Figure 1. Values of $D_{amph/cpx}$ for western Victorian xenoliths.

Amphibole and clinopyroxene major-and trace-element compositions vary systematically between the groups. In Group A samples, amphibole and clinopyroxene are relatively low in Si, Na and Cr, and high in Al and Ti. In Group B both phases are relatively enriched in Si, Na and Cr, and low in Al and Ti. Distribution of trace elements between coexisting clinopyroxene and amphibole is also found to vary systematically between the groups (Fig. 1).

Amphibole in the lithospheric mantle typically contains abundances of the rare earth elements (REE), Th and U similar to those in coexisting clinopyroxene, and much higher concentrations of elements such as Nb, Ta, and Ti. In Group A samples the ratio of REE concentrations in coexisting amphibole and clinopyroxene ($D_{amph/cpx}$) is generally higher than for Group B samples, particularly for REEs heavier than Sm. $D_{amph/cpx}$ for the high field-strength elements (HFSE: Nb, Ta, Zr, Hf and Ti) is higher in Group B than Group A, and $D_{amph/cpx}$ for Sr is lower. The differences in HFSE partitioning allow decoupling of HFSE trends in mantle processes. The different partitioning may result from the different OH contents of the metasomatising agents, and/or physical site differences in the crystal lattices of the amphibole and clinopyroxene of different compositions, as predicted from their different major-element compositions.

Petrographic section of a foliated, amphibole-bearing spinel peridotite from Gnotuk, western Victoria.

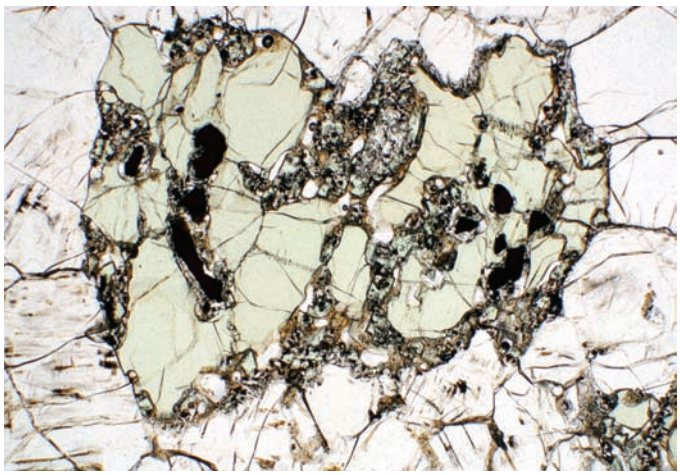

Amphibole surrounding spinel in a mantle xenolith from Bullenmerri, western Victoria. Field of view is approx. 3.5 mm.

Contacts: Will Powell, Sue O'Reilly, Ming Zhang
Funded by: ARC, Macquarie University Postgraduate Research Grant, GEMOC

Ore grades correlate with Cu and Fe isotopic data

METAL ISOTOPE STUDIES of the Candelaria Cu-Au-Fe mine, Chile were carried out as part of a larger investigation into the isotopic fractionation of Cu and Fe isotopes in hydrothermal systems. The results of this study are applicable to other Cu-Au-Fe deposits, a class of deposit in which there is currently considerable interest.

Candelaria (115 Ma old) is the richest of many Cu-Fe-Au deposits hosted by volcanic and volcaniclastic rocks in the Chilean Coastal Cordillera south of Copiapó. Ore occurs as veins, breccias, stringer bodies and replacement bodies in altered rocks within the contact metamorphic aureole of a granite. Several lines of evidence suggest that the ore-bearing fluids had a significant igneous component, probably derived from the granites, but there is also evidence for the circulation of basinal brines. Fluid flow directions are not well constrained, but the major pathway for the mineralising fluids is believed to be the Lar Fault, which crops out in the Candelaria mine pit.

Isotopic compositions of Cu and Fe were obtained *in situ* using laser ablation multi-collector ICPMS. Thirteen hand-sized samples provided by Phelps Dodge represented a ~700 metre stratigraphic section, but these samples were not obtained from a single drill core, which limits the interpretation of fluid flow. Not all samples are mineralised, although most contained pyrite. The main Candelaria open pit occurs toward the base of the section.

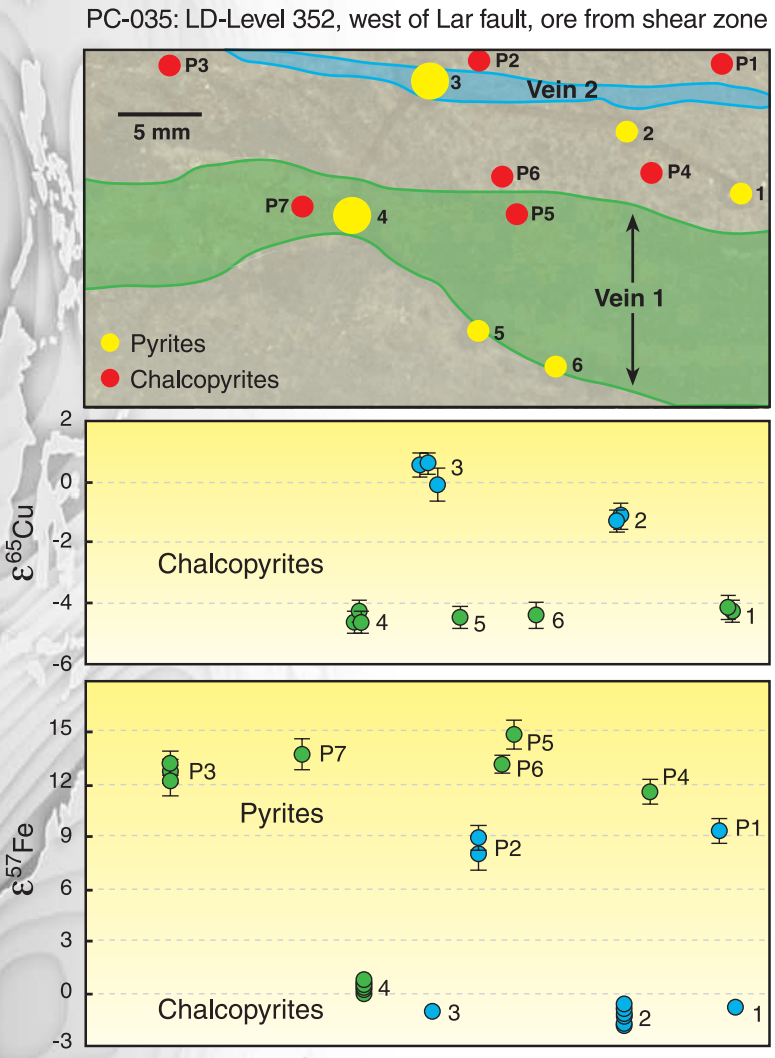

Figure 1. Photo of thin section and diagrams showing the spatial distribution of $\varepsilon^{56}Cu$ and $\varepsilon^{57}Fe$ in chalcopyrite and pyrite. Note the distinct isotopic signatures of the two different veins and the disseminated mineralisation.

Chalcopyrite $\varepsilon^{65}Cu$ varies from -11 to +6, but most values are between -8 and 0. Half of the samples contain two or more isotopically distinct chalcopyrite populations. In some samples different chalcopyrite veins have different $\varepsilon^{65}Cu$ values and these veins are isotopically distinct from disseminated chalcopyrite, suggesting numerous mineralisation events (Fig. 1).

$\varepsilon^{57}Fe$ for chalcopyrite varies from -14 to +8, but most $\varepsilon^{57}Fe$ values are between -7 to 0. In contrast, pyrite $\varepsilon^{57}Fe$ values show a much larger range, from -24 to +15. The pyrite data also form two distinct groups, with $\varepsilon^{57}Fe$ between -22 to -12 and -1 to +13 (Fig. 2). These two groups are almost totally mutually exclusive and do not occur systematically throughout the stratigraphic section. Our investigations of other ore deposits indicate that pyrite with low $\varepsilon^{57}Fe$ is found in relatively low temperature systems (<400°C), such as porphyry related skarns and the McArthur River Zn deposit (see *GEMOC Annual Report, 2001*).

Figure 2 shows how $\varepsilon^{65}Cu$ and $\varepsilon^{57}Fe$ values vary through the stratigraphic

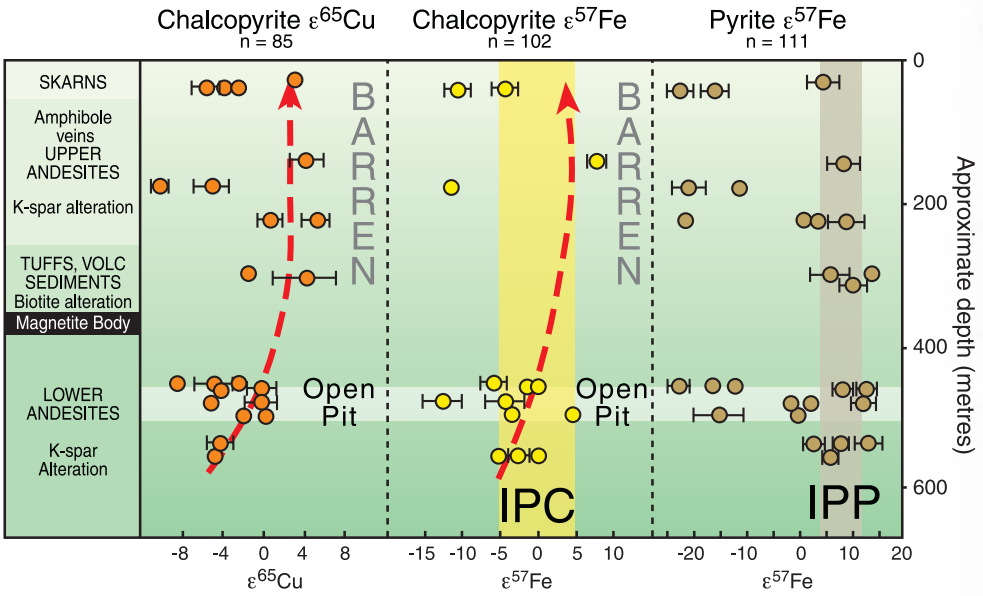

Figure 2. Diagrams showing the variation in $\varepsilon^{56}Cu$ and $\varepsilon^{57}Fe$ of chalcopyrite and pyrite through the Candelaria stratigraphic section.

interval. Also shown on this diagram are the $\varepsilon^{57}Fe$ ranges for chalcopyrite and pyrite porphyry systems (IPC and IPP, respectively). Above the "open pit" the average chalcopyrite $\varepsilon^{65}Cu$ tends to increase with distance from the ore deposit. The samples that lie on this trend, while containing some sulfide, are essentially unmineralised (i.e. BARREN). Two mineralised samples above the ore deposit do not fit this apparent trend and record low $\varepsilon^{65}Cu$ values and low $\varepsilon^{57}Fe$ values. The reason for this correlation is not clear. While we have found low $\varepsilon^{57}Fe$ in pyrite and chalcopyrite from skarn systems associated with magmatic porphyry deposits, chalcopyrite from these systems tends to have high $\varepsilon^{65}Cu$ values.

Isotopic data from the Open Pit samples may provide some insight into the fluids involved in the generation of the ore deposit. Cu and Fe isotope data for chalcopyrite define a limited range, whereas the Fe isotope data from the pyrites span approximately 35 $\varepsilon^{57}Fe$ units (Fig. 3). Pyrite from a shear zone to the west of the Lar fault has high, porphyry-like $\varepsilon^{57}Fe$, whereas pyrite to the east of the Lar fault has low $\varepsilon^{57}Fe$, like pyrite in low temperature systems. This sample also contains pyrite that is isotopically intermediate, whereas the sample in the centre contains both the intermediate and high groups. The presence of pyrite with intermediate $\varepsilon^{57}Fe$ values is highly suggestive of fluid mixing. We therefore believe that the Candelaria ore system contains two fluid components: one is similar to igneous porphyry systems and the other is similar to low temperature sedimentary systems.

Ore-grade samples at Candelaria contain sulfides that have low $\varepsilon^{65}Cu$ and $\varepsilon^{57}Fe$. It appears that metal precipitation away from the main ore zone may have been associated with brines rather than magmatic hydrothermal fluids.

Figure 3. Variation of chalcopyrite and pyrite $\varepsilon^{65}Cu$ and $\varepsilon^{57}Fe$ within the Candelaria open pit. Note the variation of pyrite $\varepsilon^{57}Fe$ from west to east.

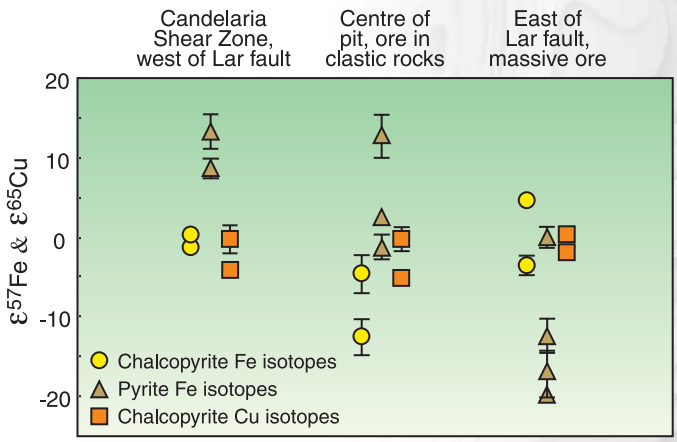

Contacts: Stuart Graham, Simon Jackson, Norman Pearson, Bill Griffin
Funded by: Industry, Macquarie University, GEMOC

Mg isotopes in olivine track fluid flow in the mantle

MAGNESIUM has three naturally occurring stable isotopes, ^{24}Mg (78.99%), ^{25}Mg (10.00%) and ^{26}Mg (11.01%), but little is known about how much the isotopic composition of Mg varies in nature, or why.

Recent developments in multi-collector inductively coupled plasma mass spectrometry (MC-ICPMS) have made it possible to measure the isotopic composition of Mg to a precision ten times better than previously possible. This has stimulated interest in how variations in the isotopic composition of Mg reflect geological and biological environments.

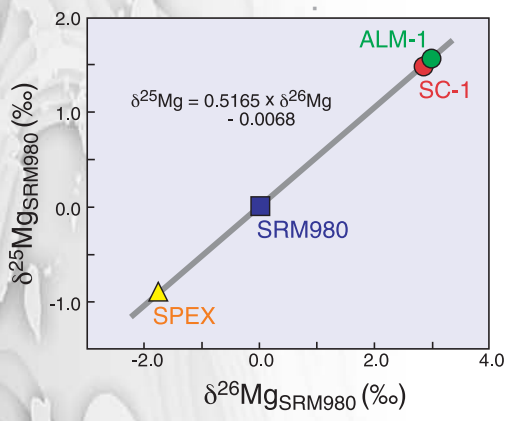

Figure 1. Magnesium three-isotope plot of standard solutions.

During 2002, we have investigated the isotopic variability of Mg in the lithospheric mantle by analysing olivine from peridotite xenoliths and megacrysts from beneath Archean cratons (Siberia, Kaapvaal, Slave), Phanerozoic fold belts (south-eastern Australia) and oceanic islands (Kerguelen Island).

Olivine from a dunite at Almklovdalen, Norway (ALM-1; Fo = 92.9), and spinel lherzolite xenoliths from San Carlos (SC-1; Fo = 91.1), Arizona, USA, were selected as potential laser standards, and analysed in solution, relative to SRM980 Mg and other high-purity Mg ICPMS standards. Solutions were introduced into the plasma using a CETAC MCN 6000 to reduce the levels of H_2O, CO_2, O_2 and N_2 in the plasma. *In situ* analysis used New Wave Merchantek LUV266 and LUV213 laser ablation systems attached to GEMOC's Nu Plasma MC-ICPMS.

Mg isotopic compositions are expressed as per mil (‰) deviation from the isotopic composition of SRM980:

$$\delta^{n}Mg = [(^{n}Mg/^{24}Mg)_{sample}/(^{n}Mg/^{24}Mg)_{SRM980} - 1] \times 1000$$

The three-isotope plot of the Mg isotope ratios (Fig. 1), shows a linear relationship between SRM980, and the solution analyses of Almklovdalen and San Carlos olivines, and high purity Mg (SPEX). The slope of this line is within error of the Terrestrial Fractionation Curve of Galy et al. (Science, 290, 2000; slope = 0.5163).

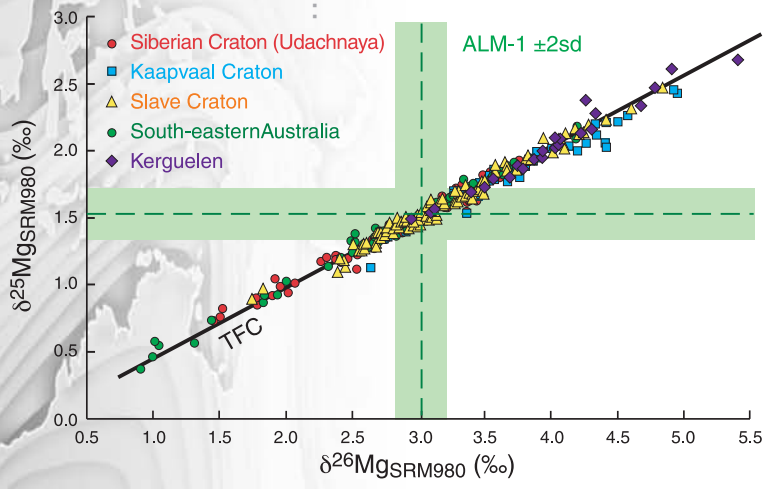

Figure 2. Magnesium three-isotope plot (relative to SRM980) of laser ablation analyses of olivine from peridotite xenoliths and megacrysts from the lithospheric mantle.

Replicate analyses of the Almklovdalen olivine gave a precision of 0.20 ‰ (2σ) for $\delta^{26}Mg$ and 0.12 ‰ (2σ) for $\delta^{25}Mg$. The precision for the San Carlos olivine is greater (0.37 ‰ (2σ) for $\delta^{26}Mg$) because of grain-to-grain differences.

The olivine analyses show significant variations in $\delta^{26}Mg$ and $\delta^{25}Mg$ in the lithospheric mantle. The overall range for the analysed samples is 0.90 - 5.40 ‰ $^{26}Mg/^{24}Mg$ and 0.35 - 2.70 ‰ $^{25}Mg/^{24}Mg$. In the three-isotope plot (Fig. 2), the *in situ* analyses of olivine grains from the lithospheric mantle lie on the Terrestrial Fractionation Curve of Galy et al. (Science, 290, 2000).

There is a broad trend from lighter Mg isotopic compositions in more depleted Archean xenoliths to heavier compositions in the Phanerozoic samples from SE Australia and Kerguelen (Fig. 3). Individual grains and samples show variations in $\delta^{26}Mg$ that are much greater than the external precision determined for ALM-1

(±0.20, 2sd). These heterogeneities suggest that the processes that control Mg isotopic fractionation are preserved on the microscopic scale.

Samples with petrographic evidence of refertilisation (eg Kaapvaal and Slave sheared peridotites) or modal metasomatism (eg SE Australian amphibole + apatite-bearing xenoliths) show large ranges in δMg values. In the spinel lherzolites from SE Australia, olivine becomes more Fe-rich in the amphibole-bearing samples, and these samples also have the largest variation in δMg (Fig. 4).

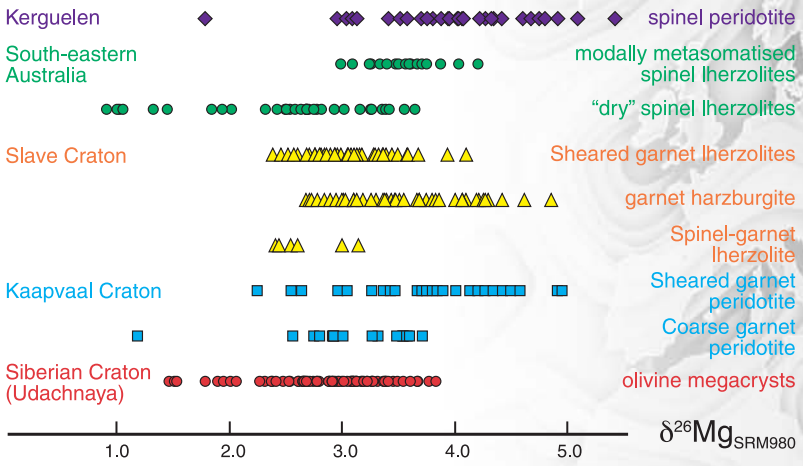

Figure 3. Range of measured δ^{26}Mg (relative to SRM980) of mantle olivine from specified localities.

Sheared peridotite xenoliths from the Kaapvaal and Slave cratons show a shift to heavier δMg values associated with the introduction of fluids with an 'asthenospheric' signature. There is a systematic variation between δ^{26}Mg, Ca content (related to temperature) and the microstructure of the olivine in sample vr40332a (Fig. 5). The variation in the Mg isotopes of the olivine suggests that parts of the sample have been modified by fluids moving along distinct pathways. Preliminary measurement of Fe isotopes in the olivine in vr50855a indicates a positive correlation between δ^{26}Mg and δ^{56}Fe.

The change in δ^{26}Mg in olivine produced by refertilisation or metasomatism provides a valuable new tool to study these processes in detail. It also helps to understand the history of single olivine grains hosting sulfides that have been dated by the *in situ* Re-Os isotope method. The data obtained so far on Udachnaya olivine xenocrysts (Publication #292; and *Research Highlights 2001*) show that sulfides thought to be affected by metasomatism are hosted by grains with higher δMg, as predicted by our other data.

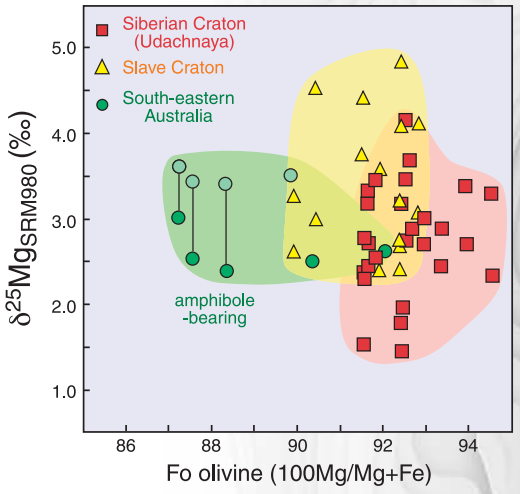

Figure 4. δ^{26}Mg versus olivine composition (Fo) for specified samples. Tie-lines show the range in δ^{26}Mg measured within individual samples showing modal metasomatism.

Contacts: Norman Pearson, Bill Griffin, Sue O'Reilly, Guillaume Delpech
Funded by: ARC, Macquarie University, Industry

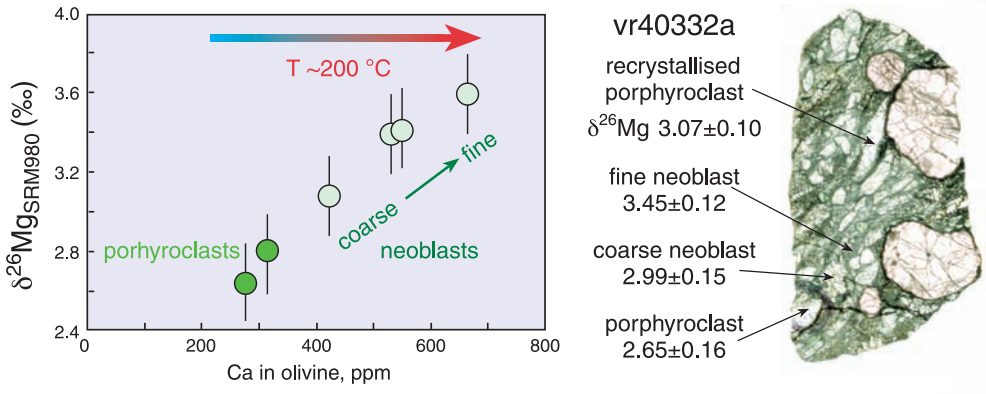

Figure 5. Variation of δ^{26}Mg versus Ca (ppm) in olivine in sample vr40332a.

Trace elements in mantle rocks revisited – a warning to modellers

THE UPPER PART of the Earth's mantle is composed of ultramafic rocks, some of which are restite, ie the material left behind in the mantle when basaltic magma is extracted. Spinel lherzolite is a common ultramafic rock in the mantle at relatively shallow depths (<60 km) and many spinel lherzolites appear to be restite that has become part of the lithosphere. To follow the origin and subsequent evolution of the mantle lithosphere, we need to better understand the origin of these spinel lherzolites, fragments of which are brought to the surface during volcanic eruptions. Incompatible elements, which are transferred to basaltic magma during melting of the mantle, are commonly assumed to image the geochemical "signature" of their mantle source. Important incompatible elements include the high field strength elements (Zr, Hf, Nb, Ta) and the rare earth elements (REE). By determining the distribution of incompatible elements in basalts from various tectonic settings, we should be able to characterize their mantle sources, and mantle-derived xenoliths provide important comparative material as inputs into such models. This, of course, assumes that incompatible elements are not reintroduced into mantle rocks by metasomatic processes after basaltic magmas were removed.

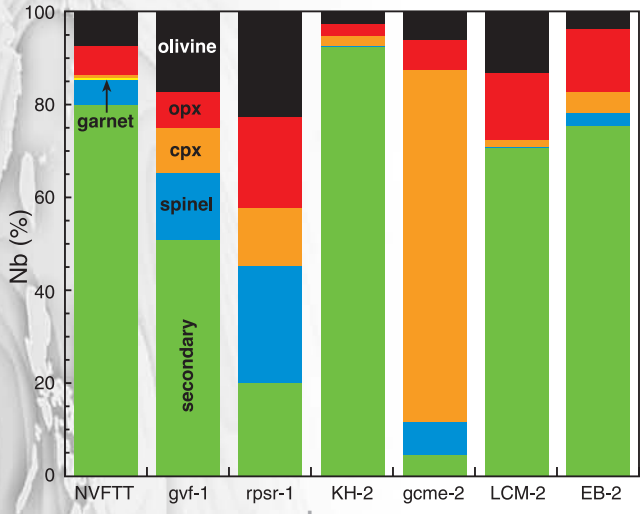

Figure 1. Nb budget in spinel lherzolites from southwestern USA.

During the past year, we have been able to test this assumption using GEMOC's laser microprobe-ICPMS techniques. Are incompatible elements really housed in the major minerals in the uppermost mantle (olivine, orthopyroxene, clinopyroxene, and spinel in order of decreasing abundance)? We have analysed both whole rocks and the individual phases in a suite of spinel lherzolite xenoliths from the southwestern United States, covering different tectonic settings representing different thicknesses and ages of lithosphere. Xenoliths range from those that show no modal evidence of mantle metasomatism (like those from Kilbourne Hole) to some that show significant evidence of metasomatism (Four Corners area of the Colorado Plateau, Grand Canyon, Lunar Crater). None, however, shows geochemical evidence of carbonatite-related metasomatism.

Figure 2. Thorium budget in mafic granulites and eclogites from the Navajo Volcanic Field.

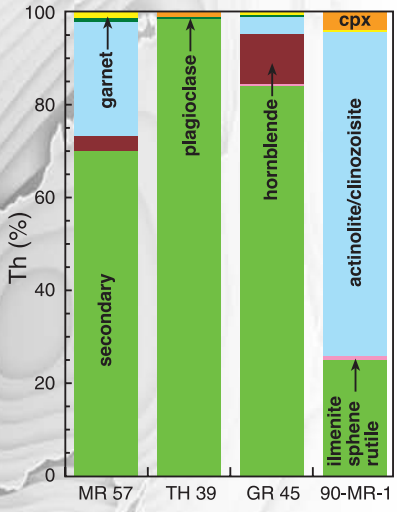

One major finding was that the least depleted (and hence least restitic) xenoliths have the most depleted incompatible element patterns, suggesting that these fertile rocks have actually experienced the least metasomatism. Like some previous studies, we found that a large fraction of the incompatible elements does not reside in any one of the four major minerals listed above. For instance, mass balance calculations using whole-rock and mineral analyses indicate that up to 90 % of Nb and Ta and 40-90 % of REE must reside in minor, very fine grained secondary phases along grain boundaries or in micro-fractures (Fig. 1). No evidence for melt inclusions was found in any of the rocks. Many of these secondary phases are much smaller than the beam size of the laser probe (≤ 30 microns). Analysis of some of the larger secondary grains around grain boundaries suggests that Ti and Fe oxides and silicates may be important hosts for Nb and Ta and traces of amphibole and sericite may house significant amounts of REE.

We also analysed lower crustal xenoliths (garnet granulite) from the Four Corners volcanic field and from Kilbourne Hole (felsic granulite) and

eclogites from the Four Corners. As with the spinel lherzolites from the same sites, we found that 30-80% of the incompatible elements in the crustal xenoliths and eclogites must reside in very fine-grained, secondary phases (Fig. 2).

Perhaps the most important conclusion from this study is that one cannot *a priori* assume that incompatible elements reside in major phases in mantle and crustal xenoliths, and hence extreme caution must be exercised in using the incompatible element distributions of these xenoliths to characterize pre-metasomatic mantle or crustal sources. Also, because restitic and fertile mantle xenoliths occur at the same site, it would appear that the lithospheric mantle sources are heterogeneous on a very small scale of centimetres to metres.

Contacts: Kent Condie, Sue O'Reilly, Bill Griffin, Norman Pearson
Funded by: New Mexico Inst. of Mining and Technology, Macquarie University, GEMOC

Trace element partitioning–time for the detail

IN RECENT YEARS the overall pattern of trace element partitioning between major silicate minerals and basaltic melts has been established for likely melting conditions in the mantle. Attention has subsequently turned to generalised models for trace element partitioning, but these need to be tied to experimentally obtained data.

Trace and minor elements in clinopyroxenes, amphiboles and basanitic melts produced in experiments at 0.5 to 2.0 GPa and 1000 to 1050°C were analysed by LAM-ICP-MS. The analyses reproduce the results of previous electron microprobe analyses by Adam & Green (Adam et al., 1994. Chem. Geol., 117, 219-233), but also provide data for many new elements, and provide a tightly coherent data-base for examining generalised models for trace element partitioning. The expanded data set was used to evaluate the trace element partitioning models of Blundy & Wood (Blundy et al., 1994. Nature, 372, 452-454) and Wood & Blundy (Wood et al., 1997. Contrib. Mineral. Petrol., 129, 166-181). Although the lattice-strain model of Blundy & Wood (1994) could be successfully fitted to our data, the thermodynamic model of Wood & Blundy (1997) does not predict the negative correlations that we found between D_{REE} and pressure. This is not explained by variations in the amounts of H_2O in our experiments. Instead, we attribute the variations in D_{REE} to volume-reducing substitutions in octahedral and tetrahedral sites that increase the activities of +3 and +4 ions, and decrease those of +1 ions, in sites of 8-fold coordination as pressure increases. We were able to quantitatively model some of these effects using a combination of simple electrostatics, Pauling bond strengths and bond-valence calculations. Notwithstanding this, it is apparent that pressure, temperature and the properties of the melt phase also influence partition coefficients independently of crystal-chemical effects.

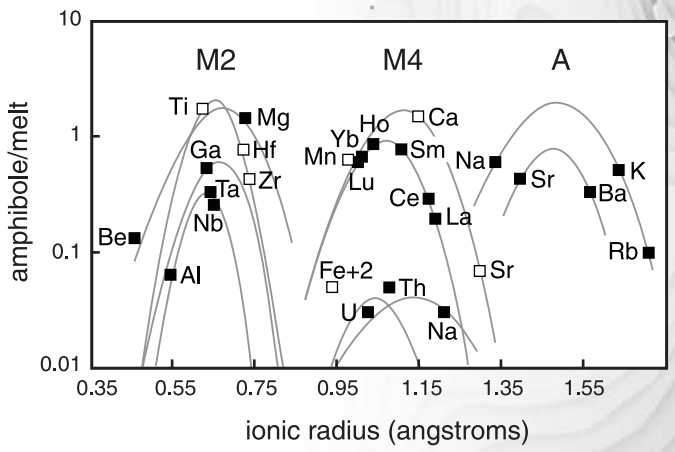

Figure 1. Amphibole/melt partition coefficients for various elements showing control by crystallographic sites.

Contacts: John Adam, Trevor Green
Funded by: ARC, Macquarie University

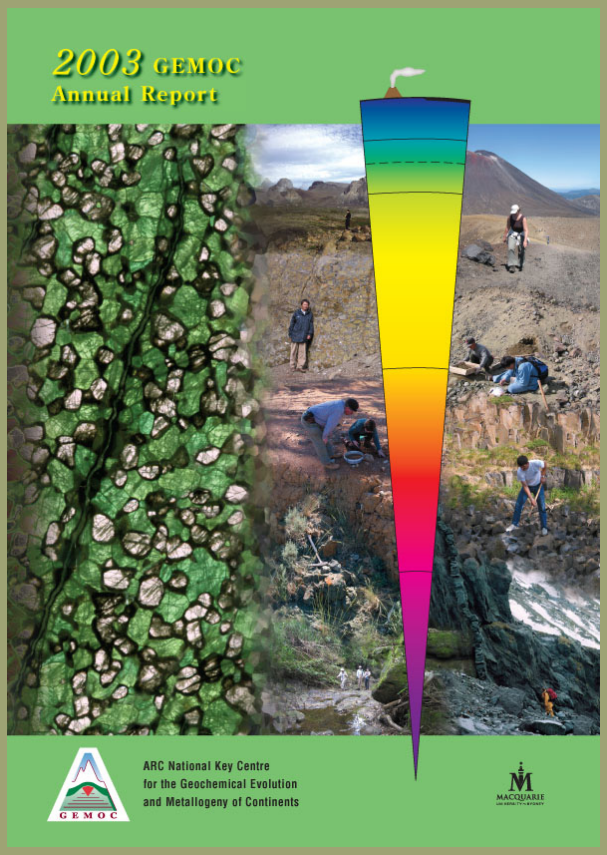

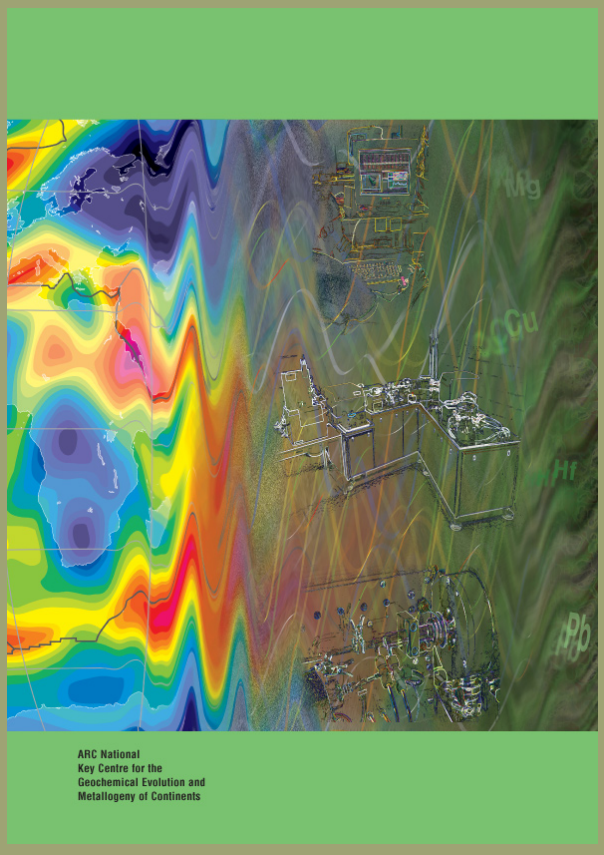

2003 Contents

Garnets, Key to the SCLM	111
The Deviant Archean	114
Taiwan and China are reunited at depth	116
RV Sonne gets to the bottom of the Campbell Plateau	118
Jostling at the edge: Macquarie Island – an exposed oceanic transform fault	120
The upper crust sheds some crumbs: a top-down perspective of the Slave Craton	122
Archean mantle betrays Norway's lithospheric age	124
Sulfur goes with the flow beneath eastern Australia: what about Re-Os ages?	125
Fluid fronts surge through the Kerguelen lithospheric mantle	126
How fast do magmas differentiate beneath volcanoes?	127
Comparative Cratonology in Canada: Slave against Buffalo	128
The Old Soak – Hf in MARID rutile unravels mantle metasomatism	130
Granitoid Genesis in the Georgetown Inlier, North Queensland	131
TerraneChron™: a competitive edge in exploration and understanding crustal evolution	133
Carbonatites beneath oceanic plateaus: trapped melts in xenoliths from Kerguelen	134

Front Cover: This year's cover emphasises the scope of GEMOC's strategy to understand the way the Earth works: from fieldwork to geochemical analysis to technology development to geodynamic modelling – and from the micron to the global.

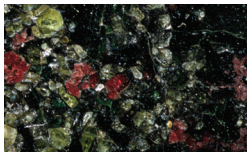

Research highlights 2003

Garnets: Key to the SCLM

THE ULTIMATE GOAL of GEMOC's 4D Lithosphere Mapping Program is to link petrology and geophysics to map the lateral and vertical heterogeneity of the subcontinental lithospheric mantle (SCLM) worldwide. The petrological data derived from studies of xenolith suites in volcanic rocks give baseline data on the distribution of rock types and composition through individual mantle sections, which ultimately can be correlated in detail with geophysical data. But good xenolith suites are scarce and widely scattered on Earth's surface, and time-consuming and expensive to study. On the other hand, many volcanic rocks contain suites of mantle-derived xenocrysts – the debris from disaggregated mantle wall rocks – that can be easily collected and rapidly analysed in statistically useful numbers. GEMOC has therefore invested considerable resources in extracting petrological data from this abundant reservoir of material, and relating it to geophysical properties like density and seismic velocity.

The most useful mineral in these suites is chrome-pyrope garnet: stable in most mantle peridotites at depths greater than 50-80 km, resistant to weathering, and easily recovered from heavy-mineral concentrates. The ambient temperature where each grain was sampled in the mantle can be estimated from its nickel content, and the information contained in the garnet's major- and trace-element composition can be put into a depth context by projecting this temperature to a local paleogeotherm, which also can be derived from the garnet concentrates themselves (Publication #92).

Over recent years the information content of garnet concentrates has been expanded in several steps. A statistical analysis of the GEMOC database (now >40,000 garnets) has defined compositional populations that can be identified with specific rock types and processes (Publication #299), and the relative abundances of these can be plotted against depth. Such a "Chemical Tomography" column for the mantle beneath the Kimberley area in South Africa (Fig. 1a) shows that the top of the section (80-120 km) is dominated by relatively fertile lherzolites. The proportion of harzburgites and depleted lherzolites increases with depth, but so does the influence of metasomatism, related to asthenosphere-derived melts infiltrating the base of the lithosphere. Rocks affected by this type of metasomatism become dominant at about 170 km, marking the base of the depleted lithosphere.

The composition (X_{Mg} = 100 Mg/(Fe+Mg)) of olivine that coexisted with each garnet grain can be calculated (Publication #222), and the mean composition plotted with depth. The results for the Kaapvaal section (Fig. 1b) compare well with data obtained from a large sample of xenoliths analysed at GEMOC. The highly metasomatised part of the section around 110 km shows a low in X_{Mg}, whereas the lower part, dominated by depleted rocks, has higher X_{Mg}, near the median values in xenoliths taken from the literature. The X_{Mg} decreases rapidly toward the base of the lithosphere, giving values like those seen in high-temperature sheared peridotite

Garnet peridotite: a sample of fertile SCLM (Top). Mantle-derived xenocrysts: a garnet concentrate from a kimberlite (Bottom).

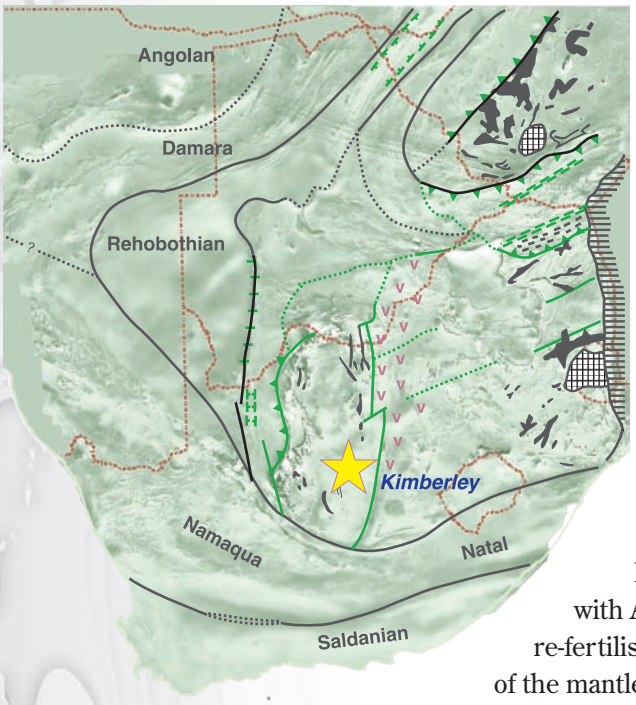

Tectonic map of southern Africa, showing terrane boundaries (green) within the Kaapvaal Craton. Star marks the area of the Group 1 kimberlites discussed here.

xenoliths from many kimberlites. These X_{Mg}-depth curves are important because olivine is the dominant phase of the SCLM, and its properties are a major control on density and seismic velocities.

Algorithms have been developed that relate the Al_2O_3 content of a peridotite to the composition of its garnet (Publications #90, 132). Figure 1c shows the results based on the Y contents of the garnets. Near the top of the section, the estimated Al_2O_3 values are close to the median of published whole-rock analyses of lherzolites, consistent with the abundance of lherzolites in that part of the section. From 125-165 km, the Al_2O_3 values are closer to the median of published harzburgite analyses, consistent with the distribution of these depleted rocks in Figure 1a.

In peridotite suites, major oxides are well-correlated with Al_2O_3 contents, reflecting processes of melt depletion and re-fertilisation. This lets us calculate the mean bulk composition of the mantle for each point on the Al_2O_3-depth curve in Figure 1c (Publication #132). Since we know the X_{Mg} of the olivine from Figure 1b (and thus the coexisting orthopyroxene) at each point, the average modal composition of each point also can be derived, using a least-squares mixing equation and average compositions for the minor clinopyroxene and garnet components.

So now we have the temperature, pressure, rock composition, mineral mode and mineral compositions at any depth in the mantle column in Figure 1a. By applying experimental data on the density and elastic properties of the constituent minerals, we can then calculate the density and seismic velocities (Vp, Vs) as a function of depth – this is the basic information needed to interpret seismic tomography, and use it to map the mantle.

Figure 2 shows the variation of these parameters with depth for the SW Kaapvaal section, calculated using the algorithms of Hacker et al. (2004; G^3 5, #QO1005). These are compared with data calculated by James et al. (2004; G^3 5, #QO1002),

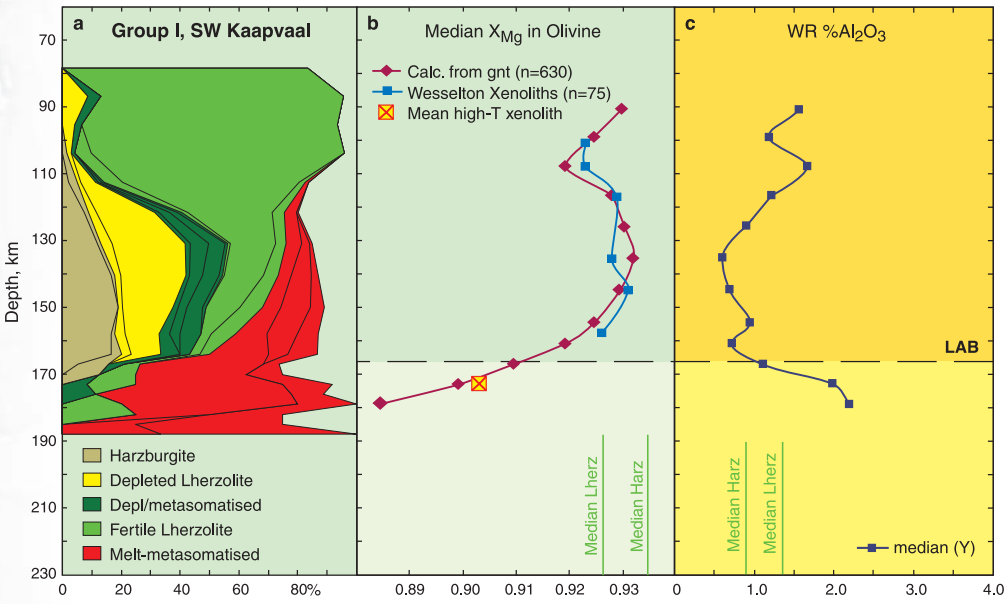

Figure 1. Chemical tomography of the Kaapvaal Craton SCLM. (a) stratigraphy of rock types and processes (b) olivine composition (c) Al_2O_3 in peridotites, calculated from Y contents of garnets

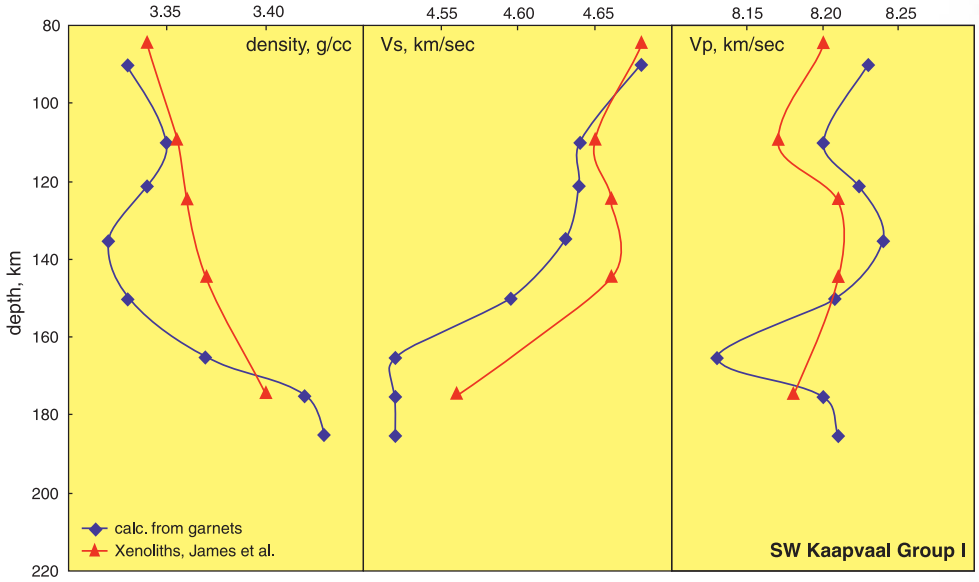

Figure 2. Density and seismic velocity beneath the Kaapvaal craton, calculated from garnet concentrate data, and from xenoliths (James et al., 2004).

using a suite of 56 xenoliths, and adjusted to the temperature-depth profile used for the garnet data. The similarities between the garnet-derived and xenolith-derived curves are encouraging, especially for the Vp and Vs data. The differences also are instructive; some reflect the choice of elastic constants in the two sets of calculations, and others the nature of the sampling. The xenolith suite specifically excludes samples with significant metasomatic effects, while these are inevitably included in the garnet data. This may explain the lower Vs and Vp predicted by the garnet data for the deeper part of the section (150-170 km). The garnet concentrates indicate a high proportion of strongly depleted rocks in the 130-150 km range, and this probably is a minimum estimate, as such depleted rocks will contribute less garnet to the sample than a similar volume of fertile (and hence garnet-rich) rocks. These depleted (low-density) rocks are not as well represented in the xenolith data, and the difference is reflected in the gap between the density curves over this depth range.

Both sets of data suggest that Vs varies more regularly and more strongly with depth in this cratonic section than Vp, so that the base of the SCLM might be more easily recognised in Vs tomography than in Vp tomography. The success of these calculations in reproducing, from garnet concentrates, the basic chemical and modal data on well-studied xenolith suites means that such petrological data can be derived for many sites worldwide, providing a network of "control points" for the interpretation of seismic tomography and other geophysical data, and the use of those data to map the SCLM.

Contact: Bill Griffin, Sue O'Reilly
Funded by: ARC Large, Industry

The Deviant Archean

UNIFORMITARIANISM is a driving force in modern geology; linked with the plate tectonics paradigm, it has provided a powerful tool for the analysis of ancient tectonic regimes. However, there are possible problems with extending the Uniformitarian model into Deep Time. To what extent can we assume that Archean tectonic processes were analogous to Phanerozoic ones? How far back in time can the plate tectonic paradigm, derived from modern observations, be extended before it breaks down?

The composition of the subcontinental lithospheric mantle (SCLM) varies in a systematic way with the age of the last major tectonothermal event in the overlying crust (Fig. 1). This secular evolution in SCLM composition implies quasi-contemporaneous formation (or modification) of the crust and its underlying mantle root, and indicates that crust and mantle in many cases have remained linked through their subsequent history. The differences in SCLM composition also imply a secular change in the mechanisms that have produced the SCLM; this implies, in turn, an evolution in the mechanisms by which continents have formed.

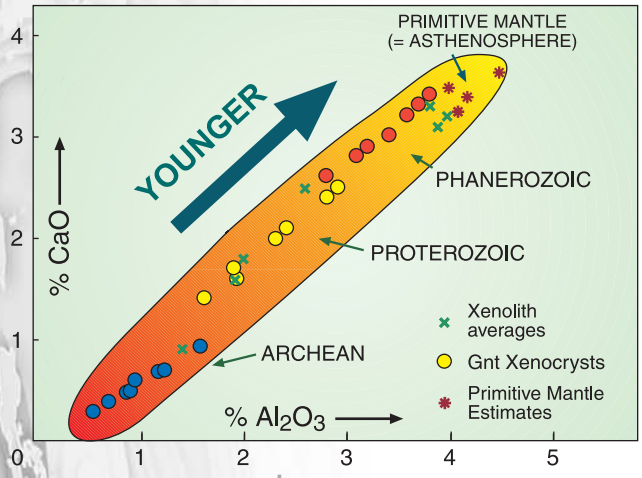

Figure 1. CaO vs Al_2O_3 for calculated SCLM compositions, showing the secular evolution in the composition of the SCLM (Publications #132, 234).

Archean SCLM is distinctively different from younger mantle; it is highly depleted, commonly is strongly stratified, and contains rock types (especially subcalcic harzburgites) that are essentially absent in younger SCLM (Fig. 2). Some, but not all, Archean SCLM also has higher Si/Mg than younger SCLM. Attempts to explain the formation of Archean SCLM by reference to Uniformitarian processes, such as the subduction of oceanic mantle ("lithospheric stacking"), founder on the marked differences in geochemical trends between Archean xenolith suites and Phanerozoic examples of highly depleted mantle, such as abyssal peridotites, island-arc xenolith suites and ophiolites (Fig. 3).

In Archean xenolith suites, positive correlations between Fe, Cr and Al imply that no Cr-Al phase (i.e. spinel or garnet) was present on the liquidus during the melting. This situation is in direct contrast to the geochemical patterns observed in highly depleted peridotites from modern environments, which are controlled by the presence of spinel during melting.

It is more likely that Archean SCLM represents residues and/or cumulates from high-degree melting at significant depths, related to specifically Archean processes involving major mantle overturns or megaplumes (Fig. 4). The preservation of island

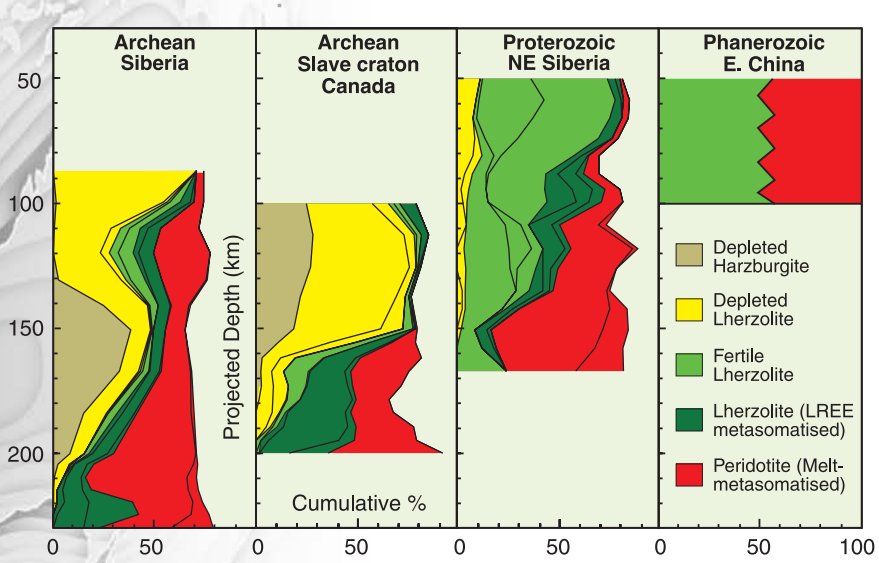

Figure 2. Chemical tomography sections constructed from the vertical distribution of garnet classes (see "Garnets: Key to the SCLM" in this Research Highlights section) in representative Archon, Proton and Tecton sections. Full details are given in Publications #299 and 303.

arc-like SCLM at shallow levels in some sections (eg Slave Craton, E. Greenland) suggests that a specifically Archean tectonic regime may have coexisted with a shallow regime more similar to modern plate tectonics. If this two-regime model is correct, the late Archean marks an even bigger change in Earth's geodynamics than generally thought; it may be when the formation of stable SCLM ended, and modern plate tectonics and lithosphere recycling became the dominant regime.

Preliminary data from *in situ* Re-Os dating of sulfide minerals in mantle-derived peridotites suggest that most Archean SCLM may have formed in a small number of such major events >3.0 Ga ago. The survival of Archean crust may have been critically determined by the availability of large plugs of very buoyant SCLM (a "life-raft model" of craton formation). Many Archean SCLM sections have been strongly affected by Proterozoic and Phanerozoic metasomatism, and much of the observed secular evolution in SCLM composition, at least through Proterozoic time, may reflect the progressive modification of relict, buoyant Archean lithosphere (Publications #132, 234, 299, 303).

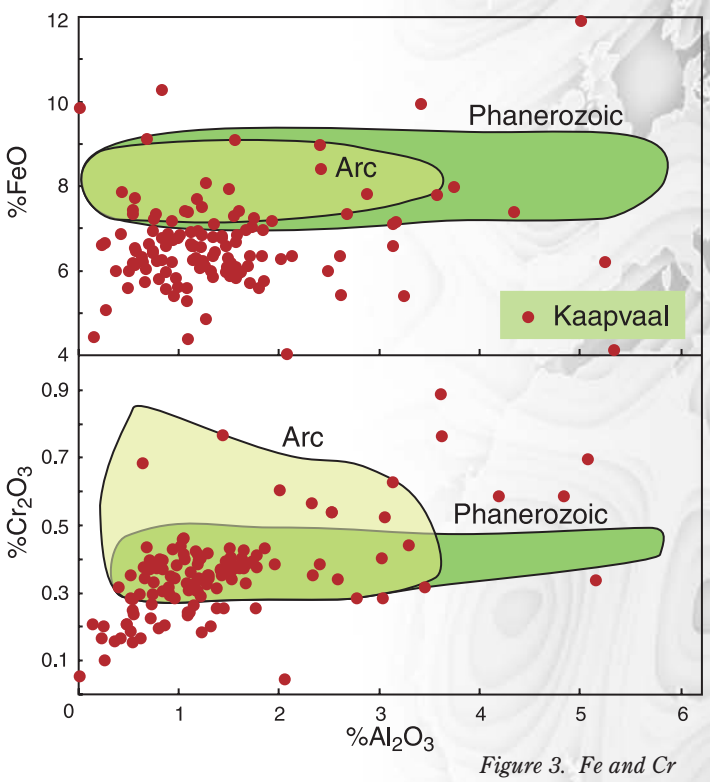

Figure 3. Fe and Cr behave incompatibly at high degrees of melting (low Al contents) in the Archean suites but not in the Phanerozoic suites, implying significant differences in the processes of mantle melting.

Contacts: Sue O'Reilly, Bill Griffin, Norm Pearson, Natsue Abe, Sonja Aulbach, Rondi Davies

Funded by: GEMOC, Macquarie University, ARC SPIRT, Large, Discovery, Industry

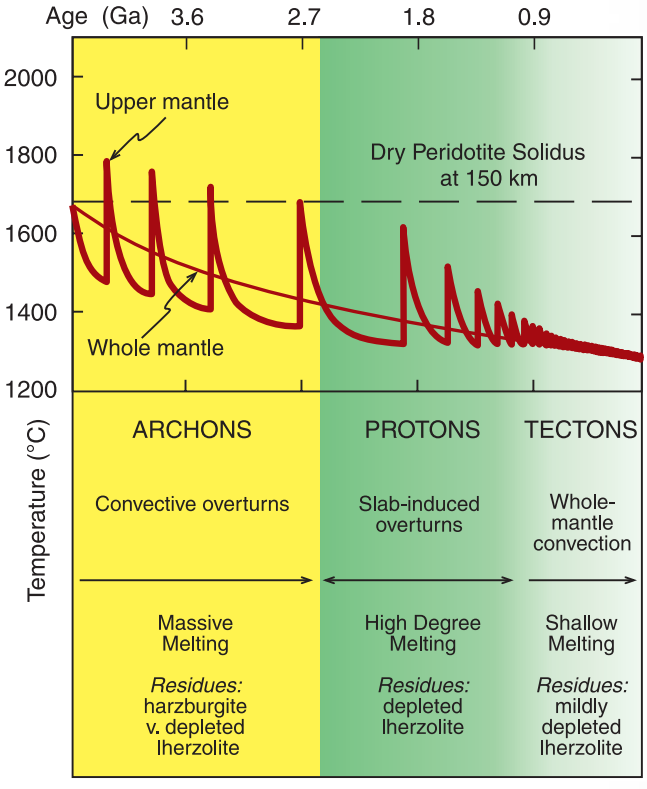

After Davies (1995) EPSL 136, 363-379

Figure 4. Model for the thermal evolution of a two-layered Earth, after Davies (1995). In an early hot Earth, heat builds up in the lower mantle faster than it can be lost from the upper mantle, leading to periodic convective overturns in which the rising lower mantle passes through the dry peridotite solidus and undergoes large-scale melting at depths ≥150 km. This provides a mechanism for the generation of Archean-type SCLM and this mechanism would cease to operate after Archean time due to the secular cooling of Earth.

Taiwan and China are reunited at depth

Photo 1. Xenolith locality (pyroclastic flow) at Tungchiyu islet, Penghu Islands, Taiwan.

EARTH'S CONTINENTS are underlain by "roots" 100-250 km thick of depleted mantle rocks, and the properties and history of these roots affect the long-term stability of the continents. Recent advances in analytical technology make it possible to measure the Re-Os age of single grains of sulfide minerals in mantle-derived rocks, and thus to trace the history of the continental roots. The crust of SE China was stretched and subsided to form the Taiwan Strait about 15 million years ago, following subduction of the Paleo-Pacific plate beneath the continental margin in the Mesozoic. Analysis of fragments of mantle rocks brought up by Miocene intra-plate basalts on the Penghu Islands in the Taiwan Strait (see *Research Highlights 2002*) has been carried out using GEMOC's novel high-precision *in situ* techniques for Re-Os isotopic analysis. The Os isotope compositions of sulfides in the mantle-derived xenoliths reveal the presence of Proterozoic subcontinental lithospheric mantle (SCLM) beneath the highly extended southeast margin of the South China block.

The mantle sulfides from Penghu Islands are mixtures of Fe-rich and Ni-rich monosulfide solid solutions (MSS), pentlandite, millerite and chalcopyrite, exsolved from high-temperature (>900°C) MSS bulk compositions. These sulfides have undergone three types of disturbance in their Os isotope systematics, which might be relevant to mantle metasomatism in the SCLM: (1) addition of Re, and of Os with an isotope composition near the present-day PUM; (2) addition of radiogenic Os, but little or no Re; (3) addition of Re with no apparent addition of Os, or with only lithospheric Os with low $^{187}Os/^{188}Os$ ratios (Fig. 1). The highly radiogenic Os in type (2) could be derived from lithospheric sources such as pyroxenites or subducted basalts, and the transporting medium may have been an oxidizing fluid derived from the Mesozoic subducting slab beneath the area. Despite the Os disturbance, both T_{MA} model ages for individual sulfides and model ages estimated from the initial $^{187}Os/^{188}Os$ ratios of Re-Os mixing lines (Fig. 1) require that some volumes of the SCLM formed prior to 2.3-1.9 Ga. Later major events in the SCLM may be recorded by T_{RD} model ages of 1.5-1.2 Ga and ca. 0.9 Ga, which are consistent with the ages of crustal tectonothermal events on the mainland

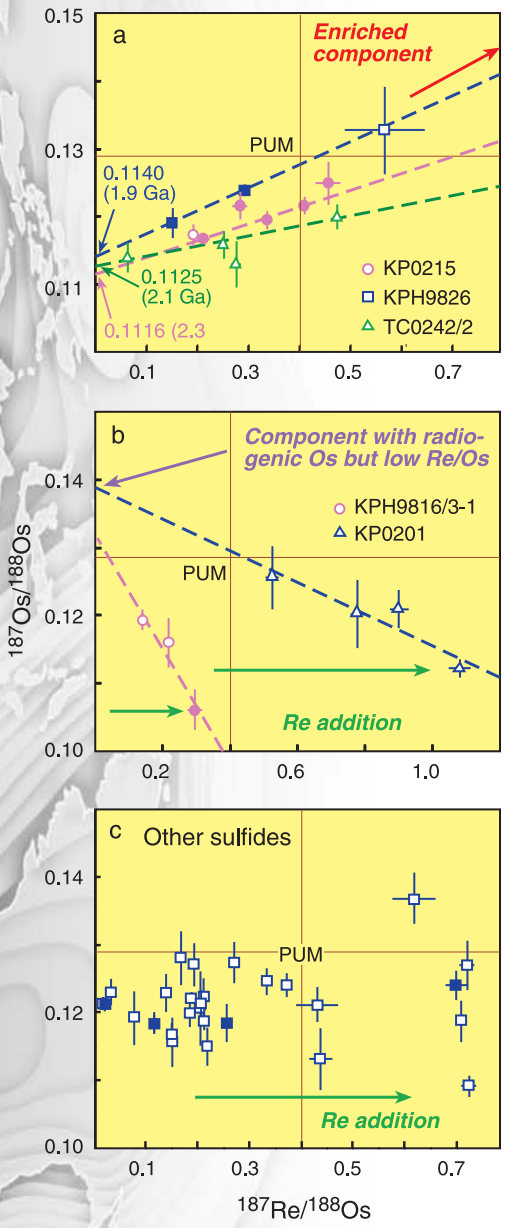

Figure 1. Plots of $^{187}Os/^{188}Os$ vs. $^{187}Re/^{188}Os$ for Penghu sulfides. Solid symbols: enclosed sulfides. Open symbols: interstitial sulfides. PUM: primitive upper mantle values. For further details see Publication #319.

South China block (Fig. 2). The correlations suggest that *in situ* sulfide Re-Os ages are dating metasomatic events in the SCLM, related to mantle thermal events that also affected the crust.

The results show that depleted parts of the SCLM beneath the Taiwan Straits retain mid-Proterozoic ages, while other, less depleted parts record only younger ages. The mixture of ages and rock types suggests that during the stretching of the lithosphere (the rigid Earth layer above the convecting mantle), the ancient continental root was partly disrupted and replaced by younger material, but stayed attached to the extending lower crust. The oldest mantle ages for the lithosphere beneath the Taiwan Strait are similar to ages from the interior of the mainland. This implies that the ancient mantle on the continental margin of mainland China survived even where major volcanic activity was constructing new crust above it during Mesozoic time. The results are directly relevant to current debates about the geodynamics of the continents, and the long-term evolution of the upper mantle.

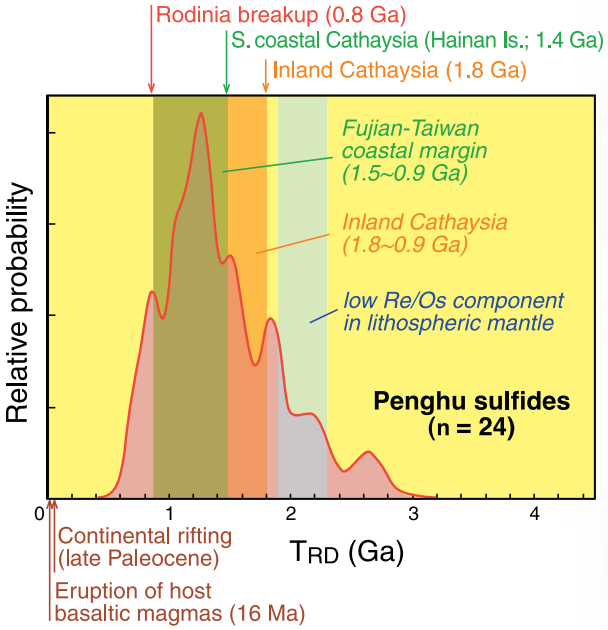

Figure 2. T_{RD} (Re depletion) model age diagram showing age correlation between the SCLM and overlying crust. The plain text above the frame gives crustal ages (U-Pb zircon); the italic text within the frame gives whole-rock Nd and Hf model ages for the crust.

Contacts: Kuo Lung Wang, Sue O'Reilly, Bill Griffin
Funded by: ARC, Macquarie University, National Taiwan University

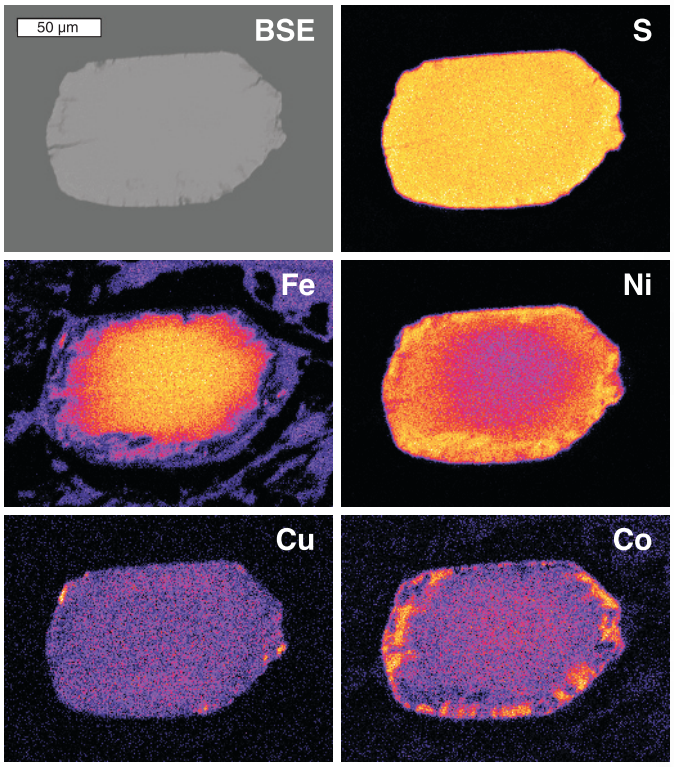

Photo 2. EMP maps of element distribution in an interstitial sulfide grain from a Penghu xenolith, Taiwan.

RV Sonne gets to the bottom of the Campbell Plateau

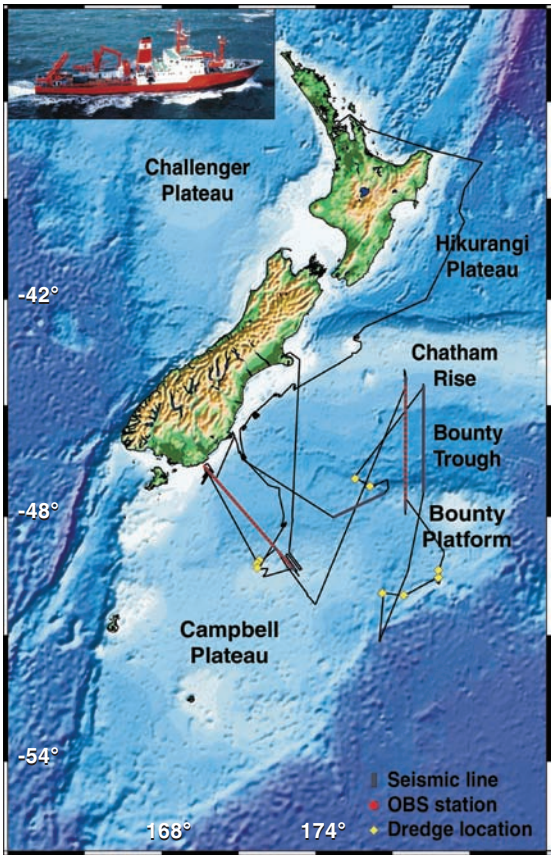

Figure 1. Ship's tracks for the duration of the SO-169 cruise, laid over the bathymetry and topography of the New Zealand region. Red dots indicate Ocean Bottom Seismograph (OBS) locations, grey lines indicate reflection seismic acquisition and yellow dots indicate geological dredge sites.

THE REGION to the east and southeast of the South Island of New Zealand comprising the Chatham Rise, Bounty Trough, Bounty Rise and the Campbell Plateau (Fig. 1) is the largest area of submerged continental crust in the world. Prior to the breakup of Gondwanaland, the Campbell Plateau and Chatham Rise were attached to the Marie Byrd Land and Thurston Island blocks of West Antarctica. The crustal structure and history of the Campbell Plateau-Bounty Trough-Chatham Rise region are poorly known, but are a key element in understanding the evolution of this Gondwanan margin from a convergent margin to continental breakup and rifted margins.

The Campbell Plateau and Chatham Rise are separated by the Bounty Trough. This trough lies parallel to the former Gondwanan subduction margin, which ran along the northern edge of the Chatham Rise (now a suture between the Chatham Rise and the accreted Hikurangi Plateau). The location of the Bounty Trough may have been dictated by a pre-existing back-arc basin, possibly Permian in age (Davy, 1993). It may have acted as a failed rift related to an early South Pacific opening. The timing of the breakup between the Campbell Plateau region and Marie Byrd Land at 84 Ma is relatively well documented by magnetic lineations off the plateau margin (Eagles et al., 2004. G^3). What is not so well understood is the process that led to the breakup. How much extension affected the area before oceanic crust developed? Questions yet to be answered include the processes involved in developing the anomalously steep continental slope on the southern margin of the Campbell Plateau; the composition of the crust-mantle boundary across the plateau; the volume, source and timing of magmatism across the area; and whether there are differences between submarine plateau margins and passive continental margins.

Catalina Gebhardt (AWI) and Tara Deen assist in the deployment of the seismic streamer.

Tara Deen participated in the research cruise of the RV Sonne that surveyed the Campbell Plateau region in January and February of 2003 with Karsten Gohl as cruise leader. This is part of a GEMOC collaboration with GEOMAR (Kiel), to investigate the relationships between the Campbell Plateau and multi-stage rifting between New

Zealand and West Antarctica.

Two coincidental Ocean Bottom Seismograph (OBS) refraction and marine reflection seismic surveys as well as two high-resolution reflection seismic lines were completed. Preliminary first-arrival models of the seismic data across the Bounty Trough indicate highly extended crust (Fig. 2).

Marine magnetic and gravity measurements were taken continuously throughout most of the cruise, and help constrain more extensive satellite gravity measurements. Swathe multi-beam sonar bathymetry and Parasound sediment echosounding data (Fig. 3) were collected along a number of profiles along with dredged geological samples. Geological samples were collected by dredging at a number of seamounts identified from multi-beam sonar bathymetry.

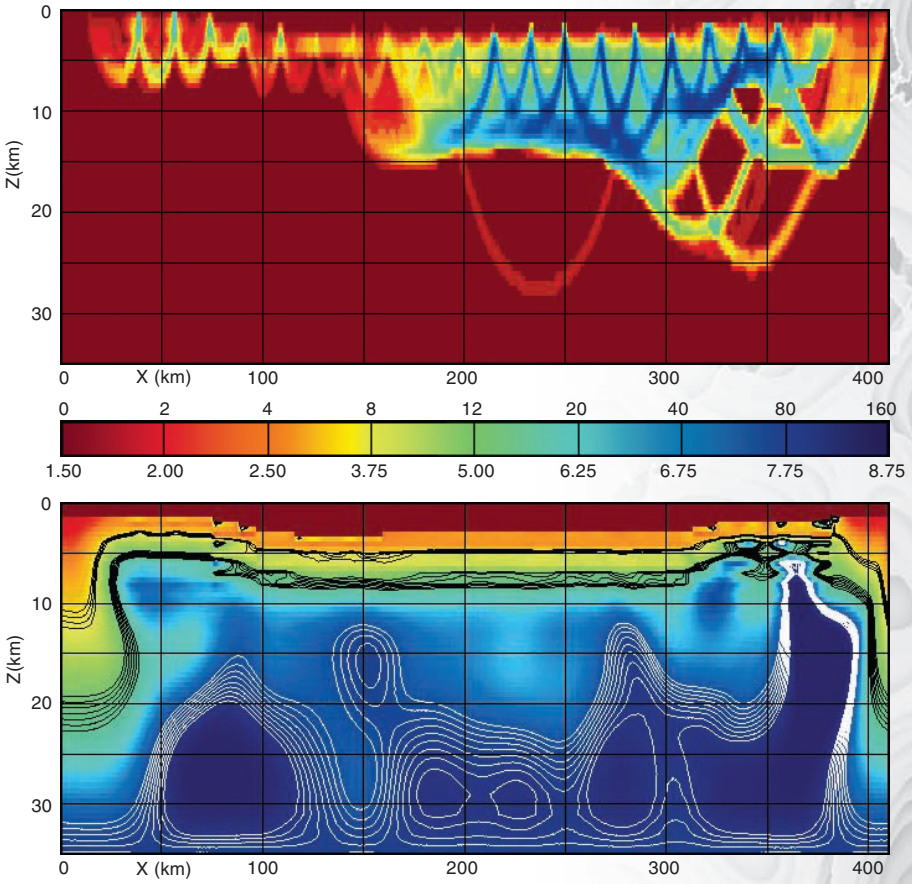

Figure 2. Preliminary first-arrival seismic tomography for the Bounty Trough. Reflections have not yet been incorporated. (Top) Quality of penetration. (Bottom) Velocity field for the tomographic inversion.

The coincidental refraction and reflection seismic lines will be integrated with analyses of the rocks dredged from seamounts on the Campbell Plateau to develop a 3-dimensional image of the crust of the Campbell Plateau/Bounty Trough region. Rock compositions will be used to calculate seismic velocities for the upper crust, which in turn can be used to interpret the seismic profiles and constrain the composition of the lower crust as well.

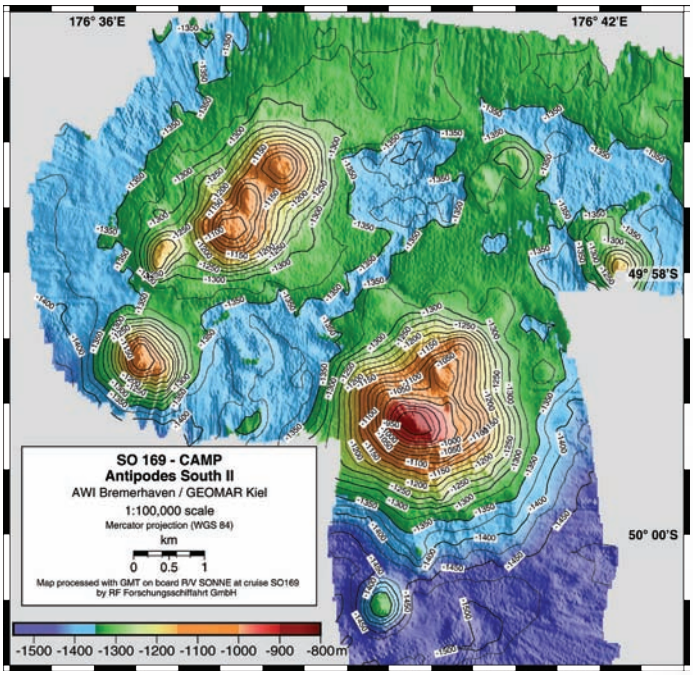

Figure 3. Multi-beam swathe bathymetry was used in the identification of dredge sites, such as these seamounts near the Antipodes Islands.

Contacts: Tara Deen, Sue O'Reilly, Bill Griffin
Funded by: ARC Discovery, Macquarie University, GEOMAR

Jostling at the edge: Macquarie Island – an exposed oceanic transform fault

OCEANIC TRANSFORM FAULTS are important features of global tectonics, but they are difficult to study because they are almost entirely under water. Even where they are (rarely) exposed on land within ophiolites, the faults have typically been deformed during obduction. Our knowledge of oceanic transform faults therefore comes mainly from bathymetry and other geophysical data, dredge samples and a few areas surveyed and sampled by submersibles.

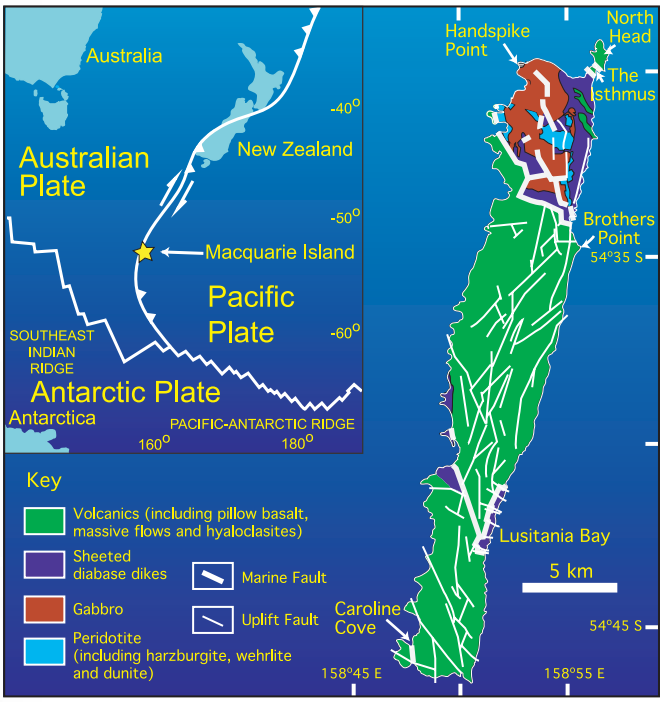

Figure 1. (a) Location of Macquarie Island indicated by a star. (b) Geologic map of Macquarie Island.

Macquarie Island, located approximately 1200 km southwest of New Zealand in the Southern Ocean (Fig. 1), forms the apex of the Macquarie Ridge Complex (MRC). The MRC is a system of ridges and troughs along the currently active Australian-Pacific oceanic transform plate boundary between the Alpine Fault of New Zealand and the Australian-Pacific-Antarctic triple junction. The island exposes the eastern side of a ~5 km high, ~50 km wide submarine ridge and lies ~4.5 km east of the major active plate boundary fault zone. It is the only subaerial exposure of non-plume-related oceanic crust that still lies within the basin in which it formed, and the transform-related structures on the island can be put in a relatively well-constrained present-day plate tectonic setting. This situation makes Macquarie Island a globally unique opportunity to examine an active oceanic transform plate boundary.

Prof. Mike Coffin (Ocean Research Institute, University of Tokyo) adjacent to elongate pillow lava flows that formed on the flanks of an ancient sub-marine volcanic edifice. Photo by Dr Nathan Daczko (Macquarie Univeristy).

The Australian-Pacific transform plate boundary fault zone, south of New Zealand, is characterised by dominantly normal faults and pull-apart basins, in apparent conflict with the regional transpressional tectonic setting. Daczko et al. (G^3 4(9),1080) proposed that the present day curvature of the transform is inherited from a pre-existing divergent plate boundary, and that the overall extensional kinematics shown by faults along the main plate boundary trace and exposed on Macquarie Island result from local stresses related to right-lateral, right-stepping, *en echelon* plate boundary faults and not to the current transpressional setting.

Mapping of recent faults affecting the topography of Macquarie Island (Fig. 1) shows the island is extensively cut by high angle normal faults forming pull-apart basins. Furthermore, evidence

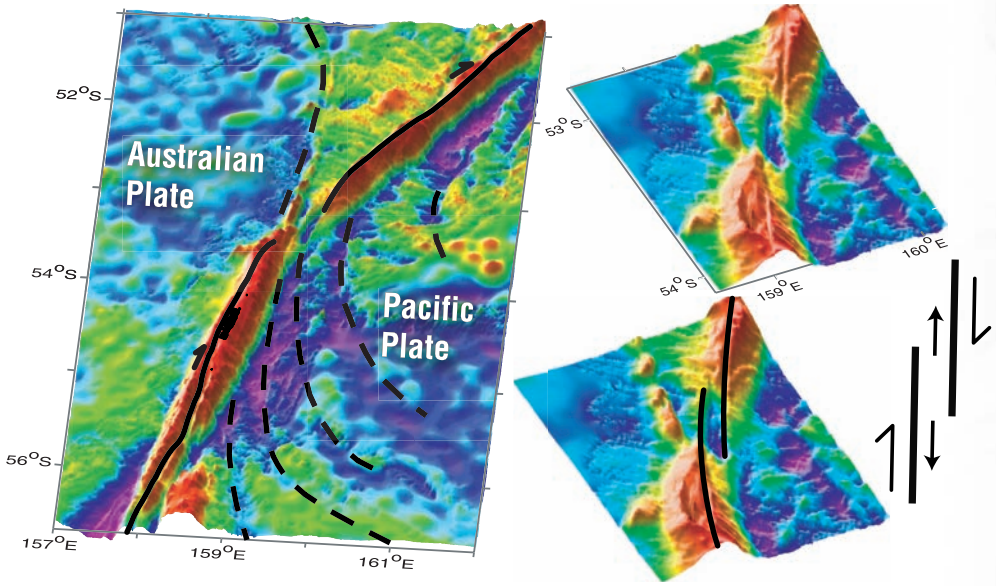

Figure 2. 3D perspective view of the MRC (see Daczko et al., G³ 4(9), 2003).

for reverse motion is rare. Using marine geophysical data, including swath bathymetry (Fig. 2), reflectivity and seismic reflection data, collected along the Australian-Pacific plate boundary north and south of the island, we have defined a 5-15 km wide plate boundary zone. A series of right-stepping *en echelon* faults within this zone lies along the main plate boundary trace. At the right-stepping fault terminations, elongate depressions (≤10 km wide and 1.2 km deep) parallel the plate boundary, which we interpret as extensional relay zones or pull-apart basins. We propose that transpression is partitioned into *en echelon* strike-slip faults at the plate boundary and a convergent component that flexes the crust, causing the anomalous bathymetric ridge and trough morphology of the McDougall and Macquarie segments of the MRC.

Contacts: Nathan Daczko (work done at Department of Geological Sciences and Institute for Geophysics, Jackson School of Geosciences, University of Texas, Austin, Texas)
Funded by: Australian Antarctic Division, University of Texas

Royal penguin rookery at Hurd Point. Photo by Dr Karah Wertz (University of Texas at Austin).

The upper crust sheds some crumbs: a top-down perspective of the Slave Craton

GEMOC RESEARCHERS have obtained a detailed picture of the composition, architecture, and temporal evolution of the subcontinental lithospheric mantle beneath the Slave craton (see *GEMOC Annual Reports 2000-2002,* Publications #121, 137, 144, 348). Provided that crustal evolution can also be well characterised, the combined data should provide valuable clues to crust-mantle genetic links. Fortunately the Slave craton is well exposed and amenable to field-based research. Detailed mapping of key areas supported by extensive U-Pb dating of zircon, baddeleyite, titanite, and monazite has allowed us to significantly advance our knowledge of crustal evolution.

The western part of the craton is underlain by a Hadean to Mesoarchean basement complex and Neoarchean supracrustal assemblages and plutons, whereas the eastern part is dominated by juvenile Neoarchean crust (Fig. 1). The largely plutonic basement block (the Central Slave Basement Complex of Bleeker et al., Canadian Journal of Earth Sciences, 1999) contains Earth's oldest rocks, the 4.03 Ga Acasta gneisses (Fig. 2). This basement block is unconformably overlain by a <200 m thick package of quartzite and banded iron formation (the Central Slave Cover Group). Widespread occurrences of this distinctive 2.85-2.80 Ga package (Fig. 1) outline the regional extent of the unconformity, which developed following volumetrically significant basement magmatism between 2.99-2.90 Ga.

The Central Slave Basement Complex evolved through a series of tectonomagmatic episodes that are constrained by U-Pb data (Fig. 3). In all mapped areas we found inherited zircon evidence of older crust-building/recycling events, even though this crust is no longer (and in some cases likely never was) exposed at the surface. The distribution of maximum crustal age, determined from igneous and inherited zircons, suggests outward growth of the basement complex from a nucleus containing the Acasta gneisses, with present-day size reached by ca. 3.3 Ga (Fig. 4). This growth pattern is broadly consistent with existing Nd and Pb isotopic data. Possible tectonic settings for basement growth have yet to be fully evaluated, but episodic magmatism is certain to have played an important role.

The basement complex is underlain by a highly-depleted mantle layer extending to 150 km depth. The western boundary of this layer is relatively unconstrained due to an absence of kimberlite pipes, but the layer thins or terminates toward the northern and southern (younger) edges of the craton.

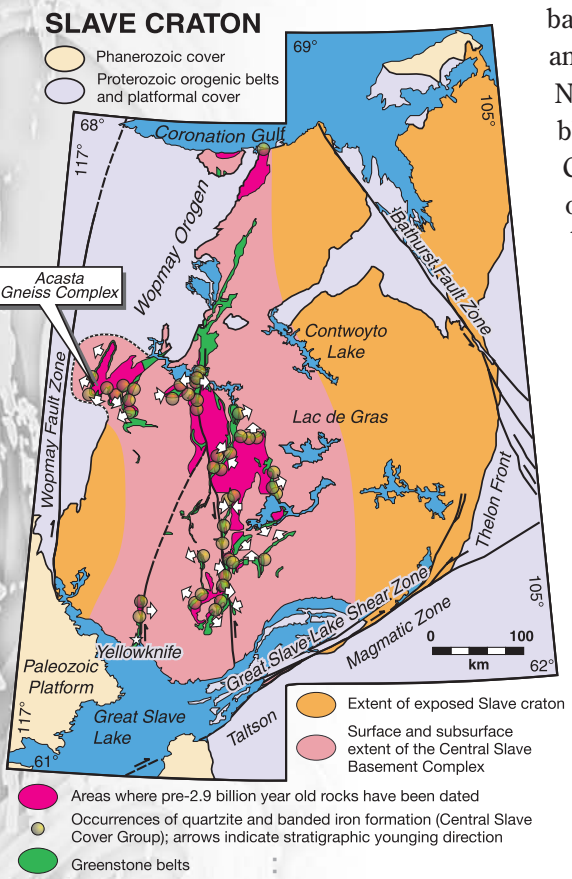

Figure 1. Map of Slave craton highlighting the surface and subsurface extent of the Central Slave Basement Complex (pink shading). Yellow circles show occurrences of the autochthonous Central Slave Cover Group, located between basement exposures (dark pink) and overlying greenstone belts (green).

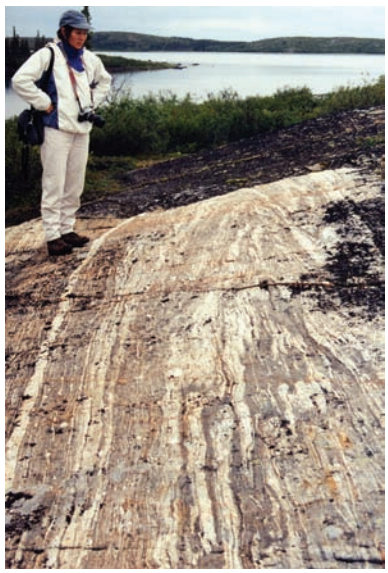

Figure 2. Contemplating folded layering in the Acasta gneisses…

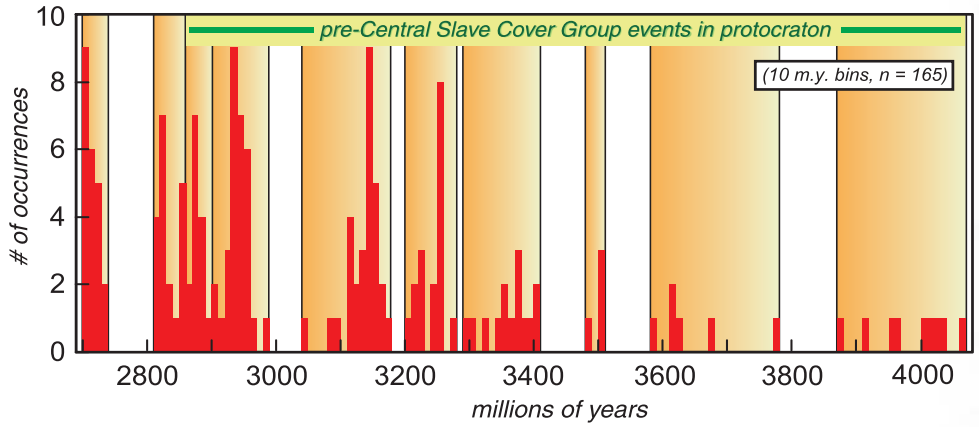

Figure 3. Histogram of all U-Pb ages for the western Slave craton. Most of the data represent igneous protolith ages. Ten age groupings have been defined; each corresponds to one or more discrete geological events.

Beneath this layer, a more fertile mantle layer extending from 150 to ~220 km depth underlies much of the craton. Emplacement of this lower layer during mantle plume activity at 3.3 Ga is indicated from a variety of data. An older age is therefore inferred for the shallow mantle layer, consistent with its location beneath similarly ancient crust. Plume emplacement of the lower layer suggests that mantle-derived magmas may have invaded the basement complex at 3.3 Ga. We are in the process of characterising crustal and mantle contributions to the magmatic episodes shown in Figure 3 by *in situ* laser ablation analysis of Hf isotopes in zircon, using GEMOC's Nu Plasma multicollector ICP-MS.

Contacts: John Ketchum, Bill Griffin, Sue O'Reilly, (Wouter Bleeker, Geological Survey of Canada)
Funded by: ARC Discovery, Lithoprobe, Geological Survey of Canada, Natural Science and Engineering Research Council of Canada

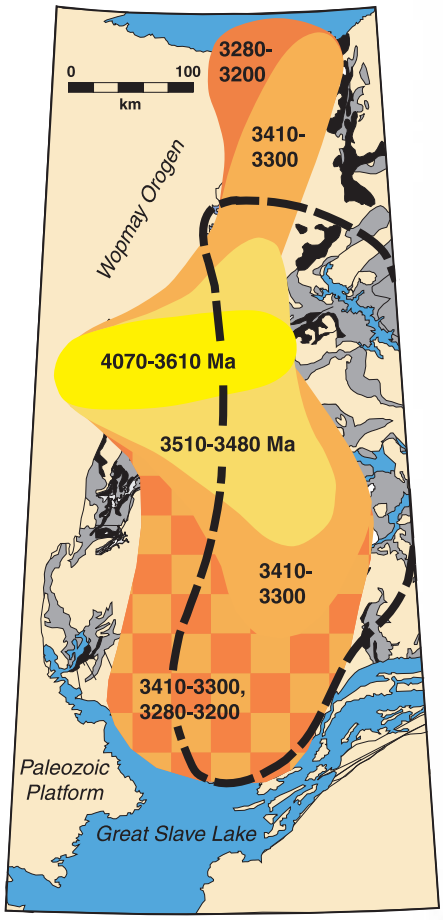

Figure 4. Contoured distribution of maximum protolith age based on the data in Figure 3, with additional input of whole-rock Nd and Pb isotopic data. Maximum age of crust appears to young outward from a central core. Heavy dashed line outlines the extent of a highly-depleted upper mantle layer (western boundary relatively unconstrained; see Publications #121, 137, 144, 348) that likely predates 3.3 Ga and may represent the original mantle lithosphere of the Central Slave Basement Complex.

Archean mantle betrays Norway's lithospheric age

OROGENIC PERIDOTITE bodies are widespread in the Western Gneiss Region (WGR) of western Norway. These bodies typically occur as small garnet-bearing volumes within larger masses of garnet-free dunite. *In situ* Re-Os analysis of mantle sulfides from the garnet peridotites has demonstrated that at least some of these fragments are Archean (see *Research Highlights 2001*). In fact, there is growing evidence indicating that all of these bodies have an Archean origin, despite being surrounded by gneisses that appear to be no older than Proterozoic.

Dunite comprises the great bulk of the WGR peridotite massifs. The Almklovdalen peridotite in southern WGR is one of the larger bodies in the region with an estimated volume of 70-80 billion tonnes and approximately 90% of this is highly refractory dunite. Unfortunately the dunite contains very little sulfide and therefore conventional whole-rock methods have been employed to date this material. Whole-rock Re-Os analysis of the dunites yields model ages that range from 2.7 to 3.1 Ga, similar to the range seen in the sulfide data for the garnet peridotites (see *Research Highlights 2001*), suggesting that these rocks experienced an Archean partial melting event.

Gusdal dunite quarry, Almklovdalen.

Previously, Proterozoic ages for the garnet-bearing peridotites and the basement crustal rocks of the WGR led to the suggestion that the mantle and crust in the southern Caledonides of Norway, as well as other terrains adjacent at the time, were coupled throughout much of the Proterozoic (Brueckner and Medaris, 1998). However, the Archean Re-Os ages now established for the Almklovdalen peridotite body provide evidence for a much older depletion event in the mantle beneath the Baltic Shield. This is intriguing as there is no geochronological evidence for the presence of Archean crust in the WGR, although the possibility has been discussed in the literature. It is possible that the peridotite bodies reflect a mantle depletion event that predated crustal growth in this part of the Baltic Shield. Alternatively, the Archean crust corresponding to this mantle depletion event may have been reworked in Proterozoic time, to the point of being unrecognisable. A third possibility is that Archean crust exists at deeper levels than those presently exposed.

A potential tool to help in determining the presence, or absence, of Archean crust in the WGR is GEMOC's *TerraneChron*™ technique (see *Research Highlights 2002*). *TerraneChron*™ utilises detrital zircon to provide timing and tectonic style information for inaccessible crustal terranes, and may prove the key to unlocking the Archean history of this part of the Baltic Shield.

Fold in dunite at Lien, Almklovdalen.

Contacts: Eloise Beyer, Bill Griffin, Sue O'Reilly
Funded by: GEMOC Macquarie, MUPGRF, ARC Large

Sulfur goes with the flow beneath eastern Australia: what about Re-Os ages?

SPINEL LHERZOLITE xenoliths hosted by Tertiary basaltic magmas have been used to characterise the composition, architecture and evolution of sub-continental lithospheric mantle beneath the New England Orogen, Eastern Australia. Studies of their detailed mineralogy and geochemical characteristics reveal regional variations in the degree of melt extraction and the type and extent of metasomatism that has affected the lithosphere.

At the Allyn River locality (Fig. 1), two distinct populations of xenoliths can be identified on the basis of microstructure, whole-rock and mineral major-element chemistry, and clinopyroxene trace-element chemistry. One group is granoblastic and shows no evidence of deformation; the other group is generally more coarse-grained, with common exsolution in pyroxene and kink-banding in olivine. These coarse-grained xenoliths contain trails of small sulfide grains (< 10 µm) along fracture planes in the silicate phases. These sulfide-bearing trails are absent in the granoblastic xenoliths: instead sulfides are found as relatively large polymineralic aggregates (~ 100 µm across) within melt pockets interstitial to the silicate phases (Fig. 2). These melt pockets have not been observed in the coarse-grained xenoliths. Equilibration temperatures calculated for the granoblastic xenoliths are lower than those of the coarse-grained samples, suggesting they represent a shallower mantle volume.

In addition to the sulfide patches, the melt patches contain variable proportions of secondary olivine ± clinopyroxene, plagioclase, K-feldspar, Mg-rich carbonate, Ca-rich carbonate, glass, ilmenite, apatite, and a titanium and chrome-rich oxide phase (spinel?). Mg-carbonates are dolomitic, suggesting a high-pressure origin. The melt patches are interpreted to represent crystallised volatile-bearing melts rich in CO_2, and would be highly mobile at mantle pressure and temperature. The close association between the sulfides and the melt patches indicates that sulfides can be highly mobile under some mantle conditions. This implies that pre-existing sulfides may be mobilised or deposited during metasomatic episodes, changing the abundance of chalcophile elements such as Re and Os, which would modify the original age information from the Re-Os system. Any Re and Os data from mantle rocks need to be interpreted within a detailed mineralogical context and a knowledge of the nature of sulfides within the rock.

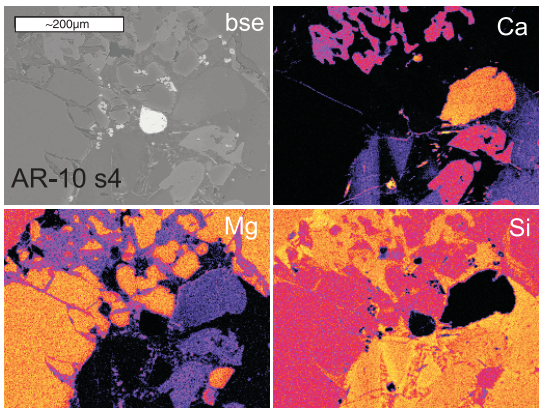

Figure 1. Melt patch in sample AR-10. The bright region in the centre of the back-scattered electron image (bse) which is black in the Si map is the sulfide patch. Beside it is a Ca-Mg-carbonate, which is also black in the Si map. Secondary clinopyroxene, some apatite, and Ti-rich chrome spinel are present also.

Contacts: Will Powell, Sue O'Reilly
Funded by: GEMOC, MUPGRF, ARC Large

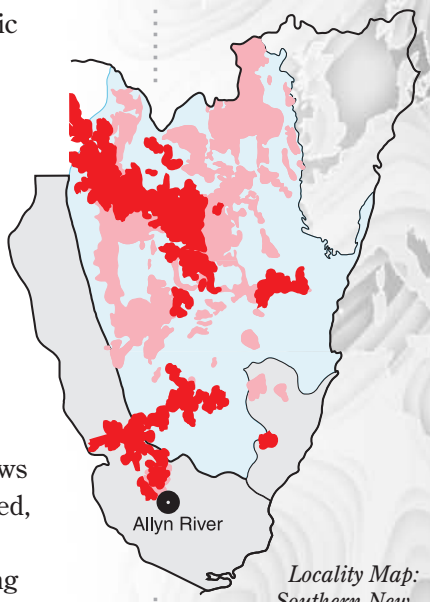

Locality Map: Southern New England Orogen, Eastern Australia. The Tamworth Belt (grey) and the Tablelands Complex (blue) represent inboard and outboard parts of a subduction complex. Granites of the New England Batholith are pink and Tertiary basalts red.

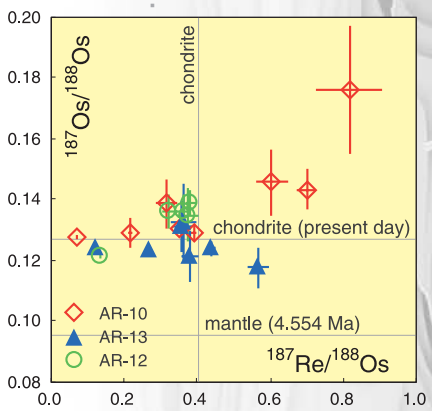

In situ Re-Os isotopic systematics of sulfides in xenoliths from Allyn River.

Fluid fronts surge through the Kerguelen lithospheric mantle

THE KERGUELEN ISLANDS are the exposed part of the Kerguelen oceanic plateau, a Large Igneous Province in the Antarctic plate domain. Its birth is related to both the spreading of the South East Indian Ridge (SEIR) overprinted by the long-lived Kerguelen plume. It provides a unique opportunity to study plume-ridge interactions and their implications for the composition of the oceanic mantle. Mantle xenoliths from the Kerguelen Islands are common in dykes or pipes of young alkaline lavas. The major and lithophile trace elements have been well-characterised over the last decade. The platinum group elements (PGE; Os, Ir, Ru, Rh, Pd, Pt) and chalcophile elements (S, Se, Cu) provide different information on the geological processes that operate in the lithosphere. This is because they are almost exclusively partitioned into a sulfide-rich melt, whereas major and lithophile trace elements have a greater affinity for silicate melts.

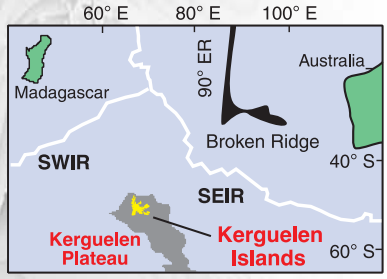

The PGE, S, Se and Cu were analysed in representative mantle xenoliths (harzburgites and dunites) for which data on major elements and lithophile trace elements in bulk-rock and separate mineral grains were already available. The harzburgites do not contain obvious sulfide grains and therefore have low S, Se, Cu contents and high Os, Ir, Ru and Rh relative to (Pd + Pt). These features indicate that these pieces of Earth's mantle are residues after a large degree of melt extraction, during which the sulfide phase was exhausted.

Some harzburgites show microstructural and geochemical evidence of refertilisation by percolation of basaltic to alkaline melts but still have concentrations of the compatible PGE (Os, Ir, Ru, Rh) lower than expected from partial melting models. This suggests a decoupling between the PGEs, major elements and lithophile trace elements during melt/rock reactions in the upper mantle. The major elements and lithophile trace elements are re-introduced into the harzburgites, while the PGE are further depleted during the melt/rock reactions. Dunite samples formed through extensive melt/rock reactions and have about the same concentrations of PGE as the harzburgites.

Some dunites were further impregnated by small volumes of highly evolved volatile-rich silicate melts, which precipitated carbonate and sulfide grains disseminated through the olivine matrix. The bulk-rock and sulfide chalcophile and PGE abundances of these rocks display unusual fractionations that suggest different sulfidation mechanisms. A group of samples with broadly chondritic S/Se and Os/Ir ratios and no enrichment in Pd over Pt ($Pd/Pt_N = 1$) contains Cu-Fe-Ni-rich sulfide melt droplets, apparently unmixed from metasomatic carbonate melt patches. In contrast, some dunites with abundant Fe-Ni sulfides have superchondritic S/Se ratios (up to 10000), coupled with superchondritic Os/Ir_N and Pd/Pt_N. This correlated behaviour of Os, Pd and S suggests transport in a S- and Cl-bearing CO_2 vapour phase.

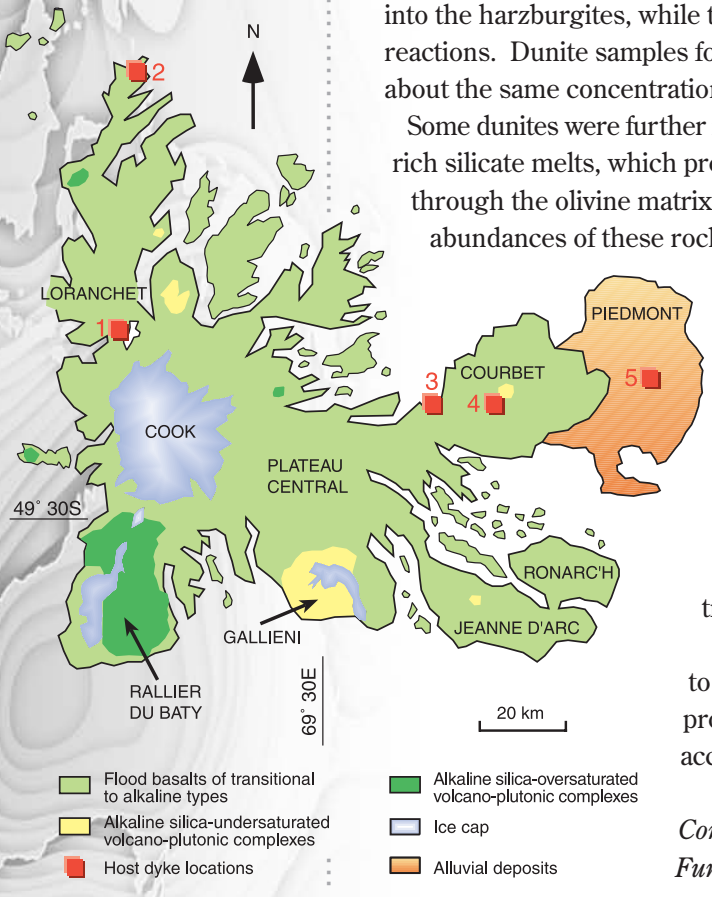

Chalcophile and platinum group elements are proving to be useful tracers of metasomatic agents in the mantle, providing further geological information that is not easily accessible from major and lithophile trace elements alone.

Contact: Guillaume Delpech, Sue O'Reilly
Funded by: GEMOC, MUPGRF, IPRS, ARC IREX, ARC Large

How fast do magmas differentiate beneath volcanoes?

THE RATES of plate tectonic processes and the vastness of geological time have led to a sense that many changes take place very slowly on Earth. However, processes ranging across melt formation and migration, volcanic eruptions (Fig. 1), erosion and water flow (Fig. 2) all occur on time scales of days to thousands of years. Thus, if we wish to study these processes and to constrain their mechanisms via detailed knowledge of their time scales, we need to apply chronometers that have very short half lives. The nuclides of the U and Th decay chains provide such tools and their application is one of the most rapidly growing areas in modern isotope geoscience.

Figure 1. Collecting young volcanic rocks from intra-caldera cones, Umnak Island, Aleutians.

The continental crust has been formed by partial melting and magma differentiation. In principle, magma differentiation could occur via a number of different processes including cooling, decompression and degassing. Research carried out by Simon Turner and Rhiannon George (now at GEMOC) with Chris Hawkesworth and Georg Zellmer has shown that the activity ratio of ^{226}Ra to ^{230}Th decreases systematically as magmas become differentiated from basalt to andesite to dacite to rhyolite. This appears to be true in a number of tectonic settings including island arcs and in continental rifts and both at the scale of a whole island arc and within individual volcanoes. ^{226}Ra and ^{230}Th are nuclides within the ^{238}U decay chain and ^{226}Ra has a half life of 1600 years. Thus, the decreases in ^{226}Ra with increasing silica in young lavas strongly suggest that differentiation of the magmas occurred within several half lives or 1600-5000 years. Such time scales are similar to numerical estimates for the cooling and crystallisation of moderate sized magma bodies in the lower to middle crust and so the Ra isotope data suggest that magma differentiation in the volcanoes studied occurs in response to cooling rather than decompression or degassing, both of which are likely to occur in weeks to a few years at most.

Figure 2. Radioactive disequilibria in surface environments such as the Kalighandaki river, Nepal reveal insights into the nature and time scales of weathering and erosion.

Greater detail can be obtained by measuring the U-series nuclides in crystals from lavas and these reveal many complexities. Results indicate that crystal grains are commonly older then their enclosing volcanic glass and many are likely to show age zoning. When the isotope data are combined with microstructural information such as grain size distributions, it can be shown that many of the grains did not grow *in situ* but were entrained by the host magma from cumulates left behind by previous magma batches. One implication is that the grains observed in a volcanic rock may often not be the ones responsible for its bulk compositional evolution. Such data also inform models for the longevity and past history of a volcano and will ultimately help in the development of better predictive models for volcano hazards.

Contacts: Simon Turner, Rhiannon George
Funded by: NERC + Royal Society at the Open University and University of Bristol (where this work was done with co-workers)

Comparative Cratonology in Canada: Slave against Buffalo

THE SLAVE CRATON and the Buffalo Head Terrane (BHT) in northwestern Canada are two ancient entities in the mosaic of provinces and terranes that makes up the North American Craton. They are currently juxtaposed, which raises the question of whether this spatial relationship is accidental or whether they were part of a single larger craton. Studies of the lithospheric mantle can help answer this question.

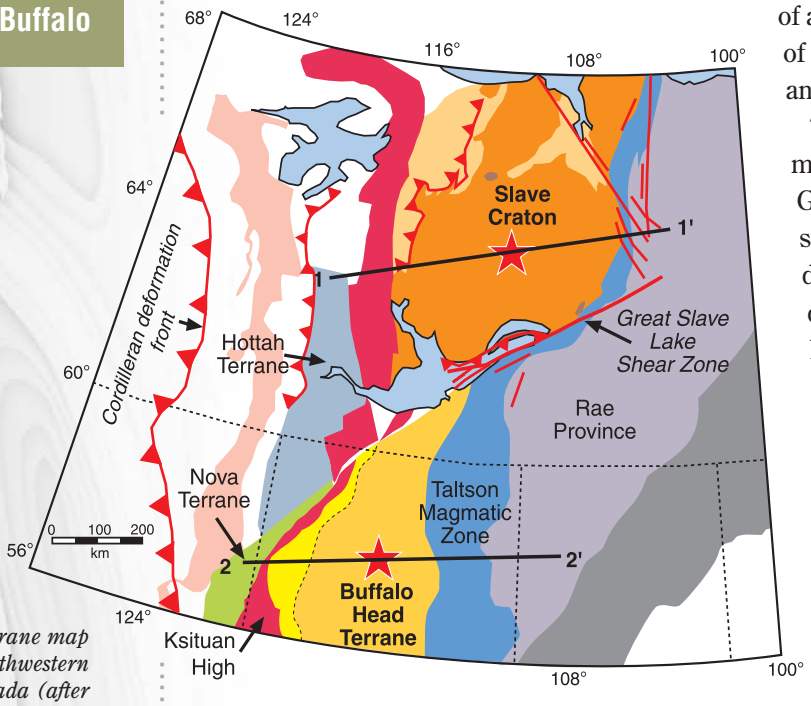

Terrane map of northwestern Canada (after Hoffman, 1987). Red stars show the Lac de Gras kimberlite locality (Slave Craton) and the Buffalo Hills kimberlite locality (Buffalo Head Terrane).

The subcontinental lithospheric mantle (SCLM) beneath Lac de Gras (central Slave Craton) is strongly layered, with an ultra-depleted shallow and a less depleted plume-related deep layer (see *Research Highlights 1997, 2000*; Publications #137, 303). Some sulfides from the deep SCLM layer lie on a 3.27 ± 0.34 Ga isochron with a supra-chondritic initial Os isotopic composition that may be interpreted as the signature of a high-Re/Os source, such as the lower mantle or outer core. This age exceeds that of the overlying crust, part of the Contwoyto terrane, but coincides with a period of major crust formation in the neighbouring Central Slave Basement Complex (CSBC), suggesting that CSBC-type deep SCLM was thrust under the younger Contwoyto terrane during 2.7 Ga collision (Publication #346; Fig. 1A-C). Proterozoic metasomatism by possibly asthenosphere-derived melts that evolved from silicate to small-volume residual melts similar to carbonatite is indicated by high Lu/Hf, but low Sm/Nd in garnet, resulting in highly radiogenic Hf and unradiogenic Nd. Interaction with melts that originated from a source similar to that of the host kimberlites preceded 50 Ma kimberlite magmatism and led to variable resetting of Nd and Hf isotope ratios (Fig. 1E).

The BHT consists

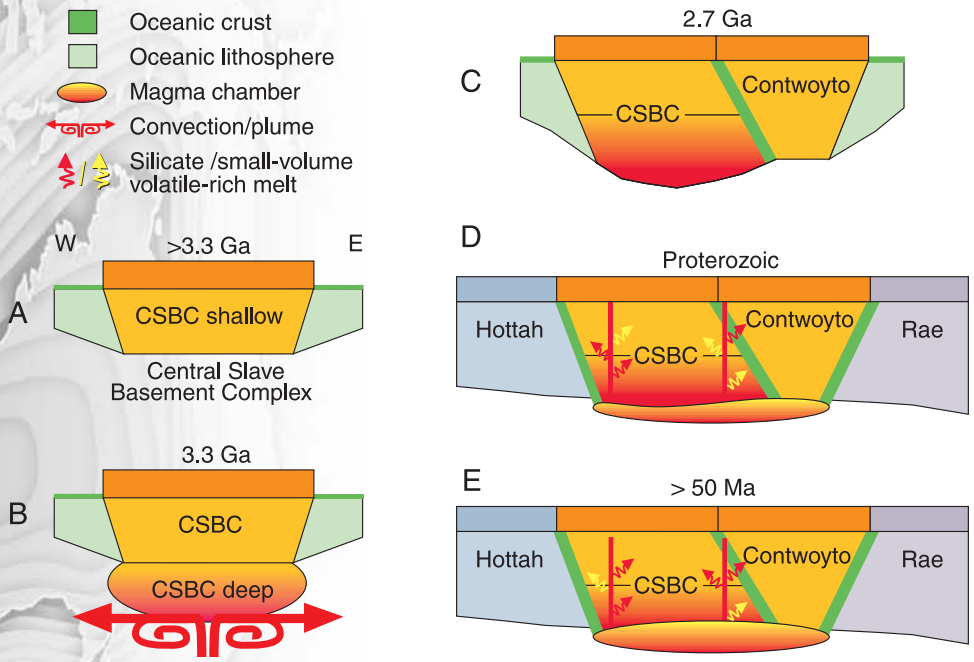

Figure 1. Evolution of SCLM beneath the central Slave Craton (transect 1-1' above).

mostly of Proterozoic basement rocks, but there are indications that this basement was continuous with the Rae province in Archean times (Fig. 2A). Peridotites from Buffalo Hills have a range in FeO, MgO and SiO_2 similar to those in the deeper layer of the central Slave craton section and this may suggest that the mantle beneath the BHT and the central Slave craton formed under similar conditions, i.e. plume subcretion. Lower mantle inclusions in diamonds from the Buffalo Hills kimberlites strengthen the plume connection (Publication #346).

As in the Slave Craton, a later (in this case Proterozoic) metasomatic event is recognised, involving silicate melts that evolved to small-volume volatile-rich melts through interaction with garnet-bearing mantle, but the importance of different metasomatic styles and their distribution with depth are different. This metasomatism may have occurred during 2.4 to 2.3 Ga rifting of the Buffalo Head Terrane from the neighbouring Rae province (Fig. 2B) and may be responsible for the evolution of some samples toward unradiogenic Nd and Hf isotopic compositions. No metasomatic processes related to subduction beneath the BHT during collision with the Chinchaga domain at 2.0-1.9 Ga are evident in mantle rocks from the BHT (Fig. 2C). However, an additional metasomatic event around 1.9 Ga may be documented by sulfide in one peridotite that has unradiogenic $^{187}Os/^{188}Os$ and gives a model age of 1.89 ± 0.38 Ga (Fig. 2D). This age coincides with the inferred emplacement of mafic sheets in the crust and suggests that the melts parental to the intrusions interacted with the lithospheric mantle. A young metasomatic event is indicated by the occurrence of sulfide-rich melt patches, unequilibrated mineral compositions, and overgrowths on spinel that are Ti-, Cr- and Fe-rich but Zn-poor (Fig. 2E; Publication #352).

In summary, there are definite differences between the two cratons: the strong layering of the SCLM beneath the central Slave craton is absent beneath the BHT, and metasomatic signatures in different depth intervals differ in style. However, there are also some parallels in the evolution of the SCLM beneath the two areas. This may indicate that plume-influenced SCLM growth and repeated metasomatism, including metasomatism precursory to kimberlite magmatism, are common milestones in the genesis and evolution of Archean to Proterozoic SCLM.

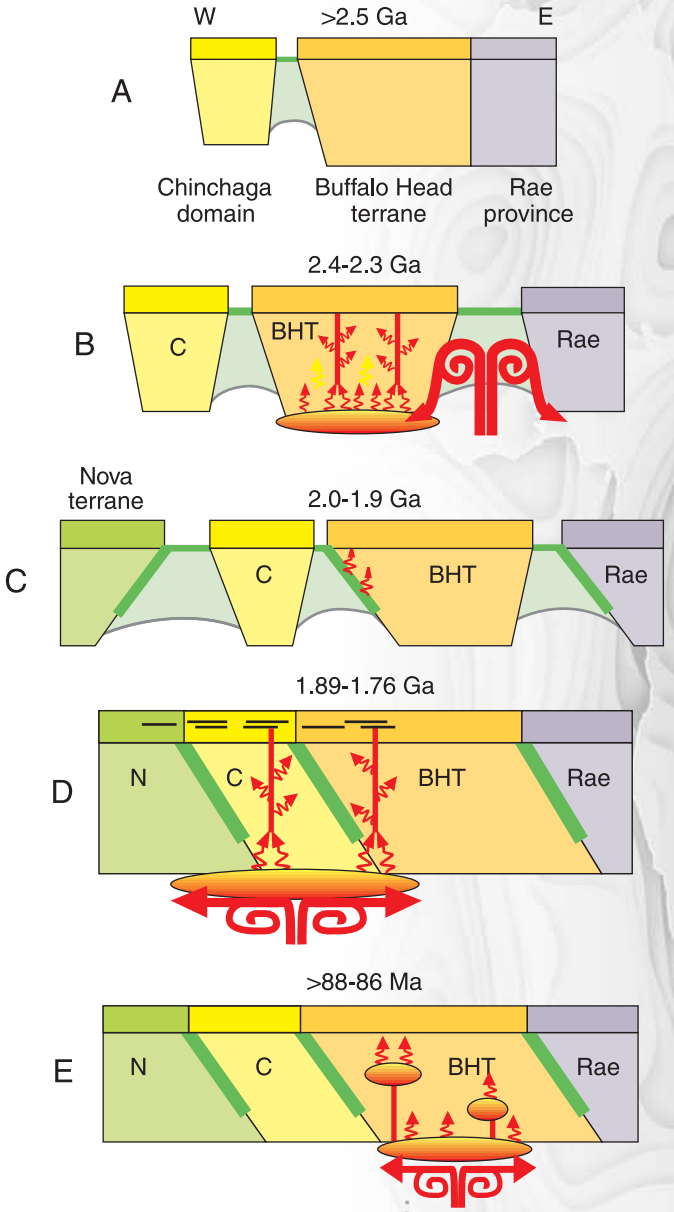

Figure 2. Evolution of SCLM beneath the Buffalo Head Terrane (transect 2-2').

Contacts: Sonja Aulbach, Bill Griffin, Sue O'Reilly
Funded by: GEMOC, IPRS, MUIPRA, MUPGRF, ARC Large, ARC Spirt, Industry

The Old Soak – Hf in MARID rutile unravels mantle metasomatism

THE GROUP I KIMBERLITES of the Kaapvaal Craton in South Africa carry many types of mantle-derived xenoliths, providing a snapshot of mantle composition at the time of eruption (ca 90 million years ago). The xenolith suite contains rare but spectacular samples of rocks known as MARID (from their mineral assemblage Mica-Amphibole-Rutile-Ilmenite-Diopside), some of which are altered to Phlogopite-Ilmenite-Clinopyroxene (PIC) assemblages. The origin of these rocks – whether metasomatic or magmatic – has been widely debated, and several detailed isotopic studies have been inconclusive. These rocks are difficult to study isotopically, because their complex history means that mineral separates may record only the average of several different processes. *In situ* isotopic analysis, with better spatial resolution, might resolve these processes, but most of the elements of traditional isotopic systems are too dilute in the main minerals to be analysed *in situ*.

However, preliminary studies showed that the rutile in MARID and PIC rocks contains 900-1500 ppm Hf, which is enough to get analyses of useful precision for $^{176}Hf/^{177}Hf$ (±0.0002, 2 sigma) using GEMOC's LAM-MC-ICPMS techniques. The rutiles are very refractory, and they have very low Lu/Hf ratios, so that the Hf-isotope composition of the rutiles can be regarded as "frozen in" at the time of crystallisation. We therefore have analysed Hf isotopes in large (0.5-5 mm) rutile grains in 9 xenoliths, showing the full range from typical MARID, through intermediate MARID-PIC samples to PIC.

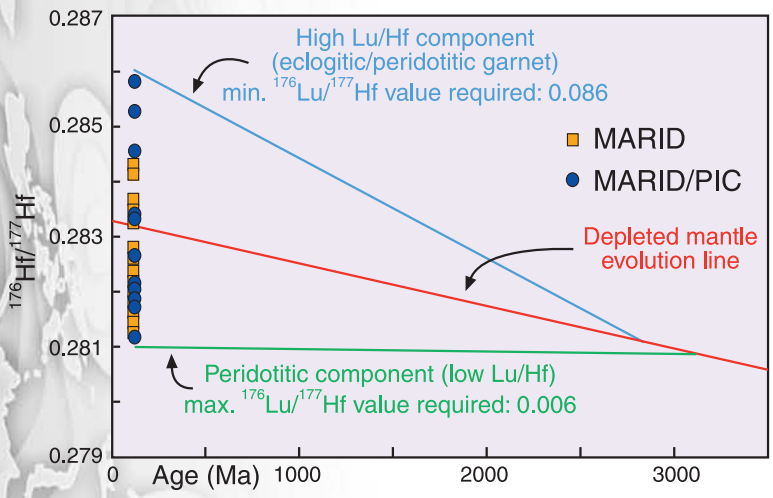

Figure 1. Hf isotope evolution plot showing composition of Hf in rutiles from MARID and PIC samples, and evolution of Hf isotopes in mantle peridotites and eclogites.

The rutiles proved to be isotopically very heterogeneous. $^{176}Hf/^{177}Hf$ ranges from 0.2812-0.2858 (Fig. 1); much of this range is found within single samples and even within single grains. The lowest values represent Hf that has been isolated from the Depleted Mantle source for about 3 Ga, similar to ages derived for the formation of the SCLM under the Kimberley area (see *2002 Research Highlights*). The highest values lie far above the mean value for the present-day Depleted Mantle, and represent Hf that has resided in a rock or mineral with high Lu/Hf for a long time. One possible reservoir is mantle garnet; with typical $^{176}Lu/^{177}Hf$ ratios of ca 0.085, such garnets could "grow" the most radiogenic Hf seen in the MARID rutiles over ca 2.8 Ga (Fig. 1).

We therefore suggest that the MARID rocks initially resulted from the interaction of an asthenospheric melt with ancient harzburgitic mantle, which has dominated their Hf budget (giving the low Hf isotopic signatures). They were later metasomatised by a fluid/melt that had caused the breakdown of eclogitic or lherzolitic garnet with high Lu/Hf, providing a source of highly radiogenic Hf (explaining the range to high Hf isotopic signatures).

During the analytical work, a single large (1.5 mm) zircon was found in one of the MARID samples. Its Hf isotope composition ($^{176}Hf/^{177}Hf$ = 0.28224±2) lies near the mean value for the rutiles, linking it to related metasomatic activity. It gave a LAM-ICPMS U-Pb age of 112±4 Ma, which corresponds to the age of the older (Group II) kimberlite magmatism in the area, and is consistent with a genetic link between MARID and Group II kimberlites (Gregoire et al., 2002. Contrib. Mineral. Petrol. 142, 603-625).

The low $^{176}Hf/^{177}Hf$ preserved in MARID rutiles also helps to resolve one of the minor controversies about the origin of kimberlites. In plots of Nd-Hf isotopes (Fig. 2), the Group I and Group II kimberlites define long trends pointing to low values. Nowell et al. (1999. Proc. VIIth Inter. Kimberlite Conf., 2, 616-624) argued that these data require a "hidden reservoir", probably located in the very deep mantle, while Griffin et al. (2000, Publication #179) suggested that this reservoir was simply the lithospheric mantle. The new *in situ* rutile data, combined with published data on MARID rocks (Fig. 2) show that the Nd-Hf isotopic systematics of kimberlites and lamproites also can be explained by contamination of asthenospheric melts with the ancient subcontinental lithospheric mantle, without any mysterious hidden reservoirs.

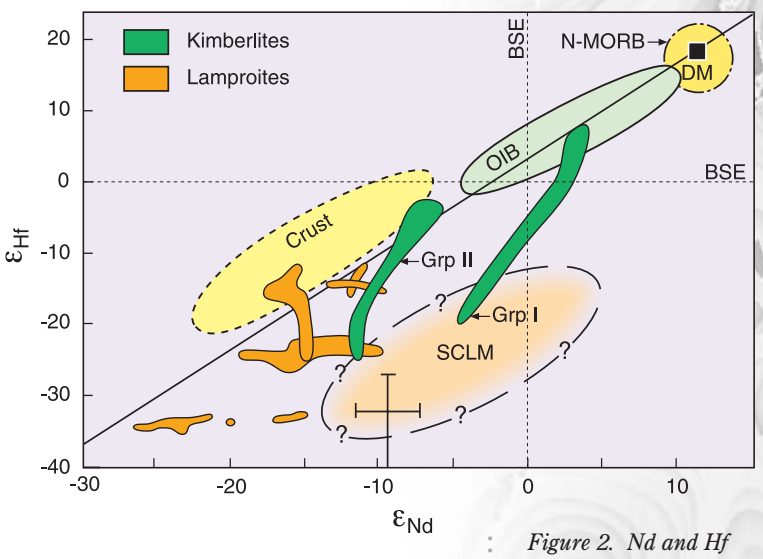

Figure 2. Nd and Hf isotope compositions of Earth reservoirs. SCLM = subcontinental lithospheric mantle, + shows MARID compositions. Kimberlite trends reflect mixing between asthenospheric melts and metasomatised SCLM.

Contact: Mathieu Choukroun, Sue O'Reilly, Bill Griffin
Funded by: ARC Discovery

Granitoid Genesis in the Georgetown Inlier, North Queensland

A WIDE VARIETY of granitoid rocks was generated in the Georgetown Inlier (Fig. 2) during three major events in Mid-Proterozoic, Siluro-Devonian and Permo-Carboniferous time. Contemporaneous mafic and felsic magmatism during these events could reflect the underplating of the continental crust by basaltic magmas (Black and McCulloch, 1990).

As part of a study of the evolution of the crust-mantle system beneath this region, three detrital zircon samples were taken from the Etheridge Province, where Siluro-Devonian I-type granites and Permo-Carboniferous I-, S- and A-type granites intruded the Proterozoic Einasleigh Metamorphics. The zircons were analysed by *in situ* LAM-ICPMS (Laser Ablation Microprobe Inductively Coupled Plasma Mass Spectrometry) for U-Pb ages, trace element patterns and Hf isotope composition (the *TerraneChron*™ approach: see *Research Highlights p133*).

U-Pb dating yielded Mesoproterozoic, Siluro-Devonian and Permo-Carboniferous ages comparable to those recognised from existing SHRIMP U-Pb zircon data. The modelling of *in situ* LAM-ICPMS trace-element data indicates that the majority of zircons are derived from granitoids with 65-75 % SiO_2, consistent with the known geology. Many of the zircons, especially in one sample, are characterised by resorbed cores of Proterozoic age overgrown by oscillatorily-zoned rims of Siluro-Devonian age (Fig. 1), offering an opportunity to study magma sources and evolution in two time slices.

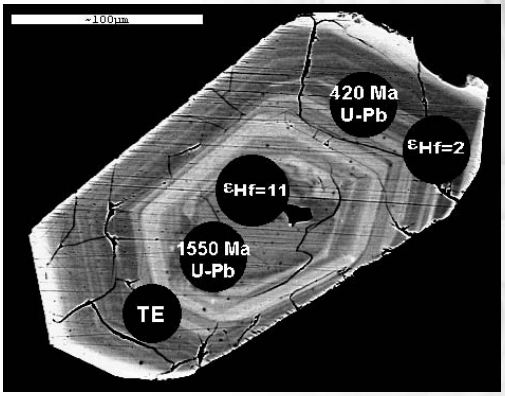

Figure 1. A backscattered electron image of a zircon grain.

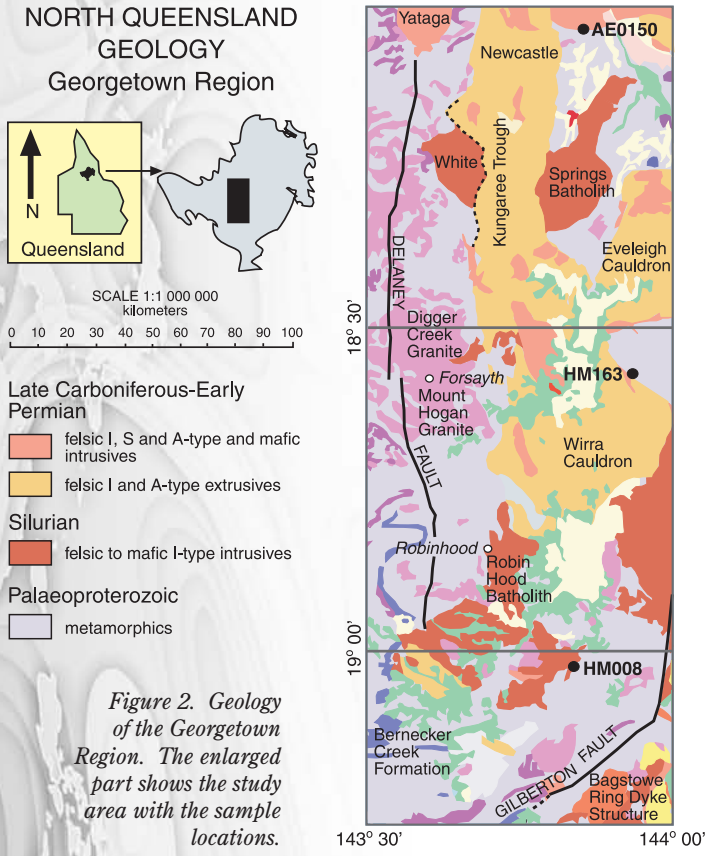

Figure 2. Geology of the Georgetown Region. The enlarged part shows the study area with the sample locations.

The Proterozoic cores in Siluro-Devonian zircons, and single grains with Proterozoic ages, are characterised by a wide spread of ε_{Hf} values, from 11.2 to -9 (Fig. 3). The lowest values give model ages (assuming an average crustal source) of more than 3 Ga, while the highest lie near the value for the Depleted Mantle at the time. This suggests mixing between magmas derived from Archean crust (low ε_{Hf}) and magmas of juvenile origin (high ε_{Hf}). The Siluro-Devonian rims, and single grains with Siluro-Devonian ages, also show a large range in ε_{Hf} from 2 to -26.5. This spread could reflect either mixing of crustally-derived and juvenile magmas, or the remelting of a heterogeneous Proterozoic crust. The observation that high- ε_{Hf} rims are found on high- ε_{Hf} cores (Fig. 3) tends to favour the latter model, and does not indicate a large juvenile contribution to the crust in Siluro-Devonian time. However, some zircons have ε_{Hf} too high to be derived from Proterozoic sources, and their trace-element chemistry indicates they are derived from mafic rocks. Basaltic underplating thus may have provided a heat source for remelting of the Archean to Proterozoic lower crust to generate most of the Siluro-Devonian granitoids.

The zircons from the Permo-Carboniferous granitoids show a much narrower range in ε_{Hf}, and a higher mean value (+7), indicating a much larger contribution of juvenile material than occurred in either Proterozoic or Siluro-Devonian time.

These preliminary results suggest that the Georgetown Inlier is underlain by Archean crust, although the surface geology is dominated by Mesoproterozoic basement rocks and Paleozoic granitoids. Its crustal evolution has involved at least three stages of strong heating, possibly associated with basaltic magma underplating and/or overplating, and reflecting the complex tectonic history of north Queensland. However, the most significant juvenile additions to the crust, after the Archean, may have occurred in Permo-Carboniferous time.

Contact: Valeria Murgulov, Sue O'Reilly, Bill Griffin

Funded by: Macquarie University, BHP Billiton, APA

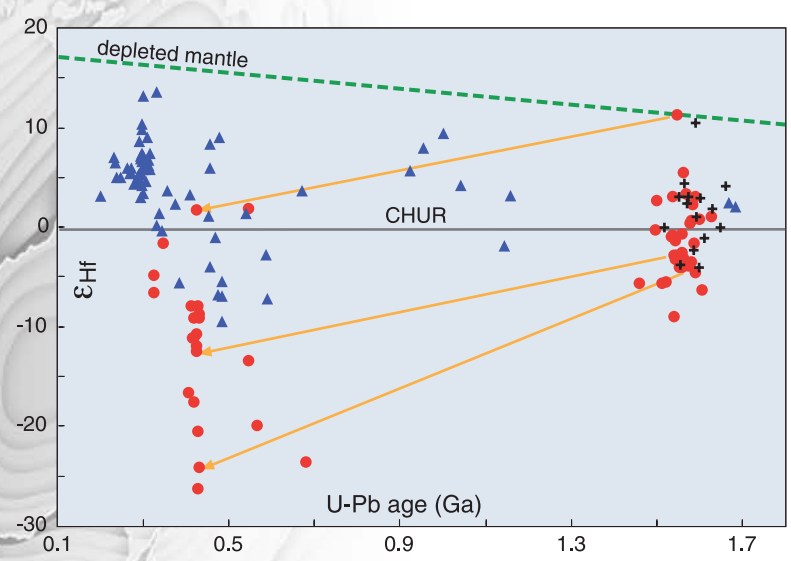

Figure 3. Plot of ε_{Hf} vs age for Georgetown zircons from three samples (circle, triangle and cross). Zircons lying below the CHUR (Chondritic reservoir) line are derived largely from crustal sources; those lying between CHUR and Depleted Mantle contain material derived from both crustal and juvenile sources. The arrows connect the Proterozoic core and Siluro-Devonian rim in representative grains.

TerraneChron™: a competitive edge in exploration and understanding crustal evolution

TERRANECHRON™ is GEMOC's unique methodology for terrane evaluation and studies of crustal evolution. It is based on the integrated *in situ* analysis of zircons for *U-Pb ages, Hf-isotopic composition* and *trace-element compositions* using GEMOC's laser-ablation-microprobe ICPMS technology. It can be applied to zircons from single rocks or to zircons separated from drainage samples judiciously collected within a defined catchment (on scales of 10 - 1000 km depending on terrane and terrain).

The zircon *U-Pb analyses* provide rapid and cost-effective age determinations with accuracy comparable to the ion microprobe; the *Hf-isotopic data* provide information on the source characteristics of the magmatic parent rock to the zircon - whether it was generated by crustal reworking or from young mantle ("juvenile") sources. The *trace elements* provide information about the composition of the magmatic rock that precipitated the zircon.

The combination of age, composition and sources of magmas for a large number of grains from drainage samples yields an "Event Signature" providing a clear fingerprint of crustal evolution events (Fig. 1).

Figure 1. Event signature diagram for S. Norway and Mt Isa.

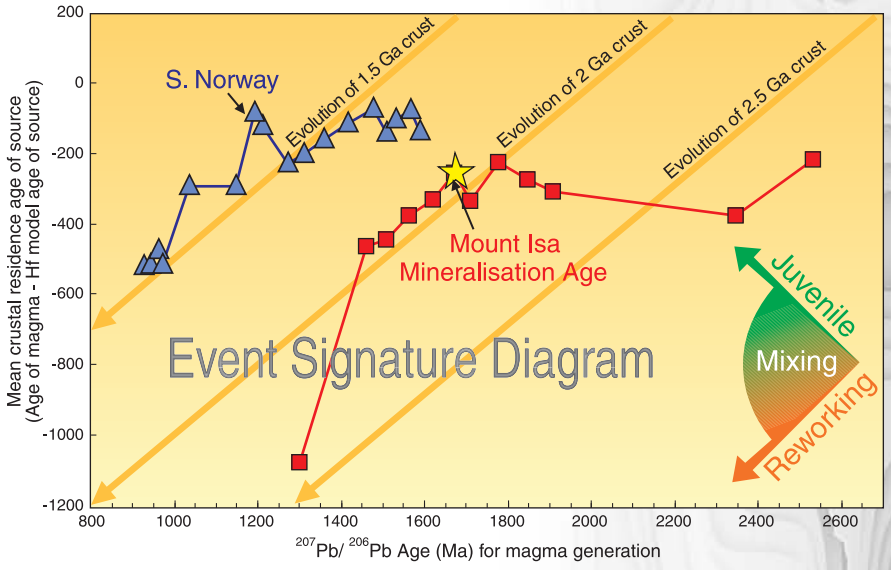

In this "Event Signature" diagram, trends toward the lower left (see key on Fig. 1) indicate tectonic events dominated by *reworking of pre-existing crustal material. Juvenile (young mantle) input* is shown by trends towards the upper left. Trends of intermediate slope imply contributions from both juvenile and pre-existing crustal sources.

Figure 1 shows results for the Mt Isa Eastern Succession (Australia) and southern Norway. ***Mt Isa's tectonic history***, as shown by these zircons, starts with a short episode of Late Archean crustal reworking, followed by several episodes of juvenile addition and mixing with reworked crust up to about 1.8 Ga, a short period dominated by crustal reworking, then a significant juvenile input at ca 1650 Ma, associated with the main Mt Isa mineralistion. This was followed by crustal reworking over a period of about 200 Ma, producing rocks such as the Williams Batholith and minor later intrusives. This pattern reflects *repeated extensional tectonism and magmatism superimposed on a pre-existing old crustal environment.*

In contrast, the Event Signature for ***southern Norway*** (a poorly mineralised area) shows no Archean prehistory, but is dominated by juvenile input from 1.6-1.4 Ga; and by crustal reworking from 1.4-1.3 Ga. This pattern reflects the *continual buildup of new crust at a convergent margin.* The Sveconorwegian (Grenville) episode started with pulse of juvenile input at ca 1.2 Ga, but the later magmatism (1.1- 0.9 Ga) was dominated by crustal reworking.

The *TerraneChron*™ methodology thus:

- Yields a synthesis of the tectonic history in the region sampled and identifies relative crust- and mantle contributions to specific magmatic episodes
- Can be used as a cost-effective reconnaissance tool in remote, inaccessible or complex terranes for evaluation of exploration potential
- Can potentially fingerprint the tectonic signatures associated with different styles of mineralisation
- Defines the timescales for crustal reworking and thermal relaxation after major crustal-generation events

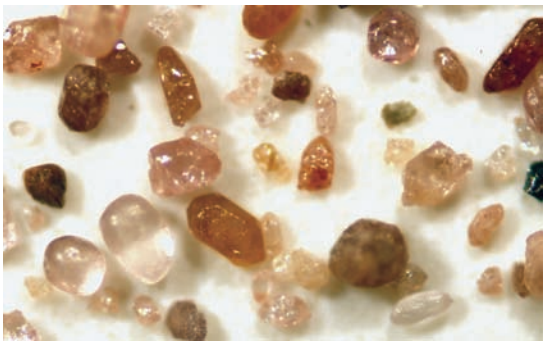

Contacts: Bill Griffin, Sue O'Reilly, Elena Belousova
Funded by: ARC Discovery, Industry, Macquarie University Collaborative Grants

Carbonatites beneath oceanic plateaus: trapped melts in xenoliths from Kerguelen

THE KERGUELEN ARCHIPELAGO is located in the southern part of the Indian Ocean. Along with Heard Island 500 km to the south, the islands lie on the huge Kerguelen-Heard oceanic plateau (25 x 10^6 km^3), which is the second largest in the world after the Ontong-Java plateau. Numerous occurrences of ultramafic to mafic xenoliths (24 outcrops) have been described in the Kerguelen archipelago with a higher concentration in the southeastern province (Ronarc'h and Jeanne d'Arc peninsula; see p.126). The Kerguelen archipelago has provided the largest diversity of xenoliths ever observed in an oceanic setting (Grégoire et al., Eur. J. Min., 9, 1996).

Some mantle-derived Kerguelen harzburgite and dunite xenoliths have bulk-rock and mineral trace-element compositions that provide evidence of carbonatitic metasomatism similar to that described in some continental and other oceanic settings. Rare xenoliths contain carbonates that are highly enriched in rare-earth elements (REE), interpreted to be quenched, evolved carbonatitic melts. One amphibole-bearing dunite xenolith containing carbonates in small interstitial pockets (100-500 µm across; Fig. 1) has been studied in detail. Mg-bearing calcite (MgO: <1.4 wt%, X_{Ca} = 0.96) with unusually high REE abundances and strong LREE enrichment occurs in the pockets; the trace element contents of these carbonates are similar to those of common carbonatite magmas (Fig. 2). The REE-rich carbonate is sometimes associated with euhedral carbonates (dolomite and Mg-free calcite), mafic silicate glass (low in alkalis) and small grains of spinel, sulfides and magnesio-

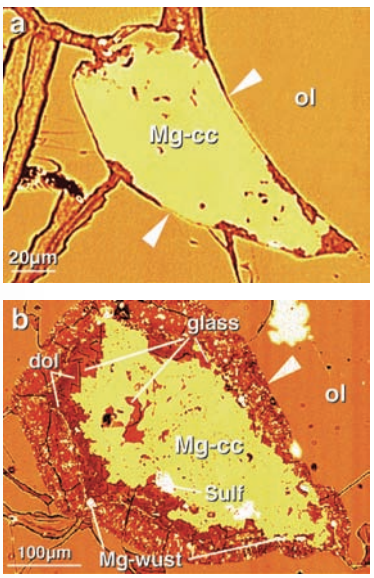

Figure 1: Back-scattered electron imaging of carbonate-bearing dunite; **a:** *anhedral Mg-bearing calcites have sharp curvilinear boundaries with olivine and totally fill the interstitial spaces;* **b:** *pocket of Mg-bearing calcite with silicate glass and rim reaction zone that consists of very fine-grained silicate phases, magnesio-wüstite, euhedral crystals of dolomite and Ni-sulfide.*

wüstite concentrated near the boundaries of the carbonate pockets (Fig. 1).

The unusual metasomatic mineral assemblage, together with the microstructural features and the chemical composition of the carbonates, suggests that the pockets of Mg-bearing calcite represent quenched carbonate melts rather than crystal cumulates from carbonate-rich melts. The associated mafic silicate glass may represent the immiscible silicate fraction of an evolved fluid produced by the dissolution-percolation of the original carbonate melt through the dunitic matrix. Unmixing of the silicate and carbonate fractions would be expected to occur as the xenoliths ascended to the surface.

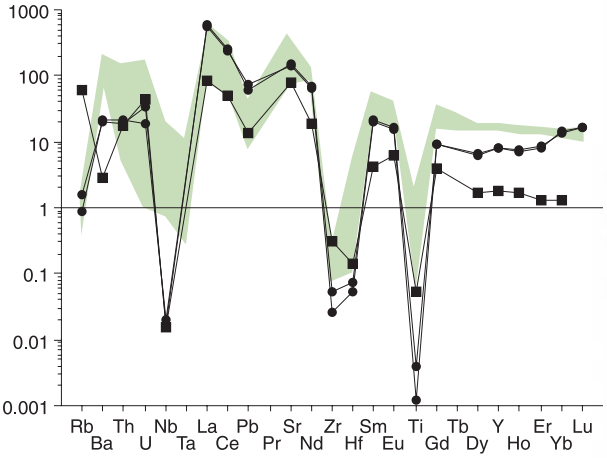

Figure 2: Trace-element patterns of Mg-bearing calcite (black symbols) compared with calcio-carbonatite from Cape Verde (Hoernle et al., 2002; shaded field). Trace-element contents normalised to Primitive Mantle, McDonough and Sun, 1995.

During the percolation, carbonate melt dissolves olivine and reacts with preexisting amphibole and spinel to produce clinopyroxene. This pyroxene is therefore inferred to be in chemical equilibrium with the carbonate melt. This allowed calculation of clinopyroxene/carbonate melt partition coefficients for a large set of trace elements at relatively low pressure (1 GPa). The results indicate a significant pressure control on REE partitioning between carbonate melt and clinopyroxene (Fig. 3) as was observed experimentally by Adam and Green (see *Research Highlights 2001*) for clinopyroxene and basanitic melt.

These data, and the recent discovery of zircon-bearing dolomitic tuff on the Kerguelen archipelago (IPEV field campaign 2002; another occurrence is known on the Cape Verde Islands) provide a new understanding of carbonate melt genesis in the oceanic mantle and the implications of these melts for mantle metasomatism.

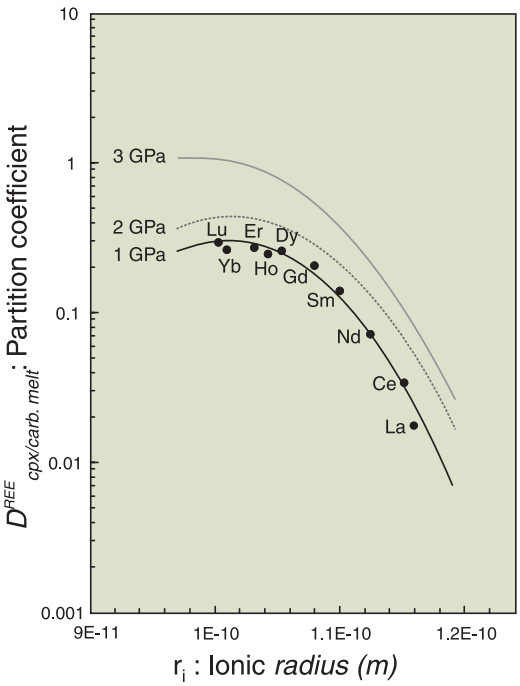

Figure 3: Plot of REE partition coefficients (D_i) between cpx and carbonate melt (Mg-bearing calcite) versus VIII-fold co-ordinated ionic radius (r_i, Shannon, 1976). Data from this study are compared with experimental results at 2 GPa (Klemme et al., 1995) and 3 GPa (Blundy & Dalton, 2000).

Contact: Bertrand Moine (Univ. Jean Monnet, St. Etienne), Sue O'Reilly
Funded by: CNRS (France), ARC Discovery

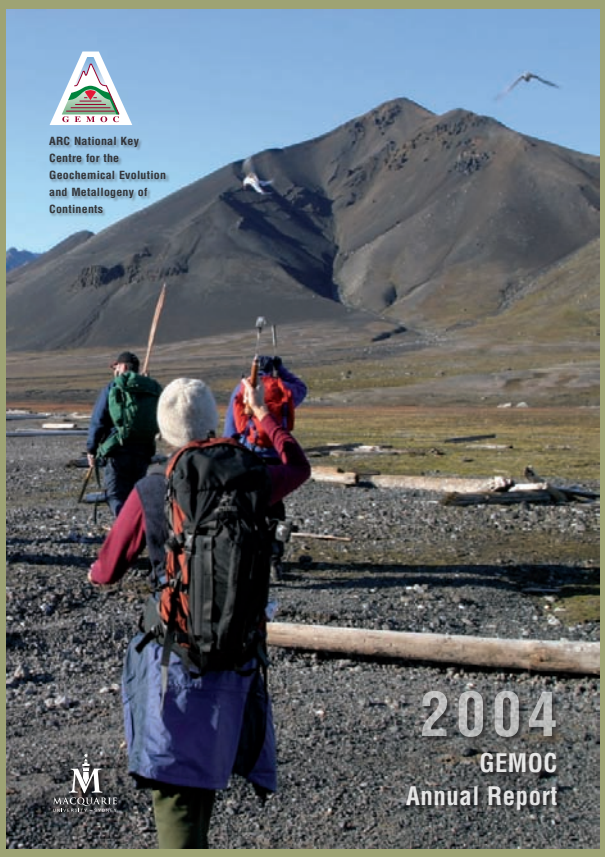

2004 Contents

TerraneChron™	137
Is there anyone down there?	138
Layered mantle beneath the Dharwar Craton: a key to ancient processes	139
Laurentian mantle fragments in Baltica's crust: zircon data support the "slam-dunk" model	140
Keeping the lid on: How long do island arc magmas degas before erupting?	142
PGE fractionation in mantle sulfides: fingerprints of metasomatic processes	144
Fault-scarp-derived volcaniclastic deposits on Macquarie Island; sedimentation at a fossil ridge-transform intersection?	146
A continental near-neighbour during Abitibi crustal growth	148
Seismic properties of the Amery Ice Shelf – How thick is it, and how does it move?	150
Tracing gold with zircon	152
Zircon – a multi-faceted tool for petrogenetic modelling	154
Kimberlites and lamproites probe the deep crust of the Dharwar Craton, south India	156
Risk management in exploration: Finding more mines for less money	158

Front Cover: The hazards of Arctic fieldwork – the GEMOC team under attack by angry Arctic terns, on their way to collect xenoliths on the Sverrefjell volcano, NW Spitsbergen. See Research Highlights for more on the 2004 Arctic Mars Analog Svalbard Expedition (AMASE).

TERRANECHRON™ is GEMOC's unique methodology for terrane evaluation. Industry continued extensive use of *TerraneChron*™ as a cost-effective tool for mapping crustal history on different scales.

Is there anyone down there?

FROM VOLCANOES in the Arctic, to meteorites, to Mars and the origins of life on Earth and other planets – this is a remarkable story about where science can lead you. In the 1980s Sue O'Reilly, Bill Griffin and a group of students worked on mantle-derived xenoliths in Quaternary basalts from the northern edge of the arctic island of Spitsbergen in the Svalbard archipelago (80°N), focussing on a remarkable glacier-bound volcano called Sverrefjell. Now GEMOC has returned to Sverrefjell as part of the international AMASE (Arctic Mars Analogue Svalbard Expedition) team, in a program to design and test instrumentation and methods for the detection of life on Mars.

Bill Griffin fingers Sverrefjell, the expedition's target volcano.

The Sverrefjell peridotite xenoliths, derived from depths of about 50 km, contain minute volumes of gases (mainly CO_2) trapped in cavities within their minerals, and analyses of these gases in 1985 showed the presence of many types of hydrocarbons – an observation that was difficult to understand at the time. Carbonate minerals in the xenoliths, in the fluid inclusions, and in volcanic vents at the surface form tiny round structures, which were originally interpreted as magmatic and/or hydrothermal in origin. When similar structures were found in Martian meteorites and described as evidence for life, one of the original Svalbard expedition, Hans Amundsen, was sceptical and he showed the Sverrefjell rocks to the meteorite group. They carried out biochemical analyses and found that the structures contained biological signatures; rather than disproving the meteoritic evidence for life on Mars, the Svalbard rocks appeared to support it.

The GEMOC field team, with two biochemists for assistance, in front of Sverrefjell.

Xenoliths galore, in a Sverrefjell dike with platy margins.

These results have led to the far-reaching hypothesis that volcanic emanations can carry hydrocarbons originally derived from the upper mantle, and that these may form the building blocks and templates for prebiotic molecules. If this is correct, it implies that life might arise on any planet with Earth-like volcanism.

Further analyses showed that many of the old hydrothermal vents in the core of the Sverrefjell volcano, exposed by glaciation, are teeming with microbial life, and biofilms coat minute cracks in the rocks to great depths. The AMASE expeditions (led by Hans Amundsen) arose from the recognition that Sverrefjell also offers an ideal Mars- analog situation where instrumentation designed for space exploration can be tested. It is cold and dry

and has both volcanic and sedimentary rocks, and hot springs along the shoreline near the volcano are full of microbes, providing several different environments for testing purposes. An impressive backdrop of red sandstones (the Devonian redbeds) adds to the Mars-like atmosphere.

The 2004 AMASE expedition included scientists (instrument designers, macro- and microbiologists, immunologists and even geologists) from the Smithsonian Institution, Cal Tech, NASA, several European universities and GEMOC; the material collected in 2004 is being studied by Nenad Nikolic, as a GEMOC PhD project. A story on the life-or-not controversy, and the AMASE expedition, appears in the May 2005 issue of the *Smithsonian* magazine.

The AMASE expedition (Hans Amundsen at left) awaits its ship, with some of its luggage.

Contact: Sue O'Reilly, Bill Griffin, Norman Pearson
Funded by: ARC, NASA, Macquarie University

Layered mantle beneath the Dharwar Craton: a key to ancient processes

During 2004 Dr EVSSK Babu of the National Geophysical Research Institute began a large-scale study of mantle structure and composition beneath the Eastern Dharwar Craton (EDC) in southern India, using xenoliths and xenocrysts from 1.1 Ga kimberlites. The kimberlites of the Kalyandurg cluster are especially rich in xenoliths, including a large and varied suite of eclogites. Besides the common bimineralic (garnet + clinopyroxene) varieties, there are many coesite ± kyanite ± rutile-bearing eclogites (Fig. 1). Perhaps the most spectacular aspect of the eclogites is their location: all of the samples appear to come from a narrow P-T range, corresponding to a layer less than 3 km thick at a depth of about 145 km. This thin layer sits in the middle of the lithospheric mantle, as defined by peridotite xenoliths and garnet temperatures from the same pipes. How can such a layer form, and in this position? Clues may lie in the trace-element geochemistry of the garnets and pyroxenes – many of the Kalyandurg eclogites have very high contents of Sr and Ba, and some show positive Eu anomalies, suggesting that they were originally formed at shallow depths before being brought down to at least 145 km. One possibility is that they represent the Archean crust of the Western Dharwar Craton, thrust into the mantle during the 2.6-2.7 Ga collision of the Western and Eastern Dharwar cratonic blocks (see "*Kimberlites and lamproites probe the deep crust of the Dharwar Craton, south India*" Research Highlight p.156); another is that the deep mafic crust of the EDC was converted to eclogite during cooling from magmatic temperatures. This dense lower crust may have delaminated, and stopped only when it reached a compositional (and density) discontinuity in the EDC lithospheric mantle. Further data on the lateral variations in mantle composition, being gathered in this project, may provide an answer.

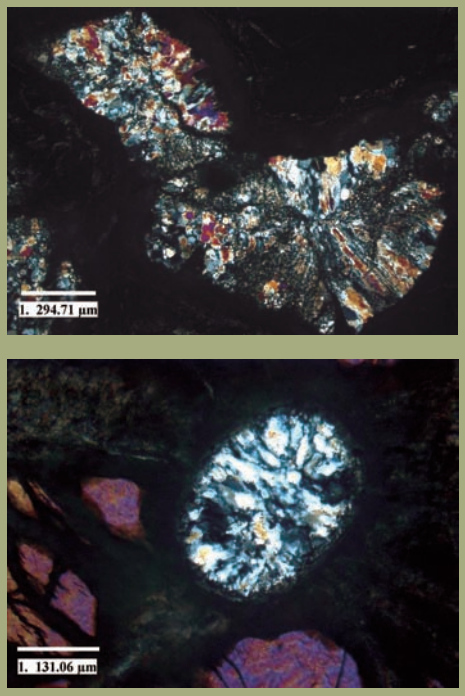

Figure 1. Inverted coesite inclusions in garnets from Kalyandurg eclogites.

Laurentian mantle fragments in Baltica's crust: zircon data support the "slam-dunk" model

MANTLE PERIDOTITE BODIES enclosed in the Proterozoic gneisses of the Western Gneiss Region (WGR) in Norway have been shown to have an Archean origin based on Re-Os dating of both whole-rock samples and their sulfides (see *Research Highlights 2002, 2003*). This discrepancy in ages between the peridotites and their host rocks raises fascinating questions about how the peridotites were emplaced into the gneisses. If they were thrust up from below the crust, we would expect there to be some Archean lower crust in the WGR, which has never been reported. An alternative is that the peridotites represent fragments of the Laurentian lithospheric mantle, scraped off into the gneisses as Baltica was thrust under Laurentia to produce the Caledonian high pressure/ultra-high-pressure (HP/UHP) metamorphism for which the WGR is famous.

This conundrum has prompted a geochronological study of the host gneisses and associated rock types to determine if there is any evidence for an Archean history for the crust in this part of the Baltic Shield. We have used GEMOC's *TerraneChron*™ technique (see *Research Highlights 2002, 2003*) which is based on the integrated *in situ* analysis of zircons for U-Pb ages, Hf-isotopic composition and trace-element compositions. This methodology has been shown to be a highly valuable tool for studies of crustal evolution and can be readily applied to tectonically complex areas such as western Norway.

Figure 1. Eloise Beyer knee-deep in her research area.

The WGR can be broadly divided into two principal lithotectonic units: (1) the HP/UHP metamorphosed Fjordane complex, a mixed assembly of gneiss, supracrustal rocks, anorthosites, augen gneisses and eclogites, exposed to the north and west; and (2) the Jøstedal complex, a more monotonous migmatitic orthogneiss unit to the east. Sample localities were selected from both units, though the Fjordane complex was of particular interest as it is this unit which contains the mantle fragments.

Detrital zircons were collected in stream sediment from several localities throughout the WGR. Preliminary results from analysis of four samples indicate a predominance of Proterozoic ages in the range 1600-1700 Ma. These ages match the period of extensive crustal formation in this area, known as the Gothian Orogeny and it is reasonable to assume that zircons of this age were sourced from rocks formed during this mid-Proterozoic event. There were also a high number of zircons with U-Pb ages in the range 1400-1500 Ma which can be correlated with a phase of intermittent mafic intrusions and possible sporadic granitic magmatism. A smaller number of zircons fall in the range 900-1300 Ma which corresponds with the extensive intrusion of dolerites and granites during the Sveconorwegian (Grenvillian) Orogeny.

The U-Pb ages give no direct evidence for an Archean-aged event in the WGR basement rocks. However, the Hf isotopic compositions of the zircon can be used

to determine the age of the sources of the magmatic parent rocks of the zircons and hence constrain the age of the deep crust. Hf isotopic data for two samples analysed to date is predominantly very juvenile, indicating that the zircon source has not undergone significant crustal reworking. Crustal model ages for the oldest group of zircons (1600-1700 Ma U-Pb ages) range from 1700-2300 Ma and show no evidence for any Archean input. The zircons with ages less than 1600 Ma have Hf compositions which suggest they were derived from a mixture of younger more juvenile material and older mid-Proterozoic crustal rock.

Figure 2. A screen concentrate with red and black rings defined by the garnet and spinel from the peridotites – the zircons are concentrated with these heavy minerals.

The lack of evidence for Archean crust in the WGR basement rocks suggests that the crust and the mantle peridotite bodies enclosed within it are not genetically related. With no evidence for an Archean lower crust, the data favour a Laurentian provenance for the peridotites (see Fig. 3). The WGR, already famous for its insights into HP/UHP metamorphism, may also contain hard physical data on the geometry and mechanisms of continental collision and the partial subduction of continental plates.

Contacts: Eloise Beyer, Bill Griffin, Sue O'Reilly
Funded by: ARC, Industry

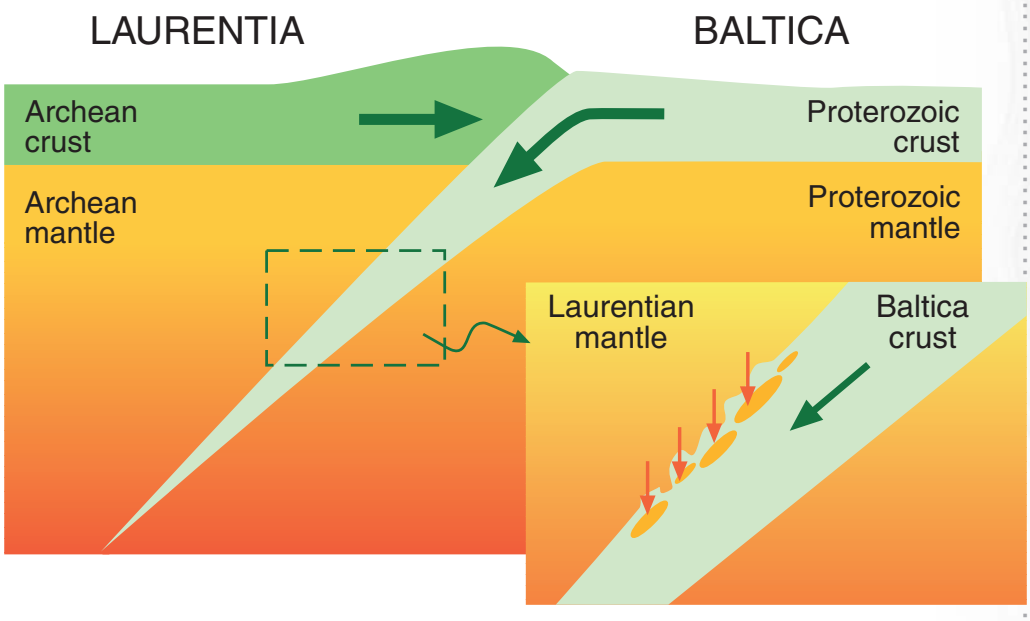

Figure 3. "Slam-dunk" model for the WGR peridotites, stuffed into the top of the descending Baltica plate.

Keeping the lid on: How long do island arc magmas degas before erupting?

AT ISLAND ARCS, fluids coming off the subducting plate facilitate partial melting in the wedge of mantle above the plate. Subsequent decompression and differentiation leads to volatile build up, degassing, the formation of hydrothermal systems and associated economic deposits, and often to violent eruptions (eg Krakatau, Tambora, Vesuvius, Mount St Helens). However, the relationships between degassing, the composition of erupted magmas and the time scales of deeper magma degassing remain unclear. For example, degassing raises the solidus, increases plagioclase stability and forces crystallisation, such that magma differentiation might be driven by degassing during magma ascent. However, volatile loss leads to increased magma density which will retard magma-crystal separation, so the link between degassing and differentiation is not straightforward. Finally, volatile build-up will be an inevitable consequence of differentiation unless it is counterbalanced by degassing – which is why the more differentiated and volatile-rich island arc magmas typically erupt most explosively.

Figure 1. Once an exsolved volatile phase exists, gases can move independently and escape from the magma through the surrounding rock or via the magma itself. A bottle neck or physical obstruction in the magmatic plumbing system can cause accumulation of gas bubbles at certain depths, which leads to potentially explosive situations.

If we can measure the time scales of these magmatic processes, we can gain important insights into the physical mechanisms at work beneath volcanoes. There has been much interest in links between the timing, composition and volume of gas emission and eruptive behaviour. Measurement of the short-lived isotope ^{210}Pb (half life = 22.6 years) can constrain the time scales of magma degassing because the decay chain from its progenitor ^{226}Ra includes the noble gas ^{222}Rn, which has a half life of only 3.8 days. ^{222}Rn is likely to be efficiently and continuously lost from a magma so long as exsolution and degassing of a major volatile species (eg CO_2, H_2O, SO_2…) is occurring. However, its short half life means that its concentrations will grow back into secular equilibrium with ^{226}Ra within a couple of weeks after degassing ends. Thus, ^{210}Pb concentrations will not "see" the effects of ^{222}Rn degassing, and ^{210}Pb/^{226}Ra will remain =1, unless the duration of degassing begins to approach the half life of ^{210}Pb. However, if the

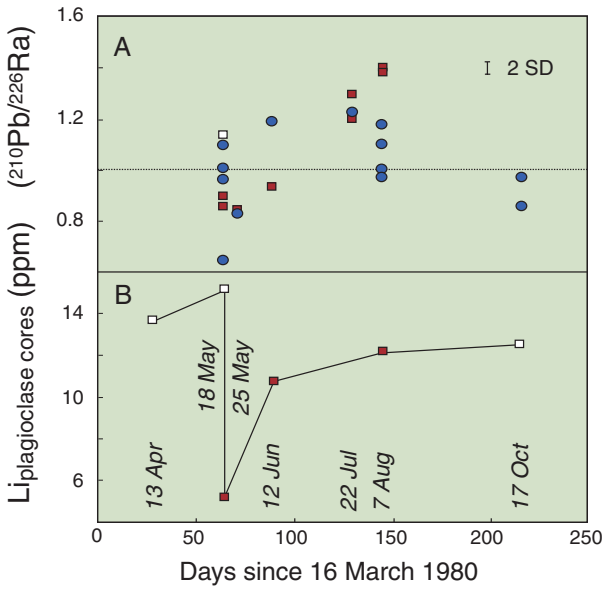

Figure 2. Variation in (^{210}Pb/^{226}Ra) in several subsequent eruptions are similar to the variation in Li concentration in plagioclase phenocrysts of those same eruptions. Both (^{210}Pb/^{226}Ra) and Li are indicators of degassing behavior of the magma. Prior to the May 18th gas bubbles with Li and ^{210}Pb accumulated, whereas on May 18th magma with low ^{210}Pb and low Li was erupted indicating a deeper degassed reservoir was tapped during this eruption. Figure after Berlo et al. (Science vol. 306).

The resurgent lava dome in the crater of Mount St. Helens, looking down the "blast corridor" of the 1980 eruption.

duration of radon degassing is on the order of several years or more significant ^{210}Pb deficits, i.e. $^{210}Pb/^{226}Ra < 1$, can be produced.

Measurements of $^{210}Pb/^{226}Ra$ in a wide range of island arc lavas from around the world show that more than 60% have significant ^{210}Pb deficits, which require degassing periods of 2-47 years. Thus it appears that most island arc magmas sit and degas for decades prior to eruption. A detailed study of Sangeang Api volcano in Indonesia indicates that this degassing post-dates magma differentiation, which occurred by crystallisation due to cooling over thousands of years deeper within the arc crust. At Mount St. Helens it appears that the $^{210}Pb/^{226}Ra$ ratio may vary with eruptive style (plinian versus effusive). Some lavas have ^{210}Pb excesses, which probably reflect the addition of ^{210}Pb via gas transport from deeper, degassing magma. ^{210}Pb excesses therefore might be used to identify volcanoes underlain by freshly emplaced magma bodies. Such information can ultimately inform models for hazard mitigation.

Contacts: Simon Turner, Rhiannon George, Tony Dosseto
Funded by: NERC, ARC

PGE fractionation in mantle sulfides: fingerprints of metasomatic processes

ANALYSES OF MANTLE SULFIDES have demonstrated the high solubility of the Platinum Group Elements (PGEs) in base metal sulphides (BMS) and show that the PGE budget of mantle rocks is fully controlled by the BMS. If they are not enclosed inside refractory silicate or oxide phases, sulfides are likely to be mobile in the lithospheric mantle and their absolute and relative abundances of PGEs can be altered by metasomatic processes. Therefore, studies of mantle sulfides may provide critical information on metasomatic processes in the mantle. Abundant primary sulfides occur both as inclusions in silicates and as interstitial grains in spinel lherzolite and pyroxenite xenoliths hosted by Miocene intraplate basalts from the Penghu Islands, Taiwan. Modally metasomatised xenoliths with amphibole can have sulfide abundances up to 1 vol.%, whereas cryptically metasomatised samples, with re-enriched trace-element patterns in clinopyroxenes, have 0.1~0.3 vol.% sulfide, well above the mantle average. These sulfides are mixtures of Fe-rich and Ni-rich monosulfide solid solutions (MSS), pentlandite, millerite and chalcopyrite, exsolved from high- temperature (>900°C) MSS bulk compositions.

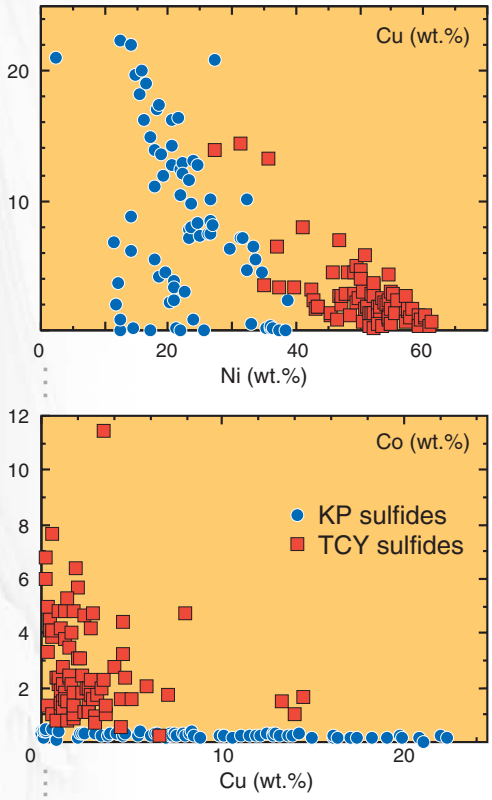

Figure 1. Bulk Ni (a) and Co (b) versus Cu in Penghu mantle sulfides.

Most Penghu sulfides are interstitial to the silicate phases, suggesting a metasomatic origin. Two distinct groups of sulfides, KP and TCY, are distinguished by their reconstructed major-element compositions (Fig. 1). The KP sulfides are Fe-Cu-rich, S-deficient MSS, whereas the TCY sulfides are Ni-rich MSS with unusually high Co contents, ranging up to 11.5 wt.% (Fig. 1). Their major-element characteristics suggest that each group of sulfides resulted from the crystallization of sulfide melts at high temperature: KP from a Cu-rich melt and TCY from a Ni-Co-rich one. Sulfides from both groups have lower Os and Ir abundances than typical residual MSS and have PGE patterns within the range of typical sulfide melts (Fig. 2); the KP sulfides have more irregular PGE patterns than the TCY sulfides, with high Ru-Rh and low Pt-Pd. The Os-isotope systematics of both groups of sulfides give Proterozoic model ages, and it seems probable that these differences in the PGE patterns reflect reaction between the sulfides and metasomatic fluids between Proterozoic and Miocene time.

The so-called P-PGEs (Pd+Pt) in the two groups of sulfides are fractionated relative to the I-PGEs (Ir + Os) but in different ways (Fig. 3a), and they have different Re-Pd relationships (Fig. 3b). Because the P-PGEs and Re are relatively incompatible elements during melting processes, these patterns suggest that both groups of sulfides have been metasomatised by silicate melts, but of different composition. Os (and Ru and Rh; not shown) behave coherently with Ir in the TCY sulfides, but in the KP sulfides, Ir and Os are only weakly correlated (Fig. 3c). This I-PGE fractionation is not likely to be caused by silicate metasomatism, considering the similar particient coefficients of the I-PGEs, so another metasomatic agent is

suggested. Aqueous fluids/low density supercritical fluids may fractionate Os from Ir (Lee, 2002; Lorand et al., 2004), and it is likely that such fluids have affected some of the KP sulfides to fractionate their I-PGEs.

Our previously published Os isotope data (see *Research Highlights, GEMOC Annual report 2003*) show these sulfides have recently undergone one unique type of Os disturbance: the addition of radiogenic Os, with little or no addition of Re. The introduction of highly radiogenic Os, which is only observed in some of the KP sulfides, may be caused by an oxidizing hydrous fluid carrying Os, but not Re. In these KP sulfides, metal/sulfur ratios are negatively correlated with $^{187}Os/^{188}Os$ (Fig. 3d), indicating that sulfides equilibrated under oxidising conditions have higher $^{187}Os/^{188}Os$. The unique metasomatic agent causing fractionation of I-PGEs coupled with enrichment in (radiogenic) Os may reflect specific processes that remain to be identified. Sulfide studies can provide more constraints on these processes, and sulfur saturation in metasomatic fluids may play a major role in controlling Re and Os (and other PGE) distribution in magmas and residual peridotites.

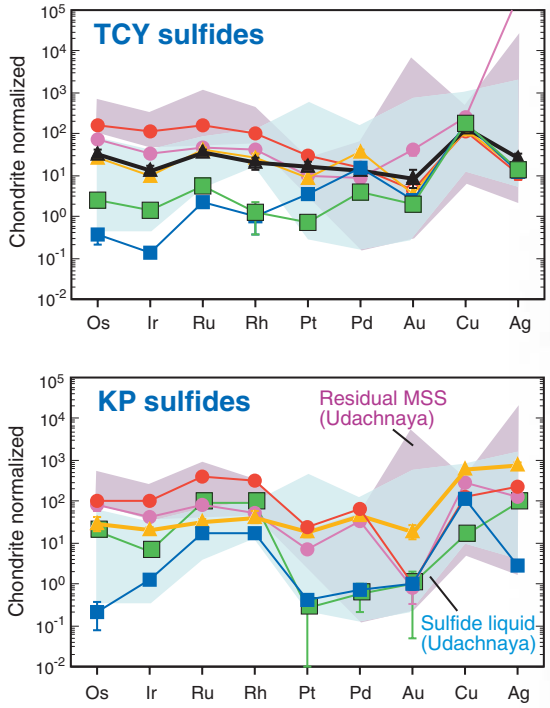

Figure 2. Chondrite-normalised PGE patterns for Penghu mantle sulfides. Data for shaded fields representing residual MSS and sulfide liquids are from Griffin et al. (2002).

Contacts: Kuo-Lung Wang
Funded by: Macquarie University (Fellowship), ARC

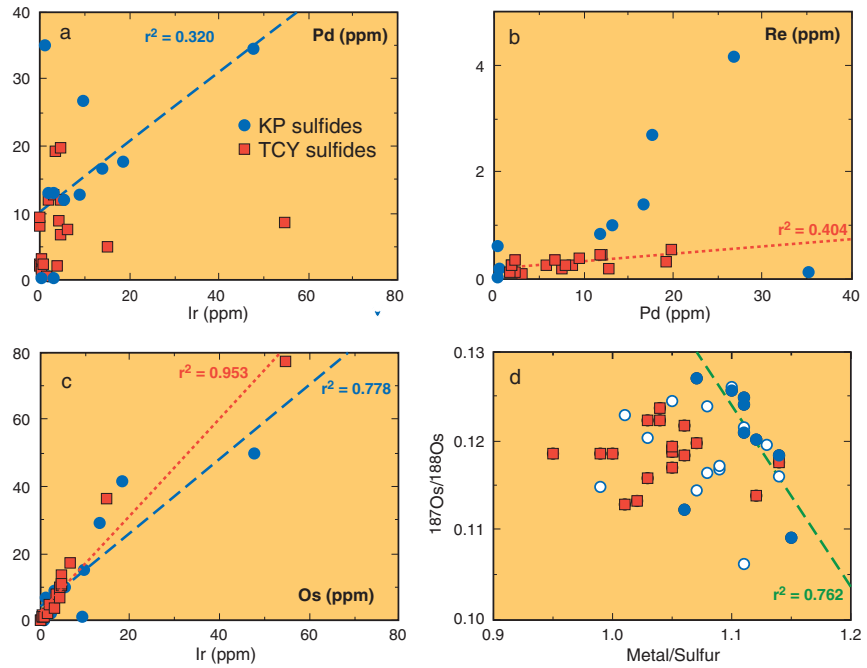

Figure 3. (a), (b) and (c) Bivariate bulk abundance plots for Penghu mantle sulfides. (d) $^{187}Os/^{188}Os$ versus bulk metal/Sulfur ratios. Solid circles: KP sulfides showing negative correlation between $^{187}Re/^{188}Os$ and $^{187}Os/^{188}Os$. Open circles: other KP sulfides. Open squares: TCY sulfides.

Fault-scarp-derived volcaniclastic deposits on Macquarie Island; sedimentation at a fossil ridge-transform intersection?

STUDIES OF OCEANIC CRUST are hindered by limited subaerial exposure. Our knowledge of *in situ* oceanic crust therefore comes from bathymetry and other geophysical data, dredge samples and in a few areas survey and sampling by submersibles. Moreover, even where rarely exposed on land within ophiolites, oceanic crust has typically been deformed to varying degrees during obduction.

Macquarie Island, located approximately 1200 km southwest of New Zealand in the Southern Ocean (Fig. 1), forms the apex of the Macquarie Ridge Complex (MRC), a system of ridges and troughs along the currently active Australian-Pacific oceanic transform plate boundary between the Alpine Fault of New Zealand and the Australian-Pacific-Antarctic triple junction. The island exposes the eastern side of the ~5 km high, ~50 km wide submarine ridge and lies ~4.5 km east of the major active plate boundary fault zone. Macquarie Island offers a globally unique opportunity to examine oceanic crust *in situ* – it is the only exposed piece of non-plume-related oceanic crust that still lies within the basin in which it formed, and in a relatively well-constrained present-day plate tectonic setting.

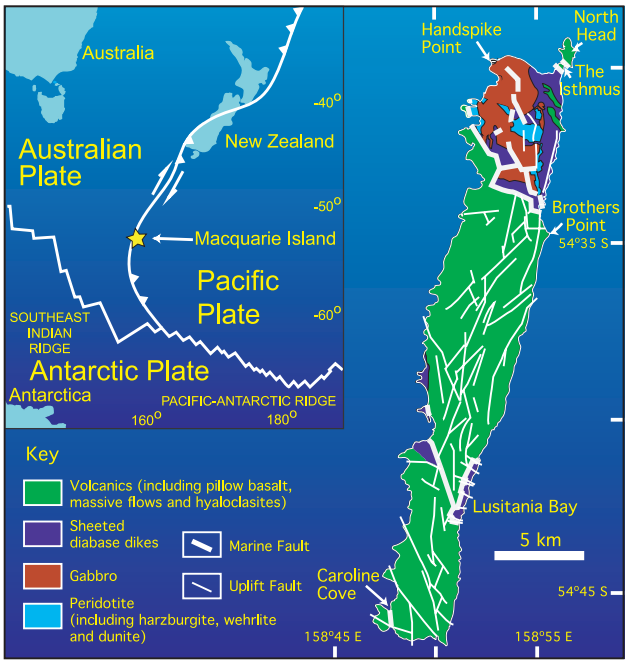

Figure 1. (a) Location of Macquarie Island indicated by a star. (b) Geologic map of Macquarie Island.

Recent research results: Upper Miocene to lower Pliocene sedimentary rocks on Macquarie Island are dominantly volcaniclastic breccia (Fig. 2a), sandstone (Fig. 3), and siltstone produced by the physical disintegration and tectonic abrasion of oceanic crust in fault zones, and mass wasting of these tectonic features. They represent small debris fans and small-scale turbidites deposited at the base of active fault scarps, related to Late Miocene to Early Pliocene seafloor spreading. Most of the sediment is derived from basalts, but diabase and gabbro clasts in some sedimentary rocks (Fig. 2b) indicate that middle and lower oceanic crust was exposed to erosion on the sea floor. A lack of exotic clasts and a low degree of clast roundness imply a local

Figure 2. (a) Volcaniclastic breccia, Unity Point. (b) Gabbro and diabase clasts in volcaniclastic breccia.

source for the sediment without input from continental rocks. Spatial relationships between sedimentary rocks and major faults associated with seafloor spreading on the island and correlations between sedimentary clast and adjacent up-thrown block compositions reflect paleo-tectonic relief for Macquarie Island crust during deposition. Our data support a model involving the deposition of these rocks at the inside corner of a ridge-transform intersection. Furthermore, a tectonic reconstruction of the Australian-Pacific plate boundary for the approximate time that Macquarie Island crust formed (10.9 Ma) also shows that Macquarie Island crust most likely formed near to a ridge-transform intersection. Sediments associated with active faulting at a ridge-transform intersection have been uplifted *in situ* above sea level along with the surrounding oceanic crust, which indicates that high-angle faults have more pronounced influence on sedimentation than do low-angle faults, in this tectonic environment (*see GEMOC publication #388)*.

Figure 3. Flame structures and graded bedding.

Contacts: Nathan Daczko (partly done at Department of Geological Sciences and Institute for Geophysics, Jackson School of Geosciences, University of Texas, Austin, Texas and Macquarie University)
Funded by: Australian Antarctic Division, University of Texas

Figure 4. Sampling hazards – female elephant seals moulting amongst rotting smelly kelp.

A continental near-neighbour during Abitibi crustal growth

THE ABITIBI SUBPROVINCE (part of the Superior craton of the Canadian Shield) is widely regarded as an example of juvenile Archaean crust generated during volcanic and plutonic activity in an ocean setting, far removed from the influence of older continental crust. However, our recent work along the southwestern margin of this subprovince casts doubt on this hypothesis.

The Kenogamissi plutonic complex is located southwest of Timmins in the Ontario segment of the Abitibi subprovince (Fig. 1). Samples of tonalite, granodiorite, granite, and diorite from this complex have zircon U-Pb primary ages ranging between 2747 ± 3 Ma and 2676 ± 4 Ma, representing nearly the entire period of Abitibi magmatic activity. Surprisingly, two of these samples also contain ca. 2850 Ma zircon grains. We believe that these zircons were derived from partially melted older continental crust during magma formation. Hf isotopic measurements were made *in situ* on dated igneous zircons from this complex. $^{176}Hf/^{177}Hf$ ratios

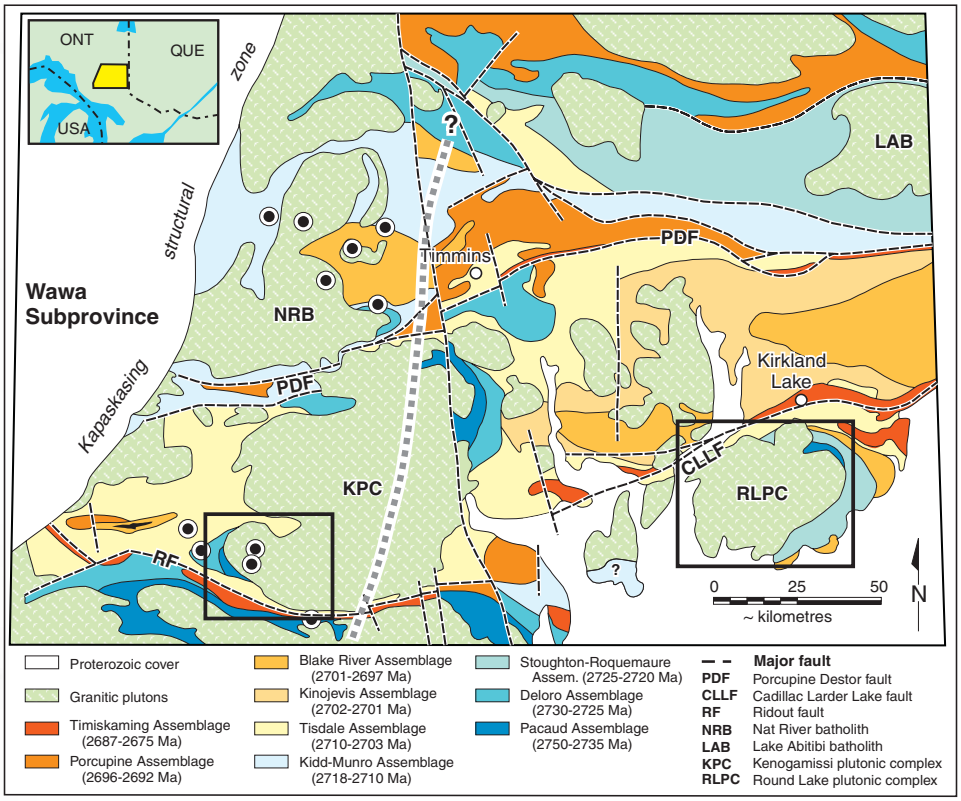

Figure 1. Geological map of the southwestern Abitibi subprovince, Ontario, Canada. The locations of two studied plutonic complexes are indicated by rectangles. Isotopic evidence for the involvement of older continental crust (≤ 2.92 Ga) during Abitibi magmatic activity is known from the locations shown by the dots. The dashed line denotes the probable eastward extent of this older crust at depth.

vary widely for individual samples (Fig. 2), consistent with final magma generation by mixing of at least two magma types: juvenile mafic melts derived from the depleted mantle, and melts of slightly older continental crust. Our *in situ* isotopic approach, combined with the radiometrically sensitive nature of the Lu-Hf system, partly explains why Hf isotopic data from individual zircons can be used to detect this older crust. In contrast, whole-rock Sm-Nd isotopic data from this region typically fails to indicate its presence. However, some of the Nd data are consistent with this interpretation, and rare 2.93-2.85 Ga inherited zircons have now been documented by other workers in both plutonic and volcanic samples from north of the Kenogamissi plutonic complex (Fig. 1).

Based on this growing evidence for the presence of older crust beneath the southwestern Abitibi subprovince, we propose the following crustal model (Fig. 3). The adjacent Wawa subprovince contains rocks as old as 2.92 Ga and is currently

separated from the Abitibi subprovince by the Kapuskasing structural zone (KSZ), an east- to southeast-verging intracratonic thrust system. Movement on the KSZ began in the late Archaean and culminated at roughly 1.9 Ga. Prior to its development, there must have been a boundary between 2.75-2.70 Ga granite-greenstone belts underlain by older crust (Wawa side) and 2.75-2.70 Ga granite-greenstone belts lacking this older basement (Abitibi side). We suggest that part of the present-day Abitibi subprovince formed above an eastward-tapering wedge of older Wawa crust. This lower crustal wedge may have formed during earlier episode of rifting and continental margin development. Subsequent tectonic activity on the KSZ left a region of autochthonous crust 'stranded' on the Abitibi side of the system, isolated from tectonically similar counterparts in the Wawa domain. Development of the KSZ was probably controlled in part by the location the older, rift-weakened(?) crustal boundary. The Abitibi subprovince thus appears to have formed in a pericratonic setting, close to and partly on top of an older continental fragment.

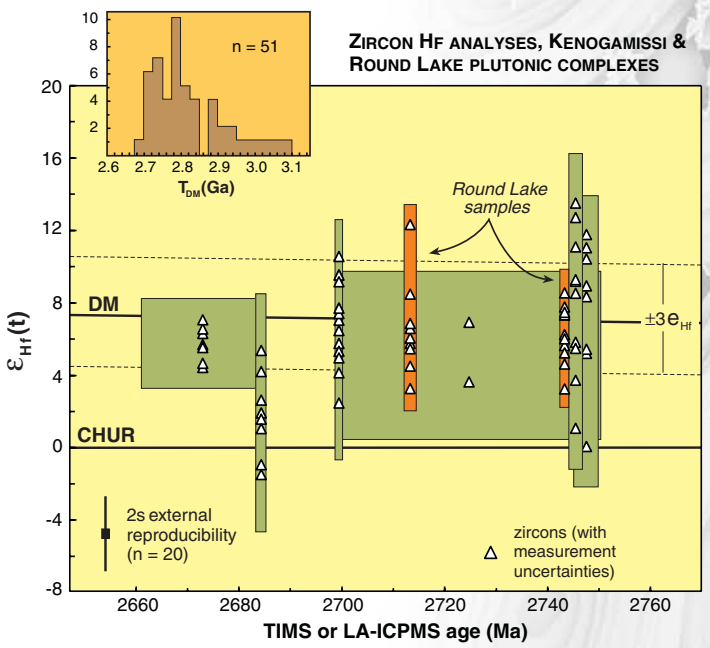

Figure 2. Hf isotopic data for igneous zircons. Most samples are characterised by a wide range of εHf, suggesting contributions of isotopically distinct magma batches to the final magma. Low εHf values (near or below CHUR) are consistent with the presence of older crust in the source region. Ca. 2850 Ma inherited zircons found in two Kenogamissi samples support this hypothesis.

Contacts: John Ketchum, John Ayer (Ontario Geological Survey), Otto van Breemen (Geological Survey of Canada)
Funded by: ARC (to O'Reilly/Griffin) and Geological Survey of Canada

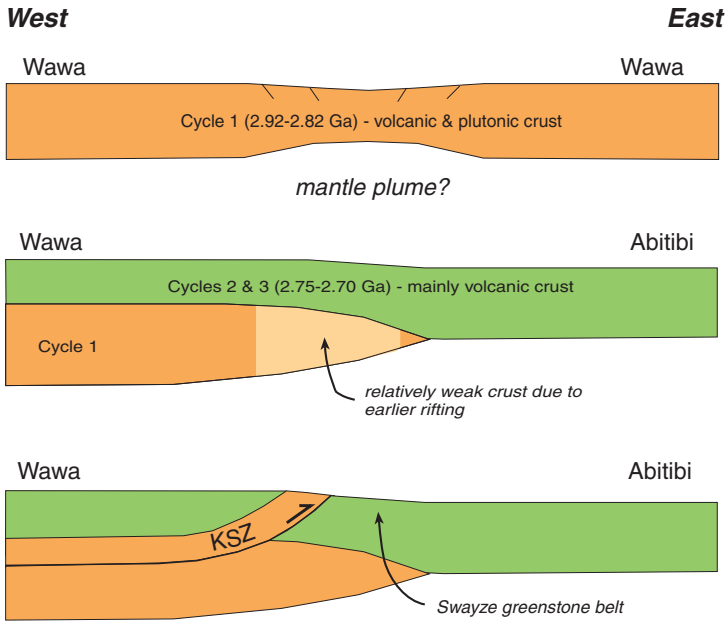

Figure 3. Schematic model of crustal development. A ≤2.92 Ga Wawa continental block was rifted to form an east-facing continental margin (alternatively, this margin was not rift-related). Subsequent growth of Abitibi crust occurred adjacent to and partly on top of this continental block. Later tectonic activity on the Kapuskasing structural zone (KSZ) created the present-day Wawa-Abitibi boundary. The Swayze greenstone belt (located west of the Kenogamissi plutonic complex) and adjacent regions may be still underlain by Wawa lower crust.

Seismic properties of the Amery Ice Shelf – How thick is it, and how does it move?

THE AMERY ICE SHELF (AIS) is located on the east coast of Antarctica, at approximately 70°S, 70°E (Fig. 1). It is the third largest embayed shelf in Antarctica, and the largest entirely in East Antarctica, and as such is one of the largest glacier drainage basins in the world. Due to this, and its thermal isolation, the AIS plays an important role in the global climate system. Knowing the structure of the AIS is important to studies of the impact of global warming on present-day ice shelves and the subsequent effect on global ocean circulation and climate. Understanding the structure of the AIS can also provide tighter control in mass balance calculations of the shelf and in ocean circulation models beneath the ice cover. The seismic geophysical technique is a powerful tool for surveying the thickness and structure of the subsurface, and this makes it perfect to investigate the AIS.

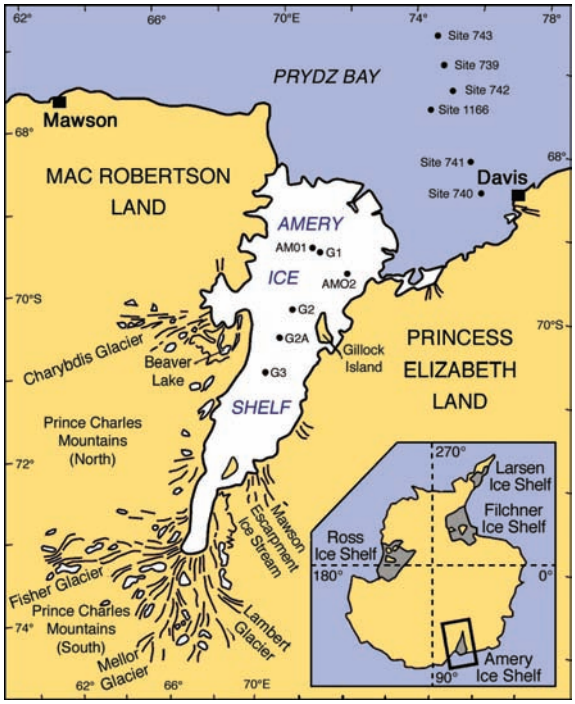

Figure 1. Map of the Amery Ice Shelf, East Antarctica. Inset: Map of Antarctica showing the major ice shelves.

A detailed seismic reflection survey was undertaken in the summer of 2002/2003 at the centre of the AIS to map the thickness of both the ice and water column, to investigate the sediment structure and most importantly to see if a delineation could be made between glacial and marine ice. The detailed seismic reflection survey was performed utilising a 24-channel spread with a 10 m geophone spacing, giving a maximum fold coverage of six. The survey successfully delineated the subhorizontal glacial and marine ice layers, with average thicknesses of 754 and 20 m, respectively. The water column is 590 m thick, placing the seafloor at a depth of 1364 m below the ice surface. A 60 m thick, subhorizontally-layered sedimentary unit can be delineated (Fig. 2).

During the 2004/2005 Antarctic summer season, seismic data were used primarily to investigate anisotropy within the ice. Anisotropy in ice refers to a difference in seismic velocity within the ice due to ice crystal orientation. As ice streams merge to become the AIS, the margins undergo stress, and ice crystals realign and elongate, meaning the ice structure is no longer homogenous, i.e. it is no longer isotropic. This could produce a measurable difference in seismic velocity with orientation relative to relict ice stream margins. These margins were picked from satellite images of the shelf, which reveal flowlines – the preserved boundaries of ice streams.

Out for a days work, photo by K. McMahon.

This season's work area was adjacent to Gillock Island (Fig. 1) where twelve sites were investigated for anisotropy using refraction surveying techniques, four regional sites were surveyed (extending the area of the shelf surveyed by Australian seismologists) and a detailed seismic reflection line was carried out, spanning ~3km of the shelf E-W over a relict stream margin. This was done using a 24-channel spread (48 for the detailed line), with a 10 m geophone spacing. For the refraction surveys, the data reveal information up to approximately 200 m depth within the ice.

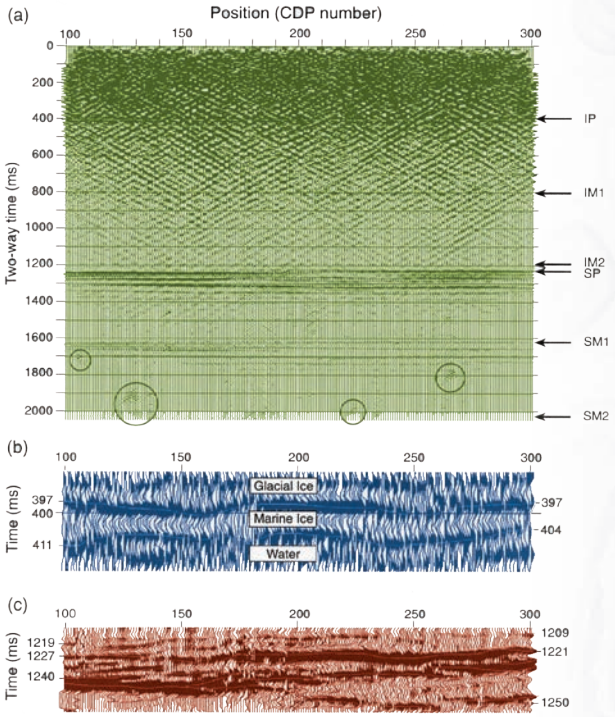

Figure 2. (a) CDP stacked section of processed reflection data showing all major reflections. Legend: IP – primary ice reflection; IM1 – first order ice multiple; IM2 – second order ice multiple; SP – primary sediment reflection; SM1 – first order sediment multiple; SM2 – second order sediment multiple. Circled objects are the deep hyperbolic reflections. (b) Detailed image of ice boundaries, with interpretation. (c) Detailed image of sedimentary layering, with interpretation.

Ray-inverse modelling is being used primarily to process the anisotropy refraction data, using a model for the ice shelf incorporating a thin snow layer overlaying firn that changes gradually to solid ice within the shallow surface material. This is more realistic than using a simple layered model, and is supported by data from ice cores elsewhere on the AIS.

The Gillock Island area of ice is older than the ice of the southern grounding zones, which will be the site for further investigation in the 2005/2006 season. This will lead to a comparison of the strength of anisotropy with age of the ice, and proximity to the zone of initial stress.

Contacts: Kathleen McMahon, Mark Lackie
Funded by: ASAC Grants 2542 and 2581

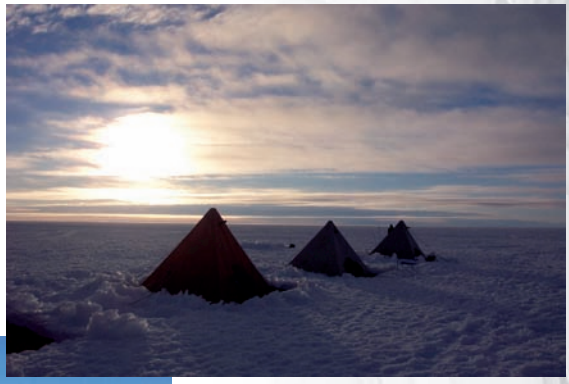

Base camp on the AIS: "Camp Tropical", Photo by K. McMahon.

Seismic work at AM01 on the AIS, Photo by K. McMahon.

Tracing gold with zircon

AS A PART OF AN ONGOING STUDY of the relationships between granites and intrusion-related gold deposits in the Georgetown Inlier, north Queensland, the Black Cap Diorite and Lochaber Granite within the Lochaber-Bagstowe Complex (Fig. 1), and the Median Dyke within the gold-rich porphyry deposit at Kidston (Fig. 1 and 2) were studied to evaluate existing models for temporal and genetic relationship between these intrusive rocks. Geologic, fluid inclusion and stable isotope studies suggest that the mineralisation and brecciation at the Kidston breccia pipe is spatially, temporally and genetically related to the north-west trending Permo-Carboniferous rhyolite dyke magmatism (Paddys Knob Dyke Swarm).

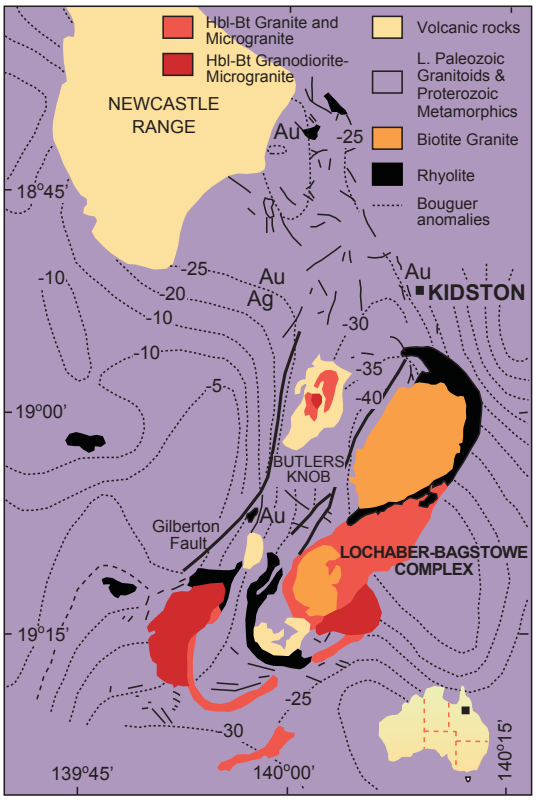

Figure 1. Regional geology of the Kidston area and the relationship of the Kidston to Permo-Carboniferous volcanism, the NW trending rhyolite dyke swarm and coincident gravity low (after Baker and Andrew, 1991.)

The U-Pb ages and Hf isotope composition of zircons are used to determine the timing and degree of crust/mantle interaction involved in the genesis of porphyry intrusions. Zircons from selected rocks were analysed by *in situ* LAM-ICPMS (Laser Ablation Microprobe Inductively Coupled Plasma Mass Spectrometry) for U-Pb ages and Hf isotope composition.

The gold-mineralised Median Dyke (Fig. 2 and Fig. 3C) within the gold-rich subvolcanic breccia-hosted porphyry deposit at Kidston has a U-Pb zircon crystallisation age of 335.7±4.2 Ma. The same rock, dated by SHRIMP I ion probe,

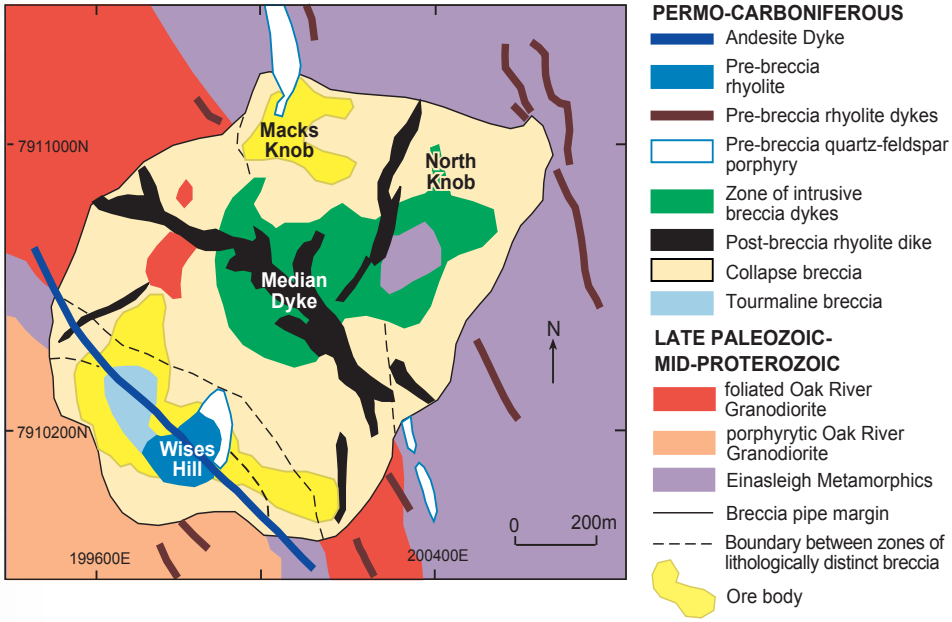

Figure 2. Surface geology of the Kidston breccia pipe (after Baker and Andrew, 1991).

yielded a $^{206}Pb/^{238}U$ age of 334.7 ± 3.3 Ma. The Black Cap Diorite (Fig. 3A) and the Lochaber Granite (Fig. 3B) within the Lochaber-Bagstowe Complex (LBC), have U-Pb zircon ages of 350.6±1.6 Ma and 338.9±2.7 Ma respectively.

The Median Dyke has ε_{Nd}=-13.45 (like other Kidston porphyries); the Lochaber Granite, ε_{Nd}=-10.68; the Black Cap Diorite, ε_{Nd} =-7.81, and the Paddys Knob Dyke Swarm have an ε_{Nd} range from -9.6 to -18.2. The range of ε_{Nd} values was interpreted to reflect either magma mixing or assimilation of highly isotopically evolved Georgetown crust (Nd model age ca 1.70 Ga) into the evolving magmas.

The range of relatively non-radiogenic Hf isotope signatures in each rock (Median Dyke, ε_{Hf}=-6.3 to -18.3; Lochaber Granite, ε_{Hf}=0.26 to -8.7; the Black Cap Diorite, ε_{Hf} =3.8 to -9.3) is interpreted to reflect magma derivation by remelting of heterogeneous deep crust. The Hf model age of 1.22-2.26 Ga suggests the source could be the regionally developed Proterozoic crust, but Siluro-Devonian granitoids were derived earlier from the Proterozoic crust (see *Research Highlights 2003*), and it therefore is difficult to distinguish between a Proterozoic or a Siluro-Devonian source rock using only Hf data. The younger Lochaber Granite could have been derived by fractional crystallisation from the older Black Cap Diorite, which has a similar Hf-isotope signature.

The Median Dyke contains zircons with a wide range of Hf isotope compositions, which barely overlaps the range seen in the Black Cap Diorite and Lochaber Granite. The chemical characteristics of the Median Dyke fall along the trends defined by the Paddys Knob Dykes and the LBC, suggesting that they are all part of the same suite and spatially, temporally and genetically related. However, the Hf-isotope data rule out a simple fractional crystallisation relationship. The less radiogenic Hf in the zircons from the Median Dyke suggests instead that magmas like the Black Cap Diorite were mixed with melts derived from Proterozoic crust with Hf model ages between 1.78 Ga and 2.26 Ga, to produce the more felsic compositions of the Median Dyke magmas.

This study illustrates once again the power of the combined U-Pb and Hf-isotope analysis of zircons as a petrogenetic tool.

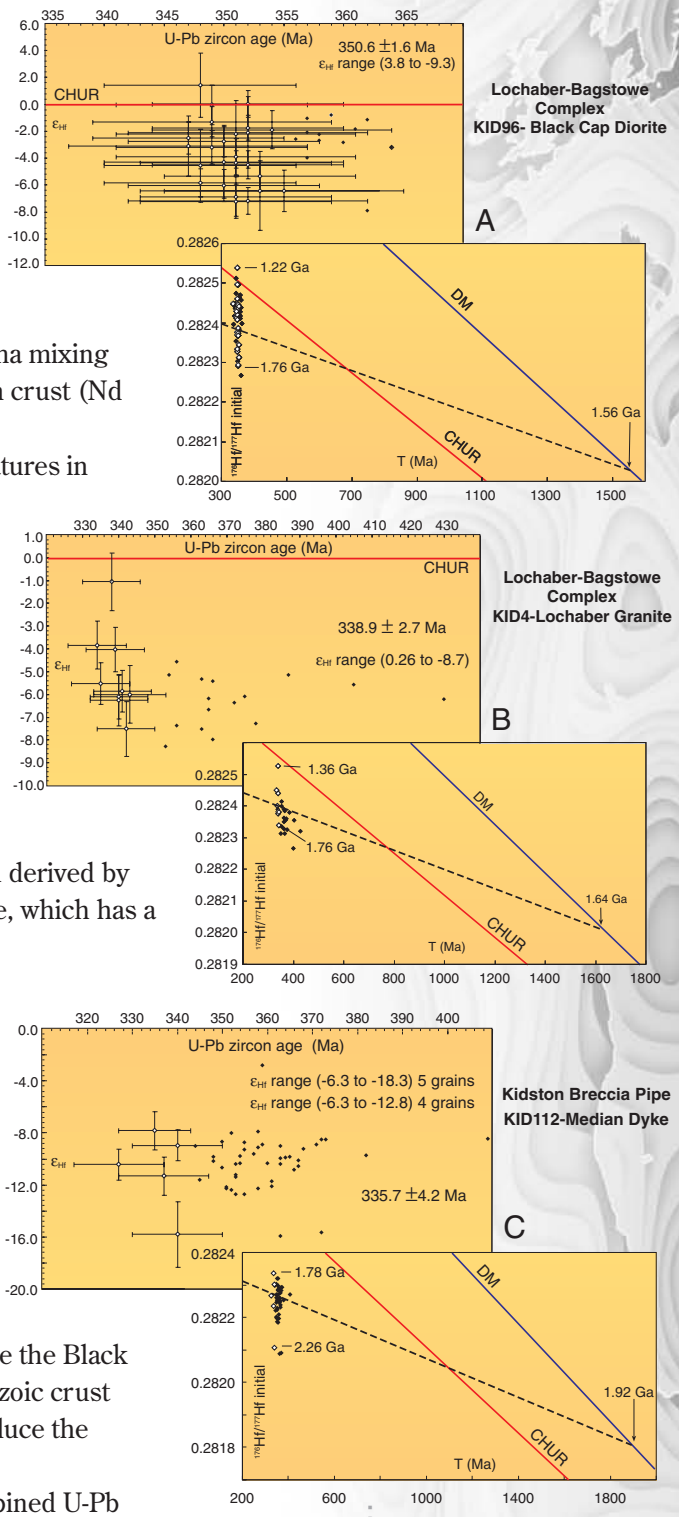

Figure 3. Plot of ε_{Hf} vs U-Pb zircon age showing the range in εHf values. Error bars shown for grains that define the age of the rock (open diamonds).

Contact: Valeria Murgulov, Phil Blevin, Sue O'Reilly, Bill Griffin
Funded by: AMIRA, ARC, Macquarie University (APA)

Zircon – a multi-faceted tool for petrogenetic modelling

PETROLOGISTS STUDYING MAGMATIC ROCKS are confronted with the end product of a complex evolution, but little obvious evidence about the sequence of processes in that evolution. However, detailed studies are showing that the crystal morphology, trace-element signatures, U-Pb ages and Hf-isotopic compositions of magmatic zircons often contain detailed records of the evolution of individual magma chambers. Zircons in S-type granitoids, such as the Berridale adamellite, Lachlan Fold Belt, eastern Australia provide an excellent example of the usefulness of zircons in tracking petrogenetic processes.

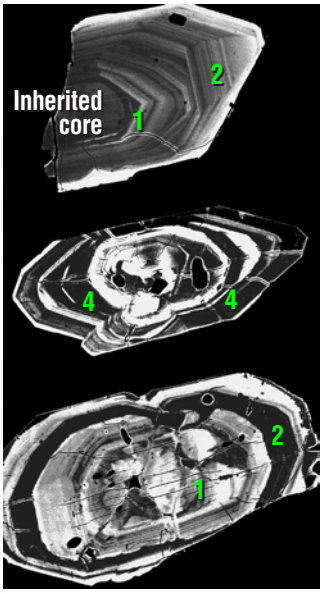

Figure 1. BSE/CL images of zircons from the Berridale adamellite, Numbla Vale. Numbers indicate zircon morphological types and an inherited core.

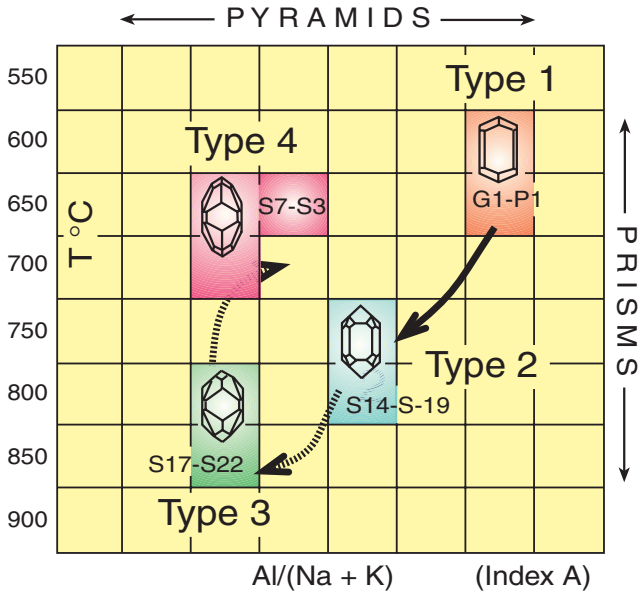

The external morphology of zircons reflects the environment of crystallisation, including magma composition and temperature. Changes in crystal morphology during crystallisation can be studied in backscattered electron/cathodoluminescence (BSE/CL) images of sectioned grains. Zircons from the Berridale adamellite have complex internal morphology (Fig. 1), which reflects changes in both the temperature and the composition of the magma and provides a qualitative record of magma evolution. The patterns suggest that zircon was crystallising as the magma cooled and became more alkaline; the late-stage heating and compositional change imply a mixing between the original magma and a new, hotter batch. *In situ* U-Pb data obtained by LAM-ICPMS distinguish age populations (Fig. 2), including some inherited grains seen as zircon cores in the BSE/CL images, and confirm that the recognized morphological Types 1-4 crystallised over a relatively short time span. The trace-element patterns of the zircons (measured by LAM-ICPMS) can characterise

Figure 2. Concordia and Tera-Wasserburg (or 'inverse concordia') plots for zircons from the Berridale adamellite.

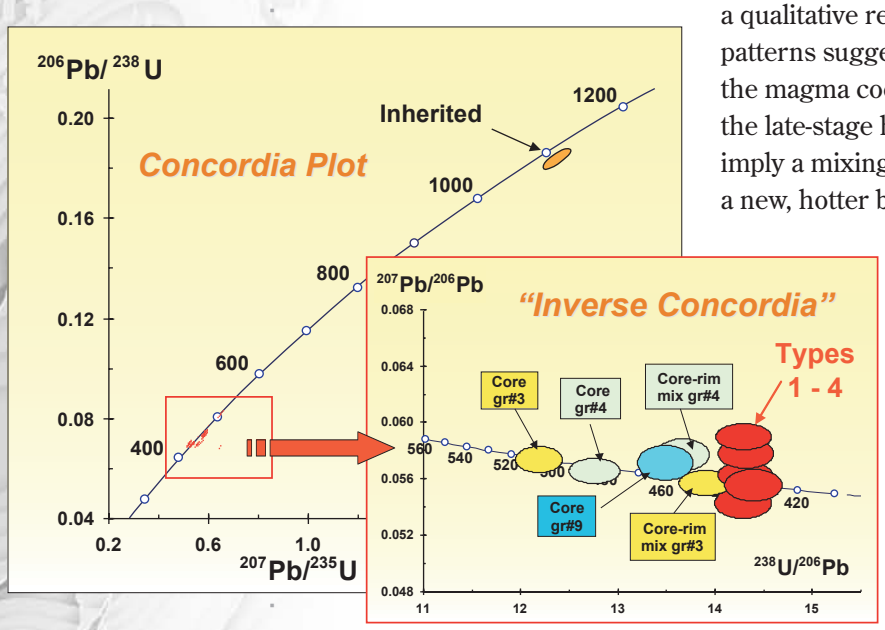

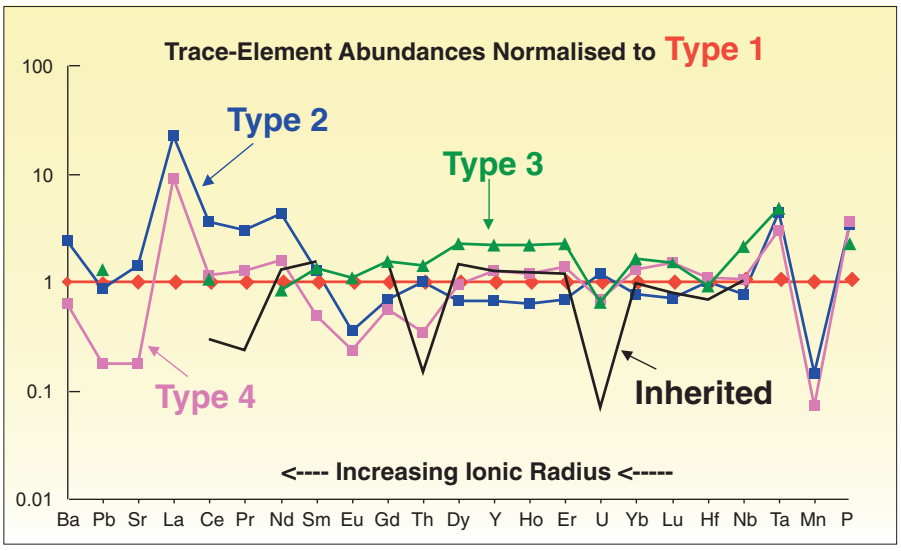

Figure 3. Average trace element patterns of zircon populations from the Berridale adamellite, where all zircon types are normalised to Type 1.

the original magma types and trace their evolution (Fig. 3). Thus from Type 1 to Type 2, the magma became enriched in LREE and depleted in HREE, and developed a negative Eu anomaly, consistent with the crystallisation of plagioclase and mafic minerals. Type 3 shows a reversal of this trend, consistent with the introduction of a new batch of magma, which then evolved toward Type 4 with more crystallisation of plagioclase. The Hf-isotope data (collected using LAM-MC-ICPMS) allow an evaluation of the relative contribution of mantle-derived and crustal-derived components in the production of the host granitoids (Fig. 4), and can help track the mixing of magmas with different sources. The rise in $^{176}Hf/^{177}Hf$ between Type 2 and Type 3 requires a new magma batch, and show that it was derived from a more primitive (mantle-like, or "I-type") source than the original magma that precipitated the Type 1-2 zircons. The zircon "tape-recorders" thus show that the S-type Berridale adamellite had two distinct sources, including a significant I-type magma contribution – information that could not have been captured using traditional petrological and geochemical techniques.

Contacts: Elena Belousova
Funded by: Industry, ARC (Australian Postdoctoral Fellowship)

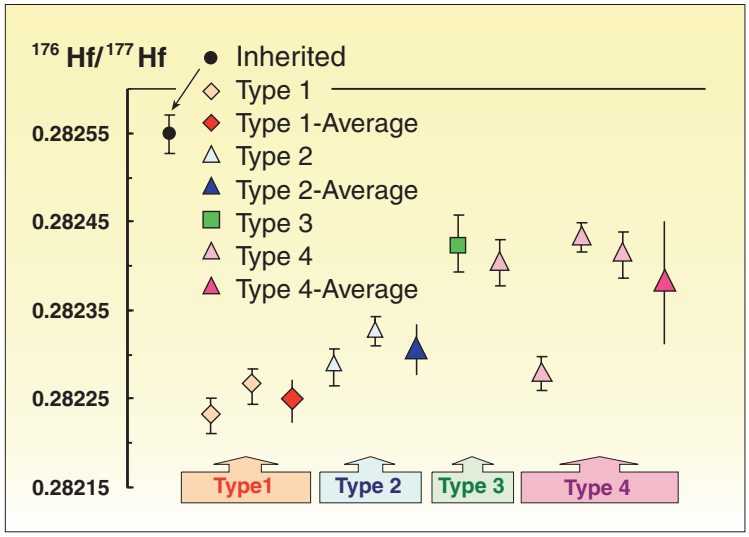

Figure 4. $^{176}Hf/^{177}Hf$ ratios in zircon populations from the Berridale adamellite.

Kimberlites and lamproites probe the deep crust of the Dharwar Craton, south India

XENOLITHS IN KIMBERLITES AND LAMPROITES provide many of our best samples of the upper mantle, but the eruption of these deep-seated magmas also can sample the inaccessible lower crust. Zircon xenocrysts in Proterozoic (1.1-1.4 Ga) kimberlites and lamproites have provided new evidence on the deep crust of the Dharwar Craton in southern India (Fig. 1), and on the tectonic relationship between intra-cratonic blocks.

The Craton is divided into two blocks; the Western Dharwar (WDC) consists of voluminous supracrustal rocks (3.3-2.6 Ga) on a largely 3.4-2.9 Ga tonalite-trondjhemite-granodiorite (TTG) basement, the Older Gneiss Complex or Peninsular Gneiss. 3.58 Ga detrital zircons in the metapelites of the older schist belts of the WDC suggest the existence of still older crust. The Eastern Dharwar (EDC) is characterised by voluminous 2.6-2.5 Ga calc-alkaline granitoids enclosing narrow tracts of 2.7 Ga supracrustals. The eastern block is believed to be thrust onto the western block along an extensive mylonite zone on the eastern boundary of the Chitradurga schist belt. Dipping reflectors seen in seismic profiles across this belt are consistent with this structure, which has been ascribed to late-Archaean (2.5 Ga) oblique convergence between the two cratons.

The U-Pb data on the zircons show considerable discordance, reflecting generally high contents of U+Th (aver. 750 ppm), and thermal disturbances during a late

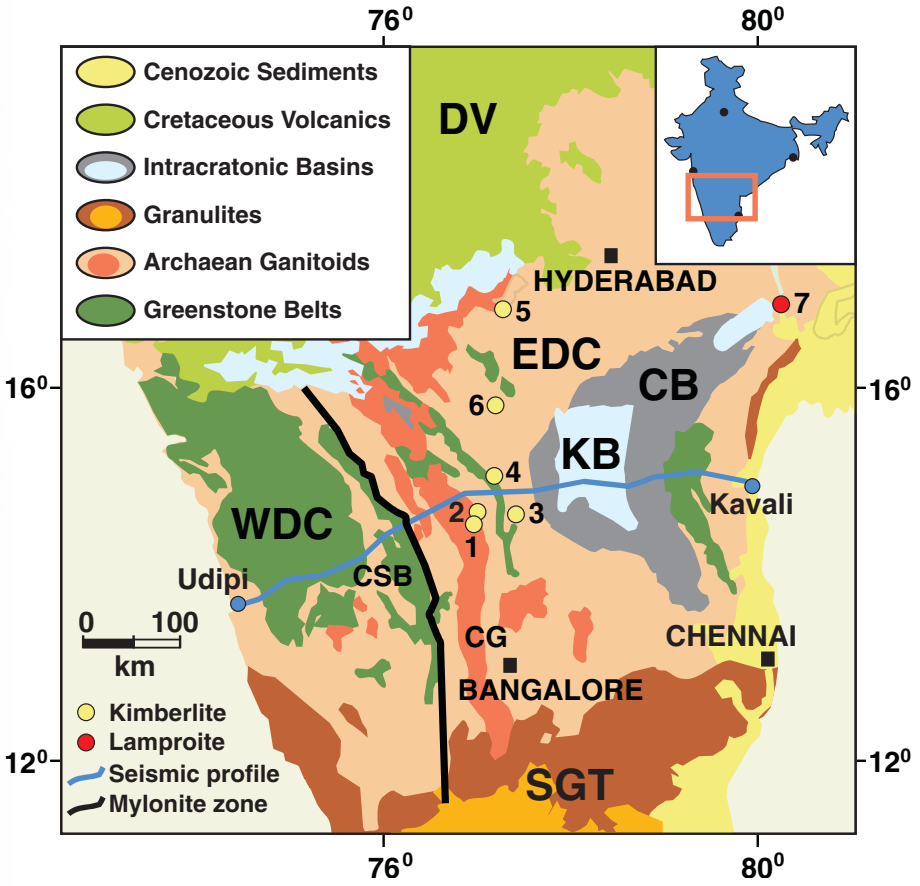

Figure 1. Location map of Southern India, showing locations of sampling sites and Deep Seismic Profile: WDC-Western Dharwar Craton, EDC-Eastern Dharwar Craton, SGT, Southern Granulite Terrain, EGGT-Eastern Ghats Granulite Terrain, CB-Cuddapah Basin, KB-Kurnool sub-Basin, DV-Deccan Volcanics, GG-Godavari Graben, CSB-Chitradurga Schist Belt and CG-Closepet Granite. Kimberlite/Lamproite clusters: 1-Kalyandurg, 2-Brahmanapally, 3-Chigicherla, 4-Wajrakarur, 5-Mahaboob Nagar, 6-Raichur and 7-Ramannapeta.

Neoproterozoic to early Paleozoic event (580-800 Ma). However, the Hf isotope compositions of the zircons, which are not affected by thermal events, allow the age data to be resolved into a major cluster of ages from 2.5-2.7 Ga and two significant groups at 3.1-3.3 Ga and 3.34-3.58 Ga (Fig. 2). Neither of the two older groups has been recognised unambiguously in the surface geology of the EDC. The 3570±15

Ma $^{207}Pb/^{206}Pb$ age of one zircon grain is the oldest reported yet from the EDC and is identical within error to the oldest zircon ages found in the WDC. Concordant to near-concordant zircons with $^{207}Pb/^{206}Pb$ ages from 2.9 to 3.3 Ga occur in all of the clusters except Wajrakarur and Ramannapeta.

The Hf isotope data for the zircons from the major 2.5-2.7 Ga populations provide strong supporting evidence for the distribution of ancient crust at depth. The trace element data indicate that these younger zircons are derived from granitoid rocks

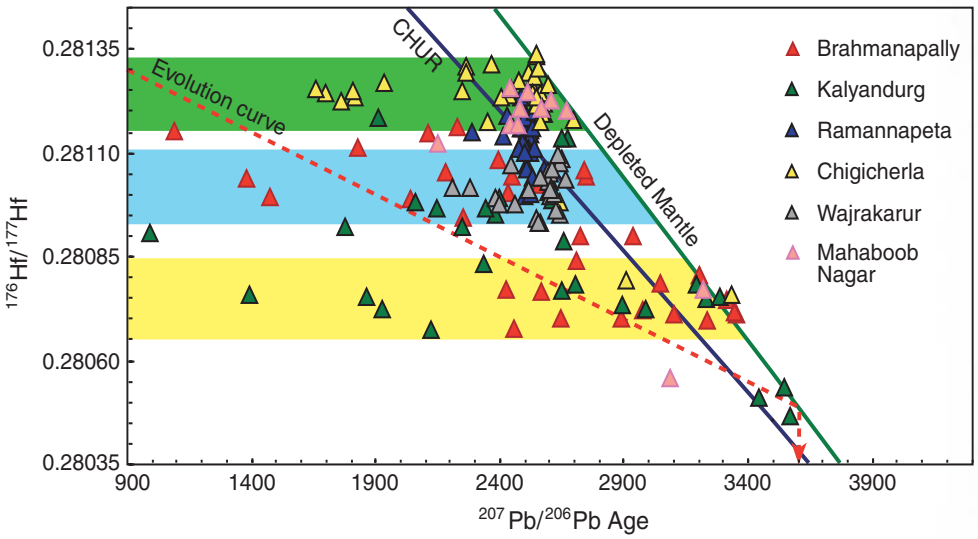

Figure 2. Plot of $^{176}Hf/^{177}Hf$ vs $^{207}Pb/^{206}Pb$ ages of zircons, with Depleted Mantle curve for reference; horizontal trends reflect Pb loss, without disturbance of Hf-isotope signatures. Dashed line indicates the evolution of a 3.6 Ga juvenile crust with $^{176}Lu/^{177}Hf = 0.015$, corresponding to the average continental crust.

with 60-75% SiO_2. Their Hf isotope compositions reflect the relative proportions of ancient crustal material, and of juvenile material, derived directly or indirectly (on a short time scale) from the depleted mantle, in the magma sources. In the Kalyandurg and Brahmanapally clusters (1, 2), the 2.5-2.7 Ga zircons show a range in model age (T_{DM}) from 2.8-3.2 Ga, indicating a significant contribution from ancient crustal material.

Similarly, the 2.6-2.65 Ga zircons of the Wajrakarur cluster (4) give T_{DM}^{C} ages of 2.95-3.3 Ga although no zircons older than 2.65 Ga were sampled. The Chigicherla (3) and Mahaboobnagar (5) clusters are dominated by 2.5-2.7 Ga zircons with dominantly juvenile Hf-isotope signatures, but even in these pipes there are grains with model ages of 3.2-3.4 Ga, and isolated grains with similar U-Pb ages. No older zircons were found in the Ramannapeta pipes, but the 2.5-2.6 Ga zircons have model ages extending back to 3.2 Ga. These non-juvenile Hf-isotope signatures imply that at least parts of the deep crust of the EDC are older than the rocks exposed at the surface.

The zircon data suggest that ancient crust, with ages extending back to ca 3.6 Ga, underlies the marginal parts of the EDC. The greatest contribution of this ancient crust to magmatism at 2.5-2.7 Ga is found in the localities (1, 2) closest to the suggested suture between the EDC and the WDC. These data, combined with the seismic profiles, strongly imply that the old crust of the WDC was thrust beneath the younger crust of the EDC, and that this continental subduction occurred before (or during?) the major EDC magmatism at 2.7-2.5 Ga.

Contacts: W.L. Griffin, S.Y. O'Reilly
Funded by: ARC Discovery, Industry, National Geophysical Research Institute (India), Boyscast Fellowship (India), Macquarie University

Risk management in exploration: Finding more mines for less money

MINERAL EXPLORATION PERFORMANCE, whether measured by discovery rate, average discovery cost, number of world-class deposits discovered, or return on exploration investment, has deteriorated significantly over the past 15-20 years. This is particularly so for the large, 'greenfields' discoveries that build companies and are crucial to the long-term, secure supply of resources. The most recent world class discovery in Australia was Olympic Dam in 1983, and the only medium to large discovery this decade was Prominent Hill in South Australia (Fig. 1).

Recent studies of the worldwide exploration and discovery records for gold and copper have concluded that the amount expended on greenfields exploration has exceeded the value of deposits discovered in both cases. In other words, greenfields exploration is overall a loss-making business, and, as a result, investors and mining company boards have become increasingly reluctant to invest in it.

We are working with our sponsor companies to investigate and develop ways to improve the financial performance of mineral exploration. However, this is not about developing new exploration technologies, but rather about building a better understanding of the specific business and management requirements of this very high risk industry. As a result, the research project involves innovative integration of geoscience, statistics, psychology, financial and business management expertise from across the university. The research is largely being funded by nine mining and exploration companies, who are contributing a total of almost $500,000 over the two years (2004-05) of the project.

Figure 1. Drilling the discovery hole at Prominent Hill, South Australia - arguably Australia's only large greenfields mineral discovery of this decade. Photo courtesy of Derek Carter, Minotaur Resources.

The main lines of investigation in the first year, and some preliminary outcomes are as follows.

1. We have been examining past exploration performance and practices, both across companies on a province basis and within individual companies. Preliminary, but consistent conclusions include, companies going back to areas that appear to have been previously thoroughly explored (Fig. 2), repeating essentially the same exploration programs over the same ground, and spending too much time and money prior to drill-testing any targets. Together, these characteristics contribute significantly to the overall cost of exploration, with little if any impact on discovery rates.

2. The mineral exploration value proposition has been modelled probabilistically, in order to provide a sound basis for estimating and reducing risk across the industry and across a company's exploration portfolio. This model will enable our sponsors to focus on a few key portfolio management tools that are critical to improving the overall return on investment. An unexpected outcome was the very low predicted sensitivity to the rate of return on investment (Figure 3). This means that any improvement in the more sensitive variables such as average probability of success has almost the same potential to deliver large financial gains as modest ones. So it is well worth the effort to make such improvements.

3. Mineral exploration is bedevilled by geological complexity, insufficient information and resultant high levels of uncertainty. Decision making under

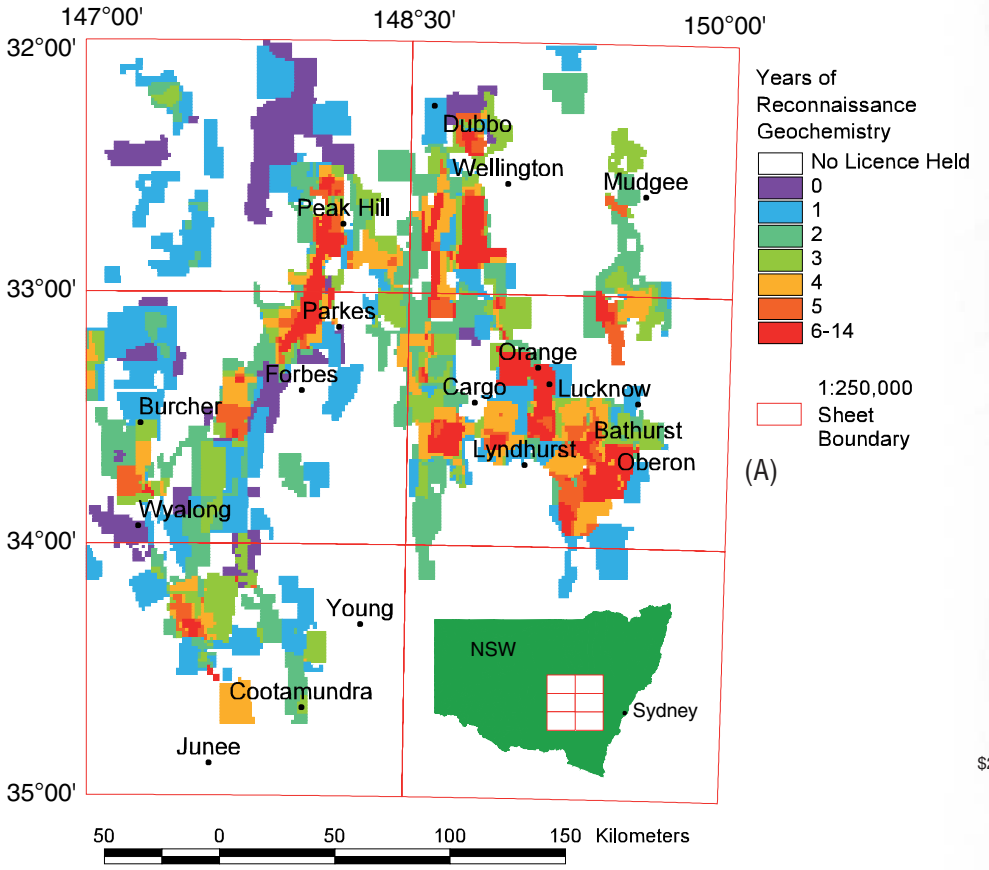

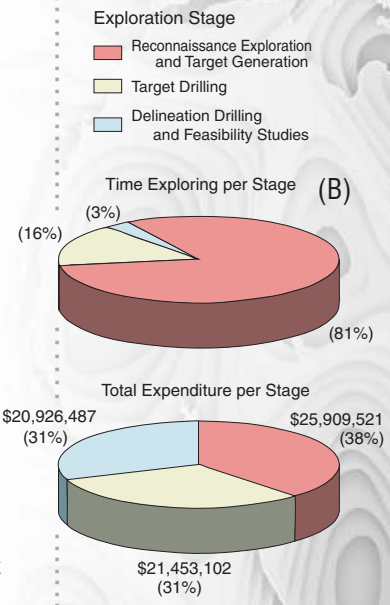

Figure 2. Lachlan Fold Belt case study: 20 years of Cu-Au exploration. (A) Evidence for repeat work (reconnaissance geochemistry in the map shown here), and (B) for spending too much time and money on pre-drill exploration stages.

uncertainty is an area in which cognitive psychologists have made significant recent gains, and we have been investigating how best to apply those gains to the specific issues around decision making in exploration. We have designed and provided an in-house workshop on Decision Making Under Uncertainty to each of our sponsors, and will undertake surveys and cognitive tests with our sponsor staff during 2005.

Contacts: Mike Etheridge, Oliver Kreuzer, Maureen McMahon
Funded by: BHP Billiton, Codelco - Chile, Geoinformatics Exploration Australia, Gold Fields Australasia, Jackeroo Drill Fund, Newmont Australia, Placer Dome Asia Pacific, Teck Cominco, WMC Resources and the Macquarie University VC Research Development fund

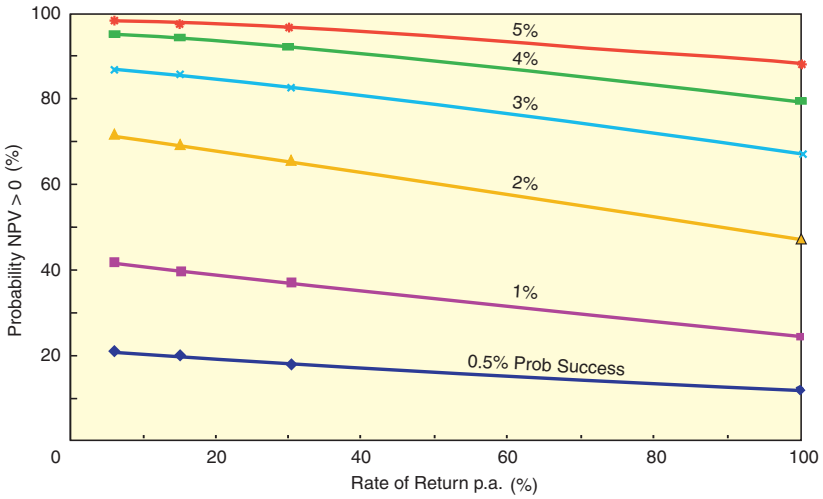

Figure 3. Example of an output from the exploration value simulation in @RISK. The graph shows the probability of achieving (NPV>0) rates of return on exploration funds invested of between 5% and 100%, at probabilities of discovery success ranging from 0.5% to 5%. This result illustrates the remarkably low sensitivity to rate of return (low slope on curves), and the high sensitivity to average probability of success (wide separation of curves).

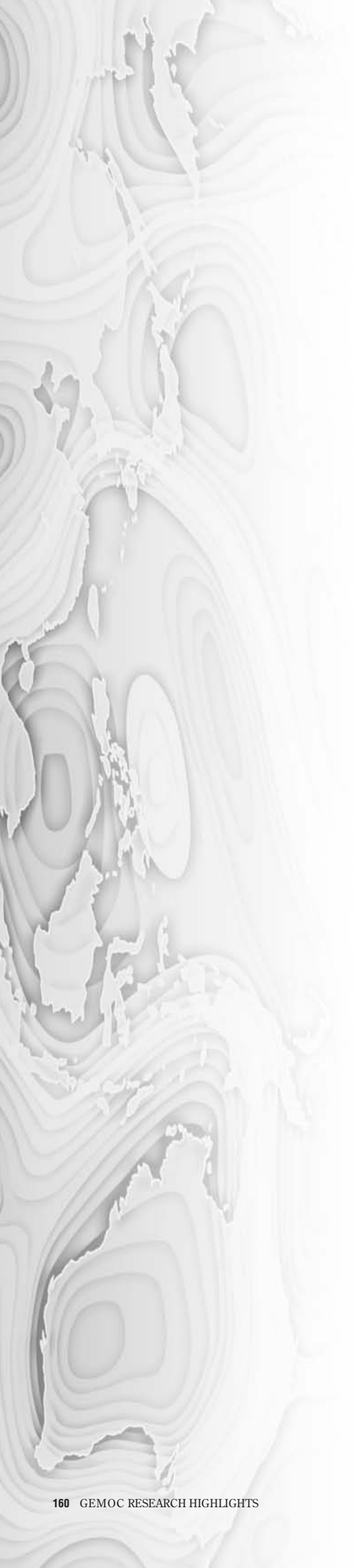

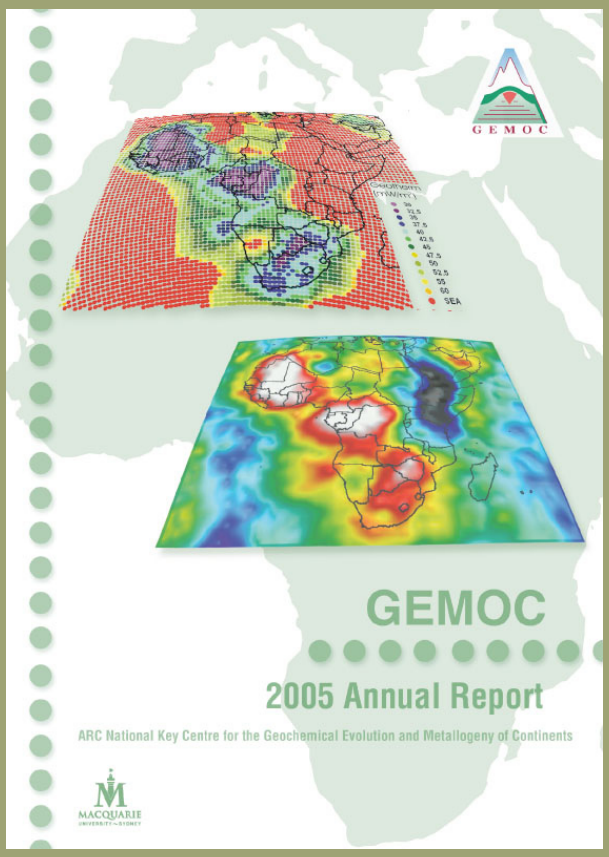

2005 Contents

TerraneChron™	162
Iron isotopes and Earth's oxygen budget	163
Trace elements are a girl's best friend:	164
Intraplate volcanism, mantle dynamics and diamond exploration	166
Hot stuff: Geotherms, density and seismic velocity	168
Isotopic ratio measurement using microbeam methods: Where do we stand and where are we going?	170
Ancient abyssal peridotites	172
Where does the Houghton Inlier belong? Zircons hold the key!	174
Following the flow: Thallium isotopes trace subduction processes	176
How fast does the mantle convect?	177
Cold adventures: Measuring ice and the crust in Antarctica	178
Erosion in the Murray-Darling basin: how long does it take to produce and transport sediments? By how much has intense land use increased erosion rates?	180
Are all mantle plumes equal in Nickel and PGE potential?	182
Re-Os isotopes in mantle xenoliths from eastern China: age and evolution of the lithospheric mantle	184

GEMOC's development of methods for the inversion of seismic tomography to constrain both mantle composition and geotherms was a major advance in 2005, done in collaboration with WMC Resources. See Research Highlights (page 30), and GEMOC publication #423.

Research highlights 2005

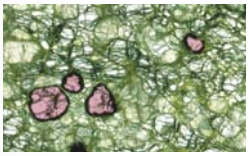

TERRANECHRON® is GEMOC's unique methodology for terrane evaluation. Industry continued extensive use of *TerraneChron*® as a cost-effective tool for mapping crustal history on different scales.

Iron isotopes and Earth's oxygen budget

AFTER THE ACCRETION OF THE EARTH from meteoritic debris, oxygen stored in the deep interior (the mantle) was released to the surface as water and CO_2, and free oxygen in the atmosphere grew to a significant level by ~2.4 billion years ago. However, we do not know how oxygen is distributed in the mantle, and how this has varied with depth and over time.

To understand how oxygen varies in the mantle, we need to measure some feature of rocks or minerals that is highly sensitive to small changes in the amount of oxygen present. The variable oxidation states of iron (Fe^{3+}, Fe^{2+} , native Fe) potentially provide such a tool, and new multiple collector inductively coupled plasma mass spectrometry (MC-ICPMS) techniques have shown correlations between the stable isotope composition of iron and its oxidation state. Recent work has demonstrated that the iron isotope compositions of spinels (an aluminium-rich oxide present in mantle rocks that hosts variable amounts of Fe^{3+}) correlate with the oxidation state of their host rock (Fig. 1); iron isotopes can therefore be used as a proxy for relative changes in mantle oxidation state. By analysing the iron-isotope compositions of minerals in mantle xenoliths originating from different depths and of different ages it will be possible to get some idea of how the level of oxidation of the mantle has changed over time. Ultimately, GEMOC scientists will be able to use this method to probe the Earth's deep interior and find out how much oxygen there is, why it's there and where it all may have come from.

Figure 1. Spinel iron isotope composition ($\delta^{57/54}Fe$; the deviation of the measured $^{57/54}Fe$ ratio from that of the pure iron standard IRMM-14 in parts per 1000) versus $\Delta logfO_2$, expressed relative to the fayalite-magnetite-quartz buffer, FMQ)

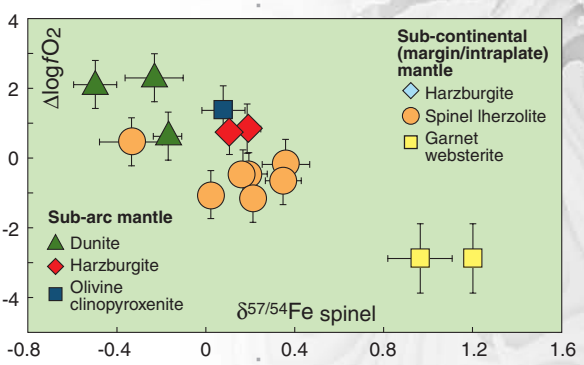

However, iron participates in a range of mass-transfer processes that take place in the mantle, such as partial melting and metasomatism, and these processes, in addition to changes in oxidation state, may influence the iron isotope signatures recorded in mantle rocks. Therefore, it is important to constrain *first* how iron isotopes behave during partial melting, in different melting environments (eg spinel versus garnet-facies peridotites) and how isotopic fractionation may be influenced by metasomatic processes. With a good understanding of how such processes contribute to the iron isotope signatures of mantle rocks, we can "deconvolve" the iron isotope compositions of mantle rocks and interpret them in terms of changes in mantle oxidation state.

As stable isotope fractionations at high temperature are believed to be extremely small (typically no more than 0.5 per mil, or a few parts per 10,000) the development of ultra-high precision MC-ICPMS techniques is required. This has been achieved at GEMOC using a standard-sample bracketing technique in conjunction with external normalisation; the standard reproducibility is now well below 0.1 permil for the $^{57}Fe/^{54}Fe$ ratio. Our next goal is to obtain iron isotope data for minerals separated from well-characterised xenoliths from the Lesotho, Kimberley and Finsch localities in the Kaapvaal craton, South Africa. These xenoliths represent variably depleted and metasomatised garnet-bearing SCLM. By studying these xenoliths, which contain garnet, olivine, orthopyroxene and clinopyroxene as major phases (Fig. 2), we can constrain the behaviour of iron isotopes during partial melting and evaluate the effects of metasomatism. Further work will focus on analysing xenoliths of different ages from different cratons with a view to evaluating how the oxidation state of the lithospheric mantle has changed with time.

Figure 2. Thin section (viewed in plane-polarised light) of sample LT98/10, a garnet peridotite xenolith from North Lesotho, Kaapvaal Craton.

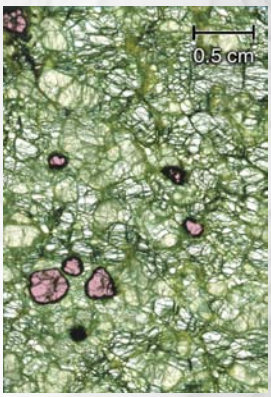

Contact: Helen Williams
Funded by: Nu Instruments Fellowship, ARC

Trace elements are a girl's best friend: How diamonds form

NATURAL DIAMOND CRYSTALS form at high temperatures and pressures in the Earth's mantle. Because diamond is chemically inert under most natural conditions, these crystals act as 'time capsules' that provide us with valuable direct samples of the mantle and records of mantle processes during diamond formation. It is now widely accepted that most, and perhaps all, diamond crystallises from fluids percolating through mantle. The structure of diamond is so tight that it excludes elements other than carbon, nitrogen and occasionally trace amounts of boron. However, during its crystallisation, diamond commonly traps small inclusions of silicate, oxide and sulfide minerals. Trace amounts of the fluids from which the diamond grew also are found, trapped in microscopic to submicroscopic fluid (±solids±vapour) inclusions. These inclusions can yield information about the chemical, isotopic and mineralogical composition of the host rocks and the nature of the fluids from which the diamond formed.

GEMOC has developed a technique for the quantitative trace-element analyses of > 40 elements in diamond by LAM-ICPMS, using a multi-element doped-cellulose standard; detection limits range to low-ppb levels for many elements. This unique method was featured as a "hot topic" lead article in the prestigious Journal of Analytical Atomic Spectroscopy in 2005 (Fig. 1; Publication #407). The technique was used to analyse >500 diamonds of different types, and from different localities worldwide, and the data provide exciting new insights into the processes of diamond crystallisation in the mantle.

The structures of polycrystalline (framesite, diamondite) and fibrous or particulate diamonds indicate that they crystallised rapidly, probably from carbon-oversaturated fluids. Their trace-element patterns are consistent with crystallisation from kimberlitic-carbonatitic melts, which may show significant compositional variation from locality to locality. However, many fibrous/particulate diamonds show an abrupt change in trace-element patterns as crystallisation proceeds. Large decreases in Nb/Ta and Zr/Hf are difficult to explain by fractional crystallisation, but can be modelled as the result of liquid immiscibility: a separation into broadly hydrous-silicate and carbonatite fluids. This process can produce very large elemental fractionations (Fig. 2). The ubiquitous development of pronounced negative Y anomalies (relative to Ho-Dy) may reflect the further separation of fluoride phases or immiscible fluoride melts.

Despite significant variation from one deposit to another, nearly all monocrystalline diamonds from localities worldwide show low LREE/HREE, Ba/MREE and Sr/LREE, as well as low Nb/Ta and Zr/Hf, suggesting that they have crystallised from the hydrous-silicate member of the proposed immiscible-liquid couple. Modelling of the conjugate Mg-rich "carbonatite" liquid shows it would have extremely high LREE/HREE and Sr (Fig. 2). The composition of this fractionated carbonatitic fluid can explain one of the unusual features of diamond-related minerals worldwide. One of the most common

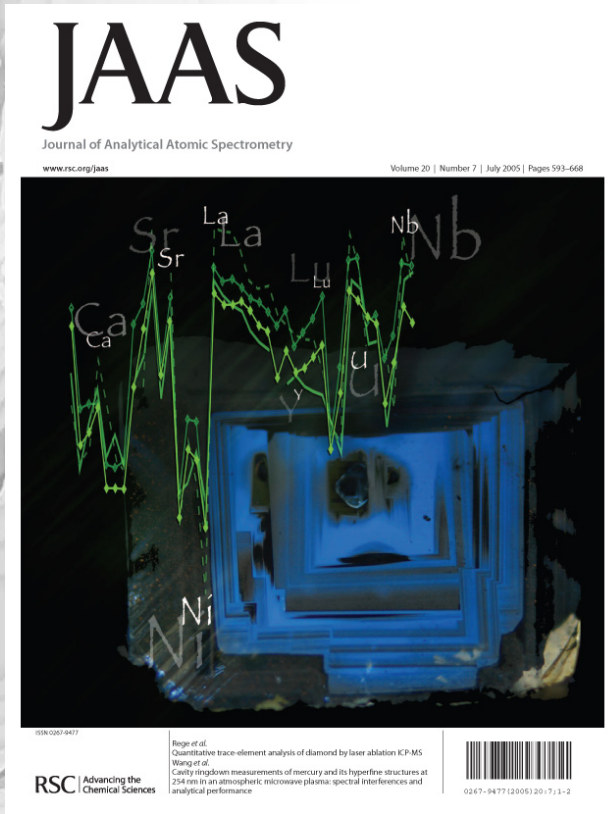

Figure 1. Rege, S., Jackson, S.J., Griffin, W.L., Davies, R.M., Pearson, N.J. and O'Reilly, S.Y. 2005. Quantitative trace element analysis of diamond by laser ablation inductively coupled plasma mass spectrometry. Journal of Analytical Atomic Spectroscopy 20, 601-610.

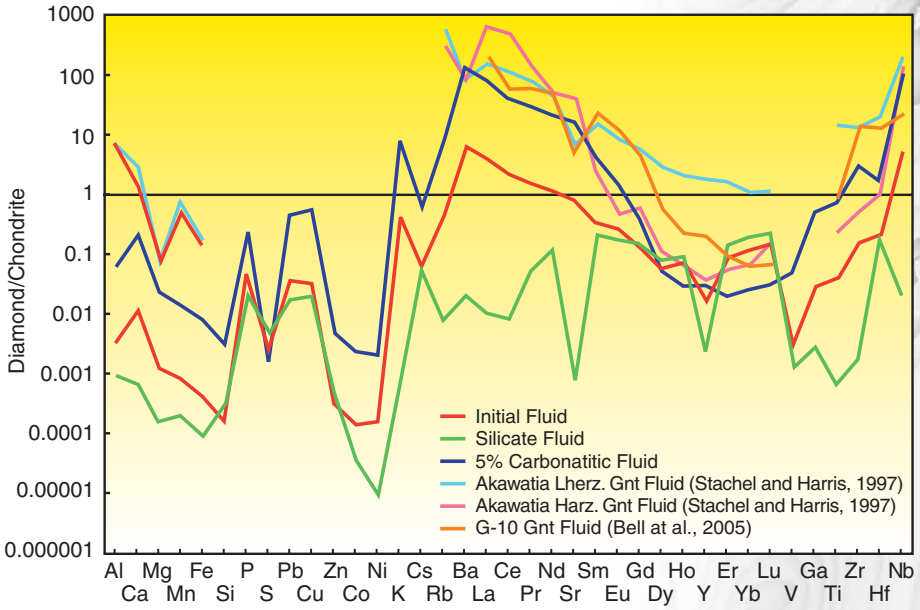

Figure 2. Diamond-related fluids. The "initial fluid" represents the mean of ca 200 fibrous/particulate/ polycrystalline diamonds worldwide, and resembles the patterns of many kimberlites and carbonatites. The "silicate fluid" represents the mean of ca 200 monocrystalline diamonds worldwide. The "carbonatitic fluid" is calculated assuming that the initial fluid separated into the silicate and carbonatitic fluids in the ratio 95:5. The fluids in equilibrium with harzburgitic (subcalcic Cr-pyrope) garnets and lherzolitic (Ca-saturated) garnets were modelled by Stachel and Harris (1997).

inclusions in diamond, and one of the most ubiquitous "indicator minerals" used in diamond exploration, is subcalcic Cr-pyrope garnet with "sinuous" REE patterns and high Sr contents (Fig. 3). Attempts to model a liquid from which such strange garnets would crystallise produce trace-element patterns with extreme element fractionations, not observed in known rocks; this conundrum has led most researchers to conclude that the subcalcic Cr-pyropes represent metasomatic modification of pre-existing garnets. However, the modeled fluids correspond closely to the immiscible "carbonatitic" end-member fluid predicted from the diamond trace-element data (Fig. 2).

It appears that the reaction of this fluid with chromite + olivine + opx in the harzburgitic mantle wall rocks can produce the unusual garnets which are a characteristic inclusion in diamonds of the peridotitic paragenesis worldwide. In contrast, metasomatism by the original kimberlite-carbonatite fluid would produce the more common lherzolitic garnets (Fig. 2). We therefore suggest that the development of immiscibility during the evolution of low-volume melts of the kimberlite-carbonatite spectrum produces conjugate fluids, one of which crystallises most monocrystalline diamonds, and the other of which interacts with mantle harzburgites to produce the most ubiquitous inclusions in peridotitic diamonds. These new models have interesting implications not only for diamond exploration, but for the origin and nature of the original Archean mantle.

Contacts: Sue O'Reilly, Bill Griffin, Sonal Rege
Funded by: ARC, Macquarie University

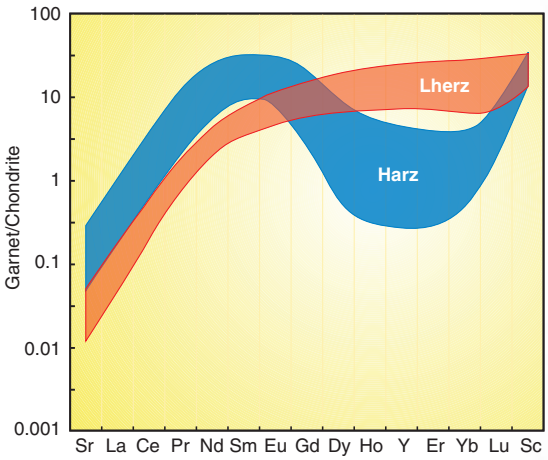

Figure 3. Trace-element patterns of garnets from lherzolites and harzburgites.

Intraplate volcanism, mantle dynamics and diamond exploration

INTRAPLATE VOLCANISM, which is not directly related to plate boundaries, can give us insights into mantle dynamics beneath the plates, and enhance our understanding of mantle-derived mineral resources, such as diamonds. The most voluminous intraplate volcanics have been attributed to hotspots - active volcanic zones not attributed to plate boundary processes. The most widely accepted origin for most hotspots is mantle plumes: hot, buoyant upwellings of mantle material that may originate as deep as the core-mantle boundary, and on reaching the surface may cause intense, localised zones of volcanism.

The most remarkable thing about these mantle plumes is that they seem to have moved very little compared to the plates, almost as if they were rooted in the deep mantle. More detailed analysis, particularly from paleomagnetic data, has shown that in fact these plumes do move, sometimes quite rapidly, as if being blown by the "mantle wind".

Three-dimensional convection simulations can determine the strength of the mantle wind, and the motion of plumes in it. Using high resolution data on past plate motions, and detailed density models of the Earth based on global seismic tomography, the mantle velocity field was calculated for the last 120 Myr. This involved a significant technological leap: backwards convection simulations are technically impossible, since thermal diffusion is an inherently one-way process. However, the use of a modified diffusion relation, and an evolutionary computation approach in which the simulations are coupled to real-world constraints on the system, overcame these difficulties.

The calculated motion of major mantle plumes is consistent with available evidence on their motion from paleomagnetism, and with the deep structure of these plumes from high-resolution tomography. Additionally, their motion explains several long-standing geodynamic conundrums, such as how to reconcile a Kerguelen-plume origin for the Rajmahal Traps in northern India, and the Ninetyeast Ridge, when the present-day position of the Kerguelen hotspot is in the wrong place to form these features. Our model of Kerguelen plume motion alleviates such problems.

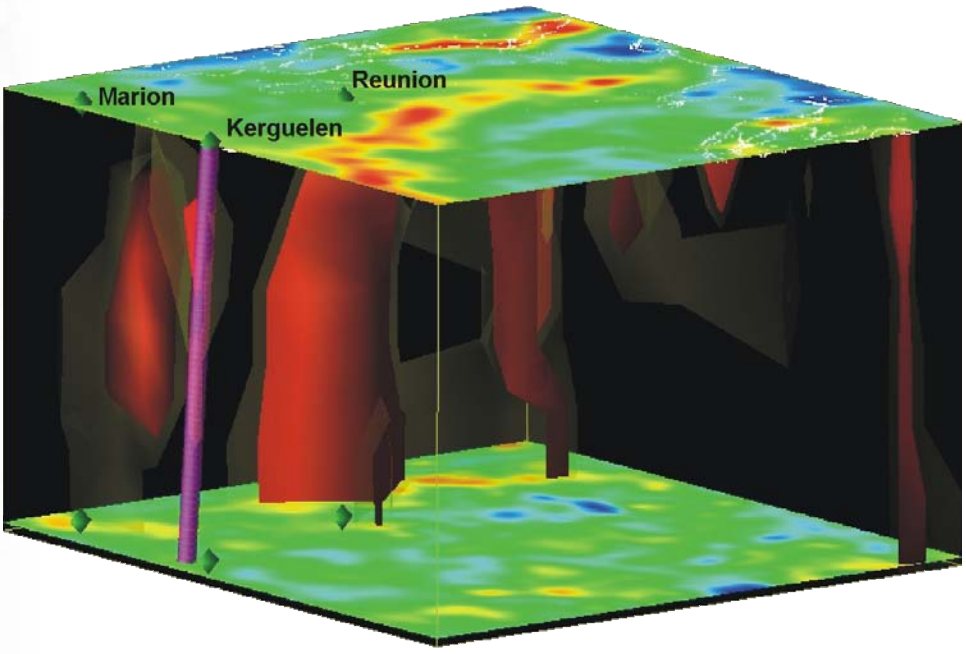

Figure 1. Velocity anomalies in the Indian Ocean and their relationship to major hotspots. The coloured slices are velocity anomaly cross-sections at 50 and 950km (red minimum velocities in given layer, blue maximum). Coastlines are shown in white. Red contours show -0.75 velocity anomalies, and yellow (translucent) contours the -0.6 anomalies. The purple tube shows the calculated tilt of the Kerguelen hotspot.

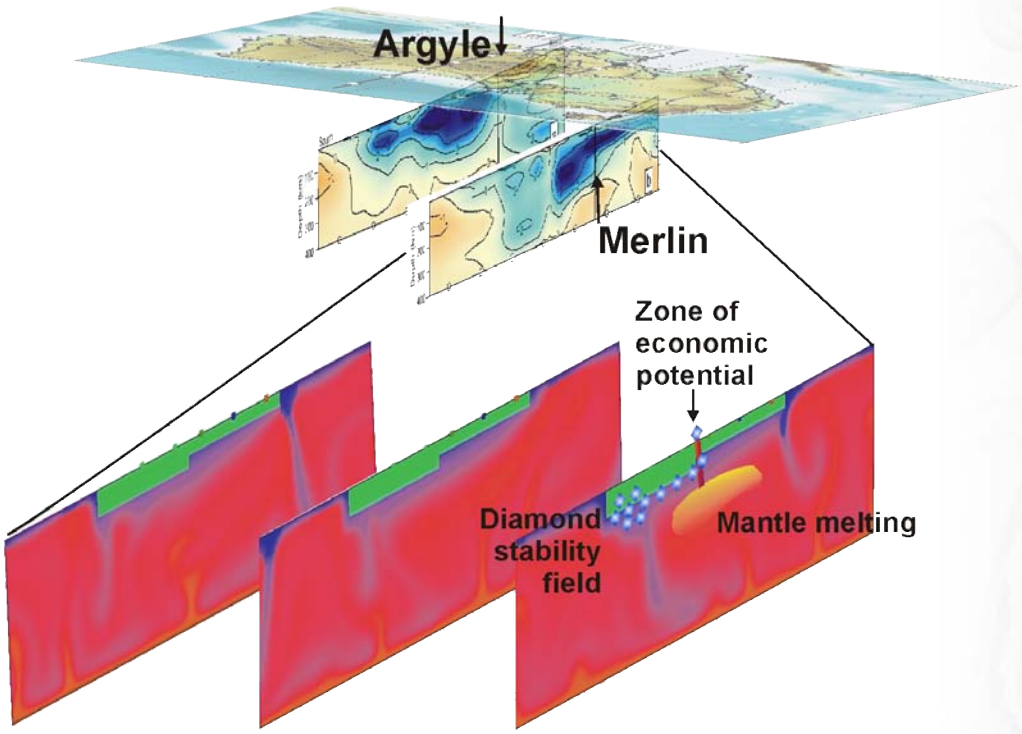

Figure 2. Vertical slices through the tomographic model of Frederik Simons, at the positions of Argyle and Merlin. Both Argyle and Merlin lie on strong gradients in lithospheric thickness. Also shown is the temperature field from mantle convection simulations incorporating a fixed continent (green). The intersection of the diamond stability field (blue diamonds) and mantle melting (yellow) indicates regions of economic potential.

The interaction of mantle upwellings with the continental lithosphere determines the surface distribution of volcanic rocks - including diamond-bearing rocks such as kimberlites and lamproites. These hot mantle upwellings also can modify the thermal state of the overlying lithosphere, potentially destroying lithospheric diamonds before they can be entrained in the rising magmas. Our simulations tracked the evolution of the thermal conditions in the lithosphere and melting in a convecting mantle. The results show that while diamonds are preferentially stable in the deepest portions of thick, cool continental lithosphere, it is very difficult to generate melt in these regions. Melting preferentially occurs when mantle can upwell to shallow depths beneath thin lithosphere - a situation not conducive to diamond stability. Therefore the regions most conducive to the sampling of diamonds by upwelling magmas are on the periphery of thick lithospheric roots. Interestingly, Australia's economic diamond deposits (Argyle, Merlin and Ellendale) all lie on the boundaries of thick lithospheric domains, suggesting a fundamental link between mantle dynamics, mantle melting, and the distribution of diamond deposits.

Contact: Craig O'Neill
Funded by: University of Sydney Postgraduate Award, NASA-MDAT and NSF grants, Macquarie University Research Fellowship

Hot Stuff: Geotherms, density and seismic velocity

MANTLE XENOLITHS PROVIDE DETAILED INFORMATION on the composition of small volumes of subcontinental lithospheric mantle (SCLM) beneath individual volcanic fields; the challenge for the geologist is to extend that information to larger volumes of the lithospheric mantle. Seismic tomography provides stunning images that carry information on the structure of the SCLM, and potentially can be used to map the deep interior. Global tomographic studies show that "roots" with high seismic velocities extend to depths of 150-300 km under Archean cratons, while younger areas typically show thinner "roots", with somewhat lower velocities and extend to lesser depths. Seismic tomography is typically interpreted in terms of thermal variations. However, calculations of seismic velocities for mantle-derived xenoliths show that variations in mantle composition can account for as much as 25% of the observed velocity range. We have developed a methodology for evaluating the relative contributions of temperature and composition, and produced maps of regional geotherm and broad compositional constraints on the SCLM from the inversion of shear-wave (Vs) seismic tomography (*Deen et al., 2006, GEMOC publication #423*).

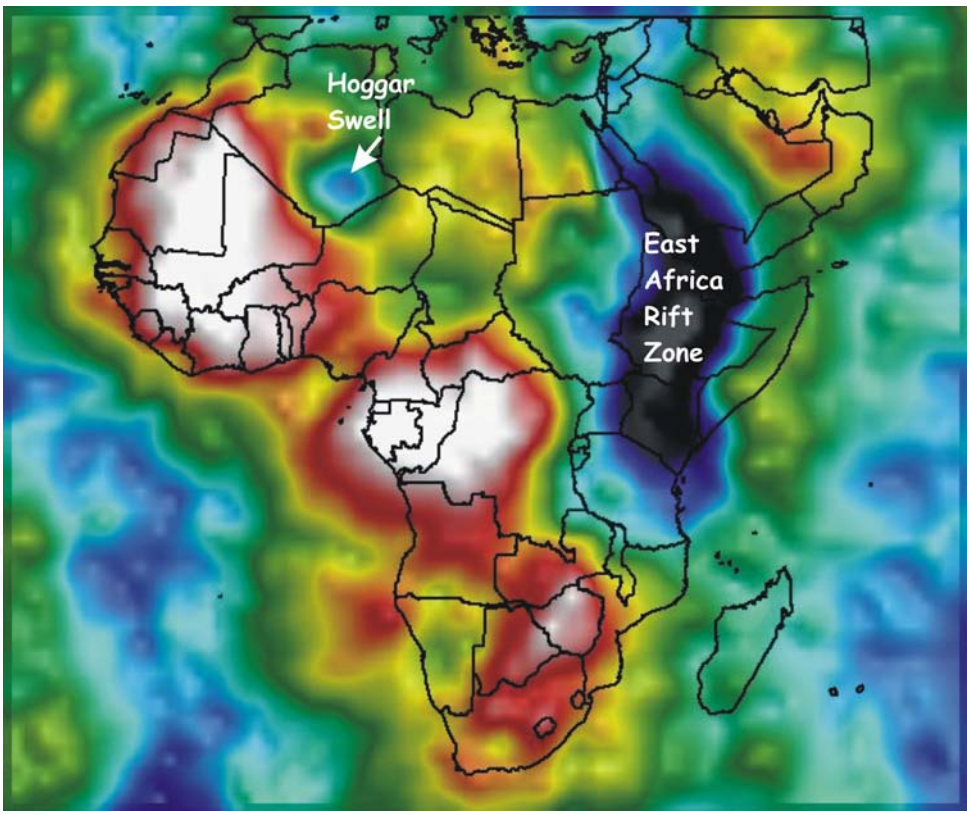

Figure 1. Distribution of shear-wave seismic velocity (Vs) for the range 100-175 km beneath Africa. Zones of relatively higher shear-wave velocity are red and white, while slower velocities are blue and black. Tomography reprocessed by WMC Resources (Perth), from Grand (1997).

The approach removes the temperature and pressure effects from the *in situ* density of the lithosphere, allowing definition of upper mantle regions showing broad differences in lithospheric composition. The methodology uses empirical model geotherms quantized in steps of 2.5 mW/m^2, and three mantle compositions corresponding to typical Archean, Proterozoic and Phanerozoic SCLM. Starting from an assumed composition for a volume of SCLM, lithospheric density at surface pressure and temperature is calculated for each geotherm at each point; the optimum geotherm is taken as the one yielding a density closest to the mean value derived from mantle xenoliths (3.31 g/cm^3). Results requiring densities or geotherms outside the known natural range of these parameters worldwide require

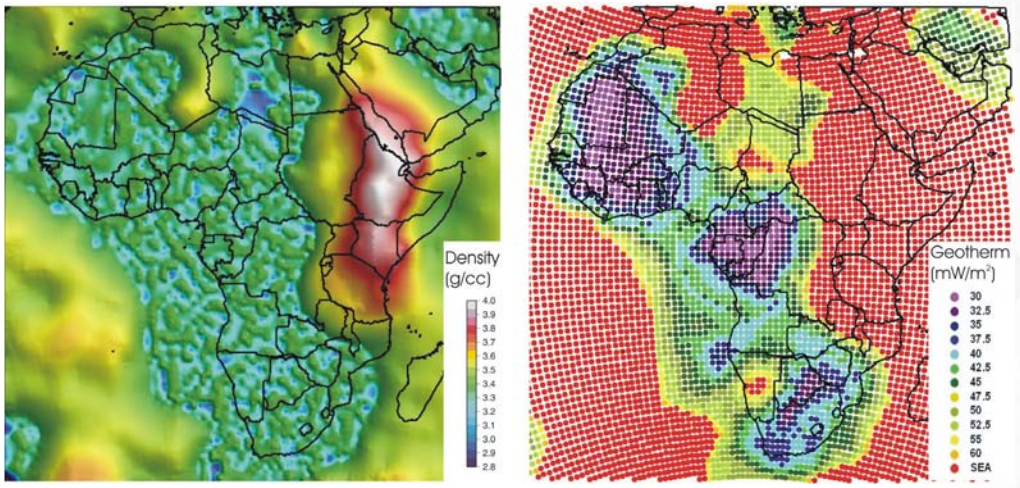

Figure 2. Calculated density (left) and corresponding geotherm values in mW/m² (right) for the lithosphere beneath Africa.

the choice of a different mantle composition. This technique, applied iteratively to a 275 km x 275 km Vs model (Fig. 1) developed by Professor Steve Grand (University of Texas at Austin; Grand, 1997 GSA Today, 7), results in maps of the geotherm and regional density, which allow interpretation of SCLM composition within broad limits. Applying this technique to the lithosphere beneath Africa (Fig. 2), thick Archon-type roots are shown to underlie the cratons, including the West African craton which has a deformed Proterzoic cover. The Kalahari craton, in contrast, has a relatively small core of Archon-type material, surrounded by mantle modified during the Proterozoic. The East Africa Rift cannot be modelled using this technique; no geologically reasonable combination of composition and temperature can produce the observed low Vs. This result implies the presence of melts or other fluids at 100-175 km in this region. The Hoggar Swell is underlain by Tecton-type mantle with a high geotherm; this feature may image a narrow hot upwelling responsible for the domal uplift and volcanism in the region. These results can be compared with local (paleo)geotherms and data on mantle composition, derived from xenolith suites (Fig. 3). Application of this technique to the SCLM beneath Africa, Siberia and North America shows good correlation with regional geological features, xenolith data and other geophysical data.

Contacts: Tara Deen, Sue O'Reilly, Bill Griffin
Funded by: Macquarie University, ARC Linkage (O'Reilly, Griffin), WMC Resources

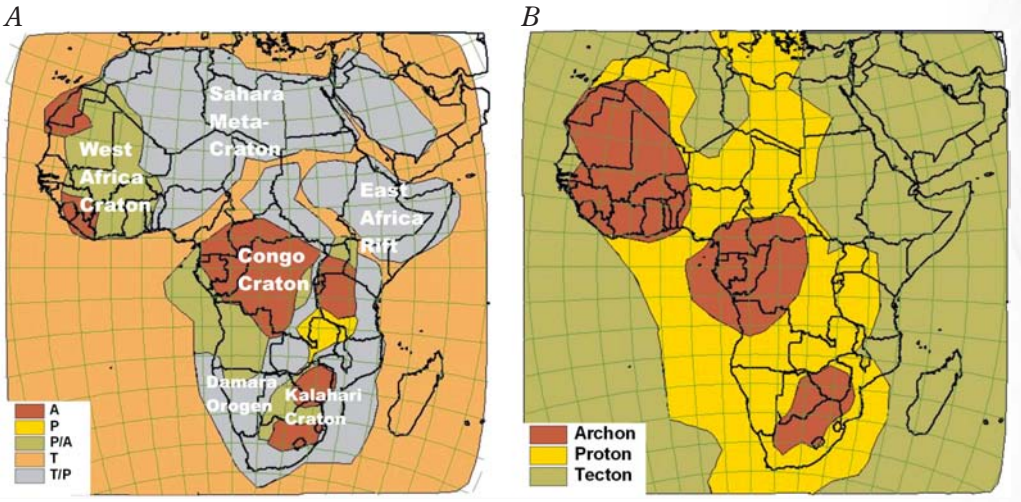

Figure 3. (A) Upper Lithospheric domains indicating the tectonothermal age of lithospheric volumes determined from mapping of geology and geophysics, labelled with broad geographical regions referred to in the text; A=Archon, P=Proton, T=Tecton, P/A=Proton-reworked Archon, T/P=Tecton-reworked Proton. (B) Generalised mantle types at 100-175 km depth, interpreted from Figure 2.

Isotopic ratio measurement using microbeam methods: Where do we stand and where are we going?

THIS WAS THE TITLE OF A SESSION co-convened by Norm Pearson at the 15th Goldschmidt Conference, held in Moscow, Idaho in May 2005. The session brought together researchers using SIMS and laser ablation MC-ICPMS for *in situ* isotope ratio analysis in the geosciences and profiled the advances that had been made by each group.

Since the late 1990s GEMOC has been at the forefront of the development of *in situ* isotope ratio measurements using laser ablation multi-collector ICPMS. The developments encompass both 'non-traditional' stable isotopes (eg Mg, Fe, Ni, Cu, Zn) and radiogenic isotopic systems (eg Sr, Nd, Hf, Os, Pb). Previous research highlights have showcased the applications of *in situ* Hf isotopes in zircon and rutile, Os isotopes in mantle sulfides, Cu and Fe isotopes in chalcopyrite and pyrite in ore deposits and Mg in mantle olivine. These new methods have had an enormous impact on our understanding of the evolution of the crust and mantle and have changed the way we study processes that recycle or modify the lithosphere.

Along the way we have also made significant contributions to understanding the fundamental processes of laser ablation (Publication #311) and investigated corrections for mass bias and isobaric overlap for plasma-source mass spectrometry (eg Publications #179, 267).

What have we learned and what does the future hold? What improvements need to be made and can be made?

The benefits to be had using laser ablation rather than conventional techniques, and the issues that must be addressed to produce high quality data, can be summerised in a table.

Advantages

- spatial resolution
- (no) sample preparation (i.e. chemical purification)
- high sample throughput
- greatly reduced (no) memory
- no solvent interferences

Disadvantages

- 'dirty' samples
- overlap corrections for parent/daughter isotopes
- matrix effects and matrix matching
- availability of suitable reference materials
- spot size vs sensitivity (precision)
- laser-induced isotopic fractionation

Figure 1.

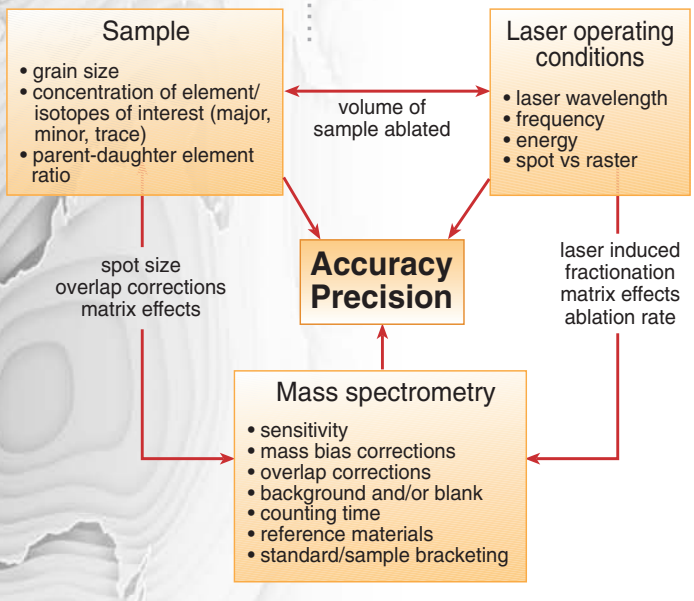

From the petrologist's viewpoint, *in situ* analysis allows the isotopic data to be interpreted in a microstructural context and in the framework of geochemical data from other microanalytical techniques. The *in situ* capabilities allow for the first time the investigation of isotopic variation at the sub-millimetre scale and in doing so have raised questions concerning the validity and interpretation of whole-rock measurements (eg Publication #326).

From an analytical viewpoint our current knowledge can be summarized in the context of the factors that control the accuracy and precision of *in situ* analysis. Ultimately accuracy and precision will depend on the interplay of several factors, including the composition of the sample, signal intensity, correction procedures and analysis time (Fig. 1).

The methods developed so far fall into two broad

groups based on the properties of the sample: (1) the analysis of stable-isotope ratios where the element of interest is a major element in the mineral and (2) radiogenic isotope measurements of an element which is present in minor or trace amounts in the mineral. At one end of the spectrum, laser ablation is a 'true' microanalytical technique with spatial resolution of 30-50 microns, which is comparable to most ion probes. As we strive to obtain the best precision for isotopic ratios of elements in low concentrations (<100 ppm) it becomes necessary to use spot sizes on the order of several hundred microns. While this still has many of the benefits outlined above, the laser effectively becomes a bulk-sampling device and within-grain variations cannot be determined unless the grain size is relatively coarse. Improvements in the sensitivity of mass spectrometers therefore are required to enable the use of smaller spot sizes. The other main issue encountered with radiogenic systems at the trace abundance level is the parent-daughter elemental ratio. The corrections for isobaric interference are a significant factor in the accuracy and precision of *in situ* measurements of Sr, Nd, Hf and Os isotopes. Figure 2 shows the combination of the uncertainties associated with signal sensitivity and interference corrections on the analytical precision of Hf-isotope measurements.

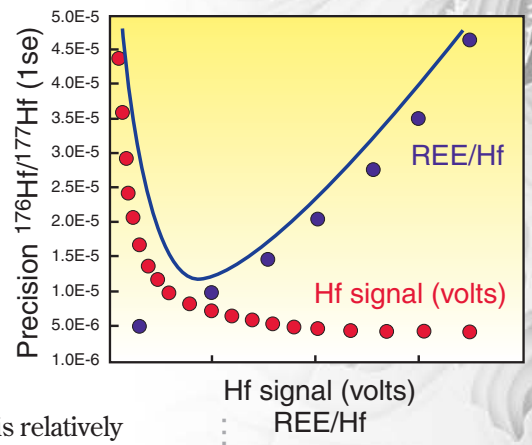

Figure 2. Internal precision for $^{176}Hf/^{177}Hf$ as a function of total Hf signal intensity and REE/Hf ratio. The curve shows the relative importance of low signal intensity and high REE/Hf as the main controls on precision.

One of the main problems faced by all microanalytical techniques is the availability of suitable reference materials, i.e. materials that are homogenous on the scale of tens of microns. As an example, since we began *in situ* analysis of Hf isotopes in zircon in 1999, we have routinely analysed two reference zircons (91500 and Mud Tank) and in the process built up large databases of results. 91500 shows considerable heterogeneity in $^{176}Hf/^{177}Hf$; the distribution is essentially bimodal with major peaks at 0.282284±22 and 0.282330±29 (2σ) (Fig. 3). By comparison, the long-term average and variance for $^{176}Hf/^{177}Hf$ of our LAM-MC-ICPMS data for the Mud Tank zircon is 0.282523±43 (2σ, n= 2190). This dataset has a single peak; although no natural zircon may be homogeneous at the scale of laser ablation, our data indicate that Mud Tank is more homogeneous than 91500.

While the Holy Grail of *in situ* isotope analysis might be to analyse the Nd-Sm or Lu-Hf systems in garnet or the Rb-Sr system in K-feldspar, this will need far greater instrumental sensitivity than is currently available, and some form of on-line chemical separation to remove isobaric interferences.

The introduction of *in situ* microanalysis of isotopic compositions is bringing about a revolution in the Earth Sciences comparable to the introduction of the electron microprobe (EMP) in the 1960s. As the development of EMP made petrologists look at the details of chemical processes, the analysis of isotopic ratios by SIMS and laser-ablation is forcing isotope geochemists to rethink the meaning of their data. While the *in situ* techniques still have the definite limitations as described above, the advantages (and the challenges) are obvious.

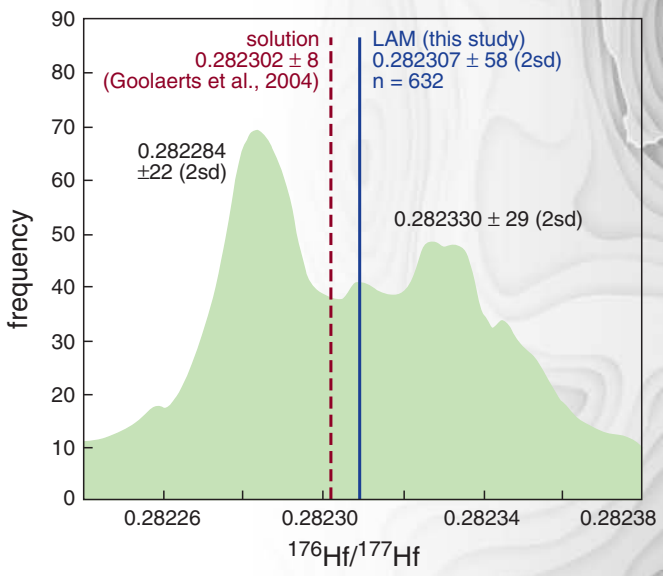

Figure 3. Cumulative-probability histogram of GEMOC's LAM-MC-ICPMS analyses of $^{176}Hf/^{177}Hf$ in zircon "standard" 91500.

Contacts: Norman Pearson, Bill Griffin, Sue O'Reilly
Funded by: ARC LIEF, DEST SII, Macquarie University, ARC Large, Discovery, SPIRT and Linkage, industry collaborations

Ancient abyssal peridotites

THE PLATE-TECTONICS MODEL has driven the study of mid ocean-ridge magmatism, as it is one of the most obvious expressions of the mantle convection associated with plate tectonics. In this model, melting of the upwelling convective mantle at mid-ocean ridges produces two complementary products: a depleted mantle residue and an igneous crust (i.e. MORB, dykes and gabbros). It is widely accepted that Abyssal Peridotites (AP) drilled or dredged from the ocean floor (eg the Ocean Drilling Program campaigns) represent this residue after MORB extraction. If so, they should provide insights into the nature, evolution and processes that affect the MORB source mantle, i.e. the convective upper mantle. Furthermore, because they are presumed to be recently incorporated into the lithosphere, their geochemistry might tell us about the evolution of the convective upper mantle.

However, a number of studies have shown that the "magmatic" history of abyssal peridotites is far more complicated than previously thought. The decay of ^{187}Re to ^{187}Os offers a new perspective on these issues. Unlike other long-lived isotopic systems such as Rb-Sr or Sm-Nd - which consist of incompatible lithophile (i.e. magmaphile) elements - Os behaves as a highly compatible element during melting and is retained in the mantle, whereas Re is moderately incompatible and enters the melt. Sulfides are the main carrier of highly siderophile elements in the mantle, including Os and Re. Recent studies have shown that several sulfide populations, characterised by different micro-structural occurrence and composition, coexist at the thin section scale and record various episodes of melting and melt/rock reaction events. Thus by establishing the Re-Os isotopic systematics of the different sulfide populations (using LAM-MC-ICPMS), we can shed some new light on the intricacy of melt extraction and percolation processes beneath mid-ocean ridges.

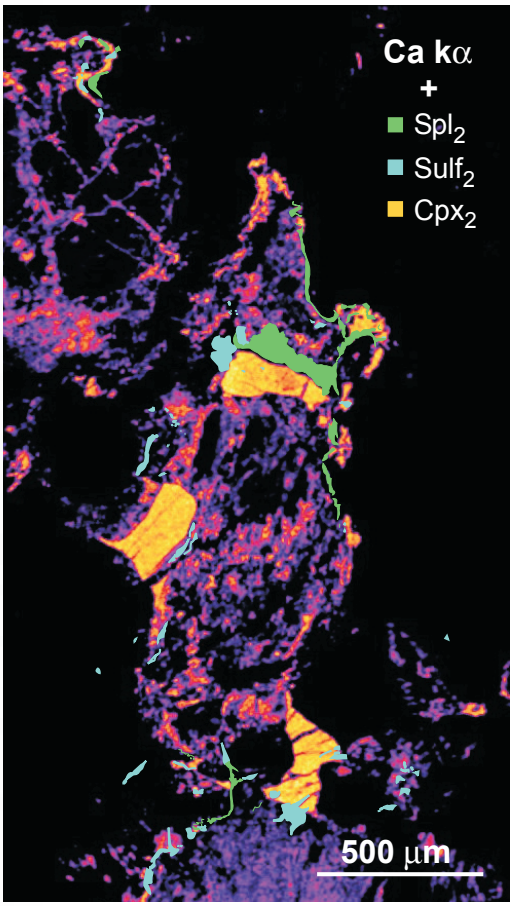

Figure 1. Chemical (Ca) map of an abyssal peridotite from Leg147 (Hess Deep, fast spreading ridge). The image shows the chemical imprint of melt percolation on the primary assemblage that makes up the AP (Ol_1-Opx_1, not shown here). Under lithospheric conditions the percolating melt crystallises secondary clinopyroxene (Cpx_2≈ "impregnation" cpx) and secondary sulfide (Type-2 sulfide ($Sulf_2$)) ± secondary spinel (Spl_2).

[Note that this metasomatism does not always lead to a fertilisation of the whole rock as commonly assumed. Indeed, the percolating melt is often characterised by a depleted REE pattern resembling those described as inclusions in olivine phenocrysts in MORBs and dubbed "Ultra- depleted Melt".]

Two populations of magmatic sulfides have been recognized in most AP or oceanic-related peridotites from all geodynamic settings. Type-1 sulfides are associated with the primary silicate assemblage; their composition and trace element abundances (eg Pd/Ir_N<1) indicate that they are residual after melting. Type-2 sulfides are associated with secondary, "impregnation" Cpx_2. This feature, along with their high metal/sulfur ratios (Ni-, Cu-rich) and their high Pd/Ir (Pd/Ir_N>1) demonstrate that these sulfides were precipitated by melt-rock reaction.

Type-1 sulfides in AP from the Kane fracture zone (Mid-Atlantic Ridge) have ^{187}Os/^{188}Os as low as 0.110. Such unradiogenic values are indicative of a long-term evolution in a low Re/Os environment (i.e. depleted lithospheric mantle) and yield

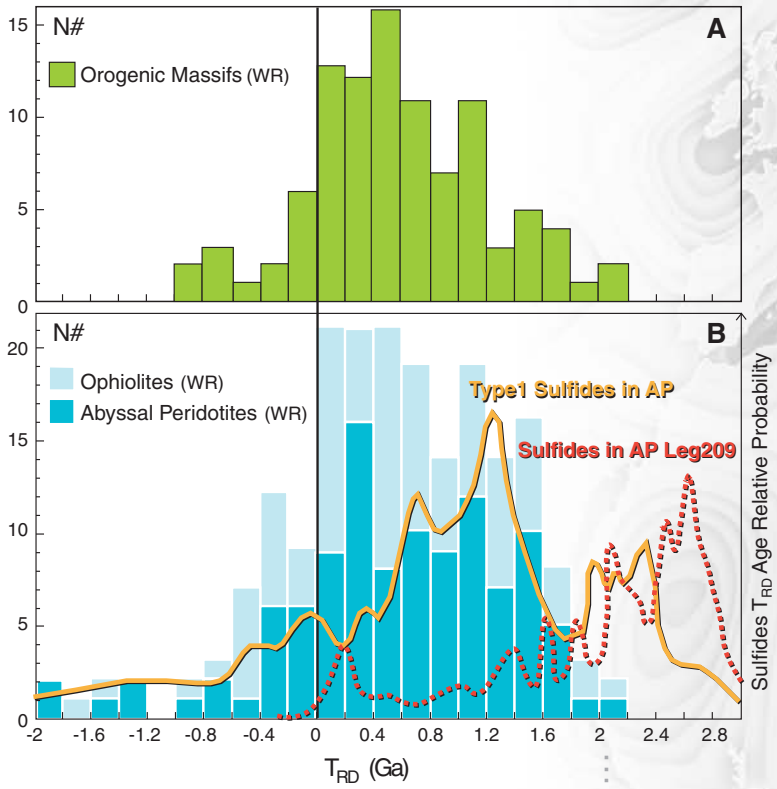

Figure 2. A, Whole-rock Re-depletion ages (T_{RD}) for orogenic massifs (Pyrenees M, Ronda, Beni Bousera). B, Whole-rock T_{RD} ages for Abyssal peridotites from worldwide occurrences (MAR, EPR, SWIR, IBM) and for ophiolites and oceanic-derived massifs (Oman, Ligurides, Horoman). The orange line shows T_{RD} age frequency for Type-1 sulfides found in AP and ophiolites from worldwide occurrences (MAR, EPR, SWIR, Ligurides). The red line shows the T_{RD} age frequency distribution for sulfides in abyssal peridotite from the recent ODP campaign Leg 209 (15°N, MAR).

Re-depletion age (T_{RD}) assumes that all Re has been removed from the residue during melting ($^{187}Re/^{188}Os_{sample}=0$) and thus yields a minimum depletion age, but is more 'robust' to addition or removal of Re by recent/secondary processes. Metasomatism or alteration cannot lower $^{187}Os/^{188}Os$; thus these old T_{RD} ages are 'robust' minimum depletion ages (i.e. not due to model artefacts).

Re-depletion ages (T_{RD}) of ca. 2.3 Ga. Type-2 sulfides in contrast have radiogenic compositions with $^{187}Os/^{188}Os$ ranging from 0.13 to 0.20. Although this typical of the Os-sulfide systematics observed in most APs worldwide, in Leg 209 (15°N-MAR), Type-2 sulfides have a narrow range of extremely unradiogenic Os yielding T_{RD} ages of ca. 2.6 Ga and are older than Type-1 sulfides (ca. 2.3Ga). Associated Cpx_2 are extremely depleted in trace elements (eg REE). This indicates that the percolating melt was here derived from an old and depleted mantle reservoir. Similar melt compositions have been found as inclusions in MORB olivine phenocrysts.

A broader survey shows that Archean or lower-Proterozoic Os model ages are quite commonly (almost systematically) found in whole-rock and/or sulfide Re-Os analyses in abyssal/oceanic-related peridotites. However, as shown in Figure 2, such age distributions are typical of sub-continental lithospheric mantle (SCLM) such as that sampled by orogenic massifs.

This observation suggests that these "oceanic" mantle sections may represent either relicts of the disrupted SCLM entrained during continental break-up, or volumes of SCLM that have been recycled through subduction and are "popping-out" later in the ocean basins. These relict "SCLM rafts/corks", which are depleted and thus less dense than the asthenospheric mantle, could be buoyant and viscous enough to maintain cohesion and 'surf' the convective upper mantle for extensive periods of time. Along with other observations, this model suggests that a significant proportion of the so-called "convective upper mantle" (the MORB source mantle) actually is ancient and highly depleted, and has a protracted history of melting and metasomatism long predating the onset of oceanic rifting.

Contacts: Olivier Alard, Sue O'Reilly, Bill Griffin
Funded by: ARC Discovery

Where does the Houghton Inlier belong? Zircons hold the key!

Elena panning for zircons in the South Para River.

A SERIES OF COLLABORATIVE PROJECTS between GEMOC and Primary Industry and Resources South Australia (PIRSA) has been aimed at building up a broad picture of the crustal evolution of the Gawler Craton. One subproject is addressing the geological affinities between the Craton and various Precambrian inliers in the younger mobile belts that fringe the eastern margin of the craton, including the Houghton Inlier and the Curnamona Province (Fig. 1). The results illustrate the power of the integrated in-situ microanalysis of Pb and Hf isotopic compositions of zircon (the *TerraneChron*® methodology) for the analysis of tectonic problems.

The methodology has been applied to detrital zircons from locally-derived stream sediments in the South Para River, which samples the Houghton Inlier. The zircons record two major events at 1718 ± 8 Ma and 1625 ± 9 Ma (Fig. 2). The details of zircon morphology and internal structure, imaged by combined cathodoluminescence/backscattered electron techniques (Fig. 3) can be used to identify the geological significance of the two age peaks. The zircons of the 1718 Ma population commonly show oscillatory zoning, typical of igneous zircons. In many grains, these oscillatory-zoned domains occur as resorbed cores, which are overgrown by structureless rims interpreted as metamorphic zircon. The 1625 Ma age population represents these metamorphic overgrowths, and single anhedral grains that lack internal structure.

Similar age populations are also found in zircons from both the Gawler Craton (syn-Kimban intrusives) and the Curnamona Province (lower Willyama Group), and the U-Pb ages alone cannot define the tectonic affinities of the Houghton Inlier. However, the Hf-isotope data on the zircons add another layer of information that can solve the problem (Fig. 4). The zircons of the 1720 Ma and 1630 Ma

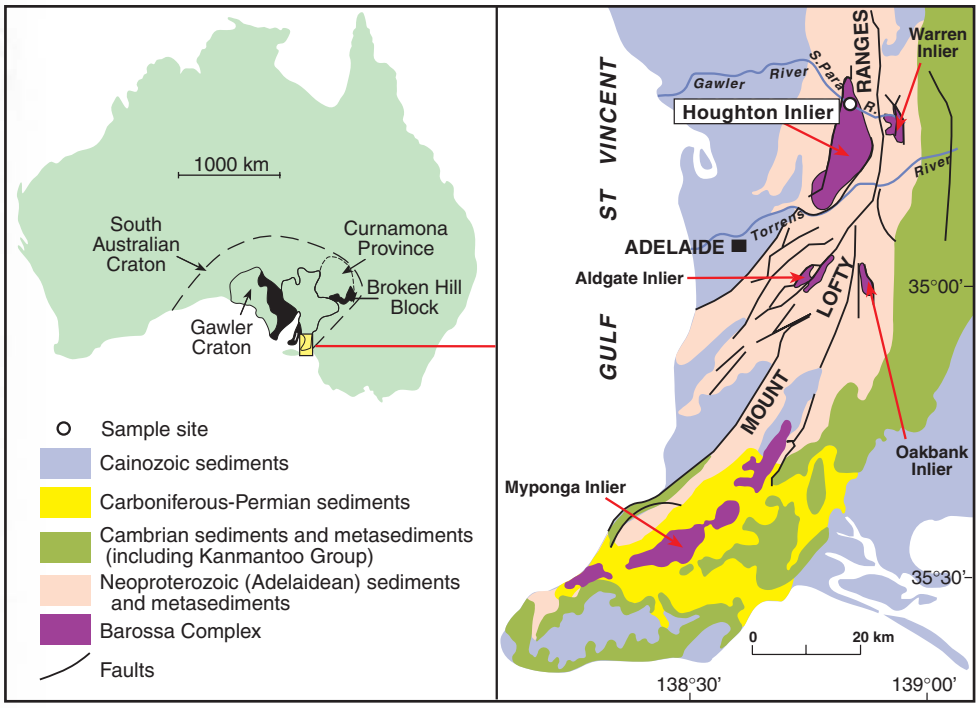

Figure 1. Sketch map of the eastern Gawler Craton, showing the location of the Houghton Inlier and the Curnamona Block.

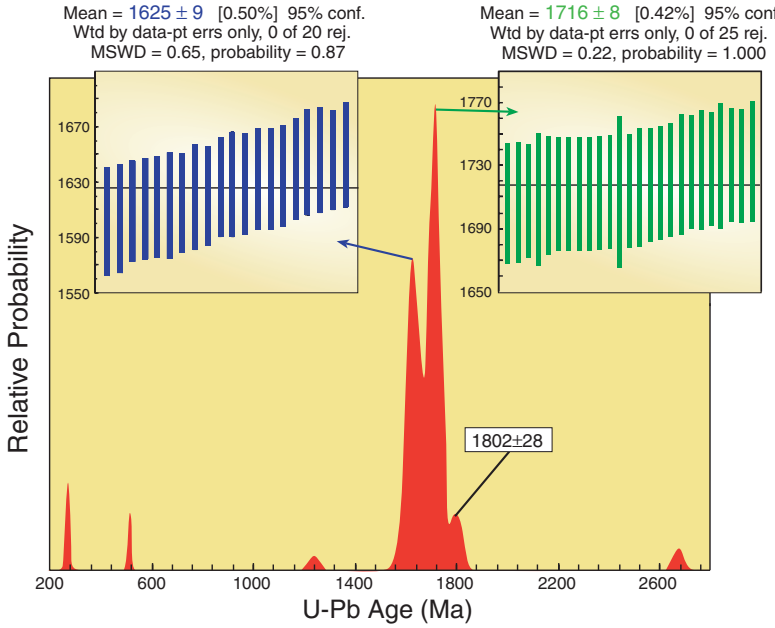

Figure 2. Cumulative-probability histogram of U-Pb data ($^{207}Pb/^{206}Pb$ ages) for zircons from the Houghton Inlier (South Para River), showing two age peaks at 1716 ±8 Ma and 1625±9 Ma.

populations from the Gawler craton show a relatively restricted range of Hf-isotope compositions with low $^{176}Hf/^{177}Hf$, reflecting derivation of the 1720 Ma magmas from much older (Archean) crust. In contrast, the corresponding zircons from the Curnamona Province rocks show a wide range of Hf-isotope compositions, extending to quite juvenile values near the Depleted Mantle (DM) line. This range of Hf-isotope compositions reflects both melting of ancient crust, and the input of juvenile material from the mantle, during the 1720 Ma magmatism in the Curnamona Province. The low $^{176}Hf/^{177}Hf$ of the zircons from the Houghton Inlier shows that they lack the juvenile component and clearly show stronger similarities to the Gawler Craton data.

The zircon data thus indicate that the Houghton Inlier is closely related to the Gawler Craton, while the Curnamona Block has experienced a different type of crustal evolution in mid-Proterozoic time.

Contacts: Elena Belousova, Sue O'Reilly, Bill Griffin
Funded by: ARC APD grant, PIRSA

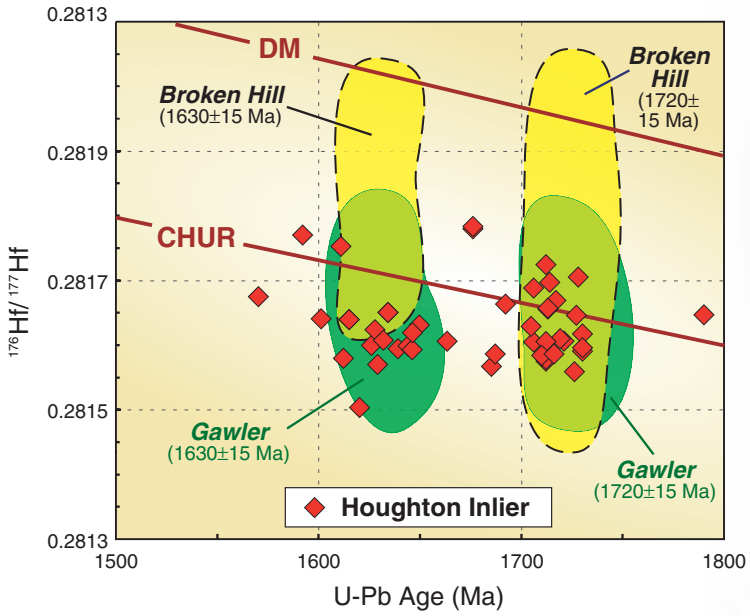

Figure 4. Hf-isotope data for zircons with U-Pb ages of ca 1720 Ma and 1630 Ma, from the Houghton Inlier (this work), the Gawler Craton and the Broken Hill area (author's unpublished data).

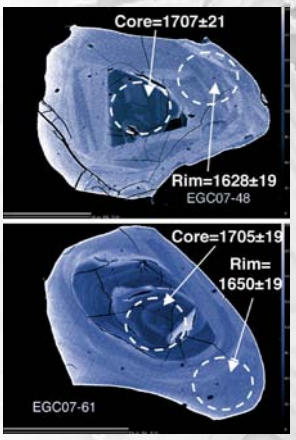

Figure 3. Combined cathodoluminescence/ backscattered electron images of zircons from the Houghton Inlier, showing oscillatory-zoned (igneous) cores and structureless (metamorphic) rims. Circles show location of laser-ablation pits; scale bar is 50 microns.

Following the flow: Thallium isotopes trace subduction processes

ONE OF THE FUNDAMENTAL PROCESSES of Earth dynamics is the subduction process, in which one tectonic plate is thrust beneath another, and down into the mantle. The subducted plate, consisting of depleted mantle, a basaltic crust derived from it, and a package of overlying sediments, has a very different chemical composition than the deeper mantle. The recycling of this crustal material back into the mantle at subduction zones must have an effect on the geochemistry of the mantle, and these effects must have changed through time.

Subducted material that enters the mantle may be eventually transported back to the Earth's surface via mantle plumes, and ocean-island basalts (OIBs) are generally thought to be the surface expression of such mantle plumes. Earth scientists have therefore long attempted to find evidence that OIBs contain components of either marine sediments or oceanic lithosphere. However, such evidence has proven elusive, probably because the subducted material becomes highly diluted in the deeper mantle and is therefore difficult to detect.

New research has found that the isotopes of thallium (Tl) provide a way to test whether any sediments or ocean crust have contributed to the generation of OIBs. Thallium has two isotopes, ^{203}Tl and ^{205}Tl, and the isotope compositions are measured relative to a standard in parts per 10,000:

$$\varepsilon^{205}Tl = 10{,}000 \times (^{205}Tl/^{203}Tl_{sample} - ^{205}Tl/^{203}Tl_{STD}) / (^{205}Tl/^{203}Tl_{STD})$$

Even though Tl is one of the heaviest elements in the periodic table, its isotopic composition varies significantly in some environments on Earth. In particular, Tl isotopes are strongly fractionated, and Tl is highly concentrated, in two important subduction components, pelagic sediments and altered oceanic crust. Therefore, this stable isotope tracer is very well suited for studying subduction processes and the recycling of oceanic crust into the mantle via subduction zones. We therefore measured the abundance and isotopic composition of Tl in lavas from Hawaii (a classic OIB locality) in order to determine if the mantle source region of Hawaiian basalts contains traceable amounts of subducted oceanic sediments or lithosphere (Publication #420).

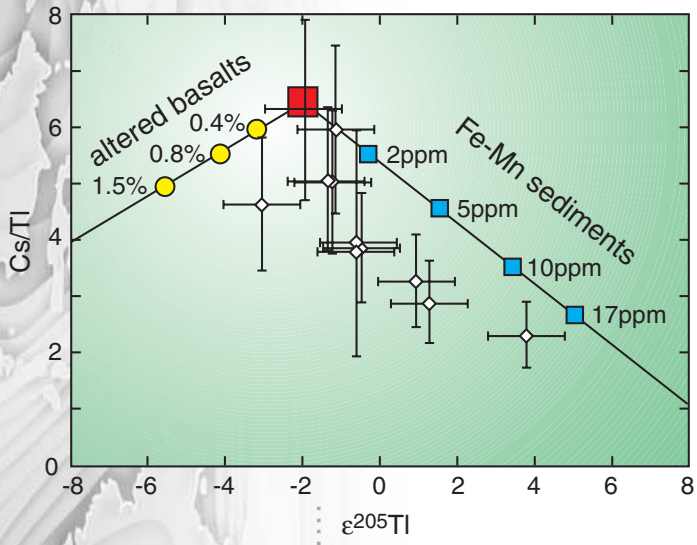

Figure 1. Tl-isotope and Cs/Tl ratios of Hawaiian picrites, showing the negative correlation between Cs/Tl and $\varepsilon^{205}Tl$. Red square shows mean MORB-source-mantle values; blue squares show effect of mixing small amounts of abyssal Fe-Mn sediments into the convecting-mantle source of the picrites; yellow dots show effect of adding altered oceanic basalts to the mantle source.

The Tl isotope compositions of the Hawaiian picrites vary from $\varepsilon^{205}Tl$ = -3.1 to +3.8, which means that the most positive values are about 6 ε-units "heavier" than the mantle represented by mid-ocean ridge basalts (MORB; $\varepsilon^{205}Tl \approx -2$). The Tl isotope compositions display a negative correlation with Cs/Tl ratios (Fig. 1). Thallium and Cs behave similarly in igneous processes and are therefore not expected to fractionate during partial melting or magma differentiation processes. As a consequence, it appears likely that a component with positive $\varepsilon^{205}Tl$ and low Cs/Tl contributed to the Hawaiian lavas. The only currently known component that can account for the decreasing Cs/Tl ratios and increasing Tl isotope compositions is ferromanganese marine sediments, which are chemical precipitates that are ubiquitous in the marine environment. The best interpretation of the data therefore appears to involve addition of marine sediments into the mantle source of OIBs, which is consistent with crustal recycling via subduction zones.

Contacts: Sune Nielsen, Bill Griffin
Funded by: PhD support at ETH, GEMOC

How fast does the mantle convect?

THE PLATE TECTONICS PARADIGM requires that Earth's mantle convects but it remains difficult to constrain either the plan-form or the rates of mantle flow, since these are not easily observed at the surface. The chemical composition of basaltic lavas erupted from volcanoes provides one of the few direct samplings of the Earths interior. One observation from such data is that rocks less than a few thousand years (kyr) old typically preserve disequilibria between short-lived isotopes of the U-series decay chains, for instance between ^{238}U and ^{230}Th (which has a half life of 75 kyr) or between ^{235}U and ^{231}Pa (which has a half life of 33 kyr). Mantle melting beneath ridges and intraplate volcanoes occurs primarily due to decompression of upwelling peridotite and the rate of melting is proportional to the rate of upwelling. Numerical models show that the extent of ^{238}U-^{230}Th and ^{235}U-^{231}Pa disequilibrium is strongly controlled by the rate of melting because this determines the amount of ^{230}Th and ^{231}Pa that are formed by decay of U in the un-melted peridotite residue. ^{230}Th and ^{231}Pa are strongly incompatible in mantle minerals, so these elements are continuously extracted from the peridodite residue and added to the melt. Thus, erupted melts have excesses of ^{230}Th and ^{231}Pa relative to their parental U and the extent of these excesses is proportional to the upwelling rate; this mechanism provides a tool to measure and map mantle upwelling rates. In studies involving Honours student Zoe Demidjuk and Professor Bernard Bourdon at ETH in Zurich, we have used U-series disequilibria to determine the mantle upwelling rate beneath Mount Gambier in South Australia and the Azores archipelago in the mid-Atlantic. The results indicate an upwelling rate of 1-2 cm per year beneath Mount Gambier and 3-4 cm per year beneath the Azores. These slow rates are consistent with the presence of relatively cool mantle plumes beneath these regions, which form part of the return flow that complements the mantle down-welling occurring in subduction zones. In the case of the Azores, the volcanoes are widely enough distributed to permit 3-D imaging of the plan-form of mantle upwelling, and thus to calculate the temperature distribution in the mantle as shown in Figure 1.

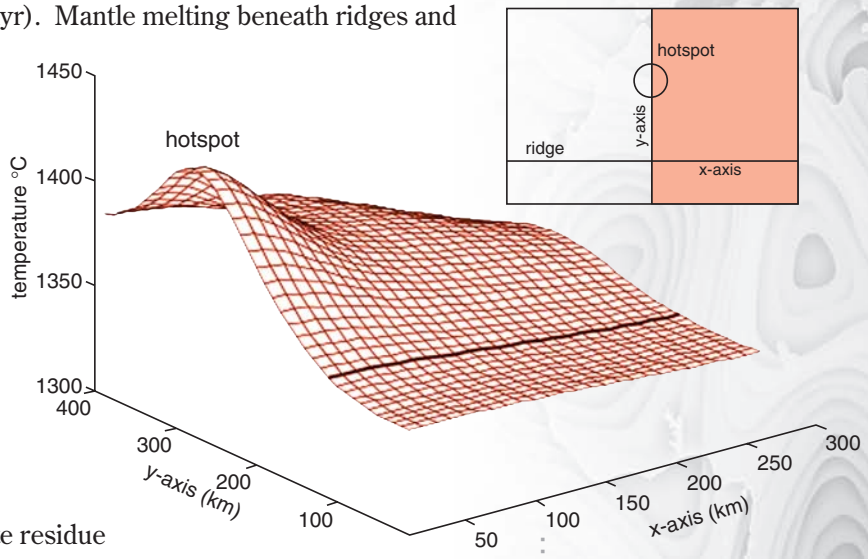

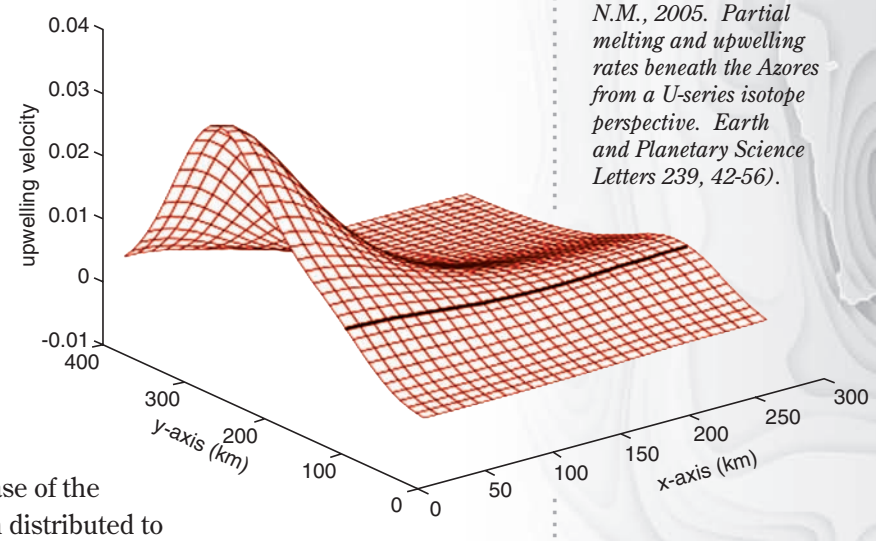

Figure 1. Temperature and upwelling velocity fields for the Azores plume inverted from U-Pa disequilibria data (after Bourdon, B., Turner, S., and Ribe, N.M., 2005. Partial melting and upwelling rates beneath the Azores from a U-series isotope perspective. Earth and Planetary Science Letters 239, 42-56).

Contact: Simon Turner
Funded by: Royal Society of UK, Federation Fellowship

Cold adventures: Measuring ice and the crust in Antarctica

THE LAW DOME IN WILKES LAND, East Antarctica, is a roughly spherical ice cap approximately 200km in diameter, with an elevation of approximately 1400 metres at its centre (Fig. 1). It is bounded to the north by the Southern Ocean and the south by the Totten-Vanderford Glacier Trough. This Trough directs ice flow from the East Antarctic Ice Sheet (EAIS) around Law Dome to be expelled at the trough's extremities, the Totten Glacier to the east, and the Vanderford glacier to the west. So the Law Dome can be treated as an individual ice cap; its ice accumulation only depends on local snowfall, and we can use it to develop models of ice cap motion and mass balance for application to larger ice caps such as the EAIS.

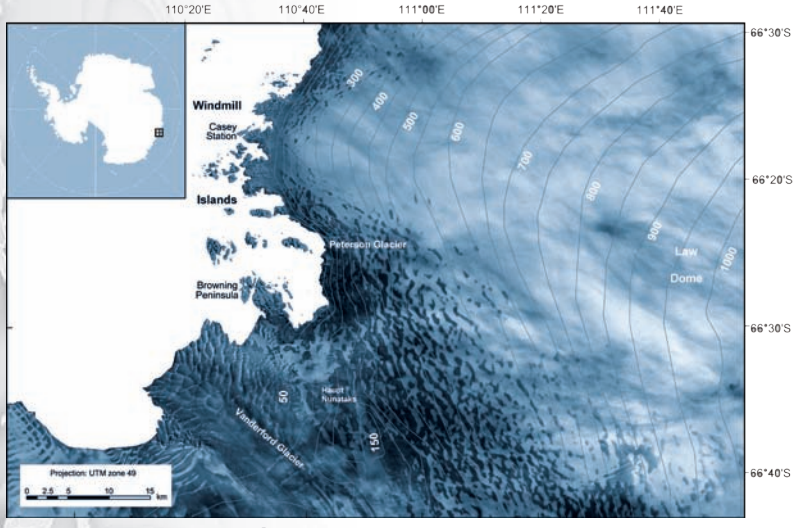

Figure 1. The Windmill Islands on the western edge of the Law Dome ice cap, East Antarctica, at approximately 66°20'S 110°30'E. (Map adapted from the Casey ice runway map provided by the Australian Antarctic Data Centre)

Law Dome has been surveyed for almost 50 years using gravity techniques. During the 2004/05 summer season, we carried out a new gravity survey coupled with terrestrial GPS and satellite measurements. The aim was to determine the effects of climate change on snow surface elevation during the past five decades, by comparing the new data with the older work. A decrease in gravity over most of the survey area is consistent with the increased snow surface elevation deduced from the GPS surveying and ICESAT. The snow surface elevation near the dome summit has increased by approximately 12 cm/yr over the 50 year period, a total of about 6m. This significant increase in elevation indicates positive mass balance in this major part of the ice cap, and probably reflects increased snowfall due to a warmer climate.

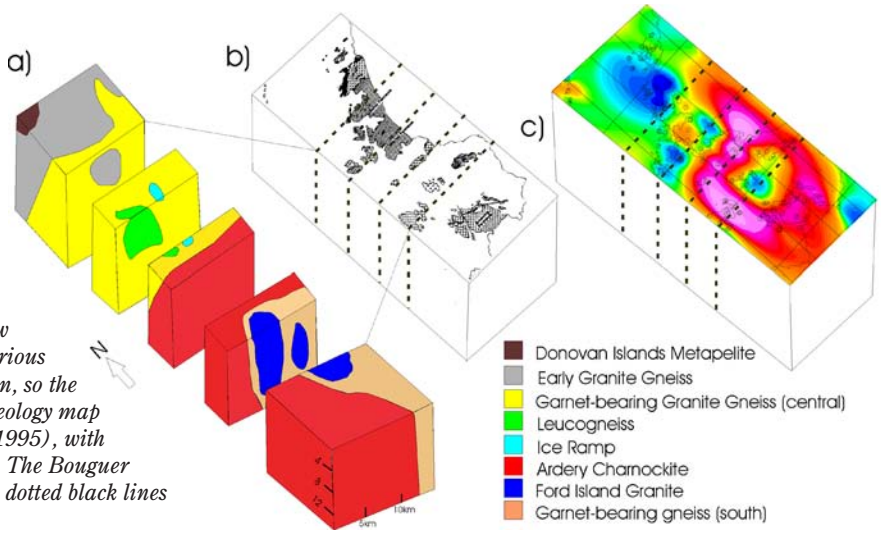

Figure 2. Block model of the Windmill Islands region and subsurface. a) The 3D model sliced along relevant east-west oriented transects to show the depth extents and orientations of the various rock units. There is no vertical exaggeration, so the sections show the true dip of contacts. b) Geology map of the Windmill Islands (from Paul et al., 1995), with dotted black lines representing the slices. c) The Bouguer anomaly map of the Windmill Islands with dotted black lines representing the slices.

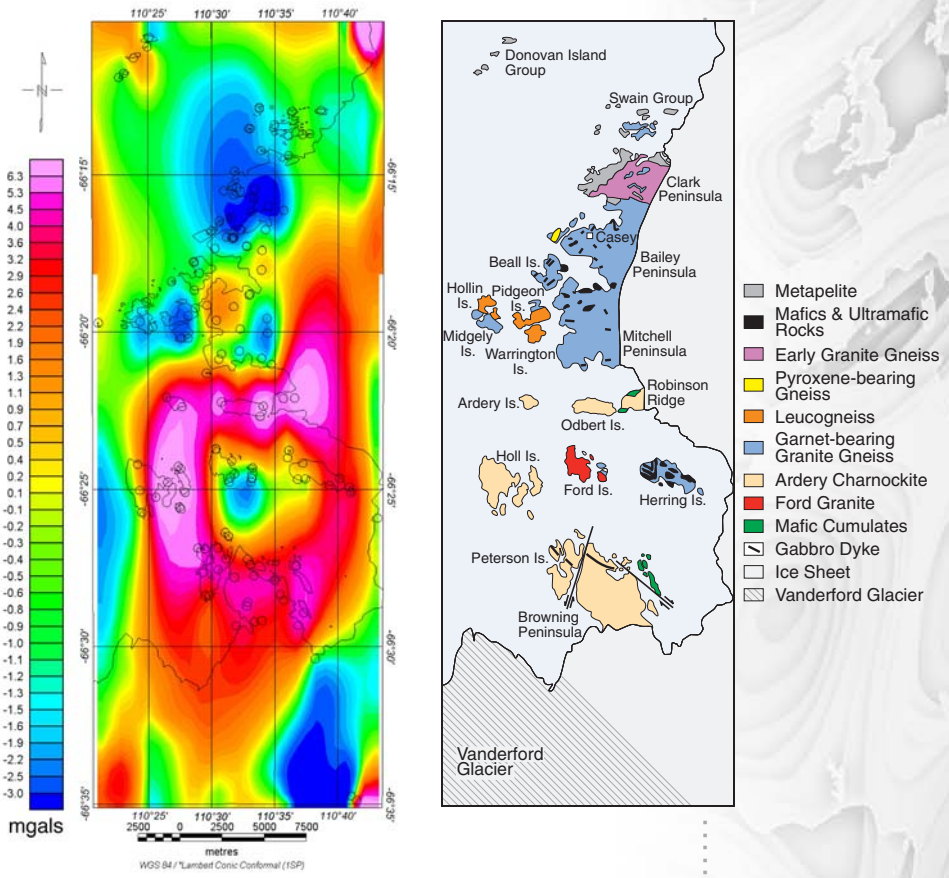

Figure 3. Bouguer gravity image of the merged 1993/94 and 2004/05 Windmill Islands gravity dataset, set alongside a geological map of the area. Correlations between the Bouguer anomalies and major geological units are evident. It can be seen that the dominant high anomaly (shown in red/pink) in the south is produced by the dense Ardery Charnockite unit, surrounding the relative low (in blue) created by the Ford Granite pluton. The ice ramp can be seen as the small low anomaly (blue) at 66°20'S 110°34'E. The Bouguer anomalies in the northern portion of the image are influenced by metamorphic rock units of varying densities, with the low anomaly on Clark Peninsula caused by the less dense Early Granite Gneiss. The small black circles represent gravity station locations.

The second component of the 2004/05 season was a gravity survey on the Windmill Islands, a group of topographically low islands and peninsulas jutting out from the western margin of Law Dome (Fig. 1). The aims of the survey were to add to the existing gravity dataset and to investigate the sub-surface geology of the Windmill Islands area. Ninety-three gravity stations were established and these data were combined with 43 stations from a 1993/94 survey to allow a complex three-dimensional subsurface model to be constructed (Fig. 2). The Bouguer anomaly image shows a strong correlation with the mapped geology of the region (Fig. 3). An intrusive charnockite unit causes the dominant positive gravity anomaly of the study area and has been modelled as extending to depths of more than 15km with sub-vertical contacts. The charnockite unit surrounds two younger granite plutons, one of which is a blind pluton. The modelling also revealed an ice ramp on the Mitchell Peninsula, defining a would-be island joined to the Law Dome ice cap.

The survey also set the foundation for future time-series gravity work in the Windmill Islands to deduce gravity and rock surface elevation changes as a result of isostatic rebound since the Last Glacial Maximum.

Contacts: Brad Bailey (pictured previous page), Mark Lackie (Macquarie University) and Peter Morgan (University of Canberra)
Funded by: ASAC Grant 2580

Taking a gravity measurement on the Law Dome ice cap along side a Hagglunds tracked vehicle.

Erosion in the Murray-Darling basin: How long does it take to produce and transport sediments? By how much has intense land use increased erosion rates?

EROSION IS ONE OF THE MAJOR PROCESSES that shape Earth's surface, moving sediments and solutes from the continents to the oceans. Soil erosion has major implications for our society; it can decrease agriculture productivity and affect water quality. Despite its importance, our understanding of the rates of erosion and the transport of sediments is still limited. Only a few attempts have been made to quantify how human disturbance (eg intensive agriculture in SE Australia over the past 100 years) has enhanced erosion. However, the recent development of tools for analysing uranium-series isotopes has made it possible to address these questions quantitatively.

Uranium-series isotopes are nuclides produced in the ^{238}U and ^{235}U decay chains (Fig. 1). Of particular interest are ^{238}U, ^{234}U, ^{230}Th and ^{226}Ra. During chemical weathering, uranium (U) and radium (Ra) are generally more soluble than thorium (Th). Consequently, solutions that have leached soluble elements from rocks (eg soil pore water, river water) will be enriched in U and Ra over Th, leaving the residual products (eg soils, river sediments) depleted in U and Ra. Thus the *activity ratios* $^{238}U/^{230}Th$ and $^{226}Ra/^{230}Th$ will be > 1 in waters and < 1 in sediments and soils. As these isotopes decay, their activity ratios will reflect both the fractionation during weathering and the time since the fractionation occurred. Hence, they can provide time constraints on erosion and weathering processes. The ^{238}U-^{234}U, ^{234}U-^{230}Th and ^{230}Th-^{226}Ra radioactive systems record weathering-related fractionation that occurred up to 1 million years, 300,000 years and 10,000 years ago, respectively; timescales are determined by the daughter half-life of each system. This allows us to tackle erosion issues with a variable time resolution.

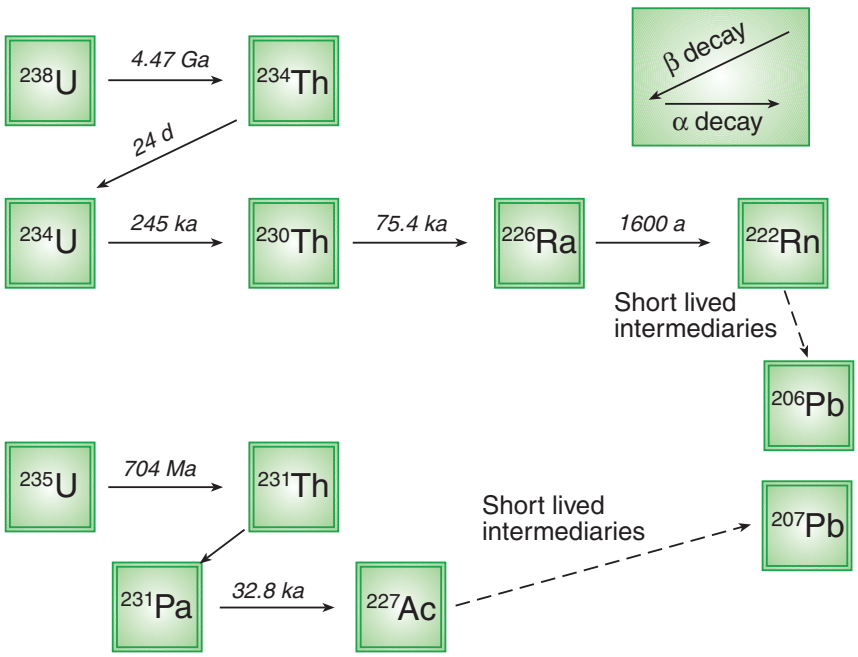

Figure 1. U-series isotopes. Of specific interest here are ^{234}U, ^{230}Th, and ^{226}Ra which have half-lives of 245 000, 75 000 and 1600 years respectively.

At GEMOC, one on-going project focuses on the Murray-Darling basin, which drains most of southeastern Australia. In a novel approach, we measured U-series isotopes in different-sized suspended particles in the river water, to understand what controls the distribution of these isotopes in river systems. This project is a collaboration with Dr Grant Douglas and CSIRO Land and Water, Perth (WA) who provided the samples.

We found that smaller suspended particles adsorb more organic matter, and that this controls the U-series isotopic composition of river colloids and suspended sediments. Using the U-series isotopic composition of these materials, we were able to correct for exchange between organic matter and silicate grains and determine the isotopic signature derived solely from weathering. Assuming that sediments are continuously weathered during their storage in the soil and transport in the river, we could infer that sediments take only ~ 10,000 years to pass through the Murray-Darling basin (Fig. 2). This age coincides with major changes in the conditions of erosion in the basin, and suggests that the U-series isotopic composition of river material records the last major change in erosion conditions, which shaped the current river system.

The U-series isotopic composition of colloids and sediments can also be used to infer long-term erosion rates (in this case, ~ 10,000 years). It turns out that long-term erosion rates are significantly lower than present-day rates measured by sediment gauging (Fig. 2). This implies a recent increase in erosion, which probably is related to the intensification of agriculture over the past 100 years.

This approach offers a novel method for quantifying the effect of European settlement on erosion rates and to identify the most stressed areas. For instance, the difference between long-term and present-day erosion rates is a factor ~ 2 in the Murray River basin, whereas present erosion rates are about ~ 100 times the long-term rate in the Darling basin. We can vary the spatial resolution of the method by simply sampling rivers that drain catchments of different size. A similar project is currently being conducted in small tropical watersheds of Puerto Rico, characterized by the largest known weathering rates. This project should allow us to understand the dependence of erosion on different climatic conditions (eg semi-arid for the Darling River, tropical for Puerto Rico) and catchment size (1,000,000 km^2 for the Murray-Darling basin, ~ 3 km^2 for Rio Icacos in Puerto Rico) (see GEMOC Publication #437).

Contacts: Anthony Dosseto and Simon Turner
Funded by: ARC Grant DP0451704

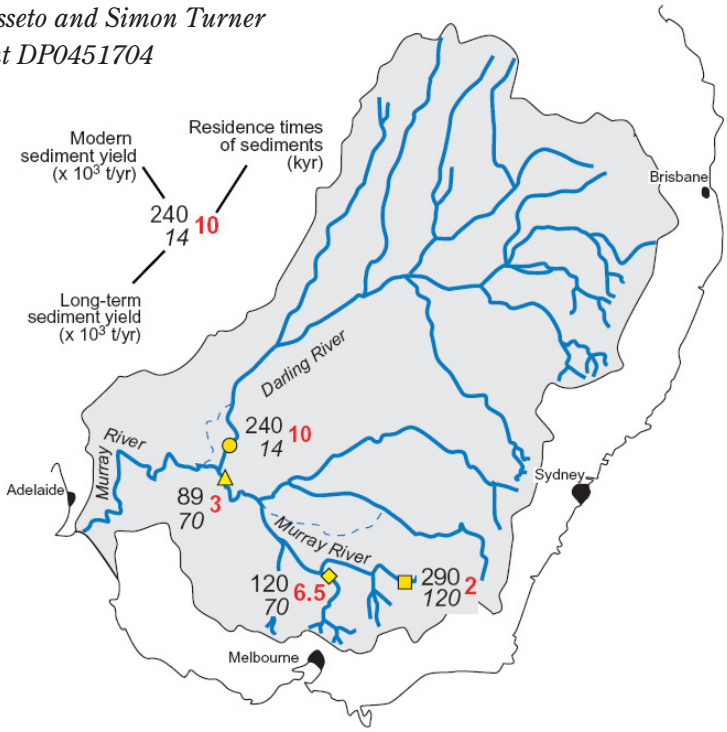

Figure 2. Modern (plain) and long-term sediment yield inferred from U-series (italics) in the Murray-Darling basin. It can be seen that the greatest increase in erosion rates occurs in the Darling River basin. Sediments have a relatively short residence time (bold) related to changes in erosion conditions at different stages of the basin history (11,000 years for the Darling basin; 3000 years for the Murray basin). The difference in residence time between the Murray River at Merbein (3000 years) and Rushy Billabong (2000 years) indicates that the average transport time of sediments between these two locations is 1000 years.

Are all mantle plumes equal in Nickel and PGE potential?

THE WORLD'S MAJOR ECONOMIC NICKEL (Ni) - platinum group element (PGE) ore deposits (eg Noril'sk, Siberia) are associated with continental flood basalts (CFBs) of large igneous provinces (LIPs). These LIPs were derived from mantle plumes (rising from the convecting mantle underneath the Earth's lithosphere and possibly as deep as the core-mantle boundary), but not all the CFBs host significant Ni-PGE deposits.

Conventional models for igneous Ni-Cu-PGE deposit propose that parental melts for Ni-PGE deposits are generated by large-degree melting of the mantle plume, with almost full dissolution of mantle sulfides, and that Ni-PGE enrichment and mineralisation reflect shallow processes. These models assume that the mantle plume is the ultimate source of Ni and PGE and focus upon processes that operated after the segregation of the magma from the mantle matrix. One implication of these models is that all mantle plumes are born equal in terms of their Ni-PGE-potential. However, detailed geochemical studies of LIPs have indicated that each plume may have a complex history and heterogeneous composition. Therefore, there may be "plumes and plumes", some being predisposed to be favourable for large-scale Ni-PGE mineralisation while others are not.

This project has taken an empirical approach, examining existing geochemical data to see whether there are fundamental geochemical differences between CFBs that are "fertile" and "barren" in terms of their Ni-PGE potential. If such differences exist, favourable geochemical signatures for the basalts with high mineralisation potential can be defined, and the mantle reservoirs and processes that produce magmas with high potential for forming Ni-Cu-PGE deposits can be explored. Geochemical data from 10 LIPs (Fig. 1) have been collected from the literature. The fertile LIPs (Bushveld, Siberia, Midcontinent, Emeishan and Karoo) host magmatic ore deposits of various type, size and grade. They commonly intruded through, or on the edges of, ancient cratonic terranes. In contrast, the "barren" LIPs erupted through both continental and oceanic settings of various ages.

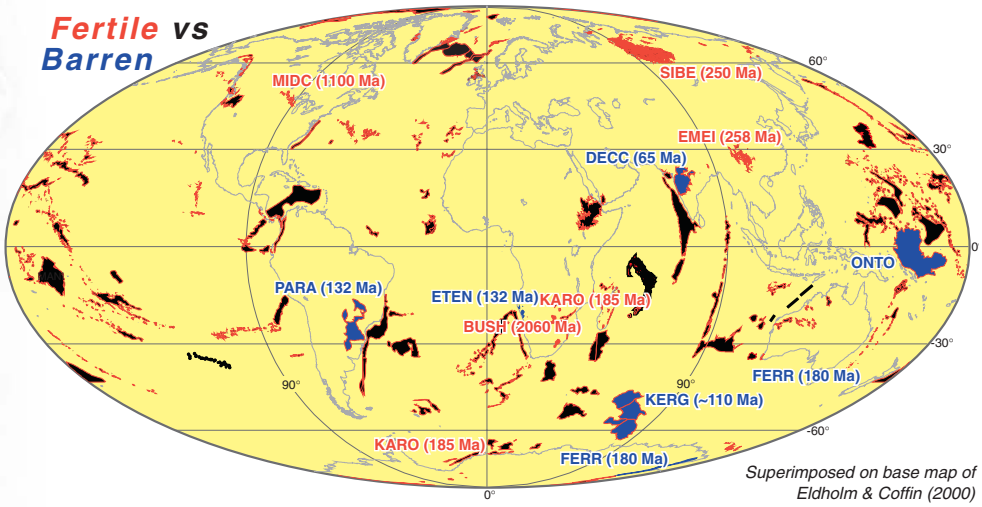

Figure 1. Distribution of fertile (red labels) and barren (blue labels) LIPs, with ages. DECC, Deccan Traps; ONTO, Ontong-Java; FERR, Ferrar; KERG, Kerguelen; ETEN, Etendeka; PARA, Parana; SIBE, Siberian Traps; MIDC, Mid-Continent; KARO, Karoo basalts; EMEI, Emeishan.

Radiogenic isotopic signatures indicate that the source for almost all LIP magmas is the deep-seated mantle plume source (FOZO), and not the more widespread depleted asthenospheric mantle (MORB) source; this confirms generally accepted models. However, several important chemical characteristics of, "fertile" and "barren" LIPs have been identified.

CFBs generated from fertile plumes generally include a relatively high proportion of primitive high-MgO melts that are low in Al_2O_3 and Na_2O, but are highly enriched in strongly incompatible elements (K, P, Ba, Sr, Pb, Th, Nb, LREE) and have elevated K/Ti, Ba/Th and Ba/Nb. They display trends of Sr-Nd-Pb isotopic variation between FOZO and an enriched mantle component (EM1; see Fig. 2). The fertile CFBs also have relatively high Os contents (≥ 0.03 to 5 ppb) and low Re/Os (< 10). In contrast, the barren LIPs contain fewer high-MgO lavas. They have high Rb/Ba ratios and show isotopic signatures of mixing between FOZO and upper continental crust (EM2). The barren LIP lavas in general have low Os contents (mostly ≤ 0.02 ppb) with high Re/Os (10 - ≥ 200).

These chemical signatures suggest that interaction between plume-related magmas and ancient subcontinental lithospheric mantle (SCLM) may play an important role in producing Ni-PGE fertility in LIP magmas, with significant contributions of Ni-PGE from pre-existing Ni- and PGE-rich sulfide phases in the cratonic SCLM. Deep recycled material may be involved in the source of barren LIPs, but they have had low degrees of interaction with old lithospheric roots. This study is continuing, with detailed examination of PGE and Os-isotope systematics.

Contacts: Ming Zhang, Sue O'Reilly, Kuo-Lung Wang
Funded by: Macquarie University, BHP-Billiton

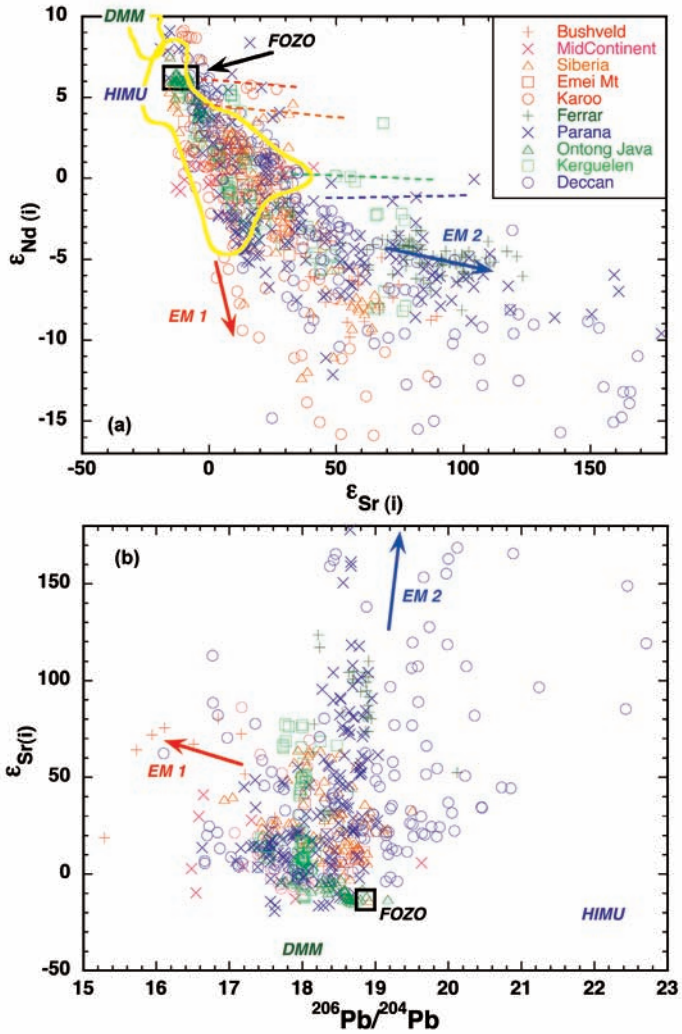

Figure 2. Isotopic data for fertile and barren LIPs, showing trends between the common mantle-plume source (FOZO) and the EM1 (fertile LIPs) and EM2 (barren LIPs) reservoirs.

Re-Os isotopes in mantle xenoliths from eastern China: Age and evolution of the lithospheric mantle

IN SITU Re-Os ISOTOPIC DATA for sulfide grains in mantle xenoliths from the Cathaysia and Sino-Korean blocks in eastern China (Fig. 2) have been used to constrain the age of the lithospheric mantle, and to investigate the linkage between crustal tectonism and fluid-migration events in the mantle. All of the xenoliths come from Mesozoic to Tertiary basalt localities. Polished sections of many xenoliths from each locality have been searched for sulfide grains; once these were analysed, the samples were polished down again, more grains were analysed, and the process was repeated.

Many xenoliths contain abundant sulfides of the "interstitial" type, (Fig. 1) which generally have Os contents too low, or Re/Os ratios too high, for reliable in-situ measurement. However, we also have found many grains, both interstitial and enclosed in the silicate phases, that have low Re/Os and enough Os to give results with acceptable precision.

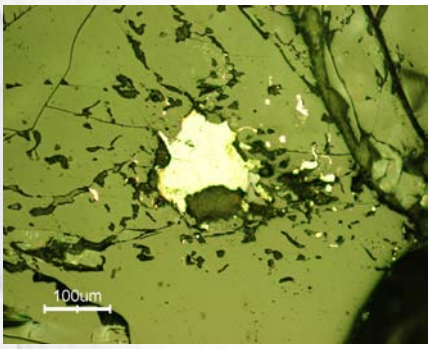

Figure 1. Interstitial sulfide in spinel peridotite xenolith from China.

The samples from the Cathaysia block, whether from the coastal region or inland, show a broad range of ages (Fig. 3) spanning from mid-Proterozoic to Paleozoic; the inland samples also show an age peak in Mesozoic time, corresponding roughly to the widespread Yanshanian magmatic event. The samples from the Sino-Korean Craton also show a wide range of ages from mid-Proterozoic onwards (Fig. 4).

The Re-Os data generally reflect the presence and modification of Proterozoic lithospheric mantle. These ages are consistent with the age of the overlying crustal basement in the Cathaysia block. However, the Sino-Korean block has generally younger lithospheric mantle underlying the Archean crustal basement. Archean Re-Os ages have been measured on mantle xenoliths from the Ordovician kimberlites at Mengyin and Fuxian (Gao et al., 2002), but none have been found in the spinel-peridotite xenoliths from Tertiary basalts. A major change in lithosphere thickness, thermal state and composition beneath the eastern half of the Sino-Korean Craton has been defined by comparison of the mantle sampled by the Ordovician kimberlites and the Tertiary basalts. Although most studies have concluded that this major modification of the lithospheric mantle occurred during Mesozoic to Tertiary time, the widespread occurrence of Proterozoic Os model ages may indicate that a major change occurred in

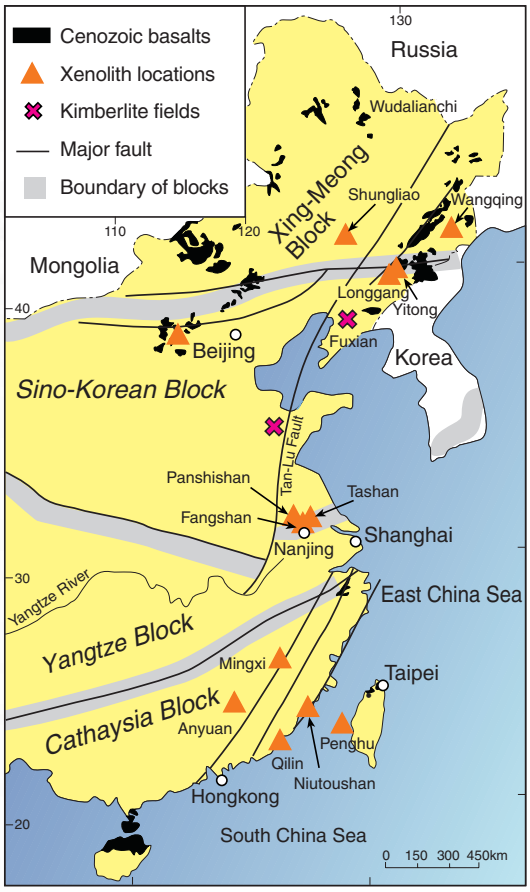

Figure 2. Sample localities.

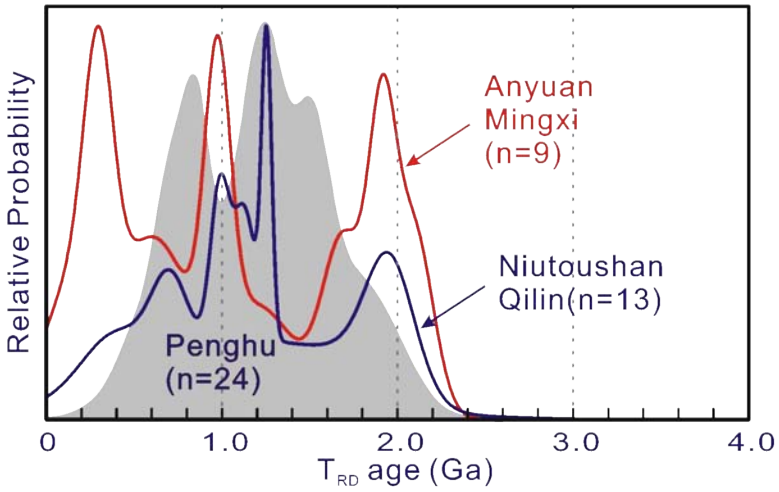

Figure 3. Distribution of model ages for low-Re/Os sulfides in xenoliths from the Cathaysia block. Penghu data are from Wang et al. (2004).

Proterozoic time. This may have affected much of the eastern half of the craton, and coincided with tectonic activity along the major suture (the Taihang Rift Zone) between the eastern and western halves of the craton. The original Archean root of the craton may have survived only in the easternmost part, where kimberlites later intruded. Much work remains to be done, but it already is clear that the lithospheric mantle beneath eastern China has had a very complex history, and is now a mixture of refractory and fertile mantle with different ages.

Contacts: Xisheng Xu, Sue O'Reilly
Funded by: ARC Discovery Project, Linkage International

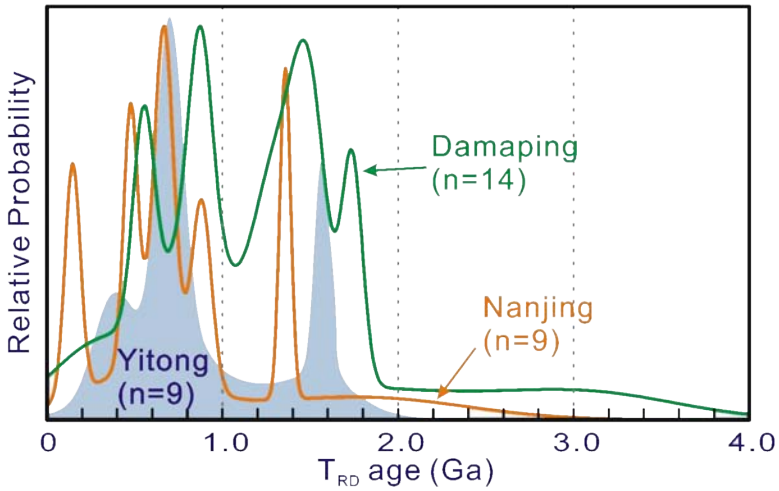

Figure 4. Distribution of model ages for low-Re/Os sulfides in xenoliths from the Cathaysia block.

2006 Contents

TerraneChron™	187
Reworking the Archean Gawler Craton, South Australia: U-Pb and Hf-isotopes in detrital zircon	188
Heavy Rock(s) in Tamworth	190
How did the Earth form?	192
Flushing the mantle: Harzburgite to lherzolite in the Lherz Massif (France)	194
Mantle "Botox" and the tale of the primitive upper mantle	196
Building an oceanic plateau: The Kerguelen Archipelago	198
Using kimberlites as drill holes: Crustal evolution beneath the Kundelungu Plateau (D.R. Congo)	200
The ghosts of lithospheres past: Imaging a changing mantle in Southern Africa	202
Eclogites in the SCLM: The subduction myth	204
Ancient mantle in modern plumes: B and Os in the Azores	206
The tenacity of cratons: a low stress home environment	208

Dynamic modelling of mantle plumes, subduction processes and the stability of continental lithosphere provides new insights into the internal workings of the Earth (see Research Highlights). At GEMOC, this type of modelling is being linked with the constraints provided by detailed studies of mantle samples. The inset shows a high-temperature clinopyroxenite exsolving lamellar garnet and orthopyroxene, and recrystallising to produce a websterite; such rocks define geotherms related to the upwelling of asthenosphere above subduction zones.

Research highlights 2006

TERRANECHRON® is GEMOC's unique methodology for terrane evaluation. During 2006 industry continued extensive use of *TerraneChron*® as a cost-effective tool for mapping crustal history on different scales.

Reworking the Archean Gawler Craton, South Australia: U-Pb and Hf-isotopes in detrital zircon

THE *TERRANECHRON*® METHODOLOGY (www.es.mq.edu.au/GEMOC/) was applied to zircons in drainage samples collected from 24 defined catchments across the Gawler Craton, South Australia. The results define the relative contribution of juvenile sources and recycled crust to the continental crust through time and constrain the role of the mantle during the Proterozoic rejuvenation of the Archean craton.

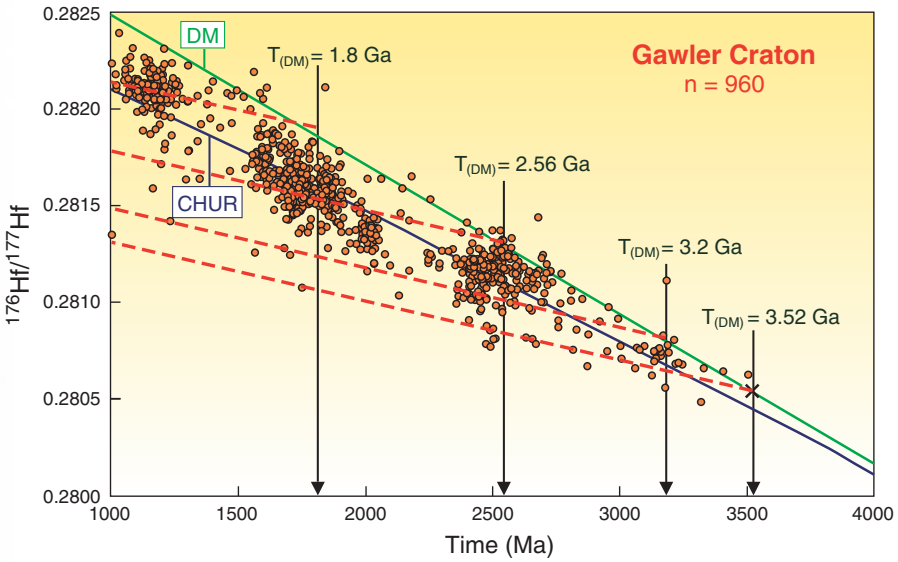

Figure 1. Hf-isotope composition vs age for detrital zircons from the Gawler Craton. Most grains in the 1500-2000 Ma range fall below the CHUR line, indicating derivation largely from older crust (2.5-3.2 Ga). Dashed lines show the evolution of average continental crust of different ages.

Widespread Hf model ages (measured by *in situ* LAM-MC-ICPMS) of about 3.5 Ga, and the presence of inherited zircon grains with comparable U-Pb ages (3.2 - 3.5 Ga), show that Archean crust as old as ca 3.5 Ga exists in the Gawler Craton. This component may now reside largely in the lower crust, where it has provided a source of crustal magmas throughout the Proterozoic rejuvenation of the craton (Fig. 1).

The Hf isotope data show that juvenile mantle-derived material represents a minor contribution to crustal generation relative to the reworking of older crust. Three periods of juvenile input can be recognised at ca 2540 Ma, 1850 Ma and 1595 Ma

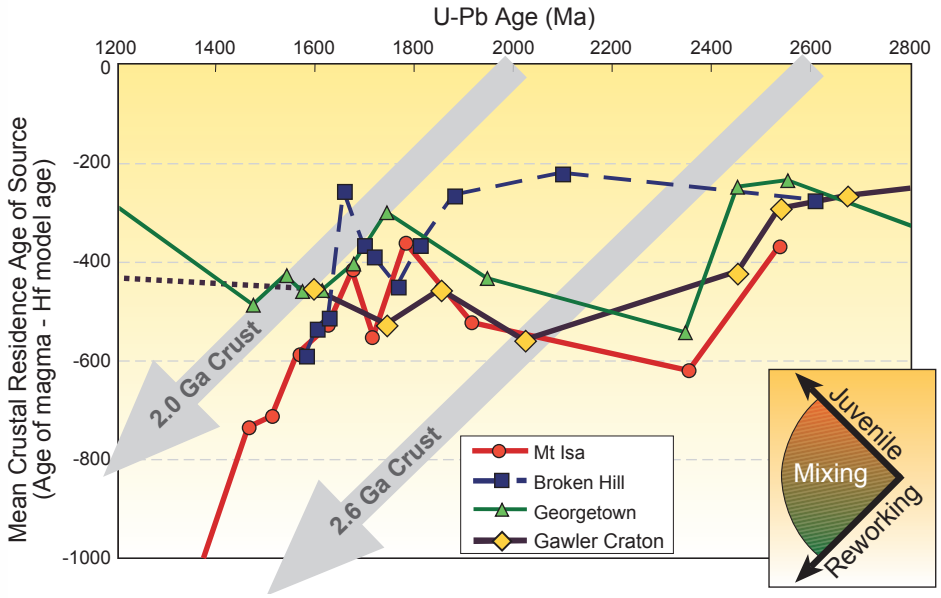

Figure 2. Event Signature curves for Australian tectonic blocks. The Gawler Craton evolved differently from the other three terrains after ca 1900 Ma; it lacks the large juvenile inputs associated with ca 1.7 Ga mineralisation events in the Broken Hill and Mt Isa blocks.

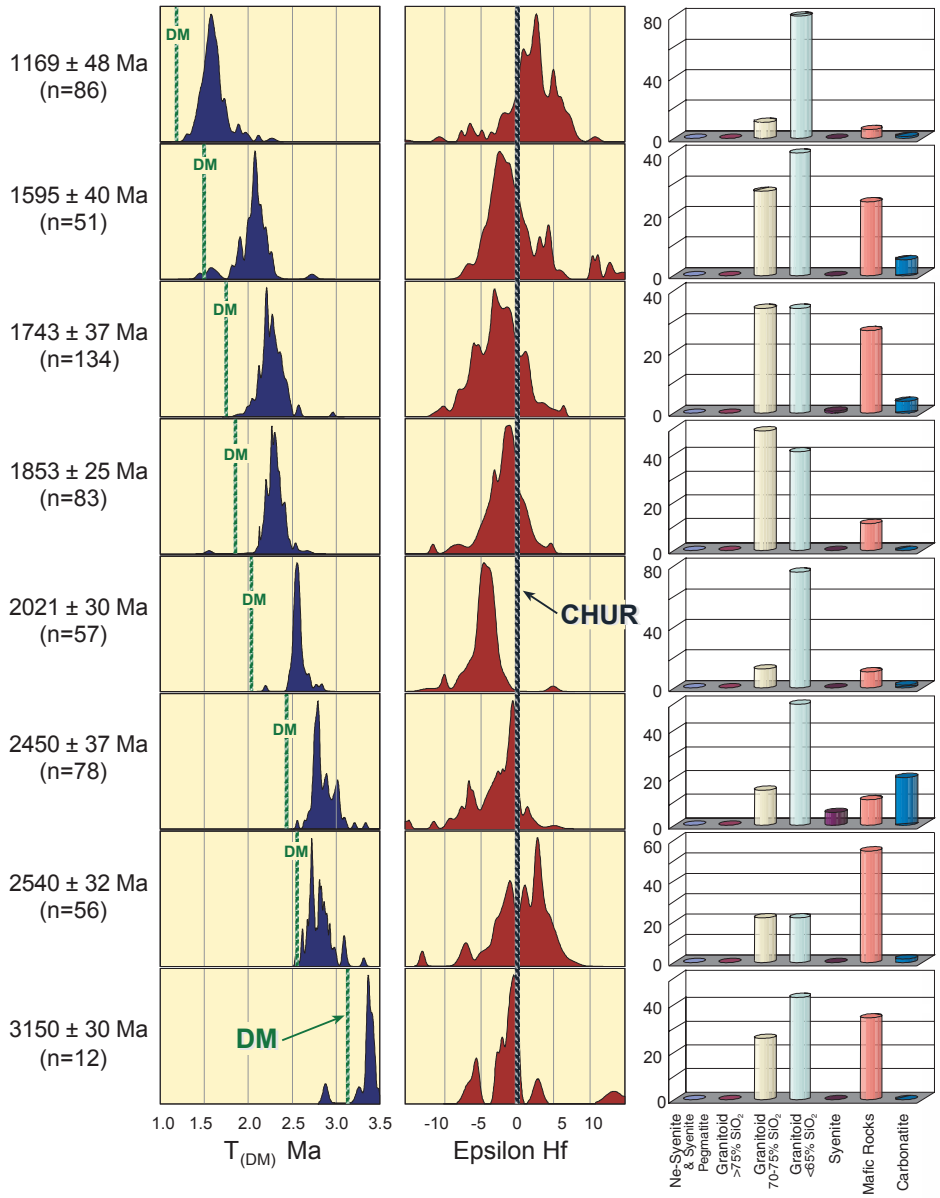

Figure 3. Model ages, epsilon Hf values and modelled rock types for the Gawler Craton in different time slices. Time slices with more mafic rocks show generally higher epsilon values, consistent with more mantle-derived magmatism.

(Fig. 2,3). However, only a minor proportion of the zircons formed during these time intervals have strongly juvenile signatures (εHf ≥ 4), and most magmatic rocks represent mixtures of remelted crustal material with mantle-derived material input.

"Event Signature" curves (Fig. 2) allow the visual synthesis of terrane evolution, and a useful way to compare the evolution of different crustal domains; they provide a new tool to advance existing plate tectonic models for the evolution of the Australian continent. Comparison of the Event Signature of the Gawler Craton with those from the Mount Isa Block and Georgetown Inlier shows some similarities in Late Archean-Early Proterozoic time, but makes it clear that the Gawler Craton evolved independently from these terrains, and from the Broken Hill Block, between ca 1800 and 1500 Ma.

Contacts: Elena Belousova, Bill Griffin
Funded by: ARC, PIRSA, Macquarie University

Heavy Rock(s) in Tamworth

MODELLING OF DETAILED GRAVITY DATA can reveal the subsurface structure of fold belts and their associated faults. For much of the period 400 – 200 Ma, the southern New England Fold Belt (SNEFB) was a convergent plate margin at the eastern edge of the Gondwana continent with a west-dipping subduction zone. The SNEFB (Fig. 1) consists of the Tamworth Belt in the west and the Tablelands Complex in the east. The SNEFB has been thrust westward over the Permian-Triassic Sydney-Gunnedah Basin, along the Mooki Fault. The Peel Fault, which trends north-northwest, separates the less deformed rocks of the Tamworth Belt from the more deformed rocks of the Tablelands Complex.

The Bouguer anomaly map of the SNEFB (Fig. 2) has two meridional linear gravity highs: the Namoi Gravity High (NGH) on the east, and the Meandarra Gravity Ridge (MGR) on the west. The NGH lies over the Tamworth Belt along its entire length and lies east of the Mooki Fault in the south and the Kelvin Fault in the north. The eastern edge of the NGH coincides roughly with the Peel Fault. To the west, the MGR lies within the Gunnedah Basin, which otherwise generally shows a relative gravity low. These gravity highs are distinct features and understanding what is causing them should help us to understand the upper crustal structure of the SNEFB.

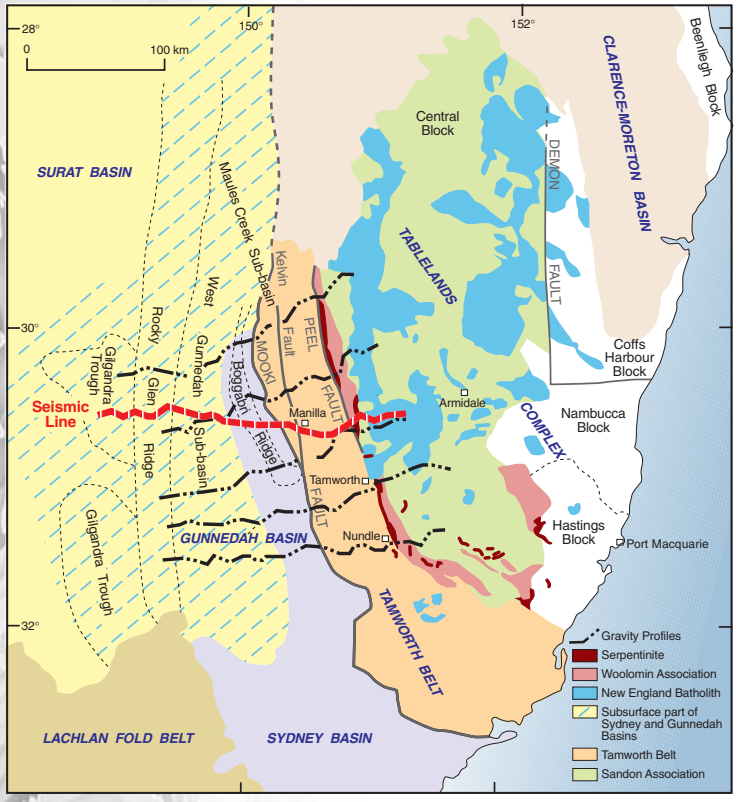

Figure 1. Generalised structural units of the southern New England Fold Belt and the Gunnedah Basin. Also shown are locations of the five gravity profiles acquired for this study and the GA seismic line BMR91-G01.

Five ENE-trending high-resolution gravity traverses (450 readings) were conducted across the belt, adjacent parts of the Gunnedah Basin and the Tablelands complex. These data were modelled together with density determinations of surface and drillcore samples. The data were first modeled using the geometry derived from the interpretation of GA's BMR91-G01 seismic line.

This modelling (Fig. 3) indicated that the gravity anomalies correlate with the densities of the exposed rock units. The Namoi Gravity High over the Tamworth Belt is produced by the high density of the rocks in this belt. These high densities reflect the mafic volcanic source of the older sedimentary rocks in the Tamworth Belt, the burial metamorphism of the pre-Permian units and the presence of some mafic volcanic units. Modelling shows that the Woolomin Association, present immediately east of the Peel Fault and constituting the most western part of the Tablelands Complex, also has a relatively high density, which also contributes to the NGH. The Tamworth Belt can be best modelled with a configuration in which the Tablelands Complex has been thrust over the Tamworth Belt along the Peel Fault, which dips steeply to the east to a depth of more than 10 km. Plutons near the Peel Fault (eg Moonbi) are also clearly delineated by the data. The Tamworth Belt is thrust westward over the Sydney-Gunnedah Basin for 15-30 km on the Mooki Fault that has a shallow dip (~25°) to the east and is consistent with the new gravity data.

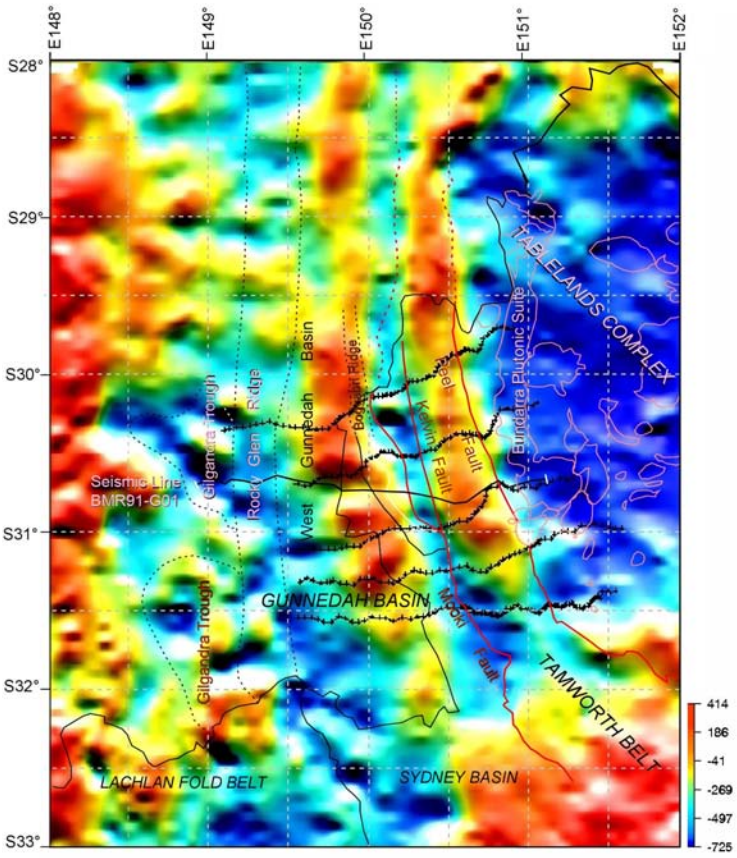

Figure 2. Bouguer gravity anomaly image covering the southern New England Fold Belt and the Gunnedah Basin, with location of the gravity profiles surveyed in this study. Unit: μm/s². Red lines indicate the Peel and Mooki Faults. Also shown is the seismic line BMR91-G01.

The Meandarra Gravity Ridge within the Gunnedah Basin was modelled as a high-density volcanic rock unit with a density contrast of 0.25 tm^{-3} relative to the underlying rocks of the Lachlan Fold Belt. The modelled unit has a steep western margin, a gently tapering eastern margin and a thickness ranging from 4.5 - 6 km. These volcanic rocks are assumed to be Early Permian in age; they may be the western extension of the Permian Werrie Basalts that outcrop on the western edge of the Tamworth Belt, and that may have formed within an extensional basin.

Contacts: Mark Lackie, Dick Flood, Bin Guo
Funded by: Macquarie University Postgraduate Research Fund

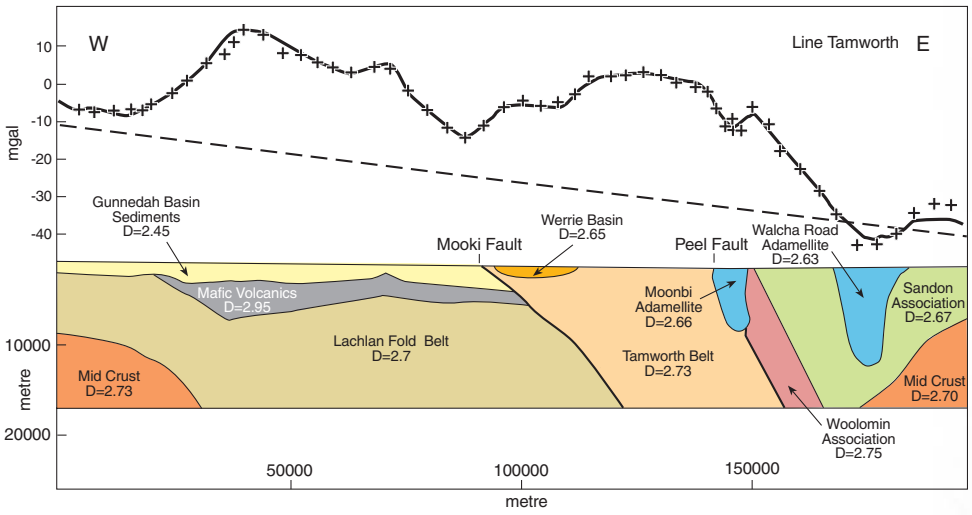

Figure 3. 2.5D gravity model along the Tamworth Profile (cross-section view) shows a good fit between the observed data and calculated profile. The Peel Fault was modelled as a steep east-dipping fault extending to mid crustal levels. Crosses represent observed data and solid line is the calculated anomaly, V/H=1.9. Density in tm^{-3}. Dashed straight line is the regional gradient.

How did the Earth form?

FROM OBSERVATIONS OF NEWLY-FORMING STARS it seems that our solar system developed from a flattened disk of dust and gas around the young sun 4567 million years ago. The mechanisms of growth of particles of dust into asteroidal (20 km diameter) bodies are not well understood, but once this size had been reached, gravitational attraction would have ensured growth to planetary-size bodies. Understanding of these processes of planetary growth and their timing can be obtained by studying the chemical compositions of the planets and asteroids and the characteristic isotopic signatures for some key elements.

Amongst the thousands of meteorites in museum collections there are about a dozen that appear to represent primitive protoplanetary material. These "carbonaceous chondrites" come from the asteroid belt between Mars and Jupiter and have compositions which closely mimic that of the Sun. They also have, for elements that condense at high temperatures from a gas of solar composition, striking affinities with the Earth, Mars and the Moon. Figure 1 shows ratios of element abundances in the silicate part of the Earth (mantle+crust) to those in carbonaceous chondrites, plotted against the temperature at which 50% of the element of interest would condense from a solar gas. Refractory elements, which condense at high temperatures, are divided into 3 groups, "lithophile", "siderophile" and "highly siderophile". Lithophile elements such as Ca, Ti, Hf, Al and the Rare Earths are those elements which did not enter the Earth's iron-rich metallic core. They are present in the same relative abundances in the silicate Earth as in the meteorites, Mars and the Moon. The siderophile elements (Fe, Ni, Mo, W etc) are all depleted in the silicate part of the Earth because they have partitioned into the core, while the highly siderophile elements (Au, Pt etc) are >99% partitioned into the core. The Earth is also depleted in volatile elements (those with low condensation temperatures) because of late volatile loss.

Figure 1. Abundance in silicate Earth versus temperature of 50% condensation.

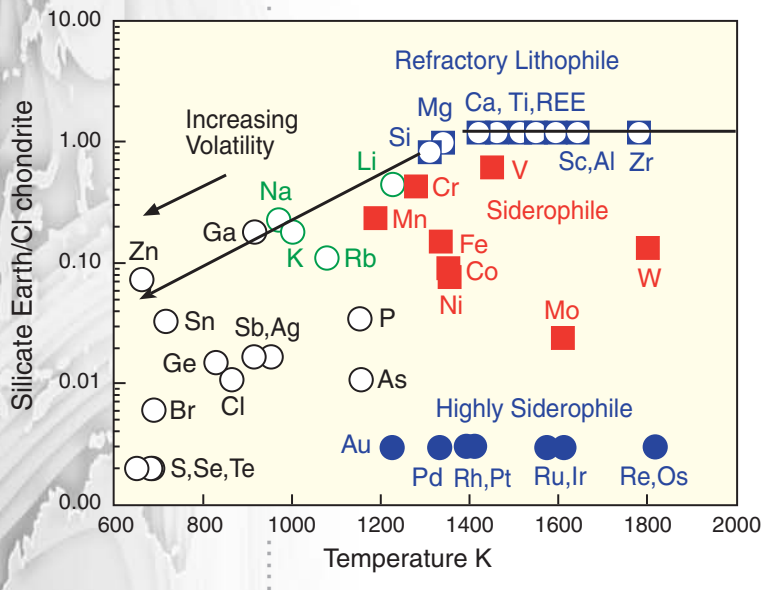

Asteroids, many of which have metallic cores like the Earth, are known to have formed within a few million years (some as soon as 1 Ma) after the beginning of the solar system. This result was obtained using the radioactive decay of ^{182}Hf (a short-lived isotope present when the solar system formed) to ^{182}W. Hafnium is lithophile while tungsten (W) is siderophile (Fig. 1). Therefore as core formed on any body, most of the tungsten was extracted to the core, leaving the silicate part with a very high Hf/W ratio. The build-up of ^{182}W during the first 50 Ma of solar system history (by which time all ^{182}Hf had decayed) then dates the time at which Hf and W were separated by core formation. Application of this method to Mars gives a time about 10 Ma after the beginning of the solar system and the Earth about 30 Ma. This then enables us to estimate the timescales of formation of asteroids (1-4 Ma), a planet 10% of Earth-size (Mars) and Earth itself.

Research at Macquarie is concentrating on studying the conditions on Earth as the metal core formed. Earth grew by initially sweeping up lots of smaller bodies,

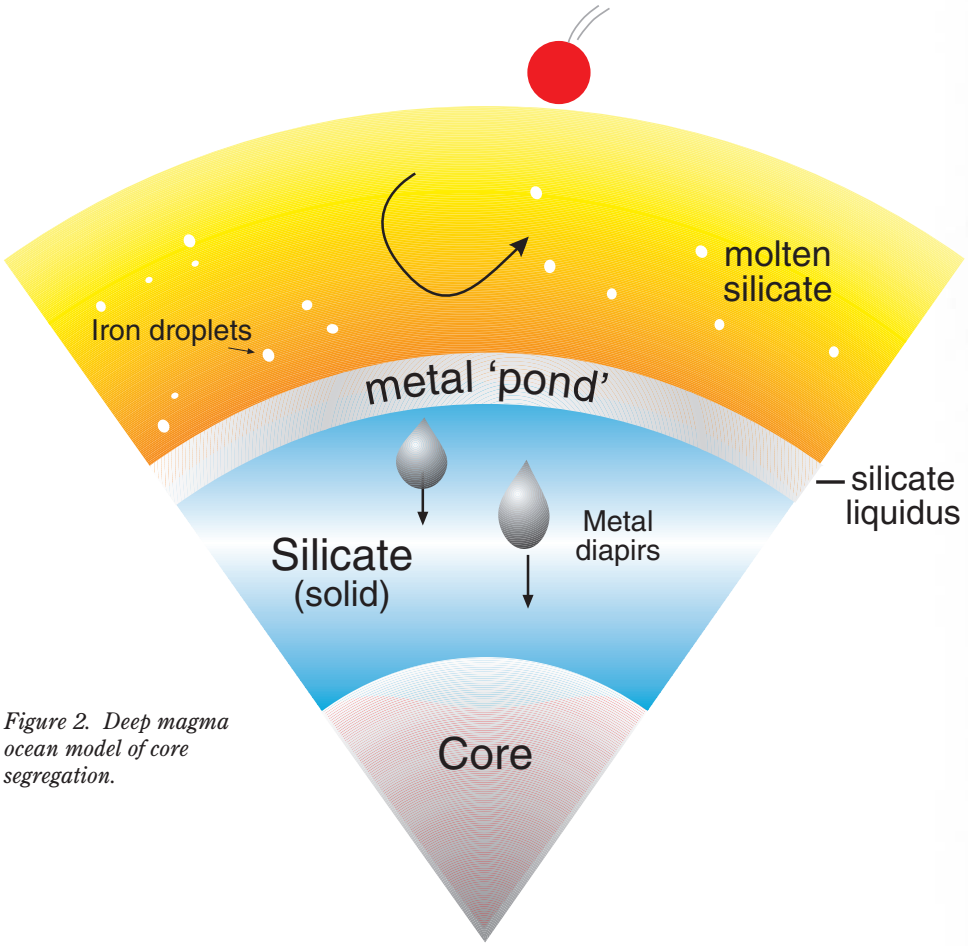

Figure 2. Deep magma ocean model of core segregation.

then progressively fewer larger and larger bodies, culminating in the impact of a Mars-sized body which generated the moon about 40 Ma after the beginning of the solar system. Our experimental work is aimed at finding the pressures and temperatures under which the siderophile element contents of the silicate Earth (Fig. 1) match those observed. We find that the metal was extracted at high pressures, probably at the base of a deep (>400 km) ocean of molten silicate (Fig. 2). This magma ocean was kept molten by the high energies of impacting bodies. We also find that the Earth appears to have become more oxidised as it grew. It is likely that the earliest atmosphere (during early growth of the Earth) was hydrogen-rich, solar-like in composition, and strongly reducing. However, this was blown away (together with many volatile elements; Fig. 1) by large impacts later in accretion, leaving the Earth to oxidise by a combination of internal and external processes.

Contact: Bernie Wood
Funded by: ARC (Federation Fellowship, Discovery Project)

Flushing the mantle: Harzburgite to lherzolite in the Lherz Massif (France)

DIFFERENTIATION OF THE EARTH'S MANTLE occurs mainly through partial melting and extraction of basaltic melts. Among the mantle rocks occurring at the Earth's surface, lherzolites are widely regarded as samples of the pristine mantle, from which no (or only small amounts of) melts have been extracted. In contrast, harzburgites are seen as refractory mantle residues left after extensive partial melting.

The Lherz Massif (Pyrenees, France; picture above) is the type locality of lherzolite. The massif is predominantly composed of layered spinel lherzolites; in the upper part of the massif the lherzolites enclose bodies of highly refractory spinel harzburgite metres to tens of metres in size (Fig. 1).

Detailed structural mapping shows that all harzburgites, even small bodies, have a constant foliation throughout the massif. In contrast, the foliation in the lherzolites is variable and generally oblique to the harzburgite foliation. This suggests that the lherzolites are secondary rocks, and that the harzburgites are remnants of a highly refractory mantle protolith, largely replaced by the lherzolites through a process of melt percolation.

Crystallographic orientations were measured by indexation of electron back scattered diffraction (EBSD) patterns at the Géosciences Montpellier laboratory. Analysis of microstructures and crystal-preferred orientations suggests that the harzburgites deformed by dislocation creep with activation of the high temperature, low stress (010) [100] slip system. Refertilised lherzolites display a much weaker alignment of the *a* axis of olivine (Fig. 2).

Figure 1. Harzburgite-lherzolite contacts are sharp and steep, and emphasised by a cm-scale websteritic layering.

These features suggest that melt percolation and melt-rock reaction started at static conditions, and produced changes in modal composition, grain growth and a weakening of the olivine fabric.

Variations of major, minor and trace elements across the harzburgite-lherzolite contacts indicate that the lherzolites were formed by a near-solidus refertilisation reaction involving crystallisation of pyroxene and spinel, and dissolution of olivine. These processes produce chemical trends in the relationships between mineral and whole-rock chemistry that are different in detail from partial-melting trends (Fig. 3).

The combination of detailed fieldwork, petrophysical analysis and geochemical

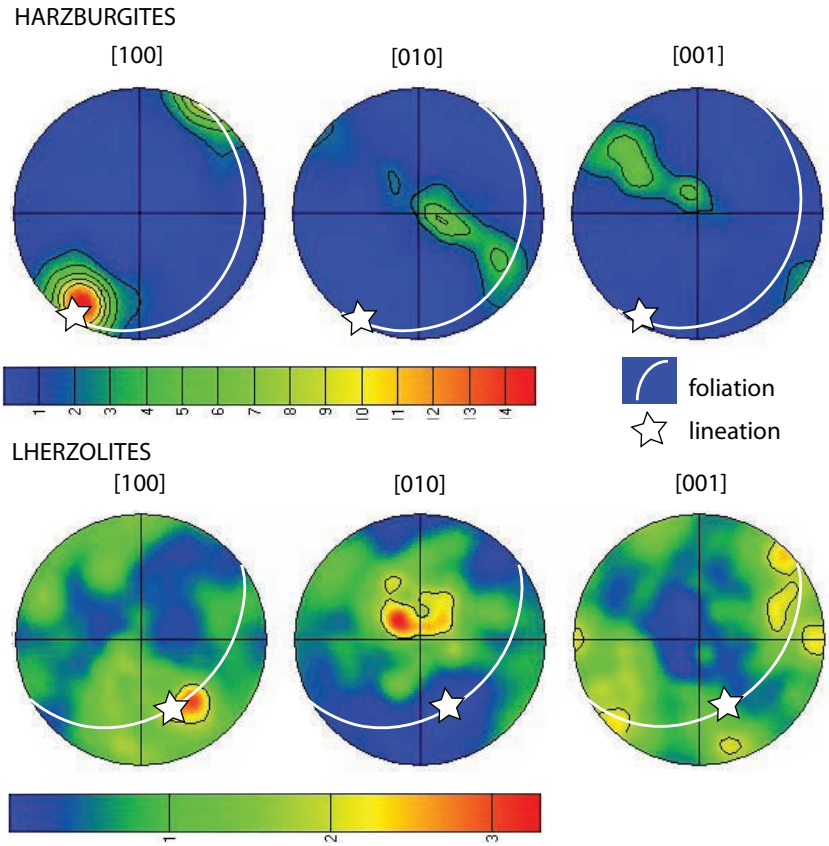

Figure 2. Illustration of the high temperature deformation in Lherz harzburgites and the weakening of crystallographic fabrics in refertilised lherzolites.

modelling reveals that the type lherzolites of the Lherz massif represent refertilised, rather than pristine, mantle. The refertilisation process has involved the interaction of refractory lithospheric mantle with upwelling asthenospheric partial melts. This study highlights the fact that melt transport and melt-rock reaction play a key role in modifying the composition of the lithospheric mantle, and that models of lithospheric mantle composition based on such lherzolites must be reconsidered.

Contacts: V. Le Roux, J.-L. Bodinier, S.Y. O'Reilly
Funded by: Bourse MENRT, INSU

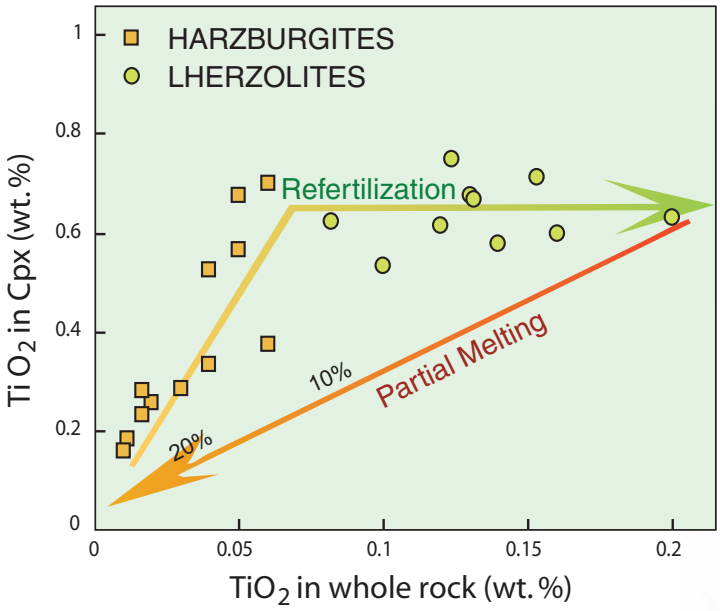

Figure 3. Modelling of partial melting versus refertilisation reaction. Orange squares, harzburgites; green circles, lherzolites.

Mantle "Botox" and the tale of the primitive upper mantle

ONE OF THE RECURRENT QUESTIONS IN PLANETARY SCIENCE is what the Earth is made of; what were the "building blocks" of our planet? Of special interest is the nature of the 'late veneer', a final meteoritic bombardment that may have been the main carrier of water and possibly life-seeds to Earth. However, the nature of this late component remains elusive, and constraints from various geochemical systems seem at first glance to be contradictory. In that respect, the siderophile elements may be one of the most promising sources of first-hand constraints on the nature of the late accreting material. The broadly chondritic relative abundances of highly siderophile elements (HSE) in the Earth's mantle are assumed to reflect the addition of chondritic material to the mantle after core formation. The HSE composition of the Primitive Upper Mantle (PUM) is thus an important goal of modern geochemistry. Current estimates of PUM for siderophile elements (PGE and Os isotopes) are based largely on two suites of mantle samples: peridotite xenoliths from Kilbourne Hole maar in Texas, and the Lherz orogenic peridotite massif in the Pyrenees (*Le Roux et al., Earth and Planetary Science Letters*, in press; see *pp. 194-195*). The Os isotopic composition of the Earth's Primitive Upper Mantle ($^{187}Os/^{188}Os$ =0.1296 ± 0.0008) is significantly higher than the ratio measured in carbonaceous chondrites (CC; $^{187}Os/^{188}Os$ = 0.1262 ± 0.0006). Taken at face value, this estimate thus rules out CC as the source of the 'late veneer' and suggests that ordinary chondrites (OC) formed the bulk of the 'late veneer'. However, carbonaceous chondrites are the only water-bearing chondrites and have a Deuterium to Hydrogen ratio (D/H) similar to the Earth's ocean (≈ 150 x10^{-6}).

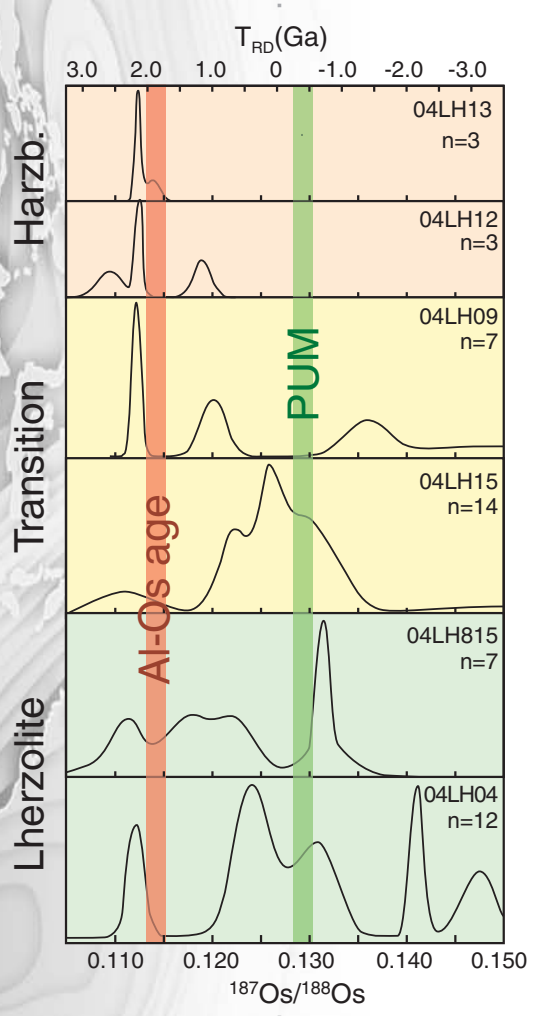

Figure 1. Os-isotope compositions of sulfide grains in samples of the primary harzburgite, the refertilised lherzolite and transitional rocks in the Lherz massif. Bars show the $^{187}Os/^{188}Os$ corresponding to the "aluminochron age" and the "PUM" estimate derived from these rocks; both are spurious.

These sorts of inconsistencies have led to proposals that the Earth was made of an unsampled type of material dubbed "Earth-chondrite" or "Earth achondrite". However, before calling upon the existence of a never-sampled material, we need to examine the robustness and significance of the PUM estimate. Indeed, the same mantle-sample suites also yield a Pd/Ir (≈ 2) much higher than any type of chondrite. Since Os, Ir, Pd and Re are all HSE and thus should behave similarly, this inconsistency raises suspicion about the nature of the data.

The Lherz Orogenic massif is the type area of lherzolite (usually assumed to represent the dominant rock type of the upper mantle) and has always been a key area for studying mantle composition and processes. However as demonstrated in the previous highlight (see *pp. 194-195*) structural, petrographic and geochemical features clearly indicate that the lherzolite suite was developed at the expense of the more refractory harzburgite via a refertilisation reaction involving precipitation of pyroxene (±spinel) and sulfide at the expense of olivine and infiltrated melt.

In situ measurement of the Os composition of rare sulfides in the harzburgites yields a constant unradiogenic Os composition indicating a T_{RD} age ≈ 2.4 Ga (Fig. 1). In contrast, the numerous sulfides in the lherzolite show a large spread of Os composition ($0.11 \leq ^{187}Os/^{188}Os \leq 0.18$). However, the unradiogenic sulfides characteristic of the harzburgite are common in the lherzolite, while extremely radiogenic Os is characteristic of Lherz's pyroxenite suite. The whole-rock composition of individual

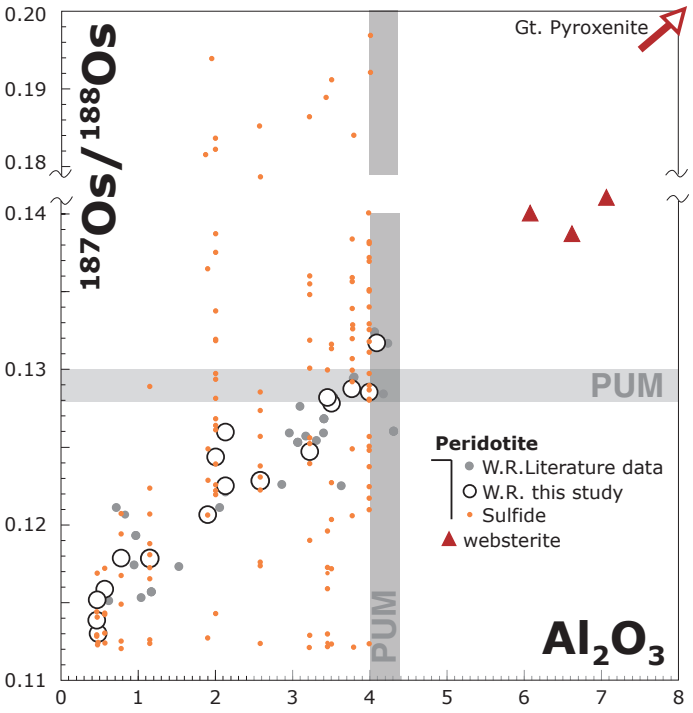

Figure 2. Al_2O_3 vs. $^{187}Os/^{188}Os$ for whole-rock samples as used to define the PUM Os composition and the Os isotopic variability of the sulfides in each sample, Red triangles are the websterite and other pyroxenites in Lherz.

lherzolite samples are intermediate between these two end members, depending on the proportion of each sulfide population (Fig. 2). This indicates that the lherzolites are in fact old, refractory harzburgites which were re-fertilised by fluids that carried radiogenic Os. This conclusion is consistent with the structural, petrographic, petrophysical and geochemical evidence presented by Le Roux et al. (in press).

Our previous work has demonstrated that the abundances of sulfides and HSE in several of the xenolith suites used to derive the Os-isotope composition of PUM have been heavily altered by metasomatic events. Together with the Lherz study, the results cast strong doubt on the robustness and significance of the currently accepted Os-isotope composition of the PUM, its bulk composition and the long-term evolution of the mantle. It appears that the "PUM" in fact represents refertilised/metasomatised, old, depleted upper mantle; it lost its "primitive" character a long time ago.

Recognition that the currently accepted model composition for the PUM is not meaningful can help to resolve some of the contradictions noted above. A better estimate of the PUM and the original bulk composition of the Earth will come through detailed studies of the budgets of siderophile and chalcophile elements in a dynamic Earth. This will need a better understanding of metasomatic processes, detailed studies of key terrestrial and meteoritic sample suites and integration with experimental studies (see *pp. 192-193*).

Contacts: Olivier Alard, Sue O'Reilly, Bill Griffin
Funded by: ARC-DP/APD

Building an oceanic plateau: The Kerguelen Archipelago

THE KERGUELEN ARCHIPELAGO, located in the southern Indian Ocean (49°S and 69°E), is the emergent part of the northern Kerguelen oceanic plateau (Fig. 1). The magmatic edifice of the Kerguelen Islands was produced over about the last 40 Ma. When the volcanic activity associated with the Kerguelen Plume started, the Kerguelen area was situated near or on the South East Indian Ridge (SEIR). The SEIR then moved away to the NE, leaving the Kerguelen Plateau in its present intraplate setting. The early magmatism was dominantly of tholeiitic-transitional affinity and became progressively alkaline to highly alkaline over time. Therefore the Kerguelen Archipelago has a complex history, superposing in time and space two types of hotspot activity. Between ~40 and ~26 Ma, the volcanism was similar to Iceland (interaction between a hotspot and a ridge); since 26 Ma, it was more similar to the Hawaiian (intraplate) hotspot type.

The Kerguelen Archipelago is made up mainly of flood basalt (80%), plutonic rocks (5%), and dykes with ultramafic and mafic xenoliths.

Over the last fifteen years, petrologic, geochemical and isotopic studies have mainly focused on the flood basalts and ultramafic xenoliths brought up from the upper mantle by alkaline basalts. These studies have characterised (i) the petrologic and geochemical heterogeneity of the mantle, (ii) the nature of the magmas and fluids circulating through the lithosphere, (iii) the different mantle sources. Geochemical studies coupled with geophysical studies have shown that the oceanic lithosphere was thickened by underplating of mafic magmas under the Kerguelen archipelago.

Gabbroic rocks (gabbros and meta-gabbro) are found at different structural levels in the oceanic lithosphere (crust, mantle/crust boundary and upper mantle), but they have been studied very little. The characterisation of these intrusive rocks (gabbroic and hypovolcanic) and related cumulate ultramafic-mafic xenoliths will help to understand the different stages of lithospheric differentiation in the context of a thickened oceanic crust. These rocks are the key to understanding how magmas evolved from their source to the surface. In a more general context, this work will also help to better constrain the formation of Large Igneous Provinces (LIP).

The gabbros and xenoliths for the initial work came from the St-Etienne

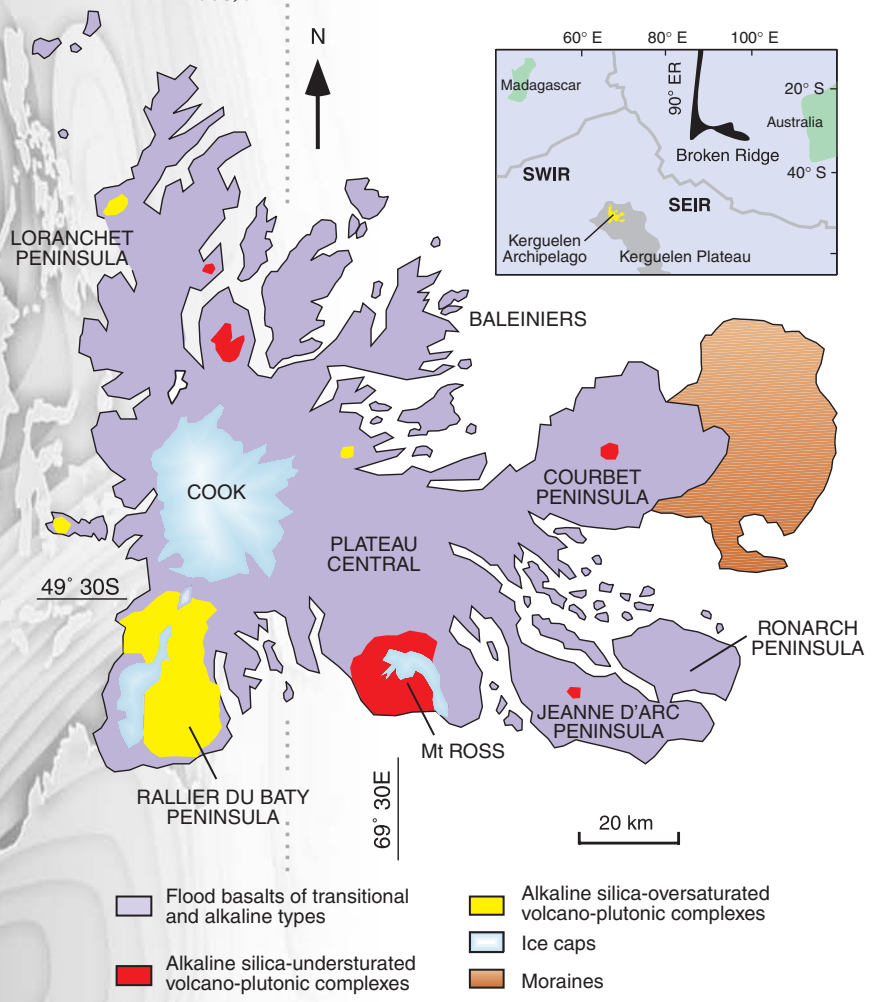

Figure 1. Simplified geological map of the Kerguelen Archipelago, after Delpech (GEMOC Research Highlights 2003).

University collection (France). Further sampling was done in December 2006 during the DyLioKer campaign supported by IPEV (Institut Paul Emile Victor). The gabbros and other plutonic rocks are exposed in massifs, sills (Fig. 2) and stratified or ring complexes. Some have also been found as xenoliths in alkali basalts.

Both *in situ* and whole-rock techniques have been used to characterise the gabbros in terms of major and trace elements (microprobe, XRF, LA-MC-ICPMS). The preliminary studies show that several types of gabbroic and intrusive rocks can be distinguished on the basis of their rare earth element (REE) composition. The REE patterns of the clinopyroxenes from different localities (Fig. 2) vary between two end-members. A tholeiitic-transitional pattern is characterised by low light REE contents (LREE, La to Sm) compared with the heavy REE contents (HREE, from Tb to Lu). A second highly alkaline pattern is characterised by high LREE/HREE. Compositions intermediate between these end-members are also observed.

Figure 2. Gabbroic sill, Val Travers, Kerguelen Island (DyLioKer campaign 2006). Photo: Damien Guillaume.

The preliminary results on the gabbroic rocks are consistent with previous studies that indicate two types of magmatic trends, from tholeiitic-transitional to alkaline, and interaction between them. Isotopic studies of the samples will help to better constrain the sources of the different gabbroic rocks, and U-Pb dating of zircon will also put better constraints on the evolution of the different sources with time.

Contacts: June Chevet, Sue O'Reilly
Funded by: iMURS, ARC-DP

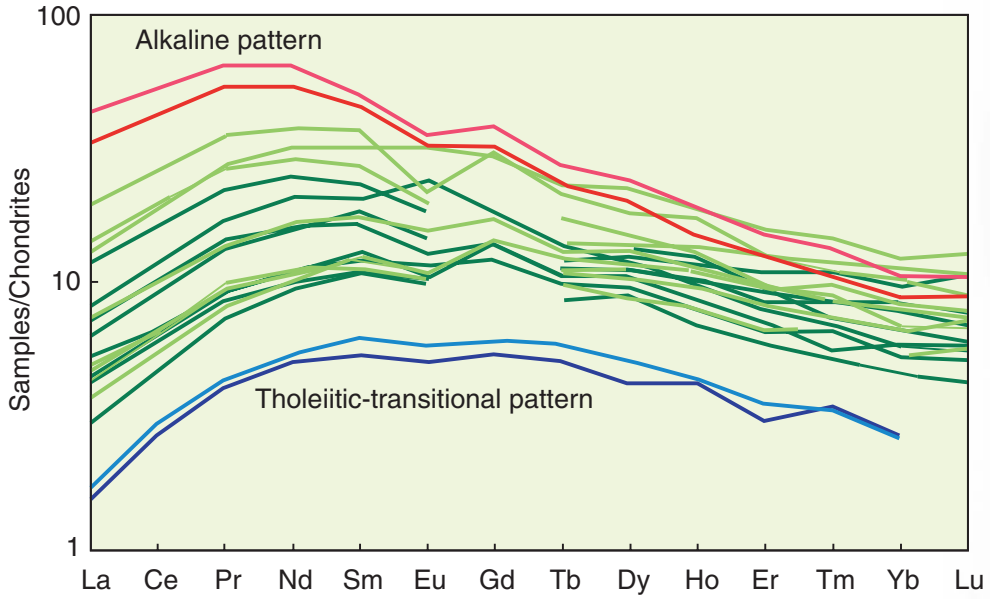

Figure 3. REE patterns measured in the cores and rims of clinopyroxenes in gabbro sampled in different localities on the Kerguelen Archipelago (red lines = alkaline composition, blue lines = tholeiitic-transitional composition, green lines = intermediate compositions).

Using kimberlites as drill holes: Crustal evolution beneath the Kundelungu Plateau (D.R. Congo)

THE KUNDELUNGU PLATEAU is located in the SE corner of the Democratic Republic of the Congo. Twenty-four kimberlitic pipes are known in the area; recent dating of perovskites at GEMOC shows that they intruded 33±3 Ma ago. The Plateau is formed of rocks belonging to the Neoproterozoic Katangan belt, which is surrounded by the Archean Congo Craton, the Paleoproterozoic Bangweulu Block, the Paleo- to Mesoproterozoic Irumide Belt, the Mesoproterozoic Kibaran Belt and Choma Kalomo Block. The Archean Zimbabwe Craton lies to the south (Fig. 1). The Gungwania and Talala kimberlitic pipes on this plateau have been used as drillholes, to obtain crustal zircons for a study of crustal evolution in the region and to constrain the age of the basement and the sedimentary provenance of the Katangan Supergroup. Zircons were separated from heavy mineral concentrates collected in streams that crosscut these pipes (Fig. 2).

229 zircons were analysed for U-Pb ages (LAM-ICPMS) and Hf isotope (LAM-MC-ICPMS) compositions. The analyses show that the oldest juvenile crust in the region is approximately 3.4 Ga old, and underwent varying degrees of recycling during Neoarchean and Paleoproterozoic times. The major Paleoproterozoic event is characterised by little production of juvenile crust; any juvenile input was essentially mafic in composition (Fig. 3). Important bimodal magmatism affected the region in the Mesoproterozoic (1 Ga) and Neoproterozoic (700-568 Ma). These events correspond to the continental extension and rifting related to the break-up of the Rodinia supercontinent (~1 Ga), the opening of the Mwashia basin (~700 Ma) and the Lufilian orogeny. The generation of Mesoproterozoic and Neoproterozoic crust involved recycling of Paleoproterozoic crust but these periods are also characterised by an important input of juvenile material (Fig. 3). The existence of a high-$^{176}Lu/^{177}Hf$ (0.059) Archean crust (eg garnet-rich rocks) in the region is suggested by the presence of zircons that lie above the Depleted Mantle line, on a line that projects back to 3.4 Ga (Fig. 3).

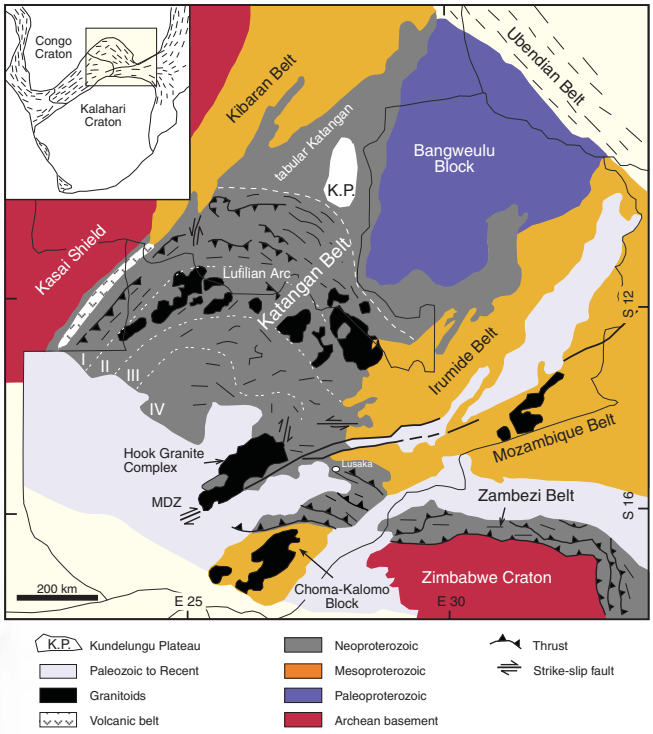

Figure 1. Simplified geological map of the Katangan belt and surrounding basements (modified after Binda and Porada, 1995), showing the location of the Kundelungu Plateau (K.P.).

The zircons in these samples may come both from the basement and from the Katangan Supergroup sediments. Morphological examination of the zircon grains in different age groups shows that the Paleoproterozoic population has the highest proportion of euhedral zircons, which implies that the basement rocks may be of this age. Most Archean zircons are rounded, indicating long transport. This does not support the presence of an Archean crust beneath the region. However, the Hf-

isotope data may indicate that an Archean crust existed at depth at least during Paleoproterozoic time (Fig. 3).

The sediments constituting the Katangan Supergroup were derived from most of the older rocks in the region including the Archean Congo Craton, the Paleoproterozoic Ubendian Belt (Bangweulu Block), the Paleo- to Mesoproterozoic Irumide Belt, the Mesoproterozoic Kibaran Belt and the Choma-Kalomo Block, with a possible minor contribution from the Zimbabwe Craton far south of the Katangan Basin. The absence of any zircons with ages < 560 Ma suggests that the Biano Subgroup sediments were deposited during the Lufilian orogeny.

Figure 2. Jacques Batumike collecting heavy mineral concentrates on the Talala River (near Talala pipe, Kundelungu Plateau).

Contacts: Jacques Batumike, Sue O'Reilly, Bill Griffin
Funded by: iMURS, IPRS, ARC-DP

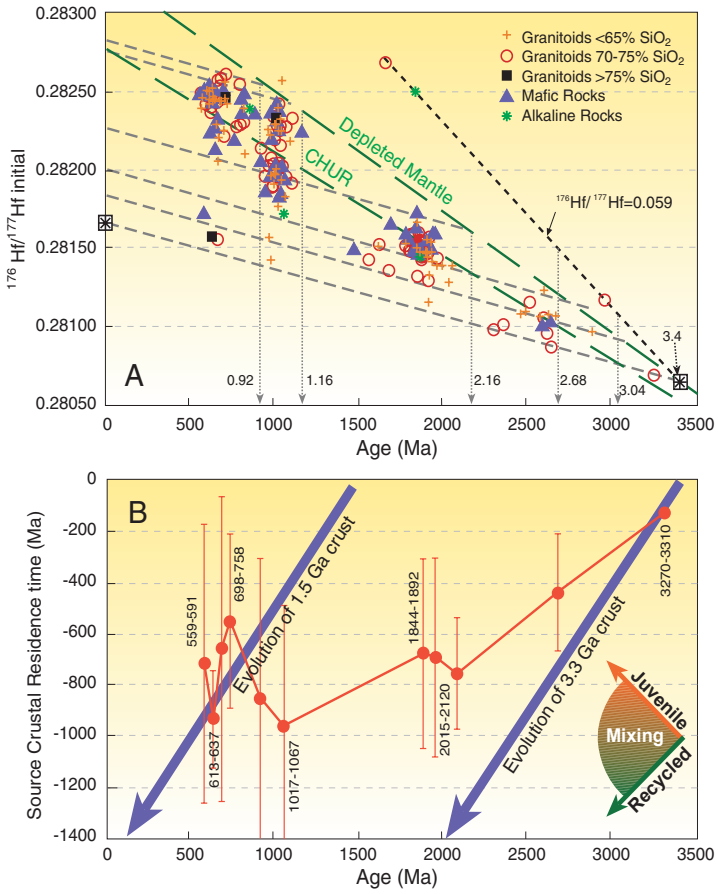

Figure 3.
A. Age, Hf-isotope and rock type data for each sample and calculated crustal ages. CHUR: Chondritic Uniform Reservoir. Dashed lines show evolution of crustal volumes with $^{176}Lu/^{177}Hf = 0.015$, corresponding to the average continental crust.
B. Event signature curve. Source crustal residence time is the time from the separation from the Depleted Mantle to the crystallisation of the zircon. In this plot, an upward trend with decreasing age indicates juvenile input, while a downward trend implies reworking of older crust. The most pronounced juvenile input occurred during the Neoproterozoic events.

The ghosts of lithospheres past: Imaging a changing mantle in southern Africa

GEOLOGISTS AND GEOPHYSICISTS view the subcontinental lithospheric mantle (SCLM) in different ways at vastly different scales. Geologists can characterise the chemistry and physical state of relatively small volumes of the lithosphere in detail, usually at the scale of an outcrop or the xenoliths sampled in a volcanic eruption. These parameters also contain a time component since the material being studied has been removed from the mantle at a specific point in time. Geophysicists must sample the SCLM in the present using methods that are sensitive to both chemical and physical properties, but at scales many orders of magnitude larger. They then must invert their data to extract information on thermal and chemical properties of the SCLM. Neither of these approaches can show detailed, large-scale maps of the properties of the lithosphere through time, due to the paucity of available material to study (geology) and limitations on sensitivity in time and space (geophysics).

Southern Africa presents a unique opportunity to rectify this; kimberlite intrusions are both spatially and temporally widespread, and provide an abundance of xenolithic material sampled in different time slices. In the southwest corner of the Kaapvaal Craton a cluster of kimberlites from two different intrusive events provides material from the same volume of mantle and allows direct comparison of SCLM composition and structure across the craton margin in two time slices (Group II kimberlites at 115-130 Ma, Group I kimberlites at 85-105 Ma) (Fig. 1). Using methods developed at GEMOC and newly available data from collaborative work with De Beers Exploration we have been able to make more detailed images of the lithosphere than was previously possible with either geologic or geophysical methods, using garnet xenocrysts extracted from the kimberlites.

Geotherms can be derived from the Ni and Cr content of the garnets. Combining these data with the distribution of garnets depleted in Y defines a "chemical" lithosphere-asthenosphere boundary. This coincides with the depth where thermobarometry on xenoliths from other localities indicates a kink in the geotherm, and there is strong enrichment in incompatible trace elements (Fig. 2). The garnet thermobarometry provides a framework on which we can overlay other garnet chemical information, such as Ti content, and also information about the calculated "whole-rock" Al content or the calculated Mg# (Mg/(Mg+Fe)) of coexisting olivine.

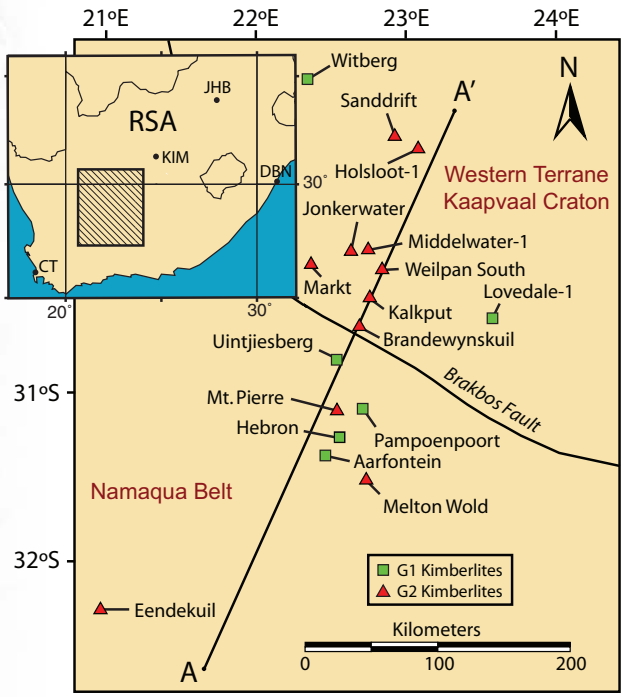

Figure 1. The study area: red triangles, older Group 2 kimberlites; green squares, younger Group 1 kimberlites. The Brakbos Fault is commonly taken as the boundary of the Kaapvaal Craton.

We have projected these data onto the cross-section indicated in Figure 1 and produced a continuous surface with a gridding algorithm. Figure 3 is the resulting image for the Mg# of coexisting olivine. This parameter is a sensitive indicator of melt depletion (high Mg#) and metasomatic refertilisation

(low Mg#). There is marked change in the SCLM between the eruption of the Group 2 kimberlites (130-115 Ma) and the eruption of the Group 1 kimberlites (105-85 Ma), reflecting a thinning and overall re-enrichment of the depleted SCLM in this area. Both images indicate that the depleted cratonic SCLM extends at least 50 km SW of the Brakbos Fault, usually taken as the craton margin.

The Mg# of olivine has particular geophysical significance because seismic velocities are very sensitive to the Mg/Fe of olivine and other upper mantle minerals. By integration of all the chemical and physical data available through garnet chemistry and mineral elasticity data, it is possible to use data such as those in Fig. 3 to calculate models of seismic wave speeds. In areas with appropriate distribution of data both spatially and temporally, we can in essence make historical seismic images of the SCLM and its evolution through time. In some cases this can be done at higher resolutions than is currently possible with geophysical methods. Continuing collaboration with De Beers Exploration will further develop these methods and extend the models across the entire Kaapvaal Craton and its surrounding mobile belts.

Contacts: Alan Kobussen, Bill Griffin, Sue O'Reilly
Funded by: iMURS, MUECRG (De Beers)

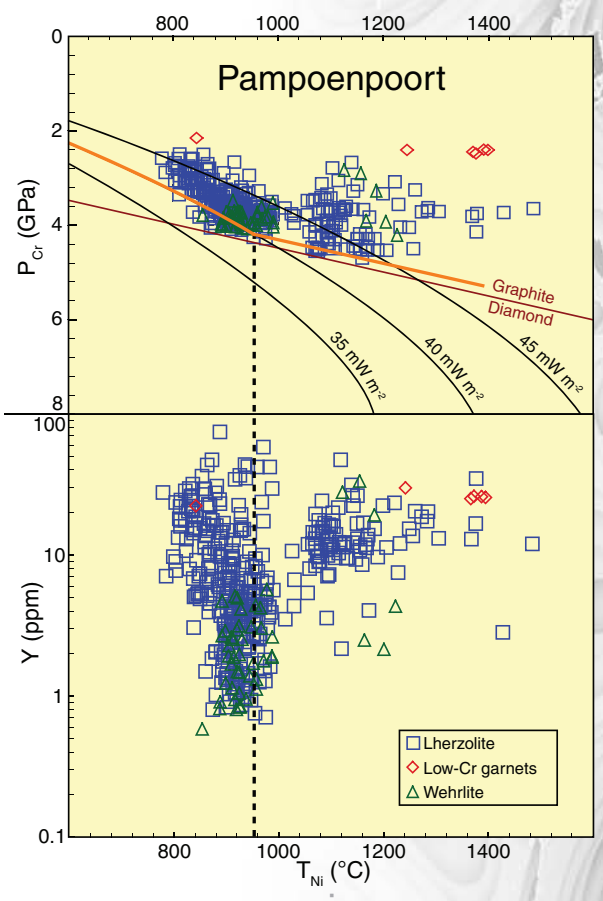

Figure 2. Derivation of the garnet geotherm for Group 1 kimberlite Pampoenpoort. A kink in the geotherm is placed at the lower limit of Y depletion, in line with observations on peridotite xenoliths.

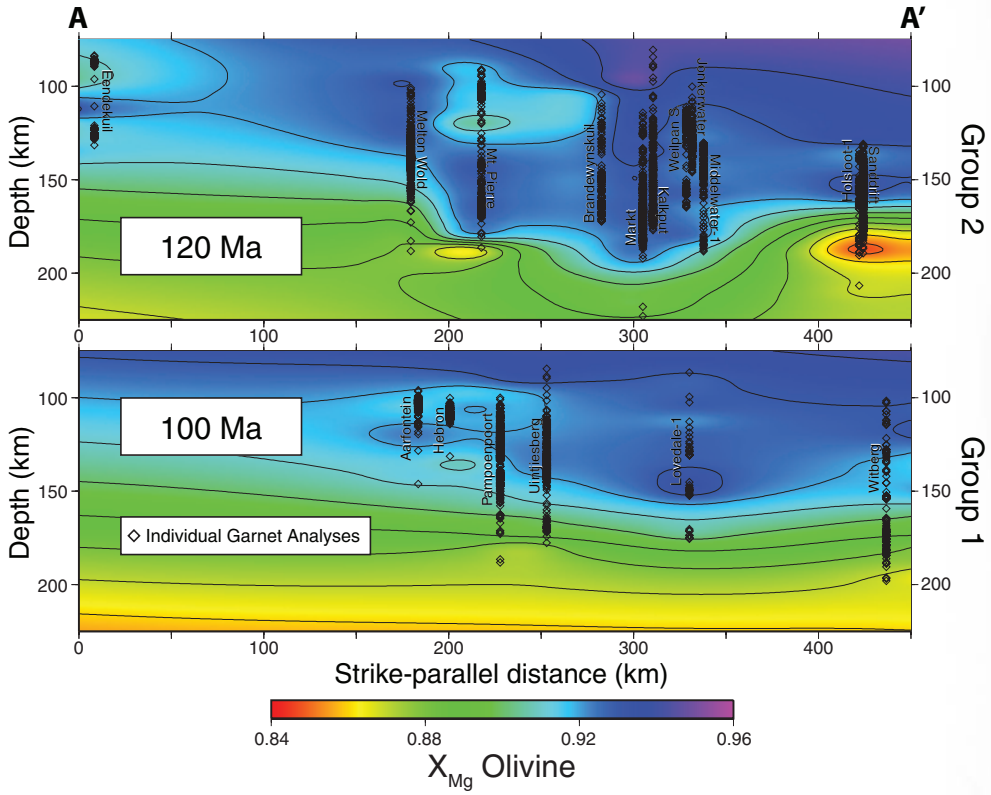

Figure 3. Vertical and lateral distribution of Mg# of olivine coexisting with Cr-garnets projected along section A-A' (Fig. 1) for two time slices.

Eclogites in the SCLM: The subduction myth

IT HAS BECOME CONVENTIONAL WISDOM that eclogite and garnet pyroxenite xenoliths derived from cratonic subcontinental lithospheric mantle (SCLM) represent fragments of subducted ocean floor, implying that the SCLM has grown by a lithosphere-stacking mechanism involving repeated shallow subduction beneath cratons. However, the implied behaviour of these ancient "slabs" is markedly different from what we observe in the modern Earth; seismic-tomography images clearly show slabs descending steeply to at least 660 km depth, rather than layering at shallow depths beneath the continents.

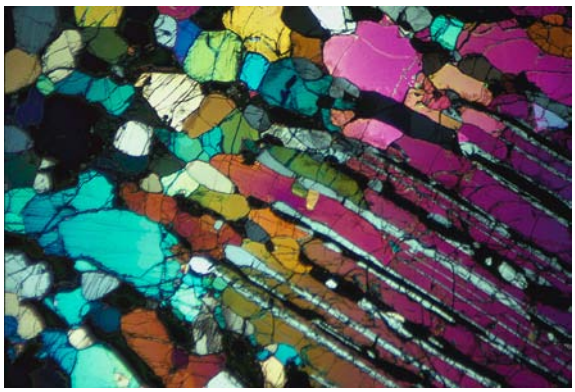

Figure 1. High-temperature clinopyroxenite (crystallised in the lithospheric mantle from mafic magma) exsolving lamellar garnet and orthopyroxene, and recrystallising to produce a websterite.

Xenolith suites in basalts from young terrains (Tectons: eg E. China, E. Australia, western USA, Hawaii) commonly contain garnet pyroxenites that display exsolution microstructures clearly reflecting their origin as high-T cumulates or crystallised melts (Fig. 1). Similar microstructures also occur in cratonic eclogites. The compositional field of Tecton garnet pyroxenites can be expressed by mixing of high-T, high-Al cpx ± opx ± gnt. This compositional field is coincident with that of nearly all cratonic eclogites (reconstructed from mineral compositions); both rock types are distinct in composition from clearly metabasaltic eclogites in HP/UHP metamorphic belts (Fig. 2). Many eclogites also have experienced episodes of metasomatism, making bulk compositions (especially trace element patterns) an unreliable guide to their origin.

Simultaneous solutions of cpx-gnt thermometers with the equations for xenolith-derived geotherms show that rather than being widely distributed in the SCLM as implied by lithosphere-stacking models, eclogites from many cratonic areas are concentrated in layers <20 km thick, co-spatial with a strong signature of metasomatism in the surrounding peridotites (Fig. 3). In many cases this combination of features defines a "lithosphere-asthenosphere boundary" marking the transition from depleted SCLM to more fertile underlying mantle. This pattern strongly

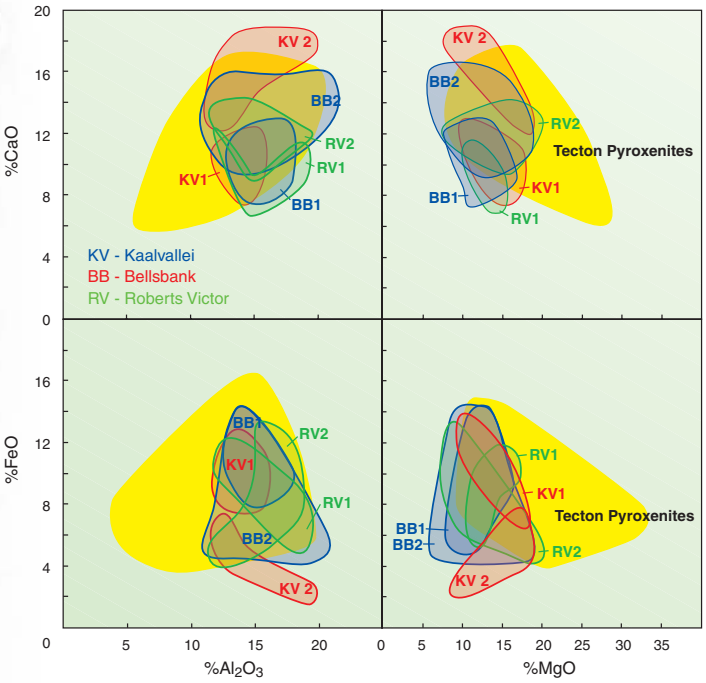

Figure 2. Compositions of cratonic eclogite suites, calculated from mineral chemistry assuming that gnt:cpx=1. Yellow shaded field encompasses data from whole-rock compositions for Phanerozoic garnet pyroxenite xenoliths in alkali basalts from SE Australia and Hawaii and pyroxenite dikes from European peridotite massifs.

suggests that the eclogites reflect the intrusion of asthenosphere-derived melts near compositional/rheological boundaries, causing metasomatism in their peridotite wall-rocks.

The strongest argument for a crustal origin for cratonic eclogites is the large spread in $\delta^{18}O$ observed in some suites; such fractionation is commonly thought to require a low-T origin. However, Mg isotopes in high-T peridotites show equally large fractionation even within single xenoliths (Pearson et al., 2006); significant isotopic fractionation clearly can take place at T >1000° C. SCLM eclogites commonly host diamonds with low-$\delta^{13}C$ carbon; this has been interpreted as biogenic in origin, but this model is not consistent with N-isotope data (Cartigny et al., 1998). The $\delta^{13}C$ variation can instead be explained by Rayleigh fractionation during redox reactions (Muroka et al., 2005). In framesites, the covariation of $\delta^{13}C$ in diamond and $\delta^{18}O$ in cogenetic silicates suggests that similar redox-related fractionation mechanisms are involved (Fig. 4); the O-isotopic signatures thus are not prima facie evidence of a shallow origin for SCLM eclogites. Eu anomalies in cratonic eclogites also have been presented as evidence of the previous presence, or fractionation, of plagioclase. However, similar anomalies are found in peridotitic phases, and may simply reflect redox processes during metasomatism.

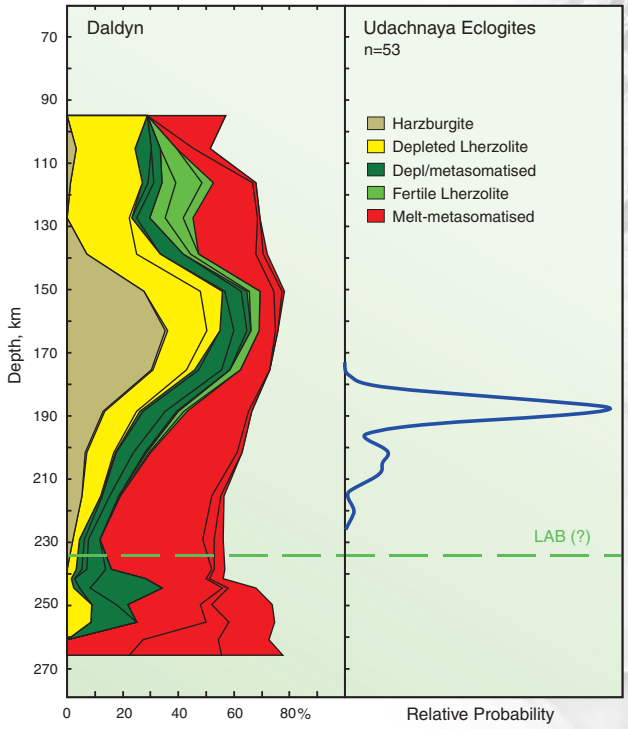

Figure 3. Distribution of eclogites in the SCLM beneath the Udachnaya kimberlite, Yakutia.

Some SCLM eclogites carry "crustal" radiogenic-isotope signatures – but so do many intraplate magmas. These signatures may reflect derivation of parental magmas from deeply subducted crust, rather than the direct emplacement of ocean floor into the SCLM. The cratonic eclogites, like the Tecton pyroxenites, may be telling us about the growth or erosion of the SCLM from below, through magmatic processes, rather than from the side, through shallow subduction.

Contacts: Bill Griffin, Sue O'Reilly
Funded by: ARC Discovery Project

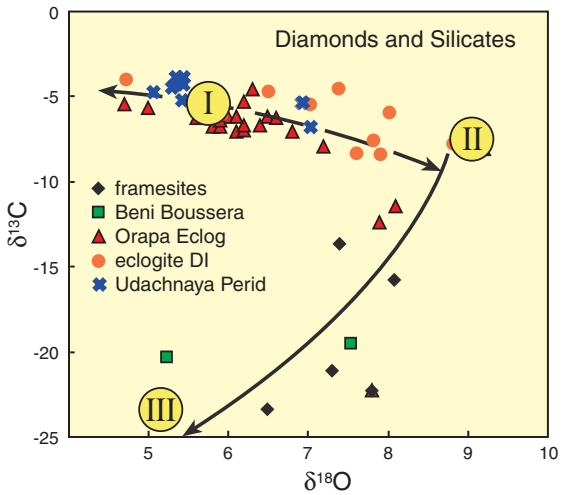

Figure 4. $\delta^{18}O$ of diamonds vs $\delta^{18}O$ in coexisting silicates.

Ancient mantle in modern plumes: B and Os in the Azores

THE DYNAMICS OF THE EARTH reflect its internal heat but the nature and time scales of mantle convection remain poorly constrained. Over the past decade tomography data have provided spectacular images of seismically fast material, associated with subducting plates. These are interpreted as the cool slabs descending through the warmer mantle, suggesting that the slabs can penetrate the 670 km discontinuity, continue into the deep mantle and pond at the core-mantle boundary. Conversely, a significant component of return flow is associated with mantle plumes; many of these, including the Azores, appear to rise from the core-mantle boundary (Fig. 1). These observations have generated a lot of interest in the possibility that subducted material is entrained in these plumes. These ideas can be independently tested by examining the composition of ocean island basalts (OIB) erupted above plumes. Radiogenic isotopes have long been employed in this search because of their potential to constrain the time scales of recycling. Many OIB have indeed been found to have signatures distinct from those of mid-ocean ridge basalts (MORB) that sample the uppermost mantle.

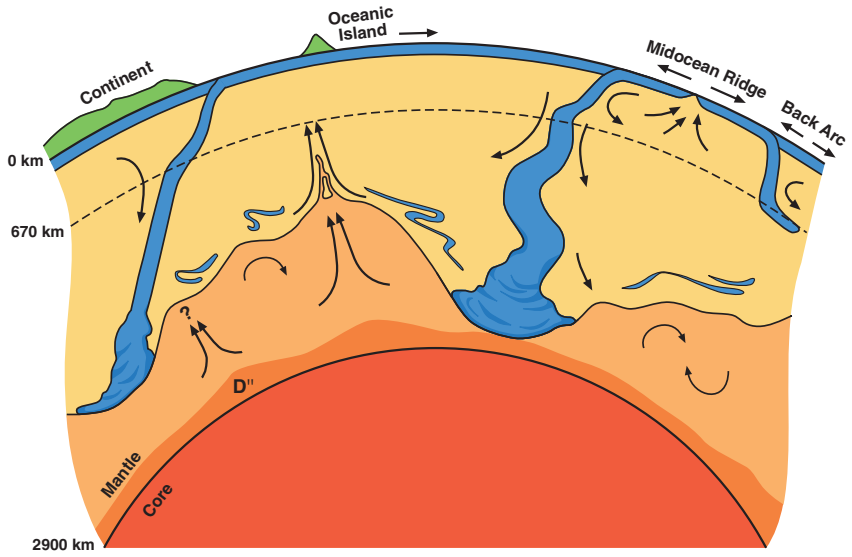

Figure 1. Cartoon of convecting mantle showing cold downwellings (subducting slabs) in blue and hot upwellings from the core-mantle boundary (plumes) in orange. Kellogg et al., 1999.

However, although such signals undoubtedly reflect the time-integrated effects of fractionated parent-daughter element ratios, the age and extent of this fractionation can rarely be sorted out. Even if this is possible, the parent-daughter fractionation is not restricted to processes occurring near the Earth's surface and could instead reflect intra-mantle metasomatism. In contrast, the isotopes of light elements, such as O, B and Li, are commonly fractionated by low-temperature processes near the Earth's surface and significant variations in the stable isotope ratios of MORB and OIB could provide evidence for contributions from recycled material. However, the range of O and B isotope ratios observed in MORB and OIB is rather restricted and observed variations often are attributed to shallow assimilation of altered oceanic crust. Furthermore, stable isotopes cannot be used to constrain the time scales of recycling.

A recent study of basalts from the Azores islands (Fig. 2) has found high Nb/B ratios and a large range in $\delta^{11}B$ ratios, which provide compelling evidence for the recycling of materials that have undergone fractionation near the Earth's surface. Moreover, $\delta^{11}B$ is negatively correlated with $^{187}Os/^{188}Os$ ratios that extend to subchondritic values (Fig. 3). The low $^{187}Os/^{188}Os$ constrains the age of the high

Figure 2. Two of the Azores islands: (left) The Caldeira das Sete Cidades on São Miguel and (below) the Island of Pico, dominated by the stratovolcano, Pico Mountain.

Nb/B, ^{11}B-enriched end-member to be ≥ 2.5 Ga. This is inferred to be melt- and fluid-depleted lithospheric mantle from a subducted oceanic plate; other Azores basalts contain a contribution from ~ 3 Ga enriched basalts (Schaefer et al. 2002, *Nature 420, 304*). The simplest interpretation is that both components are derived from an Archean oceanic plate that was subducted into the deep mantle, where it was stored until thermal buoyancy caused it to rise beneath the Azores islands.

Contact: Simon Turner
Funded by: ARC Federation Fellowship

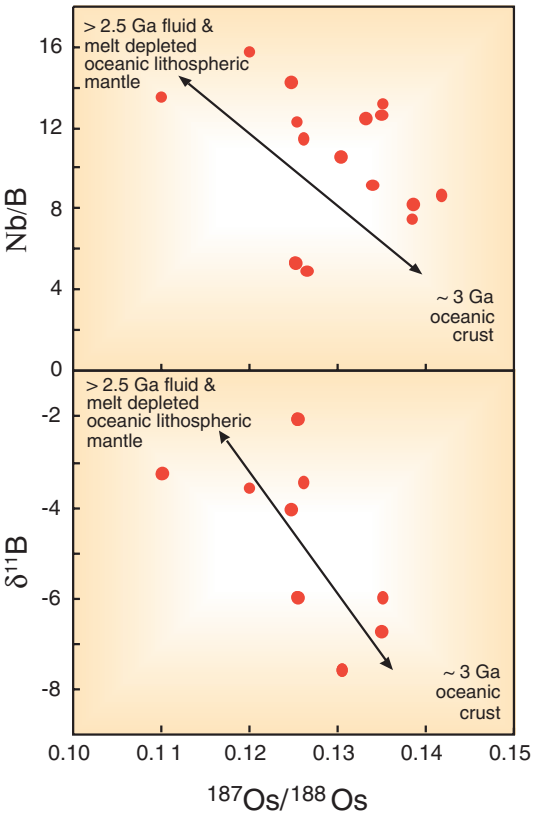

Figure 3. Variation of Os isotopes with other geochemical indices in the Azores (see text for discussion).

The tenacity of cratons: a low stress home environment?

THE CRATONIC REGIONS OF THE EARTH'S CONTINENTAL CRUST have avoided deformation for billions of years. This by itself is not remarkable – the surfaces of the Moon and Mars have avoided deformation for far longer. However, considering that the oceanic crust, representing nearly 70% of the Earth's surface, is recycled on a timescale of 100 Myr, and most continental regions are reworked over similar periods, then the survival of cratons becomes an enduring geophysical mystery.

Cratons themselves have a number of physical characteristics that may account for their strength. The crust of cratons overlies a thick, buoyant chemical lithosphere. Cratonic lithosphere exhibits extreme degrees of melt depletion, accounting for its buoyancy with respect to the mantle. The depletion also has led to very low water contents, imparting a potential 100-fold increase in viscosity compared to the asthenosphere. On top of that, cratons are cold, and their deep root regions are expected to be even more viscous and resilient as a result.

The problem arises when one tries to model cratons with these properties in a convecting mantle - they just aren't extreme enough. Buoyancy itself cannot impart strength and give rise to cratonic stability - buoyant continents either spread out under their own gravitational instability, get entrained bit-by-bit by downwelling mantle and subducting slabs, or at the least are grossly deformed by their dynamic environment. Previous mantle simulations have shown that viscosity *can* impart stability, but the high viscosities required are far beyond reasonable bounds for cratonic mantle. For plausible viscosity contrasts, the models tell us that cratons should have been heavily deformed, reworked, and even wholesale recycled under Archean mantle conditions.

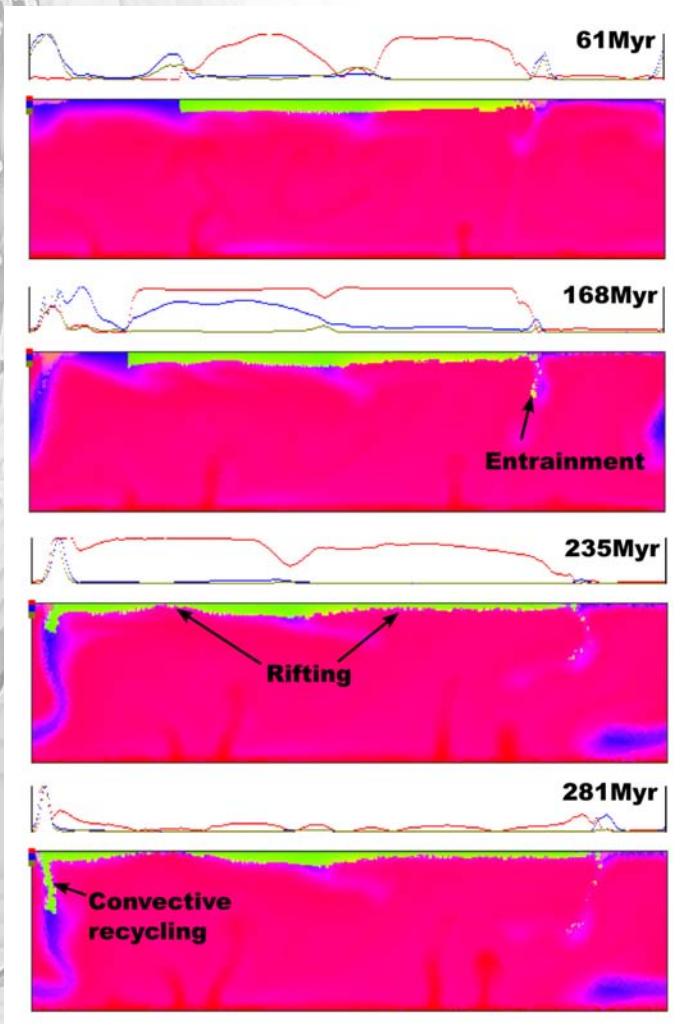

Figure 1. The fate of buoyant lithosphere without any instrinsic strength in a strongly convecting Archean mantle. Despite its convective buoyancy, the lithosphere rifts in response to the regional stress regime and is partially recycled into the mantle (O'Neill et al. 2007).

And yet the cratons are still here. What factors give rise to their remarkable tenacity? Geodynamic simulations performed at GEMOC have explored these factors in detail, and have shed light on the survival of these economically important terranes. While most previous simulations have focused on the properties of cratons themselves, few have adequately addressed their dynamic environment - the convecting mantle.

Convection in the Earth differs from simple "box" convection simulations in some important ways. Firstly, strongly temperature-dependent viscosity, with brittle/plastic failure and strain-rate weakening, is needed to simulate plates - a condition met in some previous studies. Secondly, the Earth's mantle displays a strong variation in viscosity with depth, but this effect has not been incorporated in previous craton simulations. This strongly affects the dynamics of the mantle, and the surface stress regime. Thirdly, an endothermic phase change at 670 km hinders slab penetration into the lower mantle, strongly affecting mantle dynamics and its thermal evolution. It also gives rise to a curious

phenomenon known as “mantle avalanches”, where material piled up at 670 km periodically breaks through into the lower mantle, instigating a corresponding injection of hot material into the upper mantle. These violent episodes have been associated with crustal production in the past, but represent a highly destructive surface regime for existing cratons.

The main results of the new modelling show that realistic mantle viscosity structures cushion cratons from mantle dynamics; a low-viscosity asthenosphere partly decouples the surface plates from the mantle beneath, and a viscous lower mantle mitigates the stress extremes experienced by cratons during mantle avalanche events. Under the hotter mantle conditions of the past, however, two more effects conspire against the humble craton. Firstly, the velocity of mantle convection increases - this inevitably leads to a higher stress environment for cratons. Secondly, since the phase change at 670 km is endothermic, the layering is enhanced under hotter mantle conditions, and avalanches are more violent and spectacular. But a third mechanism, previously unrecognised, acts to save cratons from these destructive effects. Mantle viscosities are highly sensitive to temperature, and under hotter mantle conditions in the past, the drop in bulk mantle viscosities would be dramatic. This acts to minimise the stresses transferred to the surface plates, and thus to cratons. The modelling shows that the magnitude of this effect far outweighs the stress increase due to faster convection, and craton stability for billions of years is not paradoxical at all in these simulations, for reasonable cratonic properties (see *GEMOC Publication #479*).

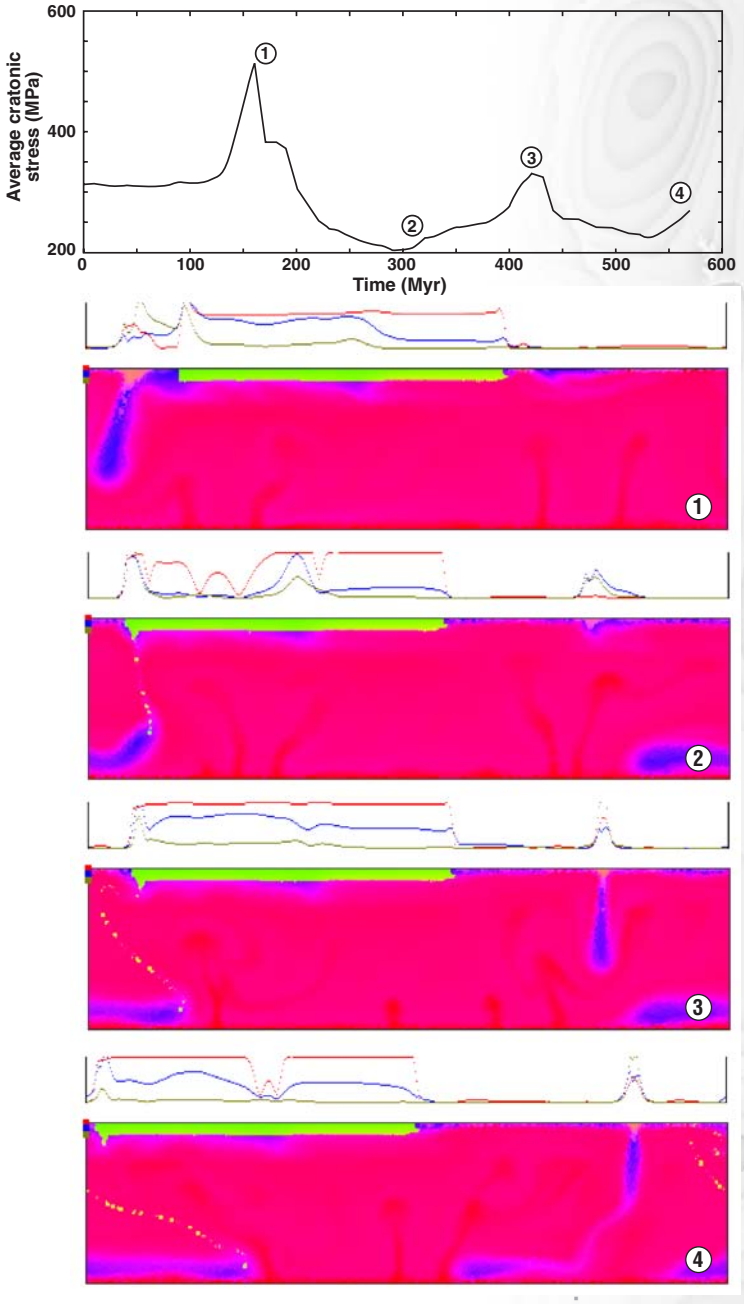

Figure 2. A stable craton with intrinsically strong roots resists tectonically violent mantle avalanches and wildly fluctuating regional stress, in part due to its physical properties, but also due to mild stresses of the ‘warm bath’ Archean mantle environment.

Contacts: Craig O’Neill, Sue O'Reilly, Bill Griffin
Funded by: Macquarie University Research Fellowship

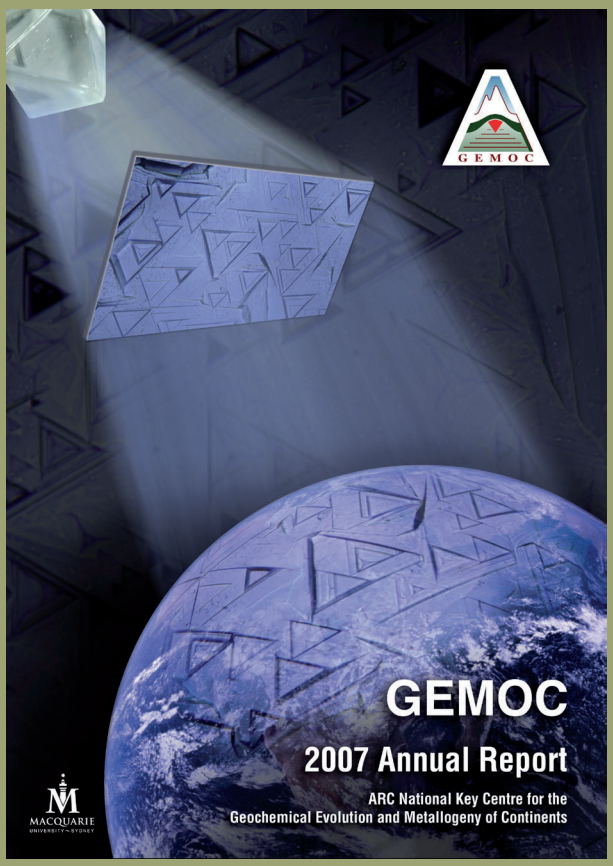

2007 Contents

TerraneChron™	212
Where on/in Earth are Diamonds? (Diamond, subcalcic garnet and mantle metasomatism)	213
Chemical impurities in gem-quality diamonds	216
Core-mantle boundary interactions: The deep mantle goes with the flow	217
Core formation, crystallisation of the mantle and oxidation of the Earth	218
Nickel Sulfide Deposits – Developing New Exploration Tools	220
Crust-mantle evolution in NW Spitsbergen: Re-Os, U-Pb and Hf isotope data	222
Extreme plate tectonics	224
Laser Microprobe -ICPMS U-Pb dating of groundmass perovskite from kimberlites	226
Sino-Australian connections billion years ago?	228
10 years of MC-ICPMS: linking the crust and mantle	230
How much potassium is in the Earth's core?	233
Heat sources in mantle plumes	234
Flawed crystals control Earth's properties	236

Front Cover: Analysis of trace elements in diamonds (see Research Highlights) is shedding new light on their origin and other features, such as the development of trigons (triangular etching features), and giving new understanding of fluid related processes deep in the Earth.

Research highlights 2007

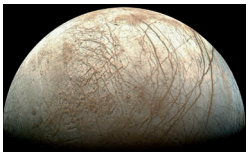

TERRANECHRON® is GEMOC's unique methodology for terrane evaluation. During 2007 collaboative research projects with industry using *TerraneChron*® yielded a wealth of information to map crustal history on different scales.

Visit the TerraneChron® web page at www.es.mq.edu.au/GEMOC/TerraneChron.html

TerraneChron®

A new tool for regional exploration for minerals and petroleum

GEMOC

- ✓ Based on zircon analyses
- ✓ Efficient and cost-effective
- ✓ Identifies regional tectonic events
- ✓ Dates magmatic episodes
- ✓ Fingerprints crust reworking and mantle input (fertility)

Contact: Bill Griffin or Suzanne O'Reilly
(bill.griffin *or* sue.oreilly@mq.edu.au)
ARC GEMOC National Key Centre
Department of Earth and Planetary Sciences
Macquarie University,
NSW 2109, Australia
www.es.mq.edu.au/GEMOC/

MACQUARIE UNIVERSITY ~ SYDNEY

What is *TerraneChron*®?

The methodology was developed by GEMOC to provide rapid, cost-effective characterisation of crustal history on regional (10-1000 km^2) scales. It is based on U-Pb, Hf-isotope and trace-element analysis of single zircon grains by laser-ablation ICPMS (single- and multi-collector) methods.

- U-Pb ages, with precision equivalent to SHRIMP
- Hf isotopes trace magma sources (crustal vs juvenile mantle input)
- Trace elements identify parental rock types of detrital zircons

What kind of samples?

- Regional heavy-mineral sampling (modern drainages: terrane analysis)
- Sedimentary rocks (basin analysis)
- Igneous rocks (dating, specialised genetic studies)

Applications to mineral exploration

- Rapid assessment of the geology in difficult or poorly mapped terrains
- "Event Signatures" for comparison of crustal histories from different areas
- Identify presence/absence of key rock types (eg Cu/Au porphyries, A-type granites….)
- Prioritisation of target areas

Applications to oil and gas exploration

In provenance studies, the information from Hf isotopes and trace elements provides a more detailed source signature than U-Pb ages alone.

- *TerraneChron*® defines the crustal history of the source region of the sediment
- Changes in direction of basin filling track regional tilting, subsidence
- Stratigraphic markers in thick non-fossiliferous sediment packages
- Proven applications in the North Sea

Where on/in Earth are Diamonds? (Diamond, subcalcic garnet and mantle metasomatism)

KIMBERLITES ARE THE MAJOR SOURCE OF NATURAL DIAMONDS, but fewer than 1% of kimberlites contain economic quantities of diamond. Even within a single kimberlite field, economic and barren kimberlites may occur within very short distance of one another, and it is rarely obvious what has controlled the small-scale distribution of diamond in the mantle volumes sampled by different kimberlites. However, a spinoff observation arising from GEMOC's ongoing 4-D Lithosphere Mapping project may have provided an important clue (*GEMOC Publication #449*).

The heavy mineral concentrates of kimberlites typically contain xenocrysts of both peridotitic garnet and chromite, derived by disaggregation of the mantle wall rocks sampled by the kimberlite. The Ni content of the garnets, and the Zn content of the chromites, can be used to measure their temperature of equilibration, and these temperatures can be translated to depth estimates for each grain, by reference to a local geotherm derived either from the garnet populations or from peridotite xenoliths. With this information, we can draw curves showing where the kimberlite picked up its load of garnet and chromite during ascent to the surface.

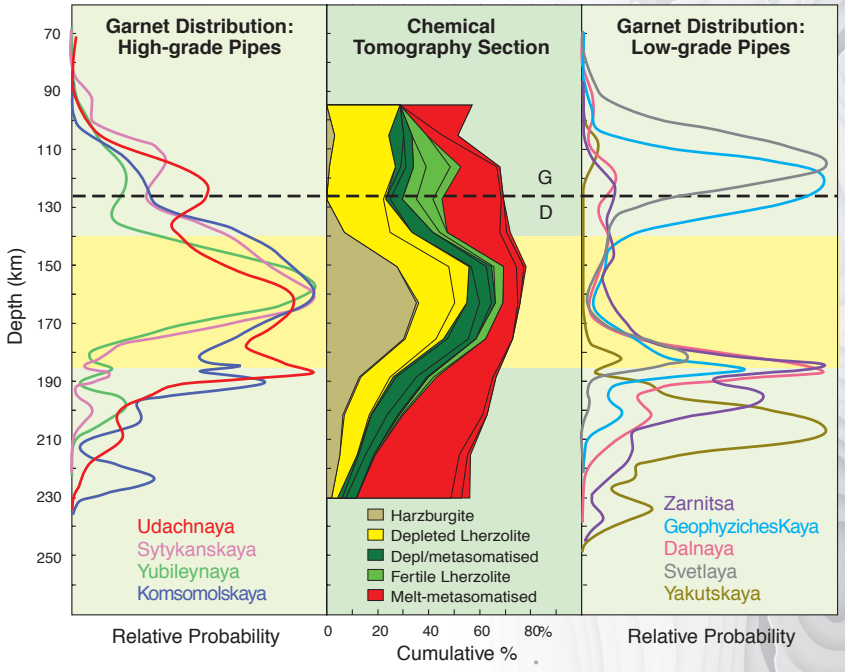

Figure 1. Chemical tomography section for Daldyn kimberlite field (9 kimberlites, 858 garnets), showing relative abundance at each depth of garnets from harzburgites, depleted lherzolites, depleted but metasomatised lherzolites, fertile lherzolites (also interpreted as metasomatic products) and lherzolites metasomatised by silicate melts. The strong concentration of harzburgitic garnets in 140–180 km depth range is marked by a shaded horizontal band. Curves show distribution of sampling depths of garnet grains entrained in high-grade (left) and low-grade (right) kimberlites from Daldyn field and adjacent Alakit field. Horizontal dashed line is graphite (G)- diamond (D) phase transition.

In the Daldyn and Alakit kimberlite fields of Siberia, strongly depleted harzburgitic rocks are largely confined to a narrow depth range of 140-190 km, whereas less depleted lherzolites dominate the mantle section above and below the harzburgitic band. Numerous studies of diamond-bearing xenoliths and mineral inclusions in diamonds from these two fields show that the vast majority of the diamonds in the pipes come from the harzburgitic band. Depth-distribution curves of garnet from these two fields (Fig. 1) show that most of the garnets in the pipes with high diamond grade come from the harzburgite-rich level, whereas the low-grade pipes contain lherzolitic garnets from deeper and shallower depth, but few grains from 140-190 km depth. Similar patterns have been found in the Archangelsk kimberlite province of NW Russia.

The distribution of chromite is quite different – it peaks in the harzburgitic layer in both the high-grade and the low-grade pipes (Fig. 2). It appears that (1) all of the kimberlites have sampled the harzburgite-rich layer; (2) chromite is ubiquitous through the layer; (3) diamond and garnet occur together, but only locally, within the layer. This suggests a genetic relationship, in which the metasomatic processes that deposit diamond also are responsible for depositing garnet. Another key observation is that chromite xenocrysts in barren kimberlites typically are more oxidised (with higher mean Fe^{3+}/Fe^{2+}) than those from high-grade pipes, and chromites included in diamond generally have very low Fe^{3+}/Fe^{2+} (Fig. 3).

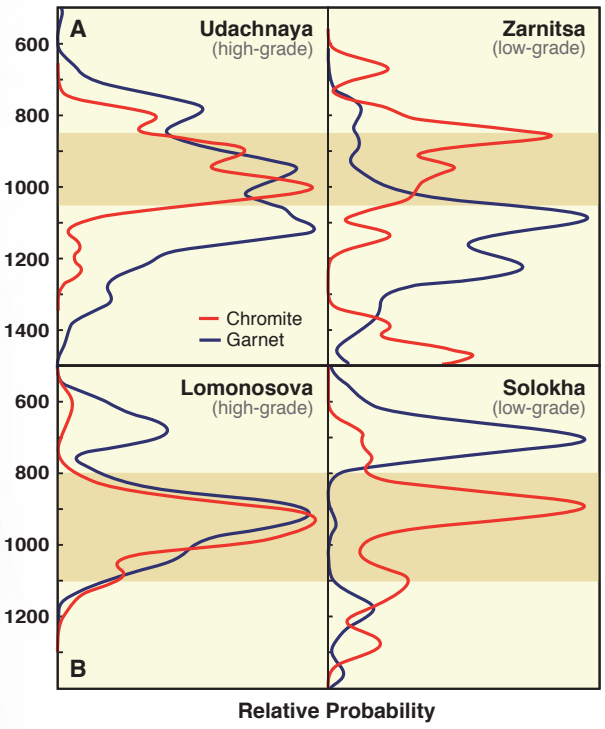

Figure 2. Temperature (depth) distribution of garnets and chromites in high- and low-grade kimberlites. A: Daldyn field, high-grade Udachnaya pipe and low-grade Zarnitsa pipe. B: Arkhangelsk field, high-grade Lomonosovskaya pipe and low-grade Solokha pipe. Shaded band shows temperature range of the depleted harzburgite-rich layer beneath each field (cf. Fig. 1).

These observations suggest that diamond and harzburgitic garnet are linked to the same metasomatic process, through generalised reactions of the type: CH_4 (in fluid) + Fe^{3+}(in chromite) + Si, Ca, Mg (in opx, fluid) → diamond + garnet + H_2O +Fe^{2+}(in chromite).

We suggest that where melts or fluids derived from below the depleted lithospheric mantle first penetrate the harzburgitic layer along fractures, CH_4-rich fluids derived from them react with the wall rocks, producing subcalcic garnet, diamond and a reduced diamond-bearing harzburgite. As the melts themselves penetrate into the lithosphere, metasomatism adds more Ca, Al and Fe, refertilising the harzburgite to produce lherzolites. Oxidation during this metasomatism would tend to destroy diamonds, producing a positive correlation between harzburgitic minerals and diamond, and a negative correlation between lherzolitic minerals and diamond, as observed in many kimberlite fields. Volumes of the harzburgitic layer that were never metasomatised would contain neither diamond nor garnet.

These processes could operate on the scale of individual melt conduits, producing very small-scale variations in diamond content within the lithosphere.

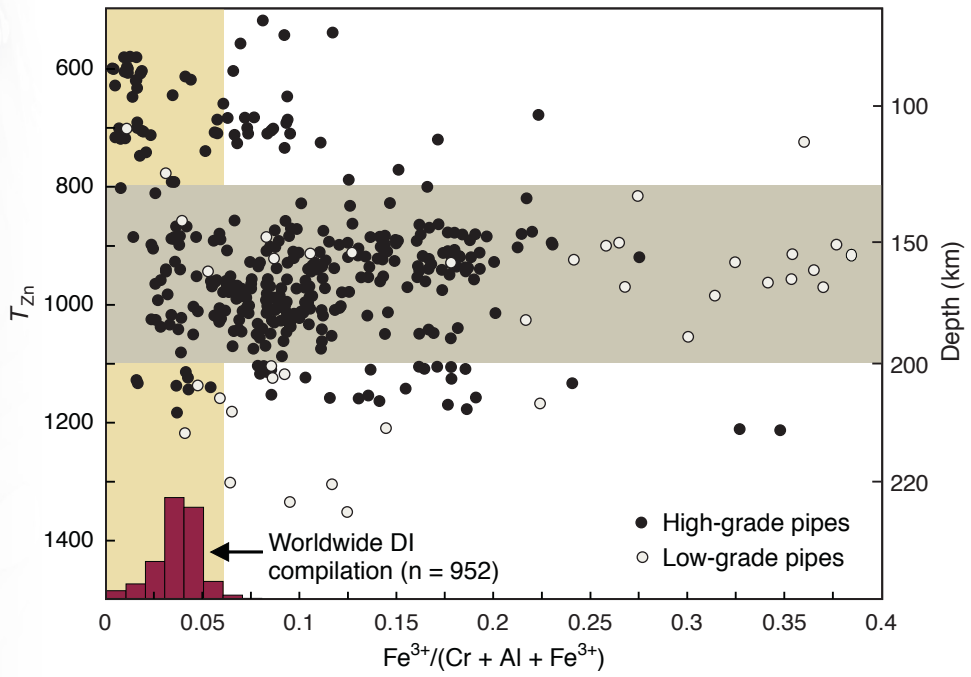

Figure 3. $Fe^{3+}/(Cr + Al + Fe^{3+})$ of chromites vs depth in kimberlites from the Arkhangelsk field. Box shows range of values in diamond inclusions (DI) worldwide; horizontal band shows depth distribution of harzburgitic rocks.

The diamond grade of later kimberlites would be dependent on their path through this heterogeneous mantle (Fig. 4). Kimberlites following old conduits that experienced mainly the first stages of the metasomatism could have high grades; those that sampled unmetasomatised volumes would be barren; those that followed well-worn magma conduits, now lined by lherzolite, might contain diamonds, but at lower grades.

This picture of the mantle suggests that it might be possible to analyse the distribution of high-grade and low-grade pipes within a single kimberlite province to map out the positions of the best structures at depth, and to target detailed brown-field exploration efforts.

Contacts: Vlad Malkovets, Bill Griffin, Sue O'Reilly
Funded by: MURF, MUNS, ARC Discovery

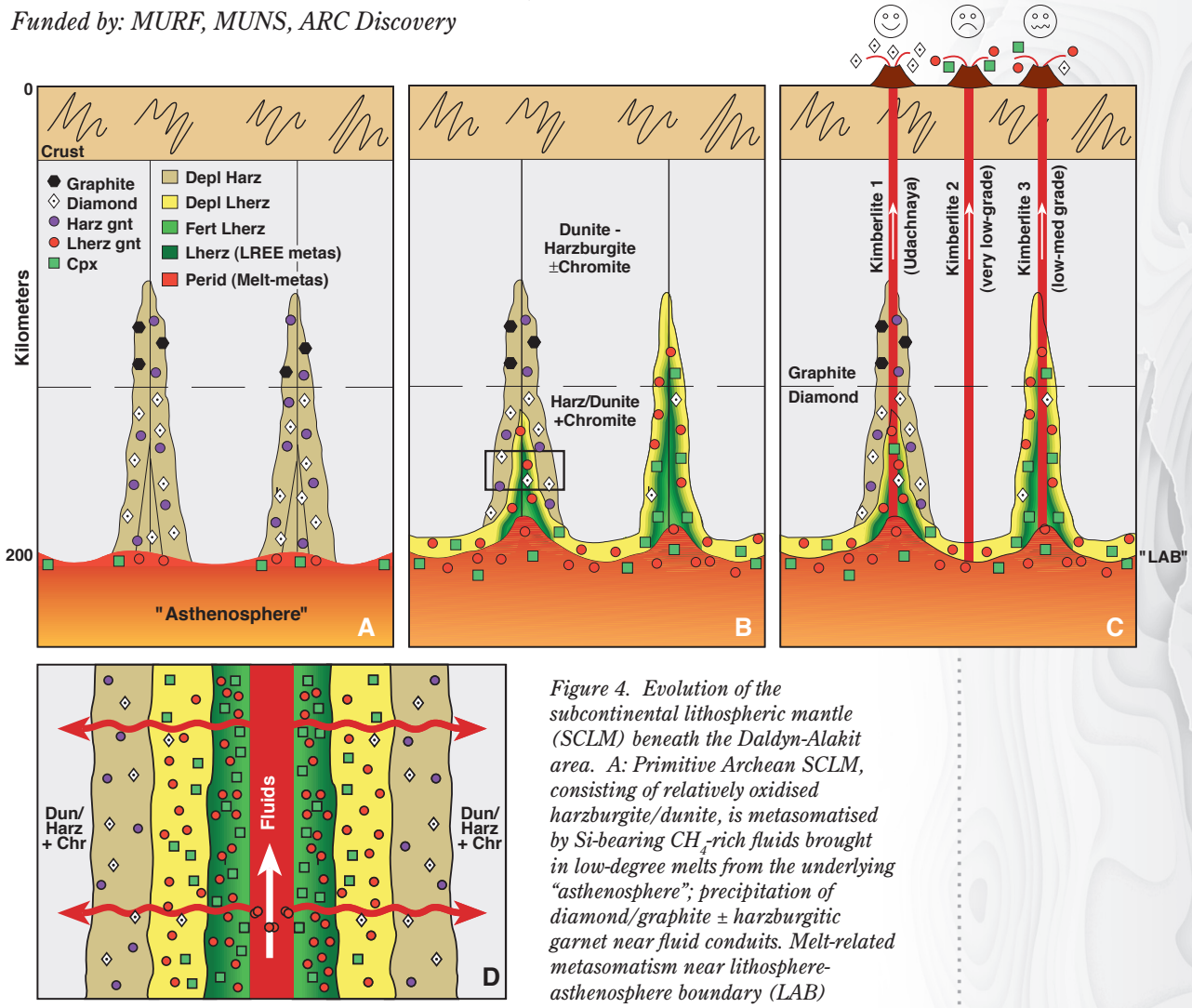

Figure 4. Evolution of the subcontinental lithospheric mantle (SCLM) beneath the Daldyn-Alakit area. A: Primitive Archean SCLM, consisting of relatively oxidised harzburgite/dunite, is metasomatised by Si-bearing CH_4-rich fluids brought in low-degree melts from the underlying "asthenosphere"; precipitation of diamond/graphite ± harzburgitic garnet near fluid conduits. Melt-related metasomatism near lithosphere-asthenosphere boundary (LAB) converts some harzburgites to fertile lherzolite by addition of Ca, Fe, Al. B: Continued input of melts/fluids; reduced harzburgite does not precipitate diamond/graphite; melt-related metasomatism refertilises harzburgite to lherzolite at base of lithosphere and along conduits (weakly in left conduit, more extensively in right conduit); relict harzburgitic diamonds in lherzolites. C: Kimberlite eruption (Devonian); high-grade pipes sample remnants of Stage-A modified mantle. Barren pipes sample least-metasomatised mantle and lack harzburgitic garnets and diamonds; some low-grade pipes sample highly metasomatised mantle with relict diamonds. D: Detail of melt conduit showing progressive metasomatism of wall rocks, first by CH_4-rich fluids expelled from melts, and then by the melts themselves. Abbreviations: Dun—dunite; Harz—harzburgite; Lherz—lherzolite

Chemical impurities in gem-quality diamonds

THE STUDY OF DIAMONDS is a very attractive topic since they can reveal unique information from the Earth's mantle. A comprehensive study of diamonds includes both simple and advanced methods as morphologic description, cathodoluminescence imagery, vibrational spectroscopy and stable isotope analyses. Recently, a methodology developed at GEMOC using LA-ICPMS (Laser Ablation Inductively Coupled Plasma Mass Spectrometry) has made it possible to investigate the very low levels of chemical impurities found in micro-inclusions within the diamonds. The technique consists of ablating the diamond surface with a laser beam, which drills a hole approximately 50 µm deep over about 2 minutes. The result is a time/space-resolved signal that reveals the chemical composition of the diamond across the depth analysed. These chemical impurities are interpreted as the composition of the fluids that once deposited that diamond in the mantle.

In our current research, the LA-ICPMS technique meets a simple and traditional method of studying diamonds: their morphology and surface textures. Diamonds are formed as octahedral and cubic crystals. Despite their well-known hardness, certain conditions (high oxygen fugacity) can corrode the surface of diamonds, forming a variety of corrosion figures, or etching pits. This dissolution can happen during the diamond's residence in the mantle and/or in the magma during its ascent to the Earth's surface. In octahedral diamonds, one of the most common corrosion figures is the trigon. These are triangular pits, either point- or flat-bottomed. The point-bottomed ones are formed at the end of crystal defects, where dislocation lines emerge from the centre of the diamond. The flat-bottomed trigons have been related to clusters of chemical impurities or crystal defects. For the first time we could test this hypothesis using LA-ICPMS.

In our investigation, we analysed gem-quality octahedral diamonds from Canada. Most of them have smooth surfaces (Fig. 1) but some have abundant flat-bottomed trigons (Fig. 2) covering some or all the surfaces. Using LA-ICPMS, we found that abundant flat-bottomed trigons occur only where a sub-surface layer is enriched with various trace elements, as Ca, Mg, Fe, K, Ba, Sr, LREE, among others. The surfaces with trigons were examined in the microscope (Fig. 3), and micro-inclusions were found distributed in a thin layer 15-20 microns beneath the surface, corresponding to depth of the flat bottoms of the trigons. The micro-inclusions are rounded and small single fractures, which can be both crystallographically [111] and randomly oriented, extend from them, producing a tadpole-like shape (Fig. 3). Such inclusions are absent beneath faces that lack trigons. The chemical composition of the micro-inclusions is similar those of carbonatitic fluids, suggesting that fluids of this composition were able to wet some surfaces of the growing diamonds, before becoming trapped beneath a new layer of "clean" diamond. The role of such mantle fluids in the formation of diamonds is a key direction for further research.

Figure 1. White octahedral diamond with smooth surface.

Figure 2. White octahedral diamond with rough surface covered with trigons, scale divisions = 1 mm.

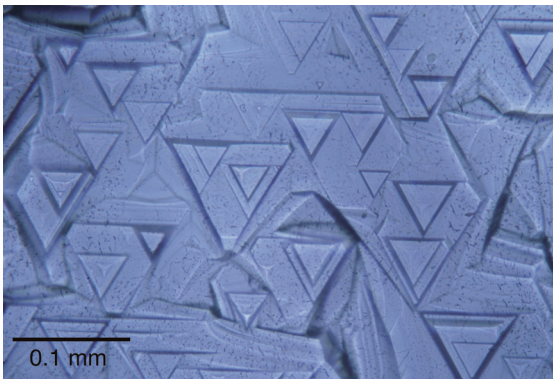

Figure 3. Surface with trigons and micro-inclusions at 15 µm beneath the diamond surface.

Contacts: Debora Araujo, Bill Griffin, Sue O'Reilly, Norman Pearson
Funded by: ARC Linkage, Macquarie University and Rio Tinto

Core-mantle boundary interactions: The deep mantle goes with the flow

OUR UNDERSTANDING OF THE EARTH'S CORE-MANTLE BOUNDARY (CMB) region has improved significantly over the past several years, due in part to the discovery of the "post-perovskite phase", a polymorphic transition in the deepest levels of the mantle. The post-perovskite mineral phase is known through experiment and theoretical calculations to be stable in the lowermost ~150 km of the mantle (the D" layer). Seismic data suggest that the CMB region is highly heterogeneous; this heterogeneity may be partly due to the structure of the post-perovskite phase, and may also reflect chemical and physical interaction between outer core liquid and the lowermost mantle. In 2007, we proposed a new mechanism of mass transfer across the CMB and suggested possible repercussions that include the initiation of deep, siderophile-element-enriched mantle plumes. We view the nature of core-mantle interaction, and the geodynamic and geochemical ramifications, as multiscale processes, both spatially and temporally (Fig. 1). On the microscale (1-50 km), the effect of loading and subsequent shearing of the CMB region where cold downwellings impinge on the outer core can drive local flow of the outer core fluid upwards into the D" layer. This process can be linked to the larger-scale processes operating on the mesoscale (50-300 km) and macroscale regimes (> 300 km). As Fe-rich liquids from the outer core infiltrate into the D" layer, they will interact with the silicates and enrich them in Fe. These processes may also impact on global mantle dynamics. Reacting Fe-rich post-perovskite material may be partially responsible for ultra-low-velocity zones (ULVZ: Fig. 1), which are zones in the D" region where silicate melt is present, and will influence the nature of thermal conduction across the CMB. Infiltration of outer-core liquids into D" also provides a mechanism for imparting a distinctive HSE chemical signature to the lowermost mantle, from where it can be transferred to plumes and the minerals enclosed in some lower-mantle diamonds (see *GEMOC publication #229*). Infiltration of core-derived fluids into the lower mantle requires shear-induced dilatancy to allow fluid movements; encouragingly, there is some new experimental evidence in support of the dilatant mechanism at elevated PT conditions.

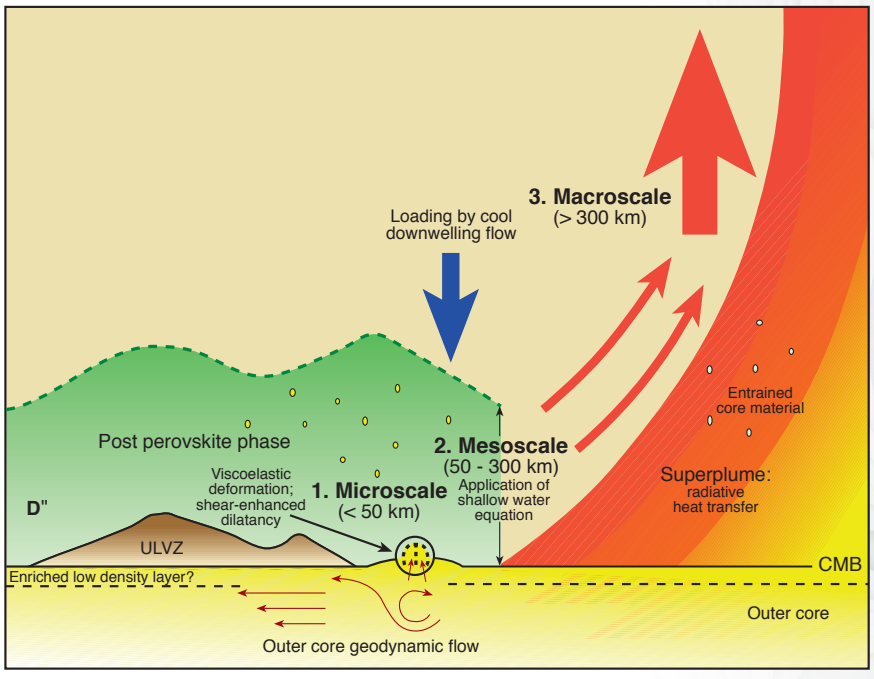

Figure 1. Summary diagram showing the proposed relationship between each of the three key length scales described above.

Contacts: Tracy Rushmer, N. Petford (Bournemouth University), David Yuen (University of Minnesota)
Funded by: MQNS and NASA

Core formation, crystallisation of the mantle and oxidation of the Earth

THE EARTH APPEARS TO HAVE GROWN FROM SMALLER ASTEROIDAL BODIES over a period of about 40 million years after the beginning of the solar system, 4567 million years ago (see *Research Highlight 2006*). Research at Macquarie is concentrating on understanding the timing and processes by which the Earth segregated its metallic core and the crust began to form from the silicate mantle. The way in which the research is done is by experimentally simulating the high pressure, high temperature conditions of, for example, metal separation and determining the partitioning of suites of important chemical elements between the metal and silicate liquids. Then, by comparing the compositions of the silicate parts of the experiment to that of the silicate part of the Earth, we can start to place constraints on how core formation occurred.

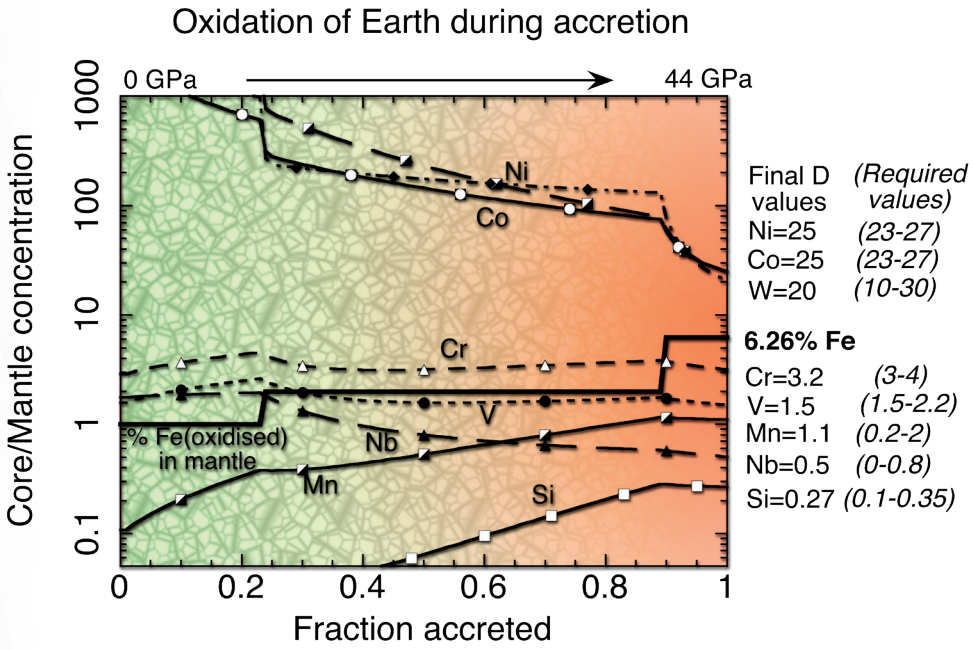

Figure 1. Changes in partition coefficients for different elements, as the Earth grew. Note the apparent increase in the oxidised-iron content of the mantle during this process.

An important requirement is a reference point for the composition of the bulk Earth. This is provided by the primitive meteorites which are chemically similar to the Sun and which have striking affinities with the Earth, Mars and the Moon (see *Research Highlight 2006*). Taking these meteorites as representatives of protoplanetary material we find that the silicate part of Earth is depleted in refractory "siderophile" elements (Fe, Ni, W, etc) because of extraction to the core but undepleted in refractory "lithophile" elements which remain in the mantle. By mass-balance we can calculate the partitioning of the siderophile elements between the core and the silicate mantle and compare the results to our experiments. The results indicate that the Earth must have started out very reduced and then become more oxidised as it grew. This is the only way we can match the core-mantle partitioning of all the well-studied elements. Figure 1 shows a typical oxidation path which correctly reproduces the core-mantle partitioning of a large number of elements. Progressive oxidation, as represented by the weight % of oxidised iron in the mantle is modeled, for simplicity in 2 steps, but in reality was probably continuous.

If the Earth became oxidised as it grew, the important questions are: (a) how

did it happen? and (b) what are the implications? The answer to the first question is that there are several possible mechanisms which call on outside influences (accretion of oxidised material, for example) and are hence unconstrained. Recent discoveries demonstrate, however, that there is a mechanism by which the Earth self-oxidised. This arises from the observation that silicate perovskite, the mineral which is stable throughout the Earth's lower mantle, has a very strong affinity for ferric iron, Fe^{3+}. We now know that this affinity is so strong that it forces Fe^{2+} to disproportionate to form Fe^{3+} and metallic iron:

$$3Fe^{2+} = 2Fe^{3+} + Fe^{0}(\text{metal})$$

Perovskite started to become stable in the Earth's interior when the planet reached 10% of its current size (about the size of Mars). Thereafter, segregation of metal to the core combined with continuous impact of accreting bodies "pumped-up" the Fe^{3+} content of the mantle. This occurred by continuous dissolution and reprecipitation of perovskite in the lower mantle (see Fig. 2).

The important point about Earth's self-oxidation is that it was caused internally rather than by, for example, subduction of oxidised material after the rise of atmospheric oxygen. This explains why all measurements of the oxidation states of materials from the mantle indicate no change since the Archean and no effect of the rise of atmospheric oxygen. The process took place earlier and was internal (see *GEMOC Publication #513*).

Contact: Bernard Wood
Funded by: Federation Fellowship, ARC Discovery, Macquarie University

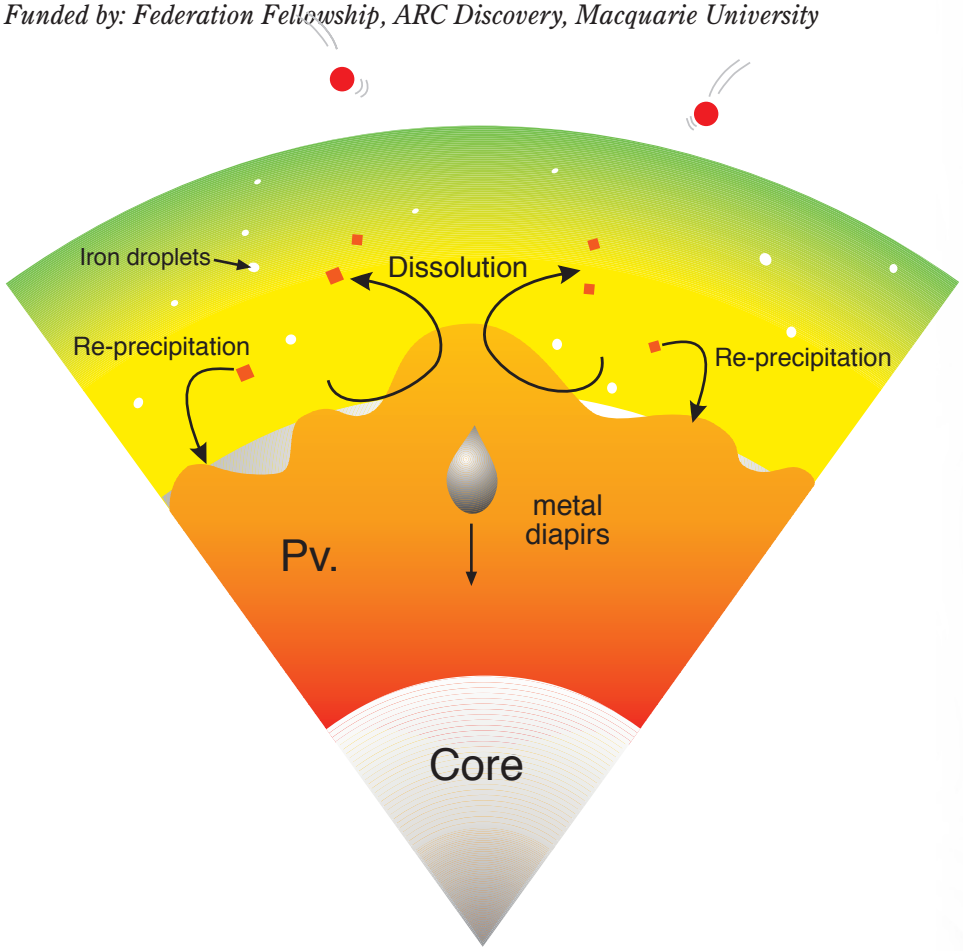

Figure 2. Cartoon illustrating the convective dissolution and reprecipitation of the high-pressure perovskite phase. As the Pv sequesters Fe^{3+} native iron (melt) is formed and sinks into the core.

Nickel Sulfide Deposits – Developing New Exploration Tools

A LARGE PROPORTION OF THE WORLD'S NICKEL PRODUCTION comes from deposits of Fe-Ni-Cu sulphides within mafic/ultramafic intrusions and flows, e.g. komatiites and komatiitic dunite bodies. The Norseman-Wiluna Greenstone Belt (NWGB), Yilgarn craton (Western Australia), is one of the world's major nickel provinces, containing over ten million tons of nickel metal, and hosts two of the world's largest komatiite/komatiitic dunite-hosted Ni-Cu-(platinum-group element: PGE) deposits. Since the first nickel boom in the 1970s exploration for more world-class deposits has continued – but the complex deformation and metamorphism of the NWGB make it difficult to understand the stratigraphic relationships and the processes responsible for Ni-Cu-(PGE) ore localisation.

A long-standing goal of research on komatiite-associated nickel-sulfide (NiS) deposits has been the development of lithogeochemical indicators that can guide exploration. Such indicators have two purposes: 1) to discriminate mineralised from barren komatiite belts, and 2) to identify vectors towards sulphide ores within mineralised sequences. Lithogeochemistry of komatiites is currently applied in NiS exploration in two distinct ways: indirectly, through identification of favourable geological environments, and more directly, through identification of signatures that record sulphide liquid segregation.

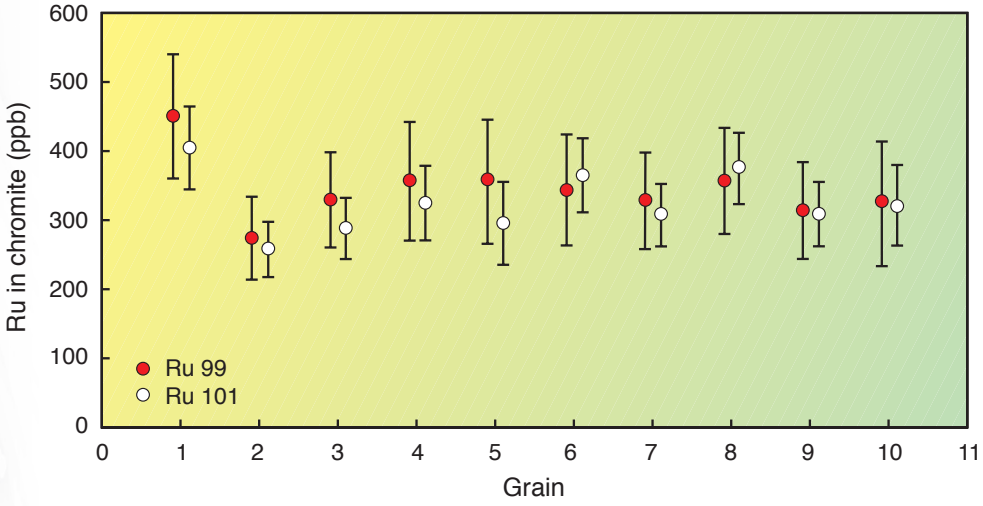

Figure 1. Ruthenium concentration in komatiitic chromite, calculated from the isotopes ^{99}Ru and ^{101}Ru. Each number represents one analysed grain. Constant Ru concentrations on the sample scale indicate that Ru occurs in solid solution, as micro-inclusions would cause scattered patterns.

The AMIRA P710A project was established to find out if the PGE distribution in mafic and ultramafic systems is related to NiS mineralisation, and to test the applicability and usefulness of PGE lithogeochemistry in the discrimination of barren and mineralised units. The project is a co-operation between GEMOC, the Centre for Exploration Targeting (CET) of the University of Western Australia and CSIRO Exploration and Mining, and is funded by BHP Billiton, Norilsk Nickel, Independence, and Meriwa.

GEMOC's contribution to this project builds on its expertise in understanding the behaviour of PGE in the mantle and its world-class micro-analytical facilities. We are investigating mechanisms of PGE fractionation in mafic and ultramafic melts, to identify PGE signatures in oxides and silicates from S-undersaturated systems and develop vectors towards the sulphur-saturated part of a system, where NiS mineralisation might occur. The study started with komatiites, representing the most primitive magmas, and will move to more fractionated magma types, such as komatiitic basalts, ferropicrites and dolerites.

The generally accepted model for NiS ore-formation in komatiitic systems requires the interaction of a sulphide liquid with a silicate melt. As PGE (Os, Ir, Ru, Rh, Pt, Pd) partition very strongly into sulphides, the remaining silicate melt will be depleted in PGE. A depleted whole-rock PGE signature might reflect interaction with a sulphide liquid, and the degree of depletion might increase towards NiS mineralisation. However, the PGE contents of melts reflect many factors, including parental magma composition, initial sulphur content, oxygen fugacity and wall-rock contamination, so a PGE-depleted signature may not necessarily reflect segregation of sulphides. Therefore, all lithogeochemical vectors currently used in exploration for komatiite-hosted NiS deposits provide inconclusive and contradictory results. Rather than using absolute levels of PGE, sulphide segregation might be recognised by using correlations of the PGE with elements that record the evolution of the magmatic system. Instead of interpreting whole-rock signatures, this study will directly use PGE signatures in primary magmatic phases (e.g. chromite and olivine) to determine if a system equilibrated with sulphides and formed a NiS deposit.

Komatiitic flow field in the Norseman-Wiluna Greenstone Belt near Kambalda (Yilgarn Craton, Western Australia).

For this purpose, a method for the *in situ* analysis of Ru in chromite by Laser Ablation ICP-MS is being developed to provide the industry with a fast but precise analytical technique in the exploration for NiS deposits. The initial results show the first convincing evidence that Ru exists as solid solution in komatiitic chromite (Figs. 1 and 2) – and suggest we can recognise chromites from barren and mineralised sequences using the Ru concentrations in chromite.

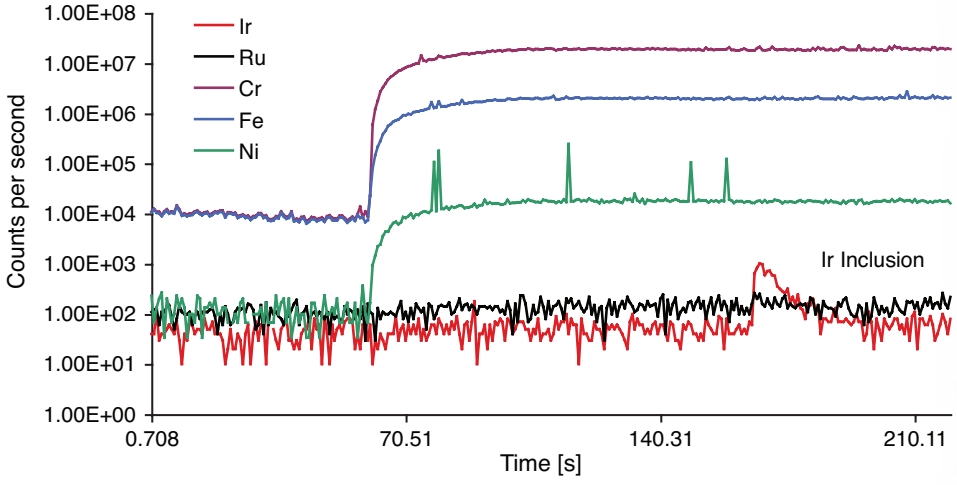

Figure 2. Time-resolved signals for several elements in a chromite from a komatiitic basalt, during a LAM-ICPMS analysis. An easily detectable Ir micro-inclusion less than 1 µm in diameter (black line) does not affect Ru abundance (red line), indicating that Ru is in solid solution in the chromite.

Contacts: Marek Locmelis, Norman Pearson, Suzanne O'Reilly, Marco Fiorentini
Funded by: Macquarie University iMURS, ARC Linkage, Industry

Crust-mantle evolution in NW Spitsbergen: Re-Os, U-Pb and Hf isotope data

SPITSBERGEN, THE LARGEST ISLAND OF THE SVALBARD ARCHIPELAGO, is located in the northern Arctic Ocean. The Svalbard archipelago lies near the north-west margin of the Eurasian plate and represents an uplifted part of the submerged Barents Shelf. The NW tip of Spitsbergen is fertile ground for studying the evolution of the uppermost mantle and continental crust during continental breakup. The exposed crustal rocks are metamorphosed igneous rocks of the NeoProterozoic to Caledonian Hekla Hoek Group. Xenoliths derived from the mantle and lower crustal are abundant in Holocene basaltic flows and pyroclastics that make up the Bockfjord Volcanic Complex. *In situ* isotopic techniques have been used to date thermal events in the upper crust (zircons from glacial streams), lower crust (zircons in granulite xenoliths) and upper mantle (sulfide inclusions in mantle xenoliths).

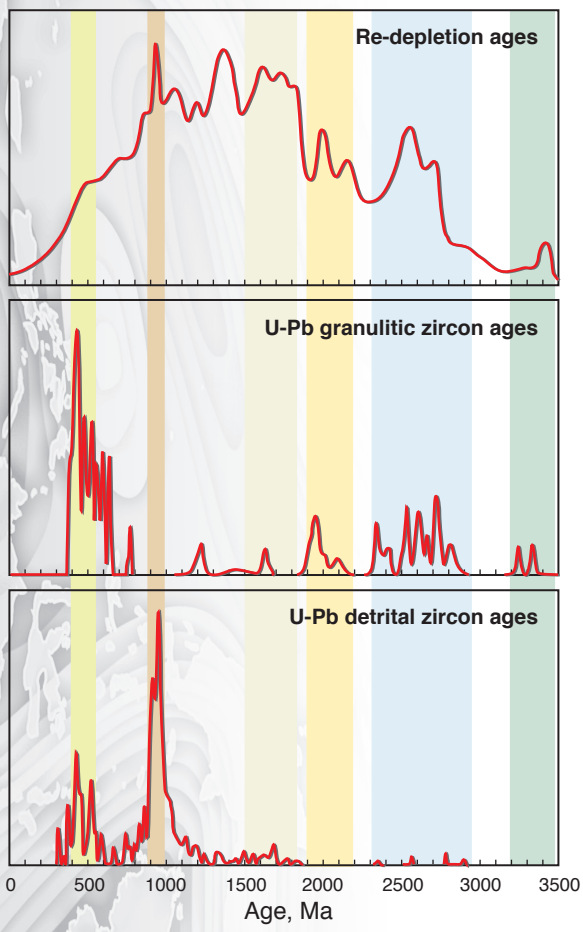

Figure 1. Thermal events recorded in sub-continental lithospheric mantle, lower upper continental crust under NW Spitsbergen, revealed from in situ Re-Os, U-Pb and Hf isotope data.

In situ U-Pb and Hf-isotope analysis have been performed on detrital zircon grains collected from outwash streams of the Adolfbreen Glacier, which drain a large area of outcropping Hekla Hoek formation. The most significant age population is Grenvillian (*ca* 0.94 Ga), and the Paleozoic component is surprisingly small, considering that Svalbard was affected by the Caledonian Orogeny (*ca* 0.41-0.32 Ga) with a climax in Silurian time. There are some scattered mid-Proterozoic ages, and a few grains with Archean ages (*ca* 2.9-2.3 Ga). On the age data alone, we could suppose that the crust is relatively young. However, the Hf isotope compositions of the zircons (Fig. 2) show that the Grenville and Caledonian zircons crystallised from magmas that were derived largely from much older crust – ranging from Mid-Protoerozoic to Archean.

Zircon grains separated from the lower-crustal granulite xenoliths give an even more surprising story. There is a large Paleozoic population, but the Grenvillian population that is so prominent in the upper crust is absent. Instead, there are important populations in the Paleo-Proterozoic (2.0-2.5 Ga) and Archean (most 2.5-3.0 Ga, extending back to ca 3.3 Ga). The Hf isotopes indicate that juvenile crust was formed mainly in Archean time, whereas the Paleozoic magmatic event involved mixing between juvenile mantle-derived magmas and the ancient lower crust. The prominence of mafic lithologies suggests that basaltic magmas underplated the crust before and during the Caledonian orogeny.

In situ Re-Os analyses of sulfides in mantle-derived peridotite xenoliths give model ages ranging Early- Mid-Archean (*ca* 3.4 Ga) to Paleozoic (*ca* 0.4 Ga) (Fig. 1). The oldest sulfide populations (*ca* 3.4-3.3 Ga and 2.8-2.4 Ga) are preserved in the most depleted peridotites and are interpreted as minimum ages for the oldest melt-depletion events. They match the prominent older population of zircon ages in the lower-crustal xenoliths. Another sulfide population between *ca* 1.8-2.3 Ga has some equivalents in the zircon data from the lower crust, but upper- crustal ages in this range are rare. The sulfide populations between *ca* 1.8-1.3 Ga have few matches in the crustal ages from zircons, and may represent mixing between younger and

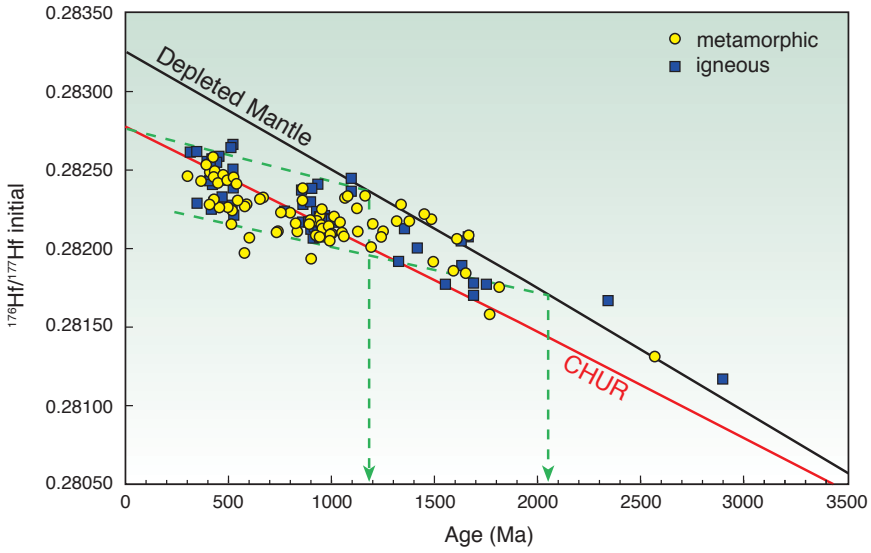

Figure 2. Hf-isotope data plotted against age, for zircons from Bockfjord. Sample taken in the outwash from Adolfbreen Glacier.

older sulfide generations. One significant age population (T_{MA} model age *ca* 0.94 Ga) correlates with the major Grenvillian crustal tectonic event seen in the zircon data (Fig. 1). The youngest sulfide population (T_{RD} model age *ca* 0.52 Ga) may represent refertilisation of the lithospheric mantle by metasomatic fluids introduced in pre-Caledonian time.

The correlation between major mantle events recorded in the sulfide populations, and thermal events recorded by magmatic zircons, suggest that several of these tectonic events, involving magmatism and reworking of older crust, affected the whole lithospheric column in this region from at least the Early/Mid-Archean to the Caledonian time (Fig. 1). While the Grenvillean and Caledonian events have effectively reworked the upper crust, the Hf-isotope data, and the ages from the lower crust and mantle, show that the older lower crust and its underlying mantle lithosphere were preserved through these major orogenies.

Contacts: Nenad Nikolic, Suzanne O'Reilly, Bill Griffin
Funded by: iMURS, ARC Discovery (O'Reilly, Griffin et al.), EPS and MQ postgraduate grants

The view from Bockfjord: Sverefjell volcano to the left, the crags of the Hekla Hoek gneisses in the distance, and Adolfbreen Glacier pushing down to the sea.

Extreme plate tectonics

WHY DOES PLATE TECTONICS OCCUR ON EARTH and not on other terrestrial planets? How long has Earth had plate tectonics? Would exosolar super-sized Earths around other stars have plate tectonics?

These questions were the impetus for work completed at GEMOC this year exploring the conditions for plate tectonics through numerical simulations (see *GEMOC publication #497*). To understand plate tectonics, we must understand the coupling between the convecting mantle and rheologically complex tectonic plates. If the driving stresses generated by the engine powering plate tectonics - mantle convection - are larger than the resistive strength of the plate, then the tectonic plate can fail, a crucial requirement for functional plate tectonics. If not, then the planet's lid will remain stagnant, much like the surface of Mars or Venus today.

The studies used a combination of scaling arguments and numerical models to explore the transition of systems from stagnant-lid into active-lid (ie. plate tectonic) modes. We found that a critical factor is the depth to the brittle-ductile transition (BDT); along with the frictional strength of the lid, this determines the resistance of the lid to convection. The BDT is related to the thickness of the elastic lithospheric, which is a known quantity on most terrestrial planets and moons. This allowed a test of the theory against a spectrum of observed bodies in the solar system. Earth itself plots clearly on the plate tectonic side of the transition - a function of its powerful internal engine and water-weakened plates. Mercury, the Moon and Mars all have lithospheres that are too thick for their feeble mantles to budge. Mars may have been active in the distant past, but only if the surface was altered by liquid water. Venus lies close to the transition, consistent with suggestions it is in an episodic mode - oscillating between active and stagnant lid tectonics. Interestingly, Io and Europa also lie close to the transition. Rugged, tilted mountain ranges on Io and non-tidal ice cracking and evidence of a lithosphere on Europa both hint that these moons of Jupiter may experience more surface tectonism than previously thought.

How different might plate tectonics have been on the early Earth? Numerical modelling also allows us to explore the behaviour of tectonic plates under the extreme thermal conditions expected for the Archaean. Starting with a model for present-day plate tectonics, with the current mantle energy budget, we systematically ran simulations for similar mantle configurations, but with increasing heat production, simulating conditions in the past. Surprisingly, plate tectonics itself breaks down in the Archean. Instead the planet goes through a transition into an episodic subduction regime, where long periods of quiescence are interspersed with periods of rapid and violent subduction. The reason is that greater mantle heat production results in higher mantle temperatures. This makes the mantle convect faster, as expected. But the viscosity of the mantle is also a strong function of temperature, and the hotter mantle becomes "runny", so it cannot effectively transmit stress to the plates.

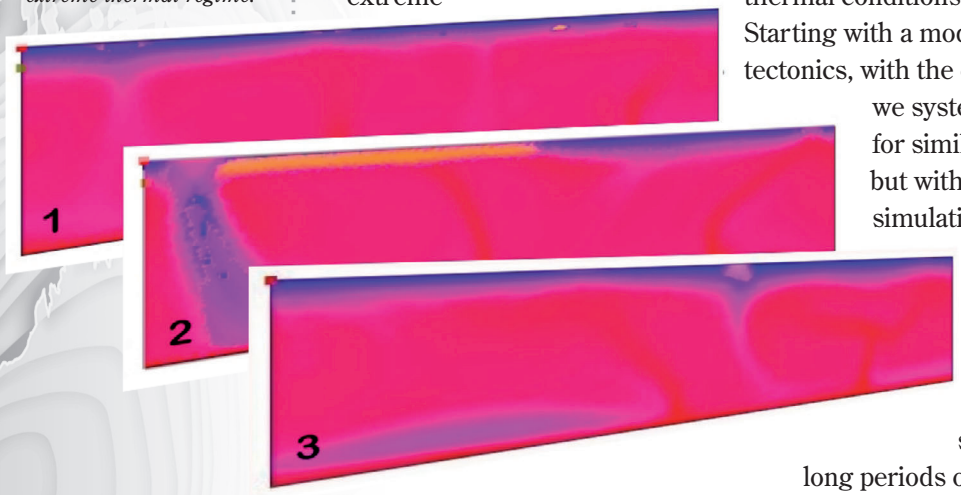

Figure 1. Simulations show that when pushed to extremes - either through heat, size or lithospheric strength - plate tectonics can break down and mantle convection enters a regime known as episodic overturn, where long periods of quiescence are interspersed with rapid subduction events, accompanied by large pulses of mantle melting and plate velocity. 1-3 shows snapshots of such an event (sowing temperature field and mantle melting). Earth may have been in such a regime in its early history due to the extreme thermal regime.

Could the Earth have operated this way? The Precambrian paleomagnetic record was reanalysed for evidence of this type of behaviour. Despite problems with the incomplete dataset, we found that Precambrian plate motions are in fact consistent with this sort of convection - which may explain many episodic features of the Precambrian geological record.

Finally, what happens if you take a planet in a plate-tectonic regime, and simply scale it to larger sizes? The problem is not trivial, and required a large suite of simulations. For larger planetary radii, and thus mass, mantle convection increases in vigour - a widely accepted result. What's more, the thickness of the lithosphere relative to the depth of the convecting mantle also decreases, and this would favour plate tectonics on giant terrestrial planets. However, there is an additional crucial factor in such systems. The brittle strength of rocks is pressure-dependent - as you go deeper into the Earth, the brittle strength of rocks increases substantially. On planets with masses larger than Earth's, and thus greater gravity and internal pressures, this effect will be even more dramatic, to the point where the surface plates will simply lock up. This regime change - from plate tectonics to stagnant lid - was dominant for the parameter range explored in our models. On Earth, plate tectonics acts as a regulatory mechanism for many atmospheric and hydrological systems, and thus the evolution of life on Earth is probably intimately tied to its tectonic regime. On super-sized versions of Earth without plate tectonics, the chances of life would be quite a bit slimmer.

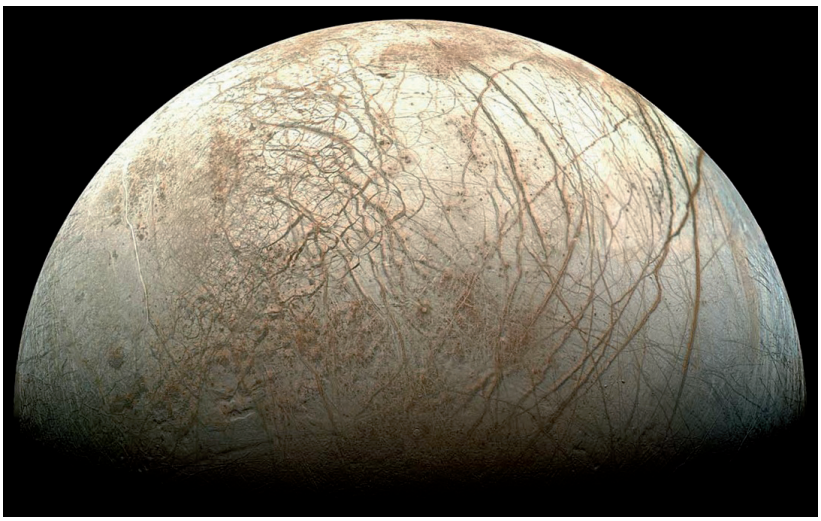

Figure 2. The study predicts that a number of smaller worlds, such as Europa (shown here), may in fact be in an episodic overturn regime, and provide evidence for active tectonism on other planetary bodies. The gradual thickening of Europa's lithosphere over the last 80 Myr, and the distribution of non-tidal surface fracture systems, support this idea. Credit: JPL.

Plate tectonics is a fundamental feature of the dynamic Earth system, but taken to extremes - either deep in the past, or for larger sized planets - it can break down, and the stability of such systems should not be taken for granted.

Contact: Craig O'Neill
Funded by: MQRF

Laser Microprobe -ICPMS U-Pb dating of groundmass perovskite from kimberlites

KIMBERLITES FORM A CLAN OF VOLATILE-RICH POTASSIC ULTRAMAFIC ROCKS that exhibit an inequigranular texture resulting from the presence of phenocrysts, xenocrysts and xenoliths set in a fine-grained matrix formed mainly of olivine, perovskite, spinels, diopside, monticellite, apatite, calcite, serpentine and/or phlogopite. The common methods of dating of kimberlites use U-Pb analysis of zircon and Rb/Sr on mica (phlogopite). Zircon ages may be older than the emplacement age of the kimberlite as zircon is not a groundmass mineral but occurs as xenocryst in kimberlite. Mica can occur as both xenocryst and groundmass phase in kimberlite. The dating of mica therefore may result in mixed ages (from combining different types of mica) or a cooling/resetting age due to the alteration of mica by late fluids.

This research focussed on development of a rapid and robust method of dating kimberlites using groundmass perovskites in thin sections (*GEMOC Publication #505*). Perovskite is one of the late-stage minerals to crystallise from the kimberlitic magma. It is found as individual crystals or overgrowths on minerals such as ilmenite. Since it is a main carrier of U and Th in the kimberlite, it offers the possibility of U-Pb dating, and because it is not an inherited mineral it is more likely to yield the emplacement age of the kimberlite.

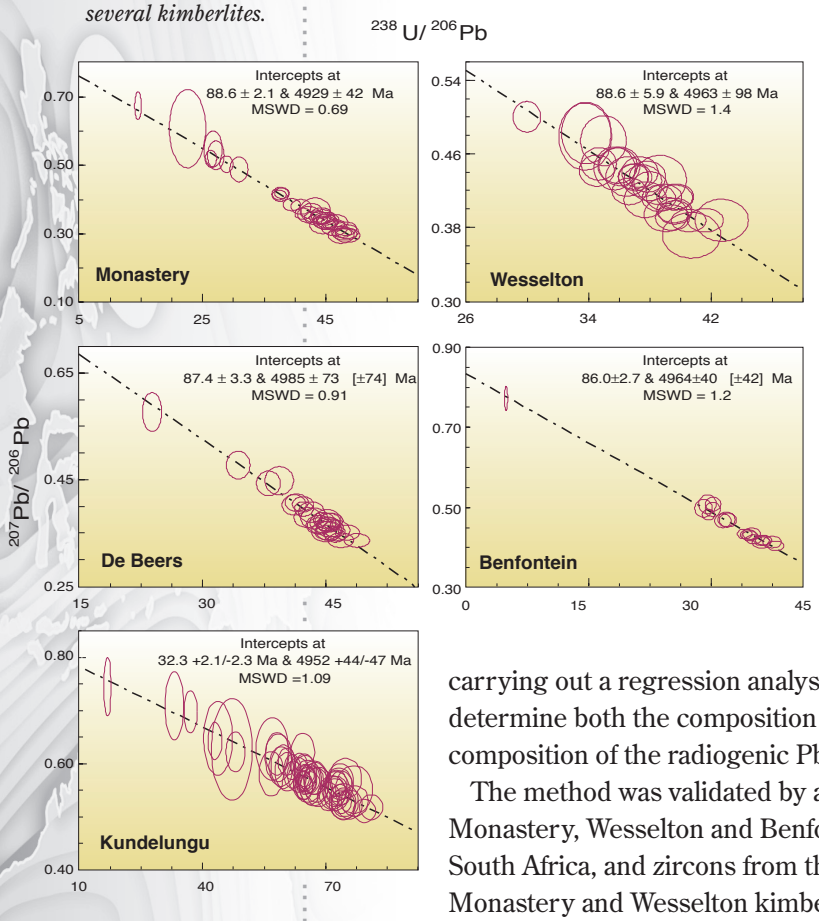

Figure 1. Inverse-concordia (Tera-Wasserburg) plots showing perovskite U-Pb analyses for several kimberlites.

The analytical techniques used are identical to those used for LAM-ICPMS U-Pb dating of zircon. The ablation is done in He which permits efficient sample transport, signal stability and reproducibility of U/Pb fractionation. Because there is no well-established perovskite standard, we used the zircon standard (GEMOC GJ-1, age 609 Ma) commonly used for zircon U-Pb dating.

Perovskite, unlike zircon, takes up significant amounts of Pb in its lattice during crystallisation, and the measured Pb-isotope composition is a mixture of this "initial Pb" and the radiogenic Pb produced by decay of U and Th. We have corrected for the initial Pb content by analysing a large number of grains, and carrying out a regression analysis in the inverse-concordia plot (Fig. 1) to determine both the composition of the initial Pb (upper intercept) and the composition of the radiogenic Pb (lower intercept; this gives the age).

The method was validated by analysis of perovskites from the De Beers, Monastery, Wesselton and Benfontein mines in the Kimberley District, South Africa, and zircons from the Monastery mine. The De Beers, Monastery and Wesselton kimberlites were previously dated respectively at 86 ± 3 Ma (K-Ar on micas), 90 ± 4 Ma (zircon U-Pb and Rb-Sr on whole-rock samples) and 90 ± 3 Ma (zircon U-Pb).

Perovskite ages for the De Beers, Monastery, Wesselton and Benfontein kimberlites are respectively 87.3 ± 3.3 Ma (n = 22; MSWD = 0.91), 88.6 ± 2.1 Ma (n = 32; MSWD = 0.69), 88.6 ± 5.9 (n = 31; MSWD = 1.4) and 86.0 ± 2.7 (n = 19; MSWD = 1.2) (Fig. 1). Zircons from the Monastery kimberlite give an age of 88.4 ± 0.9 Ma age (n = 18; MSWD = 0.76). These ages compared to those determined by different

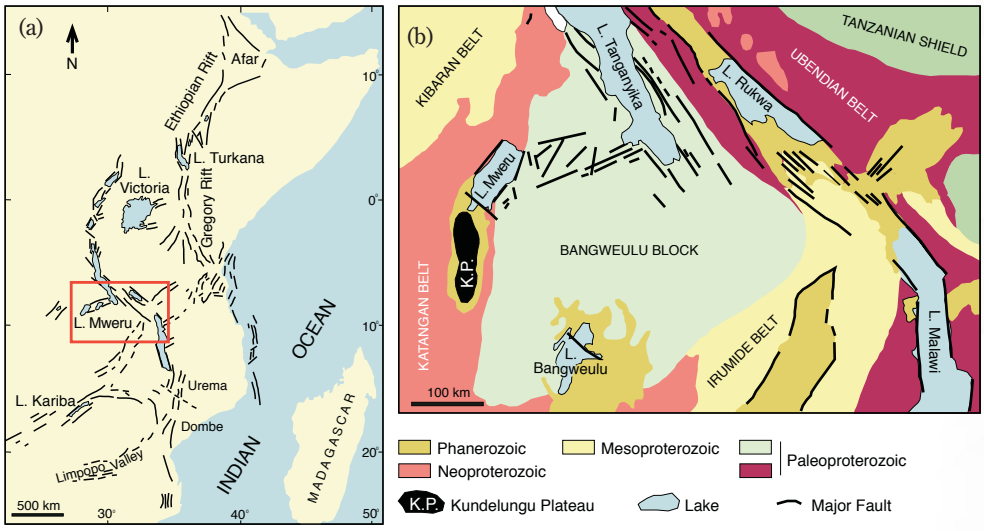

Figure 2. (a) Regional rift system in eastern Africa. Box shows area of Figure 2b. (b) Geological sketch map showing setting of the Kundelungu Plateau (KP), which is intruded by the Kundelungu kimberlites.

methods clearly support the robustness and accuracy of the method. This also indicates that the use of a zircon standard for U-Pb dating of perovskite gives robust results. The Kundelungu kimberlites (SE Congo) were dated at 32.3 ± 2.2 Ma (lower Oligocene), making them perhaps the world's youngest true kimberlites.

The $^{207}Pb/^{206}Pb$ of the initial-Pb component derived from the upper intercepts of the regression lines (see Fig. 1), 0.831 ± 0.022 for Kimberley and 0.813 ± 0.022 for Kundelungu, are similar to the values estimated for the bulk silicate Earth at around 80 Ma (0.851 ± 0.019) and 30 Ma (0.844). The value found for Group I kimberlites from Kimberley District is consistent with the average (0.80 ± 0.1) whole-rock Pb isotope composition of other Group I kimberlites in South Africa. This suggests that these kimberlites have entrained much of their lead content from the lithospheric mantle prior to crystallisation.

Kimberlites may also provide information on the regional tectonics at the time of their emplacement, as kimberlite magmatism is triggered by relatively weak extensional stresses affecting the lithosphere. The age distribution of the kimberlite intrusions may thus shed light on the tectonic evolution of the region. The age of the Kundelungu kimberlites corresponds to the initiation of the East African Rift, which has been dated at 43 Ma in Ethiopia, at 33-25 Ma in Kenya and Yemen and at 36 Ma in the Lake Turkana region (Fig. 2). The Kundelungu kimberlites are the youngest known in the continent. This implies the southward extension of the initial phase of the opening of the East Africa Rift. The Mweru Lake graben in the northern part of the Kundelungu Plateau (Fig. 2) is correlated with this early stage of the rift.

Contacts: Jacques Batumike, Sue O'Reilly, Bill Griffin, Elena Belousova
Funded by: iMURS, ARC-DP, MQ International Grant, EPS Postgraduate Fund

Figure 3. Jacques Batumike selecting kimberlite samples in SE Congo.

Sino-Australian connections 1 billion years ago?

THE CONTEMPORARY CLOSE RELATIONSHIP between Australia and China can be confidently traced back to Paleozoic times with overwhelming evidence from fossil flora and fauna and paleomagnetic data. The evidence demonstrates that several major terranes of China, including the Yangtze and Cathaysian blocks in South China and the North China Craton, were connected to Australia as a part of Gondwanaland, a super-continent that broke up about 250 million years ago. However, the location of China, and especially the South China Block (SCB), relative to the other micro-continents within the Rodinia super-continent during Neoproterozoic times remains a contentious issue; several models have placed the SCB as a "missing link" between Australia and Laurentia but in different ways (see *Li et al., Precambrian Research, 160, p. 179-210, 2008* for a summary). The paleomagnetic data do not provide unique information on the paleolongitude, nor are stratigraphic comparisons between relevant terranes definitive. Further independent evidence is required to constrain the models.

Comprehensive studies of U-Pb geochronology and Lu-Hf isotopic systematics on detrital zircons from latest-Neoproterozoic (Sinian) sedimentary rocks of the Cathaysia block in South China have been carried out using GEMOC's laser ablation technology (*GEMOC publication #518*). The detrital zircons show a range of ages and compositions, with a significant Grenvillian (ca 1 Ga) population. This suggests that there was once a Grenvillian orogenic belt, probably developed on a Neoarchean basement, along or close to the southern part of the Cathaysia block.

Minor Eo- to Meso-archean (~3.8 Ga, 3.3-3.0 Ga, ~2.5 Ga) and Mesoproterozoic (1.7 - 1.4 Ga) detrital zircon populations contained in the Sinian sediments may represent exotic input, probably derived from other continents previously linked with the South China block. U-Pb age spectra and Hf isotope compositions of the zircons indicate that they most likely came from India and East Antarctica. Comparisons with the tectono-magmatic history and compositions of crustal rocks in western Laurentia - eastern Australia and Eastern India - East Antarctica also suggest that these Chinese late Neoproterozoic sediments may have originated mainly from Eastern India and/or East Antarctica. This indicates that the South China Block was linked with the Eastern India - East Antarctica continents in the late Neoproterozoic rather than being located between the western Laurentia and eastern Australia continental blocks.

Therefore, U-Pb and Hf-isotope studies on detrital zircons provide an important

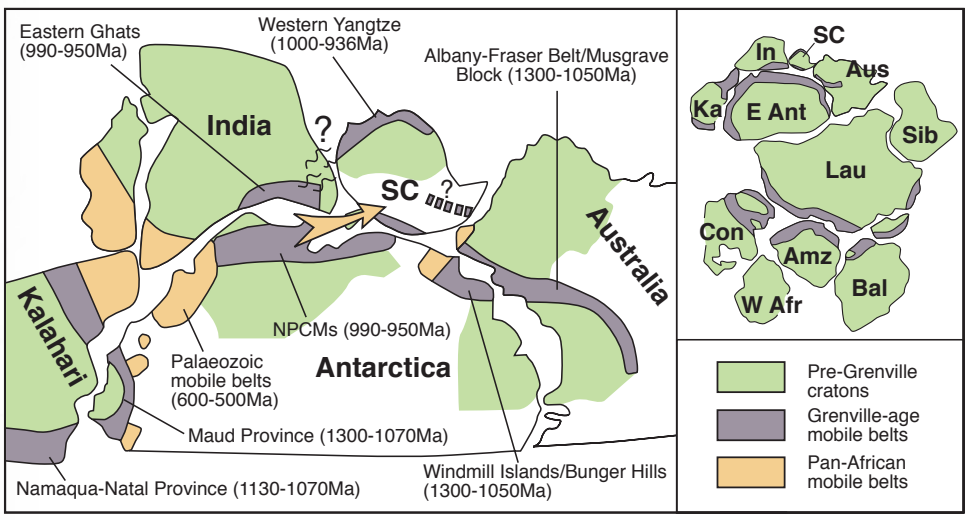

Figure 1. Reconstruction of Rodinia, with focus on the relationship between South China Block and other Rodinian terranes.

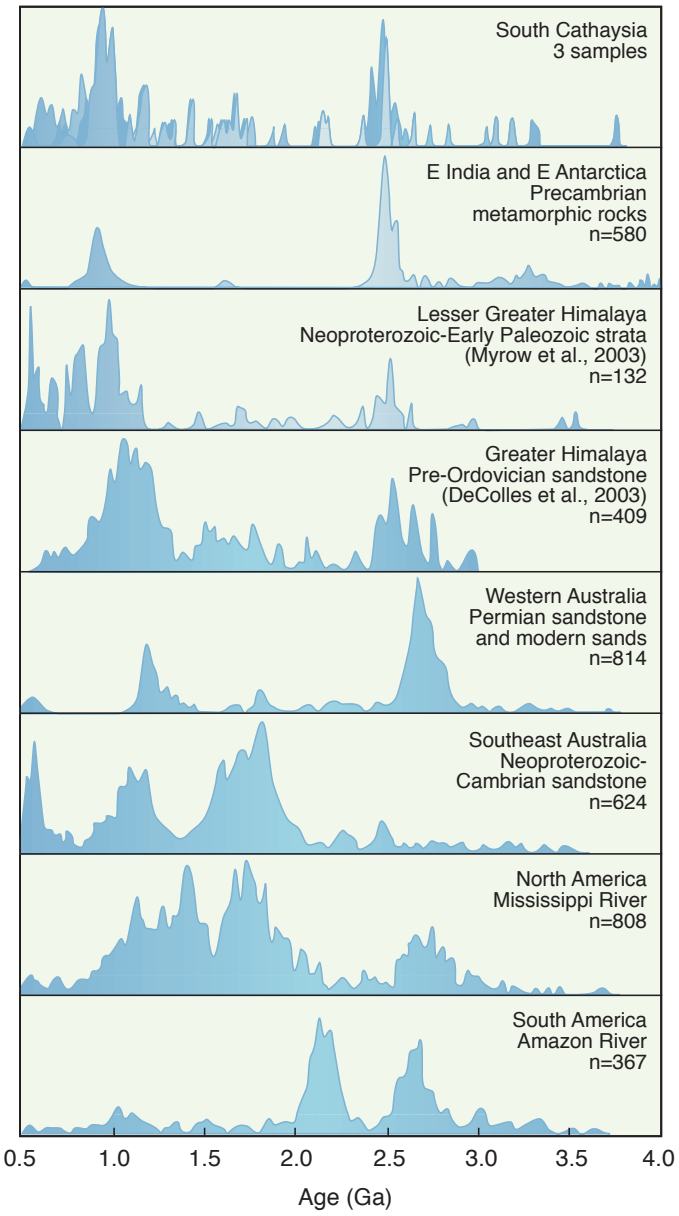

independent constraint on the palaeogeography of the South China Block in the context of the breakup of Rodinia and the subsequent assembly of Gondwana in late Neoproterozoic time, and also give insights into the historical links between the South China Block and various Australian terranes.

Figure 2. Zircon $^{207}Pb/^{206}Pb$ ages for the South China Block and other relevant locations.

Contacts: Sue O'Reilly, Bill Griffin, Ming Zhang, J-H. Yu (Nanjing)
Funded by: ARC Discovery, ARC International, NSF China, Nanjing University funds

10 years of MC-ICPMS: linking the crust and mantle

Modern geochronology has moved beyond the acquisition of dates; the goal is to understand the significance of these numbers for the geodynamic evolution of Earth at all scales. The coupling of the laser-ablation microprobe (LAM) to inductively-coupled plasma mass spectrometers (ICPMS, multicollector (MC)-ICPMS) has revolutionised geochronology and geochemistry over the last decade. These systems enable the rapid and precise *in situ* analysis of trace-element patterns and isotopic systems, while adding information related to microstructural context and major-element composition. The integration of these multiple sources of data is crucial in constraining the origin of the sample and the processes leading to its formation, so that we can understand the meaning of a date in terms of geological events.

GEMOC INTRODUCED THE MULTI-COLLECTOR ICPMS TO AUSTRALIA IN 1998, adding a second instrument in 2003. As the operation of the MC-ICPMS laboratory at GEMOC enters its tenth year it is an appropriate time to review the advances this technology has brought to isotope geochemistry and geochronology. The most significant impact has been the development of high precision *in situ* isotope ratio measurements for a range of geologically important isotopic systems (e.g. Rb-Sr, Nd-Sm, Lu-Hf, Re-Os). The way had been paved by the coupling of the laser ablation microprobe (LAM) to the single-collector quadrupole ICPMS to provide *in situ* analysis of trace element patterns and isotope ratios (e.g. U-Pb dating of zircon).

The introduction of the second generation sector-field MC-ICPMS instruments brought a number of advantages over the quadrupole ICPMS, including simultaneous detection, flat-topped peaks and greater sensitivity. All of these factors contributed to the more precise measurement of isotope ratios and made the results from the MC-ICPMS directly comparable with those obtained on the more conventional thermal ionisation mass spectrometers (TIMS). The MC-ICPMS has two great advantages over TIMS: (1) due to the high efficiency of the ICP source to ionise refractory elements, the MC-ICPMS has become the instrument of choice to investigate mass-dependent isotopic fractionation of stable isotopes of light and heavy metals (e.g. Li, Mg, Fe, Cu, Mo, Tl); (2) a LAM system can be coupled to the MC-ICPMS for *in situ* high-precision microanalysis of isotopic ratios.

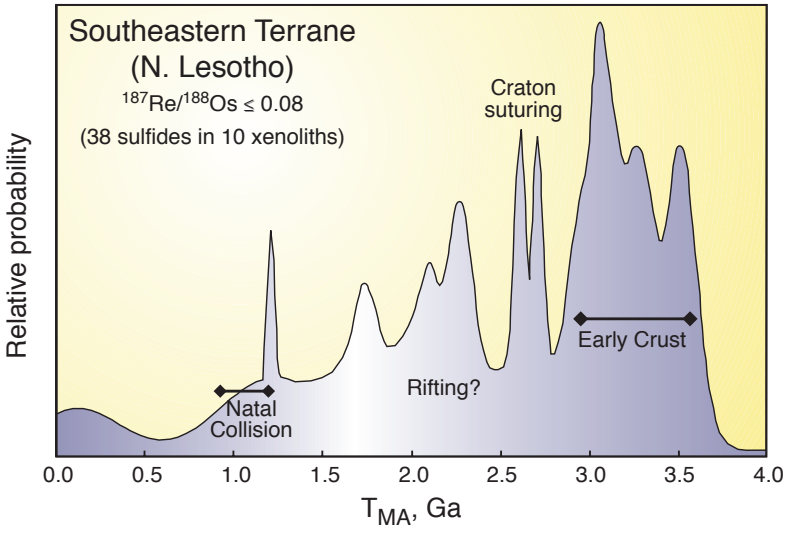

Figure 1. Re-Os model ages of sulfide grains in xenoliths from Northern Lesotho kimberlites, showing correlations with known tectonic events.

The impact of *in situ* isotope ratio analysis has advanced modern geochronology beyond the acquisition of dates. Not only does the method provide rapid and precise data, but it puts these data in a microstructural framework and allows integration with datasets produced by other microanalytical techniques. The integration of these multiple sources of data gives better constrants on the origin of the sample and the processes that produced it, so that we can understand the meaning of a date in terms of geological events.

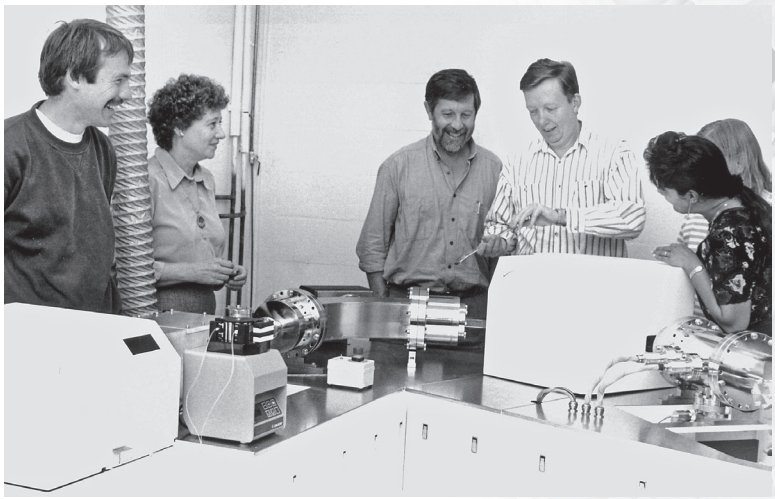

Simon Jackson, Sue O'Reilly, Bill Griffin, Norman Pearson, Ashwini Sharma and Carol Lawson at the inauguration of Australia's first MC-ICPMS (1998); Nu-05 is still in operation (photo from archives).

The two most significant developments in LAM-MC-ICPMS in the past decade have been the analysis of Lu-Hf isotopes in zircon and Re-Os isotopes in sulfides and PGE alloys. Zircon and the sulfide minerals are microscopic time capsules for the crust and mantle respectively, and the isotopic studies provide information about the evolution of each layer. By determining the timing of events in the crust and the underlying lithospheric mantle, linkages between crustal and mantle processes can be assessed and used to address key problems in geodynamics.

The analysis of Hf isotopes in igneous zircon by LAM-MC-ICPMS provides information on the sources of the parent magmas. The analytical method was first demonstrated by Thirlwall and Walder in 1995 but was not taken up again until GEMOC developed high-precision *in situ* analysis in 1999 (see *GEMOC publication #179*). The integration of the *in situ* Hf-isotope data on zircons with data on their morphology and internal structure (imaged by BSE/CL), U-Pb age and trace element composition rapidly led to the establishment of *TerraneChron*®. *TerraneChron*® is GEMOC's unique methodology for terrane evaluation and studies of crustal genesis. The combination of age, composition and sources of magma for a large number of grains is used to construct an "Event Signature" that gives a fingerprint of crustal evolution in the terrane. The *TerraneChron*® methodology typically is applied to zircons in drainage samples collected from a defined catchment. The use of drainage samples has many advantages for regional studies: nature has separated and concentrated a statistically more meaningful sample than is achievable by conventional single-rock sampling, thus giving a more comprehensive coverage of the rock types in the drainage region. This enables this type of remote-sensing mapping on a range of scales (10-1000 km^2) and in terrains ranging from mountainous (e.g. Himalayas, Andes) to alluvial plains (e.g. Yilgarn, WA; see *GEMOC publications #300, 385*).

On the global scale the combinaton of Hf-isotope data and age distributions can be used to distinguish between juvenile additions to the crust and upper-crustal rocks derived by reworking of older rocks. A compilation of results shows that since the late Archean, additions of juvenile crust have been small in comparison to the volume of reworked material. These types of data clearly are going to have a large impact on ideas about the rates of growth of the continental crust through time.

A major advance in the application of Re-Os to the mantle came with the

recognition that the Os budget of mantle-derived peridotites is controlled by trace sulfide phases, and that these rocks typically contain several generations of sulfide with widely differing Os contents and Re/Os. GEMOC pioneered the development of LAM-MC-ICPMS techniques for the *in situ* analysis of Os isotopes in individual sulfide grains and showed that different sulfide generations also have widely varying Re/Os and $^{187}Os/^{188}Os$ (see *GEMOC publications #267, 290; Fig. 1*). The implication is that whole-rock Os-isotope analyses of sulfide-bearing peridotites must represent mixtures of components with different ages and isotopic compositions. In such cases, the model ages of these rocks can only be regarded as minimum estimates of melt-depletion ages, and are unlikely to date any particular event (see *GEMOC publication #326*).

Sue O'Reilly, PhD students and overseas visitors surround Nu-05 in 2005 (photo from archives).

The development of these analytical techniques over recent years has made it possible to compare the large scale evolution of the crust and the history of its underlying mantle, where xenolith-bearing volcanic rocks are available. Studies linking crustal and mantle evolution in cratonic settings, young fold belts and rift zones (see *Spitsbergen Research Highlight*) demonstrate the potential of this approach to shed light on continental generation, modification and destruction.

Deep-seated events are commonly mirrored in the crust; Os model-age spectra from xenolith suites show age "peaks" that correspond to the ages of thermal/tectonic events in the overlying crust, suggesting strong linkages between crust and mantle (Fig. 1). Integrated studies of the timing and nature of crustal and mantle events, using these techniques, will be important for understanding the large-scale dynamics of the Earth.

Contacts: Norman Pearson, Bill Griffin, Sue O'Reilly
Funded by: ARC, DEST SII, Macquarie University and Industry

How much potassium is in the Earth's core?

THE PRESENCE OF POTASSIUM IN THE CORE is a vexing issue in Earth Science. The inner dynamics of our planet depend largely on how much energy is stored in its core. Crystallisation of the inner core, generation of the magnetic field and convection in the outer core and mantle are intimately linked to the amount of heat present in the core. Accurately describing the heat budget of the core depends on an accurate determination of the concentration of heat-producing elements. A significant amount of these elements would permit much slower rates of cooling and inner-core growth.

The presence of potassium (K) as a significant radioactive element in the core was suggested over three decades ago. However, despite numerous theoretical and experimental studies, it is still not clear whether K actually is present in the core. In particular, previous experimental studies on K partitioning between metallic and silicate liquids have yielded contradictory results concerning the fate of K during the favoured scenario of core formation in a deep silicate-magma ocean. Experimental and analytical artefacts, large extrapolation to appropriate conditions of high pressure and high temperature and the use of oversimplified chemical compositions in these studies have cast doubt on previous experimental results.

Research at Macquarie University and the Carnegie Institution of Washington (see *GEMOC publication #455*) has provided new experimental data for the partitioning of potassium in a chemical composition relevant to models of Earth's differentiation. Experiments were carried out at 2200 °C and 7.7 GPa to equilibrate a silicate melt of primitive mantle composition (fertile peridotite) with a variety of Fe–Ni–S–C–O molten alloys. As shown in Figure 1, these new data reveal a negligible effect of pressure and temperature on the partition coefficient (D_K, the weight ratio of K content in the alloy over K content in the silicate), at least over the P-T conditions of the study. These observations contrast with recent predictions based on published data, which suggest a systematic increase of K solubility in the alloy with temperature (Fig. 1). Our experimental work also indicates that the K solubility is not directly affected by the S and C contents of the alloy. However, there may be an increase in the K partition coefficient with increasing O content in the molten alloy (Fig. 2). Overall, these new results, which are appropriate for modelling core formation in a shallow magma ocean, suggest that appreciable amounts of K are unlikely to be sequestered into Earth's core during a magma-ocean event unless oxygen is a major component in the light element budget of the core.

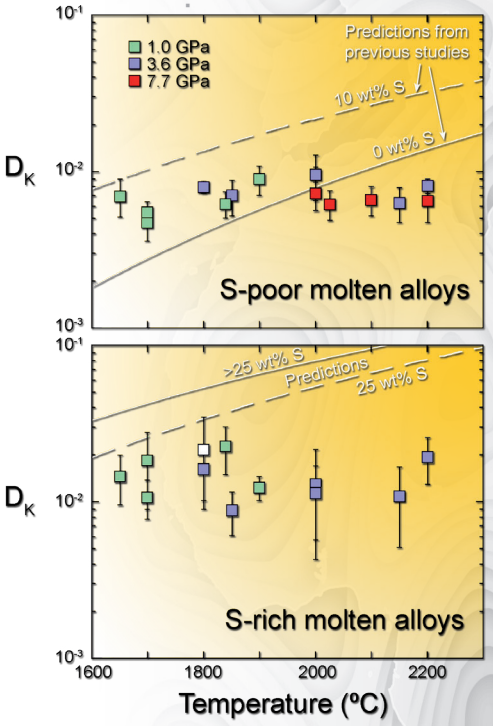

Figure 1. Partition coefficients for potassium (D_K) shown as a function of temperature. In white, data and predictions from the literature. Our new data indicate that there are no significant pressure and temperature effects on K partitioning contrary to recent predictions.

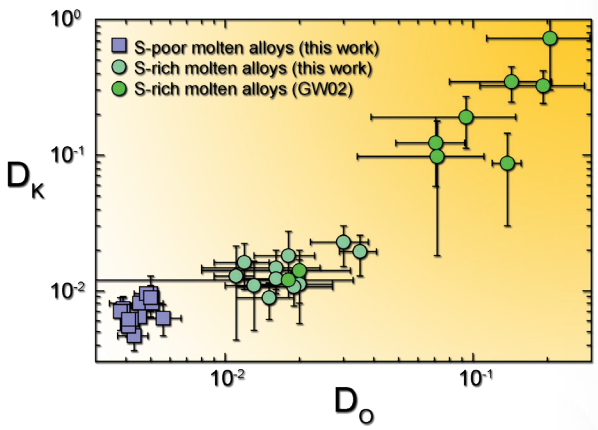

Figure 2. Potassium partition coefficient plotted as a function of oxygen partition coefficient. The observed correlation suggests that O may have a significant effect on K solubility in molten alloy.

Contact: Alexandre Corgne
Funded by: ARC, Carnegie Institution of Washington, NASA and NSF

Heat sources in mantle plumes

MELTING ANOMALIES IN THE EARTH'S UPPER MANTLE have often been attributed to the presence of mantle plumes that may originate in the lower mantle, possibly from the core-mantle boundary. Globally, mantle plumes exhibit a large range in buoyancy flux that is proportional to their temperature and volume. Plumes with higher buoyancy fluxes should have higher temperatures and experience higher degrees of partial melting. Excess heat in mantle plumes could reflect either a) an enrichment of the heat producing elements (HPE: U, Th, K) in their mantle source leading to an increase of heat production by radioactive decay or b) advective or conductive heat transport across the core-mantle boundary. The advective transport of heat may result in a physical contribution of material from the core to the lower mantle. A contribution of material from the core should result in higher Fe concentrations and coupled enrichments in $^{186}Os/^{188}Os$ and $^{187}Os/^{188}Os$ relative to the upper mantle (Fig. 1). If plumes are generated purely by differences in their chemistry (e.g. by varying HPE content), then increased abundances of U, Th, and K would lead to increased temperatures and, in turn, to higher buoyancy fluxes (Fig. 1).

Geophysical and dynamic modelling indicate that at least the Afar, Easter, Hawaii, Louisville and Samoa plumes may all originate at the core-mantle boundary. These plumes encompass the whole range of known buoyancy fluxes from 0.9 Mgs^{-1} (Afar) to 6.5 Mgs^{-1}

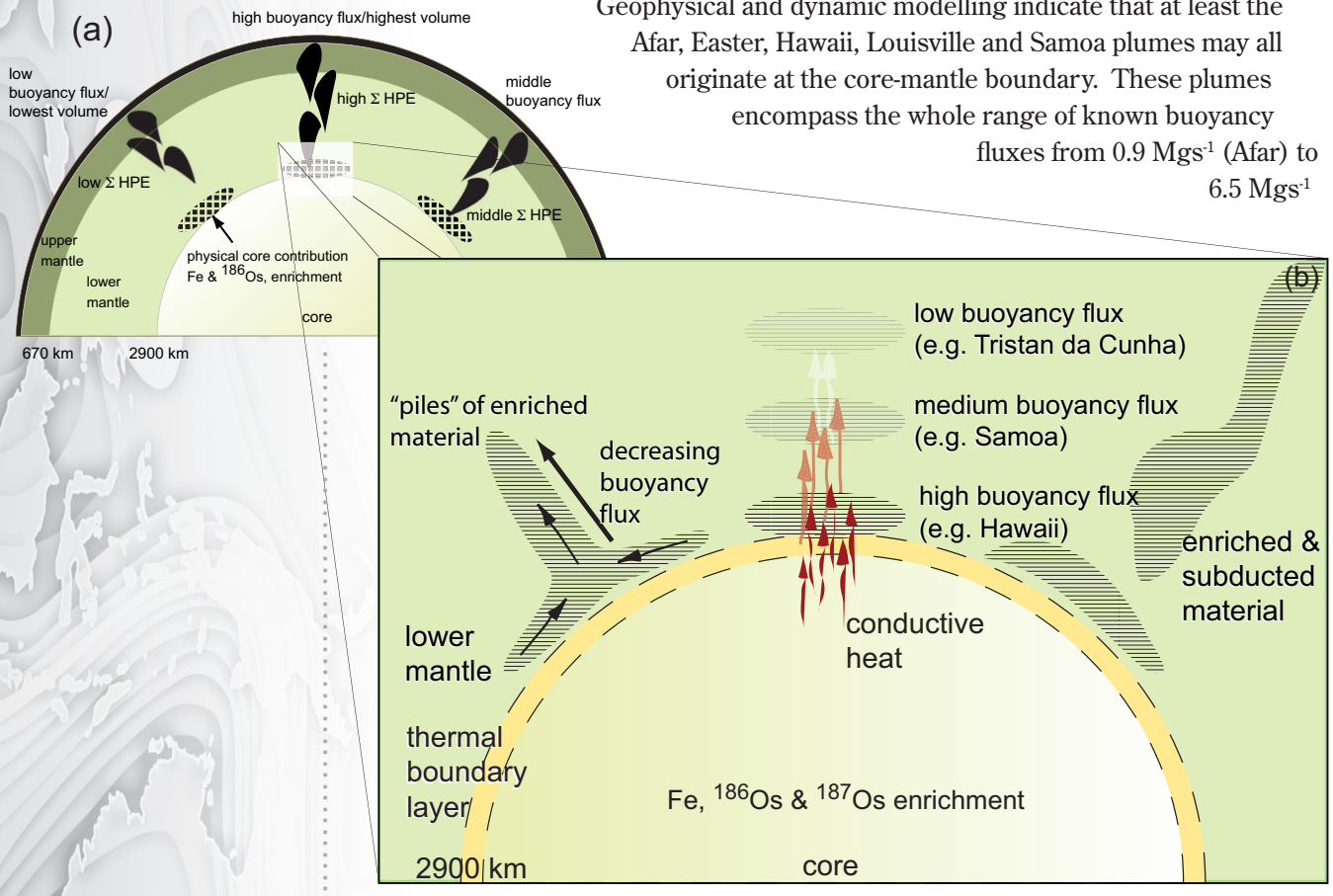

Figure 1. Model of possible effects leading to the formation and rise of mantle plumes. A physical, i.e. material, and hence, heat contribution from the core would be reflected in increased Fe, ^{186}Os and ^{187}Os, whereas a formation of mantle plumes as a result of increased concentrations of U, Th and K has been ruled out by a lack of correlation between HPE and buoyancy flux. It is most likely conductive heat transport from the core towards the mantle leads to the rise of enriched material. It has to be taken into consideration that the core-mantle boundary topography is irregular (Garcia and Souriau, Physics of The Earth and Planetary Interiors, 2000), but we suggest that the relative distance to the outermost core is the main factor of the conductive heat contribution to triggering plume generation. The formation of "piles" of enriched material may be consistent with our model, i.e. the relative distance to the core-mantle boundary may control the plume's excess heat largely independently of the shape of the enriched material along the core-mantle boundary. Not to scale.

(Hawaii) providing evidence that the buoyancy flux is largely independent of other geophysical parameters.

Major element, trace element and radiogenic isotope data for all available intraplate volcanic settings with published buoyancy fluxes (Sleep, JGR, 1990) were used in our analyses. We used the compiled GEOROC database (http://georoc.mpch-mainz.gwdg.de/georoc/) for all of our geochemical data except from the Azores. Data from the Azores were taken from a separate existing dataset. Only alkaline samples (>2 wt.% K_2O+Na_2O at 45 wt.% SiO_2 with >5 wt.% and <20 wt.% MgO were taken into consideration to avoid extended assimilation and fractional crystallisation effects. To minimise possible effects of mixing between depleted and enriched compositions, we focused on alkaline basalts rather than tholeiites. All alkaline data were fractionation-corrected to 10 wt.% MgO using a logarithmic fit.

We find that the fractionation-corrected heat producing elements (U, Th and K) and Fe are not correlated with buoyancy flux/upwelling rate (Fig. 2). This provides evidence that the excess temperatures in plumes require additional heat contribution rather than a chemical source heterogeneity. The lack of correlation between buoyancy flux and the possible core contributing tracer Fe tentatively suggests that the heat contributed may not be related to advective heat flow from the core, but may be a result of conductive heat transport from the core into the lower mantle.

The formation of thermochemical piles (Fig. 1) as proposed by geodynamic models is consistent with a heterogeneous distribution of enriched material along the core-mantle boundary and would also help to explain differences in buoyancy fluxes, where smaller piles (e.g. Azores, Canary islands) will have less internal heat, slightly higher viscosity, and hence less conductive heat transport, leading to a lower buoyancy flux than larger piles with more internal heat production, lower viscosity and higher heat contribution from the core (e.g. Hawaii).

Contact: Christoph Beier
Funded by: Humboldt Foundation, Macquarie University

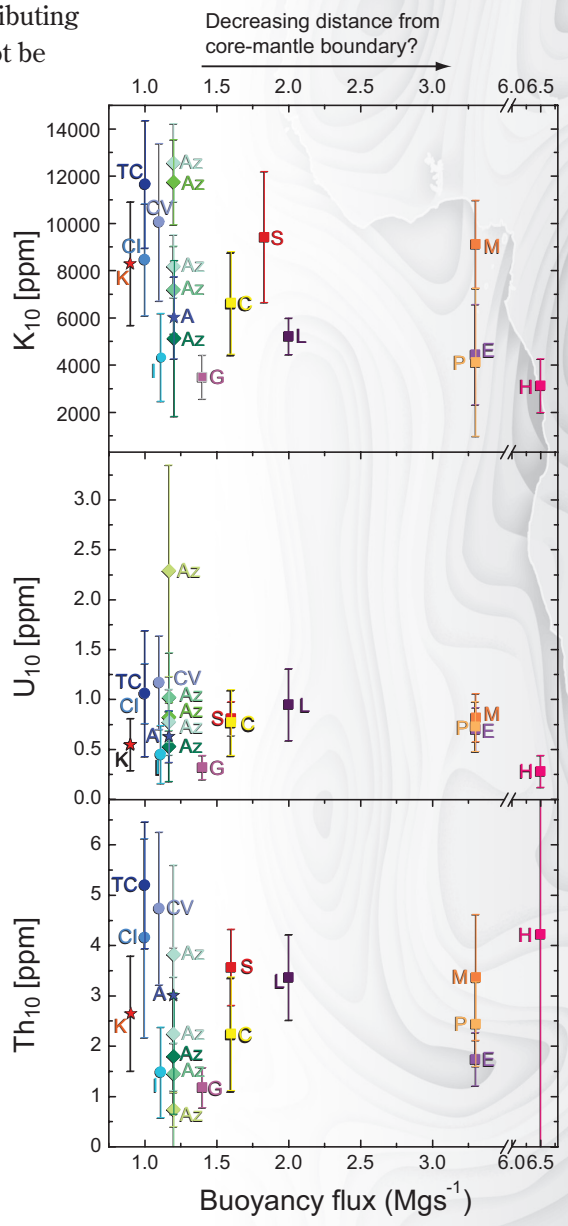

Atlantic plumes
- Iceland (I)
- Faial (Azores; Az)
- Graciosa (Azores; Az)
- Pico (Azores; Az)
- Sao Miguel (Azores; Az)
- Terceira (Azores; Az)
- Canary islands (Cl)
- Cap Verde Islands (CV)
- Tristan da Cunha (TC)

Pacific Plumes
- Hawaii (H)
- Galapagos islands (G)
- Easter islands (E)
- Lousville Seamounts (L)
- Samoa (S)
- Marquesas (M)
- Pitcairn Islands (P)
- Caroline seamounts (C)

Indian Ocean/Arabia
- Afar (A)
- Kerguelen (K)

Figure 2. Average fractionation corrected (to 10 wt.% MgO) K, Th and U concentrations [ppm] versus buoyancy flux in Mgs^{-1} of Atlantic, Pacific and Indian plumes and from the Afar plume. Error bars represent compositional range of each plume. Buoyancy flux as given in Sleep (JGR, 1990).

Flawed crystals control Earth's properties

NO MATTER HOW FLAWLESS THEY APPEAR TO THE NAKED EYE, natural crystals are never composed of atoms located in their perfect atomic arrangement. Without exception, crystals contain foreign atoms, or positions within the lattice that deviate from perfect crystal chemistry. Such imperfections are called 'defects', and there are several different types. Point defects exist when an atom normally present in the regular geometric atomic arrangement of a crystal is missing, or is present in an irregular place. Lattice vacancies, interstitial atoms and substitutional impurities are all types of point defect. The particular defect species present in a crystal is dependant on different thermodynamic parameters. Although these microscopic imperfections occur on a tremendously minute scale, their influence on the chemical, physical properties of the entire Earth is profound.

Figure 1. Scanning electron microscope images of synthetic spinel (light grey), forsterite (dark grey) and glass from experiments conducted in the High-Pressure laboratory.

Adding impurity elements – a process ubiquitous in natural systems - is a common way of introducing point defects into natural crystals. Amongst other things defects control atomic diffusion - a process by which individual atoms move through media via vacancies, interstitial impurity atoms or different interstitial positions. Understanding point defects in natural samples helps understand the accretion and subsequent evolution of our planet, and represents a fundamental area of research in the experimental petrology laboratories at Macquarie University.

Through the synthesis of Earth-forming materials (Fig. 1), studies conducted in our labs have shown that, at concentrations relevant to many natural samples, Sc^{3+} and most other trivalent cations substitute into olivine by replacing Mg^{2+}, and charge balance is maintained by the creation of metal vacancies. At slightly higher concentrations, trivalent cations are incorporated via the development of Sc^{3+}-Li^{1+} centres replacing Mg^{2+}-Mg^{2+}. Experiments aimed at understanding the defect chemistry of Li in natural samples show that Li concentrations are in excess of those which can be accounted for through the development of trivalent-Li centres. Furthermore, the results of experiments conducted at variable oxygen fugacity (fO_2) indicate that the dominant charge compensation mechanism in this regime is most likely via contemporaneous incorporation of Li on tetrahedral sites (Li'_{Mg}) and interstitially. Since olivine is the dominant host for Li in the upper mantle and isotopic fractionation is strongly dependent on crystal chemistry, these results have important implications for understanding the isotopic composition of Li in natural rocks.

Additional experiments have shown that the concentration of water in mantle olivine is strongly influenced by fO_2 and silica activity ($aSiO_2$). Our results led us to propose a reaction for the formation of protonated Fe^{3+} centres in olivine and allowed us to interpret and reconcile the results of several previous and apparently contradictory experimental studies. From a consideration of point defect equilibria we arrived at a mechanism for the incorporation of hydroxyl in olivine in a way that is appropriate for the actual range of conditions expected in the upper mantle of the Earth (see *GEMOC publications #474, 478, 480, 510*).

Contact: Kevin Grant
Funded by: Macquarie University and ARC Discovery

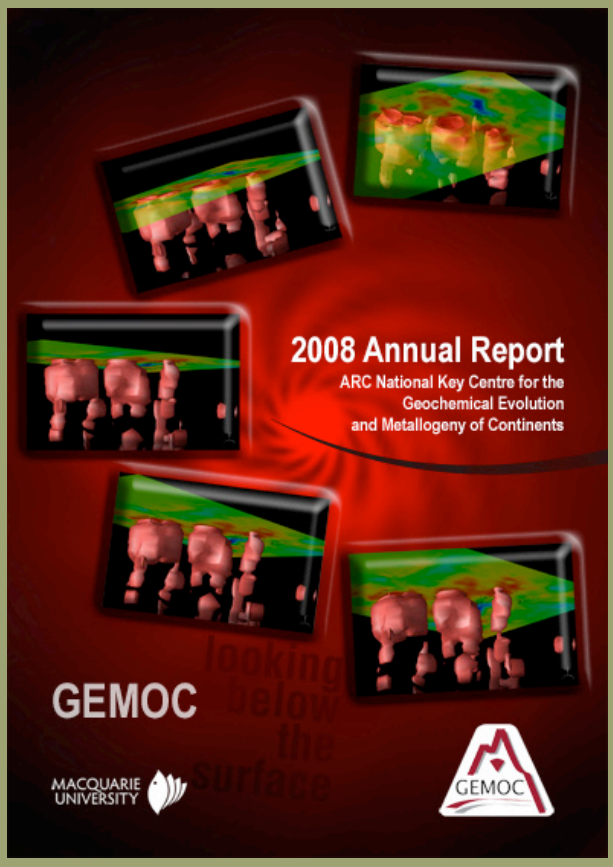

2008 Contents

How the world was made: The GLAM project 240

Ancient lithosphere blobs beneath the oceans: spelling out the geochemists' alphabet 243

Isotopic variability in mantle sources: the melt percolation recipe 245

Application of ^{186}Os to geochemistry and cosmochemistry 247

Journey in time and space beneath Kimberley South Africa 248

You can't judge a granite by its colour 250

"Decratonistion" of North China - a Mesozoic event 252

Reading geological histories in garnets 254

Deep drilling with basalts: over- and underplating of ancient crust in North China 256

Evolutionary histories of Earth and Venus - coupled convection-degassing models 258

A guide to making high-magnesium andesites 260

Multiple magma processes and TTG genesis 261

Copper isotopes blaze the trail to hidden ore deposits 262

Re-Os in sulfides tracks deep fluid interactions in old Spanish mantle 264

Melt migration transforms New Zealand's depths 266

Alloys in ophiolites wheel in new ideas on Earth evolution 268

Where are the diamonds in the Congo? 270

Front Cover: Examining the entrails --- To understand the lithospheric architecture of Africa (see Research Highlight, p240) Craig O'Neill constructed this 3-D model of the high-velocity cratonic roots down to 400 km, using Steve Grand's seismic tomography model. The West African and Congo cratons have deep robust roots; the root beneath the Kalahari craton has been greatly reduced by tectonism and metasomatism.

Research highlights 2008

TERRANECHRON® IS GEMOC'S UNIQUE METHODOLOGY for terrane evaluation. During 2008 a range of new studies including collaborative research projects with industry using *TerraneChron*® expanded our knowledge of crustal evolution and the timing of tectonic events. *TerraneChron*®*'s* success was recognised at the Australian Research Council Graeme Clarke Outcomes Award Day held at Parliament House, Canberra in May 2008.

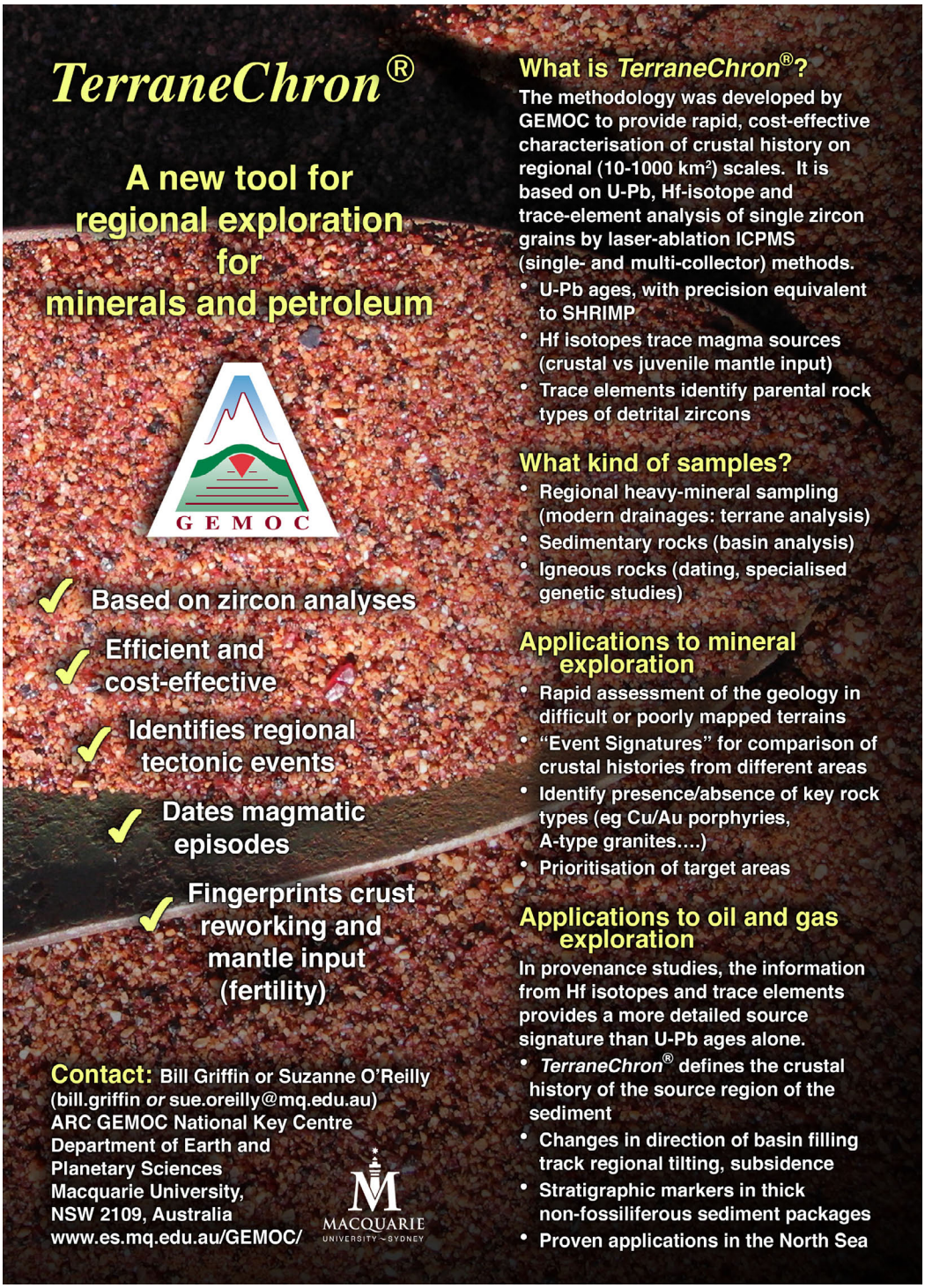

Visit the *TerraneChron*® web page at www.es.mq.edu.au/GEMOC/TerraneChron.html

How the world was made: The GLAM project

THE COVER OF THIS YEAR'S ANNUAL REPORT features one of the recent outputs of GEMOC's Global Lithospheric Architecture Mapping (GLAM) project. This major effort began 5 years ago as a collaborative research project with WMC, funded by an ARC Linkage grant. When WMC was taken over by BHP Billiton, the project continued, with BHPB sponsoring a second Linkage project that started work in 2008.

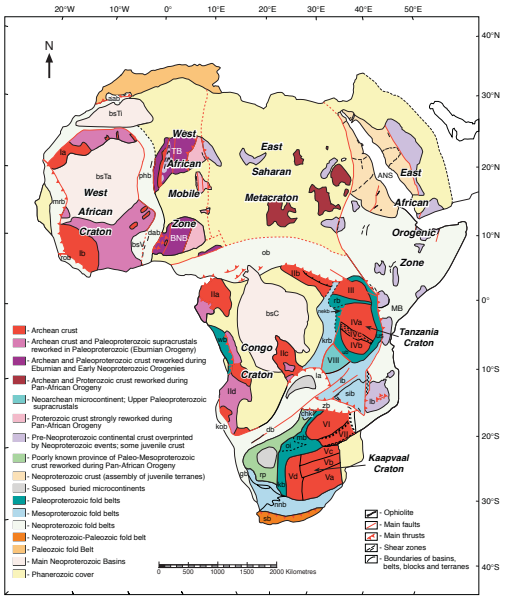

Figure 1. Lev natapov's new map of the basement geology of Africa.

The GLAM project arose from WMC's recognition that major ore deposits represent major transfers of mass and energy from the deep Earth, and that these fluxes require focusing by major, probably translithospheric, structures. This means that the most significant concepts and observations for predicting the localisation of giant ore systems are those related not to the deposit environment itself, but to the the much larger entity – the ore system. GEMOC was brought into the project because of our broad expertise in the composition, origin and structure of the lithospheric mantle.

The aims of the project are ambitious:

- To map the fundamental lithospheric architecture of the continents to depths of about 250 km
- To combine these maps with 3-D imagery and numerical dynamic modeling, to explore major geodynamic processes related to the formation and breakup of continents
- To test the relationships between lithospheric architecture, Earth dynamics and the localisation of large ore deposits

The expected outcomes include maps of lithospheric architecture at three levels: 0-100 km, 100-175 km and 175-250 km, and 3-D visualisations of selected regions (see *cover*). The construction of these maps is proceeding through several stages, which can be illustrated by our recently completed analysis of Africa (see *GEMOC Publication 547*).

(1) *A new tectonic analysis of each target area, integrating crustal geology, geochronology and tectonics*. This is based on an exhaustive literature review, using resources from GEMOC (especially Lev Natapov), the industrial sponsor, and independent consultants for specific areas. Where existing geochronology is inadequate, GEMOC's *TerraneChron*® technology is being deployed to provide new information on crustal genesis in key areas, and in particular to distinguish areas/periods where new crust was generated, or older crust was reworked. Our new map of Africa (Fig. 1) shows the type of information that is assembled and digitised in this first stage.

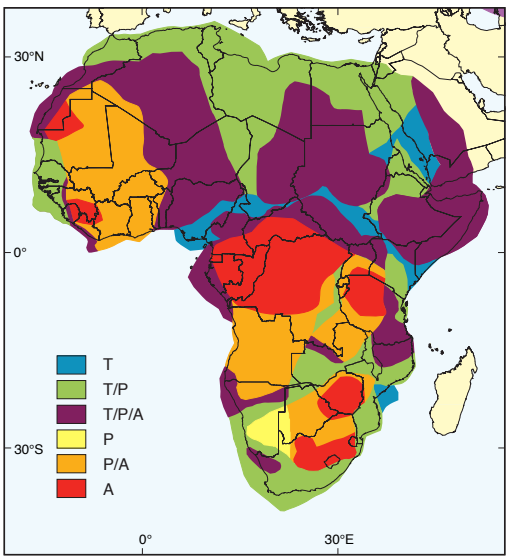

Figure 2. The tectonothermal map of Africa – see text for explanation.

(2) A map is prepared showing *upper lithospheric domains* (crust + uppermost mantle, to ≈ 100 km). The boundaries of these domains are defined on the basis of geology, topography, gravity, magnetics and derivatives of these. Using geochronological and geological data from the first stage, each domain is classified in terms of its origins and subsequent tectonic history. In Figure 2,

Archons (A) are volumes of the upper lithosphere that were formed before 2.5 Ga ago, and have escaped significant reworking since 2.5 Ga. *Protons* (P) are volumes generated between 2.5 and 1.0 Ga; *Tectons* (T) are younger than 1.0 Ga. It is especially important to recognise episodes of tectonothermal reworking; thus Archons reworked in Proterozoic time are shown as P/A, Protons reworked since 1.0 Ga become T/P, and so on. The definition of these domain boundaries is a key element in building a predictive model; Africa alone contains ca 200 upper lithospheric domains. The map in Figure 2 is a simplified version of the working files, lumping together adjacent domains with similar classifications.

(3) *Lower lithospheric domains (100-175 km)* are mapped, using a combination of seismic tomography and mantle petrology. The primary dataset is a global Vs tomographic model, generated by Prof Steve Grand (Univ of Texas, Austin) and enhanced through regridding and 3-D interpolation by WMC/BHPB geophysicists to provide exceptional resolution (see *Research Highlight, p 243)*. This dataset is supplemented wherever possible with information derived from studies of mantle-derived xenoliths in kimberlites, basalts and other deep-seated igneous rocks. The interpretation of the seismic data in terms of mantle composition, and by inference its age, has made significant progress during the project (see *GEMOC publication #548*). New Re-Os studies are being carried out on xenolith suites from a variety of areas to nail down mantle history in some contentious areas. Beneath Africa (Fig. 3) this approach has allowed the division of the subcontinental lithospheric mantle (SCLM) into volumes that are classified in the same way as the upper lithospheric domains. This analysis has outlined three major blocks of highly depleted Archon SCLM, surrounded by relatively narrow zones that have been reworked/refertilised during Proterozic time (and probably later). A major conclusion from the African study has been that much of the SCLM beneath upper lithospheric domains classified as P/A, T/A or even T/P represents strongly reworked Archean SCLM.

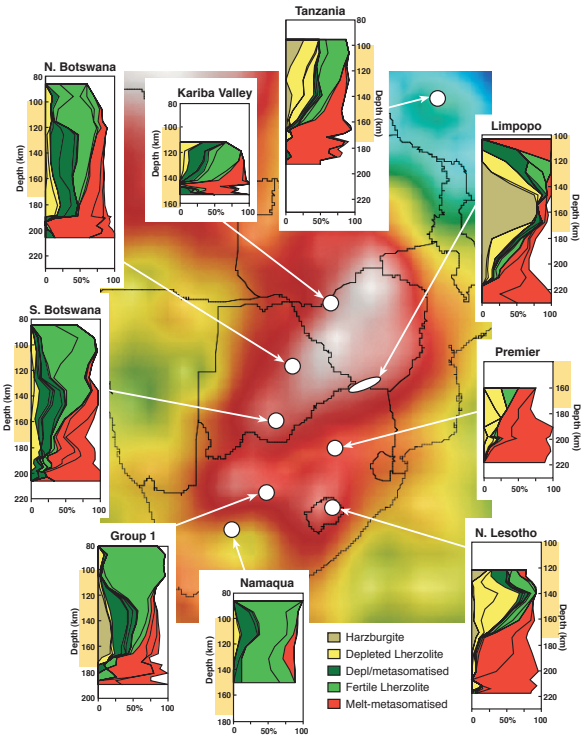

Figure 3. Vs tomographic image of the Kalahari Craton and surroundings; red to white colours show high Vs; yellow to green shows low Vs. The Chemical Tomography sections were constructed using mantle-derived xenocrysts from kimberlites; note none sample the core of the high-velocity root.

(4) Next, the project attempts to outline and classify *lower lithospheric domains (175-250 km).* This process integrates the seismic tomography and mantle petrology to map the depth of the "lithosphere-asthenosphere boundary" – which beneath cratonic areas, at least, may simply be a zone of intense melt-related metasomatism (see *GEMOC Publication #409*). 2-D cross-sections (Fig. 4) and 3-D images of Vs isosurfaces in the tomography (see *cover*) emphasise the deep roots beneath some cratonic areas,

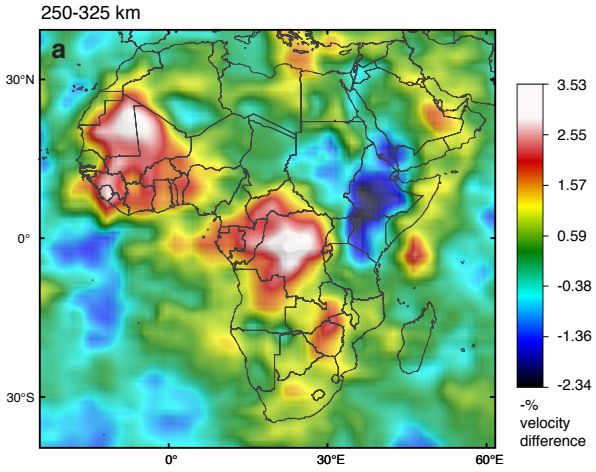

Figure 4. Section through the seismic tomography model for 250-325 km depths, showing robust roots under West African and Congo cratons, but only remnants beneath the Kalahari craton. For the full 3D model, see cover.

the steep sides of these highly depleted volumes, and the highly variable depth of the "lithosphere-asthenosphere boundary".

(5) *The maps are then interpreted in terms of mantle processes:* the primary origin of the SCLM in each domain, the location and nature of zones of mantle reworking, the tectonic environments along domain margins through time, and the "event limits" of events such as mantle plumes that have affected the SCLM. The integration of these datasets and maps results in 4-D event charts for each continental landmass, derived from the history of both mantle and crustal domains. The principle can be illustrated by a cartoon showing the changing relationships between the different domains of Africa through time (Fig. 5). This analysis emphasises that Africa is made up of several major blocks, some of which have repeatedly joined and separated along some clearly recognisable domain boundaries. These major translithospheric structures then become major foci for exploration targeting.

In the new GLAM project, numerical modeling will be used to explore how and why domain boundaries open and close, how continents extend or deform during collisions, and what mechanisms lead to the extension of some cratons out under ocean basins, and the incorporation of ancient SCLM relics beneath the Atlantic ocean (*Research Highlight, p243*). A specific aim is to incorporate realistic temperature- and depth-dependent rheology for the SCLM and the convecting mantle, and realistic strain-weakening mechanisms.

Key questions remain: why do some domains and boundaries become the sites of large-scale mineralisation and others do not? Work is in progress to assess sites of preferential magma/fluid flow along lithospheric discontinuities, the differing fertility of lithospheric domains, and how heat distribution in the lithosphere controls magmatism and hydrothermal circulation.

Ultimately, the products of the GLAM project will be collated into an atlas, accessible online.

Contacts: Sue O'Reilly, Bill Griffin, Graham Begg, Jon Hronsky
Funded by: ARC Linkage, ARC Discovery, WMC Resources, BHPB, international collaborators.

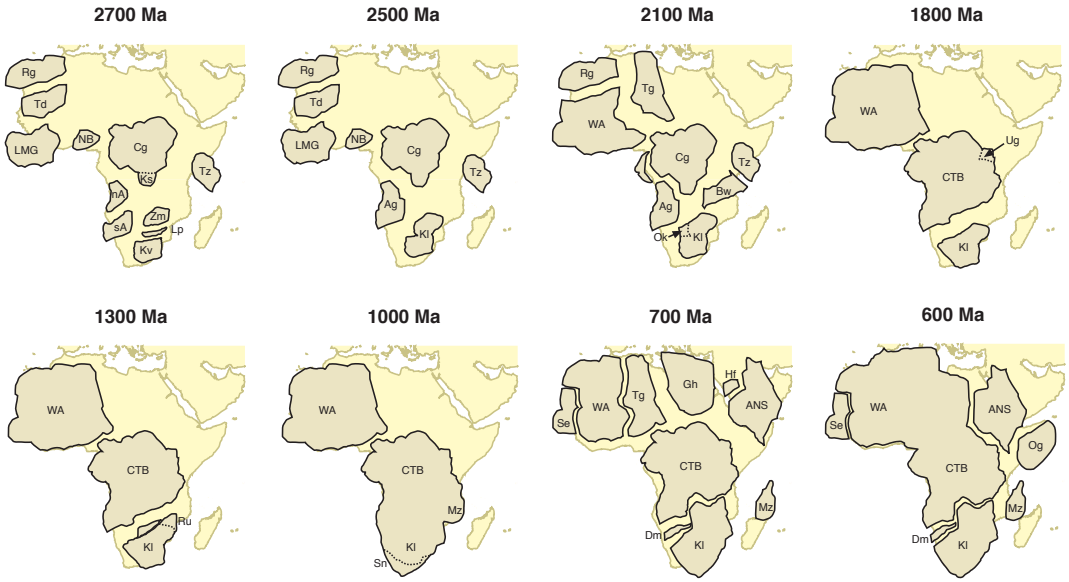

Figure 5. The assembly, breakup and reassembly of Africa's building blicks through time.

Ancient lithosphere blobs beneath the oceans: spelling out the geochemists' alphabet

The nature of continental Archean lithospheric mantle

Archean subcontinental lithospheric mantle (SCLM) is distinctive in its highly depleted composition, commonly strong stratification, and the presence of rock types (e.g. depleted, low-Fe harzburgite) absent in younger SCLM (see *GEMOC Publications #90, #132, #234, #485, #542*). Primary (unmetasomatised) Archean lithosphere is very low in basaltic components such as Al, Ca, Fe, consists dominantly of dunite and Ca-poor harzburgite and has high seismic wave velocities, mainly due to the high proportion of Mg-rich olivine (Fo 92-94). Archean lithosphere is significantly less dense than asthenosphere at any depth, and this buoyancy means that it cannot be gravitationally delaminated; it needs mechanical disaggregation (e.g. rifting) and/or metasomatic reworking to be disrupted.

Oceanic archean mantle revealed in tomographic models

Figure 1 shows tomographic slices through the oceanic lithosphere and upper mantle of the Atlantic Ocean Basin at 0-100 km, 100-175 km and 175-250 km.

In the 0-100 km section, high-velocity regions are obvious. Some are apparently continuous with continental regions (especially off southwestern Africa and southeastern South America) and some occur as discrete "blobs" within the ocean basin, from the continental margins to the mid-ocean ridge. In the layer from 100-175 km, these fast domains persist, and some also show velocity contrasts in the 175-250 km layer.

A traditional interpretation for high-velocity regions at the margins of ocean basins is the effect of cooling of the oceanic lithosphere with time and distance from the ridge. However, this cannot be the explanation for the discrete blobs that lie within the ocean basin, both away from the original rift margins and near the present-day ridge, with some extending to depths of 250 km.

We suggest that these high-velocity volumes represent remnants of depleted (buoyant), ancient continental lithosphere, fragmented and stranded during the rifting process at the opening of the ocean basin. The high-velocity domains extending out from the coastlines are not uniformly distributed along the basin edge. The most marked high-velocity regions, off SE South America and northwest and southwest Africa, appear to be continuous with their respective continental deep structure as seen

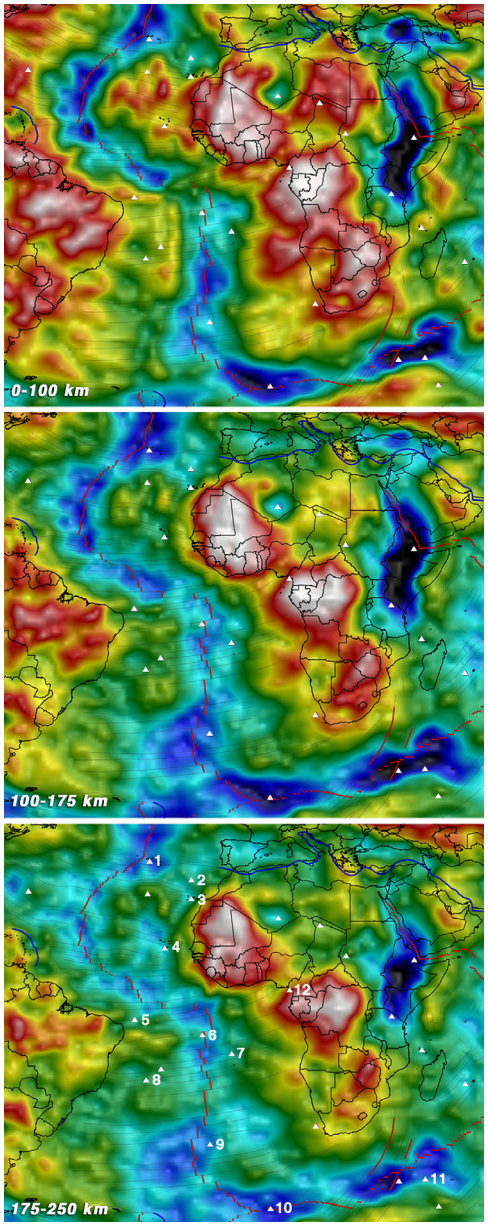

Figure 1. Tomographic model images at three depth slices for the Atlantic Ocean Basin (see text for details of the model). Note that "hot" (red-white) colours indicate higher velocities and cool colours lower velocities. Relevant OIB Provinces are: 1, Azores; 2, Madeira; 3, Canary Islands; 4, Cape Verde; 5, Fernando de Noronha; 6, Ascension Islands; 7, St. Helena; 8, Trindade; 9, Tristan da Cunha (Walvis Ridge at ~130 Ma; Richardson et al., 1984); 10, Bouvet; 11, Crozet Archipelago (Afanasy – Nikitin Rise in the Indian Ocean at Late Cretaceous, ~115-80 Ma; Mahoney et al., 1996)); 12, Cameroon Line. For more detail see GEMOC publication #576.

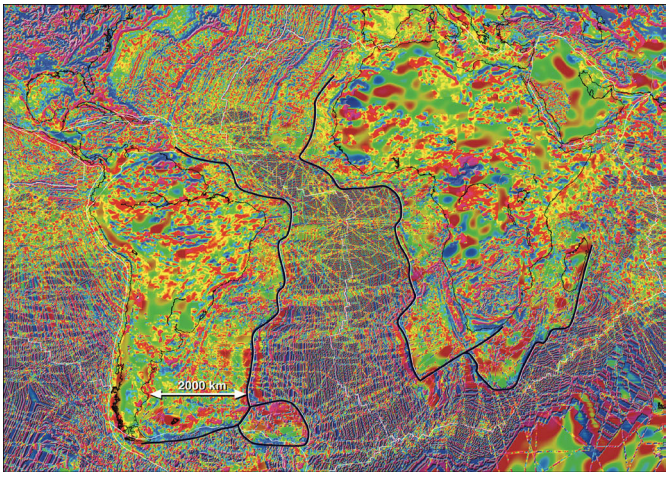

Figure 2. Modified extract from the global magnetic anomaly map (Korhonen et al., 2007. Magnetic Anomaly Map of the World Scale: 1:50,000,000, 1st edition, Commission for the Geological Map of the World, Paris, France.) showing the Atlantic Ocean Basin and Atlantic coasts of South Africa and South America. Black lines outline the regions with crustal rather than oceanic magnetic characteristics (modified from GEMOC publication #576).

in the tomographic models. The new global magnetic-anomaly map (Fig. 3) shows that these regions have a complex magnetic signature that is consistent with extended continental crust, and distinct from that of oceanic lithosphere, which is characterised by the regular magnetic striping produced at spreading centres.

Old Re-Os ages for mantle sulfides in some depleted mantle rock types beneath rift zones and oceanic areas (see references in *GEMOC Publication #576*) suggest that these high-velocity blobs (inferred to have high Mg# and low density) represent relict Archean to Proterozoic SCLM (now refertilised to varying degrees, during episodes of mantle fluid inflitration reflecting larger-scale tectonic events) that was mechanically disrupted and thinned during the formation of the oceanic lithosphere. This interpretation implies that ocean basins do not form by clean breaks at now-observed continental boundaries, but that significant volumes of buoyant old mantle are embedded within the newly generated oceanic lithosphere. The opening of ocean basins may be largely by listric faulting mechanisms, leaving significant wedges of continental lithosphere at rifted margins, and stranding domains of ancient lithosphere in the upper part of the new oceanic crust-mantle system, where they would remain as buoyant blobs.

If the higher-velocity coherent blobs observed at depths up to >150 km in the upper mantle of the Atlantic Ocean do represent remnant Archean mantle roots, this has important implications for the nature of global convection. Models involving large-scale horizontal movement would be difficult to reconcile with these observations. Instead, convection may be dominantly in the form of upwelling vertical conduits with shallow horizontal flow (Fig. 3). The locus of these conduits may be controlled by the geometry of the margins and the coherence of the buoyant lithospheric blobs.

Ocean island basalt goechemical signatures

The localised persistence of ancient SCLM beneath oceans also provides a logical explanation for the "alphabet soup" of mantle sources created by geochemists to describe the isotopic

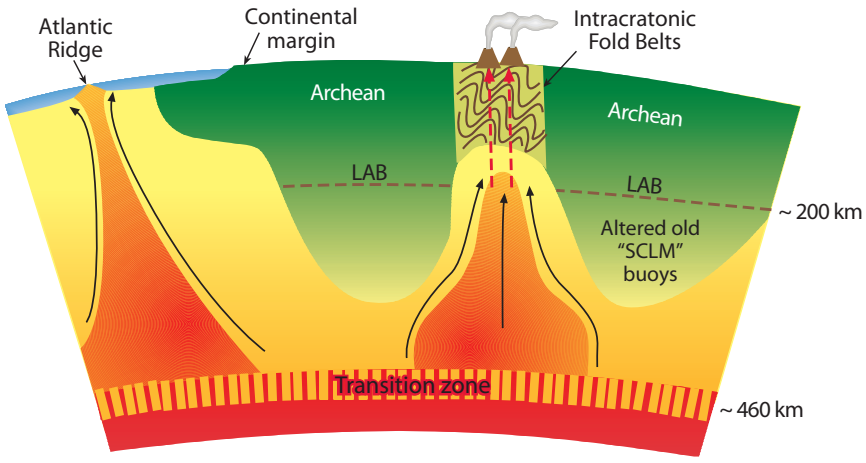

Figure 3. Cartoon indicating how high-Vs (low-density), vertically coherent regions extending to up to > 250 km could control convection pathways (modified from GEMOC publication #576).

signatures of basalts (EM1, EM2, HIMU, DMM; Fig. 4). These components are generally attributed to different geochemical reservoirs within the convecting mantle. However, all of these geochemical fingerprints are found in lithospheric material and have been well characterised in mantle xenolith studies (e.g. *GEMOC publications #60, #219*). If lithospheric volumes persist to deep mantle levels (>150 km) in ocean basins, then interaction with upwelling mantle plumes can "contaminate" magmas and fluids (Fig. 3), imposing a range of isotopic and trace-element signatures. A detailed examination of the ocean-island database from the Atlantic shows a strong correlation between "continental" signatures (EM1, EM2, etc) and the presence of high-velocity blobs in the seismic tomography (see *GEMOC Publication #576*).

This model removes the requirement for hidden source regions embedded within the convecting mantle. Magma interaction with deep ancient SCLM roots also provides a simple explanation for observations such as Archean Re-depletion model ages in oceanic basalts.

Contacts: Sue O'Reilly, Ming Zhang, Bill Griffin
Funded by: ARC Discovery, Macquarie external collaborative grants, ARC Linkage, BHPB

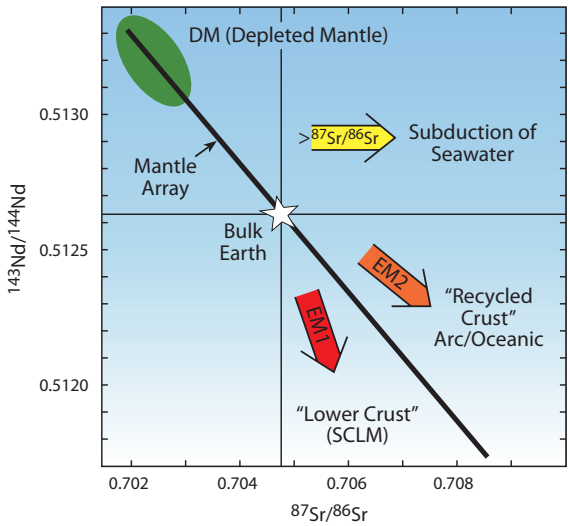

Figure 4. Isotopic components commonly observed in basaltic magmas and their fields in Nd and Sr isotopic space (for more detail see GEMOC publication #576).

Isotopic variability in mantle sources: the melt percolation recipe

MANTLE ROCKS THAT OUTCROP AT THE EARTH'S SURFACE provide direct information on the composition and evolution of the Earth's mantle. The isotopic systematics of most peridotite massifs and mantle xenoliths show a wide range of variation compared with single suites of mantle-derived lavas. Some of the isotopic variations observed in peridotite massifs are correlated with lithology, e.g. pyroxenites vs peridotites, and have been ascribed to convective mingling of subducted material with pristine material. Other small-scale heterogeneities have been ascribed to time-integrated enrichment in radioactive parent elements by percolating melts/fluids, superimposed on previously depleted rocks.

However the "instantaneous" (as opposed to "time-integrated") effect of melt transport on isotopic systematics is usually neglected, although it may theoretically generate drastic fractionation of daughter elements from different isotopic systems. Under the temperature conditions of the lithosphere–asthenosphere transition, diffusional processes may be slow, and therefore chemical and isotopic equilibrium between minerals and percolating melts may not be reached.

This type of disequilibrium has been observed in the Lherz massif, the type locality of lherzolite, located in the French Pyrenees. The lherzolites have been shown to be secondary products, produced when melts refertilised a depleted harzburgite matrix (see *Annual Report 2007; GEMOC Publication #544*). The transition zone between the harzburgites and the

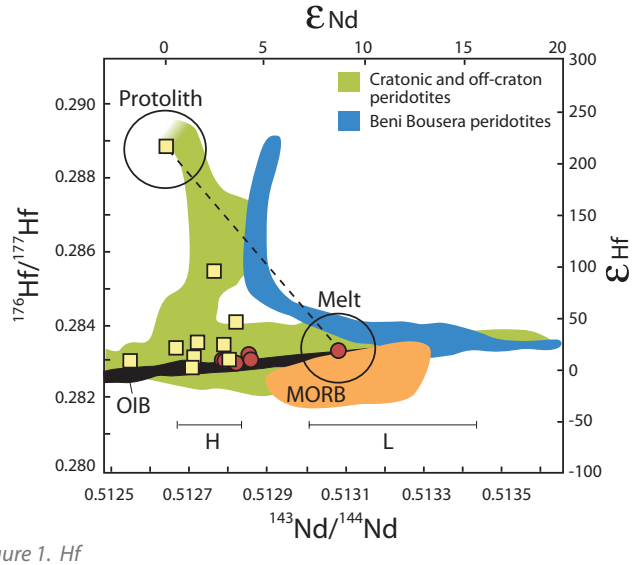

Figure 1. Hf and Nd isotopic variations at the melt percolation front in the Lherz massif.

refertilised material represents a frozen melt-percolation front that moved through the subcontinental lithospheric mantle. Isotopic signatures at the melt percolation front show a strong decoupling of Hf from Nd isotopes (Fig. 1). This decoupling cannot be accounted for by simple mixing involving the harzburgite protolith and the percolating melt (dashed line between the two circled end-members), nor by the unlikely presence of OIB-type melts at the contact, nor by a chromatographic effect.

Using one-dimensional percolation–diffusion and percolation–reaction models, we can show that these signatures represent transient isotopic compositions generated by porous melt flow (Fig. 2).

The isotopic heterogeneity observed in the transition zone between harzburgites and lherzolites can be reproduced with a realistic range of physical parameters: a melt fraction of a few percent, a percolation rate of several cm/year, percolation over distances of tens to several hundreds of meters. The Lherz example suggests that a large range of isotopic signatures may be generated at a melt percolation front, depending on chemical diffusion, isotopic homogenisation and peridotite-melt compositions. Full details are given in *GEMOC Publication #558*.

Therefore, under certain circumstances, melt-rock interactions can generate enriched, "intraplate-like" isotopic signatures in the transition zone between the two contrasting components. These results suggest that some of the isotopic signatures of mantle-related rocks could be generated by diffusional processes associated with melt transport.

Contacts: Véronique le Roux, Sue O'Reilly, Bill Griffin
Funded by: ARC Discovery, LIEF, MQRES, INSU DYETI Program, French Ministry of Research, Bourses Lavoisier

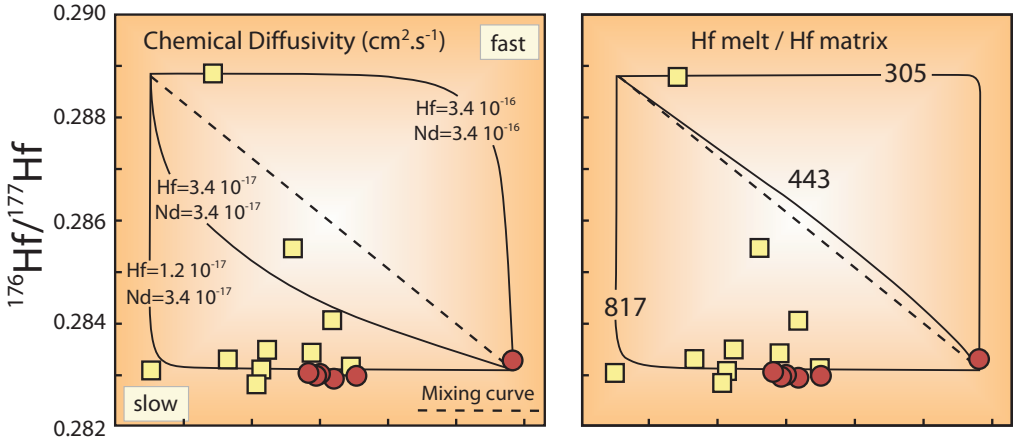

Figure 2. Modelling showing the importance of chemical diffusion and element concentrations, among other parameters, in the process of isotopic re-equilibration during percolation. Small variations in these parameters may generate a large range of isotopic variations.

Application of ^{186}Os to geochemistry and cosmochemistry

187 RE-^{187}OS ISOTOPE GEOCHEMISTRY has gained widespread utility in the geosciences over the past decade. Applications in studies of the mantle, ore deposits, organic rich sediments and meteoritics testify to the diversity of problems that can be tackled with this technique. However, another radiogenic Os isotope (^{186}Os) is formed by the decay of ^{190}Pt. This decay scheme has not been widely applied as it is technically exceedingly challenging to measure ^{186}Os anomalies. This is due largely to the combination of two factors; the half life of ^{190}Pt is ~430 billion years (ca 30 times the age of the universe) and ^{190}Pt makes up only 0.01296% of naturally occurring Pt. Therefore the amount of radiogenic ^{186}Os on the Earth is very small, and to detect any ingrowth due to this decay, we must use geochemical reservoirs that have had very high Pt/Os ratios for long periods of time. Historically the only such terrestrial reservoir was considered to be the outer core, but geochemists are increasingly recognising the presence of ^{186}Os anomalies in other terrestrial materials, such as sulfides in the lithospheric mantle.

Over the past two years, GEMOC has been attempting to establish a protocol for ^{186}Os analyses on the Triton TIMS housed in the GAU. Refinements in loading and acquisition routines have resulted in an increase in internal precision on individual analyses by an order of magnitude to ± 0.0000025 on 20 ng sample loads, a precision equivalent to that achieved by other groups conducting such work. However, this precision has been achieved on smaller sample sizes than other groups are using routinely.

With this capability we can investigate a large range of earth science problems. For example, preliminary data from Proterozoic organic rich sediments tantalisingly suggest that there may be a significant crustal reservoir of ^{186}Os which has been hitherto ignored in investigations involving potential contributions to plume derived basaltic magmatism (see cartoon). Furthermore, there is the potential to integrate the Pt-Os technique with ^{187}Os isotopic data to map out distinct lithological domains in the mantle, providing another aspect to the debate regarding the relative role(s) of the subcontinental lithospheric mantle, the asthenosphere and recycled components in mantle plumes. Finally, Pt-Os studies of differentiated meteorites can place independent constraints on the timing and rates of core formation and segregation during planetary formation. We anticipate that with further refinements in both chemistry and mass spectrometry, GEMOC will become the first laboratory in the Southern Hemisphere to routinely apply this technology, and will become a world leader in its application.

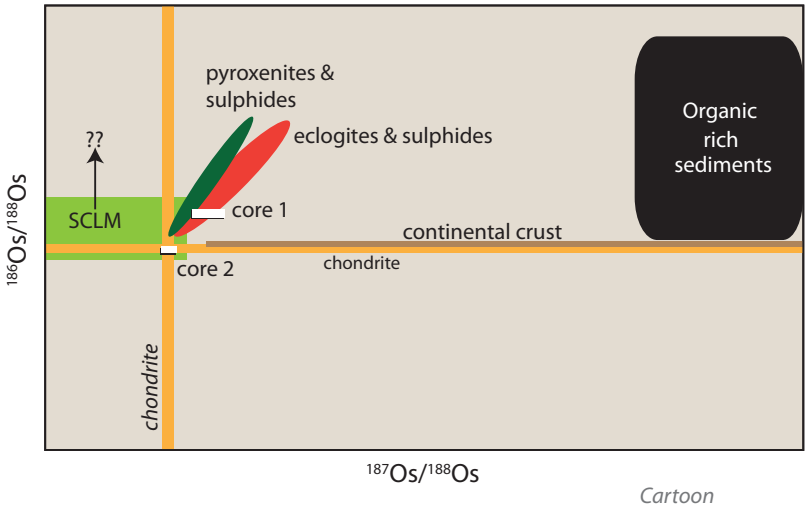

Cartoon illustrating the variation in ^{186}Os and ^{187}Os isotopes in different terrestrial reservoirs. The two core compositions are for different model Re-Pt-Os ratios dependent on partition coefficients. SCLM = Subcontinental lithospheric mantle.

Contact: Bruce Schaefer

Funded by: Monash University, Macquarie University

Journey in time and space beneath Kimberley South Africa

THE "4-D" LITHOSPHERIC MAPPING METHODOLOGY DEVELOPED AT GEMOC describes the vertical and lateral variation in lithospheric mantle chemistry using mantle xenoliths or xenocrysts carried to the surface in volcanic eruptions. Where more than one episode of magmatism occurs in the same area, this methodology also can provide insights into the temporal evolution of the lithosphere. The Kaapvaal Craton in southern Africa is an ideal natural laboratory for this methodology because many kimberlites provide samples of the lithospheric mantle. The Kimberley area in particular contains kimberlites that have erupted during two episodes of magmatism, the first at approximately 120 ± 5 Ma (Group II kimberlites), and the other at approximately 90 ± 10 Ma (Group I kimberlites). The spatial coincidence of kimberlites with different ages provides samples of the lithospheric mantle during each eruptive episode; comparison of these samples tracks the chemical evolution of the lithospheric mantle during this interval (Fig.1).

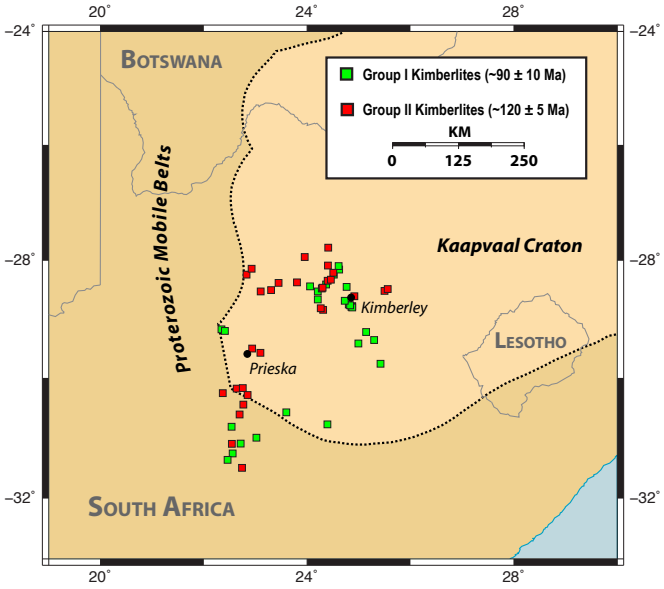

Figure 1. Cretaceous age kimberlites of the Kimberley area, South Africa.

Peridotitic garnet xenocrysts are a common component of kimberlites and are collected extensively in diamond prospecting. Application of the garnet geotherm method to suites of garnets from each kimberlite in Figure 1 places these grains in a depth context, and gives a "train" of garnets below each kimberlite, similar to a vertical borehole (Fig. 2). In addition to temperature information, the garnets also contain information on depletion and metasomatism processes in the mantle, which is the basis of chemical tomography.

Previous applications of chemical tomography have involved constructing a local paleogeotherm and then plotting garnet-derived geochemical signatures as a function of depth for each locality considered. A natural extension of this method is to correlate the compositional and metasomatic

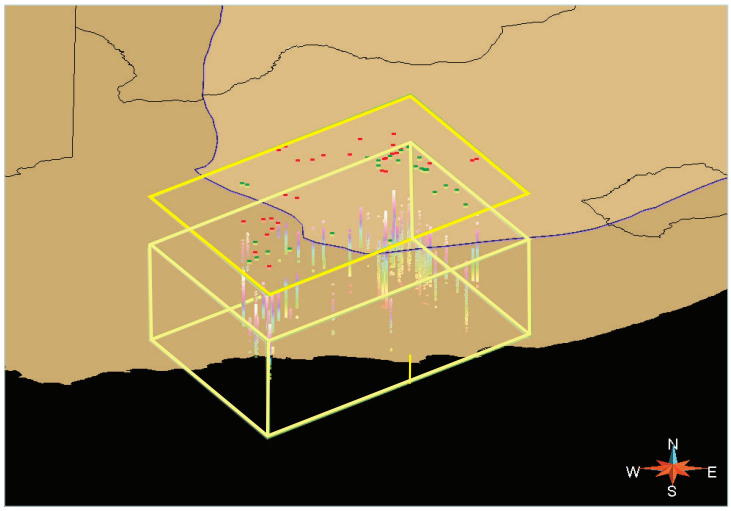

Figure 2. Perspective view toward the north of the volume sampled by the kimberlites of the Kimberley-Prieska area. The red and green squares are the same kimberlites shown in map view above, and the blue line indicates the extent of the Kaapvaal Craton. The box below the map surface indicates the volume of interest and ranges in depth from 50 to 250 km. In this volume the individual garnet xenocrysts are plotted at their calculated depths, with hotter colours indicating greater depth. The yellow rectangle indicates where the box would intersect the surface if projected upward. The angle of perspective is approximately 45° above the horizon.

signatures across multiple localities, to derive the three-dimensional distribution of rock types and metasomatism in the lithospheric mantle.

We have mapped several measures of depletion and metasomatism throughout the mantle volume sampled by kimberlites in the Kimberley-Prieska region using the Discrete Smooth Interpolation algorithm. Values for the older and younger group of kimberlites were estimated separately. One of these measures is shown in Figure 3.

Highly magnesian olivine (X_{Mg} > 0.925) is thought to represent ancient melt-depleted cratonic mantle; values less magnesian than this probably reflect later metasomatic modification. The marked shrinkage in the volume of highly magnesian mantle in the interval between the eruption of the Group II and Group I kimberlites indicates that a significant metasomatic event during this interval added iron to the mantle. This metasomatism is probably the result of interaction of the depleted mantle with mafic silicate melts (see *GEMOC publications #522 and #578*). The timing of this metasomatic event (120-90 Ma) suggests that it is related to changes in the regional stress field associated with the opening of the southern Atlantic Ocean.

Contacts: Alan Kobussen, Bill Griffin, Sue O'Reilly
Funded by: De Beers, ARC Discovery (O'Reilly, Griffin et al.), iMURS/IPRS (Kobussen)

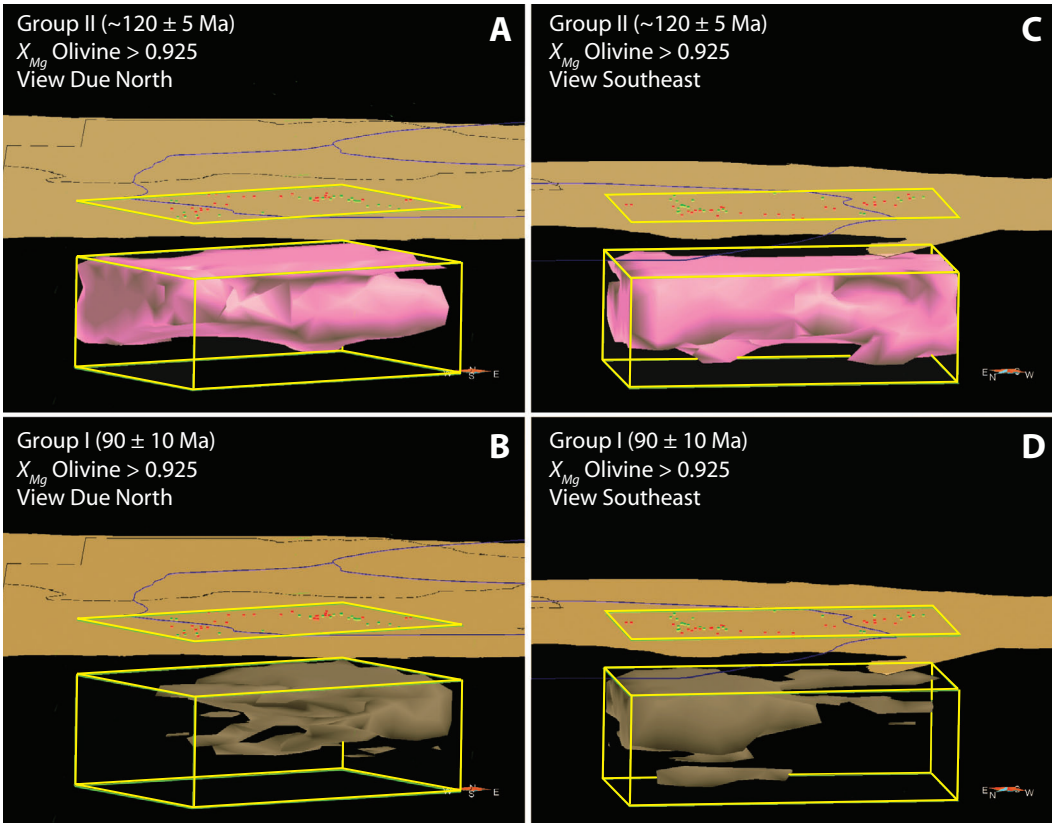

Figure 3. Perspective views of isosurfaces of X_{Mg} olivine resulting from the DSI algorithm. Areas within the shaded volumes have X_{Mg} >0.925 (a depleted peridotite composition) and areas outside have less. (A) The view due north of the volume resulting from interpolation using garnets from the Group II kimberlites. The angle of perspective is now approximately 15º. Map symbols are the same as Figure 2. (B) The same view and perspective as (A), but this time using the garnets from the younger Group I kimberlites. (C) The same volume as in (A), but viewed toward the southeast. (D) The same volume as in (B), but viewed toward the southeast.

You can't judge a granite by its colour

GRANITES FORM A SIGNIFICANT PART OF THE CONTINENTAL CRUST, yet their origin and the relative contribution of crustal and mantle-derived components to these rocks has long been hotly debated. The classification of granites into "I-type" (igneous), "S-type" (sedimentary) and "M-type" (mantle) in the 1970s went some way to recognising mineralogical and bulk-rock chemical differences that reflect source-rock characteristics. A number of studies have focussed on experimental and numerical modelling related to silicic magma generation and the ultimate source and level of magma generation. These studies have shown that both felsic residual melt fractionated from injected basalt and partial melt derived from crust adjacent to the injected basalt can be present under certain conditions in the crust.

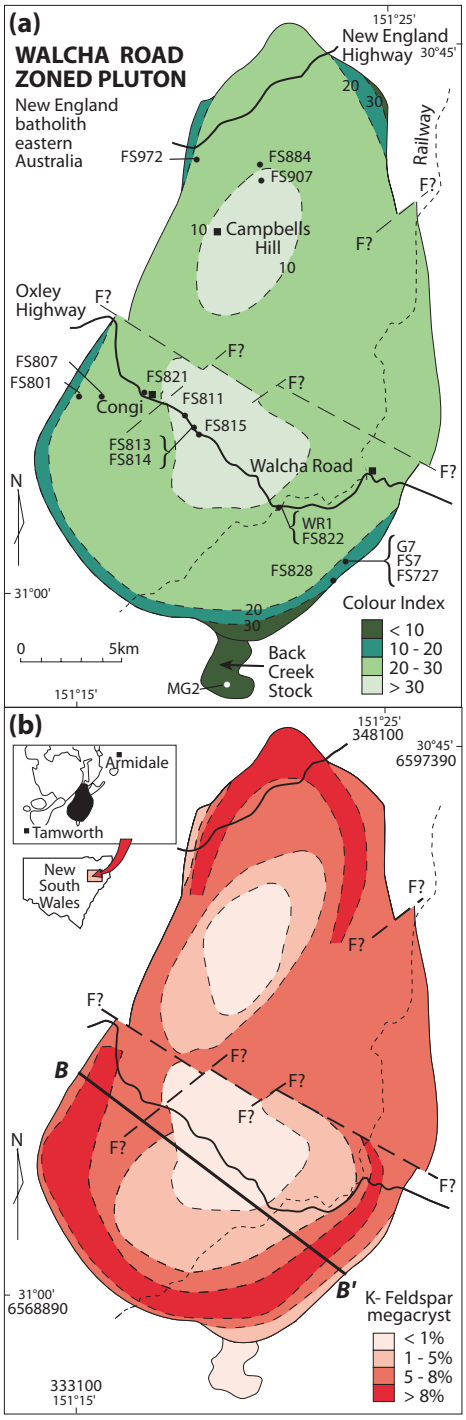

Figure 1. Simplified geological map of the Walcha Road zoned pluton and Back Creek stock, Moonbi supersuite. (a) Contour intervals for colour index; (b) K-feldspar megacryst abundance. In general the foliation, as defined by mineral elongation, follows the contact margin and contour lines. The foliation, in general, dips steeply inwards. The monzogranite pluton is zoned from a mafic margin to two felsic central zones, one around Congi and the other around Campbells Hill (modified from GEMOC publication #555).

The development of *in situ* Hf-isotope analysis in the MC-ICPMS laboratory at GEMOC (*GEMOC publication #179*) allowed reliable single-grain Hf-isotope analysis of zircon to determine the degree of $^{176}Hf/^{177}Hf$ variation within a zircon population. This technique can be applied on the scale of a hand specimen, and then extended to the pluton scale and ultimately to the total variation within a supersuite of plutons. The $^{176}Hf/^{177}Hf$ ratio of a magma, and hence of the zircon crystallised from it, is a reflection of the source(s) of the magma. Higher ratios reflect more juvenile (mantle-derived) source rocks, and lower ratios the involvement of older material (either mantle or crust). The zircons thus can record the sources of individual magma batches that went into the construction of a single pluton, or a batholith (*GEMOC publication #251*).

Single-grain zircon analyses on the large zoned Walcha Road pluton (249±3 Ma) in northern NSW (*GEMOC publication 555*) have revealed that it represents a mixture of (1) magmas derived from Neoproterozoic lower crust (I-type) and (2) residual silicic magmas (M-type) of Late Palaeozoic age (Fig. 1). The central part of the pluton has the most M-type signature, as shown in the plot of $^{176}Hf/^{177}Hf$ ratios (Fig. 2). Significantly, the mantle-derived melt component in the felsic centre of the Walcha Road pluton is silicic, rather than mafic. Wider studies have shown this to also be the case for the voluminous leucocratic Stanthorpe granite in the northern part of the batholith.

These results highlight the danger of associating mantle-like isotopic values with the

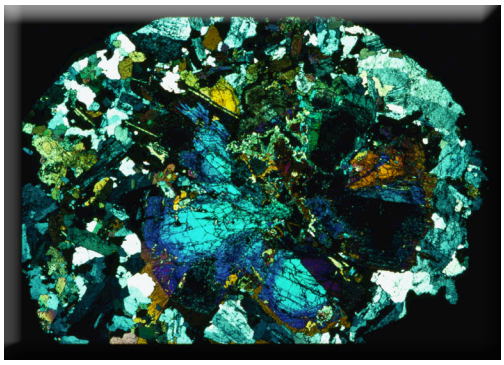

Photomicrograph of a mafic clot with radiating clinopyroxene glomerocryst overgrown by hornblende and plagioclase, magnetite ± biotite, sampled near location FS828 (see Fig. 1)

direct involvement of mafic magma. Because of the silicic composition of the residual and crustal partial melts, the mixed magma may not show the major textural and major element variations that result from mixing or mingling of felsic and mafic magmas that may be markedly different in temperature and viscosity (e.g. *GEMOC Publication #251*). Indeed, the mixing of silicic residual melts and crustal partial melts may be difficult to detect within single plutons, except by isotopic studies of zircon and other minerals that preserve isotopic disequilibrium.

Powell and O'Reilly (*GEMOC publication #419*), used Re-Os analyses of sulfides in mantle-derived peridotite xenoliths from basalts, to establish that parts of the lithospheric mantle

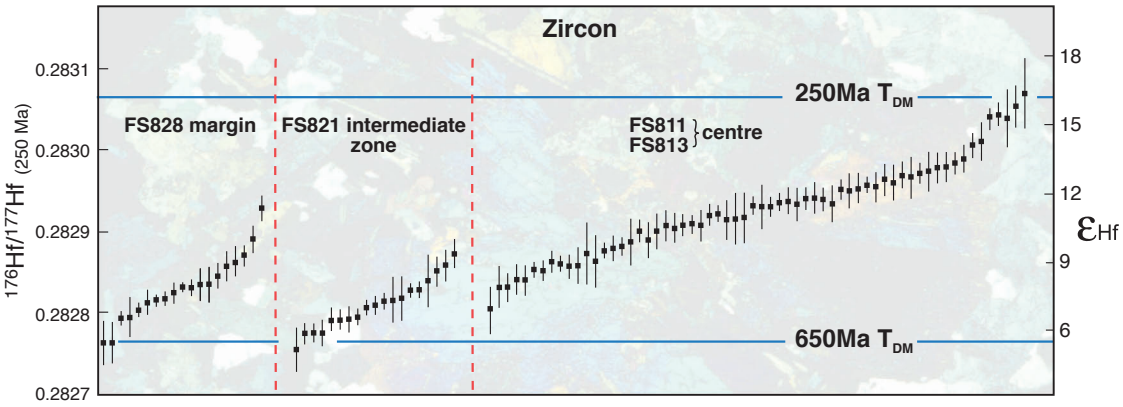

Figure 2. Plot of $^{176}Hf/^{177}Hf$ and εHf (250Ma) for zircons from the margin, intermediate zone and centre of the pluton. Error bars for individual measurements are 1SE. Data arranged in direction of increasing $^{176}Hf/^{177}Hf$. Lu-Hf T_{DM} model ages at 650 and 250 Ma are shown (modified from GEMOC publication #555).

below the New England area are at least Proterozoic in age. The Hf model ages for the older component in the Walcha Road pluton indicate the presence in the lower crust of rocks as old as Neoproterozoic. The integration of these two data sets suggests that New England may represent a microcontinental block, with a Proterozoic mantle lithosphere overlain by Proterozoic lower crust (see *GEMOC publication #555*).

Contacts: Dick Flood, Stirling Shaw
Funded by: Macquarie University

"Decratonistion" of North China - a Mesozoic event

CRATONS ARE OLD, STABLE PARTS OF THE CONTINENTAL CRUST that have survived at least since Proterozoic time and have not undergone strong magmatism or tectonism since their stabilisation. They owe much of their stability to thick roots of highly depleted peridotitic lithospheric mantle. Early in the 1990s it became apparent from studies of mantle xenoliths that the lithospheric root beneath the eastern half of the North China Craton (NCC) had been severely modified; a typical Archean root sampled by Paleozoic kimberlites had been largely replaced by a thinner, hotter and more fertile lithospheric mantle more typical of Phanerozoic mobile belts. Since those early days, the lithospheric mantle beneath the NCC has been the focus of increasingly intense research efforts, involving both petrological and geophysical studies. GEMOC and our Chinese collaborators have played a major role in this effort (see *GEMOC Publications #64, 113, 225, 339, 384, 490, 493*). Now studies of crustal rocks are providing new insights into the processes that have modified the roots of the NCC (see *GEMOC Publication #512*).

The crust of the NCC consists of several blocks of Archean rocks, stitched together in Paleoproterozoic time (1.8-1.9 Ga). The Liaodong Peninsula in the NE part of the NCC (Fig. 1) contains large volumes of Mesozoic igneous rocks, with widespread metamorphic core complexes and pull-apart basins. Hf isotope compositions of magmatic zircon grains (Fig. 2) indicate that the formation of the Mesozoic granitoids involved extensive partial melting of ancient crust. Most of the zircons from Triassic, and especially Jurassic, granitoids have εHf values <0, and could be derived from a variety of older mafic to felsic lithologies, which could be either Archean or Proterozoic in age. Many of these granitoids also contain inherited zircons with Archean to Paleoproterozoic ages. Similar low εHf values occur in Cretaceous granitoids, but these also show a range of positive εHf, up to values typical of the convecting mantle. These large ranges imply significant input of a mantle component, via magma mixing and crustal assimilation.

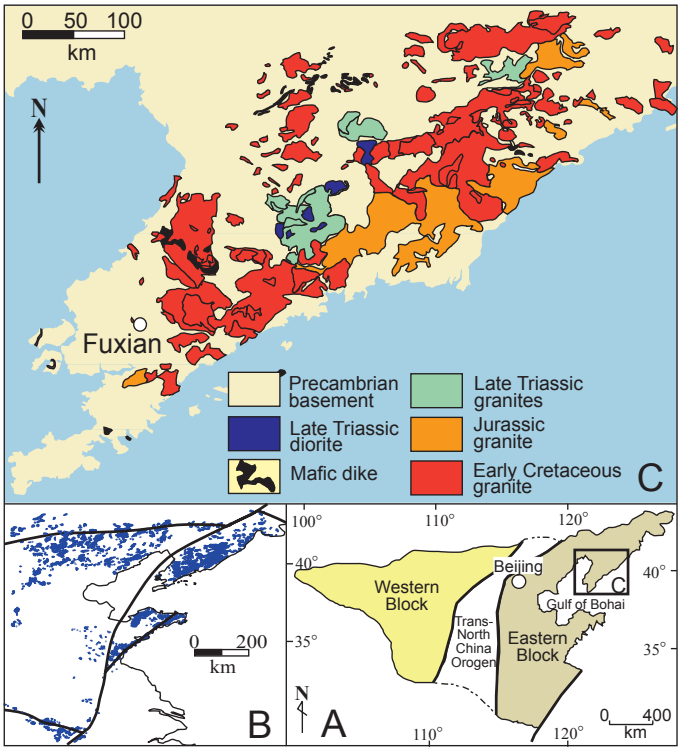

Figure 1. A: Simplified map showing major tectonic units in North China craton B: Distribution of Mesozoic intrusions in eastern North China Craton. C: Geological map showing distribution of Mesozoic intrusions in Liaodong Peninsula (modified from GEMOC publication #512).

The abundance of Mesozoic magmas, like the Tertiary basaltic volcanism, indicates that the NCC is no longer a craton in the usual sense of the term, and that the "decratonisation" of the NCC began at least 210 Ma ago. The dominance of the older crustal components in the early Mesozoic magmas suggests that the process began with heating and melting of the lower crust; heat was provided by thinning of the lithosphere and upwelling of the asthenosphere. Mantle-derived magmas may have been involved as well, but their geochemical signatures

have been strongly diluted by interaction with crustal melts. The stronger juvenile signature in the Cretaceous magmas suggests that, by ca. 125 Ma, increasing degrees of extension allowed asthenosphere-derived magmas greater access into the crust, where they could mix with melts derived from the older crust. This process has continued to the present day, culminating in Tertiary to Holocene alkali basaltic magmatism (see *GEMOC Publication #490*). The North China Craton survived as a coherent block for at least 1.5 b.y.; its decratonisation may be related to major plate-tectonic processes, including both the Triassic collision between the NCC and the Yangtze Craton, and the subduction and rollback of the Pacific plate beneath the area.

The data from the Mesozoic granitoids in the NE part of the NCC give important clues to how a cratonic root might be destroyed by the extensional processes that may accompany subduction beneath a cratonic block. However, many other Archean cratonic blocks have survived repeated episodes of subduction, collision and breakup, with their roots intact (see *Research Highlight on GLAM project, p. 240*).

Why was the NCC different? The answer may lie farther back in time. Although much attention has focussed on the evidence for an Archean lithospheric root that was sampled by Ordovician kimberlites, those data represent only two limited areas in the eastern NCC. Extensive studies of Os-isotope systematics in mantle xenoliths from other parts of the NCC, using analyses of both sulfides and whole-rock samples, have found little evidence of Archean mantle, but widespread Proterozoic model ages (see *GEMOC Publication #490*). Perhaps the roots of many of the Archean fragments that were swept into the Proterozoic assembly of the NCC had already been severely modified in that process, leaving the NCC with a less robust lithospheric root than most cratons. This could have left it more vulnerable to extension and further modification forces during the Mesozoic collision-subduction-extension events.

Contacts: Jin-Hui Yang, Bill Griffin, Sue O'Reilly
Funded by: Academica Sinica, ARC Discovery Grant, China NSF

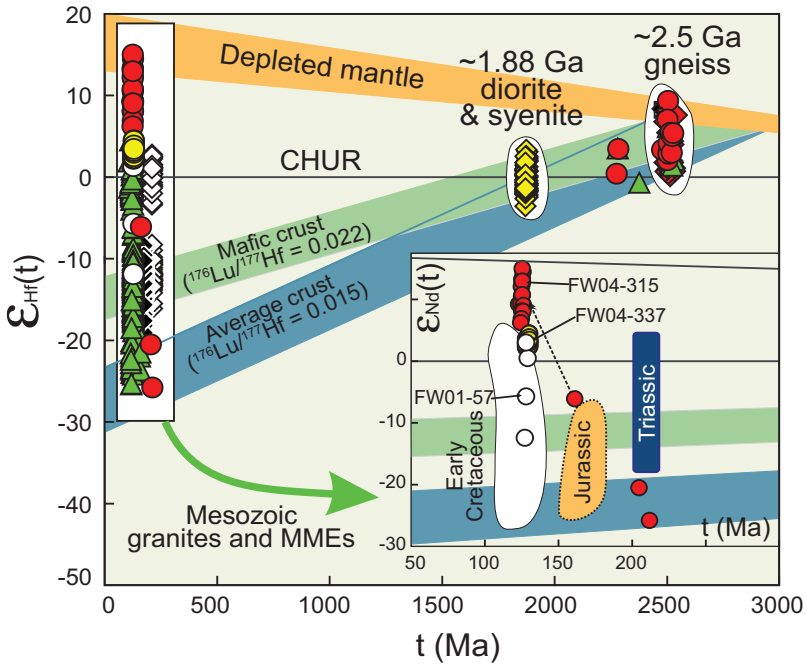

Figure 2. Plot of $\varepsilon_{Hf}(t)$ versus inferred crystallisation age of the magmatic zircons analysed in this study (published in Yang et al., 2007b, 2007c). CHUR—chondrite uniform reservoir; MME—microgranular microdiorite enclaves (modified from GEMOC publication #512).

Reading geological histories in garnets

DURING BURIAL OR SUBDUCTION, rocks experience pressure and temperature (P-T) conditions that are different from those of their formation. In response, minerals react with each other to form new minerals or to adapt their composition to one that is more stable under the new conditions. Microstructural relations among minerals and mineral composition, especially where zoning is preserved, are therefore witnesses to the geological history of the rocks and can be used to assess their P-T-time path for geodynamic reconstructions.

Garnet plays an important role in deciphering the history of metamorphic rocks because its composition can provide information about pressure, temperature and the timing of the metamorphism. Garnet is stable over a large range of bulk-rock compositions and P-T conditions. Its tight structure imposes relatively low diffusion rates on major elements and so garnet grains frequently preserve chemical zonation. A wealth of techniques has therefore been applied for deriving segments of P-T paths using the major-element composition of garnet. In addition, trace elements in garnet have been used to date metamorphic events either directly using the isotopic composition of garnet (Sm-Nd, Lu-Hf or Rb-Sr) or indirectly by linking the growth of datable accessory minerals, such as zircon or monazite, to that of garnet.

However, all the above techniques rely on the assumptions of (i) equilibrium between the growing garnet and the surrounding matrix and (ii) the closure of the rock to external chemical exchange, for example via fluids. It is therefore important to understand the processes causing garnet zoning, acquired during garnet growth or during its re-equilibration. In the case of growth zoning, does it result from P-T or bulk-compositional changes? In case of re-equilibration zoning, how fast and efficient is the re-equilibration process and what is the vector of the chemical exchange between garnet and matrix?

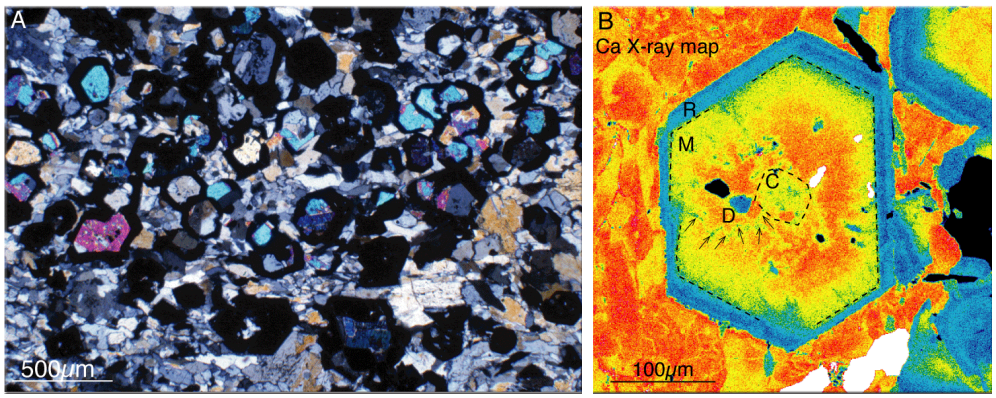

Figure 1. A- Photomicrograph (crossed nicols) of the microstructure of the eclogite; the black rings are "atoll garnet" grains, where a ring of garnet surrounds a cluster of other minerals. B- Ca X-ray map of a complete garnet (R: rim, M: mantle, C: core). The arrows point to a Ca-poor fracture in the garnet connecting the core and the matrix.

Three unusual types of garnet have been studied in terms of their microstructures and their chemical and isotopic zoning.

a) *Atoll garnets in an eclogite: dissolution-reprecipitation in an open system at peak P-T conditions* (Fig. 1).

The proposed model for atoll garnet formation involves growth of complete garnet grains along the prograde path. These complete grains display pronounced chemical zonation and numerous inclusions in the cores of the garnet grains. With changing P-T conditions, the inclusions break down (or react with their host), liberating water and creating minute fractures that cut across the garnet grains. These fractures allow infiltration of an external fluid phase, promoting (i) dissolution of garnet cores simultaneously with continuing growth at the outer margins of the grains, and (ii) growth of glaucophane porphyroblasts. Geothermobarometry

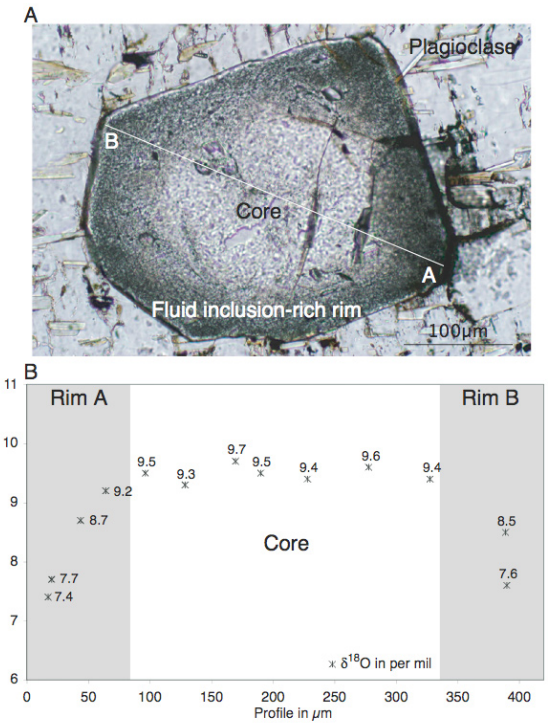

Figure 2. A- Photomicrograph of a cloudy garnet. B- $\delta^{18}O$ profile of the garnet shown in A.

using omphacite and phengite suggests that this process took place at peak P-T conditions (i.e. at about 20-25 kbar, 550°C), rather than during retrogression.

b) *Coupled dissolution-reprecipitation: zoning in oxygen isotopes and major elements in cloudy garnet from a metapelite* (Fig. 2).

Cloudy garnet crystals are interpreted to grow during the prograde path and to experience a re-equilibration at the temperature peak that essentially decreases the Ca content and $\delta^{18}O$ of garnet rims. On the basis of textural arguments (pseudomorphism, and the existence of porosity and and a fluid-inclusion-free outer rim), garnet re-equilibration is explained by a process of coupled dissolution-reprecipitation. Such a process, although recognised in zircon or feldspar, has not previously been considered during re-equilibration of metamorphic garnet; it is attractive because it allows the re-equilibration of slowly-diffusing elements such as Ca and O. As a consequence, porosity appears to be an effective pathway for element exchange between garnet and the matrix.

c) *Significance of oscillatory zoning in elongated garnet in an eclogite* (Fig. 3).

Garnet shows an unusual orientation that defines the foliation of the eclogite. The "wings" of the garnets show oscillatory zoning in Ca. The proposed model for the formation of the elongated garnets includes (i) coalescence of several grains, (ii) plastic deformation of single garnet grains, and (iii) stress-induced dissolution-reprecipitation leading to anisotropic growth. Oscillatory zoning of major elements in garnet has previously been related to varying P-T conditions along the metamorphic path (Garcia-Casco et al., 2002). In this case, the effect of varying water pressure in the rock has been tested as an alternative hypothesis using thermodynamic modelling.

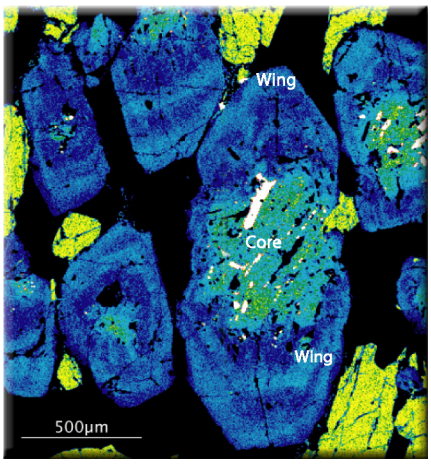

Figure 3. Ca X-ray map of an elongated garnet.

Contacts: Laure Martin and Michel Ballèvre
Funded by: ARC Discovery, CRPG-CNRS (Nancy, France), GEMOC

Deep drilling with basalts: over- and underplating of ancient crust in North China

XENOLITHS CARRIED UP TO THE SURFACE IN DEEP-SEATED MAGMATIC ROCKS provide us with windows into the composition and petrology of the deep crust and upper mantle, and tell us about processes at different depths in the Earth. It has proven much more difficult to get time constraints on these rocks – they are small, and often altered to the extent that conventional isotopic techniques give only ambiguous data. However, over recent years research with Prof Jianping Zheng, one of GEMOC's co-workers, has shown that with patience and painstaking attention to detail, zircon can be separated from many of these xenoliths, even those with mafic to ultramafic compositions. In a series of studies, he has used this "deep drilling" approach to follow the development of both the subcontinental lithospheric mantle, and the deep crust. In 2008, this technique produced a unique record of crustal evolution in the Xinyang area, near the southern boundary of the North China Craton (*GEMOC publication #519*).

The Mesozoic (~160 Ma) Xinyang volcaniclastic diatremes lie at the intersection between the Trans-North China Orogen and the Qinling-Dabie Orogenic Belt (Fig. 1), and carry a suite of xenoliths including mafic to felsic granulite, eclogite, meta-gabbro, pyroxenite and peridotite. The xenolith data show that the crust is temporally and compositionally zoned (Fig. 2). Whereas the oldest outcropping rocks are ca 2.85 Ga old, the upper part of the lower crust (to ca 30 km depth) consists of felsic granulites and rare pyroxenites that contain zircons with ages of 3.4-3.6 Ga. This "inverted stratigraphy" implies that the older crust was extensively resurfaced in Neoarchean time. The deeper (ca 30-45 km) parts of the lower crust consist of high-pressure (HP) mafic to felsic granulites and meta-gabbro, and the $^{207}Pb/^{206}Pb$ ages of most zircons in xenoliths derived from this deeper level are Paleoproterozoic (2.0-1.8 Ga). The presence of this younger layer beneath the 3.4-3.6 Ga crust suggests a major event of magmatic underplating. Hf-isotope data from the zircons (Fig. 2) indicate that this event involved both the addition of juvenile material (mafic granulites), and the remelting of older (3.0-3.8 Ga) rocks to produce intermediate to felsic granulites.

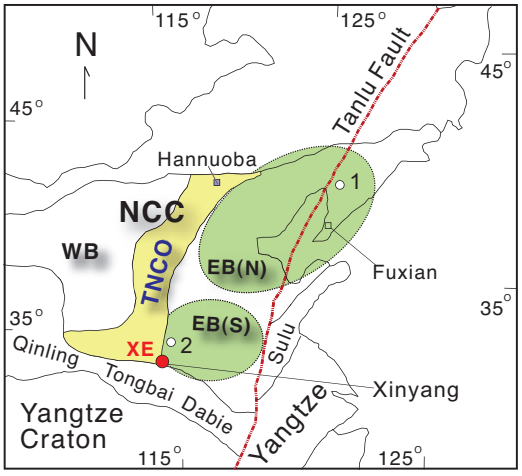

Figure 1. Major tectonic units in the eastern China: The North China Craton (NCC) is made up of the Western Block (WB) and the Eastern block (EB), which has two nuclei; these Archean blocks joined along the Trans North China Orogen (TNCO). The Xinyang xenolith locality lies on the edge of the southern nucleus (EB(S)), adjacent to both the TNCO and the Qinling-Tongbai –Dabie continental-subduction zone with UHP metamorphism.

Important populations of Paleozoic (440-260 Ma) and Early Mesozoic (228-219 Ma) zircons are interpreted as representing metamorphic zircon growth in response to thermal/metasomatic events. Mantle-derived peridotite xenoliths contain dominantly Triassic (ca 230 Ma) zircons, but rare Neoarchean grains record earlier metasomatic events in the subcontinental lithospheric mantle.

The xenolith suite thus records the growth and modification of the continental crust by overplating, underplating and metamorphism of an originally Paleo-Mesoarchean nucleus. Significant events reflected in the zircon record (Fig. 2) include at least:

1) initial formation of Paleo-Mesoarchean crust ; 2) formation of the upper crust in Neoarchean time; 3) assembly of the southern and northern parts of the Eastern Block of the North China Craton in Neoarchean time; 4) collision of the Western and Eastern Blocks of the North China Craton along the Trans-China Orogen in Paleoproterozoic time, with magmatic underplating and metamorphism in the lowermost crust; 5) subduction and collision of the Yangtze Craton with the North China Craton, which modified the lowermost crust and the upper mantle in Paleozoic and Early Mesozoic time.

This approach promises to provide many future surprises; results so far indicate that the lower crust may be significantly older than the upper crust in many parts of the world, and that the volume of ancient crust is greater than estimates derived from some models of crustal generation through time (e.g. *GEMOC Publications #339, 354, 422*).

Contacts: Jianping Zheng, Bill Griffin, Sue O'Reilly
Funded by: ARC Discovery, China NSF

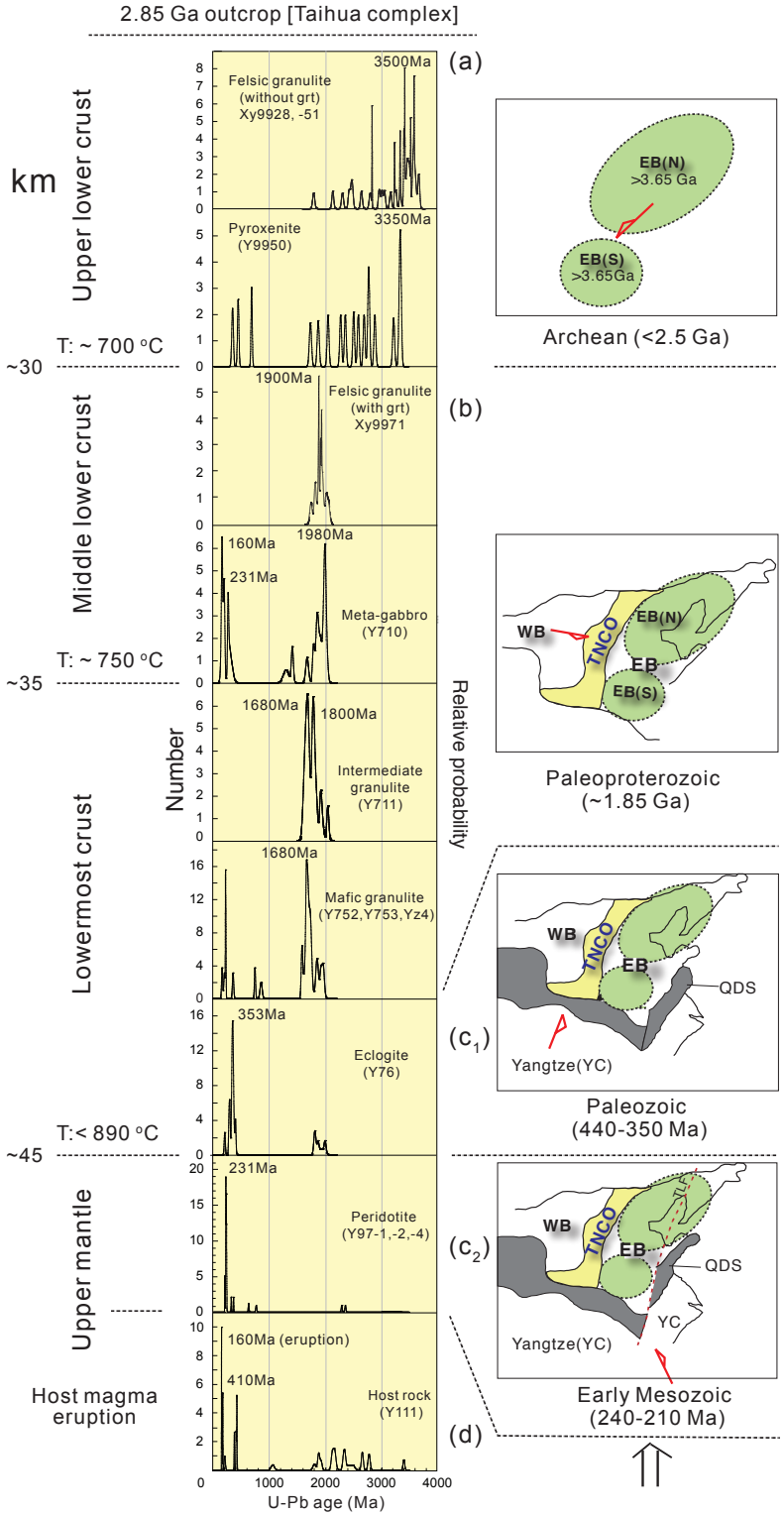

Figure 2. Cartoon showing the collision and accretion events recorded in the zircons of the Xinyang xenoliths. The original 3.5 Ga crust has been magmatically overplated (2.85 Ga) and underplated (ca 1.85-1.6 Ga), and this composite crust has been affected by Paleozoic to Mesozoic continental collision(s).

Evolutionary histories of Earth and Venus - coupled convection-degassing models

Our understanding of the divergent evolutionary histories of Earth and Venus is hindered by the sparsity of geological record - particularly the oceanic crustal record - in the deep Precambrian, and the almost complete lack of geological context on Venus. The Venera, Pioneer, and Magellan missions have increased our knowledge of Venus' surface, but Venus shows no hallmarks of plate tectonics, so interpreting these features is difficult. Cratering counts suggest nearly the entire surface of Venus was created in one event ~750 million years ago. Analyses of surface samples by the Venera landers suggest a similar bulk composition and heat budget to Earth, so this lack of tectonic activity is puzzling. It has been suggested that since Venus is dry, it may lack the lubrication of near-surface faults that Earth has as a result of pore pressure or the hydrous alteration of minerals. This would result in significantly stronger faults, and may preclude plate tectonics, so that Venus is in an episodic-overturn regime in which the entire lid is periodically recycled; this is consistent with the cratering record.

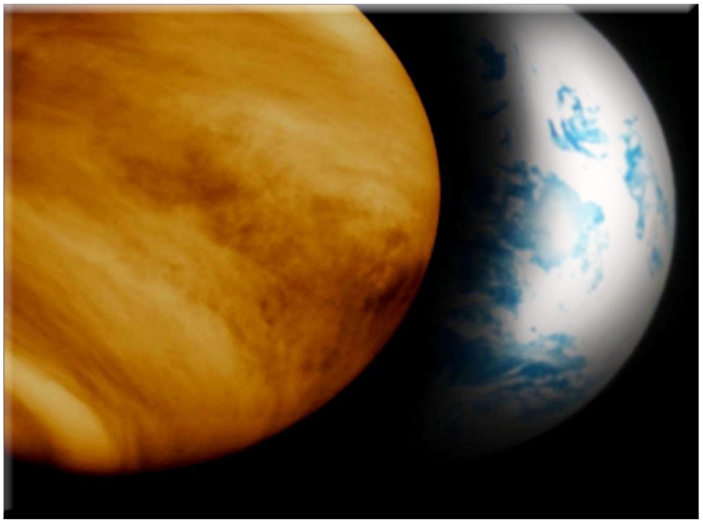

Figure 1. Venus and Earth are sister planets in terms of size and composition, but have had markedly different tectonic histories, which are reflected in their atmospheres.

Episodic mechanisms have also been postulated for the Precambrian Earth, based on the episodic nature of the preserved crustal record. While the meaning of these peaks in preservation is debated, these periods in Earth's history are also associated with massive volcanic, tectonic, and paleomagnetic disturbances. This has led to the suggestion that some episodic mechanism was at work in the distant past. Previous ideas focussed on mantle avalanches originating from instabilities in the mantle phase change at 670 km depth. Work at GEMOC (see *publication #499, 2007*) posited a new mechanism for episodic subduction, whereby the system stresses decrease with increasing heat production in the past, tipping Earth into an episodic overturn regime.

This model would imply that Earth went through a transition from episodic subduction in the early Precambrian, to modern plate tectonics as the planet cooled. The simulations also predict Venus may have in fact evolved from a stagnant-lid planet into an episodic regime, a suggestion that is at odds with traditional views of planetary evolution. It is consistent with the continental geology of Earth, but in the absence of an oceanic record, the evidence is equivocal. Furthermore, the absence of any record on Venus prior to ~750 Ma-1.2 Ga limits our geological insight into Venus' geodynamic evolution.

However, atmospheric compositions provide constraints on the history of volcanic degassing and the tectonic evolution of planets. Despite their superficial similarities, the atmospheres of Venus and Earth have evolved along significantly different paths. Without significant CO_2 sinks on Venus, ongoing volcanism has resulted in the buildup of extremely high CO_2 concentrations, which have contributed to the dehydration of Venus' surface. This dehydration, and the high surface temperatures, may contribute to the cessation of plate tectonics, as the reduction of water-weakening effects causes strong dry faults.

Venus' degassing history is to some extent recorded in its atmospheric argon signatures. Nonradiogenic ^{36}Ar is ~80 times that of Earth. Since most ^{36}Ar is primordial, this suggests

very different initial atmospheric conditions for the two planets, with Venus retaining most of its initial atmosphere due to its fortuitous impact history. On the other hand, the deficit of radiogenic ^{40}Ar (~24% escaped from the mantle, compared with ~52% for Earth), hints at a very different volcanic and tectonic history, particularly in the deepest past.

Mantle convection simulations performed at GEMOC hint at the tectonic factors behind these differences in the ^{40}Ar deficits on Earth and Venus. By modelling mantle melting and argon partitioning and degassing under different tectonic regimes, we can show that mobile-lid convection is 1.8 times more effective than episodic overturn in degassing the mantle, and 20 times more efficient than stagnant-lid convection. Coupling these results with evolutionary models for volcanism and degassing allows us to test the sensitivity of atmospheric ^{40}Ar abundances to tectonic evolution. Venus' argon budget is consistent with the planet having had stagnant-lid tectonics for the first 500 Myr of its history, and episodic overturn of the lid since then. It is not consistent with Venus having had plate tectonics for any significant portion of its history; this implies that Venus and Earth were never planetary twins but were very different planets from birth.

Earth's atmospheric ^{40}Ar deficit has often been attributed to hidden "unmixed" reservoirs in the deep mantle. However, the models show that this deficit can have a tectonic cause. The current ^{40}Ar content of our atmosphere is consistent with episodic convection till the end of the Archean, and plate tectonics since then, in agreement with geological data and previous convection modelling. If Earth's ^{40}Ar deficit does indeed have a tectonic cause, then the corollary is that its atmospheric ^{40}Ar budget is not consistent with Earth having had plate tectonics throughout the planet's history.

Contact: Craig O'Neill
Funded by: ARC Discovery, MQ University

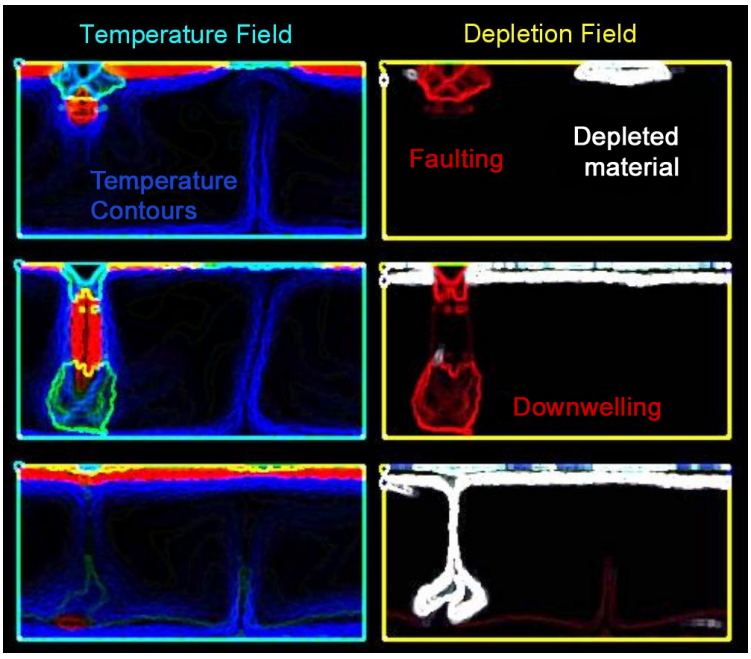

Figure 2. Time evolution of the temperature contours and depletion field for an episodic overturn simulation. Such a tectonic regime has been postulated for Venus today, and evidence suggests it has operated on Venus for the past 4 Gyr. Atmospheric and geological evidence suggest that it may have operated on Earth until the end of the Archaean, when it gave way to modern-style plate tectonics.

A guide to making high-magnesium andesites

ALTHOUGH THE MOST PRIMITIVE MAGMAS FROM MANY ARC VOLCANOES appear to be basaltic, there are a number of locations where primitive magmas are, or are inferred to be, more silica-rich andesites. Some of these are high-magnesium andesites with Mg# of around 0.7, which implies that such rocks are generated in, or equilibrated with, mantle peridotite under conditions that do not pertain beneath mid-ocean ridges. Geochemical data show that they did not form by slab melting. A review of experimental data on the melting of anhydrous peridotite showed that primitive high-Mg andesites also cannot be generated by anhydrous melting of lherzolite. A review of exisiting experimental data demonstrates that addition of H_2O alone cannot explain the increases in both SiO_2 and MgO contents (on an anhydrous basis) required to shift from basaltic to high-Mg andesitic melts in equilibrium with lherzolite residue. A much more plausible alternative is that these melts are extracted from a harzburgite residue. In order to study this further, experiments were performed at 0.6 GPa in the new high-pressure laboratories at GEMOC in which high-Mg andesitic melts were equilibrated with an olivine+orthopyroxene residue. The results showed (in the absence of H_2O) that MgO and SiO_2 contents increase in the ratio 2:1 as the degree of undersaturation in clinopyroxene increases. This is the right sign and magnitude of effect to explain the compositions of primitive high-Mg andesites. When the effects of H_2O and clinopyroxene undersaturation were added together it was possible to obtain a line in Pressure-H_2O space which describes the conditions under which a given high Mg-andesite could be in equilibrium with a harzburgite residue. Application to rocks from White Island (New Zealand), Amphlett Island (Papua New Guinea), Setouchi Belt (Japan), Mt. Shasta (USA), Adak Island and Piip volcano (Aleutians, USA) yield, for crustal thicknesses > 20 km, H_2O contents of the melts of 2-8%, in generally good agreement with the available compositions of melt inclusions.

Photo: White Island volcano, New Zealand, where high-magnesium andesites erupted in 1977.

Contacts: Simon Turner, Bernie Wood
Funding: ARC Federation Fellowships

Multiple magma processes and TTG genesis

GEOCHEMICAL STUDIES tell us that tonalite-trondhjemite-granodiorite (TTG) plutonic complexes must be formed by partial melting of metabasaltic source material, but they cannot tell us the tectonic regime in which this crust was formed, nor how large volumes of TTG magma can be generated. A solution to TTG arc crust formation requires an interdisciplinary approach to resolve the tectonic setting (slab melt versus mafic lowermost crust sources), the time and length scales for melting and extraction, and the role of melt segregation mechanisms in the formation of both Archean TTGs and more recent adakite-like magmas. We have used an experimental approach that, when coupled with numerical models (Fig. 1), allows us to address some of these issues. The experiments are designed to reproduce the local changes in bulk composition that are predicted to occur in response to buoyancy-driven melt segregation along grain edges and the associated compaction of the solid residue. We observe changes in the melt composition and proportions of melt and solid phases between earlier direct partial melting (DPM) and the new segregation equilibration experiments (MSE) on metabasalt bulk compositions.

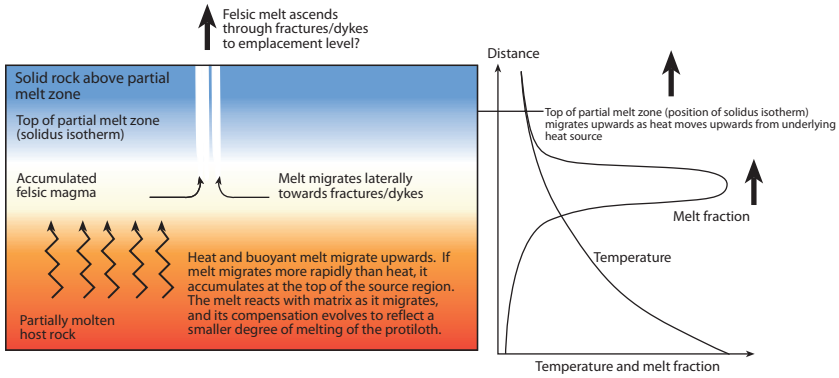

Figure 1. Felsic partial melt may segregate from a mafic host during buoyancy-driven compaction of the matrix (Jackson et al., 2005). Previous studies which suggested that this segregation mechanism is too slow (e.g. McKenzie, 1984) to yield large volumes of felsic melt neglected the chemical interaction between the melt and its matrix.

The MSE experimental results show distinct differences in the compositions of melts and solid phase and the stability of different solid phases when compared with the results from direct partial melting (DPM) experiments. The resulting melt compositions are lower in An and have higher Mg-numbers. Compared to DPM experiments, the MSE experiments show a significant reduction in hornblende and plagioclase abundances at lower temperatures (Fig. 2).

The results suggest that dynamic melt segregation and equilibrium processes may modify the modes, melt compositions, and geochemical indicators such as Mg-numbers. Both adakites and TTGs may form from partial melting of a hydrous mafic protolith, but their associated tectonic setting may be very different. This research does not support the hypothesis that links their petrogenesis through slab melting alone; nor models that require subsequent interaction of melts with the mantle wedge to increase Mg-number. The data from these melt segregation experiments demonstrate that it is possible to create variations in felsic melt compositions by partial melting and segregation processes within a mafic crustal underplate.

Contact: Tracy Rushmer

Funded by: Imperial College, UK; MQNSG

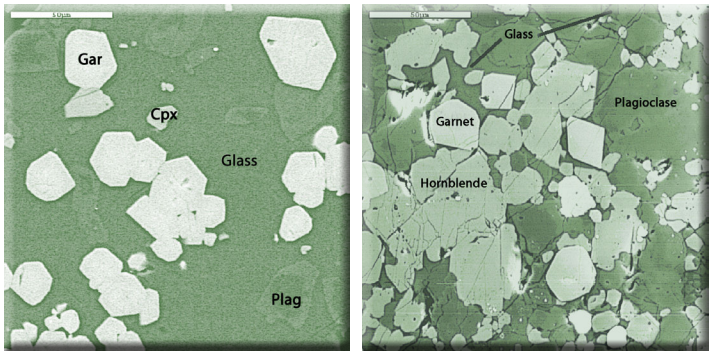

Figure 2. Comparison between direct partial melting of SC5 at 1.4 GPa and 975°C and MSE experiments. (A): JP3 melted at 1.4 GPa and at 975C% with 15% melt composition at 50:50 and 2.5 wt% water added. The synthetic (anhydrous) glass composition at 15vol% is from this SC5-8 experiment. JP3 contains 64% glass, 17% plagioclase, 12% garnet, 6% cpx, and 1% ilmenite; no hornblende is present (Table 3). (B): SC5-8 is composed of hornblende (40%), plagioclase (40%), melt (glass) 15% and garnet 5%. Glass composition in SC5-8 is granodioritic with Mg number of 26; JP3 glass is also granodioritic but with Mg-numbers averaging 31.

Copper isotopes blaze the trail to hidden ore deposits

TWO FUNDAMENTAL GOALS OF MINERAL DEPOSIT RESEARCH are to identify the sources of the metals and to understand the processes that have mobilised, transported and deposited them. To this end, geochemists have used several isotopic systems, including light stable isotopes (e.g. H, O and S) and radiogenic isotopes (e.g. Nd, Pb and Os). However, the stable isotope ratios of the metals themselves (e.g. Fe, Cu and Zn) may provide the most direct answers to these long standing questions. In the last decade, the development of multi-collector inductively coupled plasma-mass spectrometry (MC-ICP-MS) has made the high-precision measurement of metal stable-isotope ratios possible. This technique can analyse subtle variations in the stable-isotope ratios of metals in rocks and metal-bearing minerals, providing the economic geologist with a powerful new tool for investigating mineralised systems (*GEMOC publication #527*).

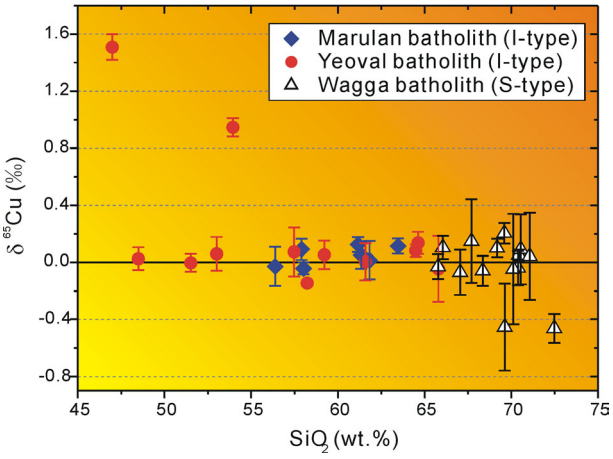

Figure 1. Variation of $\delta^{65}Cu$ against SiO_2 content for rocks from the Lachlan Fold Belt. Error bars denote 2 standard deviations.

Copper has two stable isotopes, and their ratio commonly is expressed in δ notation ($\delta^{65}Cu = (R_{sample}/R_{NIST976}-1)\times1000$ where $R = {}^{65}Cu/{}^{63}Cu$). The main area of application of Cu isotopes to date has been the study of ore-forming systems. However, the baseline values of $\delta^{65}Cu$ for different geological reservoirs (especially the crust) have not been well constrained, and this has been a major impediment to the interpretation of Cu isotope data. Furthermore, because mineralising systems influenced by low-temperature redox processes show much larger variations in $\delta^{65}Cu$ than the high-temperature mineralising systems, there is no consensus on whether Cu isotopes carry useful information for interpretation of mineralisation processes.

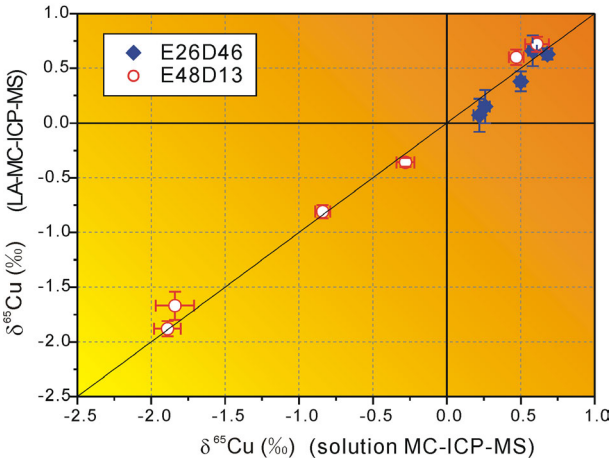

Figure 2. Comparison of the Cu isotope data measured by LA-MC-ICP-MS and solution MC-ICP-MS.

We have carried out the first systematic measurements of the $\delta^{65}Cu$ of granites (*GEMOC publication #527*). The chemical procedure developed at GEMOC has achieved quantitative recovery (100.6±1.6%), with a low total procedural blank (2.65±0.66ng) for Cu, allowing isotopic analysis of samples with as little as 10 ppm Cu. Well-characterised granites and related rocks from the Lachlan Fold Belt (LFB) in southeastern Australia were selected for analysis. The Cu-isotope ratios ($\delta^{65}Cu$ relative to NIST SRM 976) of 32 rock samples, ranging from mafic to felsic compositions, from 3 batholiths (2 I-type, 1 S-type) from the LFB, vary from -0.46‰ to 1.51‰. Most of them cluster around zero, with mean values for the I-type and S-type granites of 0.03±0.15‰ and -0.03±0.42‰ (2 sigma) respectively (Fig. 1). These data, together with Cu-isotope ratios of two loess samples, provide preliminary evidence that the baseline $\delta^{65}Cu$ of the crystalline part of upper continental crust is close to zero. The tight clustering of $\delta^{65}Cu$ in rocks from the I-type suites suggests that high-temperature magmatic processes do not produce significant Cu isotope fractionation. However, two granites with abnormally heavy Cu-isotope signatures ($\delta^{65}Cu$ up to 1.51‰) may have been affected by local hydrothermal alteration.

Copper isotopes also have been measured in sulfide minerals (chalcopyrite and bornite) from

the Northparkes porphyry Cu-Au deposit in SE Australia by MC-ICP-MS and laser ablation MC-ICP-MS. The Cu-isotope data obtained by the two techniques are consistent (Fig. 2). The results from both methods show a variation in δ^{65}Cu of hypogene sulfide minerals greater than 1 ‰. Significantly, the results from four drill holes through two separate ore bodies show strikingly similar patterns of Cu isotope variation with depth. There is a sharp down-hole decrease in δ^{65}Cu from ~ 0.8 ‰ in the low-grade ore zones (or phyllic-propylitic alteration zone) to ~ -0.4‰ at the margins of the most mineralised zones (Cu grade > 1wt. %). In the high-grade cores of the systems, the δ^{65}Cu values are more consistent at around 0.2‰ (Fig. 3). A number of hydrothermal processes, including diffusion driven by the Cu concentration gradient, precipitation of Cu sulfides from brine during cooling, partitioning of Cu into a vapour phase, and remobilisation of Cu by oxidising ground water during convection, may have contributed to the observed Cu isotopic variations (Fig. 3).

This work demonstrates that Cu isotopes show a large response to high-temperature porphyry mineralising processes, while the study on Cu isotopes in granites demonstrates that magmatic evolution does not produce significant Cu isotope fractionation. Taken together, these results suggest that Cu isotopes may be used as a vector to buried mineralisation.

Contacts: Weiqiang Li, Norman Pearson, Simon Jackson, Sue O'Reilly
Funded by: Macquarie University iMURS, ARC Discovery, MQ PGRF

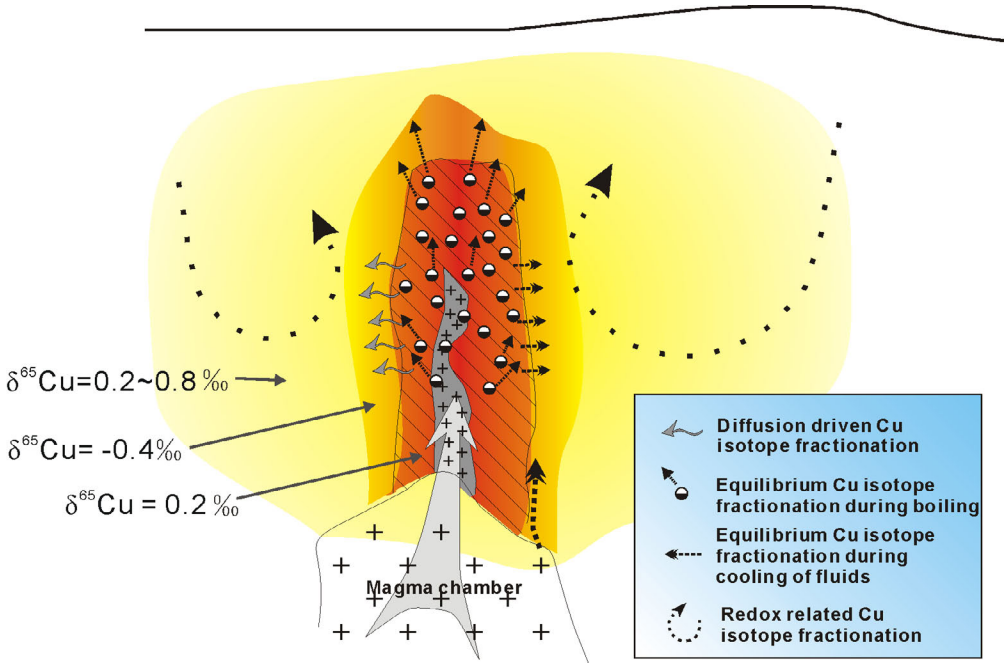

Figure 3. A summary of the pattern of Cu isotope variation in the Northparkes deposit and possible mechanisms of Cu isotope fractionation in a conceptual model for porphyry Cu deposits.

Re-Os in sulfides tracks deep fluid interactions in old Spanish mantle

THE RONDA PERIDOTITE is the largest (~ 300 km^2) known exposure of subcontinental mantle peridotites. It is located in the Betic Cordillera of southern Spain, the westernmost segment of the Alpine belt in Europe. One of the most remarkable features of this orogenic peridotite massif is the transition from highly foliated spinel-peridotite tectonites (Fig. 1a) to relatively undeformed granular peridotites (Fig. 1b), separated by a recrystallisation front. Compositional variations across this narrow transition zone indicate that the granular peridotites were produced in Cenozoic time, when partial melts derived from upwelling asthenosphere percolated into the subcontinental lithospheric mantle (the spinel tectonite domain). The Ronda massif thus constitutes a natural laboratory where we can investigate the geochemical behavior of isotopic systems during mantle lithosphere-asthenosphere interaction. We have used *in situ* isotopic analyses of sulfide minerals in the peridotites to study the effects of melt percolation on the Re-Os system.

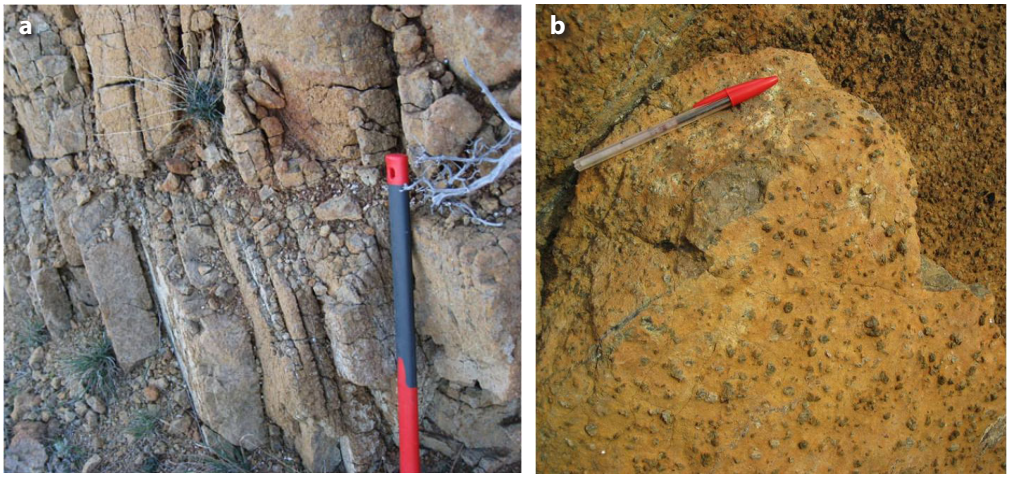

Figure 1. Field pictures of mantle peridotites from the Ronda spinel tectonite (a) and coarse-granular (b) domains.

Figure 2 shows that sulfides from both microstructural domains and the recrystallisation front show large ranges in Re/Os and Os-isotope composition. $^{187}Re/^{188}Os$ and $^{187}Os/^{188}Os$ in sulfides from the coarse-granular domain largely overlap with values in the spinel tectonites and there is no significant difference between the isotopic composition and variability of sulfides from these domains. However, some grains in samples at the recrystallisation front show an apparent decoupling between relatively high $^{187}Re/^{188}Os$ and low $^{187}Os/^{188}Os$. These sulfides are probably products of refertilisation reactions induced by percolating melts at the front, which caused significant enrichment of Re relative to Os. Aside from these effects, Re-Os systematics in the Ronda mantle peridotites apparently were largely unaffected by partial melting and melt transport induced by the Cenozoic lithospheric thinning, and mostly record more ancient tectonothermal events.

Figure 3 shows the distribution of Re-depletion ages (T_{RD}) in individual sulfides from the Ronda massif. T_{RD} ages cluster around three main peaks: 1.6-1.8 Ga, 1.2-1.4 Ga, and 0.7-0.8 Ga. Sulfides with relatively high Os contents and low Re/Os have Re-depletion ages that coincide with the two most ancient Proterozoic peaks. These grains are probably residual after variable degrees of melt extraction from the upper mantle and suggest that the Ronda peridotites underwent two main melting events at ~ 1.6-1.8 Ga and 1.2-1.4 Ga, respectively. One of these

Proterozoic episodes probably coincided with the incorporation of the massif into the refractory subcontinental lithosphere. Other grains, generally those with low Os contents and high Re/Os, suggest that a third generation of sulfides precipitated in the Ronda peridotites at ~ 0.7-0.8 Ga. These sulfides may have formed by interaction of ancient grains with younger metasomatic melts/fluids, or by crystallisation of sulfide melts and sulfide-rich fluids, and suggest the percolation of metasomatic melts/fluids in the Neoproterozoic when the massif was equilibrated at subsolidus conditions. Considering the uncertainties inherent in model age calculations, the three "events" recognised in the Ronda sulfides correspond to the range of Nd model ages recorded in the crustal basement of Hercynian Europe and northern Africa (Fig. 3). The Proterozoic Os model ages exhibited by sulfides in the Ronda peridotites thus appear to reflect different stages in the evolution of the crustal mass of Gondwana, which was later recycled in the Paleozoic.

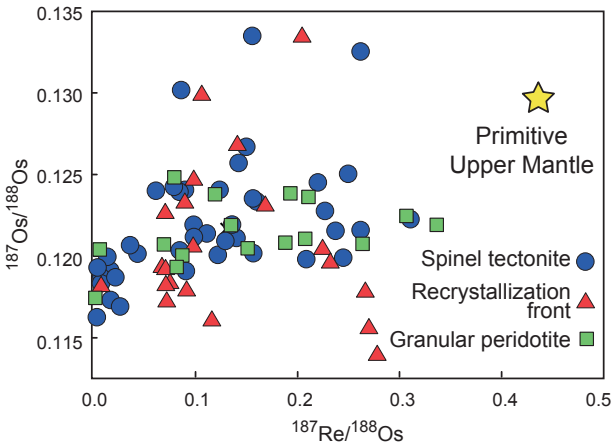

Figure 2. $^{187}Re/^{188}Os$ versus $^{187}Os/^{188}Os$ in sulfides from the Ronda peridotites.

Contact: Claudio Marchesi
Funding: University of Grenada and ARC

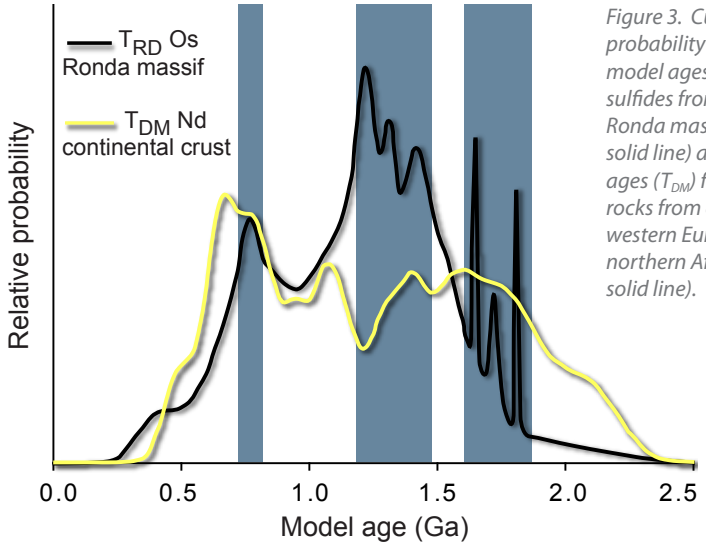

Figure 3. Cumulative probability plots of Os model ages (T_{RD}) for sulfides from the whole Ronda massif (black solid line) and Nd model ages (T_{DM}) for crustal rocks from central/western Europe and northern Africa (yellow solid line).

Melt migration transforms New Zealand's depths

HIGH-P TERRANES commonly contain a mixture of high- and low-P assemblages. The high-P assemblages are variably interpreted as part of high-P crust (i) tectonically juxtaposed against low-P rocks that never experienced high-P; or (ii) associated with low-P assemblages in adjacent crust that (a) persisted metastably during the high-P event or (b) re-equilibrated extensively during exhumation. The distinction between these models is important, because a failure to distinguish widespread metastability or extensive retrogression may lead to invalid interpretations of the tectonic and metamorphic evolution of a terrane. Furthermore, misinterpretations of the metamorphic behaviour of large volumes of crust may lead to problems and inaccuracies in geodynamic modelling of large-scale tectonic events.

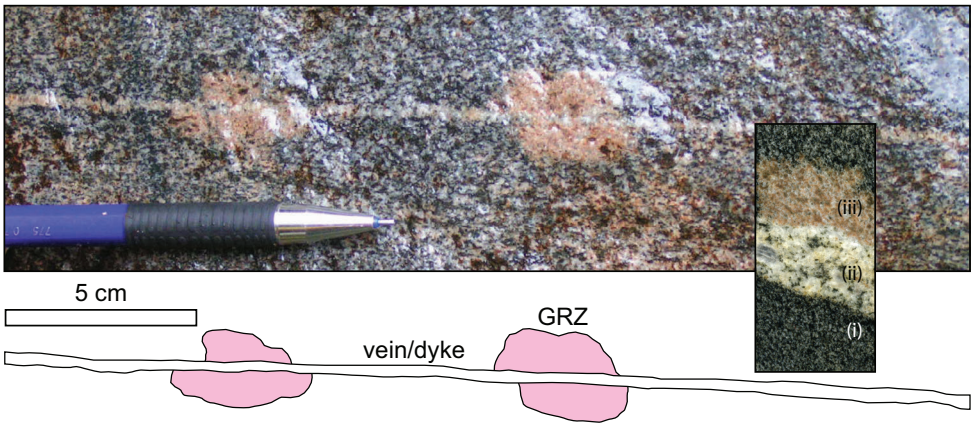

Figure 1. Outcrop photograph and sketch of a thin dyke and localised development of garnet reaction zone (GRZ) textures in irregular-shaped patches that are discontinuous and in some places are asymmetric with respect to the dyke (see flat bed scan of sample LG4051 that also shows the three key lithologies: (i) host Western Fiordland Orthogneiss (WFO), (ii) granodioritic dyke, and (iii) GRZ.

Recrystallisation of two-pyroxene hornblende granulite to garnet granulite is limited to a very small percentage (<10 %) of the crust in western Fiordland, New Zealand, suggesting that the assemblages in large parts of the deep crust persisted metastably under high-P conditions. Recrystallisation at high P is mostly associated with injection migmatite structures, in which narrow anorthositic or trondhjemitic veins and dykes cut two-pyroxene hornblende granulite facies orthogneiss. The host orthogneiss exhibits irregular, spatially restricted recrystallisation to garnet granulite along the edges of veins and dykes.

Figure 2. Back-scattered electron (BSE) images showing primary igneous and secondary textures in the dykes.

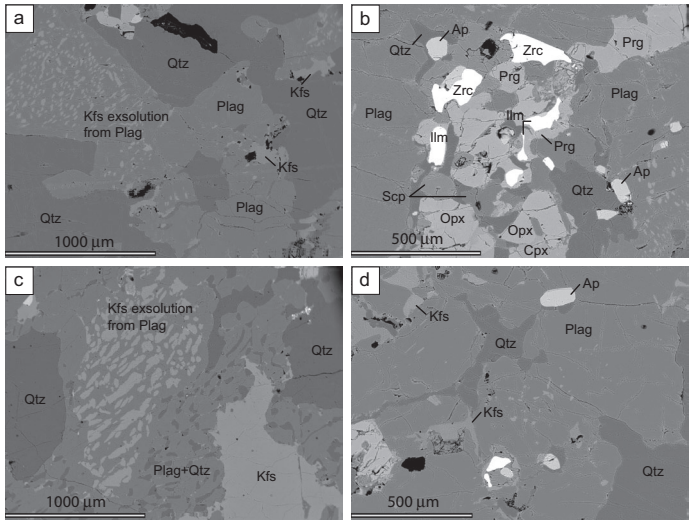

Recent research results:

A major arc batholith, the Western Fiordland Orthogneiss in Fiordland, New Zealand, exhibits irregular, spatially restricted cm-scale recrystallisation from two-pyroxene hornblende granulite to garnet granulite flanking felsic dykes (Fig. 1; see *GEMOC Publication 556*). At Lake Grave in northern Fiordland, the composition and texture of narrow (<10-20 mm across) felsic dykes that cut the orthogneiss are consistent with an igneous origin (Fig. 2) and injection of melt to form orthogneiss migmatite. New U-Pb geochronology suggests the injection of dykes and migmatisation occurred at ca 115 Ma (Fig. 3), during the latter stages of arc magmatism. Recrystallisation to garnet granulite is promoted by volatile extraction

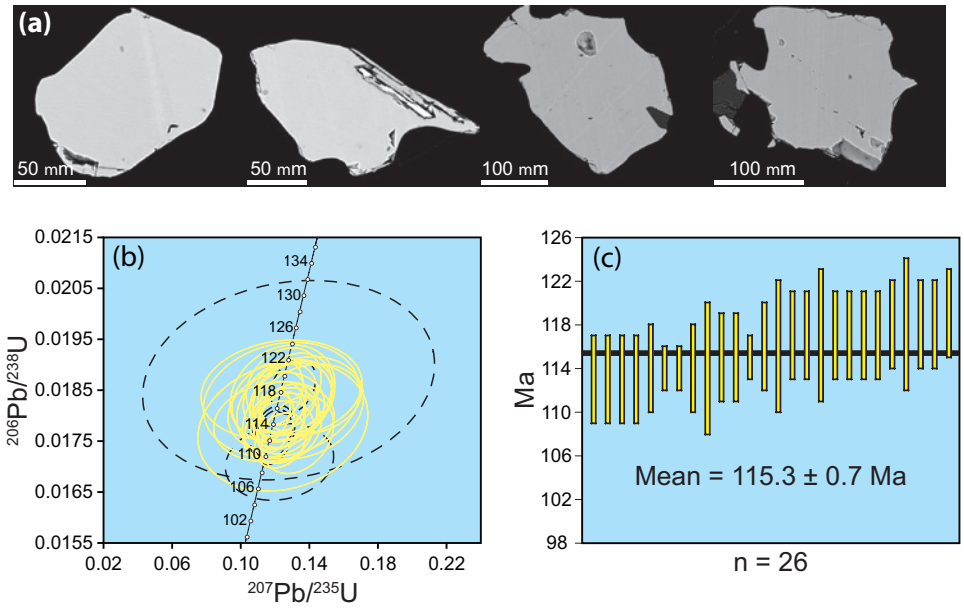

Figure 3. (a) BSE images of zircon from the narrow (< 20 mm) granodioritic dyke cutting sample LG4051 (Fig. 1). (b) U-Pb Concordia plot of a single zircon age population (n = 31). Dashed line error ellipses are excluded from the weighted mean age. (c) Weighted average mean diagram for the zircon data in (b); weighted mean by data-point errors = 115.3 ± 0.7 Ma (2σ), MSWD = 0.97 (n = 26/31) and probability = 0.5.

from the host two-pyroxene hornblende granulite via adjacent dykes and the patchily developed garnet granulite is left as a marker adjacent to the melt migration path. New modelling of mineral equilibria shows that a two-pyroxene hornblende assemblage is stable at P < 11 kbar, whereas a garnet granulite assemblage is stable at P > 12 kbar (Fig. 4), suggesting that garnet granulite may have formed with less than 5 km crustal loading of the batholith. Though the garnet granulite assemblages signify that the Western Fiordland Orthogneiss experienced high-P conditions, the very local nature of these textures indicates widespread metastability (>90 %) of the two-pyroxene hornblende granulite assemblages. These results indicate that metastable assemblages may be widespread in mafic lower arc crust during deep burial and demonstrate that the degree of reaction in the case of Fiordland is related to interaction with migrating melts.

Contact: Nathan Daczko
Funding: MQ Safety Net Grant

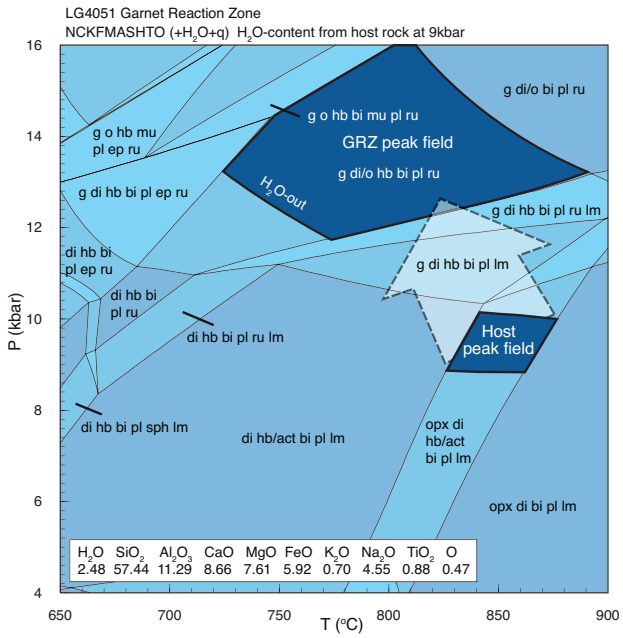

Figure 4. An H_2O-saturated combined P-T pseudosection calculated for the LG4051 host (S1) and GRZ bulk compositions. The inferred peak S1 assemblage field is outlined in bold. The inferred peak GRZ quadrivariant assemblage field g-di-hb-bi-pl-ru-q-H_2O, calculated with a fixed H_2O-content equivalent to the minimum amount of H_2O required to calculated the peak S1 assemblage at 9 kbar, is also outlined in bold. The arrow indicates a likely P-T path for the Lake Grave rocks.

Alloys in ophiolites wheel in new ideas on Earth evolution

OPHIOLITES ARE PIECES OF OCEANIC LITHOSPHERE that have been thrust onto the edges of continental plates; a complete ophiolite section consists of mantle-derived peridotites, overlain successively by mafic and ultramafic lavas and sedimentary rocks such as greywackes and cherts. The peridotitic members of the ophiolite sequences commonly contain bodies of massive chromite, in lenses, layers and veins, and the origins of these chromitites has been controversial for at least a century. The chromitites commonly contain scattered grains of Platinum-Group-Element (PGE) alloys, and these tiny grains are keys to the origins of the ophiolites. Rendeng Shi, one of GEMOC's co-workers, has used a specially built separation plant to process tons of chromites from the Triassic-Jurassic Luobusa and Dongqiao ophiolites in Tibet, releasing several hundred grains of alloy minerals, and has used GEMOC's facilities to analyse their elemental composition and their Os-isotope ratios. This has resulted in new insights into chromitite formation, the development of ocean basins, and the isotopic composition of the Earth's convecting mantle (*GEMOC publication #482*).

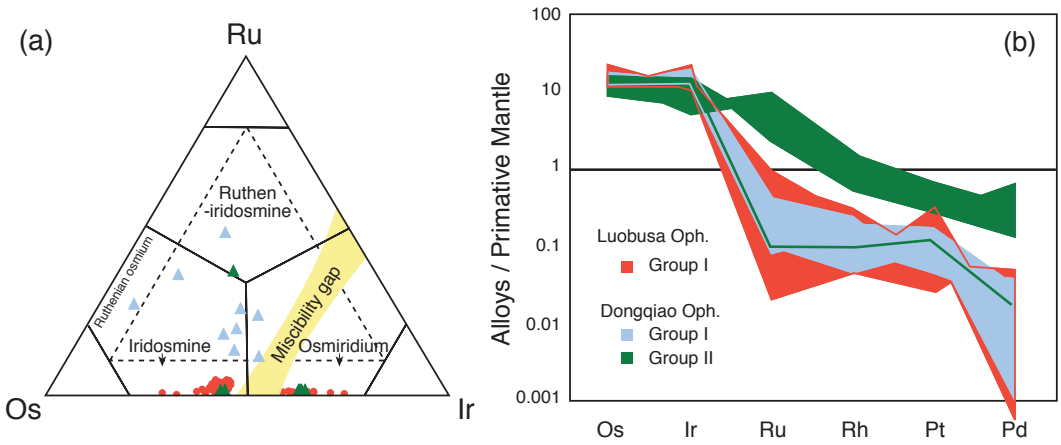

Figure 1. (a) Compositions of the analysed alloy grains from the Luobusa and the Dongqiao ophiolites in Os–Ir–Ru space. Note the two groups for Dongqiao Os-rich alloys, Group I with low Ru, and Group II with high Ru grains. (b) Primitive-mantle-normalised PGE concentrations of Group I and Group II alloys from Luobusa and Dongqiao (modified from GEMOC publication #482).

170 grains of Ru-Os-Ir alloys were analysed; most are osmiridium or iridosmine (Fig. 1). Based on elemental and isotopic compositions, two populations can be identified. Group I, found in both ophiolite bodies, has fractionated PGE patterns typical of similar alloys from other ophiolites. In contrast, Group II alloys from the Dongqiao ophiolites show PGE patterns with a "stepped" pattern, similar to those commonly seen in sulfide minerals that are residual after melting events (see *GEMOC Publication #290*). Group I alloys from both ophiolites have very homogeneous $^{187}Os/^{188}Os = 0.12645 \pm 4$ (2s; n=145), broadly consistent with the young age of the ophiolite. The Group II alloys from Dongqiao have more heterogeneous $^{187}Os/^{188}Os$ (0.12003 to 0.12194); referred to a typical Primitive Mantle evolution curve, these values yield Re-depletion ages from ca 950 to ≥1.1 Ga.

The Group I alloys are interpreted as early cumulate phases, precipitated during the crystallisation of magmas derived from the asthenosphere. In contrast, Group II alloys are inferred to reflect the breakdown of residual sulfides from the mantle section of the ophiolite, retained since a Proterozoic melt-depletion event. The signatures of such events would probably be lost by homogenisation in the convecting asthenospheric mantle, so these ancient depletion ages suggest that the Dongqiao mantle section originated as a piece of subcontinental lithospheric mantle, trapped during the opening of the Neo-Tethyan ocean (see *Research Highlight, p30*). The coexistence of the two groups of alloys in Dongqiao samples

suggests interaction between asthenosphere-derived melts and old depleted lithospheric mantle and implies that the chromitites originated through such melt-rock reactions.

The data on the Group I alloys also have implications for the Os-isotope composition of the asthenospheric mantle, the framework in which most mantle Re-depletion ages (sulfides, alloys and whole-rock samples) are usually interpreted. The two ophioites have some relatively tight age constraints; both bodies are part of the Neo-Tethyan (Triassic-Jurassic) ocean system. Dikes cutting the Luobusa chromitites have been dated to 177±31 Ma, and cumulates from the Dongqiao body have given a Re-Os whole-rock isochron of ca 240 Ma, so that the Os-isotope composition of the Group I alloys should represent the composition of the convective oceanic mantle between ca 100-250 Ma. When compared with different models for the Os-isotope composition of the mantle (Fig. 2) this value plots well below the commonly used Primitive Mantle model, and above the Carbonaceous Chondrite model. Instead, these data support the hypothesis that the Re-Os evolution of the convective oceanic mantle resembles that of Enstatite Chondrites.

With this encouraging start, GEMOC is now carrying out analyses of Os-Ir alloys from ophiolitic sequences worldwide, to cover a larger age range.

Contacts: Rendeng Shi, Bill Griffin, Sue O'Reilly
Funded by: China NSF, ARC Discovery

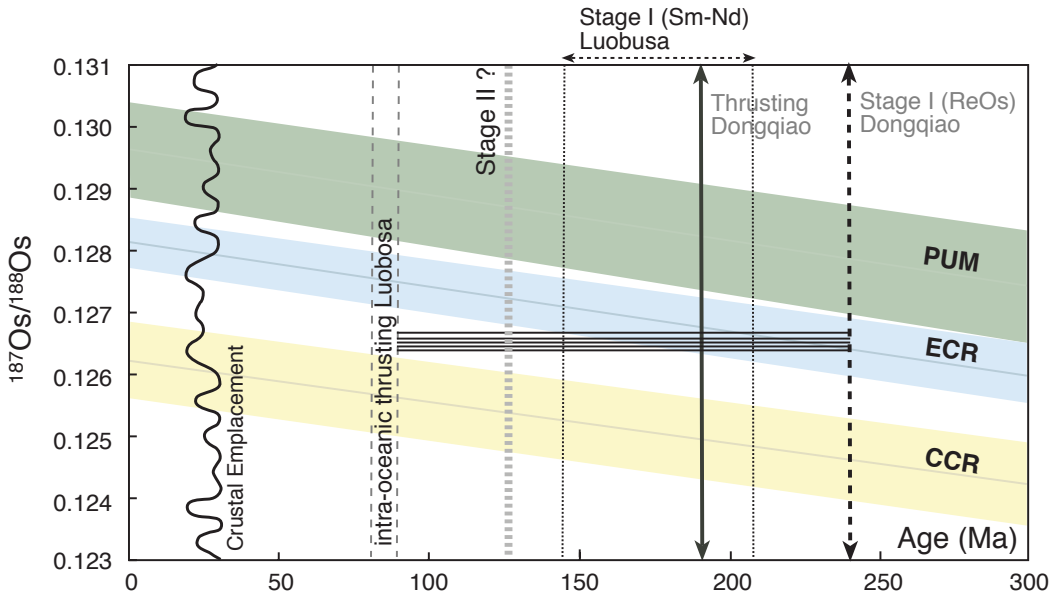

Figure 2. Models for the Re–Os evolution of the convecting mantle. Mantle evolution curves were defined as follows: CCR (Carbonaceous Chondrite reservoir) curve assumes that the Earth's mantle has an Os isotopic composition and Re/Os similar to that of carbonaceous chondrites ($^{187}Os/^{188}Os$ CC=0.1262 ± 0.0006, $^{187}Re/^{188}Os$ CC=0.392 ± 0.015 (Walker et al., 2002b)); ECR (Enstatite Chondritic Reservoir) curve is calculated using a present-day $^{187}Os/^{188}Os$ value of 0.1281 ± 0.0004 and $^{187}Re/^{188}Os$=0.421 ± 0.013 as measured in enstatite chondrites (Walker et al., 2002b); PUM (Primitive Upper Mantle) curve has a present day $^{187}Os/^{188}Os$=0.1296 ± 0.0008 and $^{187}Re/^{188}Os$=0.42. These estimates were obtained by linear regression through suites of mantle-derived peridotite xenoliths and orogenic-massif peridotites sampling mainly the Proterozoic to Phanerozoic sub-continental upper mantle(Meisel et al., 2001) (modified from GEMOC publication #482).

Where are the diamonds in the Congo?

OUR KNOWLEDGE of the nature and composition of the subcontinental lithospheric mantle (SCLM) is largely based on the study of xenoliths and xenocrysts brought to the Earth's surface by volcanism (e.g. kimberlite). Ni and Cr in pyrope garnets can be used to estimate temperature (TNi) and pressure (PCr) of equilibration. The pressure-temperature (P-T) relationships may be used to construct the geotherm. The depth of the lithosphere-asthenosphere boundary (LAB) can be estimated by Y and temperature relationship in garnet, the asthenosphere being characterised by absence of low-Y garnets (< 10 ppm). Zr, Y, Ga and Ti contents in garnets can be used in order to determine the types of metasomatism in the SCLM where the garnets were derived. The increase in Zr accompanied by increases in Y and Ti indicate melt metasomatism whereas an increase in Zr with low to moderate Ti, Y and Ga characterise phlogopite metasomatism (Griffin et al., 1992, CMP 110 and *GEMOC publication #1*). Garnets can be categorised into 5 groups based on their inter-element correlations: depleted harzburgites, depleted lherzolites, depleted/metasomatised lherzolites, fertile lherzolites and melt-metasomatised peridotites (*GEMOC publication #299*).

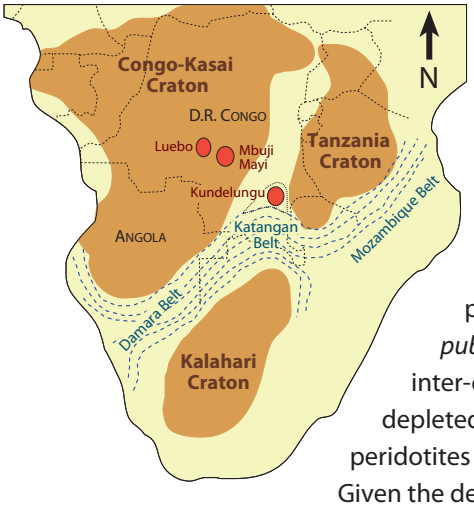

Figure 1. Sketch geological and locality map for sub-Saharan Africa showing the main cratonic areas (brown).

Given the depth at which the garnets equilibrated and the geochemical process and rock type indicated by the composition of the garnets, the proportion of the garnets reflecting individual rock types and processes at particular depths can be calculated. This allows the construction of a section through the lithosphere showing the variation in the proportions of rock types or types of processes with depth. These sections have been described as "Chemical Tomography" (see *GEMOC publication #409* for more information).

Garnets included in diamond are characterised by high XMg [Mg/(Mg+Fe)], and show sinuous rare-earth element (REE) patterns with enrichment in MREE and depletion in HREE. Malkovets et al. (2007, *GEMOC publication #449*) suggested that the presence of abundant chromite associated with garnets showing these characteristics indicate the presence of diamond.

This study applies this methodology to data from xenocrystic peridotitic pyrope garnets

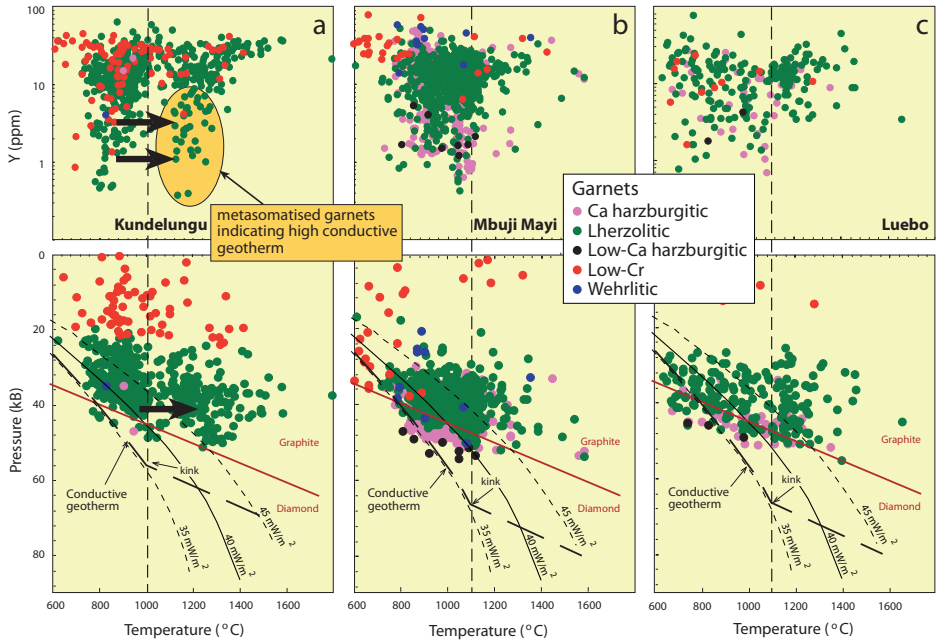

Figure 2. Conductive geotherms for Kundelungu (a), Mbuji Mayi (b) and Luebo (c). Note the geotherm is 35 mW/m² for all the region and the presence of low-Y garnets with high temperature in Kundelungu but not observed in Mbuji Mayi and Luebo.

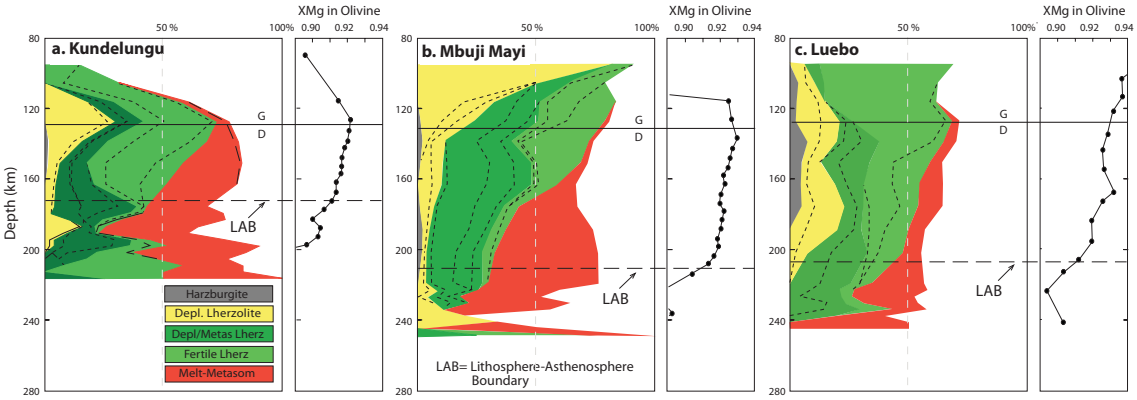

Figure 3. Subcontinental lithospheric mantle chemical tomography for Kundelungu (a), Mbuji Mayi (b) and Luebo (c). The horizontal line marked G-D gives the depth for the graphite-diamond stability field in the region. The LAB depth is drawn based on the decrease in XMg in olivine coexisting with garnet.

from Kundelungu, Mbuji Mayi and Luebo in the southern part of the Democratic Republic of the Congo (Fig. 1; *GEMOC publication #565*). Because the Mbuji Mayi and Luebo regions are located inside the Congo-Kasai Craton whereas Kundelungu is outside of the craton, this study provides an opportunity to compare the composition and structure of the lithospheric mantle and kimberlite peridotitic diamond potential in two different geological settings. The data allow the following conclusions:

1. Despite the location in two different tectonic settings, Kundelungu, Mbuji Mayi and Luebo are characterised by low, cratonic-type conductive geotherms (Fig. 2), but the deeper parts of the Kundelungu section have been thermally disturbed.
2. The lithospheric mantle beneath the Kundelungu area (off-craton) is relatively thin and fertile compared with that represented by garnets from Mbuji Mayi and Luebo (on-craton) (Fig. 3), and may represent refertilised Archean cratonic lithosphere as also shown by zircon data (*GEMOC publication #464*).
3. The disturbance of the initially low geotherm in Kundelungu is correlated with the upwelling of melts related to the opening of the East African Rift.
4. The mantle sections beneath the Kundelungu, Mbuji Mayi and Luebo regions were affected by melt-related and phlogopite-related metasomatism but these effects, and especially the melt-related metasomatism, were most pronounced in Kundelungu.
5. The Mbuji Mayi and Luebo areas have higher peridotitic diamond potential as shown by abundant harzburgitic garnets with characteristics similar to those of garnets included in diamond and abundance of chromite (Fig. 4 for Luebo).
6. The apparent scarcity of diamonds in the kimberlites of the Kundelungu Plateau as indicated by the scarcity of harzburgitic garnets and chromite is attributed to the heating and melt-related metasomatism that has affected the lithosphere in the region. Some of Kundelungu lherzolitic garnets have characteristics similar to garnets included in diamond (Fig. 4).

Figure 4. Nd/Y-Sc/Y and Nd/Y-T(Ni) plots for Kundelungu (a,b) and Luebo (c,d) garnets. Note the presence of lherzolitic and harzburgitic garnets similar to diamond-inclusion garnets, plotting within the diamond-stability field.

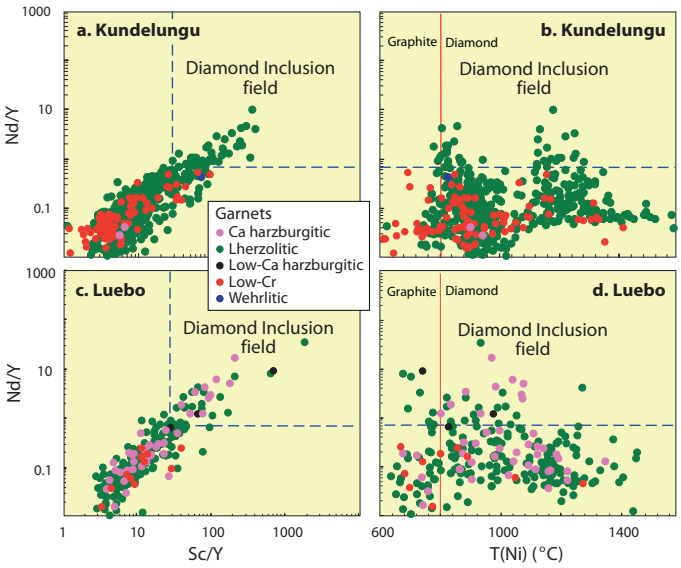

Contacts: Jacques Batumike, Bill Griffin, Sue O'Reilly
Funding: ARC Discovery and Linkage grants (SYO'R and WLG), iMURS, IPRS, PGRF and Macquarie International travel grant (JMB)

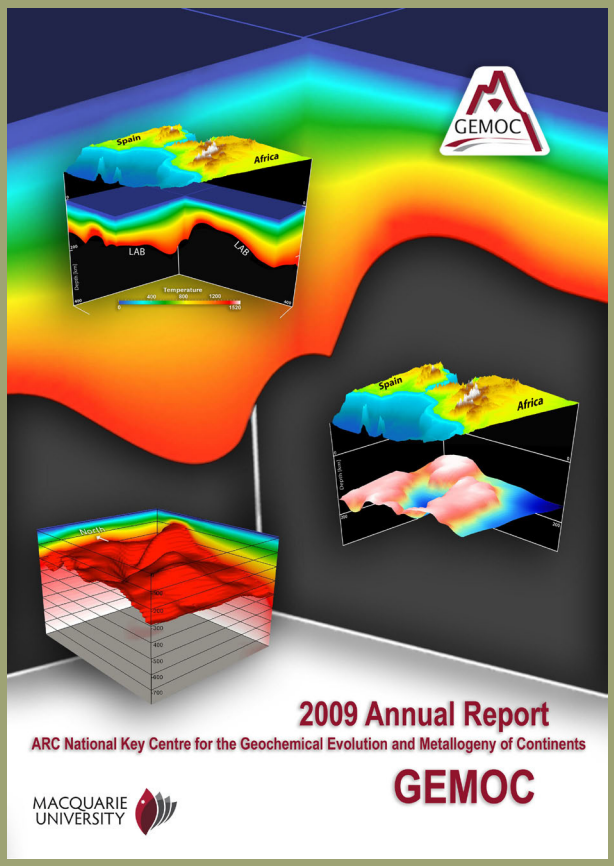

2009 Contents

A novel linking of geochemical and geophysical data to resolve thermal and compositional structures of the Earth's upper mantle 275

Heat, light and energy - Geothermal resources in Eastern Australia's Basins 278

Hot, cold, or different? New constraints to interpret upper mantle seismic data 280

Timescale of early core formation: Numerical modelling of liquid metal micro-segregation processes 283

Geological swap meet: transforming geochemical data into geophysical observables in southern Africa 284

Ancient continental lithospheric mantle beneath oceanic islands – Cape Verde Archipelago 286

A translithospheric suture in the vanished 1-Ga lithospheric root of South India 288

Metasomatic hide and seek: Origins of the Roberts Victor eclogites 290

Dating problems with ancient perovskites rescued by SIMS 292

Short-lived isotopes reveal off-axis magmatism at the East Pacific Rise 294

Apatite trace element fingerprints reveal Transhimalayan magmatic processes 295

The Gawler Craton, South Australia: Unexpected discoveries and mysteries 296

Zircons lay bare the secrets of the ancient Yangtze Block 298

Platinum-group elements nobly unravel komatiites 300

Front Cover: Three dimensional thermal structure of the lithosphere beneath the Atlantic-Mediterranean Transition Region constructed with the geophysical-petrological software LitMod3D (see Research Highlights page 31 and page 36). LitMod3D uses seismic, petrological, and surface geophysical information as constraints. The highly irregular lithosphere-asthenosphere boundary reflects the complex tectonic evolution that characterises this region.

Research highlights 2009

TERRANECHRON® IS GEMOC'S UNIQUE METHODOLOGY FOR TERRANE EVALUATION. During 2009 a range of new studies, including collaborative research projects with industry, using *TerraneChron*® expanded our knowledge of crustal evolution and the timing of tectonic events.

Visit the *TerraneChron*® web page at www.gemoc.mq.edu.au/TerraneChron.html

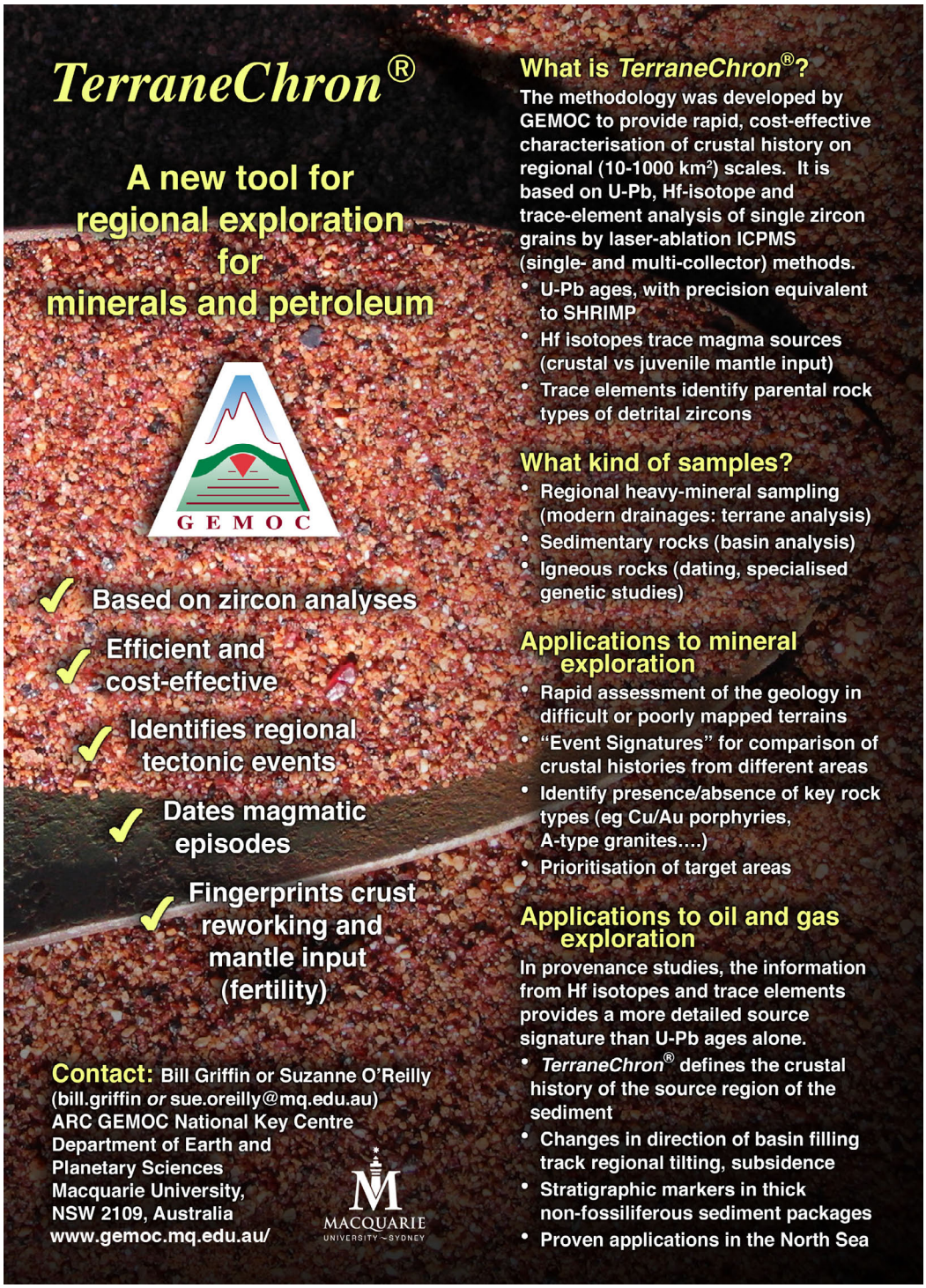

A novel linking of geochemical and geophysical data to resolve thermal and compositional structures of the Earth's upper mantle

THE DETERMINATION OF THE THERMAL AND COMPOSITIONAL STRUCTURES of the Earth's mantle in space and time is a fundamental goal of modern geophysical modelling. These data are the basis for any evolutionary model of the Earth, as well as for understanding the relationships between geophysical observables (e.g., gravity, seismic velocity) and the physical state of the Earth's interior. They also provide critical information on how the lithospheric-sublithospheric system would respond to perturbations arising from tectonic shortening, rifting and sublithospheric convection. Much of our current knowledge about the present-day thermal and compositional structure of the lithospheric and sublithospheric upper mantle has been based on three independent approaches: i) modelling of geophysical observables such as gravity, surface heat flow (SHF), elevation, or some combination of these; ii) interpretation of seismic data using an appropriate combination of "observed" seismic velocities (usually shear waves) with mineral physics, laboratory data, and thermodynamic concepts; ii) geochemical and thermobarometry studies of mantle xenoliths (see *GEMOC publications #521 and 622*). If the assumptions behind all these methods were correct, any modelled section of upper mantle should produce consistent results, no matter which methodology is applied. However, large discrepancies between predictions from these three different methods still are the rule rather than the exception (see *GEMOC publication #521*).

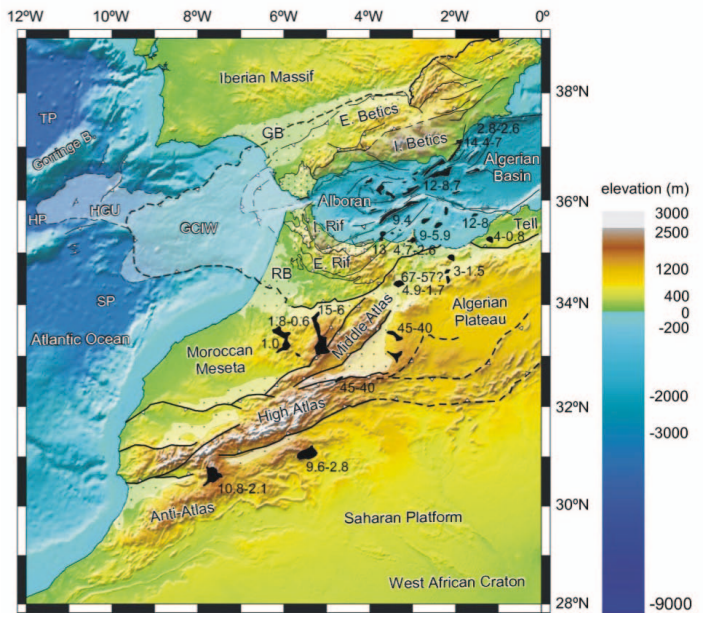

Figure 1. Elevation map with the principal tectonic domains of the Betics, Rif and Atlas Mountain belts, together with the Cenozoic volcanic rocks (black areas) and their age. Cenozoic sedimentary basins are depicted by dotted areas. Guadalquivir Basin (GB), Rharb Basins (RB), Gulf of Cadiz Imbricated Wedge (GCIW), Horseshoe Gravitational Unit (HGU), Seine (SP), Horseshoe (HP) and Tagus (TP) abyssal plains.

One way to overcome these difficulties and obtain more consistent and robust models is to fit simultaneously and self-consistently all the available geophysical and petrological observables (i.e., gravity anomalies, geoid height, SHF, electrical conductivity, seismic velocities, xenolith data and elevation). A simultaneous fit of all these observables reduces the uncertainties associated with the modelling of each of them alone, or with the combinations of pairs commonly used in the literature (see above). It also allows us to distinguish, and have a better control on, thermal or compositional density variations at different depths, since these observables are differently sensitive to shallow/deep, thermal/compositional density anomalies. However, an integrated modelling approach that can include all of these parameters in a self-consistent manner represents a major technological and conceptual challenge. Current research at GEMOC attempts to fill this gap by developing and applying a new integrated geophysical-petrological methodology based on a robust and consistent combination of thermodynamic and physical models. The first full 3D forward version has been recently applied to the Atlantic-Mediterranean Transition Region (AMTR, see *GEMOC publication #627*), and the main results are summarised here.

The AMTR comprises a narrow region along the transition between the western Mediterranean and the Atlantic Ocean along the westernmost segment of the African-Eurasian

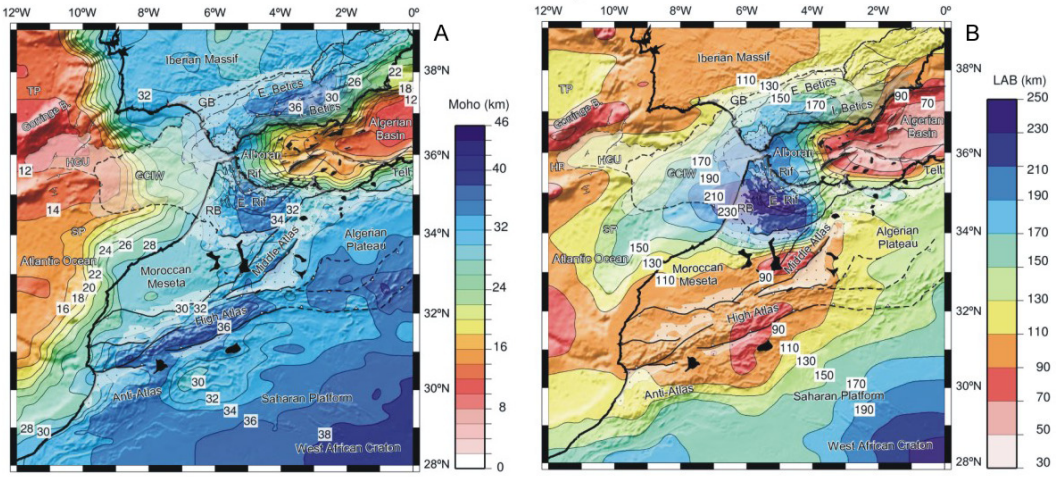

Figure 2. A) Moho depth map superimposed on the structural map with the main tectonic units and volcanism (see Fig. 1). Isolines every 2 km. B) Map of the depth to the Lithosphere-asthenosphere boundary superimposed on the structural map with the main tectonic units and volcanism. Isolines every 20 km.

plate boundary (Fig. 1). It is characterised by a diffuse transpressive contact between the African and Eurasian plates, including a wide band of active deformation. Traditionally, the AMTR has been considered as a zone comprising the Alboran Basin, the Betic and Rif orogens, and the Gulf of Cadiz (Fig. 1). However, some authors have included the adjacent Atlas Mountains on the basis of the similarities in the type and ages of the lavas in south-eastern Iberia and north-western Africa, including the Atlas.

Maps of the depths to the LAB and the crust-mantle boundary of our final best fitting model are shown in Figure 2. The depth of the crust-mantle boundary shows a very heterogeneous crust in the modelled region, with thickness variations of > 25 km. The resulting LAB topography is characterised by strong lateral gradients in the northern, southern and eastern limits of the thick lithosphere imaged beneath the Gulf of Cadiz, the Betics and the Rif (170-240 km). These regions coincide with the contact between the Iberian Variscan Massif and the Betic chain in the north, the contact between the Middle Atlas and the external Rif domain to the south, and the contact between the Betic-Rif orogen and the Alboran Basin to the east. This lithospheric thickening, with a reduced magnitude, continues to the southwest, encompassing the NW Moroccan margin (140-170 km). The thinnest lithosphere obtained in this model is in the eastern Alboran Basin, where the LAB depth is about 70 km. Moderate lithospheric thicknesses are obtained in the SW Iberian Variscan Massif (90 km) and the Atlas Mountains, particularly in the central High Atlas and eastern Anti Atlas (90 km), and the Middle Atlas (<80 km). The eastern branch of the Atlas does not seem to be affected by a lithospheric thinning. The lack of a spatial correlation between the thicknesses of the crust and lithospheric mantle (Fig. 2) in large parts of the model suggests a previously unrecognised decoupling of these two layers. Whereas the Moho depth map essentially mimics topography, with maximum values beneath the Eastern Betics, Rif and Atlas mountains, the LAB map shows a remarkably different pattern, with NE-SW thickening along the western Betics, Rif, Rharb Basin, and Moroccan Atlantic margin, and thinning along

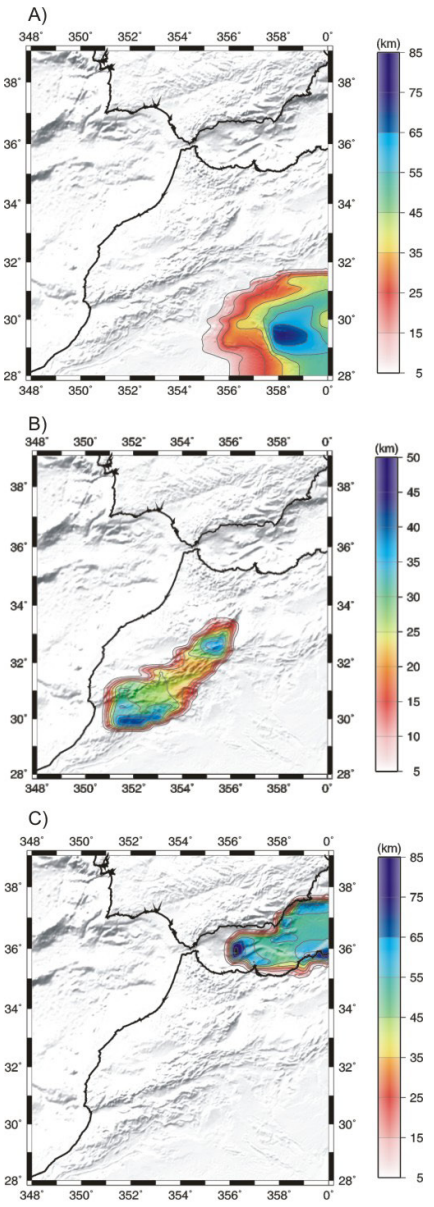

Figure 3. Thickness map of anomalous mantle layers (i.e. mantle domains with different compositions from the background mantle). All layers are defined from the Moho depth downwards. A) West African Craton/Mobile Belt. B) Atlas Mountains. C) Alboran Basin.

the Eastern Alboran Basin and Middle, High and Anti Atlas. It is therefore likely that this lack of a thickness correlation results from the overlapping of different tectonic processes, which incorporate a sub-lithospheric component (see *GEMOC publication #627*).

Interestingly, most of the Miocene mafic lavas (Fig. 1) seem to be spatially related to regions where the lithospheric mantle has been thinned (Fig. 2), suggesting a causal relationship between mantle upwelling and alkaline magmatism. Geochemical analysis indicates that these magmas have a common mantle source, forming a deep reservoir extending from the Canary Islands to the Western Mediterranean. Therefore mantle melting and alkaline volcanism would be related either to small-scale convection involving the deep reservoir, or to small plumes acting as 'escape valves'. This implies that the thinning beneath some parts of the High Atlas, Middle Atlas and Anti-Atlas is probably responsible for, or related to, the observed alkaline volcanism rather than acting as an effective corridor through which magma displaces laterally from a unique reservoir located in the Canary Islands.

Our analysis indicates that the average bulk composition of the lithospheric mantle corresponds to that of a typical Tecton (i.e. Phanerozoic) domain, with the exceptions of the Sahara Platform, the Alboran Basin, and Atlas Mountains. The presence of these distinct lithospheric domains (Fig. 3) is required to reduce the residuals between measured and calculated regional observables such as gravity, geoid and elevation. These heterogeneities are related to either secular compositional variations (Sahara Platform) or recent mantle metasomatism (Atlas Mountains and Alboran Basin), and allow a fairly good reproduction of the measured Pn-velocities of the uppermost mantle and the regional travel-time tomography models (Fig. 4).

Although our methodology represents the first petrological-geophysical self-consistent approach in 3D, it still is a forward method (based on a recursive run of user-guided forward models). The non-linearity of the physical problems involved (see *GEMOC publication #605*) means that any true inversion scheme must be based on either systematic or stochastic exploration of the parameter space, i.e. running several successive forward models. In the 3D case, the high number of degrees of freedom (e.g. the petrophysical and compositional parameters of each body, and the depth of each node defining the limits of the layers), as well as the relatively long time required to run each forward model (~30 min), makes the inversion approach unviable at present. However, preliminary results indicate that a sophisticated combined forward-inversion technique is possible. This will make the modelling process much easier, and will provide a robust means to evaluate uncertainties as well as allowing us to model larger regions of the Earth.

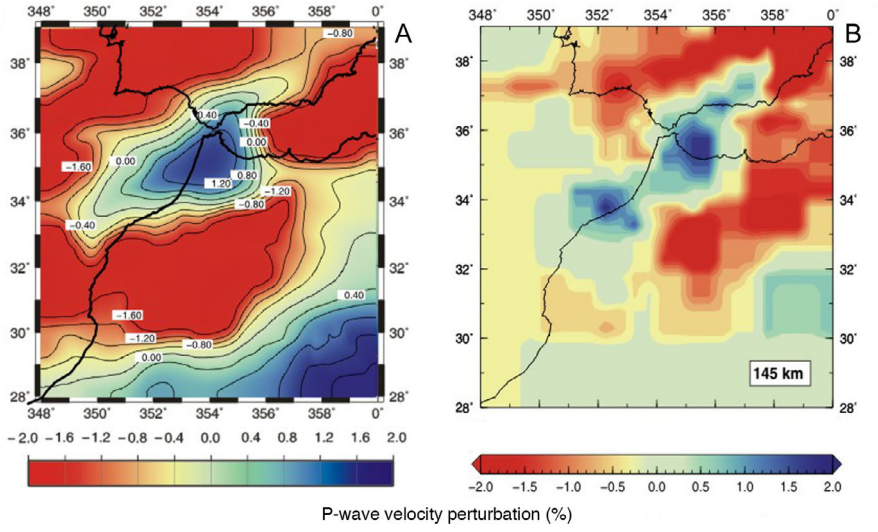

Figure 4. A) Synthetic P-wave velocity anomalies predicted from our model at 145 km depth. B) Horizontal slice of P-wave velocity anomaly obtained from a seismic tomography study (Villaseñor et al., 2003).

Contact: Juan Carlos Afonso
Funding: Macquarie University

Heat, light and energy - Geothermal resources in Eastern Australia's Basins

COAL FROM THE SYDNEY-GUNNEDAH-BOWEN BASIN SYSTEM has been a major resource for Australia's energy industry for the better part of a century, supplying the largest percentage of NSW's base-load power. More recently, developments in the extraction of methane and natural gas from coal beds has seen a resurgence of interest in these deposits.

The move from a fossil-fuel based energy system to a renewable energy economy will involve a range of energy solutions, and one of the most promising for delivering base-load power is geothermal energy.

Traditionally, geothermal industries have focussed on the exploitation of obvious, near-surface energy sources, such as active volcanic fields; examples are New Zealand and Iceland. However, advances in scientific drilling have seen deeper levels of the crust become viable heat sources, and some of the most prospective areas in Australian are within sedimentary basins.

While commercial interest recently has been focussed on the extraordinarily hot Cooper Basin in central Australia, many of Australia's East-coast basins have the advantage of being near the largest population centres. The connected Sydney-Gunnedah-Bowen Basin system is one of the largest tectonic basin systems in Australia, and in places it contains extremely thick sedimentary sequences, ideal areas for trapping crustal heat at depth.

Recent work at GEMOC has been aimed at developing crustal-scale models of the architecture of the Sydney and Gunnedah system. These models, combining information from hundreds of drill cores and detailed gravity modelling, incorporate detailed lithological information on the

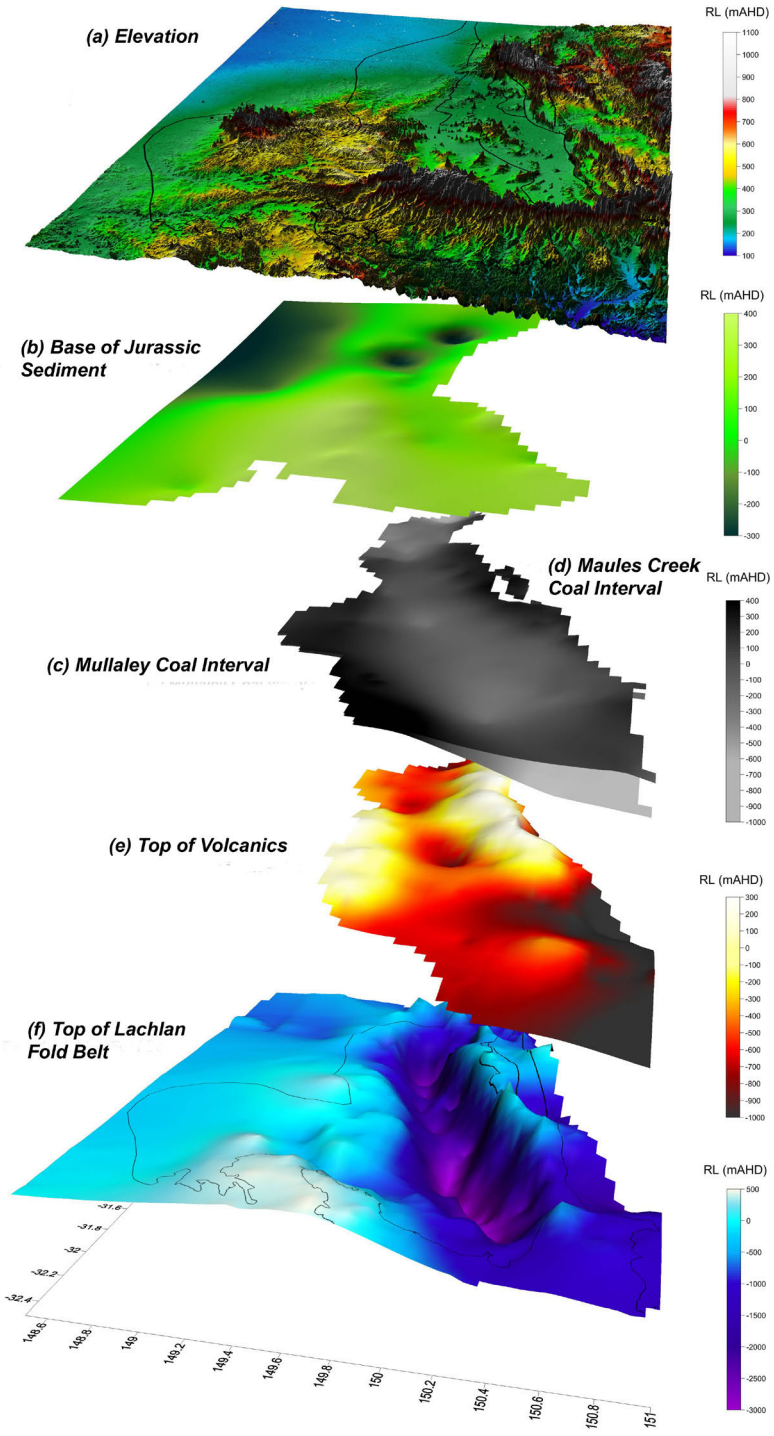

Figure 1. Architecture of the Gunnedah Basin, viewed from the south. Stacked model 3D surfaces of the Gunnedah Basin (in mAHD), blanked to their approximate extent. (a) Elevation with basin outline; (b) Base of Jurassic sediment; (c) Top and base of the Permian Mullaley Basin coal interval; (d) Top and base of the Permian Maules Creek Coal interval; (e) Top of rift volcanics; (f) Top of Lachlan Fold Belt basement with Gunnedah Basin outline.

sedimentary pile and have constrained the structure of the basin in 3D at an unprecedented scale. These models have become the basis for thermal models of the sedimentary basin system. Existing geodynamic codes have been 'rewired' to import complex geological models; coupled with sparse thermal constraints available in parts of the basin, these show the detailed 3D thermal structure of these systems.

These results have been surprising. Conventional wisdom holds that the highest temperatures would be found directly beneath the thickest sedimentary "blanket", but these simulations suggest that instead the lateral temperature gradients within a basin cause heat to refract around such layers. Heat preferentially goes around a coal layer, for instance, rather than through it. In addition, large gradients in the basement are also the sites of elevated temperatures at depth, as heat preferentially moves around the thick insulating blanket of basin sediments. The results also show a lower correlation between surface heat flow and temperatures at depth than commonly assumed, often due to these lateral geometric effects. Heat flow measurements over a coal layer, for instance, may be low, despite high temperatures beneath the insulating coal layer. Without detailed thermal modelling, it is difficult to extrapolate shallow temperature measurements to depth.

This project is currently expanding into the Bowen Basin, and will soon be able to address the thermal history of these basins through time, which has clear potential for the coal/gas maturation history. Additionally, such detailed thermo-structural models will enable us to constrain the stress state of these basins in greater detail - relevant to intraplate earthquakes in areas such as Newcastle. The detailed thermal and sedimentary structure models will also enable us to simulate the deep, hot aquifers of such basins - identified as a potential geothermal resource in their own right, and also an important and under-appreciated factor in basin-scale groundwater systems.

Contacts: Craig O'Neill, Cara Danis
Funding: ARC Discovery, APA

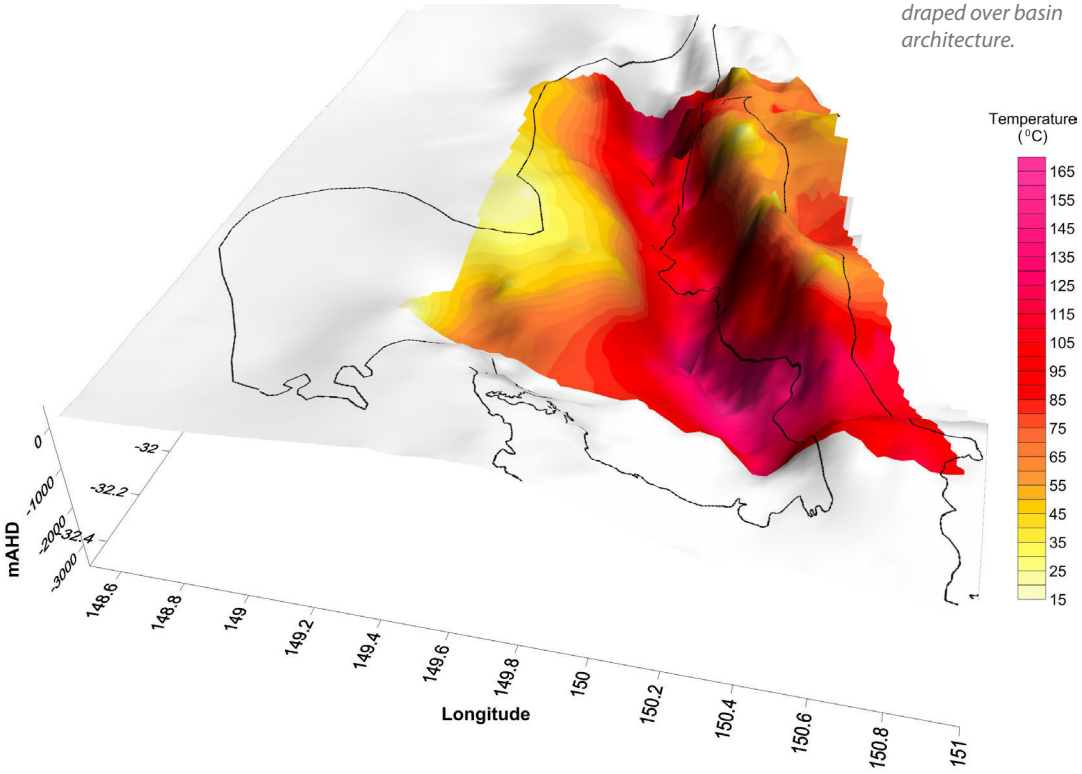

Figure 2. Temperature at the top of the Lachlan Fold Belt Basement, draped over basin architecture.

Hot, cold, or different? New constraints to interpret upper mantle seismic data

THE SEISMOLOGICAL STRUCTURE OF THE EARTH'S UPPER MANTLE is highly heterogeneous, and much of this heterogeneity reflects the lithosphere's thermal and compositional structure. Since lithospheric discontinuities commonly correlate with the location of seismically active zones, major tectonic boundaries, foci of magma intrusion and major ore deposits (see *GEMOC Publication #547*), their detection is important for ore and energy exploration and natural hazard assessment. However, limitations on resolution, and trade-offs between temperature and composition complicate the seismological characterisation of the small-scale (ca 300 km) distribution of compositional and thermal anomalies in the upper mantle.

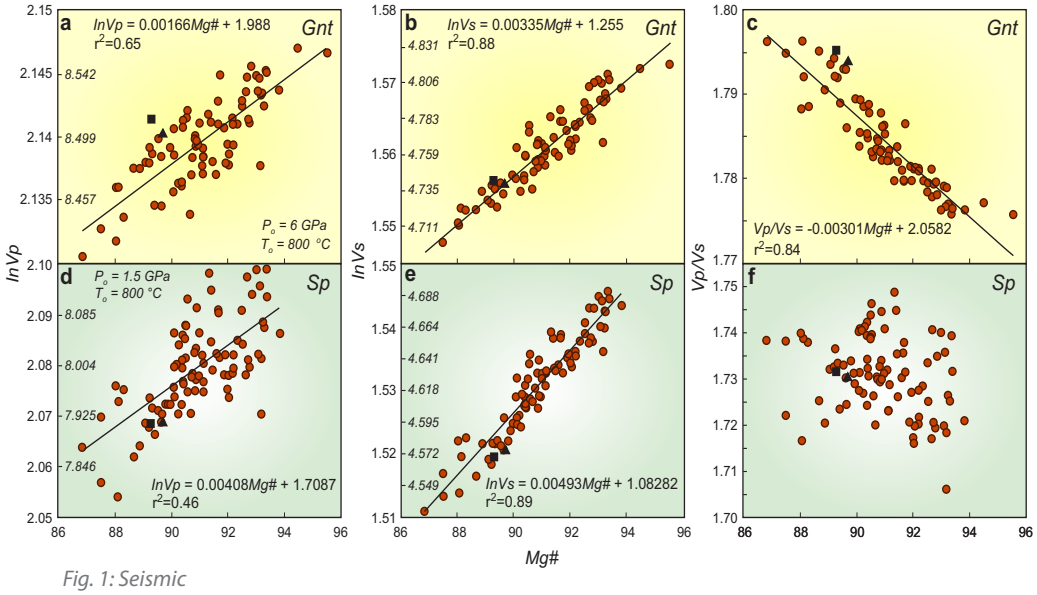

Fig. 1: Seismic velocities versus bulk Mg#. a, b, c Vp, Vs, and Vp/Vs versus bulk Mg# for peridotites within the garnet (Gnt) stability field. d, e, f Vp, Vs, and Vp/Vs versus bulk Mg# for peridotites within the spinel (Sp) stability field. Numbers within the boxes are absolute velocity values in km s-1.

A fundamental problem is the lack of reliable quantitative relationships or indicators (derived from seismic data) that can distinguish between compositional and thermal contributions to variations in seismic velocity. In this context, parameters such as the ratio of compressional-wave to shear-wave velocity (Vp/Vs) or the Poisson's ratio are commonly thought to be reliable indicators of compositional variations in peridotites. Although these parameters have been successfully applied at crustal P-T-X conditions (where X is composition), their extension to general upper mantle conditions has serious limitations due to the effects of temperature-dependent non-elastic behaviour and phase stability.

In order to give some insights into these problems we have carried out a systematic assessment of the effects of temperature and composition on densities and seismic velocities in peridotites, applying thermodynamically self-consistent and hybrid methods, the latest mineral physics databases, and experimental results on the non-elastic behaviour of olivine aggregates at seismic frequencies (see *GEMOC Publications #521, 542, 605, 622, 627*). We have used a xenolith dataset that spans a range of composition (Mg# values from ~ 88 to 95) covering most of the expected variability within the lithospheric mantle.

Figures 1d, e and f illustrate the compositional dependence of Vp, Vs, and Vp/Vs within the spinel stability field. Although the general behaviour of both Vp and Vs with Mg# is similar to that observed within the garnet stability field, Vp/Vs shows no apparent correlation. Since spinel is stable in peridotitic rocks to depths of ~ 50-60 km under most circumstances, and down to ~ 100 km in strongly depleted rocks, we cannot apply correlations derived for garnet-bearing peridotites in seismic studies of the uppermost mantle.

We have analysed different anomaly ratios from our data set and find that ρ/Vs (where ρ is density) displays the best correlation with Mg# (Figs. 2a, b). Furthermore, the ratio between the compositional and thermal (anharmonic) derivatives of ρ/Vs is similar to, but more reliable than (i.e. less scatter), the Vp/Vs case. Although ρ/Vp also correlates well with composition (particularly in the case of garnet-bearing assemblages; Figs. 2c, d), our results reveal several previously unrecognised advantages of using ρ/Vs rather than ρ/Vp as a general indicator of compositional anomalies. Foremost among these are (i) the greater sensitivity of Vs to temperature variations; (ii) the larger compositional derivative of ρ/Vs; (iii) the smaller scatter of ρ/Vs in the spinel field; and (iv) the similarity in the anharmonic derivatives ∂(ρ/Vs)/∂Mg# and ∂(ρ/Vs)/∂T of both spinel- and garnet-bearing assemblages. While the first two factors ensure a better response to temperature and compositional variations, respectively, the last two eliminate the problem of phase stability. Despite these advantages, the indicator ∂lnρ/∂lnVs is also affected by attenuation, although considerably less than Vp/Vs, as discussed below.

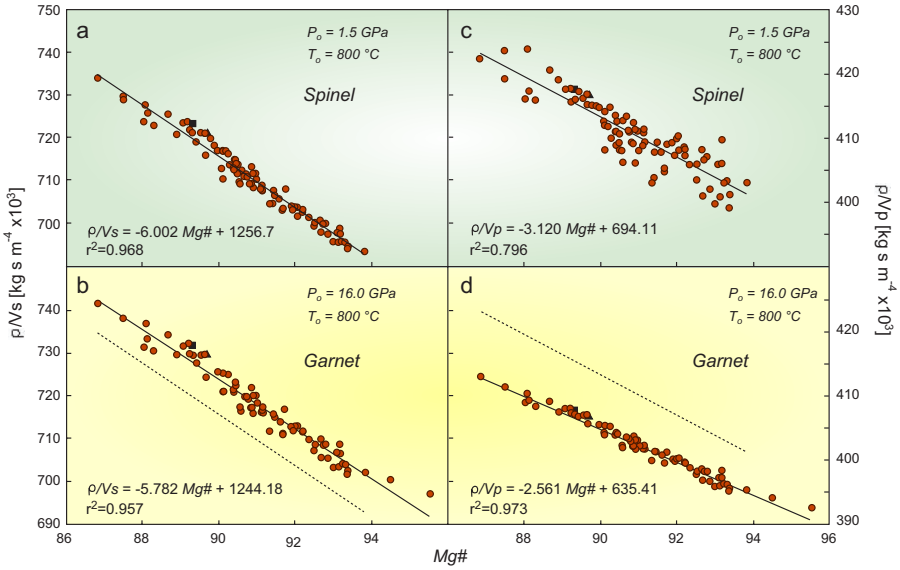

Figure 2. A, B, Ratio of density to shear wave velocity [kg s m^{-4} x10^3] versus bulk Mg# for the same samples shown in Fig. 1. The correlation is significant ($r^2 > 0.9$) in both spinel and garnet stability fields. The derivative ∂(ρ/Vs)/∂Mg# is remarkably similar in both fields. This is clearly visible when the two regression lines are plotted in the same panel, as done in B (the dashed line is the regression line from A). C, D, Ratio of density to compressional wave velocity (absolute values) versus bulk Mg#. Note that although the correlation is significantly poorer than in the ρ /Vs case within the spinel stability field, it is slightly better (greater r^2) in the garnet stability field.

The anelastic behaviour responsible for seismic wave attenuation becomes important in olivine-rich rocks at temperatures ~> 900 °C. Since all of the sublithospheric UM and up to 40% of the subcontinental lithospheric mantle have temperatures above this limit, any attempt at constraining mantle composition from seismic data must include attenuation effects. Shear waves are more strongly affected by anelasticity than compressional waves, and therefore both Vp/Vs and Poisson's ratio become strongly dependent on temperature at T >~ 900 °C. Figure 3 shows that a change of 300 °C within the anelastic regime translates into a fictitious change of ~ 6-7 units in Mg# if anharmonic estimates are used for the conversion. This change covers the entire range of common peridotitic compositions in the UM. The ratio ρ/Vs is appreciably less sensitive to anelastic effects and therefore gives a smaller fictitious Mg# change (Fig. 3b). However, due to the non-linear effects of temperature on shear modulus, the graphs for both Vp/Vs and ρ/Vs steepen with increasing temperature. Therefore, the common practice of interpreting observed variations of Vp, Vs, and/or Vp/Vs in the UM in terms of compositional variations with no consideration of anelasticity and phase stability is likely to produce erroneous conclusions.

In the light of the above considerations, can we distinguish thermal from compositional anomalies in the UM? The data presented here show that previous models based on seismic parameters produce results that are not meaningful for spinel-bearing peridotites or for olivine-rich assemblages at T >~ 900 °C. On the other hand, the ratio ρ/Vs is a more robust compositional indicator, but requires bulk density as an independent input. Since both density

and elastic moduli depend on bulk composition, any model (inverse or forward) of these properties requires a framework that guarantees a self-consistent coupling among P, T and X (bulk and phase). Current joint inversion methods are not well suited because they rely on long-period normal-mode observations, while studies based on the combination of short-period body waves and gravity anomalies model these two geophysical fields through scaling factors and therefore are not self-consistent. Recently-developed techniques that combine geophysical and petrological modelling within a consistent thermodynamic framework (see *GEMOC Publications #605 and 622*) are particularly promising, although more detailed studies on the effects of intrinsic attenuation, fluid content and thermodynamic modelling of mantle assemblages are needed.

Contact: Juan Carlos Afonso
Funded by: Macquarie University, Spanish research projects, NSERC, ARC

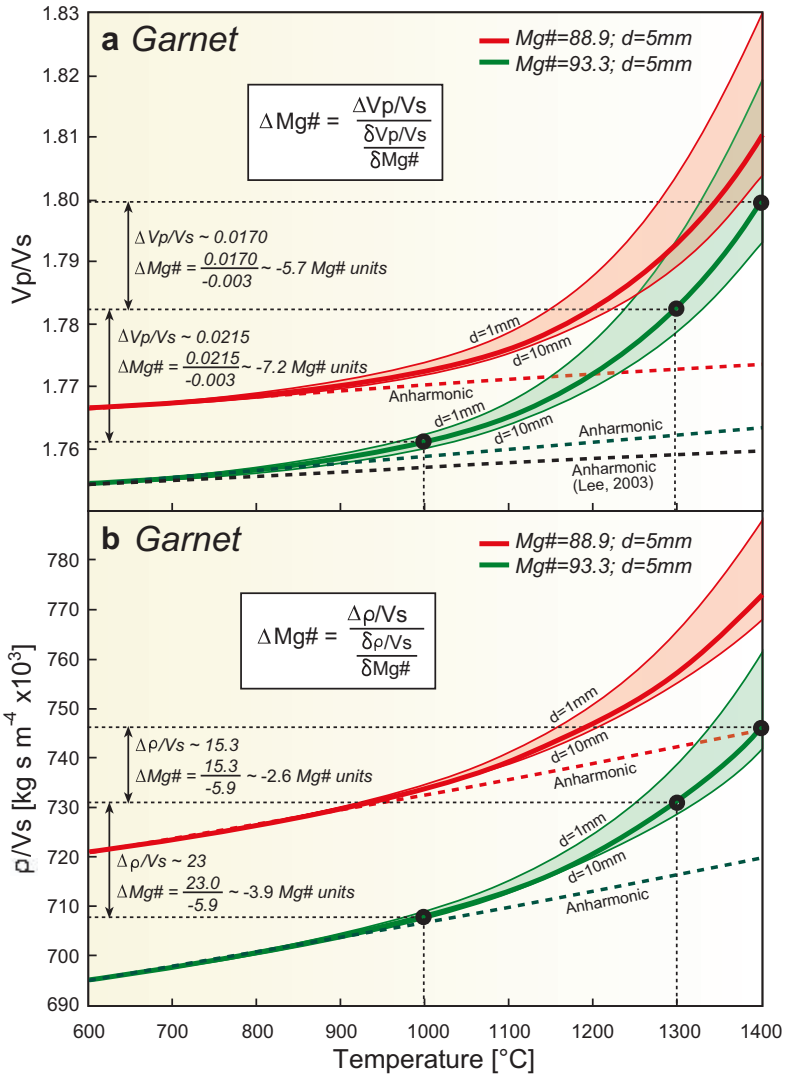

Figure 3. A) Vp/Vs versus temperature for two representative samples with Mg# = 88.9 (red colour) and 93.3 (green colour) within the garnet stability field. Reference pressure is Po = 4 GPa. The envelopes enclose Vp/Vs values for grain sizes between 1 and 10 mm. The anharmonic approximation is shown with dashed lines. The black circles denote Vp/Vs values for the same sample (i.e. no change in composition) separated by ΔT = 300 °C (1300 °C – 1000 °C) and 100 °C (1400 °C – 1300 °C) within the anelastic regime. B) ρ/Vs [kg s m^{-4}] versus temperature for the same samples shown in A). The anharmonic behaviour is shown with dashed lines.

Timescale of early core formation: Numerical modelling of liquid metal micro-segregation processes

OUR UNDERSTANDING OF DIFFERENTIATION EVENTS OCCURRING EARLY IN THE SOLAR SYSTEM has been greatly enhanced by using short-lived radioisotopes. The rapid decay in these systems gives us fine-scale temporal resolution of melting and differentiation events. Data from the short-lived radioisotope systems suggest that planetary differentiation (represented by iron meteorites which are considered to represent the cores of planetesimals) must have started within ~1.5 Myr of the beginning of the solar system. The results also require that the physical segregation of the core(s) was very rapid. Both percolative flow and deformation-driven flow have been shown to be important in core formation. For a more robust analysis of the speed at which metallic liquid migrated, we need to perform additional numerical studies. We have examined the preserved textures in the Kernouve meteorite (an H6 ordinary chondrite) before and after experimental deformation. The original, static state provides a snapshot of porous flow at the beginning of melting with no applied stress; after experimental deformation the textures show that focused metallic liquid flow has occurred, producing veins of metal in the silicate matrix.

Our modeling results show that the textures in the undeformed rock reflect migration of the metallic liquid by porous flow into high-permeability and low-pressure sites of initial melting and the flow velocity becomes position-dependent. If we modify the matrix permeability in the numerical model, we find that the highest average migration velocities (10^{-5} m/s) correspond to the highest permeability (10^{-9} m^2). When deformation textures are included in the modeling, channel flow becomes important and most liquid metal moves through channels (Fig. 1), as demonstrated by the experiments. Under these conditions flow velocities are higher (10^{-3} m/s). For a planetesimal 200 km across, metallic iron can segregate within 30 (channel) to 30,000 (porous flow) years, providing flow is continuous. Another important aspect is the production of silicate melt as the planetesimal continues to heat. When silicate melt is produced, the porous-flow mechanism of segregation shuts off, unless impacts can produce stresses high enough to trigger deformation at high strain rates. High strain rates can overcome the strength of the silicate mush matrix, and deformation would shift back to fracture (albeit transient) rather than plastic flow.

Contact: Tracy Rushmer
Funded by: ARC Discovery

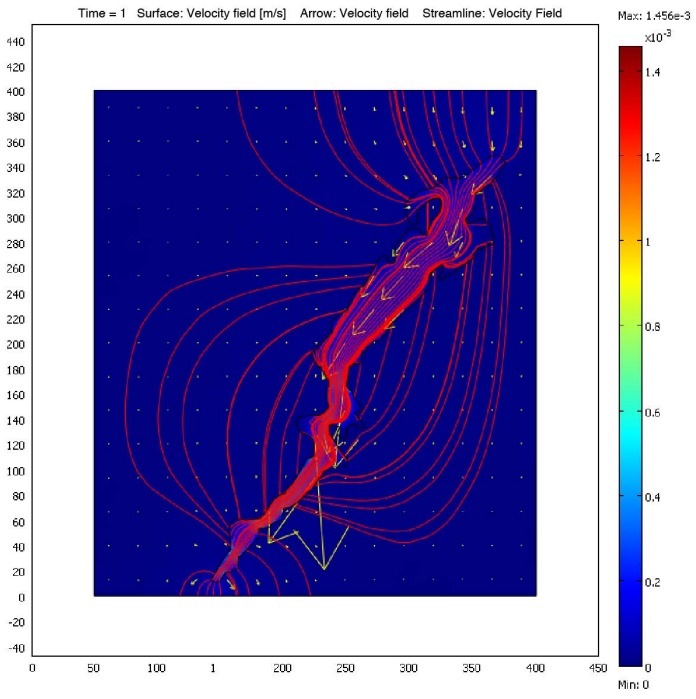

Figure 1. Numerical result of a simulation of the 2D velocity field made using a geometry in which melt flow is confined largely to a vein formed during sample deformation in the laboratory. Some background matrix flow also takes place. The implication is that this geometry reflects textures likely to dominate in an environment where planetesimals are in frequent collision. For this calculation, matrix permeability = 10^{-10} m^2 using a liquid metal viscosity in vein 10^{-3} Pa s corresponding to 14 wt% S at T = 1500 K and 1 GPa.

Geological swap meet: transforming geochemical data into geophysical observables in southern Africa

THE KAAPVAAL CRATON IN SOUTHERN AFRICA is one of the most-studied fragments of Archean crust and mantle in the world. Detailed seismic and geochemical surveys of the craton provide an unprecedented view of this ancient system from different perspectives. However, the question remains: how well do these perspectives agree with one another?

The "4-D" lithosphere-mapping methodology developed at GEMOC provides a framework to convert geochemical data directly into seismic data in order to compare these data sets. Lithosphere mapping principles were applied to two sets of peridotitic garnet xenocrysts collected from the heavy mineral concentrates of kimberlites along a transect through southern Africa (Fig. 1). The first set of garnet xenocrysts comes from 33 Group II kimberlites with a median age of ~119 Ma and records the thermal and compositional state of the lithosphere after a long period of quiescence. The second set of garnet xenocysts comes from 31 Group I kimberlites with a median age of ~90 Ma and records major metasomatism and heating of the lithosphere, particularly near the craton margins (for details see *GEMOC publication #578*).

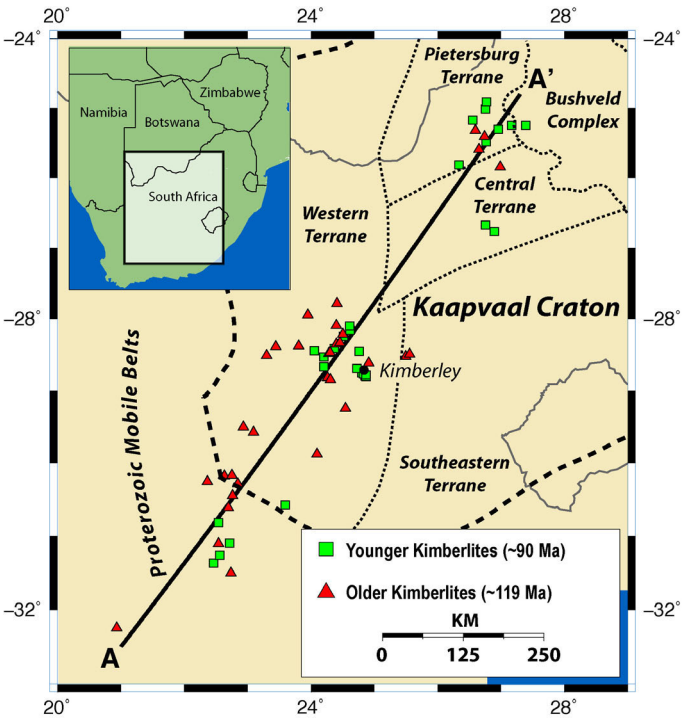

Figure 1. A simplified tectonic map of southern Africa showing the location of the Kaapvaal Craton, the locations of the two sets of kimberlites, and the path of the profiles in Figures 2 and 3.

Using the geochemical information contained in the two sets of garnets, a whole-rock bulk composition was calculated and converted into modal mineral estimates using a Gibbs free-energy minimisation algorithm. Anharmonic seismic velocities were then calculated from pressure, temperature, and mineral elasticity data and corrected for anelastic effects due to grain size, temperature, and seismic wave frequency (see *GEMOC publication #521*). The seismic velocity images resulting from each set of garnets are shown in Figure 2.

The seismic images echo the changes in the thermal and compositional data described above. Seismic velocities derived from garnets hosted in the older kimberlites are uniformly higher than those from garnets hosted in the younger kimberlites. The reduction in velocity is primarily related to a rising geotherm and thermal disequilibrium at the base of the lithosphere resulting from metasomatic activity preceding the eruption of the second set of kimberlites. Comparison of the garnet-derived velocities with modern seismic observations (Fig. 3) indicates that the localised thermal anomaly causing the low velocities 90 Ma years ago has dissipated to form a broad low-velocity zone between 175 and 250 km depth beneath the

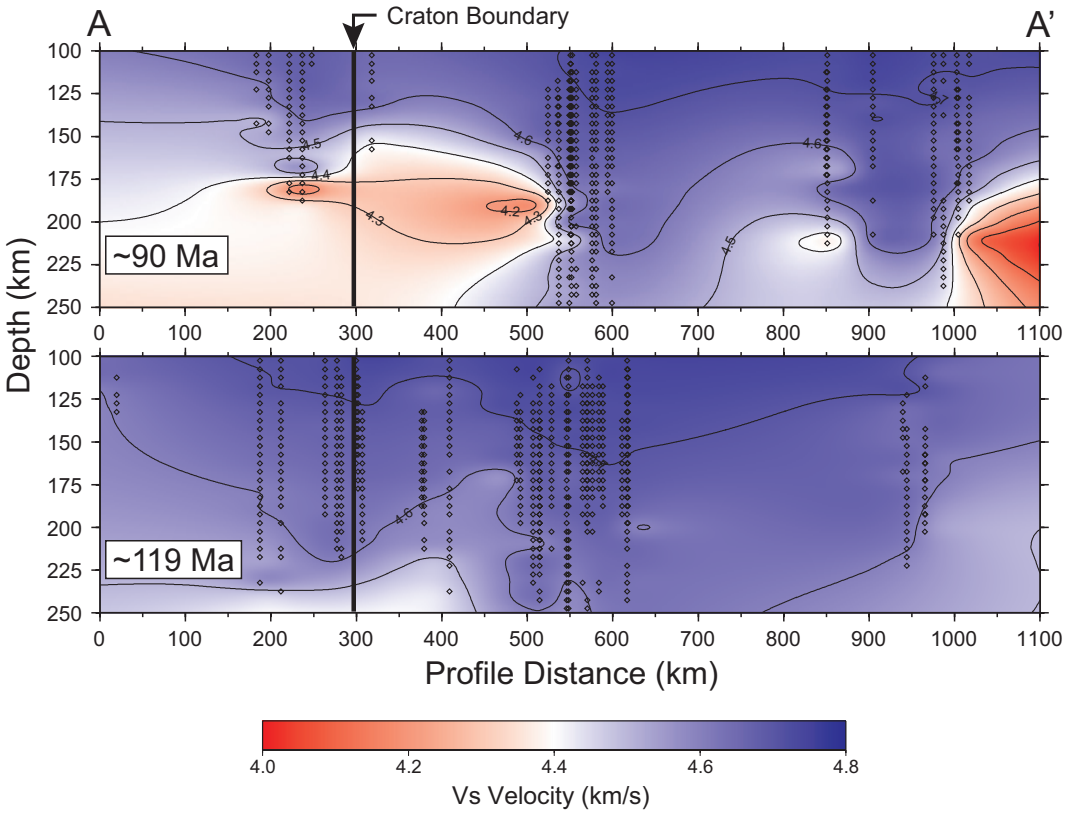

Figure 2. Shear wave velocities calculated from garnet xenocrysts hosted in the older set of kimberlites (bottom panel) and the younger set of kimberlites (top panel). Diamond symbols on the profiles indicate the depth range of garnet data from each kimberlite. The heavy vertical black line indicates the location of the craton boundary as mapped at the surface.

Kaapvaal Craton. Ongoing thermal modeling at GEMOC aims to reveal the timing and extent of the thermal perturbation and related metasomatism beneath southern Africa from the Late Mesozoic to the present.

Contacts: Alan Kobussen, Juan Carlos Afonso, Bill Griffin, Sue O'Reilly
Funded by: ARC Discovery, ARC Linkage, DeBeers Exploration, Macquarie University

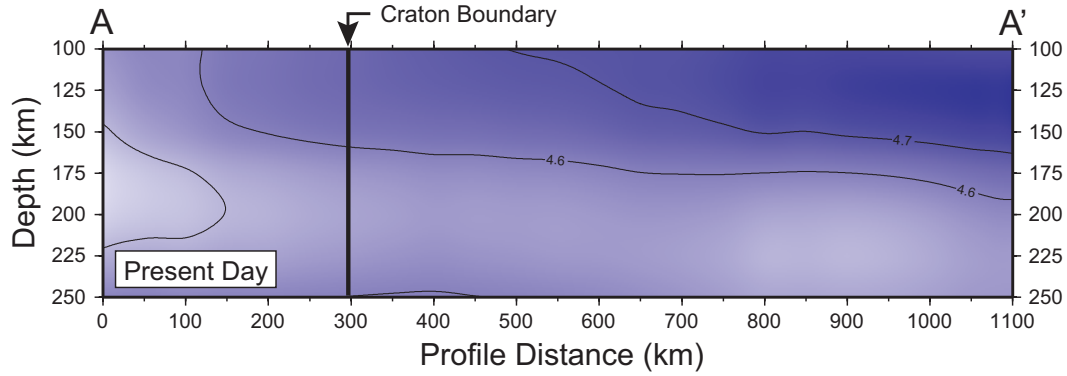

Figure 3. Seismic tomography model of velocities along the same profile as Figure 2 using modern seismic observations in southern Africa (S. Fishwick, personal communication). The colour scale is the same as Figure 2.

Ancient continental lithospheric mantle beneath oceanic islands – Cape Verde Archipelago

THE CAPE VERDE ISLANDS LIE IN THE ATLANTIC OCEAN OFF WEST AFRICA, in a clearly oceanic setting. The lavas of some islands carry mantle-derived xenoliths of depleted peridotites (low in Ca, Al, Fe and other basaltic components), petrologically similar to those derived from cratonic lithospheric mantle. Oceanic lithospheric mantle, in contrast, consists mainly of less-depleted peridotites (lherzolites and harzburgites) formed by the extraction of mid-ocean ridge basalts. *In situ* Re-Os analyses of individual sulfide grains from depleted xenoliths from the island of Sal yield Re-depletion model ages ranging mainly from Neoproterozoic to Archean. Their age distribution mirrors the tectonic history of the western margin of the West African Craton and the corresponding continental margin of Brazil. These data suggest that part of the Cape Verde Archipelago is underlain by a fragment of ancient subcontinental lithospheric mantle (SCLM), left stranded in the oceanic lithosphere during the opening of the Atlantic Ocean (*GEMOC Publication #625*). Contamination of magmas by this ancient continental root can explain the unusual isotopic characteristics of some Cape Verde lavas without recourse to recycled continental material in the sources of mantle plumes.

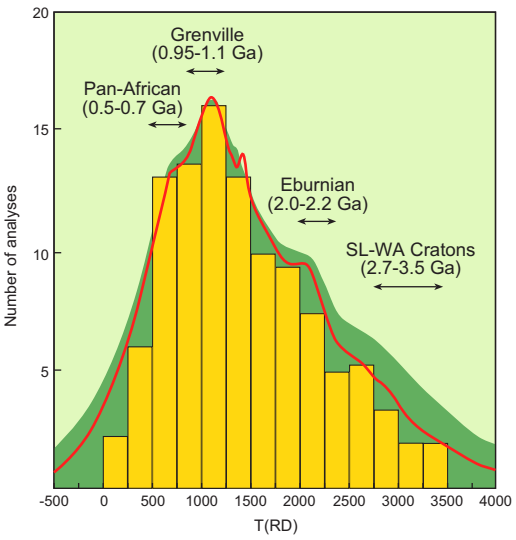

Figure 1. Age histogram (n=135) and cumulative probability plot of T_{RD} (rhenium depletion) age (n=108) for mantle sulfides (after GEMOC Publication #411).

The sulfide Re-Os age data from the Cape Verde mantle xenoliths (Fig. 1) broadly reflect the timing of events characterising the tectonic history of the Atlantic suture, and especially of the West African margin. The oldest Archean ages correlate with the ancient rocks of the West African Craton; the peak around 2 Ga correlates with the Birrimian volcanism and the Eburnian orogeny along the margins of the craton. The major Neoproterozoic peak (ca 1 Ga) matches the collision of the West African and Sao Luis Cratons and related volcanism; the youngest group of ages (550-800 Ma) corresponds to the breakup of the continent along the earlier suture, and the opening of the Iapetus Ocean. The dominance of Neoproterozoic ages is consistent with the position of the Cape Verde Archipelago closer to the inferred former suture between Africa and South America, where pre-existing SCLM would have been most strongly modified.

The broad spread of model ages between ca 1800-1300 Ma (ca 30 % of the data) may reflect either reactions between successive sulfide generations (i.e. mixed ages), or episodic metasomatism of the SCLM. In any case, the existence of possible "mixed ages" requires the presence of an older (cratonic) component. This possibility is also suggested by recent global tomographic mapping which show a high-velocity region below the Cape Verde Archipelago (Fig. 2).

The presence of a domain of Archean-Proterozoic SCLM beneath the Cape Verde Islands suggests that the opening of the ocean basin did not involve a clean break, with generation of new oceanic lithosphere directly overlying the underlying convective mantle. Depleted Archean to Proterozoic SCLM is buoyant relative to the convecting mantle (see *GEMOC Publication #228*), and detached fragments are thus unlikely to sink; instead they may "surf

the convecting mantle" (see *GEMOC Publication #411*) as the ocean opens. Such fragments of relict SCLM may be widespread in the ocean basins.

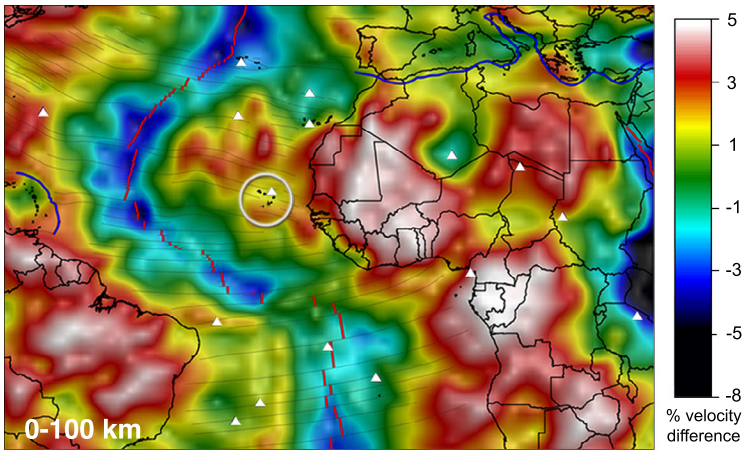

Figure 2. Seismic tomography (Vs) image of northern Africa and the adjacent Atlantic Ocean at 0-100 km (after GEMOC Publication #547) showing high-velocity regions in the ocean basin. (Note colour reversal with hot colours indicating high velocity).

We suggest that during rifting, before true oceanic crust has been formed, rising MOR-like melts impregnate the pre-existing SCLM, causing a progressive heating and rheological weakening. A combination of rifting and ductile extension could produce an intermingling of old pieces of SCLM and new oceanic lithosphere. Geological and geochemical studies of the Lanzo peridotite massif (Piccardo et al., Lithos, 94, 181-209) provide a possible analogue. Lanzo may represent a transition between old SCLM and oceanic lithosphere; extending SCLM was modified by magmas, causing a progressive thermo-chemical erosion of the SCLM.

The presence of an SCLM remnant beneath the Cape Verde islands also can explain the complex isotopic signatures of the magmatic rocks. Geochemical signatures typical of ancient SCLM components have been recognised in some lavas on Sal (Holm et al., J Petrology, 47, 145-189) and the interaction of rising magmas (derived from the convecting mantle) with the SCLM could impart these signatures.

If such SCLM remnants are widespread in the ocean basins, they offer an alternative interpretation of the origin of EM1 and EM2 components (geochemical signatures of recycled crust) in ocean-island basalts. Rather than reflecting continental components subducted into the lower mantle and sequestered until tapped by rising plumes, these signatures may simply indicate contamination of rising magmas by relatively shallow SCLM remnants (see *GEMOC Publication #576*).

The new Re-Os data resulting from this study, coupled with those from abyssal peridotites, suggest that the traditional picture of oceanic lithosphere as the residues of basalt extraction at mid-ocean ridges is probably an oversimplification. Instead, the development of ocean basins may involve disruption of continental lithosphere and incorporation of relict SCLM domains in oceanic regions (Fig. 3). The repeated opening and closing of oceans, commonly along older sutures, must have left many SCLM remnants of different ages within the ocean basins. This process will produce significant compositional and geochronological heterogeneity in the oceanic lithosphere over time.

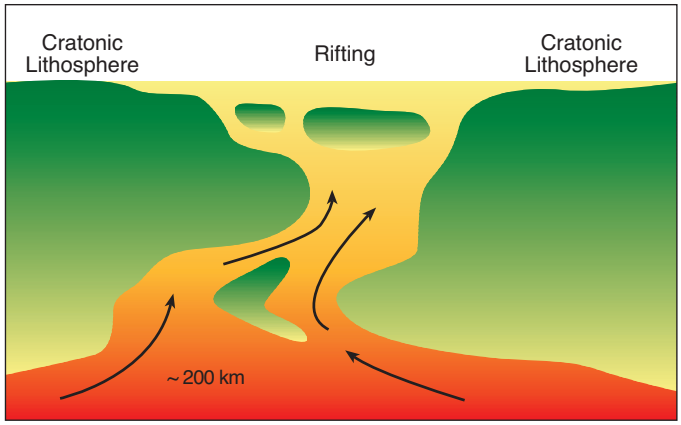

Figure 3. Cartoon showing possible oceanic rifting mechanism with listric faulting at cratonic margins and stranding of ancient subcontinental lithospheric mantle remnants in the ocean basin (after GEMOC publication #576).

Contacts: Sue O'Reilly, Bill Griffin, Massimo Coltorti, Norman Pearson, Costanza Bonadiman
Funded by: ARC Discovery, Italian Government research grants

A translithospheric suture in the vanished 1-Ga lithospheric root of South India

GARNET XENOCRYSTS AND ECLOGITE XENOLITHS from 15 kimberlites (1.0-1.1 Ga in age) have been used to map the composition and structure of the subcontinental lithospheric mantle (SCLM) along an 80-km traverse across the eastern margin of the Closepet Granite in Andhra Pradesh, southcentral India (see *GEMOC Publication #567*; Fig. 1, 2). The SCLM at the SW end of the traverse is more depleted (abundant harzburgites, mean X_{Mg} of olivine ≈93.5, mean whole-rock Al_2O_3 ≈1.5%) than that at the NE end (fewer harzburgites, X_{Mg} ≈ 92, Al_2O_3 >2%) (Fig. 3). The depleted layer thins from ca 195 km thick in the SW, to ca 170 km in the NE, although geotherms derived from the xenocrysts are similarly low (ca 35-37 mW/m^2). The middle of the traverse is underlain by a strongly refertilised SCLM with a higher geotherm (ca 40 mW/m^2) and extensive evidence of metasomatism (high Ti, Zr, lower Mg#; Fig. 4). At the SW end of the traverse, the kimberlites contain abundant eclogites; P-T estimates show that these are tightly concentrated in a layer from 175-190 km depth, and coincide with a zone of melt-related metasomatism. In the central part of the section, the eclogites also are abundant, but are distributed through the highly metasomatised section from 90-160 km depth.

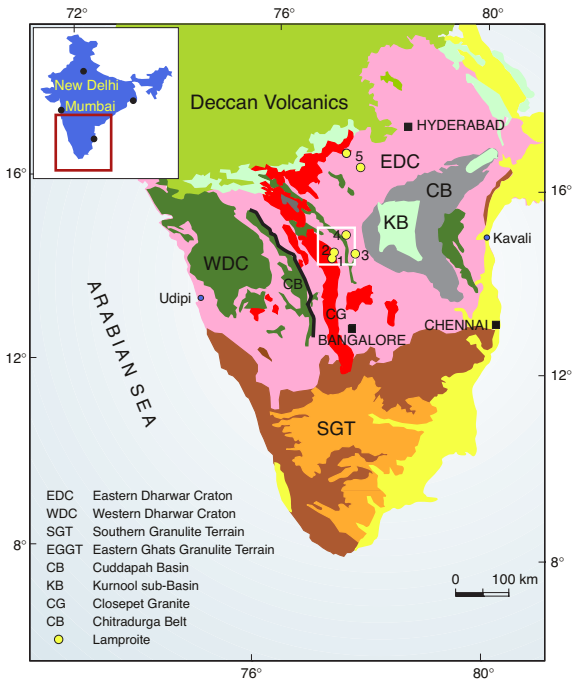

Figure 1. Geological sketch map of India, showing the location of the Dharwar craton; box outlines the area shown in Figure 2.

These data suggest that the kimberlites at either end of the traverse sampled two distinct lithospheric blocks, perhaps coinciding with the Eastern and Western blocks of the Dharwar Craton. The zone of refertilised SCLM between them is interpreted as the cratonic suture, metasomatised by mafic melts (now eclogites). At either end of the traverse, such melts ponded at the base of the SCLM, but they were able to penetrate higher into the SCLM along the ancient suture. If this suture dips 70-80° to the east, its surface outcrop would lie within the area now intruded by the Closepet Granite. The "tilt" of the proposed cratonic suture may reflect overthrusting of the Eastern Dharwar Craton crust up to 100 km to the west.

Recent geophysical data (seismic, MT) suggest that the depleted lithospheric root beneath the Dharwar Craton

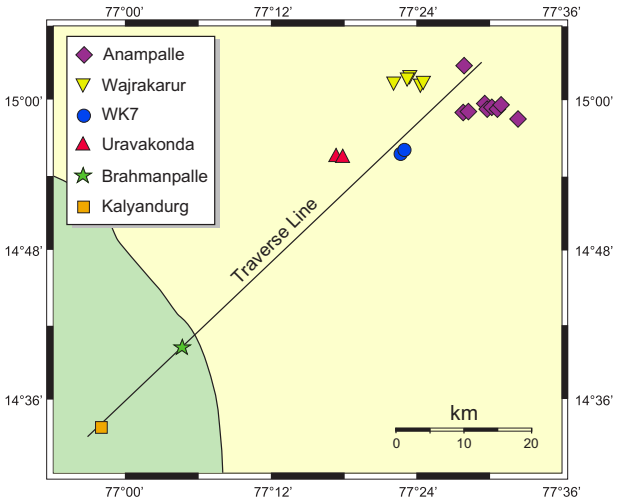

Figure 2. Locations of kimberlite clusters studied. Pale green indicates outcrop area of the Closepet Granite.

that was sampled by the 1.1 Ga kimberlites is no longer present. The removal or major modification of this root could have occurred during the breakup of Gondwanaland, and may help to explain India's rapid northward drift before it collided with Asia. India thus joins the North China Craton as an example of the destruction of an Archean continental keel.

Contacts: Bill Griffin, Sue O'Reilly, Alan Kobussen
Funded by: ARC Discovery, MQRESIndia

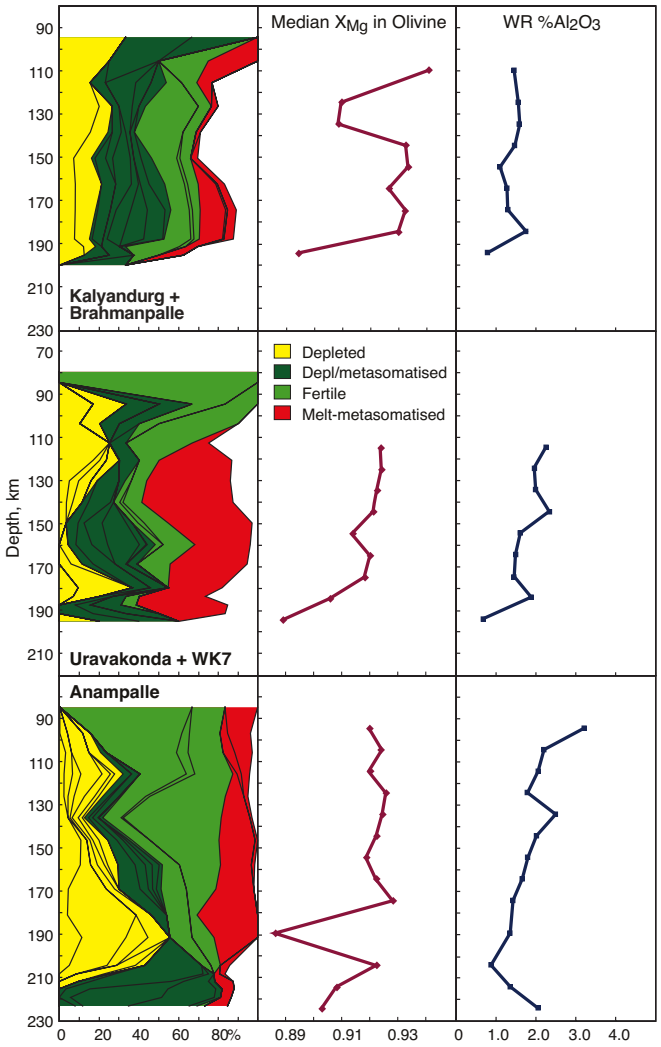

Figure 3. Chemical Tomography sections, illustrating the vertical distribution of geochemical signatures in peridotitic garnets. The mean X_{Mg} of coexisting olivine and the mean whole-rock Al_2O_3 content are calculated from garnet data.

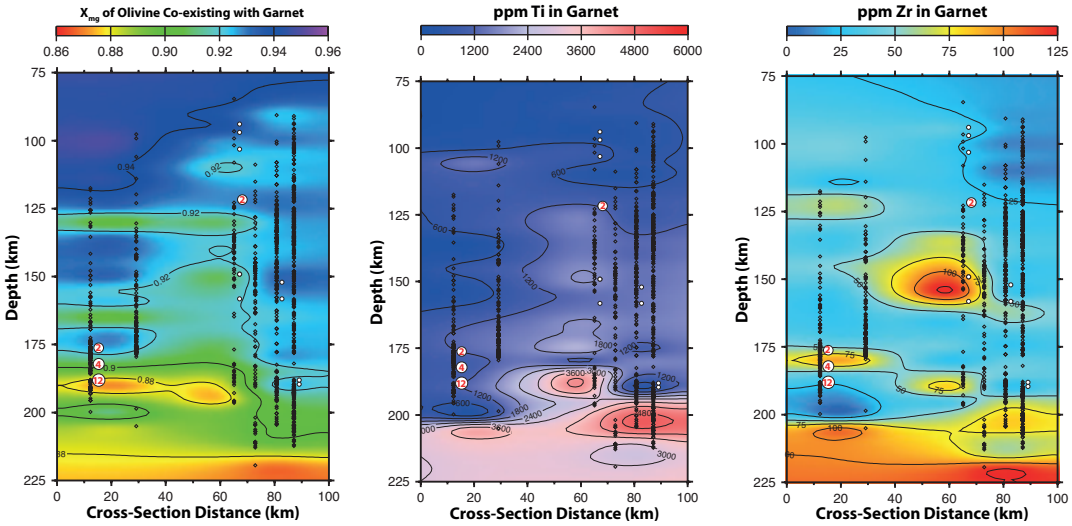

Figure 4. Lithosphere mapping. Diamonds, individual data points. Circles, eclogites (numbers show >1 sample with similar depth estimate). Contour filtering blocks are 20 km wide by 5 km deep. (a) Median calculated X_{Mg} of olivine coexisting with Cr-pyrope garnets. (b) Distribution of Ti in peridotitic garnets. (c) Distribution of Zr in peridotitic garnets.

Metasomatic hide and seek: Origins of the Roberts Victor eclogites

ECLOGITE (THE HIGH-PRESSURE METAMORPHIC EQUIVALENT OF MAFIC ROCKS SUCH AS BASALT) is an important constituent of the subcontinent lithospheric mantle (SCLM) although its abundance is low (1-3 vol%). A clear picture of its origin will help us to understand the origin of the ancient SCLM, one of the key questions in Earth Sciences. Extensive studies of these rocks have generated two contradictory hypotheses about their origin; one regards eclogites as deep-seated magmatic rocks, while the other regards them as components of subducted oceanic slabs. Eclogite xenoliths are very abundant in the Roberts Victor kimberlite in South Africa, and previous studies have provided many observations and analyses. These provide a basis for a new approach to the "eclogite problem", using a large collection of samples housed at GEMOC.

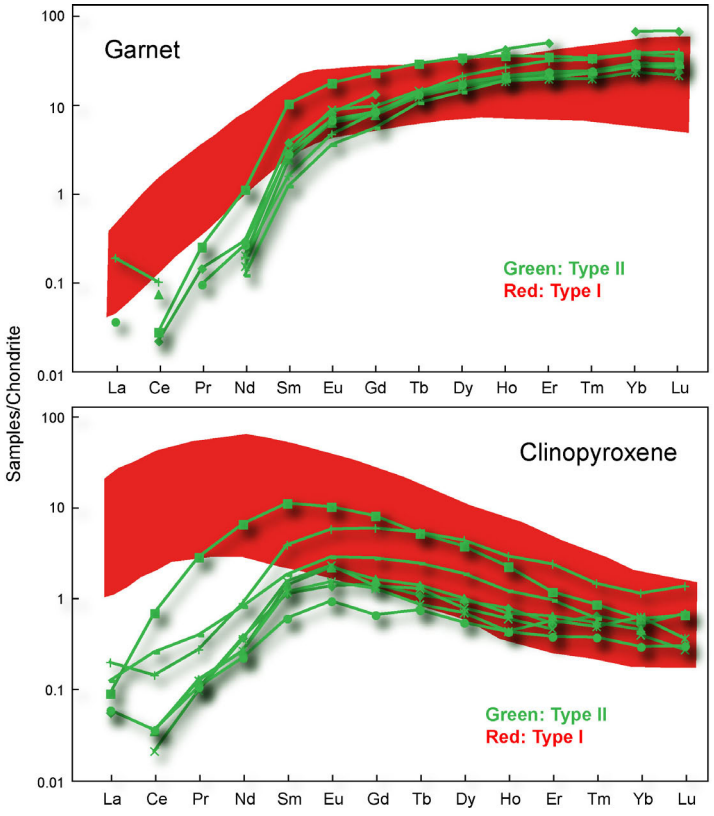

Figure 1. Chondrite-normalised rare earth element patterns for garnet and clinopyroxene from Type II (green lines) and Type I (red areas) eclogites from Roberts Victor mine.

The Roberts Victor eclogites can be divided into two types based on differences in microstructure and mineral composition; the abundance of Type II is low, about a quarter of Type I. Type II eclogites have low Na in gnt and low K in cpx, while Type I have high values. Type II eclogites are generally fresh and show equilibrated microstructures. Rutile exsolution in gnt and cpx, and gnt exsolution in cpx, are only found in Type II eclogites. Type I eclogites, in contrast, are not in textural equilibrium, have many fluid inclusions and contain altered cpx. Only Type I eclogites contain diamond, graphite, sulfides and apparently-primary phlogopite.

All the minerals are homogenous within each sample. The depth of each sample was estimated by projecting the P-T locus calculated from the gnt-cpx thermometer to the local geotherm derived from peridotitic xenoliths and garnets. Type II eclogites are homogeneously distributed from 170-200 km depth, but Type I are strongly concentrated in a layer at 180-190 km depth, just beneath the lithosphere-asthenosphere boundary (180-200 km).

Reconstructed whole-rock compositions show that Type I eclogites are richer in Mg and K than Type II; there are also significant differences in trace-element patterns between the two types. Type II garnets have higher mean ΣREE than those of Type I, but Cpx from Type II has lower REE concentrations than those from Type I, and ΣLREE/ΣHREE is much lower (Fig. 1). O- isotope ratios also show differences between the two types of eclogites. Type II eclogites have $\delta^{18}O < 4.3‰$ and those of Type I have mantle values (ca 5.4) or higher (Fig. 2).

Sr, Nd and Hf isotopes of gnt and cpx were analysed in small acid- leached grains. Although Eu anomalies are absent or very small in gnt and cpx (Fig. 1), they are pronounced in the leachates from both phases in both types of eclogites. Previous reports of Eu anomalies in such eclogites probably represent contamination on grain boundaries or in cracks within the minerals.

The Nd-Hf data for Type I eclogites define two-point isochron ages (Sm-Nd 127±21 Ma; Lu-Hf

128±13 Ma; Fig. 2) that are identical to the kimberlite eruption age (128 Ma). Lu-Hf isochron ages for three Type II eclogites (1354±9 Ma; Fig. 3) may suggest a connection to the Namaqua-Natal Orogenic Belt south of the Kaapvaal Craton; other Type II eclogites show more obvious partial re-equilibration. These differences immediately suggest that Type II eclogites have retained their initial isotopic compositions (modified by radioactive decay) whereas the isotopic systems of the Type I eclogites were actively re-equilibrating at the time of their entrainment in the kimberlite. This is consistent with the petrographic and mineralogical evidence of fluid metasomatism in the Type I eclogites. Initial isotopic ratios at the time of kimberlite eruption also show marked differences between Type II and Type I; initial $^{87}Sr/^{86}Sr$ is 0.7060-0.7064 in Type I and 0.7013-0.7030 in Type II.

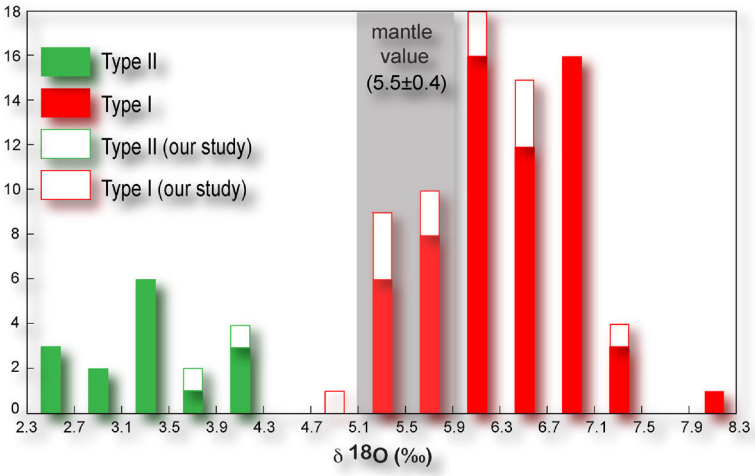

Figure 2. O isotopic compositions of Type II and I eclogites from Roberts Victor mine. Solid squares are the data from MacGregor and Manton,1986; Ongley et al.,1987; Jacob et al., 2003 and Schulze and Helmstaedt, 1988; Open squares are the data from our study.

These data and observations, combined with the detailed study of sulfide minerals suggest that Type I eclogites were being actively metasomatised at the time of the kimberlite eruption. Inter-element correlations suggest that the metasomatism was adding Mg, K, Na, Ti, S, C (diamonds) and LREE. Some samples from the same depth range (the present Type II eclogites) appear to have escaped this process and preserved their original characteristics.

The calculated fluid in equilibrium with Type I eclogitic gnt and cpx is LREE-enriched and shows trace-element patterns similar to those of fibrous diamonds and carbonatitic/kimberlitic melts. The Sr- and O-isotope values are also consistent with reaction between Type II eclogites and carbonatitic melt (typical $\delta^{18}O \approx 6$ - 7; $^{87}Sr/^{86}Sr \approx 0.706$ -0.707) to form Type I eclogites. Type II eclogites therefore are the key samples for studying the origin of this eclogite suite, since they may represent the protoliths. Type I, in contrast, are heavily metasomatised rocks, and retain little evidence of their primary origin.

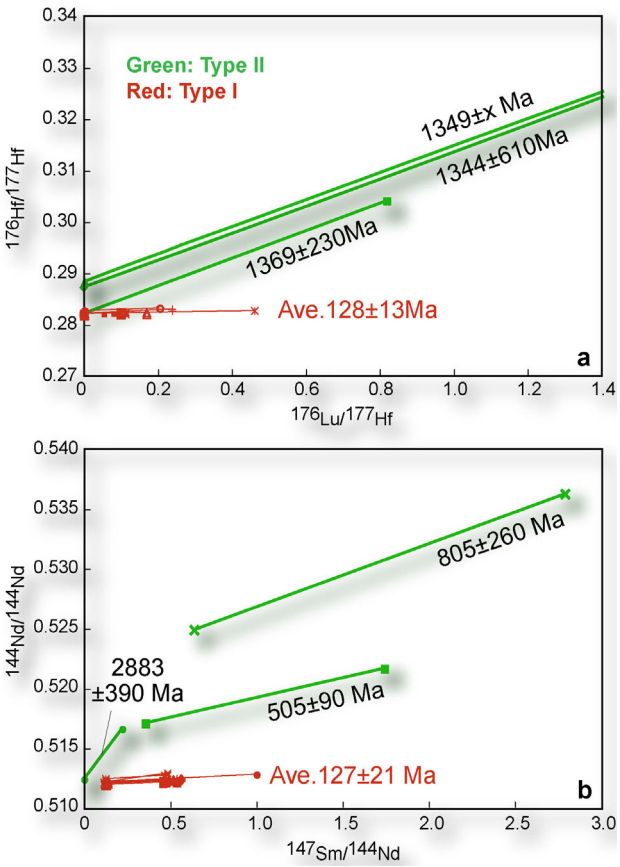

Figure 3. Garnet-clinopyroxene Lu-Hf (a) and Sm-Nd (b) isochron ages of Type II (green line) and Type I (red line) eclogites from Roberts Victor mine.

Contacts: Jinxiang Huang, Yoann Greau, Bill Griffin, Sue O'Reilly
Funded by: ARC Discovery (O'Reilly and Griffin), MQRES, EPS Postgraduate Fund

Dating problems with ancient perovskites rescued by SIMS

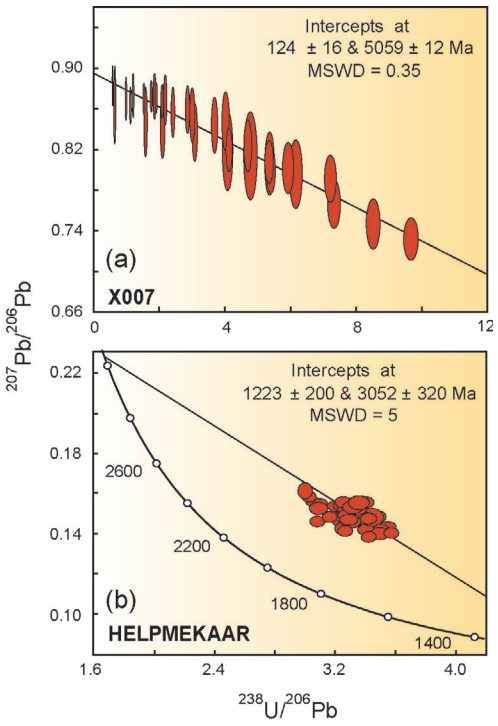

Figure 1. U-Pb inverse-Concordia diagrams showing (a) the typical example of kimberlitic perovskite dating using the in situ LAM-ICP-MS method, example from the X007 kimberlite; (b) U-Pb inverse-Concordia diagram from the Helpmekaar kimberlite.

KIMBERLITES, OUR MAIN SOURCE OF NATURAL DIAMONDS, are notoriously difficult to date, because they are chaotic mixtures of foreign mineral and rock material, enclosed in a (usually altered) magmatic matrix. Perovskite ($CaTiO_5$) grains in the groundmass of kimberlites are usually interpreted as having crystallised from the kimberlite during its rapid cooling after emplacement in the shallow crust. The perovskites have high contents of uranium, and potentially can be used to date the emplacement of the kimberlite by U-Pb isotopic analysis. This approach could avoid the complications of inheritance or mixed ages associated with traditional zircon and mica dating methods. The drawback to perovskites is that (unlike zircon) they also soak up lead ("common Pb") from the magma, so that they contain a mixture of common Pb and radiogenic Pb produced by the decay of U and Th, which complicates the dating.

In recent years the use of laser ablation microprobe-inductively coupled plasma mass spectrometry (LAM-ICPMS) U-Pb analysis to date kimberlitic perovskite has become increasingly popular (see *2009 Annual Report*). It can provide very precise ages in a fraction of the time used by other techniques, allowing its widespread application. For these analyses, it is assumed that perovskite is concordant in the U-Pb system. A linear regression is calculated through the data points; the upper intercept of this line with the Concordia curve on a Tera-Wasserburg plot (Fig. 1) gives the common-Pb composition and the lower intercept gives the inferred crystallisation age (Fig. 1a).

This procedure works well as long as the data points show sufficient spread in U/Pb ratios and common-Pb contents to define a line. If this is not the case, a common-Pb correction is required for each analysis. In TIMS (thermal ionisation mass spectrometry) or SIMS (secondary ion mass spectrometry, or "ion-probe") analysis this can be done by measuring the abundance of the non-radiogenic isotope ^{204}Pb, assuming an isotopic composition for the common-Pb component, and subtracting the calculated common-Pb abundance from the analytical data. However, the LAM-ICPMS method cannot accurately measure the ^{204}Pb contents due to an interference with ^{204}Hg in the Ar carrier gas. This problem became apparent during our attempts to obtain more precise emplacement ages for some old kimberlites, in the Kuruman field of South Africa.

The non-diamondiferous Kuruman Kimberlite Province is comprised of 16 small pipes and dikes that were intruded across the western edge of the Archean Kaapvaal Craton (Fig. 1). Despite being recognised as some of the oldest kimberlites in the world (~1.6-1.7 Ga), there are only limited geochronological data for the Kuruman Province. Unfortunately, the Kuruman perovskites are relatively homogenous in terms of U and common-Pb contents, which results in a limited range of data points on the Concordia plot. Furthermore, the Kuruman perovskites commonly show evidence of mild, fine-scale alteration and LAM-ICPMS U-Pb analyses of these grains typically scatter results to younger discordant ages. Regression of such data results in large errors in the lower-intercept ages and unrealistically low upper-intercept common-Pb compositions (Fig. 1b). As such, for the Kuruman perovskites, a common-Pb correction is required for each analytical spot.

This may suggest that perovskite is not as resistant to weathering and alteration as was previously thought and that the U-Pb isotopic system in perovskite may be reset by alteration. The LAM-ICPMS analysis uses volumes ca 30 microns across and 30-40 microns deep, and we suspected that the analysed volumes were including altered material, even if the grains looked good on the surface. An alternative approach clearly was required, and was made possible by our collaborator (Jin-Hui Yang) in the SIMS lab at the Chinese Academy of Sciences, Beijing.

The application of SIMS to U-Th-Pb perovskite geochronology has been relatively limited. However, recent developments in calibration protocols using well-characterised standards (see Li et al., Chemical Geology, 269, p. 396-405, 2010) have allowed the smaller analytical sampling volume used by SIMS to be combined with precise measurements of ^{204}Pb, providing a promising tool for detailed *in situ* perovskite geochronology.

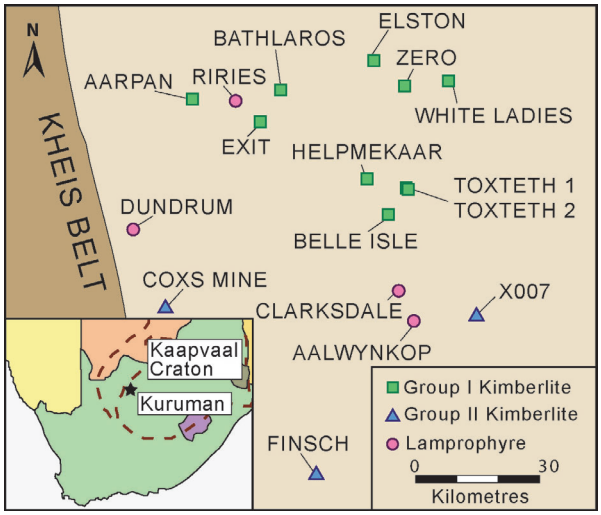

Figure 2. Map showing the location and petrographic classification of the Kuruman kimberlite province.

Perovskites from the Kuruman kimberlites were re-analysed using SIMS to target only the most pristine parts of each grain and the results were then corrected for ^{204}Pb. The Bathlaros kimberlite yielded a ^{206}Pb/^{238}U age of 1594±27 Ma (n=7; MSWD=0.22; Fig. 3a); this is younger than the 1694± 42 Ma phlogopite isochron age, upon which the age of the Kuruman Province is currently defined. The Elston (Fig. 3b) and Helpmekaar (Fig. 3c) kimberlites have ^{206}Pb/^{238}U perovskite ages within error of each other at 1689±26 Ma and 1651±21 Ma, respectively. The Zero kimberlite yielded an older emplacement age of 1832±37Ma (Fig. 3d). The SIMS results thus show a considerable range (~200 Ma) in emplacement ages within the Kuruman Province and reveal a previously unrecognised trend of increasing kimberlite age from east to west across the Province.

Figure 3. U-Pb inverse-Concordia diagrams for the Kuruman kimberlites obtained using HR-SIMS data.

The recent LAM-ICPMS dating of kimberlite perovskite has produced many precise and apparently accurate ages, but these have all been from relatively young kimberlites (≤1 Ga; *GEMOC publication #505*; Wu et al., 2010, Lithos, 115, 205-222). The failure of this method in the case of the Kuruman kimberlites, even when "unaltered" grains were analysed, suggests that the U-Pb system in older perovskites may be disturbed by metamictisation – the breakdown of the crystal structure under α-particle bombardment as U and Th decay – as is seen in many zircons.

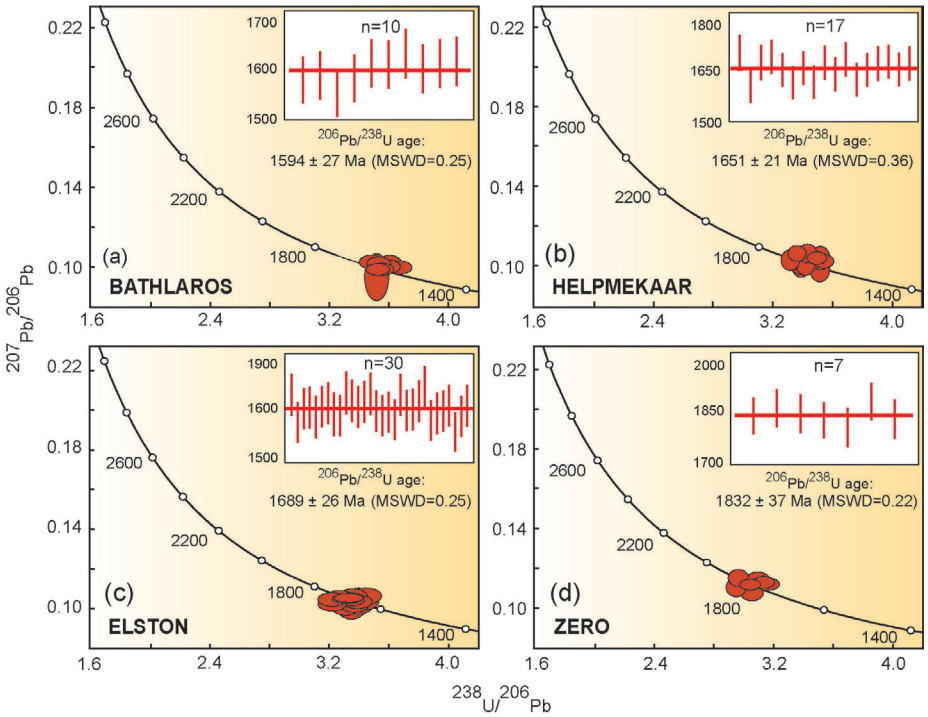

Contacts: Cara Donnelly, Bill Griffin, Sue O'Reilly, Jin-Hui Yang
Funded by: ARC Discovery (O'Reilly and Griffin), MQRES, EPS Postgraduate Fund, Industry

Short-lived isotopes reveal off-axis magmatism at the East Pacific Rise

More than 70% of global volcanism consists of basalts erupted at mid-ocean ridge ridges (MORB) and this is generally thought to be confined to a narrow axial zone due to efficient magma focusing from a much broader, triangular melting volume. However, the dynamics of melting and melt transport remain a subject of debate. In this regard, studies of short-lived U-series isotopes have proven especially useful because of their potential to constrain melting rates and melt extraction porosity.

One of the most intensively studied ridges is the fast-spreading (11.1 cm/yr) East Pacific Rise (EPR) which appears to be underlain by axial magma chambers. The EPR axial summit trough is only 10-100 m wide, yet geophysical surveys indicate that the oceanic crust continues to thicken (by a factor of ~ 2) away from the ridge axis. This demands the occurrence of off-axis magmatism either by intrusion or by volcanism. This inference has been supported by observations from submersible vessels, and by earlier U-series dating that yielded ages younger than those predicted by combining the distance of the sample from the axis with the local spreading rate. For example, in the region 9-10°N, U-series data demonstrate the persistence of volcanism up to 4 km from the ridge axis.

In order to explore these substantial matters further, we have undertaken U-series analyses of samples from traverses across the EPR at 9°30′N, 10°30′N and 11°20′N. The results show that about 50% of the 34 samples analysed must have erupted off-axis and at least 14 formed within a few km of their current position. Thus, the data confirm geophysical suggestions that magmatism extends significantly off axis (up to 30-50 km). The implication is that magmatism is not as efficiently focused beneath the ridge as is generally believed. There is a decrease in "primary" U-series disequilibria in samples inferred to have formed off-axis and simple modeling suggests that this can be explained by a decrease in melt-column length and fertility as the overlying lithosphere thickens with age (Fig. 1).

Contact: Simon Turner
Funded by: ARC Discovery

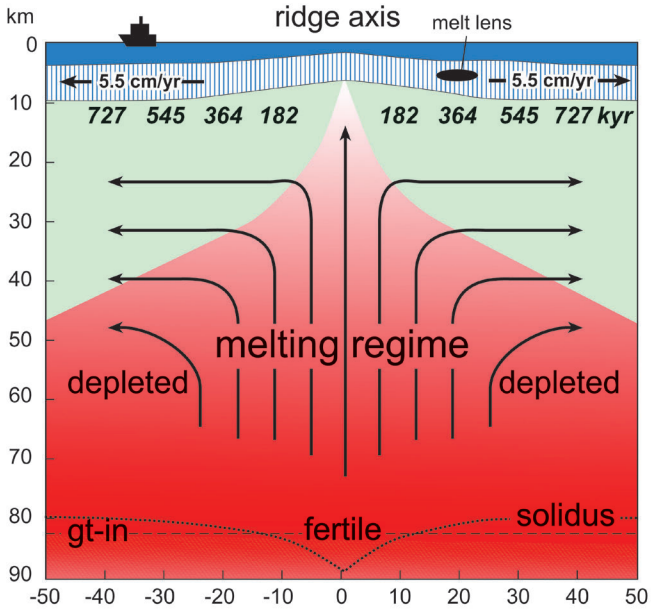

Figure 1. True-scale illustration of the melting model explored in light of the East Pacific Rise traverse data, showing schematic mantle flow lines. The oceanic crust thickens away from the ridge axis following the thermal plate model (age is given in italics). Shown are the location of the spinel to garnet transition and the melting region that is required to dip into the garnet peridotite zone on the basis of the large ^{230}Th excesses observed in erupted lavas. It is also assumed the melt extraction in the central upwelling region results in more depleted peridotite moving away from the axis. The location of a melt lens identified from seismic observations is also shown. Ship not to scale.

Apatite trace element fingerprints reveal Transhimalayan magmatic processes

A (collision-type) adakite from Zedong, southeast of Lhasa.

ACCESSORY MINERALS, THOUGH TINY AND SPARSE, concentrate specific geologically-interesting trace elements such as rare earth elements and can give critical constraints on the details of igneous processes in magma chambers. This approach provides information about igneous petrogenesis that is not accessible through conventional bulk-rock analysis. Apatite, although less intensively studied than zircon, may be the next candidate for such expanded applications. In terms of its common occurrence, stability during magma evolution and chemical diversity, apatite is comparable with zircon and even better in some respects.

To get a better idea of the relationships between magmatic processes and the geochemical characteristics of apatite, we have analysed minor- and trace elements in apatites from a range of plutonic rocks in the Lhasa terrane of southern Tibet. The Lhasa terrane consists primarily of Paleozoic to Mesozoic sedimentary rocks, intruded by ubiquitous igneous rocks. These may be categorised into three principal rock types on the basis of geochemistry and/or occurrence: (1) S-type granites, (2) I-type Gangdese granitoids, (3) (collision-type) adakites, with uniquely high Sr/Y ratios and heavy-REE depletion.

View of the Lhasa terrane, Wuyu, Nanmulin County, northeast of Xigaze.

Apatite retains geochemical information about the host magma through the course of magmatic evolution: F, Mn, Sr and rare earth elements in apatite systematically vary with the composition of its host magma and thus have high potential as petrogenetic tracers. More specifically, F and Mn contents in apatite can be used as an indicator of magma aluminium content or differentiation index. Combined with Sr and REE data, which also show significant variations in apatite from different rock types as well, these elements are useful for constructing "discrimination diagrams" (Fig. 1). The variations of Sr and REE in apatite with bulk rock aluminium content reflect competition with other major and accessory minerals in silicate melts, including plagioclase and monazite. These variations therefore are useful for more detailed investigations of petrogenetic processes such as fractional crystallisation and magma mixing (see *GEMOC Publication #609*). Magma mixing is signaled by inconsistent Eu anomalies, Sr abundances and REE patterns relative to bulk rock composition.

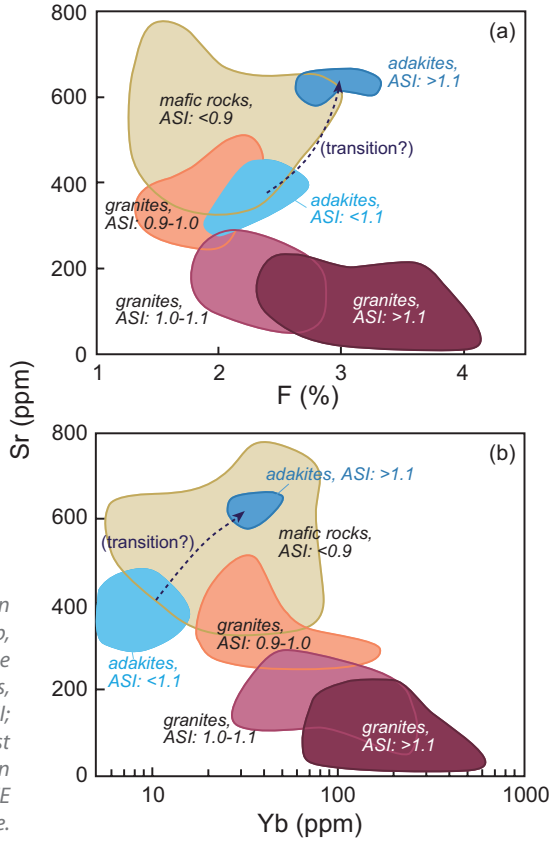

Contacts: Mei-Fei Chu, Norman Pearson, Bill Griffin, Sue O'Reilly
Funded by: ARC Discovery

Figure 1. Two examples of "discrimination diagrams." (a) F and (b) heavy REE, e.g. Yb, abundances in apatites generally increase with aluminosities of host plutonic rocks, e.g. the aluminum saturation index (ASI; molecular $Al_2O_3/(Na_2O+K_2O+CaO)$. In host rocks of similar aluminosity, apatite from an adakite has higher Sr and lower heavy REE than one from a granite.

The Gawler Craton, South Australia: Unexpected discoveries and mysteries

ZIRCON GRAINS FROM MODERN AND ANCIENT DRAINAGES OF THE GAWLER CRATON, South Australia have been studied to unravel the evolution of this craton. The study has defined the relative contributions of juvenile sources and recycled crust to magmatic activity as a function of time, and constrained the role of mantle inputs during the Proterozoic rejuvenation of the Archean Gawler Craton (see *GEMOC Publication #600*).

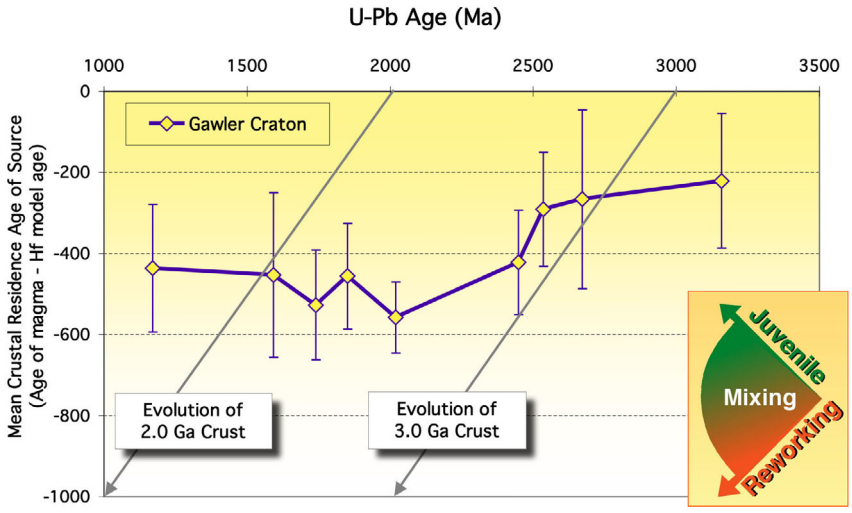

Figure 1. 'Event Signature' curve for the Gawler Craton; mean magma source residence time (Age - T_{DM}) is plotted against time. The mean crustal residence time is given by the age of the given event peak minus the mean T_{DM} model age for that peak.

The integration of Hf-isotope data with U-Pb age spectra showed that the crustal evolution was dominated by long periods of crustal reworking, and that crust generated in the Paleoarchean (3.2–3.5 Ga) was largely reworked during Proterozoic time (Fig. 1). There were three periods with some juvenile mantle input at ca 2540 Ma, 1853 Ma and 1595 Ma. However, these juvenile mantle inputs provided a minor contribution to the crustal volume, compared to the major role played by the reworking of older crust.

Modelling of the composite age spectrum derived from the detrital zircons allows definition of six major geological events in the Gawler Craton, spanning the period 2550-1550 Ma (Fig. 2). Besides those previously well-recognised events, we identified a minor age peak at ~3152 Ma. This Archean age is also strongly supported by Hf-isotope data – many zircons have model ages ca 3.2 Ma. This conclusion was later confirmed by the Geosience Australia discovery of the oldest rocks reported from the Gawler Craton; an outcrop in the Eyre Peninsula has been dated to 3150 Ma.

We also found a major peak at 1169 ± 48 Ma represented by a prominent zircon population (Fig. 2). This appeared to be the only event that had not been reported previously in the Gawler Craton and is a mystery remaining to be resolved. There is a possibility that this age population might represent zircons that were transported from the Musgrave Province, where a Grenville-age event is well documented. However, zircons of this age are found not only in the samples

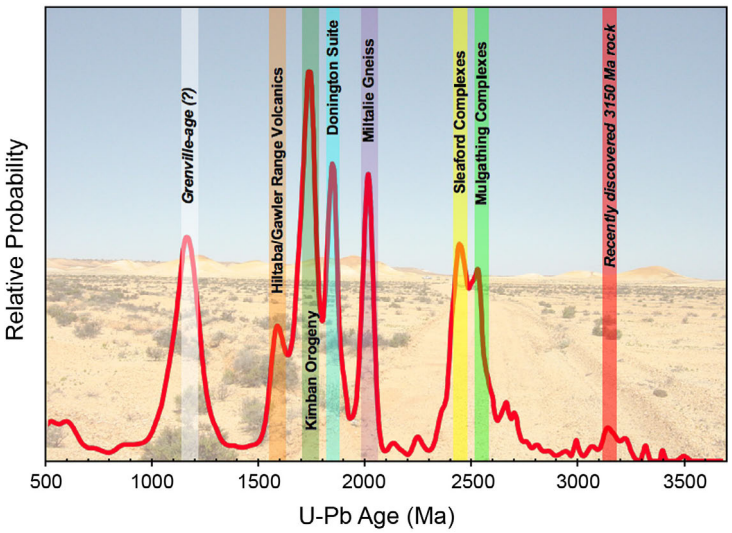

Figure 2. Relative probability plot of U-Pb age data for zircon from the Gawler Craton.

from drainages situated near the Musgrave Province, but across the Gawler Craton as far as the Gawler Range Volcanics Domain and the southern part of the Olympic Domain, over 700 km SE of the Musgrave Block. Moreover, other age populations, and especially the 1300-1400 Ma event that is prominent in the Musgrave Province, are not found in the Gawler samples. This observation alone makes it improbable that the 1169 Ma age population is derived from the Musgrave province. Further investigations to find rocks of this age within the Gawler Craton will be necessary to resolve this ambiguity.

Contacts: Elena Belousova, Bill Griffin, Sue O'Reilly
Funded by: PIRSA, ARC Linkage

TerraneChron® sampling in the Gawler Craton

Zircons lay bare the secrets of the ancient Yangtze Block

THE YANGTZE CRATON OF SOUTH CHINA is usually regarded as a Proterozoic block with minor Archean remnants, but this interpretation is based mainly on inference, because most of the craton is obscured by much younger sediments. However, there are several late Proterozoic basins lying around the edge of the craton, and the detritus in these is believed to be derived from its now-covered interior. A Nanjing University- GEMOC collaboration has been investigating these basins, using integrated U–Pb dating, Hf-isotope and trace-element analysis of detrital zircons to identify ancient crustal remnants and the provenance of clastic sediments, and to provide an overview of crustal evolution in the now-covered parts of the Yangtze Block.

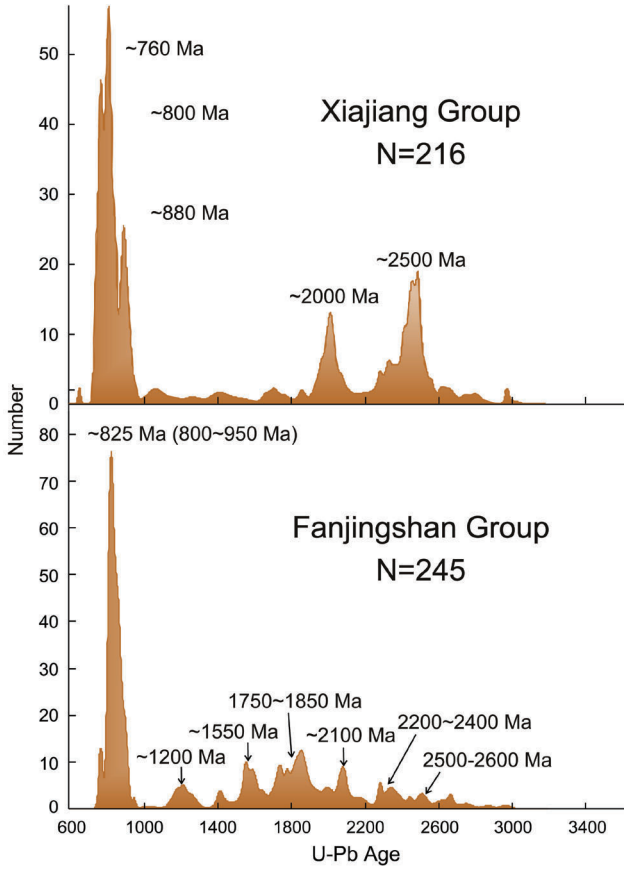

Figure 1. Probability density plots comparing U-Pb ages for detrital zircons.

The Fanjingshan and Xiajiang sediments in the southeastern part of the Yangtze Block have been studied during 2009. The zircon dating indicates that the Fanjingshan Group, which previously was regarded as 870 Ma old, actually was deposited in a ~800 Ma rift basin similar to other contemporaneous basins in the Yangtze Block. The regional unconformity separating the Fanjingshan Group from the overlying Xiajiang Group is dated to 800~740 Ma and is probably related to rifting processes during the breakup of Rodinia (830~740 Ma).

Detrital zircons from these two sedimentary groups have different age populations. We have identified seven main age populations in the Fanjingshan Group: 0.85~0.8 Ga, 0.95~0.86 Ga, 1.3~1.1 Ga, 1.6~1.5 Ga, 1.8~1.7 Ga, 2.1~2.0 Ga, 2.4 ~2.2 Ga and 2.6~2.5 Ga. There are fewer age peaks in the Xiajiang Group: ~760 Ma, ~800 Ma, ~880 Ma, ~2000 Ma and ~2500 Ma (Fig. 1).

The trace-element analysis indicates that most zircons in the Fanjingshan Group were derived from granitoids, with a few from mafic rocks. However, the dominant source rock of zircons from the Xiajiang Group changes from the lower to the upper part of the group. The proportion of mafic rocks increases upward through the sequence, suggesting bimodal magmatism in the region.

Based on the zircon U-Pb dating and Hf-isotope results for the Fanjingshan and Xiajiang groups, the distinguishing features of Precambrian crustal evolution in their respective source regions are summarised in the Event Signature curves of Figure 2a. They have similar Archean origins. The oldest continental crust in the Yangtze Block may have started to form in early Archean or even Hadean time. A previously unrecognised source (~4.3 Ga) is suggested by the Hf model ages of the oldest zircons. During late Archean time (2.4~2.6 Ga), some juvenile material was added to the crust in the source areas for both the Fanjingshan and Xiajiang groups. After this time the two source regions have followed different evolutionary paths.

In the source regions of the Fanjingshan Group, the juvenile Archean crust was reworked during Paleoproterozoic time (2.1~1.7 Ga). An important input of juvenile mantle-derived material occurred in the early Mesoproterozoic (1.6~1.4 Ga). This is the first documentation of early Mesoproterozoic juvenile crust in South China. Afterwards, both reworking and some

juvenile growth of crust took place from Mesoproterozoic (~1300 Ma) to mid-Neoproterozoic (~800 Ma) time.

In the source area of the Xiajiang Group, the Archean crust was reworked in Paleoproterozoic time (2.0-2.1 Ga), but the 1.6-1.4 episode is essentially absent. The most significant input of juvenile crust occurred in early Neoproterozoic time (850~1000 Ma). This episode of juvenile-crust formation was followed by crustal reworking until ~800 Ma. The last magmatic activity in this area involved a new juvenile contribution at 790~740 Ma. The curves show that crustal evolution of the source area of the Xiajiang Group is quite similar to that of the Yichang area reported by Liu et al. (2008; AJS, 308, 421-468).

The possible source areas for these sedimentary rocks are the Yangtze Block and the adjacent Cathaysia Block (Fig. 2b). Although similar mid-Neoproterozoic and Paleoproterozoic age populations (0.85~0.8 Ga, 1.8~1.7 Ga) are found within both the Yangtze Block and the Cathaysia Block, the detrital zircon spectra in this study show remarkably little material of Grenvillian age (0.95~1.0 Ga) whereas rocks of this age are abundant in the Cathaysia Block. The crustal event signature summarised in Figure 2b shows a different geological evolution than the one recorded by the zircons studied here (see *GEMOC Publications #615 and 477)*. The euhedral morphology of zircons in all age windows from the Fanjingshan and Xiajiang sediments also suggests that their primary sources were not far from their site of deposition. Therefore, the (now unexposed) Yangtze Block is considered to be the main source for the sediments in the Fanjingshan and Xiajiang groups. The differences in the sources for some detrital material between these two groups, and with exposed basement in the Yangtze Block that the sources for these zircons lie within different, now-covered, parts of the Yangtze Block.

Contacts: Lijuan Wang, Sue O'Reilly, Jin-Hai Yu
Funded by: ARC Discovery (O'Reilly and Griffin), MQRES, EPS Postgraduate Fund

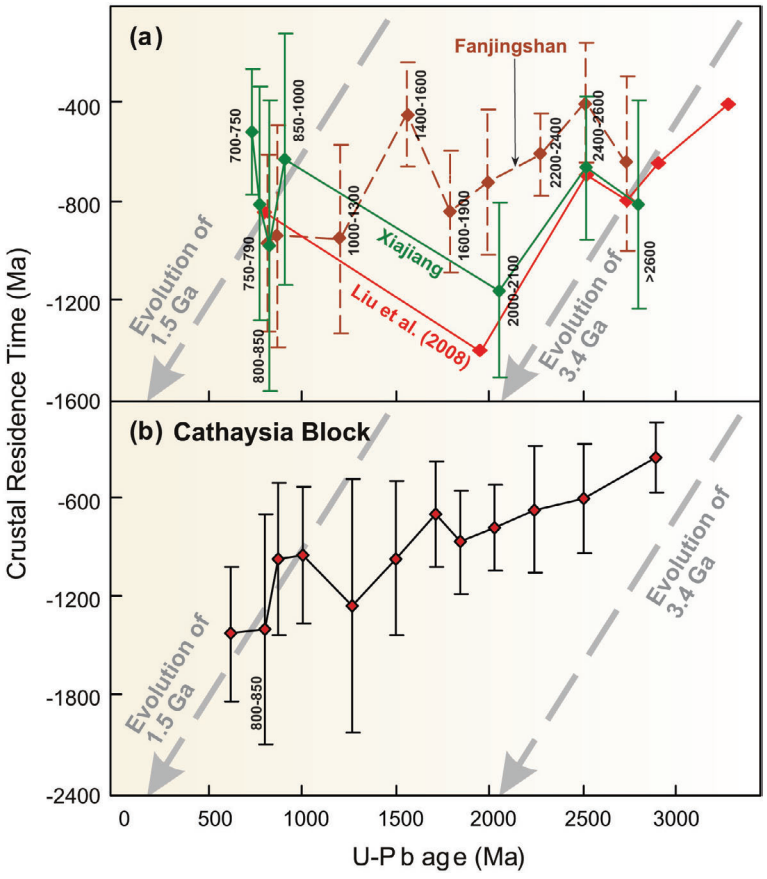

Figure 2. "Event signature" curves combining zircon ages with calculated crustal model ages for the study area, the Yichang area (Liu et al., 2008) and Cathaysia Block (Yu et al., 2009; Xu et al., 2007). Crustal residence time is the time between the separation of the source from the Depleted Mantle and the crystallisation of the zircon. In this plot, an upward trend with decreasing age indicates juvenile input, while a downward trend implies reworking of older crust.

Platinum-group elements nobly unravel komatiites

PLATINUM-GROUP ELEMENTS (PGE: Ru, Rh, Pd, Os, Ir, Pt) are important as petrogenetic tracers in the study of Earth's accretion history, core-mantle interaction, mantle differentiation processes, and the Re-Os isotopic system that is widely used to date mantle depletion events. They are industrially important commodities in their own right, and have been identified as potential pathfinders for Ni-Cu-sulfide mineralisation. However, owing to their low abundance and complex behavior, PGEs remain among the least understood elements in geochemistry, mainly because of the difficulties of producing accurate and precise analyses. Research at GEMOC has developed novel analytical approaches for low-level PGE analysis in order to investigate the behaviour of PGEs during the fractionation of komatiites and komatiite-derived magmas, with a particular focus on the role of chromite in the fractionation and concentration of Ru.

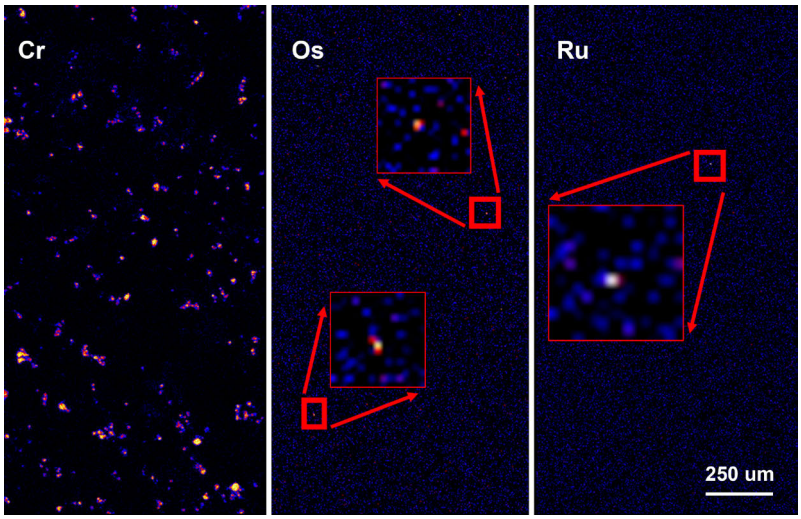

Figure 1. X-ray fluorescence maps showing the distribution of Cr Ka (as an indicator of chromite), Os and Ru in a komatiite. The maps were obtained using a beamline on the Australian Synchrotron.

In sulfide-saturated systems, the behaviour of the strongly chalcophile PGE is well established; it is dominantly controlled by their strong partitioning into sulfide melts relative to silicate magmas. However, little is known about the fractionation of PGEs in sulfide-undersaturated systems, mainly because the PGE contents of mineral phases that record the magmatic evolution of a system are generally below the detection limit of conventional analytical techniques. Accordingly, most studies have been limited to using whole-rock PGE signatures from S-poor rocks. Although this gives a rough idea about the PGE behavior, it leaves a lot of questions unanswered, particularly as primary magmatic whole-rock signatures can be overprinted by metamorphism, alteration, and weathering. Moreover, the presence of minute platinum-group minerals can distort the whole-rock PGE signatures of S-poor rocks (Fig. 1).

A more informative way to investigate PGE behaviour is to determine the PGE signatures and/or concentrations of primary mineral phases as these signatures are less likely to be overprinted by secondary processes. However, it has been widely debated over the past decades if PGE can exist in solid solution in non-sulfide phases at all, or if measured PGE concentrations in oxides and silicates are exclusively related to the presence of inclusions. This needs to be established, as only PGE in solid solution will record the evolution of a magmatic system, and therefore can be used to better understand

Archean lava lake outcrop from Kurrajong, Western Australia.

the behaviour of PGE during fractionation.

The analytical approach for low-level PGE analysis in mineral phases at GEMOC combines (1) *in situ* laser ablation (LA) ICP-MS analysis of chromite and silicate grains to determine PGE concentrations at low ppb levels and the spatial distribution of PGE within the grains; and (2) Carius-tube digestion and isotope-dilution ICP-MS analysis of mineral concentrates to confirm the accuracy of the *in situ* studies. The study has demonstrated that Ru can exist in solid solution in chromite with concentrations up to several hundred ppb and that the fractionation of Ru in S-poor systems is controlled by the crystallisation of chromite. The laser ablation ICP-MS data show that Ru concentrations in chromite grains in individual samples are, within analytical uncertainty, the same on sample- and grainscale (Fig. 2). These results suggest that Ru is bound as solid solution in the crystal lattice of chromite, as the occurrence of Ru-bearing micro-inclusions would produce a greater variability within and among grains of the same sample. This hypothesis is supported by the fact that time-resolved LA-ICPMS analyses show a uniform distribution of Ru in komatiitic chromite indicated by a constant signal intensity of approximately 40-50 cps above background, whereas it was possible to establish the presence of Ir-inclusions distinctly smaller than 1 µm using the same analytical procedures (Fig. 3). This indicates that the absence of Ru-bearing micro-inclusions in the analysed chromites is a real feature and not the result of sampling bias. It could be argued that Ru may be evenly distributed as nano-particles in chromite – and not necessarily bound in the crystal lattice as solid solution. However, our data give similar results for many samples from different localities. If Ru was hosted as nano-particles rather than being in solid solution, a greater variability would be expected. Therefore, we suggest that Ru can exist in solid solution in chromite with concentrations up to several hundred ppb.

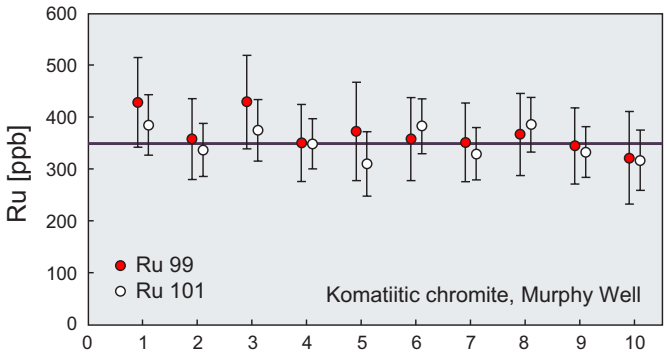

Figure 2. Ruthenium in chromite from the Murphy Well komatiite flow in Western Australia as analysed by laser ablation ICP-MS. The solid line shows the average Ru concentration obtained by Carius-tube digestion and isotope-dilution ICP-MS analysis and confirms the accuracy of the in-situ studies.

These outcomes are the first of their kind and open up new avenues of research related to the role of chromite in the fractionation and concentration of Ru in mafic and ultramafic systems.

Contacts: Marek Locmelis, Norman Pearson
Funded by: ARC Discovery (O'Reilly, Griffin and Pearson), MQRES, EPS Postgraduate Fund

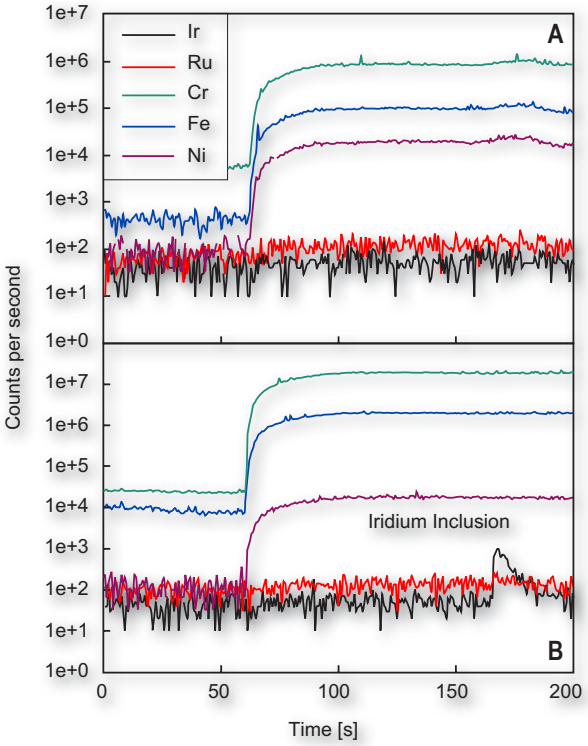

Figure 3. Time resolved analysis record obtained by LA-ICP-MS illustrating (A) the absence of any PGE-bearing micro-inclusions in chromite from Murphy Well, and (B) the presence of an iridium-bearing micro-inclusion in a chromite grain from a komatiitic basalt flow at Collurabbie (Western Australia).

2010 Contents

TerraneChron™	304
When the Earth moves: Applications to geothermal exploration (Western USA)	305
Continents can't subduct!…or can they?	308
The Lithosphere-Asthenosphere boundary: Can we sample it?	310
Out of Africa: Garnets reveal insights into Earth's oldest mantle	312
What's new? - *TerraneChron*® pinpoints when and where continental crust really grew	314
The Earth's first continental crust	316
On the edge: Continent roots and giant Nickel deposits	318
Noble method updates the Ni exploration toolkit	320
Zircons from the roof of the world unearth Himalayan evolution	322
The Big Bang - New insights into the 1912 eruption of Katmai volcanoe	323
Journey from the centre of the Earth: xenoliths reveal the velocity of magmas	324
Core formation in partially molten planetesimals: A complex network analysis	326
Catastrophic overturn on Enceladus	328
Brilliant imaging: new facets of diamonds' deep inner secrets	330

Front Cover: A collage of images reflecting GEMOC's work over 15 years: from mantle petrology to lithosphere evolution, modern volcanology to the genesis of giant ore deposits, and on to the cutting-edge geochemical, geophysical and planetary studies – and from micron to global to planetary scales.

Research highlights 2010

TERRANECHRON® IS GEMOC'S UNIQUE METHODOLOGY FOR TERRANE EVALUATION. During 2010 a range of new studies, including collaborative research projects with industry, using *TerraneChron*® expanded our knowledge of crustal evolution and the timing of tectonic events.

Visit the TerraneChron® web page at http:// www.gemoc.mq.edu.au/TerraneChron.html

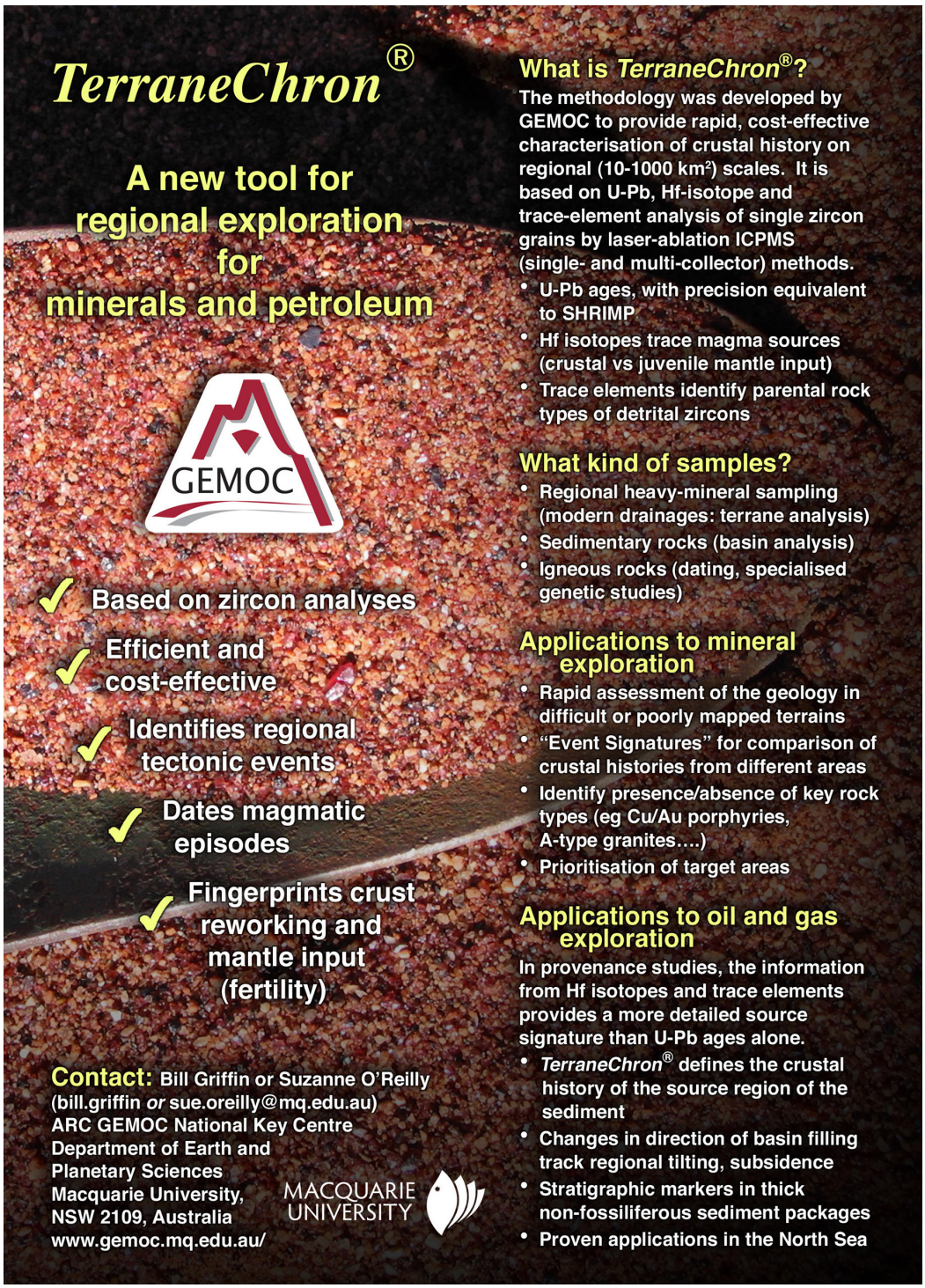

When the Earth moves: Applications to geothermal exploration (Western USA)

SEISMIC WAVES ARE THE MAIN TOOL USED TO REVEAL INFORMATION about the underground structure of the Earth, because they can penetrate into the deep interior and be received by seismographs. Seismic tomography is a technique for constructing three dimensional structure of the Earth's interior using these waves. It is analgous to the CT scanning used in medicine to look inside our bodies. Traditional seismic tomography uses natural earthquakes as sources to image internal structure. However, earthquakes are mainly located at tectonic plate boundaries, and this makes it difficult to image the shallow structure of the crust, especially in the top 10 km of the Earth, in aseismic regions such as the Australian continent. The advent of ambient noise tomography in 2005 revolutionised seismic tomography. This new method uses the microseismic noise produced by ubiquitous minor ground motions, the so-called

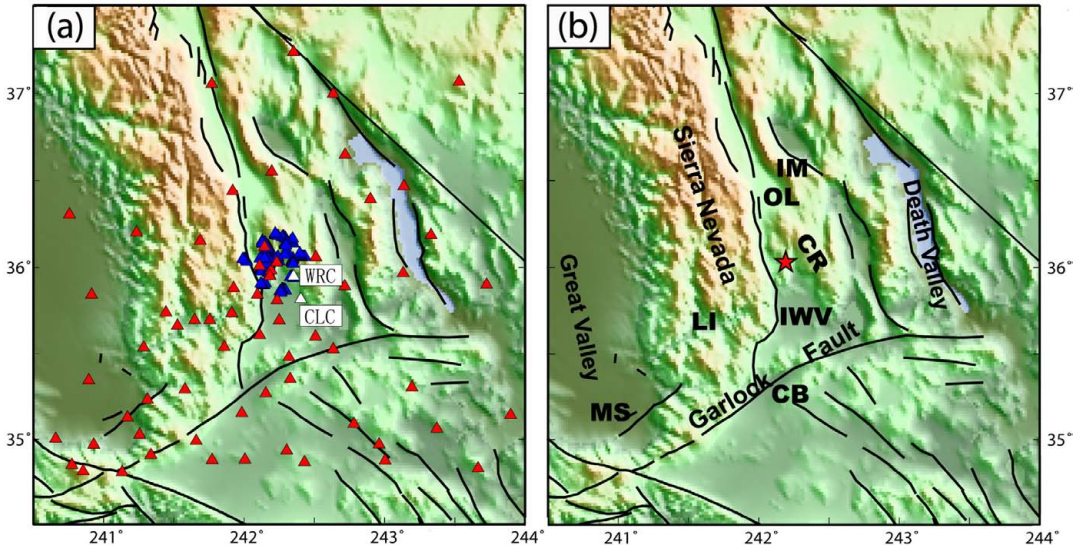

Figure 1. (a) Distribution of seismic stations (triangles) in the Coso Geothermal Area and surrounding areas used in this study. Black lines denote faults. (b) Place names mentioned in text: CB: Cantil Basin; CR: Coso Range; IM: Inyo Mountains; IWV: Indian Wells Valley; LI: Lake Isabella; MS: Maricopa sub-basin; OL: Owens Lake.

ambient noise, to map seismic velocity along the path between any two seismic stations, independently of earthquakes. It is especially useful for imaging the shallow levels of the crust, where the most abundant natural resources are located, such as mineral deposits, oil and gas reservoirs, and geothermal fields.

The Coso Geothermal Area lies at the southwestern corner of the actively deforming part of the Basin and Range Province of North America; it is within the Eastern California Shear Zone (Fig. 1). It also lies in the part of the Basin and Range that has experienced the most recent significant volcanism. The Coso Range contains one of the young magmatic centres along the western margin of the Basin and Range; its activity started about 4 Ma ago but entered a phase of bimodal volcanism about 1 Ma ago. The recent magmatic activity produced high temperatures beneath the Coso Geothermal Area, and commercial power development began there in the 1980s. The power plants are currently producing 270 MW from four geothermal power plants. To characterise the geothermal resource and generate electricity more efficiently in the future, numerous geophysical studies have been carried out over the geothermal field. However, two main questions still remain: the depth of the magma chamber acting as the heat source and the relationship of magmatism to faulting or shearing at depth.

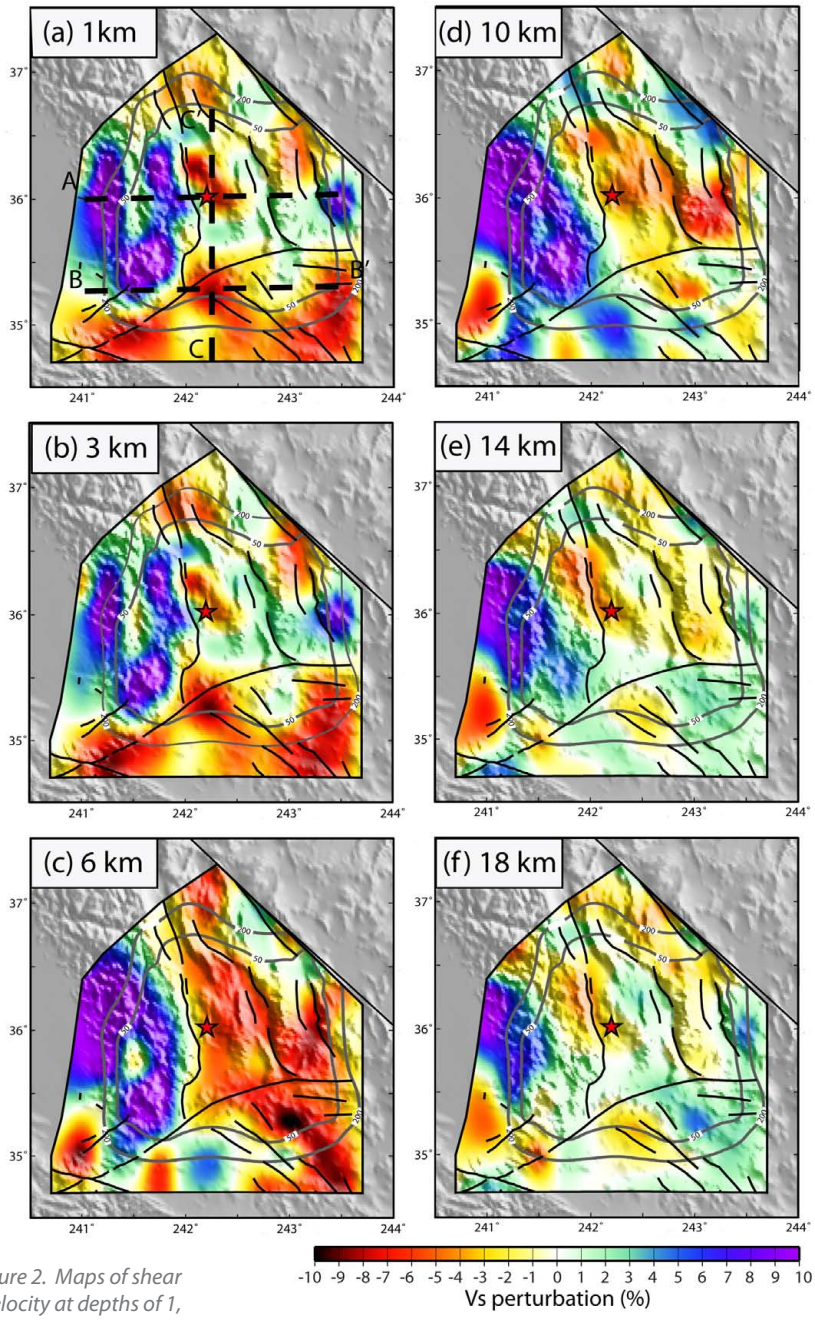

Figure 2. Maps of shear velocity at depths of 1, 3, 6, 10, 14 and 18 km, plotted as perturbations to averages at each depth: 1 km (2.867 km/s), 3 km (3.174 km/s), 6 km (3.319 km/s), 10 km (3.452 km/s), 14 km (3.524 km/s), 18 km (3.574 km/s). Two grey contours of resolution at scales of 50 and 200 km are plotted in each map. The three dashed lines in Fig. 2a show the surface locations of the three vertical transects shown in Fig. 3.

In this study, ambient noise tomography was adopted to image shallow structures beneath the Coso Geothermal Area and surrounding areas using all the stations nearby (Fig. 1; see *GEMOC Publication #702*). The purpose was to constrain the depth of any magma chambers underlying the area. The resulting 3D shear-velocity structure from this study is shown as maps of shear velocities at depths of 1, 3, 6, 10, 14 and 18 km (Fig. 2) and three vertical shear-velocity transects whose surficial positions are indicated in Figure 2a. Warm colors in these figures represent lower seismic velocities, indicating either high temperature or the presence of magma; cold colors represent higher seismic velocities indicating lower temperature.

Low velocities in the entire depth column beneath the Coso Range are quite close to the position of the Coso Geothermal Field (Fig. 3). In particular, a feature with very low velocity is imaged in the top 2 km. The appearance of this anomaly, even though the dominant surface exposures are granite, suggests profound alteration of the crust in the area and/or significant influence from shallow magmatic or hydrothermal fluids. Although the entire crustal column beneath the Coso Geothermal Area appears to have depressed Vs speeds (Fig. 3), there is an indication of a stronger low-velocity zone between depths of 6 and 8 km. This may reflect a deeper magmatic anomaly underlying the shallow geothermally-induced anomaly in the top 2 km. The absence of really low velocities below ~14 km (Fig. 2e) tends to support a shallow-magma interpretation.

An intriguing feature that emerges in this study is the low velocities between about 6 and 8 km depth under much, but not all, of the Basin and Range Province (Fig. 2c, 3). This feature correlates well with the extent of sizeable exposures of Neogene and Quaternary volcanic rocks (Fig. 4), strongly suggesting a magmatic origin. Within the area well-resolved by this study, only the older Miocene volcanic centre in the southern Sierra Nevada and some small centres in the eastern Sierra Nevada remain outside this zone. It is implausible that this entire feature represents uniformly distributed melt at these depths, but local accumulations of melt seem consistent with very low electrical resistivity found near these depths north of Coso. This anomaly probably represents crust profoundly reworked by igneous processes over the

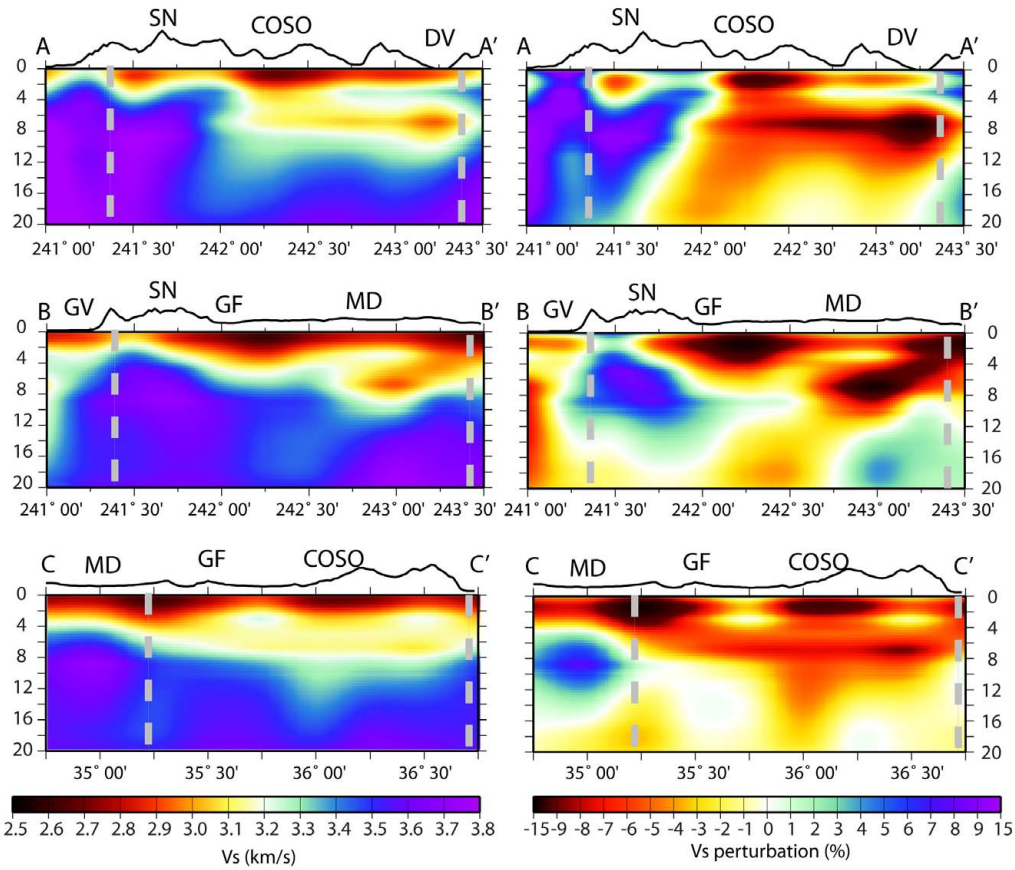

Figure 3. Vertical transects of shear velocities plotted both as absolute values (left) and as perturbations relative to the 1D Vs averages (right). The two dashed gray lines in each plot enclose an area where the imaging has a lateral resolution of 50 km. The locations of the cross-sections are shown in Fig. 2a. Abbreviations: COSO: the Coso Geothermal Area; SN: the Sierra Nevada Mountains; DV: Death Valley; MD: the Mojave Desert; GV: California's Great Valley; GF: the Garlock Fault.

past few million years. The modern low velocities may represent some combination of melt, alteration, magmatic fluids and high temperatures.

In summary, beneath the Coso Geothermal Area, shear velocities are generally depressed. A prominent low-velocity anomaly is resolved clearly within the top 2 km, probably resulting from geothermal alteration at shallow depths. The low-velocity anomaly between 6 and 12 km indicates the location of a magmatic body. No magmatic body is imaged below 14 km depth. Low velocities in the broad regions surrounding Coso at depths near 7 km underlie areas with Miocene to recent volcanism. This project has proven the usefulness of ambient-noise tomography for geothermal exploration; the method can be also applied anywhere in Australia in the future to investigate the underground structures relevant to geothermal energy exploration.

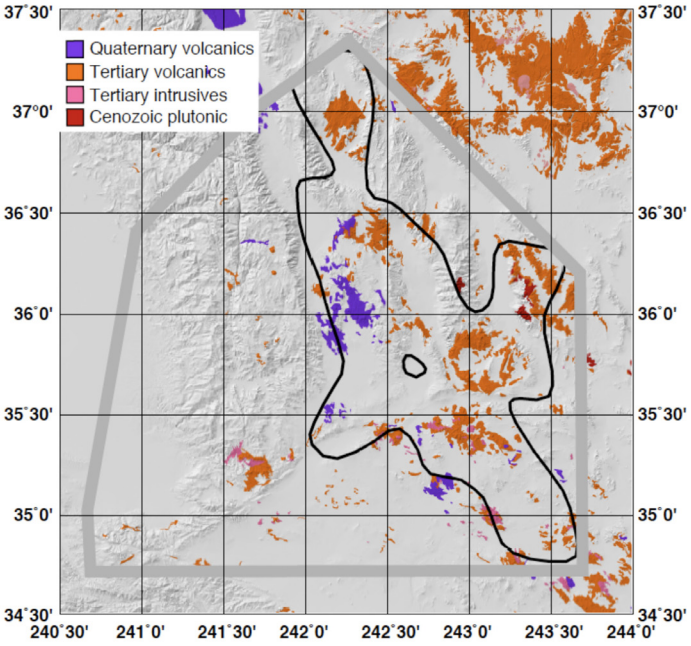

Figure 4. Exposures of Cenozoic igneous rocks in eastern California compared with outline (black) of low Vs (<~3% at 6 km depth, Fig. 2c). The extent of the inverted region is shown by the grey outline.

Contact: Yingjie Yang
Funded by: Macquarie CoRE funding

Continents can't subduct!...or can they?

We commonly assume that continental crust cannot be subducted to significant depths, due to its high relative buoyancy. However, clear field and petrological evidence shows that relatively large sections of continental crust have been subducted to depths >100 km and then exhumed, at numerous locations worldwide. The discovery of metamorphic diamonds (Kokchetav massif, Russia; Western Norway…) and especially of pyroxene exsolution in garnets (e.g. Western Norway, Sulu metamorphic belt (China)) further demonstrated the possibility of ultra-deep subduction of continental crust to depths >250 km. The possibility of continental material being subducted to depths of the transition zone, and perhaps even into the lower mantle, is supported by geochemical and isotopic signatures in magmas erupted in island arcs, presumably from source regions at depths >300 km, and by experimental data at extremely high pressures. These studies indicate there may be a "depth of no return" for continentally-derived materials at around 8.5–9 GPa (270 km), where dense silicates start to form. However, the actual amount of continental material that can be subducted below the point of no return, and its final fate, have never been assessed with coupled thermomechanical-thermodynamic numerical models. This is the objective of an ongoing GEMOC research project (for more details see *GEMOC Publication #659*).

To allow direct comparisons with geological, geochemical and geophysical evidence, numerical simulations need to include realistic thermophysical properties for all the materials involved in the model. Therefore we couple our thermo-mechanical solvers with thermodynamic datasets that account for all expected metamorphic reactions and phase changes. Earlier models made use of thermodynamic databases strictly suitable only at pressures <3 GPa, while we use an in-house database valid up to ~25 GPa that includes

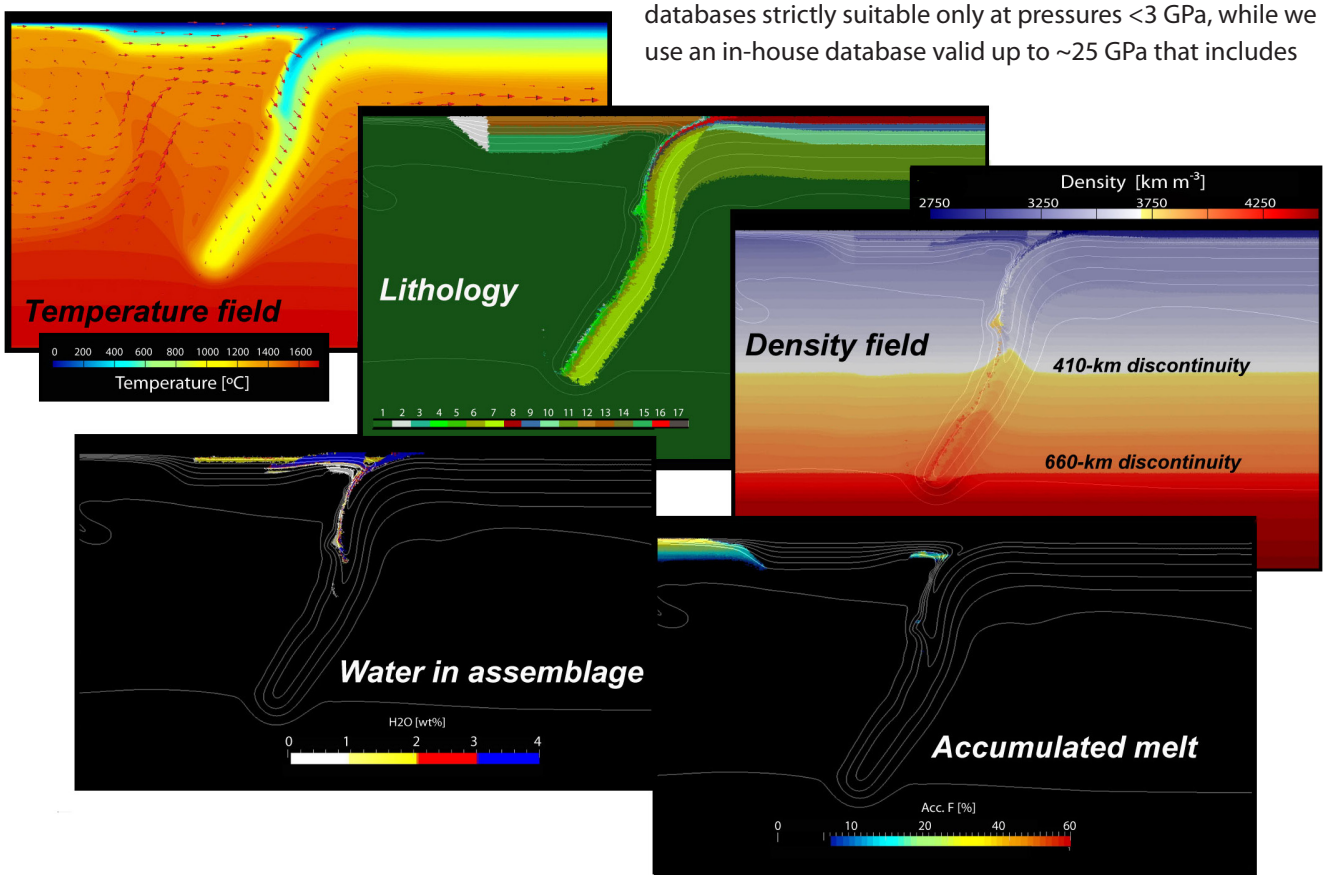

Figure 1. Snapshot from one of our simulations showing the thermal, density and compositional fields. The amount of bound water in the assemblages and accumulated melting in the mantle are also shown. The simulations were carried out with a modified version of the Underworld platform (http://www.underworldproject.org).

all major phases obtained in UHP experiments on compositions relevant to the continental crust. Importantly, we have not imposed velocity boundary conditions to either force or stop continental subduction, so the velocities obtained in our simulations emerge self-consistently from the balance between internal forces in our numerical domain.

We have run a total of 80 simulations (Fig. 1) to test different aspects of the problem (effects of compositional variations in the mantle, passive-margin geometries, types of continental sediments, etc.). The main results can be summarised as follows:

(1) The buoyancy increase due to subduction of continental material may not be the only explanation for the typical decrease in convergence velocity observed in collisional settings after the continental crust arrives at the trench. Delamination of the lithospheric mantle at lower crust levels after a period of continental subduction can result in a similar pattern of convergence velocities. This scenario is favoured in settings dominated by slab rollback.

(2) The thermal structures of the continental plate and passive margin play important roles in the evolution and final configuration of the collision. The colder temperatures in a thick continental plate give it an extra strength, which overcomes the effects of its negative buoyancy. Thus, the overall effect of increasing the thermal thickness of the continental plate is to reduce convergence velocities, stalling subduction and impeding deep recycling of continental material.

(3) When both the arc and the continental plate are free to move (e.g. bounded by mid-ocean ridges), the system evolves as forward subduction rather than as slab rollback. Although the circulation patterns in the sublithospheric mantle and in the mantle wedge are significantly different in these two cases, the general pattern and absolute values of the resulting convergence velocities are similar. Replenishment of fertile mantle in the mantle wedge and enhanced partial melting are favoured in forward-subduction scenarios.

(4) The composition of the continental lithospheric mantle exerts a moderate influence on the overall evolution of the collision system. Since the highly depleted part of the continental mantle seems to be restricted to shallow depths (<60–80 km), the thermal effect is usually more important and the overall buoyancy of the lithospheric mantle at the beginning of the collision is negative.

(5) The rheology of the continental crust is a major factor controlling both the duration of continental subduction and the volume of continental material that can be subducted. Strong crusts favour deep subduction of continental materials while soft crusts tend to accumulate at shallow depths. In the latter case, the decoupling between the upper crust and the rest of the lithosphere effectively restricts the increase in the positive buoyancy of the slab, which remains negatively buoyant at all conditions.

(6) Subducted continental crust remains buoyant with respect to the surrounding mantle down to depths of ~250–300 km. Potential detachments from the slab will therefore result in upwelling of these continental portions. However, the characteristic cold temperatures in the uppermost part of the slab result in a strong mechanical coupling between the crustal and mantle components, making detachment more difficult.

(7) Subducted continental crust that reaches depths >250–300 km becomes significantly denser than the surrounding mantle, due to the appearance of high-density phases. This provides extra negative buoyancy to the slab and inhibits the return of subducted crust to the surface (the point of no return).

“The rheology of the continental crust is a major factor controlling both the duration of continental subduction and the volume of continental material that can be subducted.”

Contact: Juan Carlos Afonso
Funded by: Macquarie CoRE Funding

The Lithosphere-Asthenosphere boundary: Can we sample it?

THE LITHOSPHERE-ASTHENOSPHERE BOUNDARY (LAB) represents the base of the Earth's lithosphere, the rigid and relatively cool outer shell characterised by a conductive thermal regime, and isolated from the convecting asthenosphere. Chemically, the LAB should divide a

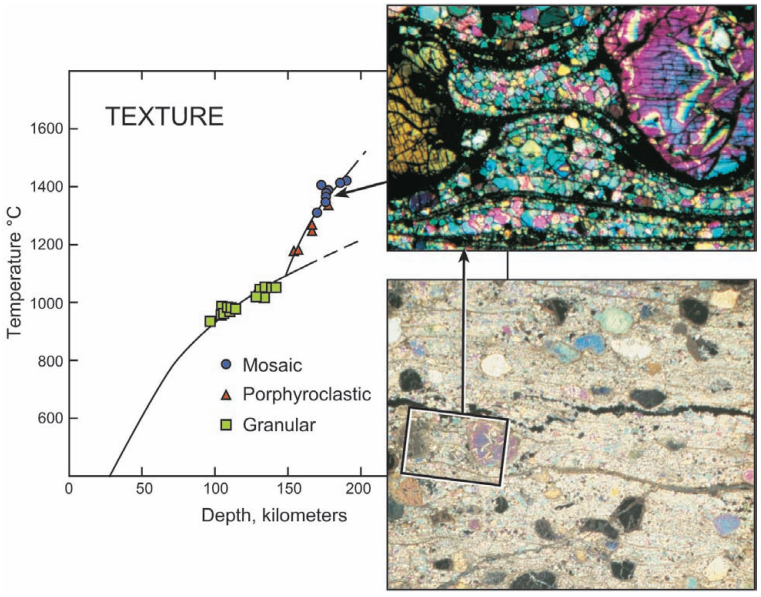

Figure 1. The original Lesotho xenolith geotherm of Boyd and Nixon (1975) showing the conductive low-T limb defined by granular-structured garnet lherzolites and the "kinked" limb defined by high-T sheared peridotites such as PHN1611 (photomicrographs). Base of upper photomicrograph is 0.5 mm.

lithospheric mantle that is variably depleted in basaltic components from a more fertile asthenosphere. In xenolith suites from cratonic areas, the bottom of the depleted lithosphere is marked by a rapid downward increase in elements such as Fe, Ca, Al, Ti, Zr and Y, and a rapid decrease in the median Mg# of olivine (Figs. 1,2), reflecting the infiltration of mafic melts and related fluids (*GEMOC Publication #650*). Eclogites and related mafic and carbonatitic crystallisation products are concentrated at the same depths as the maximum degrees of metasomatism (Fig. 3), and may represent the melts responsible for the refertilisation of the basal lithosphere. This refertilised zone, which lies at depths of ca 170-220 km beneath Archean and Proterozoic cratons, is unlikely to represent a true LAB (*GEMOC Publication #576*; http:// www.mantleplumes.org/LithosphereRemnants.html).

Re-Os isotopic studies of the deepest fertile peridotite xenoliths show that they retain evidence of ancient depletion events; seismic tomography data show high-velocity material extending to much greater depths beneath cratons. The cratonic "LAB" probably represents a level where asthenospheric melts have ponded and refertilised the lithosphere, rather than marking a transition to the convecting asthenosphere. Our only deeper samples are rare diamond inclusions and some xenoliths inverted from majoritic garnet, which are

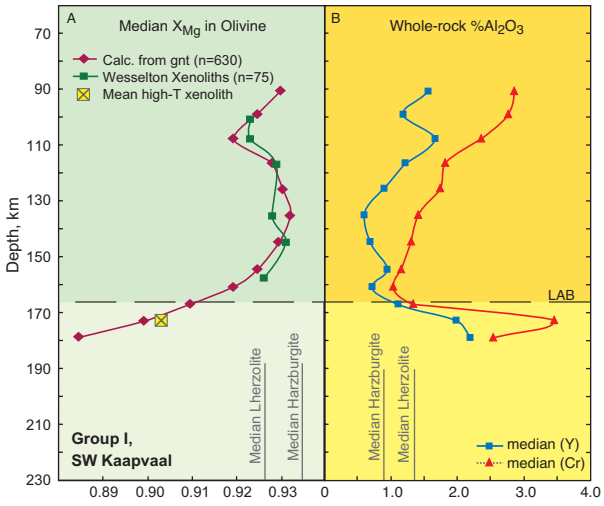

Figure 2. Geochemical parameters that can be derived from the compositions of xenocrystic peridotitic garnets. (A) X_{Mg} of coexisting olivine vs depth (GEMOC Publication #222) (B) Median whole-rock Al_2O_3 contents vs depth in the same kimberlites (GEMOC Publication #132).

unlikely to represent the bulk composition of the asthenosphere.

In younger continental regions the lithosphere-asthenosphere boundary is shallower (commonly at about 80–100 km) and more clearly marked. In regions of extension and lithosphere thinning (e.g. eastern China, eastern Australia, Mongolia), upwelling asthenosphere may cool to form the lowermost lithosphere, and may be represented by xenoliths of fertile garnet peridotites in alkali basalts worldwide. It has also been shown experimentally that the LAB beneath cratons is coincident with the depth where the mantle solidus is exceeded for some compositions, and this is the level where segregation of carbonate-rich fluids can occur (e.g. *Wyllie, JGR 85, 1988; Gudfinnsson and Presnall, JGR 101, 1996*). The presence of carbonate-rich fluids, in addition to mafic melts, at this level provides a possible explanation for the magnetotelluric signals that suggest the LAB may be detected by lower resistivity (*Jones et al., Lithos 120, 2010*). Gaillard et al. (*Science 322, 2008*) demonstrated that carbonate melts are much more highly conductive than silicate melts, and that small amounts of carbonate melt will wet grain boundaries, providing a physical-chemical basis for the magnetotelluric signals at these depths.

The increased conductivity commonly observed at about 90 km in young tectonic lithospheric regions and from about 180 to 220 km in cratonic regions also may coincide with the level at which fluids may segregate because there is a sharp drop in the water-storage capacity of mantle wall rocks, coupled with the onset of small degrees of partial melting in the presence of water (e.g. *Green et al., Nature 467, 2010*).

The LAB is a movable boundary. It may become shallower due to thermal and chemical erosion of the lithosphere, assisted by extension (Fig. 4). Refertilised lithospheric sections, especially where peridotites are intermixed with eclogite, may be subject to gravitational delamination. The lithosphere-asthenosphere boundary may also be deepened by subcretion of upwelling hot mantle (e.g. plumes). This process may be recorded in the strongly layered lithospheric mantle sections seen in the Slave Craton (Canada), northern Michigan (USA) and the Gawler Craton (Australia).

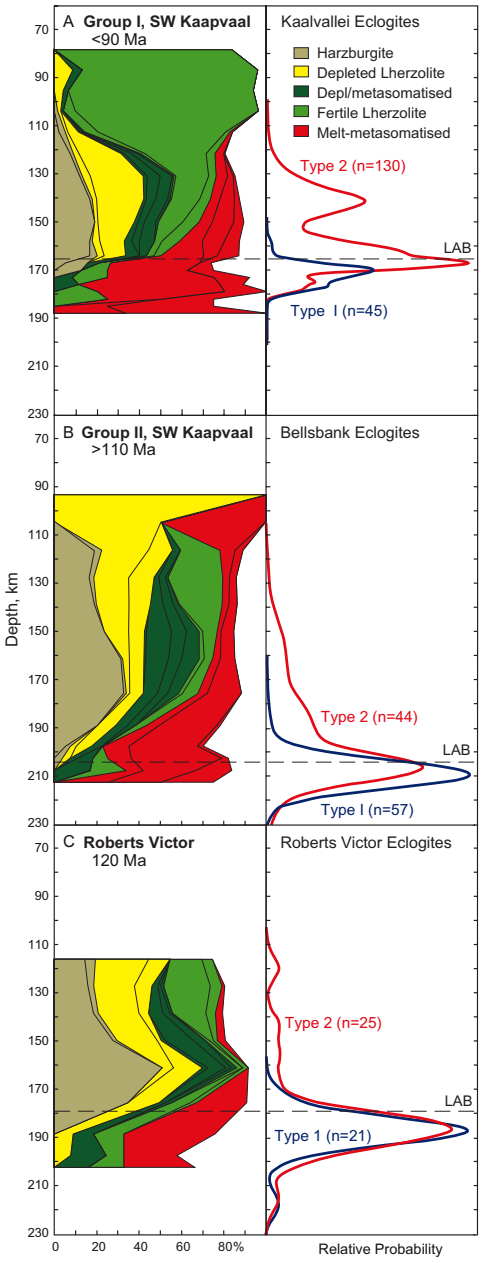

Figure 3. Distribution of eclogites in representative mantle sections. (Data from GEMOC Publication #461)

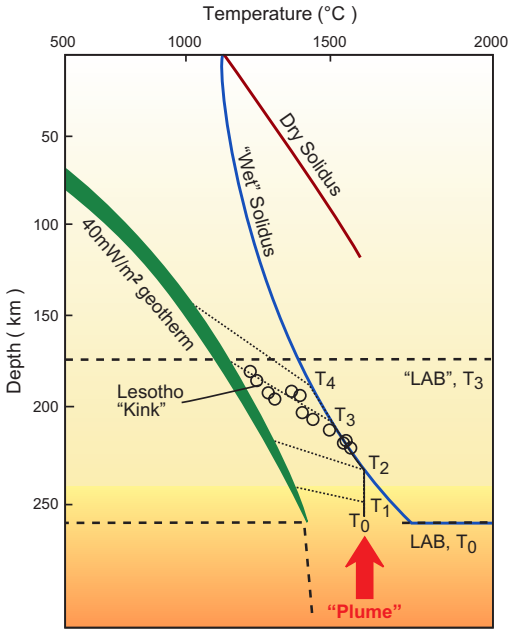

Figure 4. Development of a kinked geotherm by impingement of a thermal pulse on the base of the lithosphere; the accompanying refertilisation front moves up through the lithosphere to establish a new "LAB" and a (temporarily) kinked geotherm.

Contacts: Sue O'Reilly and Bill Griffin
Funded by: ARC Discovery Project and Linkage Grants, BHP-Billiton, MQ PhD Scholarships

Out of Africa: Garnets reveal insights into Earth's oldest mantle

Most of our knowledge about the composition, structure, thermal state and processes in the subcontinental lithospheric mantle (SCLM) has been obtained by analysing mantle-derived xenoliths and xenocrysts, brought to the Earth's surface in volcanic rocks such as kimberlites. Xenolith studies are often costly and time consuming, and it is often difficult to obtain enough samples for a statistically representative xenolith suite. A more accessible source of information is the xenocrysts derived from the disaggregation of mantle xenoliths. As xenocrysts are far more abundant than xenoliths, they are useful in characterising the SCLM sampled by kimberlites that lack mantle xenoliths.

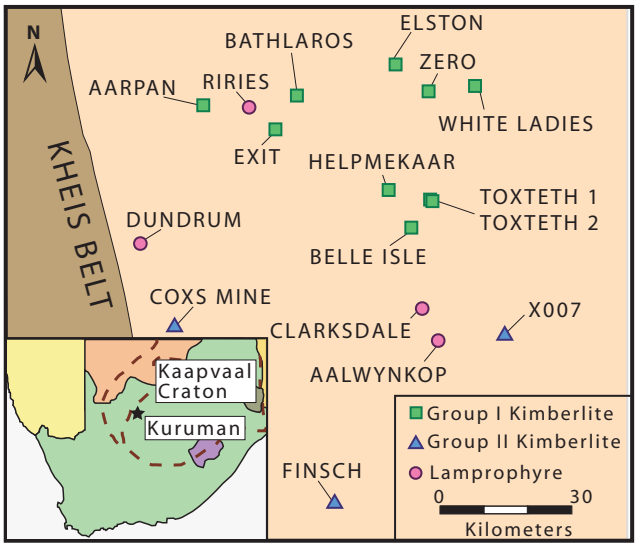

Figure 1. Location and classification of intrusions in the Kuruman Province of South Africa.

Pyrope garnet xenocrysts are particularly useful, because the Ni and Cr contents in some garnets can be used to estimate equilibrium temperature (T_{Ni}) and pressure (P_{Cr}) conditions and these P-T data can be used to construct a geotherm. With this framework, the Ni contents of other garnets can give a T, and projection of the T to the geotherm gives a depth estimate for the individual grains. The Y content of garnets can be used to estimate the depth of the lithosphere-asthenosphere boundary (LAB), as low-Y garnets (< 10 ppm) are restricted to the lithosphere. Furthermore, the trace-element (i.e. Zr, Y, Ga and Ti) contents in garnets can be used to identify different types of metasomatism that affected the SCLM where the garnets were derived. Garnets can be subdivided, based on inter-element correlations, into five groups: depleted harzburgites, depleted lherzolites, depleted/metasomatised lherzolites, fertile lherzolites and melt-metasomatised peridotites (*GEMOC Publication #299*). The proportion of garnets from these five categories can then be mapped as a function of depth, to construct "chemical tomography" sections that show geochemical variation with depth in the lithospheric section.

The Kuruman Kimberlite Province (Fig. 1) lies on the western margin of the Kaapvaal Craton and contains some of the oldest known kimberlites (~1.6 to 1.8 Ga; *Shee et al., 1989, Proc. 4th Int. Kimb. Conf. p 60-82; GEMOC Publication #662*). While most kimberlites intrude through SCLM that has undergone many episodes of metasomatism (*GEMOC Publication #449*; *Foley, 2008, Nature Geoscience, 1, 503-510*), the Kuruman Province may provide a unique opportunity to examine a relatively undisturbed section of the SCLM. This study utilised the major- and trace-element compositions of mantle-derived garnets from Kuruman intrusions, which represent two distinct geochronological and petrogenetic groups, namely Proterozoic kimberlites and Cretaceous orangeite. The data provided several key observations:

(1) The Proterozoic kimberlites sampled SCLM with low conductive geotherms (~40 mW/m^2; Fig. 2a,b), but these were thermally disturbed at shallow depths, consistent with the lack of diamonds in these kimberlites.

(2) The Proterozoic kimberlites sampled a lithospheric thickness of ~170 km, while the X007 Cretaceous orangeite sampled a thinner (~145 km) SCLM that had a lower conductive geotherm (~37.5 mW/m^2; Fig. 2c).

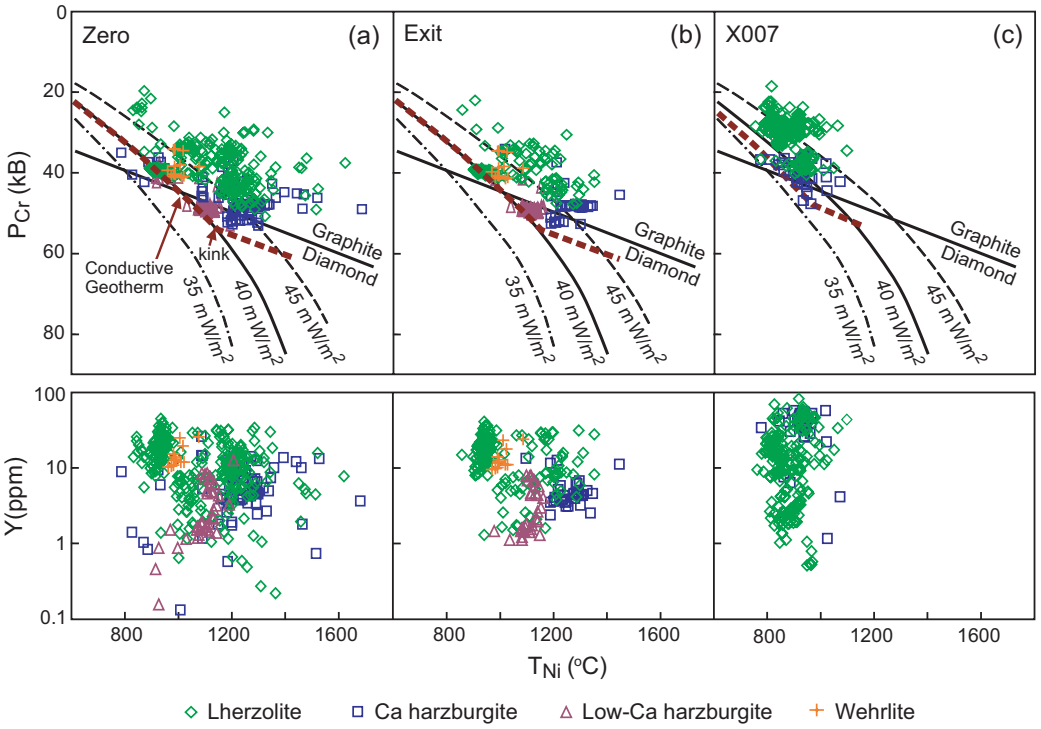

Figure 2. Conductive geotherms from the (a) Proterozoic Zero kimberlite, (b) Proterozoic Exit kimberlite, and (c) Cretaceous X007 orangeite. Note the higher 40mW/m² geotherm for the kimberlites relative to the younger orangeite intrusion.

(3) Chemical tomography (Fig. 3) reveals that the SCLM sampled by the Proterozoic kimberlites (i) was highly depleted; (ii) had experienced extensive phlogopite-related metasomatism; and (iii) had not experienced significant melt-related metasomatism, even at great depths.

(4) The SCLM sampled by the Cretaceous X007 orangeite contained much less harzburgite and had experienced more extensive metasomatic modification, producing more abundant lherzolites.

These observations are consistent with the concept of the secular chemical evolution of the SCLM, whereby older depleted lithosphere is progressively refertilised by asthenospheric-derived melts over time (*GEMOC Publication #303*). As such, the Proterozoic Kuruman kimberlites provide an excellent example of relatively unmodified ancient SCLM and represent an important, rarely observed, point of reference for the chemical evolution of the SCLM.

Contacts: Cara Donnelly, Bill Griffin
Funded by: ARC Discovery Project Grant and Linkage, iMURS, PGRF

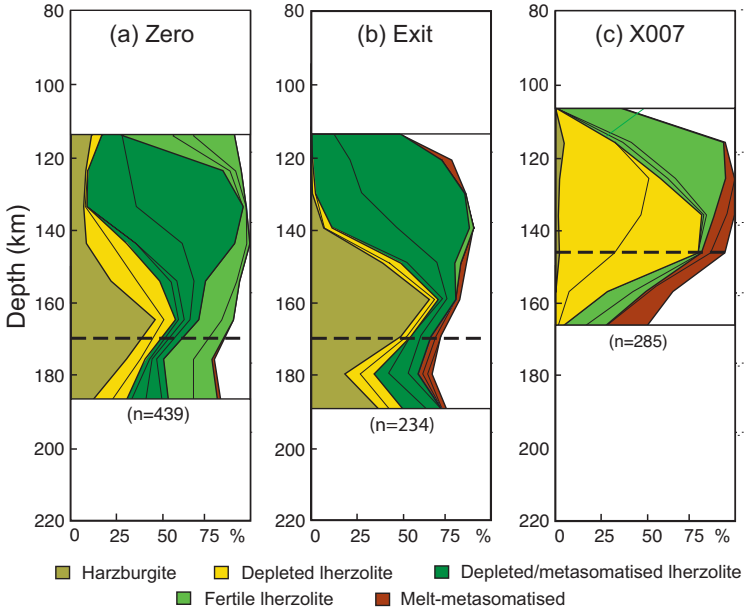

Figure 3. SCLM chemical tomography for the (a) Proterozoic Zero kimberlite, (b) Proterozoic Exit kimberlite, and (c) Cretaceous X007 orangeite. Note the more fertile compositions and shallower LAB (derived from Y contents in garnet) of the younger X007 orangeite, relative to the kimberlites.

What's new? - *TerraneChron*® pinpoints when and where continental crust really grew

THE CONTINENTAL CRUST IS AN "END PRODUCT" OF THE CHEMICAL DIFFERENTIATION of the Earth's primitive mantle through time; the question of crustal growth rate thus bears directly on the nature and timing of this differentiation process. It is not enough to just measure the relative volumes of crust with known ages, because some of the crust may be juvenile (i.e. derived from the convecting mantle), while other parts may be derived by recycling older crust. To understand the growth of the crust through time, we need to determine the sources of the magmatic rocks that went into making the crust: do these represent juvenile additions, or recycling, or perhaps the mixing of juvenile and recycled material? The U-Pb and Lu-Hf isotope systems in zircon give us a powerful tool for answering questions like this. *In situ* microanalysis of the U-Pb system can give us the age of a single zircon grain, while the isotopic composition of its Hf tells us whether its parent magma was generated in the mantle, or by remelting of older crust.

GEMOC's *TerraneChron*® program (integrated U-Pb, Hf-isotope and trace-element analysis of zircon) has built up a worldwide database of about 14,000 analyses of zircon, derived largely from detrital sources. This has been used to examine processes of crustal evolution on a global scale, and to test existing models for the growth of continental crust through time (Fig. 1; *GEMOC Publication #671*). In this study we introduced a new approach to quantitatively estimating the proportion of juvenile material added to the crust at any given time during its evolution. However, no zircon database, even our very large one, can be completely representative of the upper crust, because the samples have not been taken randomly. To overcome this sampling bias, we have normalised our data to the relative areas of Archean, Proterozoic and Phanerozoic crust that have been mapped in GEMOC's GLAM project

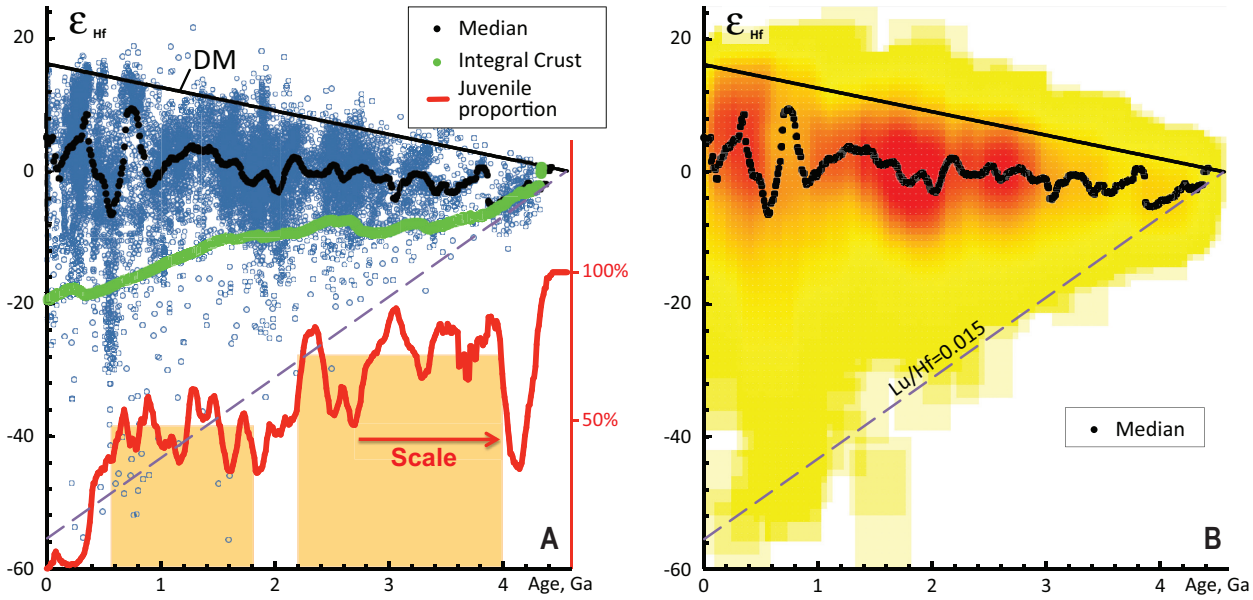

Figure 1. ε_{Hf} versus zircon U-Pb age for all zircons in the database (N=13,844): (A) the green line is the calculated integral ε_{Hf} of the crust and the red line is the calculated juvenile proportion (right-hand scale); (B) data are illustrated by a two-dimensional histogram with each element/cell representing 50Ma × 1 ε_{Hf} unit and the window of smoothing is 250 Ma × 5 ε_{Hf}, where the full dataset is taken as 100%. More intense colours (into red) indicate higher density of the data. Dashed line shows the evolution of "average crust" from 4.56 Ga.

(see *GEMOC Publication #547*). This estimate has then been used to model the crustal growth rate over the 4.56 Ga of Earth's history. The model suggests that there was little episodicity in the production of new crust, even though plots of the magmatic ages of rocks show marked peaks at some time intervals (Fig. 2).

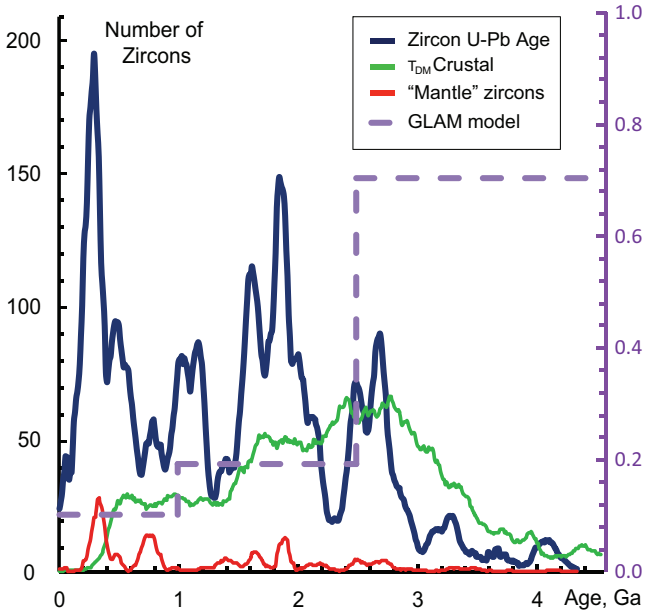

Figure 2. Relative probability curves (left scale) of U–Pb zircon ages (blue line), T_{DM} C model ages (green line) and number of zircons with juvenile Hf-isotope compositions (red line; defined as grains with εHf=0.75×εHf DM). Proportions of the continental lithosphere formed during three major time intervals derived from GLAM mapping are shown by the dashed line (right axis).

The distribution of age-Hf isotope data from zircons worldwide implies that at least 60% of the existing continental crust separated from the mantle before 2.5 Ga (Fig. 3). However, taking into consideration new evidence coming from geophysical data, the formation of most continental crust early in Earth's history (at least 70% before 2.5 Ga) is even more probable. Thus, crustal reworking has dominated over net juvenile additions to the continental crust, at least since the end of the Archean. This explains the increasing number of zircons with non-radiogenic Hf-isotope compositions (with ε_{Hf} lower than -20) found throughout post-Archean time. Moreover, the proportion of juvenile material in newly formed crust decreases stepwise through time: it is about 70% in the 4.0 – 2.2 Ga time interval, about 50% from 1.8 – 0.6 Ga, and possibly less than 50% since 0.6 Ga (Fig. 1A). These changes maybe related to the formation and breakup of supercontinents. This study thus represents a major advance in our understanding of the genesis of the continental crust through time.

Contacts: Elena Belousova, Bill Griffin

Funded by: ARC Linkage Project Grant and industry projects

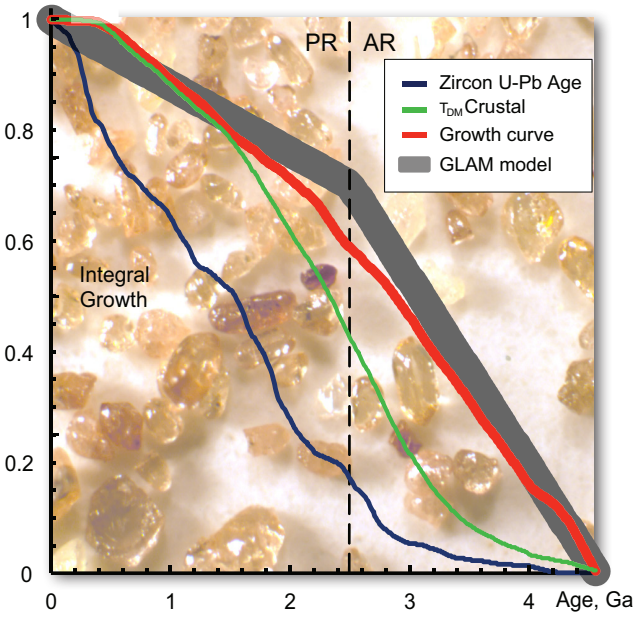

Figure 3. The integrated crustal growth curve (red line) derived in this study, compared with the GLAM (Global Lithospheric Architecture Mapping) model shown as a grey band. Integrated curves for the zircon U-Pb age data and crustal model age are shown for comparison.

The Earth's first continental crust

THE EARTH'S OLDEST CONTINENTAL CRUST IS COMPOSED PRIMARILY OF FELSIC ROCKS of the tonalite-trondhjemite-granodiorite series (commonly known as TTGs). These granitoids typically occur as plutons that are encompassed by belts of metamorphosed mafic volcanics (known as greenstones). In spite of their close association, the exact relationship between the TTG granitoids and surrounding greenstones is problematic. This is partially because original stratigraphic contacts are rarely preserved in such old rocks. Another problem is that, although it is generally believed that TTG magmas were produced by the partial melting of an older basaltic crust, the tectonic environment in which this occurred is unknown and appears not to have any modern analogues. We have approached these difficulties by obtaining specifically relevant experimental and geochemical data for greenstones from one of the oldest known greenstone belts (the Nuvvuagittuq belt of northern Quebec, dated at 4.28 billion years). Our objective is to test for a direct genetic link between the greenstones and a closely associated but younger (3.66 billion years) tonalite (PC-103) of the TTG series.

A significant characteristic of the Nuvvuagittuq greenstones is their resemblance to much younger volcanic rocks called boninites, which are now exclusively associated with subduction zones (and hence with plate tectonics). Two samples of Nuvvuagittuq greenstone were used as starting materials for the experiments. These included PC-227 and PC-162 which are among the most mafic and least altered of the Nuvvuagittuq greenstones. For comparison, experiments were also conducted on a modern boninite from northern Tonga. The experiments were undertaken at GEMOC using powdered samples of natural rock. They were conducted in end-loaded piston-cylinder apparatus using conventional techniques. Analyses of the run products and starting materials were done by electron microprobe and ICP-MS at the GEMOC Geochemical Analysis Unit.

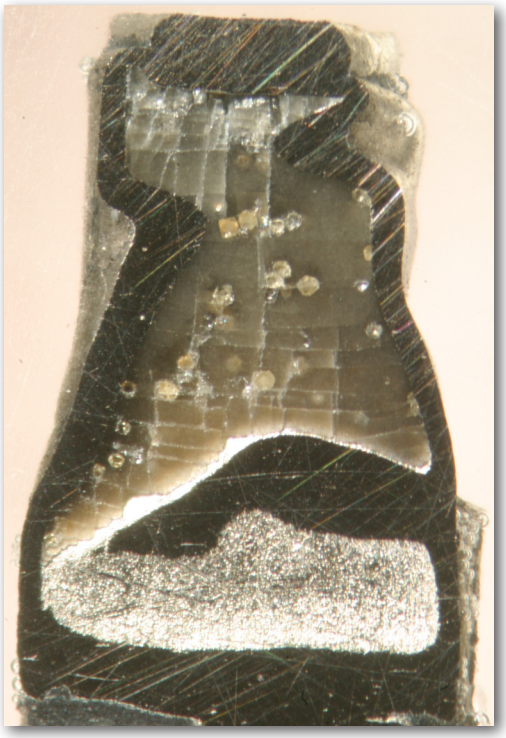

Figure 1. A longitudinal section through an experimental capsule showing the outer metal capsule (made of silver-palladium alloy) and rounded crystals of yellow garnet in a tonalitic glass.

At temperatures of 950 °C to 1050 °C and pressures of 1.5 GPa to 2.0 GPa, the greenstones and boninite undergo between 30 % and 45 % partial melting and produce residual garnet ± clinopyroxene ± orthopyroxene (Fig. 1). The partial melts have tonalitic compositions and are similar in many respects to the natural tonalite PC-103. They have similar concentrations of most major elements and also produce similarly shaped patterns on mantle-normalised plots of incompatible element concentrations (Figs. 2 and 3). The latter may reflect a familial connection between the original greenstones and associated tonalite. This is because the comparatively high degrees of partial-melting needed to form the tonalitic melts have relatively little effect on the relative concentrations of most incompatible elements. It is only the influence of residual garnet that is needed to produce the distinctively inclined heavy Rare Earth patterns that characterise both the experimental and natural tonalite compositions.

Although the overall concentrations of incompatible elements in the experimentally-produced melts are lower than those of the natural tonalite, this is due to our use of the most mafic and incompatible-element-poor greenstones as starting materials. On average, the Nuvvuagittuq greenstones are considerably more enriched in incompatible species than our starting materials, although the relative concentrations of most elements are similar. If this factor is taken into account (compare Figs. 2 and 3), it seems likely that the TTG PC-103 inherited many of its primary geochemical characteristics from an earlier fractionation event that also produced the basaltic Nuvvuagittuq lavas (now represented by the greenstones).

Although modern magmas compositionally similar to the Nuvvuagittuq greenstones are associated only with subduction zones, our experiments do not provide additional support for the existence of plate tectonics on Earth during the Hadean. Instead, they are consistent with continental crust formation that involved some kind of crustal re-cycling process during the Hadean. Regardless of whether this process was plate tectonics (or something else) it must have replicated many of the magmatic consequences of modern plate tectonics, including arc-like basaltic magmas. It must also have occurred on a sufficiently large scale that it was able to exert a major compositional influence on the first continental crust.

Contacts: John Adam, Tracy Rushmer
Funded by: ARC Discovery Project Grant

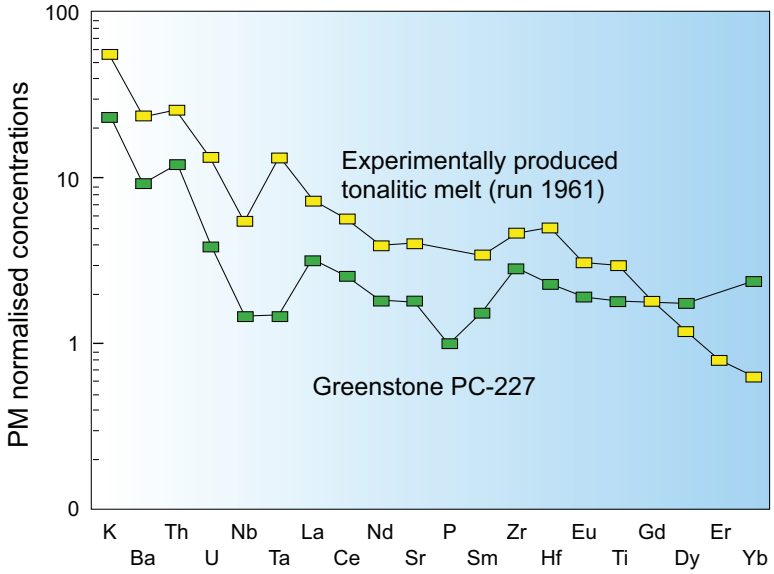

Figure 2. Mantle-normalised concentrations of incompatible elements in the greenstone PC-227 and an experimentally produced tonalitic melt that resulted from partial melting of PC-227.

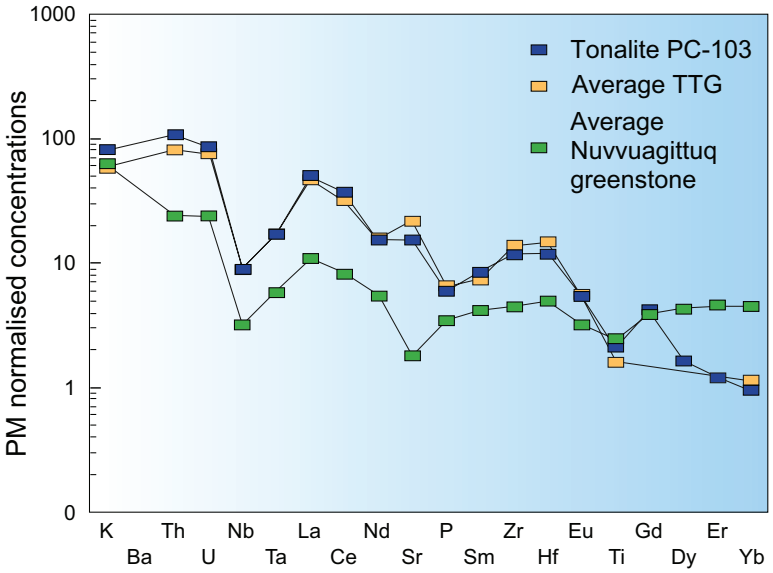

Figure 3. Mantle-normalised incompatible element concentrations in the tonalite PC-103, an estimated average TTG, and in an average Nuvvuagittuq greenstone.

On the edge: Continent roots and giant Nickel deposits

THE LOCATION OF MAGMATIC NI-CU-PGE SULFIDE DEPOSITS is closely related to lithospheric architecture, particularly the deep roots of sub-continental lithospheric mantle (SCLM). Giant deposits are found close to the margins of cratons, the large (100s to 1000s of km across) stable blocks

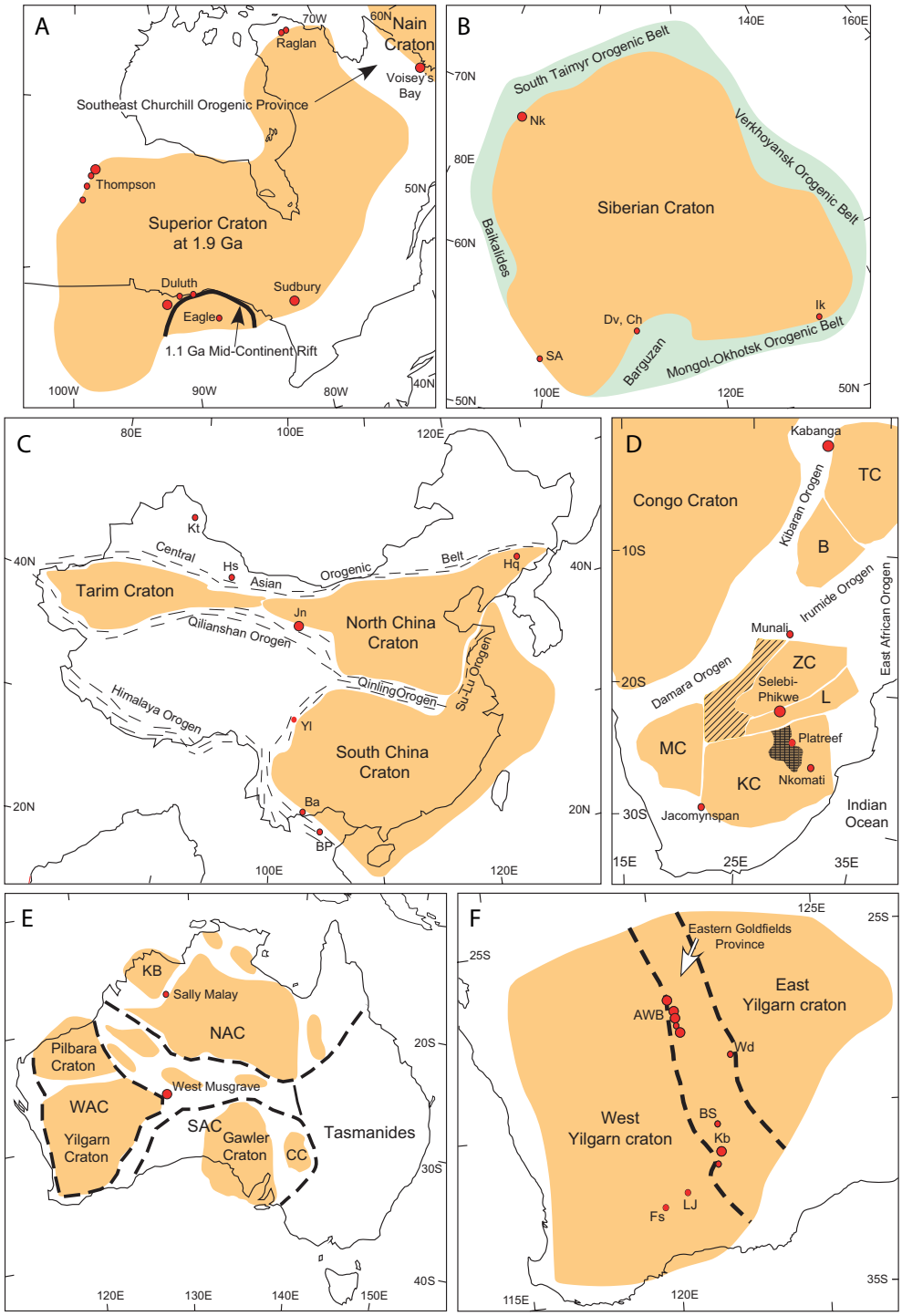

Figure 1. Examples of cratonic/lithospheric architecture (orange polygons and dashed polygons) and the location of nickel sulfide deposits (red dots; size reflects relative deposit size for each region). See GEMOC Publication #664. A) Proterozoic deposits of North America at ca 1.9 Ga. B) Siberian craton. Lighter grey is area of Middle to Late Proterozoic and/or Phanerozoic orogenic reworking and possible terrane accretion. C) Cratons of China; flanking Phanerozoic orogens are patterned. D) Cratonic architecture of southern Africa. E) Proterozoic deposits of Australia. F) Neoarchean deposits of the Yilgarn craton, Australia .

produced by the amalgamation of smaller chunks of thick lithosphere (mantle root plus overlying crust) during Precambrian tectonic collisions (Fig. 1). These deposits are associated with mafic-ultramafic rocks, especially the massive outpourings of magma known as Large Igneous Provinces. The metal quantities and grades observed in such deposits require segregation of a magmatic sulfide melt from a very large volume of parental ultramafic melt. This requires a high degree of melting at depths of 100 km or less; this and the large melt volumes involved are consistent with a mantle-plume origin. Some small- to medium-sized deposits may be associated with melting of upwelling asthenosphere following delamination of the lithospheric mantle. Segregation of the sulfide liquid from the melt may be triggered by interaction with crustal rocks. This liquid eventually forms disseminated or massive sulfide accumulations in the host mafic or ultramafic rocks.

All deposits formed during periods of active regional tectonism, most commonly under mildly compressional to transpressional conditions. The timing and tectonic setting of the deposits are consistent with a plume impact (craton margin) model involving 5 stages (Fig. 2):

1. Mantle plume impact and upward flow towards areas of thinner lithosphere
2. Plume decompression melting at shallower levels
3. Melt transfer into the (upper) crustal environment via active trans-lithospheric faults and an interconnected intrusion (sills) network
4. Variable interaction of melts with crust
5. Nickel sulfide precipitation and accumulation

Most large deposits formed in intracontinental settings, or with (former) passive margins at the edge of small marginal basins. The rarity of large deposits associated with the margins of large oceans or with subduction-zone environments reflects either poor preservation or (with the latter) limitations on plume interaction with continental lithosphere. The model provides a coherent predictive framework for mineral exploration.

Contacts: Graham Begg, Jon Hronsky, Bill Griffin and Sue O'Reilly
Funded by: BHP Billiton (and previously by WMC Resources), and Discovery, SPIRT, and Linkage grants from the Australian Research Council

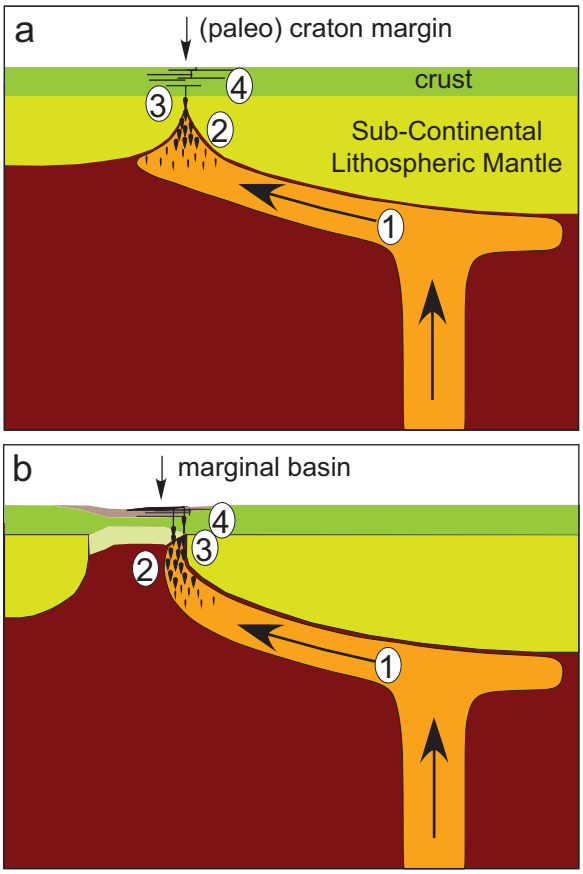

Figure 2. Generalised model showing formation of nickel sulfide deposits at tectonically active margins of thick (>150 km) lithospheric blocks (mostly cratons; after GEMOC Publication #664). In scenario a) the blocks are contiguous, whilst b) depicts a small, intervening marginal basin. The former encourages evolution of the melt via ponding and wallrock interaction at all crustal levels, with resultant deposits found mostly within mafic host rocks. The latter (b) favors shallower melting of the plume, direct melt access to the upper crust, and therefore typically ultramafic host rocks.

Noble method updates the Ni exploration toolkit

KOMATIITES CONTAIN SOME OF THE WORLD'S LARGEST NICKEL-SULFIDE DEPOSITS and the development of reliable lithogeochemical indicators to guide exploration has been a long-standing goal. A common lithogeochemical approach is to identify whole-rock signatures that record sulfide segregation, and use these to predict if a system has reached sulfide saturation and therefore is worth exploring for nickel sulfide deposits. For this purpose the platinum-group elements (PGE: Os, Ir, Ru, Rh, Pt, Pd) are of great interest. The PGE are chalcophile and partition very strongly into segregating sulfides, which produces a PGE depletion in the remaining silicate melt. However, PGE abundances in ultramafic melts and/or rocks reflect a complex range of factors including magmatic processes and emplacement dynamics, alteration, metamorphism, and weathering. As a consequence, whole-rock signatures depleted in PGE may not reflect the segregation of sulfides. Moreover, the changes in whole-rock PGE geochemistry are mostly too subtle and too ambiguous to be used in exploration, because their low concentrations (a few parts per billion) are a challenge to the analyst.

Rather than working with whole-rock signatures, GEMOC is using its state-of-the-art micro-analytical facilities to probe minerals that record the geochemical evolution of ultramafic systems. *In situ* mineral analysis by laser ablation ICP-MS enables measurement of PGE concentrations down to the low ppb level in spots a few microns across. The research focuses on the role of chromite in the fractionation and concentration of ruthenium (Ru) because chromite can host Ru in solid solution (see *Research Highlights 2009*). The Ru content of chromite should therefore reflect if the chromite crystallised in a sulfide-undersaturated (barren) or sulfide-saturated (potentially mineralised) system.

To test this idea, we have analysed chromite in a wide range of komatiites from the Eastern Goldfield's Superterrane (EGST) in the Yilgarn Craton of Western Australia. The EGST contains some of the world's largest komatiite-hosted nickel deposits. Numerous previous studies and an intense mineral exploration history make this an excellent natural laboratory for the investigation of komatiite geochemistry. Laser ablation ICP-MS data show that chromites from barren komatiites (Agnew, Kurrajong, Murphy Well and Sullivans) have Ru concentrations between 120 and 420 ppb (Fig. 1). In contrast, the Ru contents of chromites from the world-class nickel deposits at Mount Keith (Fig. 2), Kambalda, Black Swan, and Betheno are below the detection limit of the laser ablation ICP-MS (down to

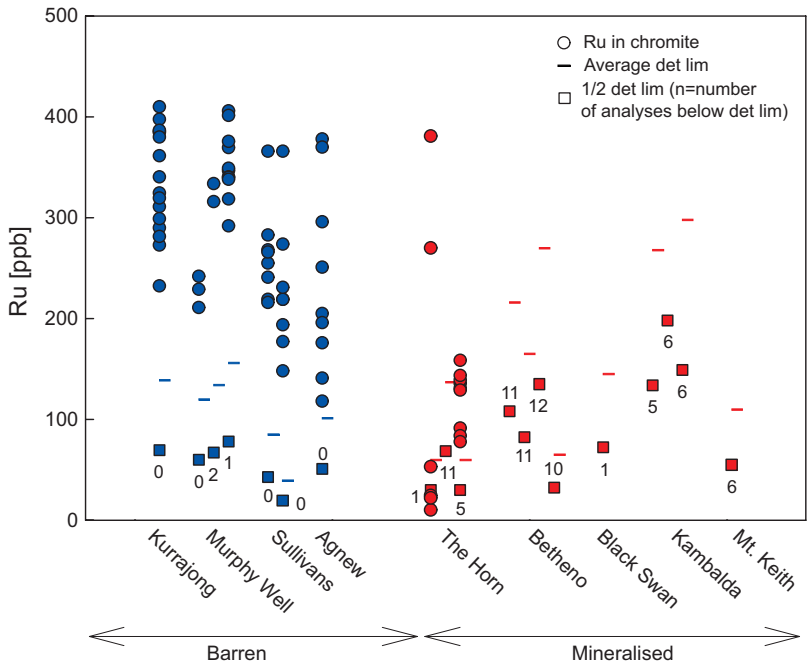

Figure 1. Ruthenium variation in chromite as observed in barren (blue symbols) and mineralised (red symbols) komatiites from Western Australia.

5 ppb, depending on grain size and measurement conditions). The one exception found so far is a nickel deposit at The Horn, where the chromites have Ru concentrations mostly between 10 and 150 ppb; this is still distinctly lower than the mean concentrations observed in chromites from the barren komatiites.

The results suggest that the partitioning of ruthenium into chromite is dominantly controlled by the sulfide content of the system. In sulfide-saturated systems, the chalcophile Ru will dominantly partition into sulfides, whereas in the absence of sulfides, Ru partitions into chromite. Therefore, Ru concentrations in chromite can be used in the exploration for nickel-sulfide deposits, based on the empirical evidence that Ru-enriched chromites are associated with barren systems. This method can be applied directly to polished sections and/or grain mounts and therefore provides a rapid and cost-effective tool in the hunt for nickel-sulfide deposits.

Contacts: Marek Locmelis, Norman Pearson
Funded by: ARC Discovery Project Grant (O'Reilly, Griffin and Pearson), MQRES, EPS Postgraduate Fund

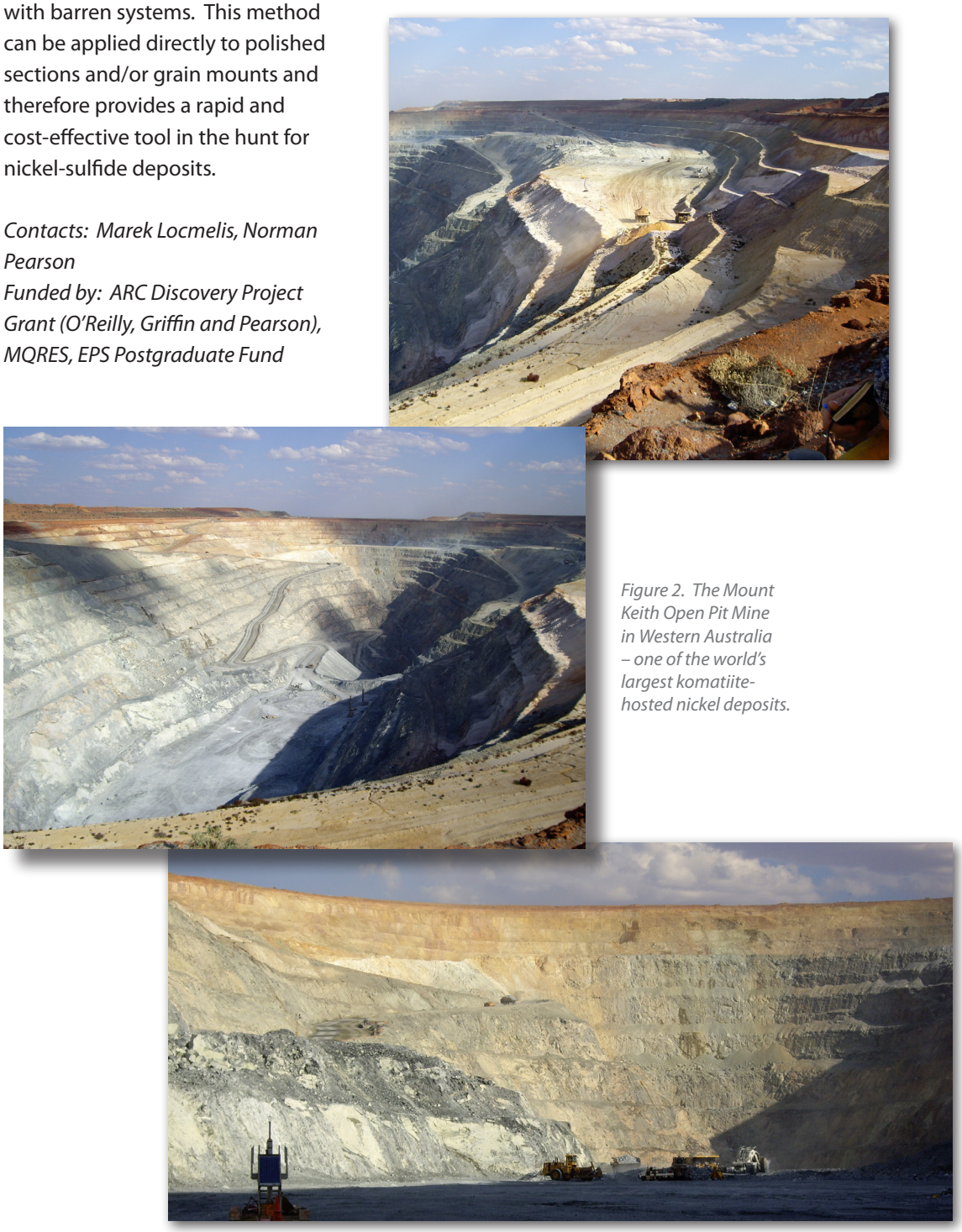

Figure 2. The Mount Keith Open Pit Mine in Western Australia – one of the world's largest komatiite-hosted nickel deposits.

Zircons from the roof of the world unearth Himalayan evolution

THE TIBETAN PLATEAU, one of the most remarkable places to visit in Asia for travellers, is known as the roof of the world. The formation of such a high broad uplift naturally attracts geologists' curiosity. Following decades of investigations, we know that it formed during the collision between the Indian and Eurasian plates. However, some details remain controversial, for instance: when did these two plates collide, (from Late Cretaceous to Oligocene), and what mechanisms support the immense relief? Now, *in situ* analysis of Hafnium isotopes in zircon, commonly a trace mineral, combined with the isotopic analysis of Hafnium and Neodymium in its host rocks in the southern part of the Lhasa terrane, offer us new answers to these questions.

In this study, we analysed rocks from the south Transhimalayan batholiths, including Gangdese granitoids and Oligo-Miocene adakites. Our integrated Hf and U-Pb isotope analyses of zircon crystals, together with Hf and Nd isotopes of their host rocks, show a secular change in the magma sources that can be related specifically to the encroachment of the Indian plate into the southern part of the Tibetan orogen during the continental collision.

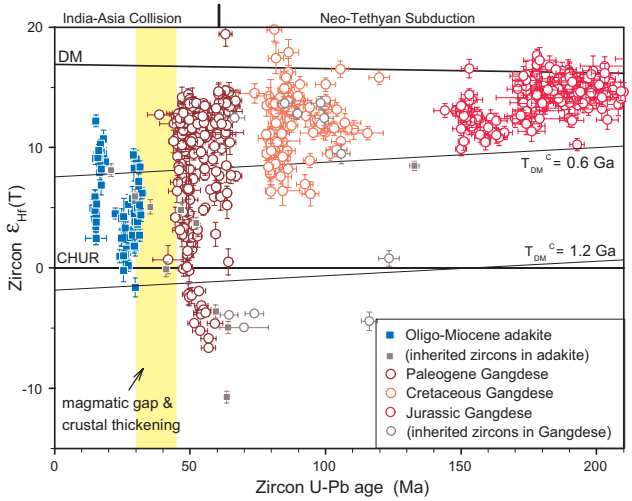

Figure 1. In situ Hf and U-Pb isotopic data for zircons from Gangdese granitoids and Oligo-Miocene adakites in the southern part of the Lhasa terrane.

The magmatic zircons, crystallised between ca 200 Ma and 50 Ma, mainly show depleted mantle-type Hf-isotope characteristics but this changes markedly in the Paleogene (Fig. 1). The Hf-isotope shift is interpreted as reflecting the subduction of the Himalayan sediments, driven by the approach of the Indian plate, and thus signals the initiation of the India-Asia collision by 55 Ma.

Our data also indicate that the crust of southern Tibet thickened significantly between ca 45 - 30 Ma, before emplacement of the post-collisional adakites (Mg-rich silicic igneous rocks). These adakites exhibit Hf-Nd isotopic systematics different from the previous Gangdese magmatism, suggesting mixing of melts from (a) the juvenile Gangdese mafic crust and (b) incorporated Himalayan sediments, with zircon residues fractionating Nd and Hf abundances during crystallisation (Fig. 2). See *GEMOC Publication #730.*

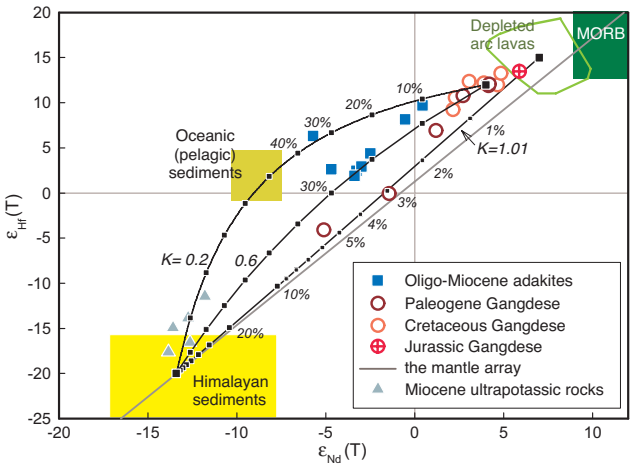

Figure 2. Whole-rock $\varepsilon_{Hf}(T)$ vs $\varepsilon_{Nd}(T)$ plots of the Transhimalayan rocks, showing how the adakites fall along mixing curves between the older Gangdese magmas and Himalayan sediments.

Contacts: Mei-Fei Chu, Norman Pearson, Sue O'Reilly
Funded by: ARC Discovery Project Grant

The Big Bang - New insights into the 1912 eruption of Katmai volcano

In June 1912, the biggest and one of the most compositionally diverse eruptions of the last century took place in the Katmai group of volcanoes on the Alaska Peninsula. In the space of 60 hours, 13 km^3 of rhyolite, dacite and andesite magma were explosively ejected, producing an ash cloud covering 77,000 km^2 that extended as far east as Greece and filled the Valley of Ten Thousand Smokes. The eruption started with a crystal-poor rhyolite followed by a gradual increase in the proportions of dacitic and andesitic material. The eruption took place from a vent at the site of the present-day Novarupta dome, but the magma came from beneath the summit of Mount Katmai 10 km to the east. As the magma moved out, the summit started to collapse some 11 hours after the onset of the eruption, finally forming a 5.5 km^3 caldera. New geochemical data are now giving a very detailed picture of the lead-up to this massive volcanic eruption.

View along the Valley of Ten Thousand Smokes towards Mount Katmai.

The entire major- and trace-element range in the successive magmas can be modeled by 80-90% closed-system crystal fractionation over a temperature interval from 1279 to 719 °C at 100 MPa, starting with about 65 km^3 of parental basaltic magma. Numerical thermal models suggest that, for wall rock temperatures appropriate to this depth, this volume of magma would cool and crystallise by 90% over this temperature interval within a few tens of thousands of years. However, a significant range in $^{87}Sr/^{86}Sr$, ($^{230}Th/^{238}U$) and ($^{226}Ra/^{230}Th$) in the magmas requires open-system processes. The U-series isotopes indicate that crustal residence times for some dacites were close to 8000 years, whereas the rhyolites appear to be significantly older (50-200 kyr). Thus, magmas that erupted within only 60 hours of one another in 1912 had resided in their crustal magma chambers for quite different time spans. Nevertheless, because they were emplaced in the same thermal regime, they all evolved along similar liquid lines of descent from parental magmas with similar overall compositions. The system was built up progressively with multiple injections of mafic magmas, which provided both mass and heat; some of the heat led to melting of older silicic material that provided much of the magma mass for the rhyolite. Although this scenario is increasingly recognised as a common one, it cannot be deduced from field observations or major- and trace-element compositional variations. Only the data from short-lived radioactive isotopes are sensitive to processes such as protracted magma build-up, differentiation, assimilation and eruption.

Aerial view of Mount Katmai showing the caldera that formed during the 1912 eruption (Captain Budd Christman, NOAA Corps).

Contact: Simon Turner
Funded by: National Environment Research Council, UK

Journey from the centre of the Earth: xenoliths reveal the velocity of magmas

THE RATES AT WHICH MAGMAS RISE THROUGH THE CRUST AND UPPER MANTLE cannot be measured directly, but can be estimated by several indirect means, based on observations from mantle-derived xenoliths in alkali basalts, kimberlites and related rocks (*GEMOC Publication #666*). These magmas are generated in the convecting mantle at depths from about 90 to 200 km, commonly are not fractionated during their ascent and may incorporate fragments of the lithospheric mantle as they travel through it.

Figure 1. Angular xenoliths of spinel peridotite in alkali basalt from Batchelor Crater, Queensland, Australia.

At upper mantle temperatures and pressures (depths of 50-250 km and temperatures of 1000-1300 °C), mantle rocks have been shown to deform plastically, at least in response to long-term stresses. However, the entrainment of xenoliths in an ascending magma requires that fragments of rock be broken off the walls of magma chambers or conduits, a process that implies brittle fracture in response to short-term stresses. This brittle response is evidenced by the typically angular to subangular shapes (Figs. 1,2), resulting in polygonal and facetted xenoliths (Fig. 3), and the common linear contact surfaces of veins in xenoliths (Fig. 4). Significant rounding is restricted to xenoliths from breccias or those associated with the more explosive eruptions such as maars, diatremes, and some cinder cones. Xenoliths in kimberlites are typically more rounded than those in basalts, but many display planar faces (Fig. 3). This rounding appears to reflect tumbling of xenoliths during turbulent ascent and eruption. However, we infer that at the time of their entrainment, most xenoliths are angular, and originated by brittle fracture.

The mineral assemblages and mineral chemistry of many xenoliths can be compared with experimental studies to derive the depth and temperature at which they were picked up by the ascending magma. These xenoliths therefore can provide constraints on the shallowest depths of magma generation and segregation, and on how rapidly magmas get to the surface.

Figure 2. A composite xenolith showing spinel peridotite veined by basaltic magma that crystallised in the mantle, within a volcanic bomb from Mt Shadwell, Victoria, Australia. Note the originally straight sides (emphasised by white dashed lines) and the rounded edges of the xenolith due to abrasion in the magma. The spinel peridotite areas appear rounded due to reaction with the invading basaltic magma.

The rates of ascent of magmas are equivalent to the residence times of xenoliths in the magma after their entrainment. These rates can be estimated by a variety of methods using the physical and compositional parameters of the xenoliths. Mantle-derived peridotite, eclogite and pyroxenite xenoliths are relatively dense, and the magma must be ascending more rapidly than the xenoliths can sink through it. These calculations suggest an average ascent rate through the whole lithosphere (mantle and crust) in the range of 0.2 to 0.5 metres per second (about 0.5 to 2 km/hour). The ascent rates through

the shallow crust may be much higher; >20 metres per second and up to supersonic speeds (≥300 metres per second) in the uppermost crust.

Residence times of xenoliths in the magma also can be estimated using calculations based on temperature-related diffusion phenomena (chemical zoning, grain-boundary adjustment) observed in xenoliths; all of these approaches suggest ascent rates in the range of 0.2 to 0.4 metres per second.

Figure 3. Xenolith from kimberlite showing polygonal shape with planar surfaces.

It has been suggested that high contents of CO_2 in magmas provide a significant "propellant effect" to assist xenolith transport. This is not correct, because the density and viscosity of the mixed magma-fluid system are lower than those of unmixed magmas. However, the exsolution of CO_2 both provides heat that helps to prevent the magma from cooling during ascent, and enhances crack propagation. Magmas representing significant proportions of partial melting, such as tholeiitic basalts, rarely carry mantle-derived xenoliths; this probably reflects ascent rates that are too slow to hold (or possibly incorporate) high-density xenoliths entrained in the magma.

In summary, magmas carrying mantle xenoliths must reach the surface within a maximum of about 8 to 60 hours after picking up these dense fragments from depths of about 200 to 80 km depth. See *GEMOC Publication #666.*

Contacts: Sue O'Reilly, Bill Griffin
Funded by: ARC Discovery Project Grants

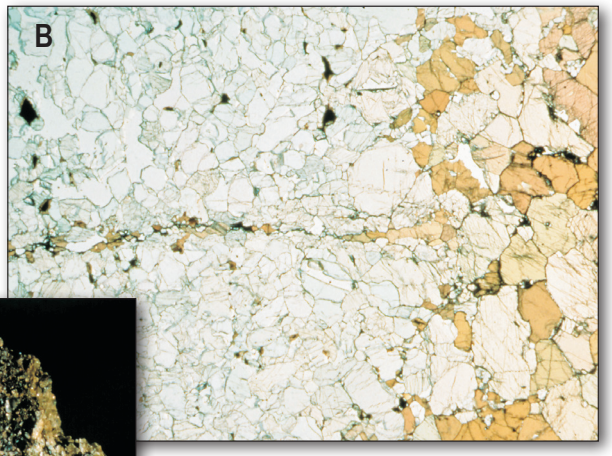

Figure 4. A: Spinel peridotite xenolith showing straight-sided vein of garnet pyroxenite (basaltic magma crystallised within the mantle). B: Photomicrograph of thin section of a peridotite showing an amphibole-rich vein with thin offshoot. Note the straight sides on both the large and small veins. Field of view is 2.5 cm across.

Core formation in partially molten planetesimals: A complex network analysis

THE SEGREGATION OF METALLIC CORES FROM SILICATE MANTLES is one of the earliest, and most important, differentiation processes in the evolution of terrestrial planetary bodies. Although a magma-ocean model is commonly used for efficient core formation, more recent scenarios using calculations from extinct radionuclides (e.g. ^{26}Al, ^{60}Fe) call for segregation of the core from partially molten silicate – a silicate "mush matrix". This segregation scenario requires growth of molten core material into blebs large enough to overcome the strength of the mush matrix so that separation can occur. The geochemical ramifications can be significant because bleb size will control the degree of equilibration. In collaboration with colleagues from the Mathematics Department at the University of Melbourne (A. Tordesillas and D. Walker), we have developed an innovative approach that combines partial-melting experiments on natural materials with complex-network analysis to quantify the growth of metallic melt regions in a silicate mush matrix. The presence of silicate melt is a significant transition point in the segregation of liquid metal and we are characterising this by using graph-theoretic techniques from Complex Networks. Properties of the networks have been constructed from the experimental data to determine whether the molten metal and silicate zones are tending to mix or separate, as manifested in the liquid metal blebs growing during melting and deformation of the rock sample (Fig. 1).

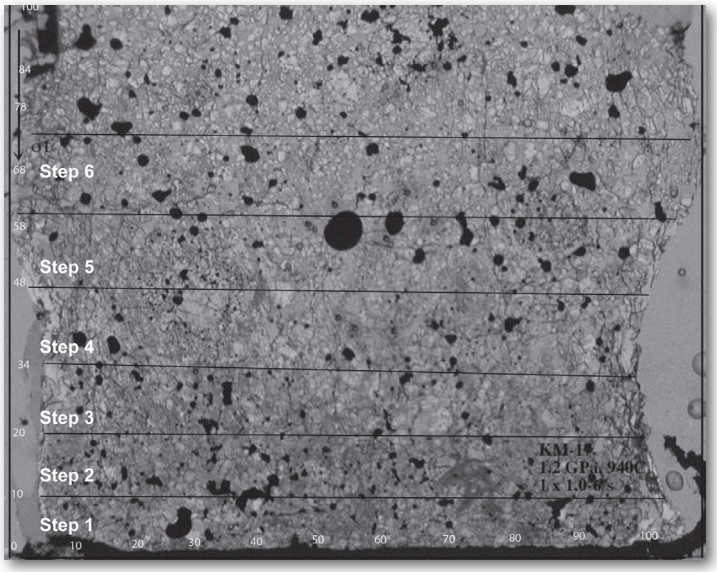

Figure 1. A backscattered-electron image of experiment KM-17, deformed at 940°C, 1.2 GPa and at 1.0 x 10^{-6}/s. Metal-sulfide eutectic quench liquid is most common and forms blebs in the silicate glass in the middle of the sample. The grid is placed on top of the sample and data collected at every point (100 data points per line by approximately 10 lines per step). Steps were chosen by the changes in the modes of melt and liquid vs unmelted material and go from step 1, where no melt or liquid metal is present, to step 6 where silicate melt fraction is the highest.

Complex Network Analyses: A basic network or graph consists of nodes, with some pairs of nodes connected by a link. Here, the networks are constructed from textural information collected at distinct sampling sites located at the intersection points of a near-regular sampling grid placed on the experimental sample. The sampling sites are then assigned to the nodes of a complex network. The topological structure of such a network is uninteresting. However, if we then label each node as a "type" according to the sampled data, i.e., node type indicates silicate melt, liquid metal, etc. then there are useful network measures to summarise the patterns of connections between node types (Fig. 2). One such measure is the assortativity, which quantifies a node's 'preference' to attach to other nodes of the same type. In complex networks, the statistics that are most associated with assortativity arise from the question of whether network nodes of the same degree (number of links attached to a node) are typically connected to each other. A random network where there is no discernable pattern of mixing has an assortativity measure of zero. We performed this analysis on the experimental data to establish whether separation of liquid metal from silicate melt (positive assortativity) or mixed (negative or zero assortativity) has occurred in the silicate mush matrix under deformation.

Results: For the assortativity coefficient, we found that the sample subnetworks evolve to a highly disassortative network due to the early dominance and residual presence of type 1 (solid silicate) within the sample. This is expected as it is a mush, so that solid silicate remains even in the

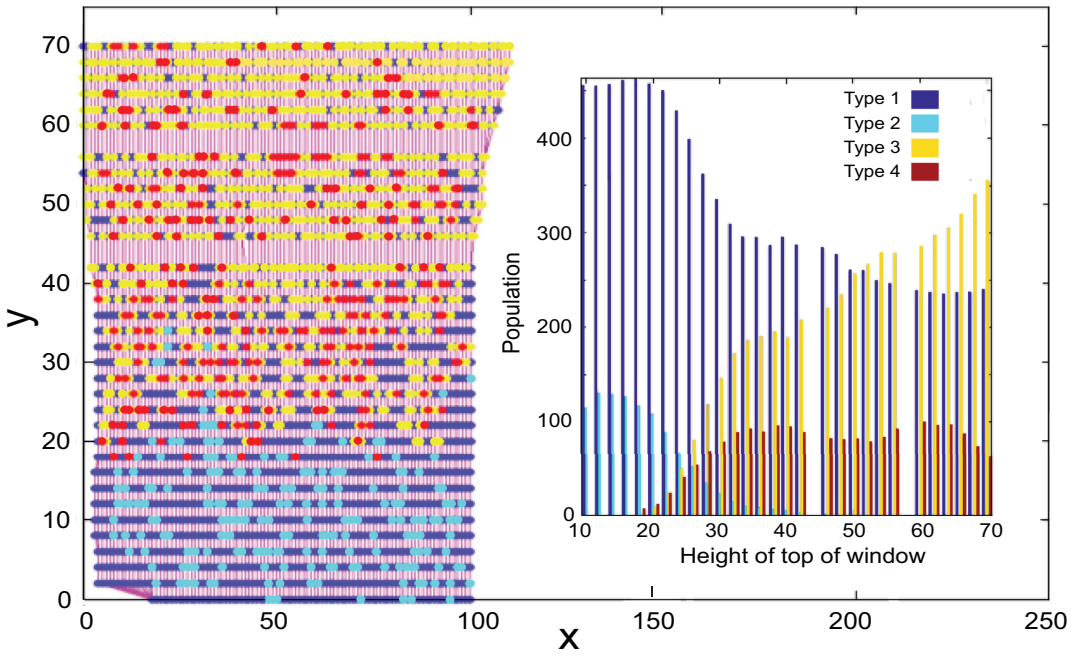

Figure 2. Full sample grid showing spatial distributions of type 1 (solid silicate), type 2 (solid metal), type 3 (liquid silicate) and type 4 (liquid metal). 29 windows "slide up" the sample, starting from the bottom of the sample (step 1) and ending at the hot spot with the highest melt fraction of both metal and silicate (step 6). The change in the population of each type as the window moves up is shown in the inset: in step 1, type 1 is dominant with some type 2, but by step 6, type 3 is dominant with some types 1 and 4.

highest temperature zone. For the subnetwork of liquid metal and silicate melt, we observed an assortativity coefficient around zero for heights above *y*=20 (types 3, silicate melt, and 4, liquid metal, are absent from the sample below this height) which is indistinguishable from a random mixing pattern. A simple randomisation test of the assortativities of surrogate random networks, each constructed by assigning node types 3 and 4 randomly, confirmed this. At heights beyond *y*=60, we find that the experimental sample with respect to node types 3 and 4 had evolved to a pattern with a significant positive assortativity coefficient (Fig. 3). In this area of the sample, there is significant "clumping" of the silicate melt and the liquid metal in the sample with respect to height (i.e. with increasing temperature and deformation). At *y*=60 and above, the zone of the highest strain and concentrated deformation, we find the highest fraction of silicate melt.

This novel approach has allowed us to quantify the texture by treating the four-phase system as a complex network. We see a "clumping" of metallic liquid and of silicate liquid as the proportion of silicate melt increases (from steps 1 to 6 in the sample) and deformation is concentrated in this weaker partially molten zone (step 6). The clumping processes may be driven by a combination of low pressure (dilational sites) in the mush zone, developed during deformation, and contrasts in surface energy and viscosity between the silicate melt and metallic liquid. The analysis of the textural data in step 6 shows that the network is assortative; the nodes of the same type are more likely to be connected together. This analysis can allow us to extract unambiguous network trends that can then predict the growth of blebs in the presence of silicate melt. This can then be used in calculations that include a modified Stokes Law to predict sinking rates for core formation in partially molten planetesimals.

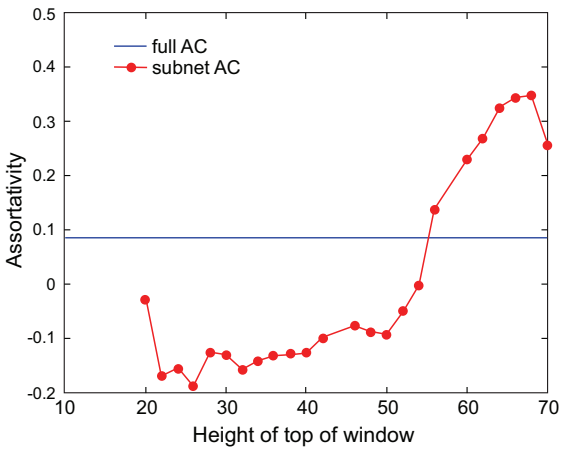

Figure 3. Assortativity coefficient of the 29 sliding window subnetworks consisting of nodes of types 3 and 4 only (from Fig. 2, nodes of types 3 and 4 do not exist below y=20). The blue line shows the equivalent value of the assortativity coefficient for the global network comprising all types for the entire sample (window size is the full sample).

Contact: Tracy Rushmer
Funded by: ARC Discovery Project Grant

Catastrophic overturn on Enceladus

New research at GEMOC has explained the enigmatic behaviour of Enceladus, Saturn's sixth-largest moon. This tiny ball of ice and rock is only 500 km across—and yet it hosts a level of geologic activity comparable to Earth.

Enceladus's south pole erupts water-rich geysers into Saturn's ring system, from a region carved up by unusually warm fractures known as 'tiger stripes'. Thermal imaging of the moon's surface by the Cassini space-probe indicates that Enceladus is losing far more heat than it should be generating - a fundamental disparity in the thermal balance of the body. What's more, the south pole terrane is geologically young - cratering statistics indicate that it is less than 100 Myrs old, and perhaps much younger. In contrast, heavily cratered plains on Enceladus yield ages of up to 4.2 Ga - as old as any surface in the outer solar system, while the moderately cratered plains of Sarandib Planitia and Samarkand Sulcus yield ages of 170–3,750 Myrs and 10–980 Myrs, respectively. The episodic distribution of ages of different terranes on Enceladus implies that Enceladus has experienced localised periods of surface activity, interspersed with periods of relative inactivity.

In a paper published in Nature Geoscience in 2010 (*GEMOC Publication #621*), we proposed a model to resolve the discrepancy between Enceladus's heat production and heat loss. In this model, the massive heat loss at the moon's south pole can be explained by a periodic tectonic regime, resulting in geologic eruptions - such as those now visible on Enceladus - occurring every billion years or so.

As Enceladus orbits Saturn, the massive planet's gravitational pull causes the icy moon to flex, generating tidal heat on the satellite. Enceladus's orbit is not circular, so as it goes around Saturn its orbital distance changes, and the gravitational force that it feels changes slightly. As a result Enceladus is constantly squeezed and stretched, generating a lot of heat, like a squash-ball being squeezed in a hand. Radioactive decay - which powers most of Earth's tectonism, is only marginally important on Enceladus.

Despite its high range of tidal heating, Enceladus is still losing many times more heat than tidal sources can account for. Either something is unaccounted for, or the heat being released today is not matching the steady-state production rate. Instead, Enceladus may be in the middle of a 'pulse' of transiently enhanced heat loss well above its background average.

The new research suggests what we are seeing on Enceladus now is a transient period of active lid behaviour—a brief episode of

Figure 1. Cassini photograph of Enceladus, showing the relatively young South Pole Terrane, exhibiting a sub-linear 'Tiger-stripe' fracture system, and much older heavily cratered plains to the north. (Credits: NASA)

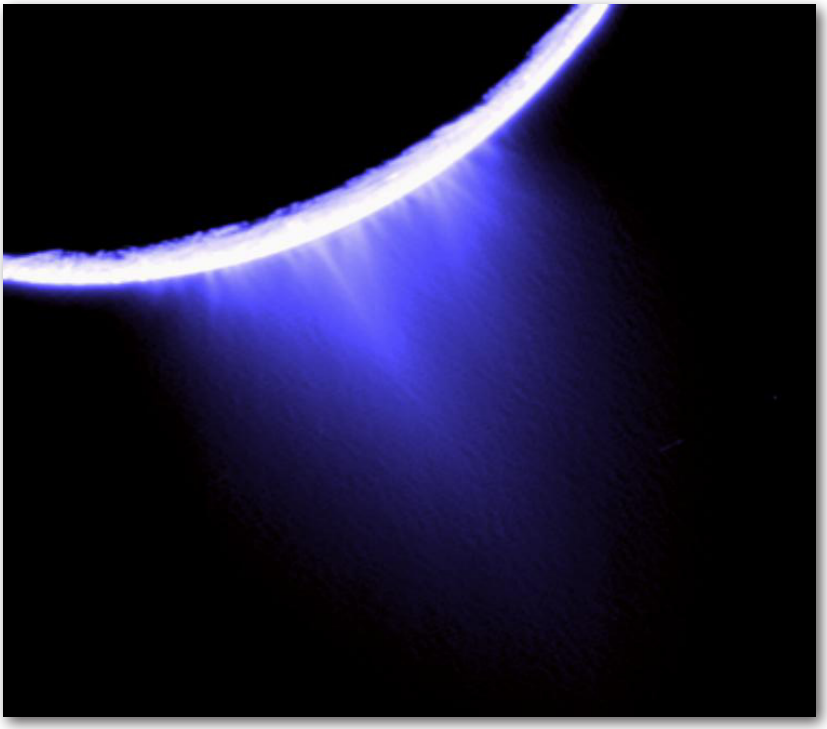

Figure 2. Water-rich geysers emanating from the 'Tiger-stripe' fractures in the South Pole Terrane. Image from UV Camera. (Credits: NASA)

tectonic activity that resurfaces a limited area of the moon. In the new model, heat is pent up inside the interior over billions of years, building up to a critical level and then escaping in one big pulse of activity. The models show that episodic partial-lid recycling occurs for plausible lid strengths and Enceladus's estimated supply of tidal energy. The localised nature of such overturn episodes, their periodicity of 0.1–1 billion years and an anomalous heat flow during these episodes are consistent with Enceladus's geology and modelled heat supply.

The models suggest that the pulses of activity would last for around 10 million years - a blink of an eye, geologically. Outside these active episodes, Enceladus would exhibit a more dormant, stagnant-lid mode of convection - not unlike many other icy moons. But if this periodic tectonic behaviour is endemic to icy satellites with evidence of partial resurfacing throughout the solar system, the other satellites also should show signs of episodic resurfacing. Indeed, Ganymede, Rhea and Miranda all show signs of episodic resurfacing deep in their geological past, and so transient tectonics in the outer solar system may be more common than previously thought.

Contact: Craig O'Neill
Funded by: Macquarie CoRE funding

Brilliant imaging: new facets of diamonds' deep inner secrets

DIAMONDS, ALONG WITH THE MINERAL AND FLUID INCLUSIONS they can contain, represent the deepest direct samples from the Earth's mantle. Studying these diamond "capsules" as well as their contents has shed light on the chemistry of mantle fluids. A principal technique in the world of diamond research is infrared (IR) spectroscopy. This is a very simple technique for observing and quantifying the impurities that commonly occur in the diamond lattice, including both nitrogen and hydrogen. It is now the main technique used for diamond classification, which is based upon the abundance and nature of the nitrogen impurities.

Developments in IR analytical capabilities have made the mapping of these impurities far easier and quicker than ever before. The most modern equipment, as used in GEMOC, can collect thousands of point spectra across a single diamond in a single working day. However, for quantitative anaysis, the raw FTIR spectra must be deconvoluted. This has produced a requirement for an automated method that can accurately deconvolute thousands of spectra and quantify the most common impurities. We have developed an open-source (i.e. free to access) software routine (DiaMap) that automatically deconvolutes the spectra and quantifies the main nitrogen and hydrogen impurity features of a diamond. This includes the nitrogen concentration and aggregation state, the size of the platelet peak (interstitial carbon aggregates formed as a by-product of nitrogen aggregation) and the relative abundance represented by the main hydrogen peak.

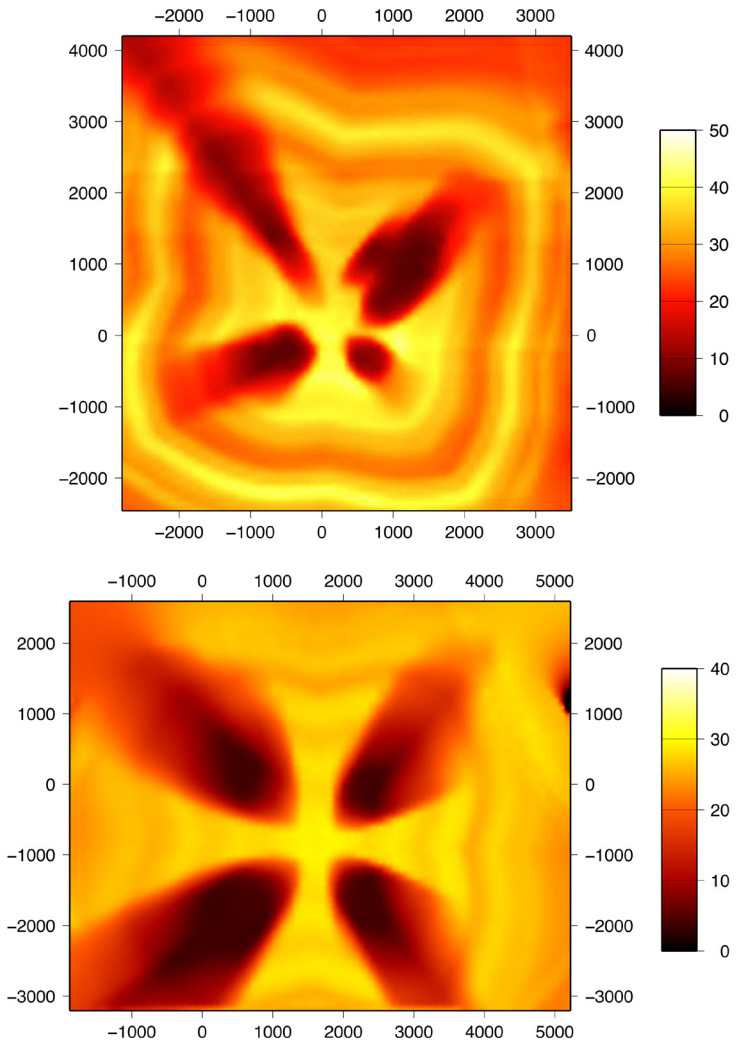

Maps of diamond MC06 (top) and MC12 (bottom), made up of thousands of infrared spectra, showing the relative intensity of the dominant hydrogen band (3107 cm^-1) in diamond. The hydrogen concentration correlates with cuboid growth, which is a different growth mechanism to that which produces perfect, octahedral gem quality diamonds.

Application of this technique has already shown some interesting results with respect to diamonds of mixed-habit growth. These are diamonds that show periods of smooth faceted octahedral growth and rough, hummocky cuboid growth, occurring at the same time. This often results in a center cross feature, which may or may not be obvious to

the naked eye. A common feature observed in these types of diamonds is that platelet concentrations are much lower in cuboid sectors relative to contemporary octahedral sectors. No satisfactory reason for this has ever been given, but the most recent idea suggests that the high concentrations of hydrogen in cuboid sectors inhibit nitrogen aggregation, resulting in reduced platelet production. However, our new IR mapping shows that aggregation state of N can be the same in contemporary sectors, while platelet concentrations are lower in the cuboid sectors. This leads to the more logical conclusion that other defects (disc-like cracks), which are only found in cuboid sectors, are responsible for reducing the quantity of interstitial carbon atoms and therefore lowering the platelet concentrations. This has serious implications for another commonly utilised diamond classification method, based on platelet concentrations.

The application of this IR mapping method, in combination with other techniques like laser ablation mass spectrometry (LA-ICP-MS) to measure trace elements, cathodoluminescence imaging to reveal growth stratigraphy, and secondary ion mass spectrometry (SIMS) to measure carbon isotopic ratios, will reveal further information about the role of fluids in the mantle.

Contacts: Dan Howell, Craig O'Neill, Bill Griffin
Funded by: ARC Discovery Project Grant

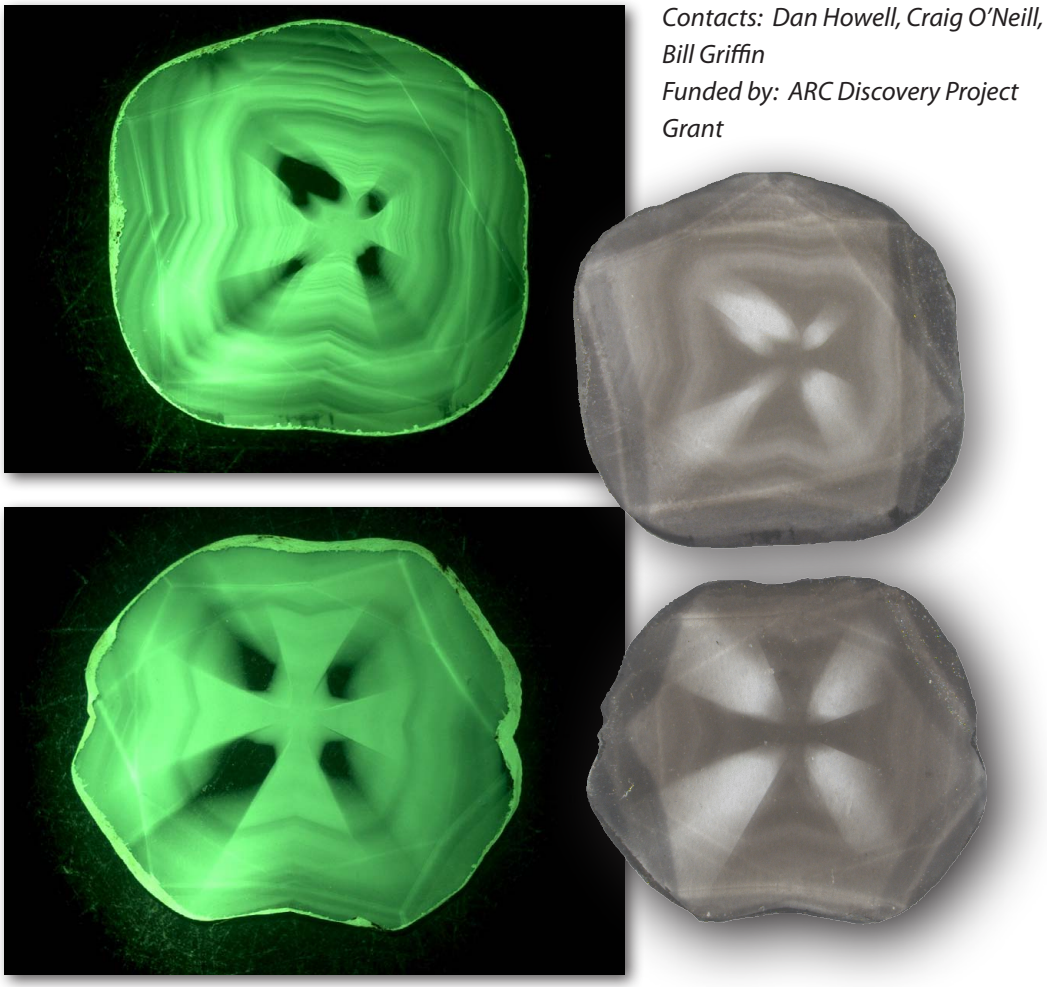

Images of sample MC06 (top) and MC12 (bottom) taken under UV light. The luminescence comes only from the cuboid sectors (shown to be hydrogen-rich by the IR maps) while the octahedral sectors appear black. The cross feature that appears by luminescence is the reason these mixed-habits diamonds are commonly referred to as "star" or "centre-cross" diamonds.

ARC National
Key Centre for the
Geochemical Evolution and
Metallogeny of Continents